

Journal of

Tropical Biodiversity and Biotechnology

VOLUME 8 | ISSUE 3 | DECEMBER 2023

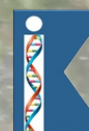


PUBLISHED BY



UNIVERSITAS GADJAH MADA
FAKULTAS BIOLOGI

IN COLLABORATION WITH



KBI

KONSORSIUM BIOTEKNOLOGI
INDONESIA
INDONESIAN BIOTECHNOLOGY CONSORTIUM

Credits

Editor	Miftahul Ilmi Ardaning Nuriliani Furzani Binti Pa'ee Sri Nopitasari Liya Audinah Annisaa Widyasari Tanti Agustina
Copyeditor and Language Editor	Salwa Shabria Wafi Almaulidio Tazkia Dina Syarifah Rosana
Layout Editor	Salwa Shabria Wafi Muchamad Ulul Azmi
Cover Photo	Ratih Tryas Intani
Editorial Board	Prof. Dr. Wibowo Manguwardoyo Prof. Dr. Budi Setiadi Daryono, M.Agr.Sc. Prof. Dr. Jonathan A. Anticamara Prof. Jean W. H. Yong, Ph.D. Dr. Farid Asif Shaheen Ts. Dr. Kamarul Rahim bin Kamarudin Assoc. Prof. Dr. Wong Wey Lim Dr. Phoon Lee Quen Sukirno, M.Sc., Ph.D. Dr. rer. nat. Andhika Puspito Nugroho Assoc. Prof. Dr. Ruqiah Ganda Putri Panjaitan Dr. Abdul Razaq Chasani Dr. Ratna Stia Dewi Dr. Alona Cuevas Linatoc Prof. Madya Ts. Dr. Muhammad Abdul Latiff Bin Abu Bakar Ts. Dr. Siti Fatimah Binti Sabran

Table of Contents

Short Communication

- Notes on The Current Distribution and Abundance of The Frog Genus *Leptophryne* spp. (Anura: Bufonidae) in Gede Pangrango National Park jtbb84031
Mohamad Isnin Noer, Ratih Tryas Intani, Priya Yuga Prasetya, Ahvita Dwi Lestari, Boby Darmawan

Research Articles

- Stomata characters of sugarcane (*Saccharum officinarum* L.) mutants of GMP3 variety at PT Gunung Madu Plantations, Lampung, Indonesia jtbb79860
Mahfut Mahfut, Putri Kendari, Admi Syarif, Sri Wahyuningsih, Endah Susiyanti
- Comparison of Light Intensity under the Canopy between Sal (*Shorea robusta*) and Akashmoni (*Acacia auriculiformis*) in Agroforestry Stands: Effect of Tree Size and Distance from Individual Trees jtbb78063
Md. Al Forhad Islam, Md. Najmus Sayadat Pitol, Md. Nabiul Islam Khan
- The Status, Trends, and Limitations of Philippine Mollusk Production and Trade Based on Available Databases and Publications jtbb73325
John Alberto H Ordinario, Jonathan A. Anticamara
- Region of Nuclear Ribosomal DNA (*ITS2*) and Chloroplast DNA (*rbcL* and *trnL-F*) as A Suitable DNA Barcode for Identification of *Zingiber loerzingii* Valeton From North Sumatera, Indonesia jtbb76956
Eko Prasetya, Lazuardi Lazuardi, Fauziyah Harabap, Yuanita Rachmawati, Yusnaeni Yusuf, Said Iskandar Al Idrus, Puji Prastowo
- Herbaceous Diversity in the *Gumuk* Ecosystem in Ledokombo District-Jember Regency with Varied Land Use Type jtbb77888
Wiwini Maisyaroh, Luchman Hakim, Sudarto Sudarto, Jati Batoro
- In Silico* Approach for DNA Barcoding using Phylogenetic Analysis of *Coelogyne* spp. based on the *matK*, *rpoC1*, *rbcL* and *nrDNA* Markers jtbb73130
Apriliana Pratini, Anggiresti Kinasih, Maura Indria Meidianing, Febri Yuda Kurniawan, Endang Semiarti
- Birds Species on Vertical Stratification of Mangrove Vegetation Nusa Lembongan, Bali Indonesia jtbb78394
I Ketut Ginantra, I Ketut Muksin, Martin Joni
- Induction of Synthetic Polyploids of Porang (*Amorphophallus muelerri* Blume) and Assessment of Its Genetic Variability Using Morphological Data and RAPD Molecular Marker jtbb82238
Suyono Suyono, Imey Tamara Indivia, Ruri Siti Resmisari, Fitriyah Fitriyah, Didik Wahyudi
- In Silico* Analysis of *Phalaenopsis Orchid Homeobox1* (*POH1*) Functional Gene for Shoot Development in *Phalaenopsis* Orchid jtbb83934
Nuzlan Rasjid, Febri Yuda Kurniawan, Saifa Usni Putri, Aniesta Linggabuwana, Ireneus Seno Prasajo, Endang Semiarti
- In silico* Screening of Potential Antidiabetic Phenolic Compounds from Banana (*Musa* spp.) Peel Against PTP1B Protein jtbb83124
Rico Alexander Pratama, Junaida Astina, Arli Aditya Parikesit
- Cobalamin and Thiamine Effect on Microalgae Biomass Production in the Glagah Consortium jtbb81949
Tri Wahyu Setyaningrum, Arief Budiman, Eko Agus Suyono

- Spatial Distribution of *Cedrela Odorata* Smaller Trees Affects Forest Regeneration in Exotic Tree Plantations in Central Côte d'Ivoire jtbb84322
Bi Tra Aimé Vrob, Abdoulaye Koné
- The Diversity of Scarabaeid Beetles (Scarabaeidae: Coleoptera) in The Lowland Rainforest Ecosystem of Sorong Nature Tourism Park, West Papua, Indonesia jtbb78230
La Ode Fitriadiansyah, Tri Atmowidi, Windra Priawandiputra, Sib Kabono
- Comparison of Soil Arthropod Diversity and Community Structure in Various Types of Land Cover in Malang Region, East Java, Indonesia jtbb79496
Bagyo Yanuwidi, Subarjono Subarjono, Nia Kurniawan, Mubammad Fathoni, Agus Nurrofik, Miftah Farid Assiddiqy, Abdul Mutholib Shabroni
- Profiling of Single Garlic Extract Microencapsulation: Characterization, Antioxidant Activity, and Release Kinetic jtbb79072
Sri Rahayu Lestari, Abdul Ghofur, Siti Imroatul Maslikah, Sunaryono Sunaryono, Amalia Nur Rahma, Dahniar Nur Aisyah, Ikfi Nibayatul Mufidah, Nadiya Dini Rifqi, Nenes Prastita, Dewi Sekar Miasih, Alif Rosyidah El Baroroh
- Maturation of Female Yellow Rasbora (*Rasbora Lateristriata* Bleeker, 1854) Using Oodev at Different Doses in Feed jtbb75916
Juniman Rey, Slamet Widiyanto, Bambang Retnoaji
- Bioremediation of Mercury- Polluted Water in. Free Water Surface-Constructed Wetland System by *Englena* sp. and *Echinodorus palifolius* (Nees & Mart.) J.F. Macbr. jtbb88143
Dwi Umi Siswanti, Budi Setiadi Daryono, Himawan Tri Bayu Murti Petrus, Eko Agus Suyono

Review Article

- Advancement in Plant Tissue Culture-Based Research for Sustainable Exploitation of Well-Known Medicinal Herb *Bacopa Monnieri* jtbb74937
Abhijith Vinod, Shivika Sharma, Vikas Sharma
- Extremophilic Cellulases: A Comprehensive Review jtbb74986
Subham Mohanta, Megha Babuguna, John David Baley, Shivika Sharma, Vikas Sharma

Short Communications

Notes on The Current Distribution and Abundance of The Frog Genus *Leptophryne* spp. (Anura: Bufonidae) in Gede Pangrango National Park

Mohamad Isnin Noer^{1*}, Ratih Tryas Intani², Priya Yuga Prasetya², Alvita Dwi Lestari², Bobby Darmawan³

1) Biology Department, Faculty of Mathematics and Natural Sciences, Universitas Negeri Jakarta. Jl. Rawamangun Muka, 13220. Indonesia.

2) Undergraduate student, Biology Department, Faculty Mathematics and Natural Sciences, Universitas Negeri Jakarta. Jl. Rawamangun Muka, 13220. Indonesia.

3) Ministry of Environment and Forestry, Indonesia. Jl. Kebun Raya Cibodas, Cimacan, Kec. Cipanas, Kabupaten Cianjur, Jawa Barat 43253

* Corresponding author, email: mohamad.isnin@unj.ac.id

Keywords:

Leptophryne

Gede Pangrango National Park

endemic

Indonesia

niche segregation

Submitted:

24 April 2023

Accepted:

10 June 2023

Published:

20 October 2023

Editor:

Ardaning Nuriliani

ABSTRACT

We reported the current distribution of *Leptophryne* spp. in Gede Pangrango National Park. *Leptophryne cruentata* was recorded in Cibodas (Cikundul waterfall and Goa Lalay), Selabintana (Cibeureum Waterfall), and Goalpara (Rasta Waterfall), whereas *Leptophryne borbonica* was only reported from a creek at lowland forest of Bodogol. Goa Lalay and Rasta waterfall were explicitly reported as new distribution locations of *Leptophryne cruentata*. It was strictly found at a higher elevation usually within reach of waterfalls that generate substantial background noise, except in Cibodas in which *Leptophryne cruentata* can also be found in two noisy creeks located at a fairly great distance from waterfalls (100 – 170 meters).

Copyright: © 2023, J. Tropical Biodiversity Biotechnology (CC BY-SA 4.0)

Gede Pangrango National Park (GPNP) is an important area in providing resources and shelters for many endemic and rare species. The very few unchanging features of this park over decades help sustaining a huge number of important species by providing them a lot of resources and tranquillity of habitats. *Leptophryne cruentata* is one of the endemic frogs of Java, Indonesia. This frog currently reported only presents in West Java following the recent study that split this cryptic species into two different species (Hamidy et al. 2018). *Leptophryne cruentata* is the only amphibian species listed in protected species in Indonesia. Due to small area of distribution and significant increase of population during decades, this species categorised as Critically Endangered in red lists of IUCN. Its distribution in West Java has been documented in Gede Pangrango, Halimun Salak, and Ujung Kulon (Kurniati 2002; Kurniati 2006), but its population is more prolific in Gunung Gede National Park (Mumpuni 2001; Kusrini et al. 2017), thus, encouraging conservation efforts in this area is more principle. One of the conservation actions required to be addressed is updating the population of *Leptophryne cruentata* and identifying the novel distribution of this frog in GPNP (Iskandar & Erdelen 2006; Kusrini et al. 2007b; Kusrini et al. 2017; Saputro et al. 2021).

The distribution of this frog in this GPNP could probably be more widespread which is indicated by newly anecdotal areas reported being occupied by *Leptophryne cruentata*. The possibility of discovering this frog in other locations in GPNP is also promising because there are so many areas in GPNP considered to be potential habitats for *Leptophryne cruentata* (Saputro et al. 2021). Moreover, additional information on habitat features, such as elevation and noise, are pivotal to be addressed since *Leptophryne cruentata* are strongly associated with waterfalls and high elevation (Iskandar & Erdelen 2006; Kusrini et al. 2007a).

In addition to *Leptophryne cruentata*, GPNP is also a habitat for its sister species, namely *Leptophryne borbonica*. *Leptophryne borbonica* is not an endemic frog and is not listed as species that requires a greater concern on its distribution and population as its widespread distribution and relatively high in number (Inger & Stuebing 1997; Iskandar 1998; Malkmus 2002; Ardiansyah et al. 2014).

Thus, the occurrence of *Leptophryne borbonica* in this park has been neglected for decades, based on our knowledge, their distribution is only documented in Bodogol (Ardiansyah et al. 2014) and Cibereum (Cibodas) (Kusrini et al. 2017). Therefore, a study that investigates and updates the information on this frog is necessary.

In this study, we aimed to explore various areas in GPNP that are potentially utilised by *L. cruentata* and *Leptophryne borbonica*. We also aimed to address niche segregation between two frog species based on data on their distribution as well as incorporated several habitat parameters that likely has a strong functional link with their distribution and abundance.

The study was conducted in August – December 2022 at 11 sites in GPNP (Figure 1). We performed consecutive surveys at Cibodas, Selabintana, Goalpara, and Bodogol. We visited 5 locations in the Resort of Cibodas, 3 locations in the Resort of Selabintana, and 1 location in the Resort of Goalpara. All locations surveyed in this study were presented in Table 1 including resort information and the type of water body.

We conducted daily and nightly observations using visual encounter surveys to record the presence of *Leptophryne cruentata* and *Leptophryne borbonica* in 11 locations (Table 1). Daily observations were used exclusively to record the presence of *Leptophryne cruentata* since this frog is active and easily captured during the day. We performed daily observations between 08.00 – 12.00. Night observations were conducted between 19.00 – 23.00 to detect the presence of *Leptophryne bor-*

Table 1. Eleven sites surveyed in this study for the presence and abundance of *Leptophryne* spp. Information on the type of water bodies from all sites was also recorded.

No	Sites	Resort	Type of water bodies	Elevation zone
1	Ciwalen	Cibodas	Creek	Submontane
2	Telaga Biru	Cibodas	Creek	Montane
3	Rawa Gayonggong	Cibodas	Creek	Montane
4	Goa Lalay	Cibodas	Creek	Montane
5	Cibeureum	Cibodas	Waterfall	Montane
6	Pondok Halimun	Selabintana	Stream	Submontane
7	Paseban Flying Fox	Selabintana	Stream	Submontane
8	Cibeureum	Selabintana	Waterfall	Montane
9	Rasta	Goalpara	Waterfall	Submontane
10	Cisuren	Bodogol	Creek	Lowland
11	Cikaweni	Bodogol	Creek	Lowland

bonica. We performed 3 – 5 visits for each location to ensure the validity of detection.

We estimated the abundance of each species of *Leptophryne* spp. based on one day/night calculation by investigating exhaustively all the individuals obtained in each sampling location. Since both species of frogs are territorial and rarely change their position for several hours, we can ascertain that the probability of individuals being resampled was negligible. We marked the location of all recorded individuals using GPS. We also measured the level of background noise for each location by placing Extech 407736 Digital Sound Level Metre in the centre of each location. We extracted altitude information on each individual location from Digital Elevation Model provided by Shuttle Radar Topographical Mission (SRTM) in USGS. Annual temperature and precipitation were collected by analysing raster images captured in 2018 from Bioclim (<https://www.worldclim.org/data/bioclim.html>).

We used QGIS version 3.18.2 to visualise the distribution of both frogs on a 2D map of Gede Pangrango National Park. Digital Elevation Model (DEM) was classified into 4 categories following Kusrini et al. (2017) using Raster Calculator Tool in QGIS to easily visualise the distribution of the frogs in four different zones in GPNP (alpine, montane, sub-montane, and lowland forest). We also provided statistical comparisons of occurrence site parameters (elevation, annual temperature, annual precipitation, and background noise level) by generating 95% confidence intervals, based on 1000 bootstrapped estimates, around median values. Analysis was performed using R version 4.2.2 (R Project for Statistical Computing, <http://www.R-project.org>).

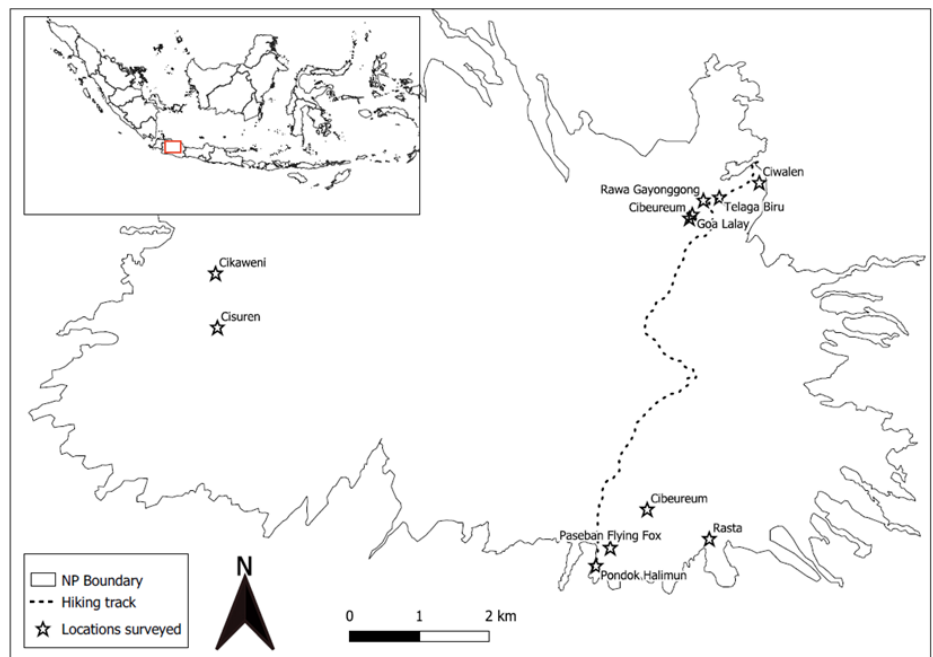


Figure 1. Map of 11 locations visited in this study indicated by stars. Locations covered the montane, sub-montane, and lowland forest of Gede Pangrango National Park.

Distributional records of *Leptophryne cruentata* in GPNP were relatively more widespread than its sister species. *Leptophryne cruentata* was documented in 4 of 11 locations visited during a course of study (Figure 2). We recorded the presence of *Leptophryne cruentata* on Cibodas trail scattered at three different sites, Cikundul waterfall, a creek near Cibeureum, and Goa Lalay. Within the Selabintana and Goalpara resorts,

Leptophryne cruentata was only recorded in one location respectively, Cibereum waterfall and Rasta waterfall. The number of individuals was slightly greater in Cibodas (N=23) relative to Goalpara (N=11) and Selabintana (N=9) respectively. In Goalpara and Salabintana, *Leptophryne cruentata* is exclusively found only within waterfall habitats (no more than a radius of 100m from waterfalls), whereas this frog in Cibodas was not only observed within reach of waterfalls but also documented in fast-slowing creeks at Goa Lalay (n=3) and Cibereum (n=15) which located far enough from waterfalls. *Leptophryne cruentata* tended to avoid Cibereum waterfall as shown by the absence of this frog in this location, the presence of *Leptophryne cruentata* was recognised in Cikundul waterfall (n=5) located just a few meters behind the Cibereum waterfall. We also observed variation in the coloration of *Leptophryne cruentata* in Cibodas (Figure 3). *Leptophryne borbonica* was obtained only at Cisuren, a slow-moving creek, in the lowland forest of bodogol. We did not record the presence of this frog in Cikaweni.

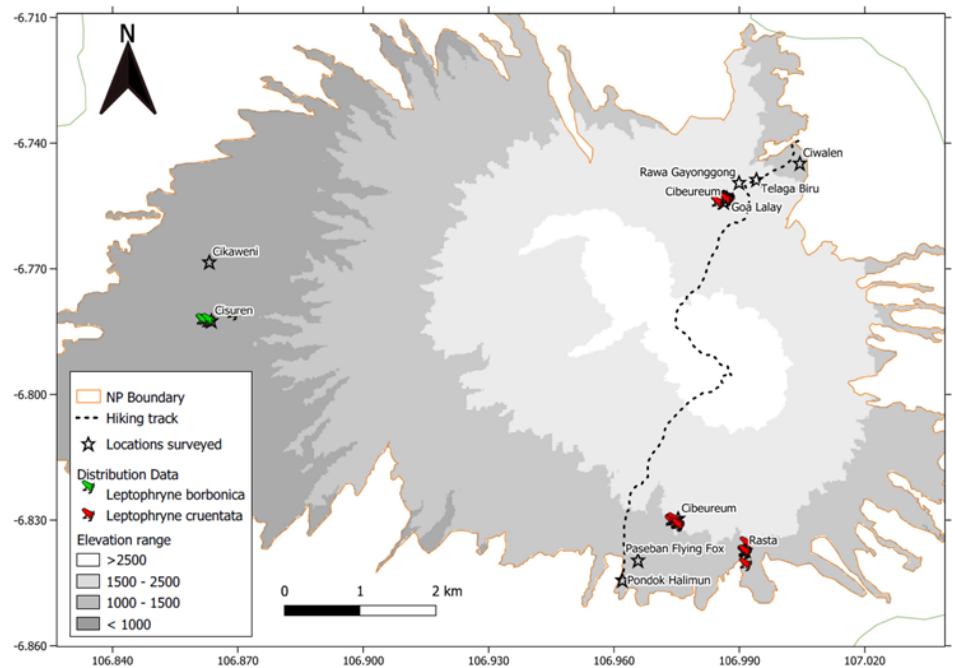


Figure 2. Distribution map of *Leptophryne* spp. showing that *Leptophryne cruentata* has a more widespread distribution than *Leptophryne borbonica*. *Leptophryne cruentata* also exhibits a high association with higher altitudes (montane and sub-montane zone), whereas *Leptophryne borbonica* occurred exclusively in lowland forests.

Information on the distribution of *Leptophryne cruentata* and *Leptophryne borbonica* had been rarely explicitly studied and usually concentrated only on small or specific areas, making the centre of conservation priorities inadequate. Yet, a recent study also reported the distributional changes of some species of frogs driven by many factors after 40 years (Kusrini et al. 2017), highlighting the importance of monitoring the distribution of frogs regularly. Focusing on *Leptophryne cruentata* we found even just only 10 years after (Kusrini et al. 2017), the distribution of this frog has changed. In our study, *Leptophryne cruentata* was reported in Cibereum and Goa Lalay and absent in Rawa Gayonggong. Distribution of this frog in Cibereum was documented in two sites, rapid creeks near the main waterfall and Cikundul waterfall.

In addition, we also recorded new distribution of this frog in Selabintana and Goalpara that had not been explicitly reported by pre-

vious studies (Liem 1971; Kusrini et al. 2017). Meanwhile, the occurrence of *Leptophryne borbonica* was recorded only in a slow-moving creek in the lowland forest Bodogol, namely Cisuren. Our finding demonstrated that the distribution of this frog has experienced substantial changes demonstrated by our failure to detect the occurrence of *Leptophryne borbonica* in Cikaweni (Bodogol) and Cibodas as these sites were previously reported as distributional sites of *Leptophryne borbonica* (Kusrini et al. 2007b; Ardiansyah et al. 2014). The lowland forest of Bodogol still retains its natural condition, but intense intrusion from the forest edge driven by man-made activities could probably force the frog to move to a higher elevation or cooler environment (Sulaeman et al. 2019; Erfanda et al. 2019; Muliani & Krisnawati 2022).

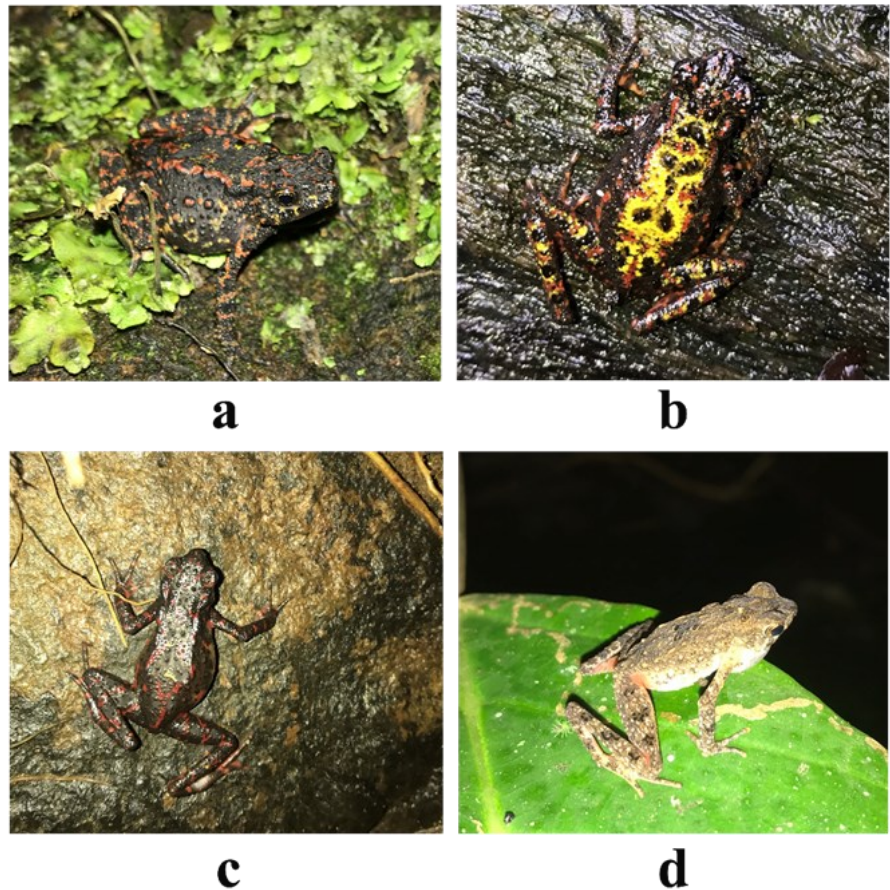


Figure 3. *Leptophryne cruentata* (a – c) and *Leptophryne borbonica* (d). Variation in coloration was shown in *Leptophryne cruentata* (a - b), some individuals of *Leptophryne cruentata* were observed adhering to vertical rocks in Goalpara waterfalls (c).

The absence of *Leptophryne cruentata* in Rawa Gayonggong reported in our study is probably linked to a low level of vegetation cover and the scant number of seepages. *Leptophryne cruentata* has been reported to prefer habitats that are facilitated with greater canopy cover (Saputro et al. 2021) and provided with an adequate number of flowing seepages or creeks. The association between *Leptophryne cruentata* and aqueous habitats has been previously studied and reported the absence of this frog in Lebak Saat due to the dryness condition in this location (Kusrini et al. 2017).

As seen on the map, both species did not exhibit niche overlap as indicated spatially by the different sites of distribution. The sites occupied by *Leptophryne cruentata* were not shared with *Leptophryne borbonica*.

Niche segregation was also explained by differences in the selection of elevation, annual precipitation, annual temperature, and noise as their habitats. *Leptophryne cruentata* inhabited highland forests with substantial noise backgrounds generated by waterfalls or fast-flowing creeks (Table 2). Even though both species showed a high preference for rocky creeks, *Leptophryne borbonica* tended to choose slow-flowing creeks with low to medium-level of noise backgrounds. In addition to the differences in site selection, both species also have different ways of foraging. *Leptophryne cruentata* can be obtained actively foraging and socialising during the day and night, whereas *Leptophryne borbonica* actively foraged only at night.

Leptophryne cruentata covered a wide range of distribution compared to *Leptophryne borbonica*. However, the occurrence of this frog is limited in the montane and submontane zones, none of *Leptophryne cruentata* was recorded in lowland forests as the only habitat for *Leptophryne borbonica*, based on our study. We did not perform observation on both species of frogs in the Alpine zone (Lebak Saat and Rawa Denok), thus, we cannot explain the distributional pattern of these frogs in a broader context. Despite Lebak Saat being known as a historical site for *Leptophryne cruentata*, however, the latest study confirmed the absence of this frog in this area (Iskandar & Erdelen 2006; Kusrini et al. 2017). The difference in niche selection between these two frog species is probably driven by the preference of both species for different environmental features. *Leptophryne cruentata* tend to prefer habitats at higher altitudes that facilitate a high level of moisture (Kusrini et al. 2007b). While its sister species, *Leptophryne borbonica* usually inhabits a stream in the lower elevation of mountain forest that did not provide a high level of moisture (Inger & Stuebing 1997; Iskandar 1998; Malkmus 2002).

The population of *Leptophryne cruentata* was greater in Cibodas compared to any other sites, however, the frogs in Cibodas scattered in three sub-sites. In Selabintana, we did not find the frog in other sub-sites other than Cibereum. A similar pattern was also documented in Goalpara. We could not confirm the absence of this frog in other sites other than Rasta Waterfall since we did not survey any other potential sites in this area due to several constraints that limit our sampling efforts. Overall, the number of *Leptophryne cruentata* estimated in this study was relatively lower compared to previous studies (Liem 1971; Kusrini et al. 2007), indicating the population of this frog is decreasing. Despite the widespread distribution of *Leptophryne cruentata* at various sites in GPNP, their overall number is still distressing.

These findings can be used as baseline information for conservation authorities to widen their area of concerns other than Cibodas as potential habitats for *Leptophryne cruentata*. Decreasing population and

Table 2. Summary of median values and upper and lower 95% confidence intervals (in parentheses, derived from 10,000 bootstrap samples) for four parameters recorded at four locations.

Species	Location	Background Noise	Annual Temperature	Annual Precipitation	Elevation
<i>Leptophryne borbonica</i> (N = 8)	Bodogol	63.05(53.3 - 69.7)	23.23485(0)	297(297 - 325)	821.5(738 - 896)
<i>Leptophryne cruentata</i> (N = 23)	Cibodas	68.2(64.8 - 81.3)	18.91216(0)	373(0)	1661(1632 - 1703)
<i>Leptophryne cruentata</i> (N = 9)	Goalpara	73.2(66.8 - 73.2)	17.24538(0)	338(0)	1384(1381 - 1389)
<i>Leptophryne cruentata</i> (N = 11)	Selabintana	75.8(73.2 - 83s.5)	17.24538(0)	343(0)	1501(1488 - 1526)

distribution sites of its sister species, *Leptophryne borbonica*, are an important issue that needs to be addressed in order to prevent the local extinction of this species in the future.

AUTHOR CONTRIBUTION

M.I.N. designed the study and supervised all the processes. M.I.N. also conducted the analysis and wrote the paper with assistance from all authors. R.T.I., P.Y.G., and A.D.L. assisted in conducting field observation and providing the data. B.D. helped in providing information about locations potentially selected for study and conducted literature reviews.

ACKNOWLEDGMENT

We thank the Ministry of Environment and Forestry, Indonesia for the access, permission, and support during field observation. We also thank Mang Ae and other officers of Gunung Gede National Park that help us during field observation.

CONFLICT OF INTEREST

We declared that this research has no conflict of interest.

REFERENCES

- Ardiansyah, D. et al., 2014. Kelimpahan Kodok Jam Pasir *Leptophryne borbonica* di Sepanjang Aliran Sungai Cisuren, Bodogol, Taman Nasional Gunung Gede Pangrango. *BIOMA*, 10(2), pp.10–17. doi: 10.21009/Bioma10(2).2
- Erfanda, M.P. et al., 2019. Distribution record of *Leptophryne borbonica* (Tschudi, 1838)(Anura: Bufonidae) from Malang, East Java: description, microhabitat, and possible threats. *Journal of Tropical Biodiversity and Biotechnology*, 4(02), pp.82–89. doi: 10.22146/jtbb.45355
- Hamidy, A. et al., 2018. Detection of Cryptic taxa in the genus *Leptophryne* (Fitzinger, 1843)(Amphibia; Bufonidae) and the description of a new species from Java, Indonesia. *Zootaxa*, 4450(4), pp.427–444. doi: 10.11646/zootaxa.4450.4.2
- Inger, R.F. & Stuebing, R.B., 1997. *A field guide to the frogs of Borneo*, Natural History Publications.
- Iskandar, D.T., 1998. *The amphibians of Java and Bali*, Bogor: Research and Development Centre for Biology LIPI.
- Iskandar, D.T. & Erdelen, W.R., 2006. Conservation of amphibians and reptiles in Indonesia: issues and problems. *Amphibian and Reptile Conservation*, 4(1), pp.60–87. doi: 10.1514/journal.arc.0040016
- Kurniati, H., 2002. Frogs and Toads of Ujung Kulon, Gunung Halimun and Gede-pangrango National Park. *Berita Biologi*, 6(1), pp.75–84. doi: 10.14203/beritabiologi.v6i1.1172
- Kurniati, H., 2006. The Amphibians Species in Gunung Halimun National Park, West Java, Indonesia. *Zoo Indonesia*, 15(2). doi: 10.52508/zi.v15i2.112
- Kusrini, M.D. et al., 2007a. Preliminary study on the distribution and biology of the bleeding toad, *Leptophryne cruentata* Tschudi, 1838. *Frogs of Gede Pangrango: A Follow up Project for the Conservation of Frogs in West Java Indonesia. Book 1: Main Report*, p.32.
- Kusrini, M.D. et al., 2007b. The amphibians of Mount Gede Pangrango National Park. *Frogs of Gede Pangrango: a follow up project for the conservation of frogs in West Java, Indonesia, Book 1*, pp.11–31.

- Kusrini, M.D. et al., 2017. Elevation range shift after 40 years: The amphibians of Mount Gede Pangrango National Park revisited. *Biological Conservation*, 206, pp.75–84. doi: 10.1016/j.biocon.2016.12.018
- Liem, D.S.S., 1971. The frogs and toads of Tjibodas National Park, Mt. Gede, Java, Indonesia. *Philippine Journal of Science*, 100, pp.131–161.
- Malkmus, R., 2002. *Amphibians & Reptiles of Mount Kinabalu (North Borneo)*, Koeltz Scientific Books.
- Muliani, L. & Krisnawati, I., 2022. Development Model of Special Interest Tourism Packages Through The Exploration Of Local Wisdom In Desa Wisata Wates Jaya. *The Journal Gastronomy Tourism*, 9(2), pp.56–67. doi: 10.17509/gastur.v9i2.52212
- Mumpuni, M., 2001. Keanekaragaman Herpetofauna Di Taman Nasional Gunung Halimun, Jawa Barat. *Berita Biologi*, 5(6), pp.711–720. doi: 10.14203/beritabiologi.v5i6.1078
- Saputro, P.B. et al., 2021. Potential Suitable Habitat Distribution for Two Endemic and Highly Threatened Species of *Leptophryne* (Amphibia; Bufonidae) in Java. *Zoo Indonesia*, 28(2). doi: 10.52508/zi.v28i2.4097
- Sulaeman, M., Sulistijorini, S. & Rahayu, S., 2019. Habitat suitability for *Hoya* spp.(Apocynaceae) in the Bodogol Conservation Area, West Java. *Biosaintifika: Journal of Biology & Biology Education*, 11(1), pp.91–99. doi: 10.15294/biosaintifika.v11i1.13021

Research Article

Stomata characters of sugarcane (*Saccharum officinarum* L.) mutants of GMP3 variety at PT Gunung Madu Plantations, Lampung, Indonesia

Mahfut^{1*}, Putri Kendari², Admi Syarif³, Sri Wahyuningsih², Endah Susiyanti⁴

1)Department of Biology, Faculty of Mathematics and Natural Sciences, University of Lampung. Jl. Prof., Dr. Ir. Soemantri Brodjonegoro, No. 1. Gedong Meneng, Kec. Rajabasa, Bandar Lampung, Lampung, 35145

2)Postgraduate Student of Biology, Faculty of Mathematics and Natural Sciences, University of Lampung. Jl. Prof., Dr. Ir. Soemantri Brodjonegoro, No. 1. Gedong Meneng, Kec. Rajabasa, Bandar Lampung, Lampung, 35145

3)Department of Computer Science, Faculty of Mathematics and Natural Sciences, University of Lampung. Jl. Prof., Dr. Ir. Soemantri Brodjonegoro, No. 1. Gedong Meneng, Kec. Rajabasa, Bandar Lampung, Lampung, 35145

4)Division of Agronomy, Research and Development, PT. Gunung Madu Plantations. KM 90 Terbanggi Besar, Gunung Batin Udik, Terusan Nunyai, Lampung, 34167

* Corresponding author, email: mahfut.mipa@fmipa.unila.ac.id

Keywords:

Colchicine

GMP3

Indonesia

Saccharum officinarum L.

Stomata

Sugarcane

Submitted:

07 December 2022

Accepted:

29 March 2023

Published:

04 September 2023

Editor:

Furzani Binti Pa'ee

ABSTRACT

The induction of colchicine mutations is one method of breeding. PT Gunung Madu Plantations, for example, has induced mutations of commercial sugarcane (*Saccharum officinarum* L.) varieties, however, investigations on the impact of colchicine on stomatal characters have received less attention. Therefore, this study aimed to analyse the stomata character of 21 sugarcane mutants of the GMP3 variety at PT Gunung Madu Plantations, Lampung, Indonesia with a focused look at stomata aperture width, stomata length and width, number of stomata, stomatal density, and stomata index. The collected data were analysed using cluster and Principal Component Analysis (PCA) through MVSP software. This study showed that all GMP3 mutants had Graminae-type stomata. In terms of stomata length and width, the average size of the GMP3 variety mutant was greater than that of the control. The diversity of stomata characters is fairly high due to differences in stomata size between GMP3 and control mutants. With a similarity index of 0.20, the phenetic analysis of 21 mutants of the GMP3 variety revealed that the relationship between mutants and controls was getting further. A six-character principal component analysis revealed that axis I's total variation accounted for 40.54 percent of the variation and had an eigenvalue of 2.43, whereas axis II's contribution to the variation was 19.02 percent and had an eigenvalue of 1.14. The findings indicate that stomata are excellent taxonomic evidence for identifying and analysing sugarcane varieties induced by colchicine-induced breeding.

Copyright: © 2023, J. Tropical Biodiversity Biotechnology (CC BY-SA 4.0)

INTRODUCTION

Sugarcane (*Saccharum officinarum* L.) is a monocotyledonous plant with has the highest sucrose and the lowest fiber content (Lubis et al. 2015). Therefore, it is widely used as the main raw material in the sugar industry. The consumption of sugar in the country has been continuously increasing as the population grows as well as consumption per capita has increased 1.5 times, reaching 14.5 kg per capita per year. However, the increase in sugar consumption has not been matched by an increase in

sugar production. Based on sugarcane production data from 2017-2021, it is currently around 2.1-2.3 tons/ha with sugar recovery of around 7-8% (Central Bureau of Statistics 2021).

PT Gunung Madu Plantations (PT GMP) is one of the sugar industries attempting to increase production by assembling high-yielding sugar cane varieties through its research and development department, including several commercial varieties such as GMP1, GMP2, GMP3, GMP4, GMP5, GMP6, and GMP7. The GMP3 is the most commercial and dominant variety, comprising approximately 30% of the total land area. However, according to the field data, this variety has a low quality, low sugar yield, an agronomic appearance on small stems, and narrow leaf width (PT Gunung Madu Plantations 2016; Windiyani et al. 2022).

As widely stated in the literature Mugiono (2010), plant breeding is one of the ways to improve the quality of a variety. The primary principle of a sugarcane breeding program is to obtain transgressive segregation that exhibits maximum heterosis from across. Furthermore, adequate genetic diversity is essential to producing superior sugarcane varieties (Carsono et al. 2022). Therefore, plant breeding can be conducted through mutation induction using the chemical mutagen, such as colchicine (Kamwean et al. 2017). Colchicine can be used to induce mutations to obtain polyploid plants. Colchicine can improve the characteristics of plants with better traits in breeding programs (Sivakumar 2018). Sattler et al. (2016), showed that corn induced by colchicine experienced an increase in stomata density, and an increase in stomata length and width. The character of stomata in plants that have experienced polyploidy has a character of larger cell size, especially seen in epidermal cells and cell nuclei (Bagheri & Mansouri 2014).

PT GMP induced mutations with the colchicine mutagen in sugarcane GMP3 variety, but this effect of colchicine has not been tested further, tested whether the induced sugarcane has changed, especially in stomatal characters. So based on these problems, this study aims to analyze stomatal characters in 21 mutant variety of GMP3.

MATERIALS AND METHODS

Plant materials

The plant materials investigated in this study were twenty-one mutants of GMP3 varieties, one control, 0.1% and 0.2% colchicine concentrations. The twenty-one varieties of these mutants are Mutan1, Mutan2, Mutan3, Mutan4, Mutan5, Mutan7, Mutan8, Mutan9, Mutan10, Mutan11, Mutan12, Mutan13, Mutan15, Mutan16, Mutan17, Mutan18, Mutan19, Mutan21, Mutan22, Mutan23, and Mutan24, aquadest, immersion oil, glycerine, and clear nail polish. In each sample mutant taken for observation there is 3 leaf sample. Leaves samples collected from the experimental garden of field-acclimatized PT GMP. Observation of stomatal characters was observed when the sugarcane mutant of the GMP3 variety was 9 months old, and the leaves used were young leaves in the middle of the leaves. This research was conducted at the botanical laboratory of PT GMP in Lampung, Indonesia.

Method

Leaf stomata characters were observed from the paradermal part, making microscopic incisions on the paradermal part of the leaf (Munir et al. 2011; Arzani et al. 2013; Chikmawati 2013; Arofatum et al. 2020; Mahfut et al. 2023). The first step was to take the leaf and clean it using 70% ethanol. Then the bottom of the leaf was placed on a slide, covered with transparent nail polish, and dripped with glycerine and covered with a

cover glass. Light microscopic observations (Model: Olympus, magnification 10 x for the ocular and 40 x for the objective) were used to observe the specimens (Pitoyo et al. 2018). The stomata characters observed were stomata aperture width, stomata length and width, number of stomata, stomata density, and stomata index (Arofaturun et al. 2020). In this research, the number of repetitions for each character measured from each mutant was carried out at 5 times the anatomical observations in a broad field of view.

Data analysis

Stomata characters were analysed quantitatively (stomata aperture width, stomata length and width, number of stomata, stomatal density, and stomata index) and qualitatively (stomata type) in a descriptive form to identify variations in stomata characters observed using MVSP (Multivariate Statistics Package) software v.3.2 to construct a phenetic dendrogram and for Principal Component Analysis (PCA). The dendrogram was built using the Jaccard coefficient, and the similarity index for genetic distance analysis used the Unweighted Pair-Group method with the arithmetic average (UPGMA) method, while the PCA Scattered plot was constructed using the Euclidean Distance algorithm.

The formula for calculating stomata density is as follows (Suhaimi 2017):

$$\text{Stomata density } (\mu\text{m}) = \frac{\text{Number of stomata}}{\text{Broad field of view}}$$

Meanwhile, the formula for calculating the stomata index is as follows (Tambaru 2015):

$$\text{Stomata index } (\mu\text{m}) = \frac{\text{Number of stomata}}{\text{Number of epidermal cells} + \text{Number of stomata}} \times 100$$

RESULTS AND DISCUSSION

Stomata characters

Based on the stomata observations, the GMP3 variety has Gramineae stomata type, which shows the length of the axis of the neighbouring cell is parallel to the stomata axis (Figure 1). The type of stomata of the GMP3 mutants obtained in each 0.1% and 0.2% colchicine treatment did not show changes in the shape of the stomata. This indicates that colchicine does not affect the stomata's shape. According to Moghbei et al. (2015), the type of olive leaf stomata obtained on each treatment, which is submersion and drops at various concentrations (0.25%, 0.5%, 0.75%, and 1%), did not change the shape of the stomata. This is because colchicine does not affect all parts of the cell, just a few cells or random cell mutations. According to Syukur et al. (2015), colchicine does not affect all cells or cause random cell mutations. Cells that are actively dividing are sensitive to colchicine, whereas differentiated cells are less sensitive to this mutagen. According to Moghbei et al. (2015), the sensitivity of each plant species to colchicine application will be different even from the existing plant part.

Based on the data results (Table 1), the width of the stomata aperture in the GMP3 mutant has a value range of 1.06-2.06, an average of 1.67 with a standard deviation of 0.38. Several types of GMP3 mutants had smaller stomata aperture (1.06-2.06 μm) compared to controls (2.54 μm). This is because the concentration of colchicine given to these mutants is too high, so that colchicine will inhibit the process of enlargement or opening of stomata.

In terms of stomatal length, the GMP3 mutant has a range of 17.33

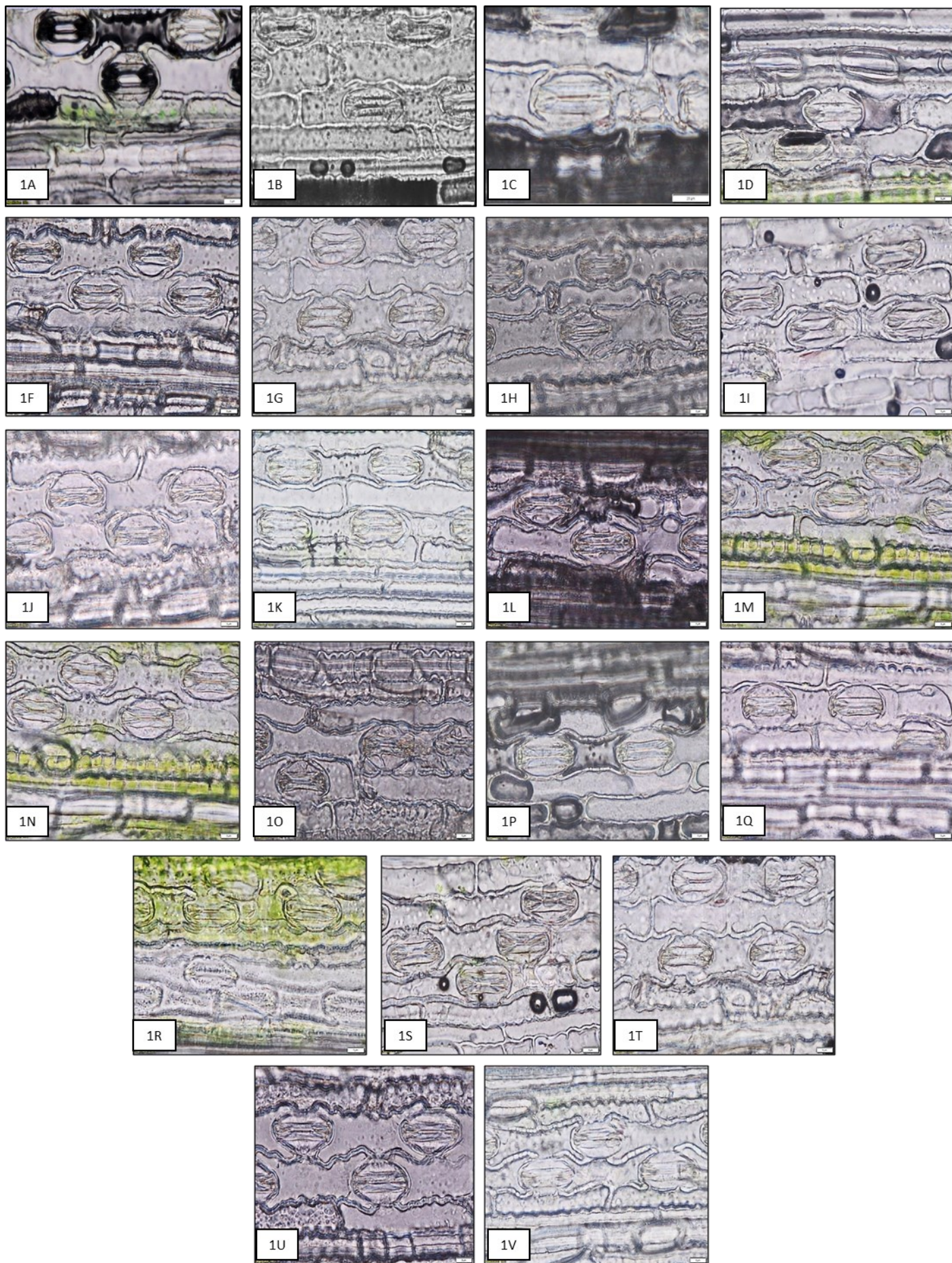


Figure 1. Structure of stomata in GMP3 variety and 21 GMP3 mutant varieties.

Note: 1A:GMP3, 1B: Mutan1, 1C: Mutan2, 1D: Mutan3, 1E: Mutan4, 1F: Mutan5,1G: Mutan7, 1H: Mutan8, 1I: Mutan9, 1J: Mutan10, 1K: Mutan11, 1L: Mutan12, 1M: Mutan13, 1N: Mutan15, 1O: Mutan16, 1P: Mutan17, 1Q: Mutan18,1R: Mutan19, 1S: Mutan21, 1T: Mutan22, 1U: Mutan23, 1V: Mutan24. Bar = 1 μ m.

Table 1. The average value of stomata characters in the GMP3 variety and 21 GMP3 mutant varieties.

No.	Variety Name	Stomata Aperture Width (µm)	Stomata Length (µm)	Stomata Width (µm)	Number of Stomata	Stomata Density (mm)	Stomata Index (%)
6.	GMP3	2.54	19.20	11.71	77	392	0.32
1.	M / C 0.1/2H/01	1.30	18.72	9.12	95	484	0.41
2.	M / C 0.1/3H/15	1.10	19.39	11.62	87	443	0.39
3.	M / C 0.1/3H/16	2.06	19.78	10.13	74	377	0.30
4.	M / C 0.1/3H/02	2.21	17.90	9.07	97	494	0.38
5.	M / C 0.1/3H/10	1.63	18.43	10.80	77	392	0.32
7.	M / C 0.1/3H/04	1.06	18.72	12.82	79	402	0.34
8.	M / C 0.1/3H/07	2.06	19.73	9.74	89	453	0.41
9.	M / C 0.1/3H/06	1.73	17.33	10.75	59	300	0.30
10.	M / C 0.1/3H/03	1.97	18.96	11.86	72	366	0.34
11.	M / C 0.1/3H/14	2.26	18.34	8.59	91	463	0.38
12.	M / C 0.1/3H/02	1.15	21.02	10.61	93	473	0.40
13.	M / C 0.1/3H/08	1.44	18.58	10.03	84	428	0.41
15.	M / C 0.1/3H/05	1.54	18.38	10.27	88	448	0.42
16.	M / C 0.1/3H/01	1.44	18.38	11.52	84	428	0.39
17.	M / C 0.1/1H/01	1.44	20.74	10.75	82	417	0.39
18.	M / C 0.1/2H/01	2.21	18.43	9.65	97	494	0.45
19.	M / C 0.2/1H/04	1.44	18.58	10.05	95	484	0.41
21.	M / C 0.1/3H/09	1.87	18.86	10.46	98	499	0.42
22.	M / C 0.2/3H/10	1.63	18.43	10.80	80	407	0.44
23.	M / C 0.1/3H/12	1.44	21.31	9.00	73	371	0.30
24.	M / C 0.1/3H/11	2.11	17.9	8.54	89	453	0.43
	Average	1.67	18.94	10.29	85	432	0.38
	Std. Dev.	0.38	1.03	1.10	10.11	51.66	0.04

Note: M= Mutant, C = Colchicine, 0.1-0.2%: = Colchicine concentration, H = Day

-21.31, an average of 18.94 with a standard deviation of 1.03, while the GMP3 mutant stomata aperture width has a range of 8.54-12.82, an average of 10.29 with a standard deviation of 1.10. Meanwhile, the stomata's size of the GMP3 mutant variety increased in length and stomata aperture width compared to the GMP3 variety (Table 1). This suggests that colchicine affects the character of stomata's length and width. Although in this study colchicine affected the length and width of stomata, the induced colchicine at a concentration of 0.1-0.2% could not yet be indicated as a superior variety of sugarcane because each character measured was not more than 1.25 times. This is in accordance with what has found by Miguel and Leonhardt (2011) that polyploid orchidaceae plants are those that have stomata that are wider and longer than control plants by at least 1.25 times the length of control plants. Polyploidy plants with stomatal character can be characterized by the size of their cells getting bigger and visible in the epidermal cells, and cell nucleus (Suryo 2009).

The number of stomatal characters based on the data (Table 1) has a value range of 59-98, an average of 85 with a standard deviation of 10.11, while the density of stomata in the GMP3 mutant has a value range of 300-499, an average of 432 with a standard deviation of 51.66. Some GMP3 mutants have more stomata numbers than GMP3 variety, while some mutants also have higher stomata density than GMP3 variety (Table 1). It can be said that colchicine can induce polyploidy formation in GMP3 variety. According to Gantait et al. (2011) reported the stomata and epidermal cells of *Gerbera jamesonii* Bolus cv. are greater in size than those of diploid plants, their stomatal density is higher than that of diploid plants. The value of olive leaf stomata density obtained in

the colchicine treatment has increased stomata density (Rohmah et al. 2017). Stomata density in plants is closely related to plant resistance to drought stress, while stomata size and stomata density are closely related to plant resistance to water stress (Yanny et al. 2022). Based on this research, it shows that the colchicine-induced mutant causes drought resistance by having high stomata density.

The GMP3 mutant stomatal index characters have a value range of 0.30-0.45, an average of 0.38 with a standard deviation of 0.04. Some GMP3 mutants had a higher stomatal index than the control (Table 1) and colchicine at a concentration of 0.1-0.2% caused the stomatal index to increase from 0.30-0.45%. This is because the colchicine-induced mutant causes an increase in the size of the stomata. As found by Moghbei et al. (2015) that the stomata index on olive leaves treated with 0.2-0.5% colchicine increased the size of the stomata index from 0.21-0.24%. An increase in stomata size indicates an increase in stomata frequency in plant mutations. The number of stomata affects the density of stomata. Stomata density is high if the number of stomata increases. According to Asif and Khalil (2019), there is harmony between stomata size and stomata frequency, the larger the size of the stomata, the higher the stomata frequency. It was found that a dose of 75 Gray was given to the mutant plantlets, and the resulting stomata frequencies ranged from 54.47 to 77.4. Hanafy and Akladious (2018) obtained the stomata frequency range of *Trigonella foenumgraecum* to be 93.23-159.39 for the mutated plants.

Colchicine induction in GMP3 mutant variety showed larger stomata size, increased number of stomata, and high stomata index (Table 1). Sattler et al. (2016) stated that colchicine-induced maize experienced an increase in stomatal density, length, and width. This shows that colchicine can be used as a reference for sugarcane breeding because sugarcane plants with larger stomata can increase the rate of photosynthesis where the effect of this rate of photosynthesis is able to increase the growth and productivity of sugarcane plants (Prabowo et al. 2022).

Phenetic analysis

The similarity index of 21 GMP3 mutant varieties and GMP3 variety ranged from 0.20-1.00 (Table 2). The higher similarity index indicates the results of the phenetic analysis between samples are getting closer, while the lower similarity index indicates the results of the phenetic analysis are getting farther away (Hamidah et al. 2016).

Analysis of kinship relationships aims to group between plant populations based on the same character or characteristics to determine whether they are closely related or distantly related. The coefficient of similarity can be used to determine how distant or close a group is related. Genetic distance and kinship, as indicated by the coefficient of similarity, are correlated. The closer the kinship between people, the lesser the genetic distance, and the greater the similarity coefficient value (Purnomo et al. 2020; Mahfut et al. 2021).

The results show that M9, M5, M24, M18, M11, M4, M17, M2, M22, M21, M19, M15, M13, M12, M10, and M3 are the only ones to possess the similarity index of 1.00. This similarity between GMP3 mutations and GMP3 variety explains their close association. The characteristics of stomata length, stomata aperture width, and stomata index were found to be similar. According to Purnomo et al. (2012), the greater the similarity index indicates no difference between the objects being compared. This indicates that some mutants of the GMP3 variety are closely related.

Table 2. Similarity index on GMP₃ varieties and 21 mutants of GMP₃ varieties.

	GMP ₃	M1	M2	M3	M4	M5	M7	M8	M9	M10	M11	M12	M13	M15	M16	M17	M18	M19	M21	M22	M23	M24	
GMP ₃	1.00																						
M1	0.16	1.00																					
M2	0.33	0.40	1.00																				
M3	0.75	0.00	0.40	1.00																			
M4	0.16	0.50	0.40	0.20	1.00																		
M5	0.25	0.00	0.25	0.33	0.00	1.00																	
M7	0.20	0.25	0.50	0.25	0.25	0.50	1.00																
M8	0.50	0.60	0.50	0.33	0.60	0.00	0.16	1.00															
M9	0.25	0.00	0.25	0.33	0.00	1.00	0.50	0.00	1.00														
M10	0.75	0.00	0.40	1.00	0.20	0.33	0.25	0.33	0.33	1.00													
M11	0.16	0.50	0.40	0.20	1.00	0.00	0.25	0.60	0.00	0.20	1.00												
M12	0.33	0.75	0.60	0.16	0.40	0.25	0.50	0.50	0.25	0.16	0.40	1.00											
M13	0.33	0.75	0.60	0.16	0.40	0.25	0.50	0.50	0.25	0.16	0.40	1.00	1.00										
M15	0.33	0.75	0.60	0.16	0.40	0.25	0.50	0.50	0.25	0.16	0.40	1.00	1.00	1.00									
M16	0.16	0.50	0.75	0.20	0.50	0.33	0.66	0.33	0.33	0.20	0.50	0.75	0.75	0.75	1.00								
M17	0.33	0.40	1.00	0.40	0.40	0.25	0.50	0.50	0.25	0.40	0.40	0.60	0.60	0.60	0.75	1.00							
M18	0.33	0.75	0.33	0.16	0.75	0.00	0.20	0.80	0.00	0.16	0.75	0.60	0.60	0.60	0.40	0.33	1.00						
M19	0.33	0.75	0.60	0.16	0.40	0.25	0.50	0.50	0.25	0.16	0.40	1.00	1.00	1.00	0.75	0.60	0.60	1.00					
M21	0.33	0.75	0.60	0.16	0.40	0.25	0.50	0.50	0.25	0.16	0.40	1.00	1.00	1.00	0.75	0.60	0.60	1.00	1.00				
M22	0.33	0.75	0.60	0.16	0.40	0.25	0.50	0.50	0.25	0.16	0.40	1.00	1.00	1.00	0.75	0.60	0.60	1.00	1.00	1.00			
M23	0.25	0.00	0.25	0.33	0.00	0.00	0.00	0.20	0.00	0.33	0.00	0.00	0.00	0.00	0.00	0.25	0.00	0.00	0.00	0.00	1.00		
M24	0.33	0.75	0.33	0.16	0.75	0.00	0.20	0.80	0.00	0.16	0.75	0.60	0.60	0.60	0.40	0.33	1.00	0.60	0.60	0.60	0.00	1.00	

There are two main categories into which the GMP3 mutant accessions can be divided: cluster A and cluster B (Figure 2). The 18 accessions in Cluster A, which has a similarity index of 0.25, are M7, M9, M5, M24, M18, M8, M11, M4, M16, M17, M2, M22, M21, M19, M15, M13, M13, and M1. The similarity of this kinship relationship is based on the similarity of the characters of the width of the stomata opening and the length of the stomata. Sub Cluster I of Cluster A is made up of M7, M9, and M5, whereas Sub Cluster II is made up of M24, M18, M8, M11, M4, M16, M17, M2, M22, M21, M19, M15, M13, M13, and M12. Cluster B has a similarity value of 0.30. The closeness of this kinship relationship is based on the similarity of the characteristics of the width of the stomata opening, the number of stomata, and the density of stomata which consists of 4 accessions, including GMP3, M23, M10, and M3. Two sub-clusters of Cluster B exist: Sub-Cluster I, which only contains M23, and Sub-Cluster II, which contains GMP3, M10, and M3.

The dendrogram's clustering pattern reveals distinct distinctions between GMP3 and its variant mutations. In this case, the GMP3 variety as a commercial variety, showed a clear separation from the mutant group of the GMP3 variety. At the similarity index of 0.25 (Figure 2), the two clusters formed. Clusters A and B are grouped with a similarity coefficient of 0.20. The two clusters are similar in that they have high stomatal density and high stomatal index. The distinctive features in cluster A were the length and width of the stomata, which are both large and narrow stomata opening. While in cluster B the length and width of the stomata are small, and the number of stomata is large. The clustering pattern based on the dendrogram shows the grouping of GMP3 mutants based on the similarity of stomata characters. Many comparable GMP3 mutants will have a higher similarity value, which is why they are grouped together in the same cluster or subcluster. Because of variations in stomata characteristics, the findings of the cluster analysis revealed that the mutants of the GMP3 variety did not cluster in a single cluster.

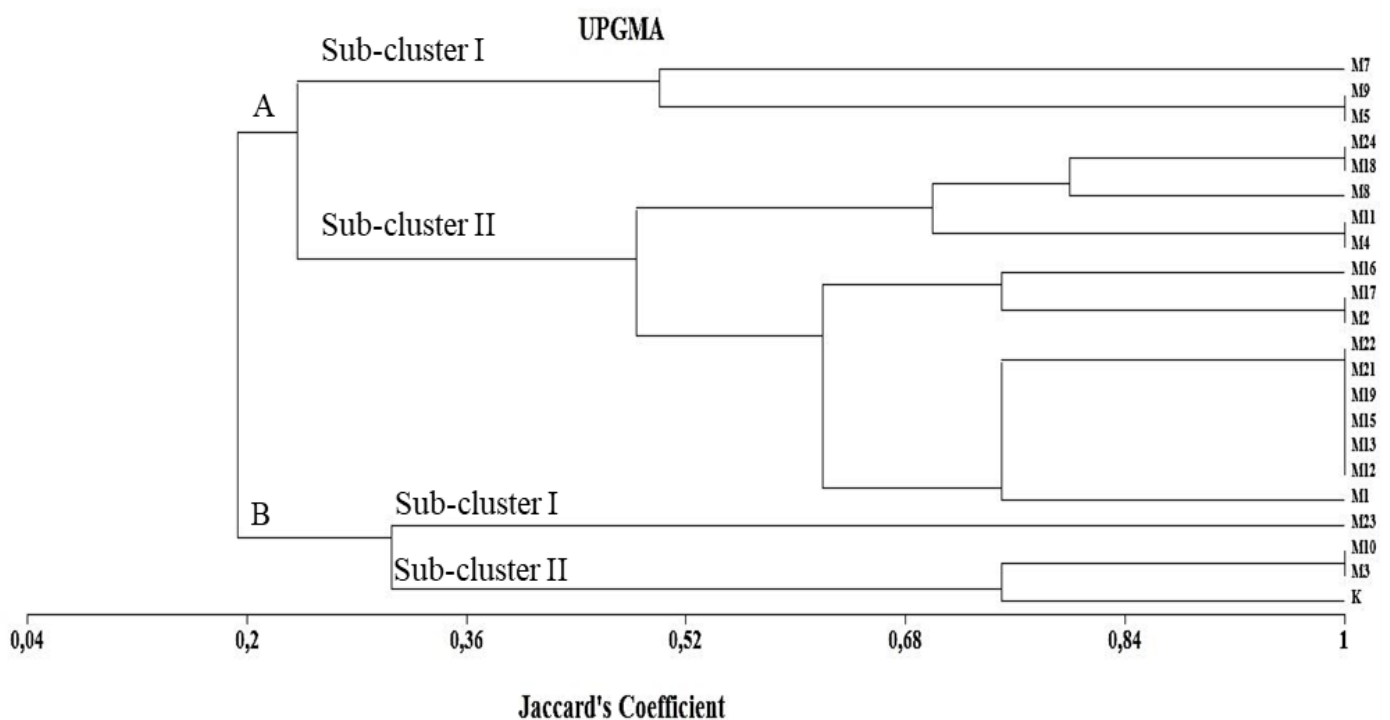


Figure 2. Dendrogram of phenetic relationship of 21 GMP3 mutants and GMP3 variety using Jaccard's coefficient.

Principal Component Analysis (PCA)

The grouping of GMP3 varieties and GMP3 mutant varieties are divided into two clusters (Figure 3), Cluster I consisting of GMP3, M7, M9, M10, M17, and M23 based on the characters of stomata length and stomata aperture width. Cluster II consists of M2, M8, M11, M16, M22, and M24 which are grouped based on the character of the number of stomata, stomata index, and stomatal density. According to Sari et al. (2016), the length and direction of the arrows indicated the stomata characters that most influence the grouping. Arrows pointing to a particular group indicate the most influential stomata character. The length of the arrow is directly proportional to the character of the stomata. The characters that play a role in the grouping of GMP3 mutant accessions are presented in Table 3.

PCA is used to indicate the distance between groups in the specimen under study. According to Adebisi et al. (2013) and Hamidah et al. (2016) PCA is also used to determine the character of stomata that plays a dominant role in group formation.

There are two characters are playing an important role in grouping GMP3 mutant varieties (Table 3). These two characters, namely stomata aperture width (LBS) and stomata cell length (PS) were simultaneously able to separate all samples on PC1 and PC2. In the main component analysis, there is an eigenvalue that shows the percentage value of the contribution of each grouping (Sultan et al. 2010). Eigenvalue of >0.02 indicates the most important character in cluster grouping (Stevens & Tello 2014). The size of the eigenvalues shows the influence of each character, which can be seen from the short length of the projection formed (Sari et al. 2016). The six stomata characters were varied by 40.54 percent with the help of the total variation on axis 1, which had an eigenvalue of 2.43, and by 19.02 percent with the help of the total variation on axis II, which had an eigenvalue of 1.14.

Based on the findings of this study, the characteristics that influence sample separation between cluster analysis and principal component analysis share commonalities aside from the cluster grouping pattern (I and II). Jalil et al. (2020) stated that there is congruence between the

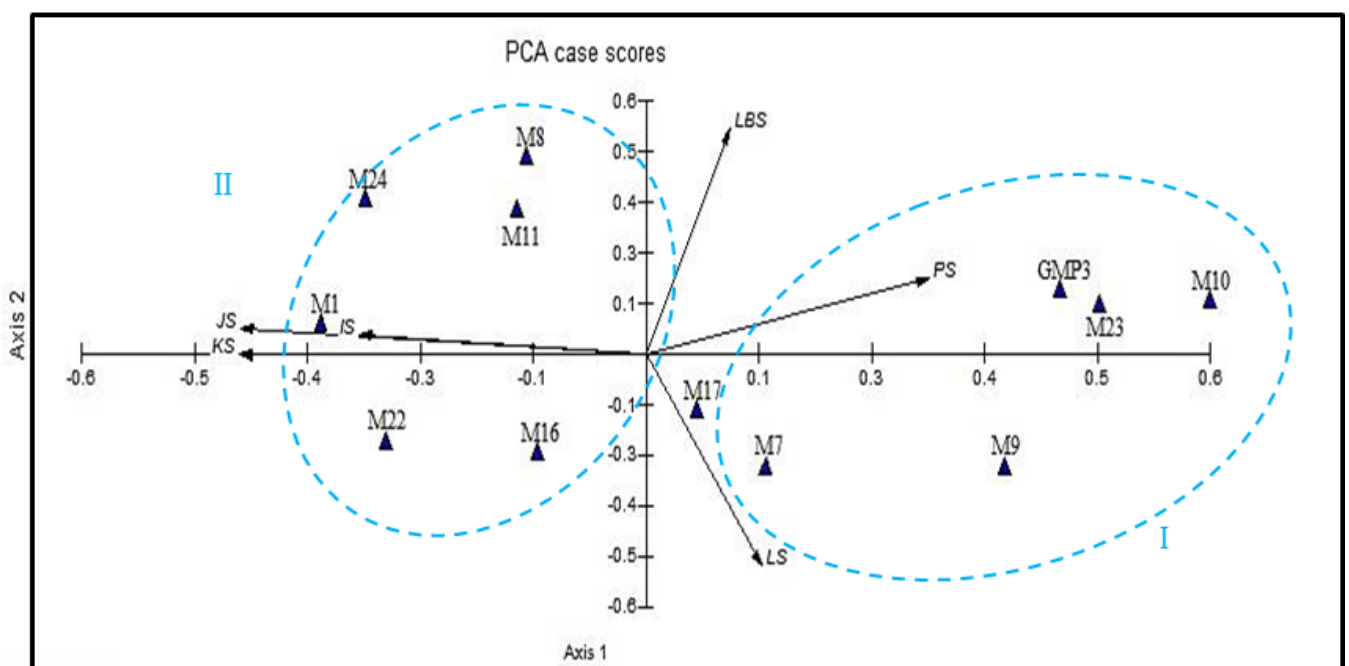


Figure 3. Principal Component Analysis on 21 mutants GMP3 varieties and varieties of GMP3 based on the characters of the stomata.

results of cluster analysis and principal component analysis. Both analyses can separate a number of botanically similar species and are widely used techniques for discovering cluster structures in numeric taxonomy.

Table 3. Characters that play a role in grouping GMP3 mutant varieties.

Character Code	Character Name	PC1	PC2
LBS	Stomata Aperture Width	0.117	0.706
PS	Stomata Cell Length	0.395	0.235
LS	Guard Cell Width	0.162	-0.661
JS	Number of Stomata	-0.567	0.081
KS	Stomata Density	-0.568	-0.003
IS	Stomata Index	-0.401	0.061
	Eigenvalues	2,433	1,141
	Percentage (%)	40,544	19.023
	Cum. Percentage (%)	40,544	19.023

CONCLUSION

In conclusion, the current study's findings revealed that 21 mutants of the GMP3 variety possessed a range of anatomical characteristics, including greater stomata size, smaller stomatal opening width, high stomatal density, a large number of stomata, and a high stomata index.

AUTHORS CONTRIBUTION

M. data validation, reviewing and final manuscript preparation. P.K. set up the experiment, carried out the entire experimental work, analyzed and interpretation of data, writing-editing. A.S, S.W, and E.S. guide in setting up the experiment and manuscript preparation. All authors have read and approved the manuscript for publication.

ACKNOWLEDGMENTS

The authors would like to express their gratitude to the Institute for Research and Community Service of the University of Lampung for financially supporting this applied research, grant number 777/UN26.21/PN/2022. They also appreciate the funding assistance provided by PT. Gunung Madu Plantations (GMP), Lampung, Indonesia for the research collaboration, grant numbers 023-00/GMP/I/2021, 013-00/GMP/I/2022, and 025-00/GMP/I/2023.

CONFLICT OF INTEREST

The authors declare that they have no competing interests.

REFERENCES

- Adebisi, M.A. et al., 2013. Evaluation of variation in seed vigor character of the West African rice genotype (*Oryza sativa* L.) using multivariate technique. *Am J Plant Sci.*, 4, pp.356-363. doi: 10.4236/ajps.2013.42047.
- Arofatur, I.N., Rugayah, R. & Chikmawati, T., 2020. Leaf stomata variation in *Desmos* Lour. and *Dasymaschalon* (Hook. F. & Thomson) Dalla Torre & Harms species (Annonaceae). *Biodiversitas*, 21(7), pp.3317-3330. doi: 10.13057/biodiv/d210756.
- Arzani, K. et al., 2013. Study of foliar epidermal anatomy of four pistachio rootstocks under water stress. *Idesia*, 31(1), pp.101-107. doi: 10.4067/S0718-34292013000100012.

- Asif, A. & Khalil, A.M.Y., 2019. Generation of mutant lines of *Nigella sativa* L. by induced mutagenesis for improved seed yield. *Industrial Crops and Products*, 13(9), pp.111-252. doi: <https://doi.org/10.1016/j.indcrop.2019.11>.
- Bagheri, M. & Mansouri, H., 2014. Effect of induced polyploidy on some biochemical parameters in *Cannabis sativa* L. *J Biotechnol Appl Biochem.*, 175(5), pp.2366-2375. doi: 10.1007/s12010-014-1435-8.
- Carsono, N. et al., 2022. Agronomic characteristics and genetic relationship of putative transgenic rice lines of cv. Fatmawati with the Glu-1Dx5 Transgene. *Biodiversitas*, 23(1), pp.291-298. doi:10.13057/biodiv/d230135.
- Central Bureau of Statistics, 2021. *Indonesian Sugarcane Statistics*. Central Bureau of Statistics.
- Chikmawati, T., 2013. Stomata and cytological features of *Spathoglottis plicata* from Java Island. *J Trop Life Sci.*, 3(2), pp.87-92. doi: 10.11594/JTLS.03.02.03.
- Gantait, S., Mandal, N. & Bhattacharyya, S., 2011. Induction and identification of tetraploids using in vitro colchicine treatment of *Gerbera jamesonii* Bolus cv. Sciella. *Plant Cell Tissue Organ Cult.*, 106(2), pp.485-493. doi: 10.1186/s43141-021-00269-1.
- Hamidah, H., Tsawab & Rosmanida, 2016. Analysis of *Hylocereus* spp. diversity based on phonetic methods. *AIP Conference Proceedings*, 1854. doi:10.1063/1.4985403.
- Hanafy, R.S. & Akladios, S.A., 2018. Physiological and molecular studies on the effect of gamma radiation in fenugreek (*Trigonella foenumgraecum* L.) plants. *J Genet Eng Biotechnol.*, 16(2), pp.683-692. doi: <https://doi.org/10.1016/j.jgeb.2018.02.012>.
- Jalil, M. et al., 2020. Distribution, variation, and relationship of *Curcuma soloensis* Valetton in Java, Indonesia based on morphological characters. *Biodiversitas*, 21(8), pp.3867-3877. doi: 10.13057/biodiv/d210856.
- Kamwean, P. et al., 2017. Chaging of morphological characteristic and biomass properties in *Pennisetum* grassland soil. *Soil Sci Soc AmJ.*, 68, pp.1429-1436. doi:10.3923/JA.2017.23.31.
- Lubis, M.M., Mawarni, L. & Husni, Y., 2015. Response to growth of Sugarcane (*Saccharum officinarum* L.) against tillage on two conditions of drainage. *Jurnal Agroekoteknologi*, 3(1), pp.214-220. doi: 10.32734/jaet.v3i1.9385.
- Mahfut et al., 2021. Identification of *Dendrobium* (Orchidaceae) in Liwa Botanical Garden based on leaf morphological characters. *Journal of Tropical Biodiversity and Biotechnology*, 6(1), pp.1-6. doi: 10.22146/jtbb.59423.
- Mahfut, Hidayat, M.M. & Arifannisa, S.J., 2023. Study of orchid resistance induction using Rhizoctonia against ORSV infection based on anatomical characters of roots and leaves. *Asian Journal of Plant Sciences*, 22(2), pp.239-249. doi: 10.3923/ajps.2023.239.249.
- Miguel, T.P. & Leonhart, K.W., 2011. In vitro polyploid induction of orchids using oryzalin. *Scie Horror.*, 130, pp.314-319. doi: 10.1016/J.scienta.2011.07.002.
- Moghbei, N., Khalili, M.B. & Bernard, F., 2015. Colchicine effect on the DNA content and stomata size of *Glycyrrhiza glabra* var. glandulifera and *Carthamus tinctorius* L. *J Genet Eng Biotechnol.*, 13(1), pp.1-6. doi: 10.1016/j.jgeb.2016.02.002.
- Mugiono, 2010. *Plant Breeding With Mutation Techniques*. Isotope and Radiation Technology Research Center. Jakarta.

- Munir, M. et al., 2011. Foliar epidermal anatomy of some ethnobotanically important species of wild edible fruits of northern Pakistan. *J Med Plant Res.*, 5(24), pp.5873-5880.
- Pitoyo, A. et al., 2018. Morphological, stomata, and isozyme variability among taro (*Colocasia esculenta*) accessions from the southeastern part of Central Java, Indonesia. *Biodiversitas*, 19(5), pp.1811-1819. doi: 10.13057/biodiv/d190532.
- Prabowo, H. et al., 2022. Stable isotope analysis to assess the trophic level of arthropod in sugarcane ratoon agroecosystem. *Biodiversitas*, 23(6), pp.2871-2881. doi: 10.13057/biodiv/d230613.
- PT Gunung Madu Plantations, 2016. *Company history*. Gunung Madu Press.
- Purnomo et al., 2012. Phenetic analysis and intraspecific classification of Indonesian water yam (*Dioscorea alata* L.) germplasm based on morphological characters. *SABRAO J Breed Genet.*, 44(2), pp.277-291.
- Purnomo et al., 2020. Phenetic analysis of cultivated taro (*Colocasia esculenta* L. Schott) accessions based on morphological characters. *SABRAO J Breed Genet.*, 52(3), pp.231-247.
- Rohmah, A. et al., 2017. Influence of Colchicine Present toward Stomata Characters of Oliv Leaf (*Olea europaea* L.). *Jurnal Ilmiah Bioscience Tropic*, 2(2), pp.10-17. doi:10.33474/e-jbst.v2i2.81.
- Sari, N. et al., 2016. Variation and intraspecies classification of edible Canna (*Canna indica* L.) based on morphological characters. *AIP Conference Proceedings*, 1744. doi: 10.1063/1.49535155.
- Sattler, M.C. et al., 2016. The polyploidy and its key role in plant breeding. *Planta*, 243, pp.281-296. doi: 10.1007/s00425-015-2450-x.
- Sivakumar, G., 2018. Upstream biomanufacturing of pharmaceutical colchicine. *Critical Review in Biotechnology*, 38(1), pp.83-92. doi: 10.1080/07388551.2017.1312269.
- Stevens, R.D. & Tello, J.S., 2014. On the measurement of dimensionality of biodiversity. *Glob Ecol Biogeogr.*, 23(2), pp.1115-1125. doi: 10.1111/geb.12192.
- Suhaimi, S., 2017. *Evaluation of Morphology, Anatomy, Physiology and Anatomy of Forage Plants Obtained by Colchisin Treatment*. Universitas Diponegoro.
- Sultan, H.A. et al., 2010. Stomata and phytochemical studies of the leaves and roots of *Urginea grandiflora* Bak. and *Pancratium tortuosum* Herbert. *Ethnobot Leaflet*, 14, pp.826-835. doi: 10.1.1.1.683.9435.
- Suryo, H., 2009. *Cytogenetics*, Gadjah Mada University Press.
- Syukur, M. et al., 2015. *Plant Breeding Techniques*. Jakarta: Penebar Swadaya.
- Tambaru, E., 2015. Identification of morphological and anatomical characteristics *Flacourtia inermis* Roxb. in the Unhas Tamalanrea Makassar campus area. *Journal of Natural and Environmental Science*, 6(11), pp. 35-41.
- Windiyan, I.P. et al., 2022. Morphological variations of superior sugarcane cultivars (*Saccharum officinarum* L.) from Lampung, Indonesia. *Biodiversitas*, 23(8), pp.4109-4116. doi: 10.13057/biodiv/d230831.
- Yanny, D.L. et al., 2022. Increasing the diversity of marigold (*Tagetes* sp.) by acute and chronic chemical induced mutation of EMS (Ethyl Methane Sulfonate). *J Biodiversitas*. 23(3):1399-1407. doi:10.13057/biodiv/d230326.

Research Article

Comparison of Light Intensity under the Canopy between Sal (*Shorea robusta*) and Akashmoni (*Acacia auriculiformis*) in Agroforestry Stands: Effect of Tree Size and Distance from Individual Trees

Md. Al Forhad Islam¹, Md. Najmus Sayadat Pitol^{2*}, Md. Nabiul Islam Khan¹

1)Forestry and Wood Technology Discipline, Khulna University, Khulna-9208, Bangladesh.

2)Mangrove Silviculture Division, Bangladesh Forest Research Institute, Muzgunni, Khulna-9000, Bangladesh.

* Corresponding author, email: najmus.sayadat@bfri.gov.bd, najmus.sayadat@gmail.com

Keywords:

agroforestry
canopy
Interception
light environment
RPAR

Submitted:

28 September 2022

Accepted:

10 April 2023

Published:

08 September 2023

Editor:

Furzani Binti Pa'ee

ABSTRACT

Agroforestry is now inevitable for meeting the snowballing demand for food of the growing number of people worldwide. The light environment is the most important driving force for the growth and development of crops in agroforestry stand. The present study aims to quantify the light interception in two different agroforestry types, where one was composed of *Shorea robusta* (Sal) with *Ananas comosus* and another was *Acacia auriculiformis* (Akashmoni) with *Ananas comosus*. The relative Photosynthetically Active Radiation (PAR) was measured by a pair of quantum sensors in four directions from some individual trees. Spatial variation of PAR was also explored in both stand types. The results revealed that RPAR did not significantly ($P>0.05$) vary among four directions of individual trees in *S. robusta* but the *A. auriculiformis* showed a significant difference ($P<0.001$) along the four directions. Also, RPAR was significantly different ($P<0.001$) at different distances from individual trees under the canopy of both tree species. When the stand-level spatial variation of RPAR was considered, *A. auriculiformis* (0.177) and *S. robusta* (0.171) showed no significant difference ($P>0.05$) in the light environment. Our findings explored that both the tree species would be suitable species for agroforestry practices in the area. For the betterment of the natural *S. robusta* forest responsible authorities should encourage people to avoid *A. auriculiformis* plantations near the natural *S. robusta* forest which will enhance the conservation of *S. robusta* cover in its natural habitat.

Copyright: © 2023, J. Tropical Biodiversity Biotechnology (CC BY-SA 4.0)

INTRODUCTION

The present world is facing significant challenges of food, fuel wood, fodder and other agriculture and forest products due to global population growth. It is very problematic to fulfill food and forest product demand with detaching practice of agriculture and forestry because of land scarcity (Licker et al. 2010). There are approximately 80-120% rise in global food demand by 2050 because of global population growth and alteration of dietary intake (Tilman et al. 2001; FAO 2006; Foley et al. 2012). In this challenging global situation, agroforestry practice is one of the best options to meet those challenges (Dufour et al. 2013) worldwide as well as in Bangladesh. Agroforestry has numerous benefits including biodiver-

sity conservation (George et al. 2013), food production, carbon sequestration (Nair et al. 2009), effective resource use (Munz et al. 2014) and soil improvement (Udawatta et al. 2008). Agroforestry also plays an important role to promote green economy, sustain agriculture landscape (Schroth & Mota 2013), stimulate long-term sustainable and renewable forest management (Gold 2017), and reduce soil erosion and desertification (Branca et al. 2013). Generally, people prefer fast-growing cover crops that can reduce nutrient losses and soil erosion in the establishment of agroforestry stands (Fageria et al. 2011). But the best combination of trees and crops are still unknown in agroforestry system of Bangladesh.

Madhupur Sal (*Shorea robusta*) forest is the largest belt of *Shorea robusta* forest in Bangladesh situated in Tangail and Gazipur district (Rahman et al. 2009). Land tenure and encroachment become a serious problem in this forest management and conservation. The local people started to convert the forest area into agricultural land through clear-felling, without any permission from the government or forest department (FD) (Safa 2004). In this situation, Bangladesh forest department (BFD) decided to give access to the local people for agroforestry practice in existing forest areas to protect the Madhupur Sal forests from further degradation.

In agroforestry practice, light environment is a significant driver for the growth and development of crops (Forester 2014). It also found that the harvest product of tree-crop intercropping was better than in monoculture crops, exclusively a new pattern for light utilization (Whiting 2011). Trees and crops compete for various growth resources mainly light that drives the energy available for photosynthesis and transpiration (Alam et al. 2018; Liu et al. 2021). However, the photosynthetically active radiation (PAR), light interception and light use efficiency increase the yield of intercropping (Marshall and Willey 1983; Gao et al. 2010; Ceotto et al. 2013; Du et al. 2015; Wang et al. 2015). In most cases, the tree canopies are responsible for light environment regulation because they work as a light barrier to crops. Light interception also controls energy balance and microclimate, which are crucial parameters of agroforestry practice for the growth and development of crops (Alam et al. 2018). In agroforestry plots, the growth of crops is influenced by the amount of photosynthetic photon flux density (PPFD) reaching the agricultural produce because their lights are intercepted by plantation crops (Willson 1999). It assumed that the light environment may vary because of species variation, density, crown volume, leaf area index, spacing, distance from tree, and height from ground. However, the knowledge of light environment in agroforestry system remains unclear.

Considering the significance of light intensity in output of agroforestry schemes, the present study aims to sketch of the light environment and its impact on two different agroforestry tree-crop combinations broadly practiced in the study area. These two tree-crop combinations are *Shorea robusta* with *Ananas comosus* and *Acacia auriculiformis* with *Ananas comosus*. *Shorea robusta* is a deciduous large tree. The diameter at breast height (DBH) varied from 1.5–2 m with an average height ranging from 18–32 m. The bole is clean, straight and cylindrical with often bearing epicormic branches and a spherical crown (Sharma et al. 2019). The leaves are 10–25 cm long and 5–15 cm broad. In wetter areas, *S. robusta* is evergreen; in drier areas, it is dry-season deciduous, shedding most of the leaves from February to April, leafing out again in April and May. On the other hand, *Acacia auriculiformis* is an evergreen tree that grows between to 15–30 m tall, with a trunk up to 12 m long and 50 cm

in diameter. The trunk is crooked and the bark is vertically fissured. It has dense foliage with an open, spreading crown. Mature leaves are linear to very narrowly elliptic and falcate with a dark green color. The leaves are glabrous, 8–22.5 cm long (average 10–20 cm) and 10–52 mm wide (average 12– 30 mm) (Orchard & Wilson 2001). The objectives of this study were to explore the variation of RPAR in the tree level and stand level, as well as explore the effect of crown volume, distance from tree and above ground biomass of individual trees on the RPAR on two types of agroforestry stands. We hypothesized that there is no significant difference in relative Photosynthetically Active Radiation (RPAR) under the canopy between the two tree species. We also hypothesized that RPAR would not vary among four directions and distance from individual trees.

MATERIALS AND METHODS

Description of the Study Area

The study was conducted in the Madhupur Sal forests (locally known as Madhupur Garh), Bangladesh's largest belt of Sal forests (Figure 1). *Shorea robusta* is the dominant species and usually forms 75% of the total tree individuals in the natural forest patches (Rahman et al. 2019). The area is located between 24°30'–24°50' N and 90°00'–90°10' E (Rahman et al. 2017). The area is slightly elevated and the maximum height of about 18 - 20 m from the mean sea level. The soil is yellowish red sandy clay and becomes compacted and harder when dries but melts with the rainfall and becomes soft and tenacious (Mondol 2021). All physio-chemical characteristics (soil colour, soil texture, pH, organic matter, nitrogen, phosphorus, potassium, and sulphur) of uncovered and encroached areas soil are low here in comparison to the forests covered areas (Mondol 2021). The mean annual temperature is 26°C and the average of monthly maximum and minimum temperatures are 27.5°C and 18.5°C respectively (Rahman et al. 2019).

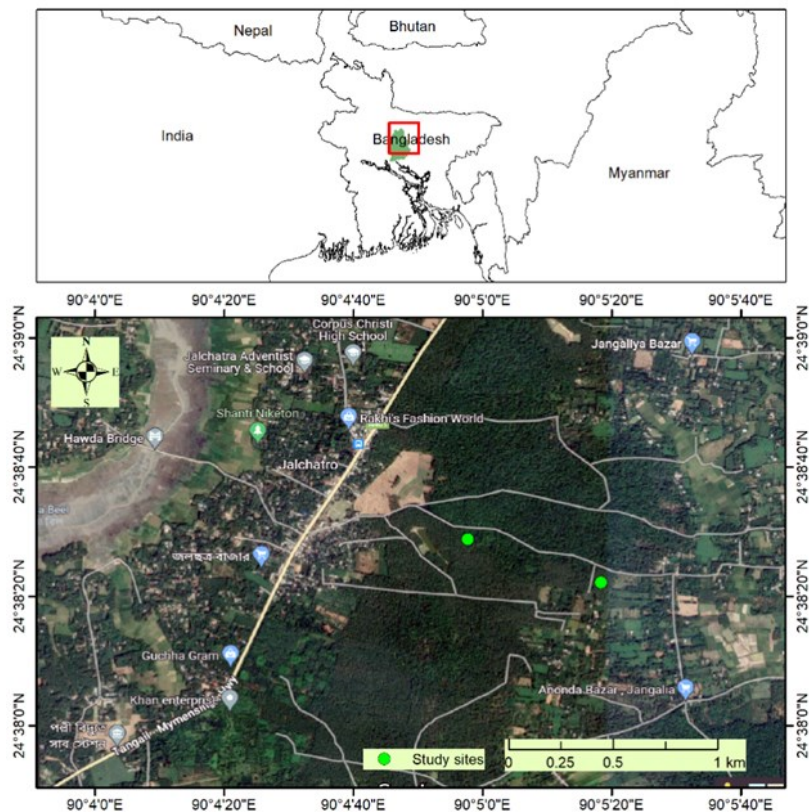


Figure 1. Map of the study sites (adapted from Google maps, maps.google.com).

Sampling Design and Data Collection

The sampling was conducted in two sample plots with total area 800 m². Each plot was divided into twenty subplots with 1m² size (Figure 2). Both sampling plots were located in agroforestry area; one was constituted with *Shorea robusta* and *Ananas comosus* and the other one was constituted with *Acacia auriculiformis* and *Ananas comosus*. Those plots were located in Dokhola range in Madhupur Sal forest, Tangail. All trees height, DBH, crown height and crown width were measured and recorded from those two plots. We consider an individual is a tree where the DBH of the trees is more than or equal to 5 cm (DBH \geq 5 cm). Wood density of *Shorea robusta* and *Acacia auriculiformis* were collected from secondary data sources available at Global Wood Density Database (Chave et al. 2009; Zanne et al. 2009).

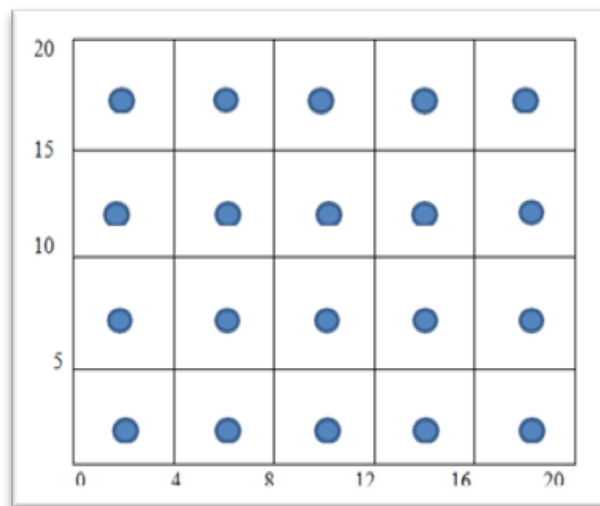


Figure 2. Photosynthetically Active Radiation (PAR) measurement points in a 20 m x 20 m plot layout.

Measurement of Photosynthetically Active Radiation (PAR) at Plot Level and Tree Level

The Photosynthetically Active Radiation (PAR) measurements were performed from 11:00 a.m. to 1:00 p.m. on sunny days during the last week of October 2017. Each plot was divided into 20 subplots. And the PAR is measured by a pair of horizontally placed quantum sensors (LI-190SA; LI-COR, USA) and in each subplot, 25 observations of photosynthetically active radiation (PAR) were taken using a data logger (LI-1400; LI-COR, USA) (Figure 3). At tree level, the individual trees were selected randomly from those two plots. First 10 trees of *Shorea robusta* were selected randomly from the first plot and 10 trees of *Acacia auriculiformis* were selected randomly from the second plot. PAR measurement of the individual tree was performed at varied distance from the tree in four perpendicular directions (north, south, east and west) with one meter interval in each direction from tree to 5 meter distance. In each direction data was obtained at 5 points and repeated in the four perpendicular directions (Figure 3). Data were recorded in a data logger (LI-1400; LI-COR, USA).

Relative Photosynthetically Active Radiation (RPAR) Measurements

Relative Photosynthetically Active Radiation (RPAR) for each direction of every tree was measured by using Beer-Lambert law (Khan et al. 2004).

$$\text{RPAR} = \text{UC/OC}$$

Where RPAR= Relative Photosynthetically Active Radiation (the value varies from 0 to 1);
 UC= Photosynthetically Active Radiation at under canopy or selected point;
 OC= Photosynthetically Active Radiation at open canopy or full sunlight.

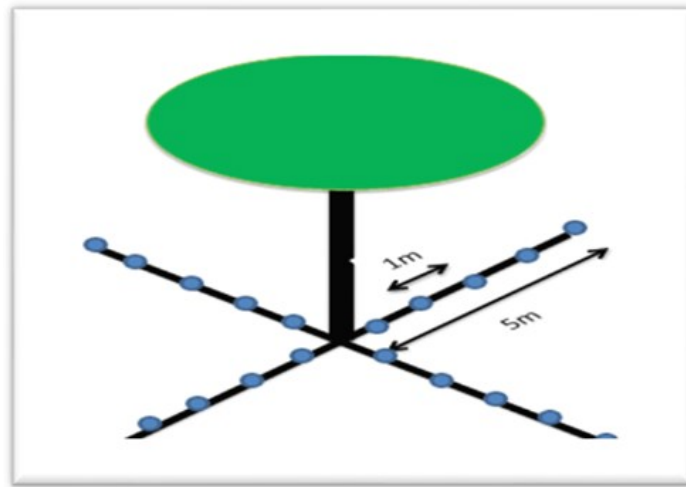


Figure 3. Photosynthetically Active Radiation (PAR) measurement points in four directions at tree level.

Crown Area Measurement

The crown diameter (CD) was calculated by using measuring tape. First, the extension of canopy was calculated in two directions from tree base to get the crown diameter. The crown base and crown top were measured by using Suunto Clinometer. The difference of crown base and top was the crown diameter. Crown Area (CA) was estimated by the following equation,

$$CA = \frac{\pi}{4} (CD)^2$$

Where, CA = Crown Area; CD = Crown Diameter.

To get the crown volume (CV), crown area was multiplied by crown height.

Aboveground Biomass Measurement

Chave et al. (2005) established a set of allometric equations for measuring the biomass of tropical trees. The equations were frequently used for measuring the above ground biomass (Pitol et al. 2019; Pitol & Mian 2023; Azad et al. 2021) worldwide. We also used the equation recommended by Chave et al. (2005).

$$AGB (Kg) = 0.0673 \times (\rho D^2 H)^{0.972}$$

Where, AGB = Aboveground Biomass (Kg); ρ = Wood density ($g\ cm^{-3}$); D = Diameter at breast height (cm); H = Height (m).

Statistical Analysis

A two-way-ANOVA test was performed with relative Photosynthetically Active Radiation (RPAR) as response variable against distance and direction as explanatory factors. Pearson's correlation was performed among different tree related variables, such as DBH, height, aboveground biomass, crown size, and distance from individual trees. An independent sample t-test was performed to find any significant difference of spatially distributed RPAR under the canopy of the two tree species. The statistical analysis of data was performed using the R programming language (R Core Team 2021).

RESULT

Tree Level Variation of Light Intensity in Two Species

RPAR shows strong correlations ($P < 0.01$) to different tree level variables, such as DBH, height, aboveground biomass, crown size, and distance from individual trees. It was found that DBH, height, aboveground biomass, crown size, and distance from individual trees significantly affect the light environment (RPAR) in both the species *Acacia auriculiformis* and *Shorea robusta*. While the effect of crown volume of *A. auriculiformis* on RPAR was not significant ($P > 0.05$) (Figure 4).

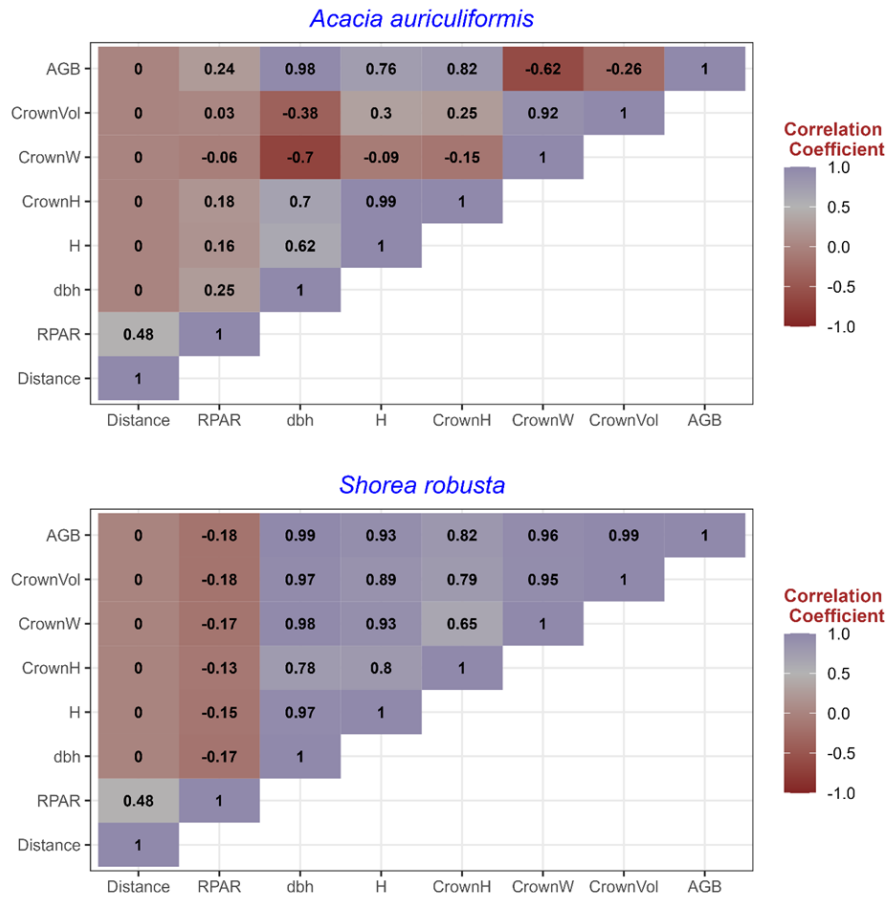


Figure 4. Pearson's correlation matrix among different tree level variables in *Shorea robusta* and *Acacia auriculiformis*. Distance = Distance from individual tree in meter, RPAR = Relative Photosynthetically Active Radiation, DBH = diameter at breast height (cm), H = height (m), crownH = crown height (m), crownW = crown wide (m), crownVol = crown volume (m^3), AGB = Above-ground biomass (kg)

RPAR do not significantly ($P > 0.05$) vary among four perpendicular directions of individual trees in *Shorea robusta* while *Acacia auriculiformis* showed a significant difference ($P < 0.001$) among four perpendicular directions (Table 1). Also, there was significant ($P < 0.001$) effect of distance from individual trees on the RPAR intensity under the canopy of both tree species. However, the combined effect of distance and direction on RPAR was not significant for *Shorea robusta* ($P < 0.241$). There was a significant ($P < 0.001$) effect found between the RPAR and combined effect of distance and direction for *Acacia auriculiformis* (Table 1).

Spatial Variation of Light Intensity

The result of the analysis showed no significant difference ($P > 0.05$) in the light environment of *Shorea robusta* with *Ananas comosus* and *Acacia auriculiformis* with *Ananas comosus* stand (Figure 5), having the average

Table 1. Two-way ANOVA of RPAR against distance and direction of individual trees in two species

Factor	<i>F</i>	<i>P</i>
<i>Shorea robusta</i>		
Distance	589.45	<0.001***
Direction	2.1072	0.097 ^{ns}
Interaction (Distance: direction)	1.3985	0.241 ^{ns}
<i>Acacia auriculiformis</i>		
Distance	618.182	<0.001***
Direction	4.193	<0.01**
Interaction (Distance: direction)	18.416	<0.001***

** significant at 0.01 level; *** significant at 0.001 level; ^{ns} not significant

RPAR of 0.171 in *S. robusta* and 0.177 in *A. auriculiformis*. The tree density of *Shorea robusta* was 625 stem ha⁻¹ with aboveground biomass of 168.75 ton ha⁻¹ whereas the density of *Acacia auriculiformis* was 900 stem ha⁻¹ with aboveground biomass of 36.646 ton ha⁻¹. Although, the scenario of tree density and aboveground biomass of both tree species were different the average RPAR in both stands were similar and the height of *Ananas comosus* in two plots was also very close, ranging from 1.06 to 1.13 m.

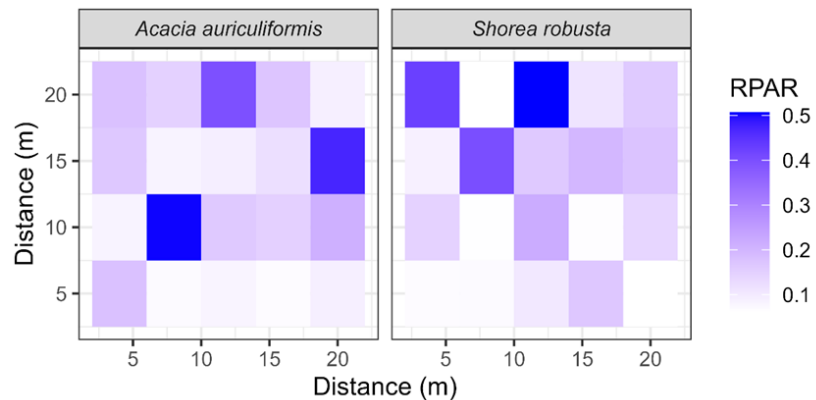


Figure 5. Stand level mean RPAR distribution in *Shorea robusta* and *Acacia auriculiformis*.

The Average RPAR Distribution with Direction

The light environment of individual tree of *Shorea robusta* and *Acacia auriculiformis* in four directions was relatively similar in trend (Figure 6). However, the results suggested that RPAR in the south direction of *A. auriculiformis* shows a distinct pattern and all other cases were similar.

The overall penetration of light at tree level is higher in *A. auriculiformis* than *S. robusta* (Figure 7) at 5 m distance from individual trees but quite similar when coming close to the trees. It was observed that the RPAR exponentially increase with increasing distance from the tree for both *S. robusta* and *A. auriculiformis* (Figure 7).

Relationship of RPAR to Aboveground Biomass with Different Distance

The aboveground biomass with different heights from the ground had significant effect on RPAR of both trees. The Figure 8 displayed the relationship between aboveground biomass and the RPAR with different distance. At 5 m distance for all tree and measured biomass the RPAR was high (> 0.5). At 4 m distance from *A. auriculiformis* the RPAR increased gradually with an increase for the aboveground biomass but fluctuate for *S. robusta*. Most of the cases the RPAR was slightly higher (> 0.3) for *A.*

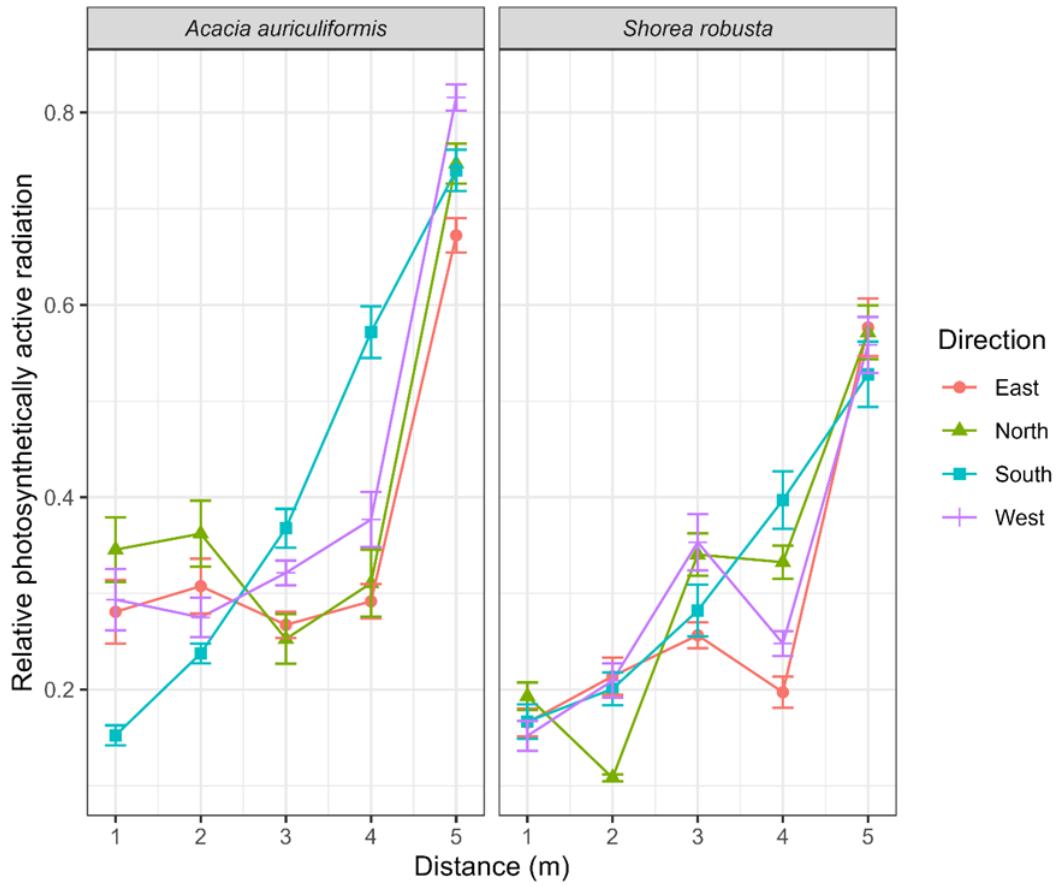


Figure 6. Relationship of RPAR to distance from the trees in four directions in *Shorea robusta* and *Acacia auriculiformis* where X-axis denotes the distance from tree, Y-axis denotes the RPAR and four colors denotes the four directions

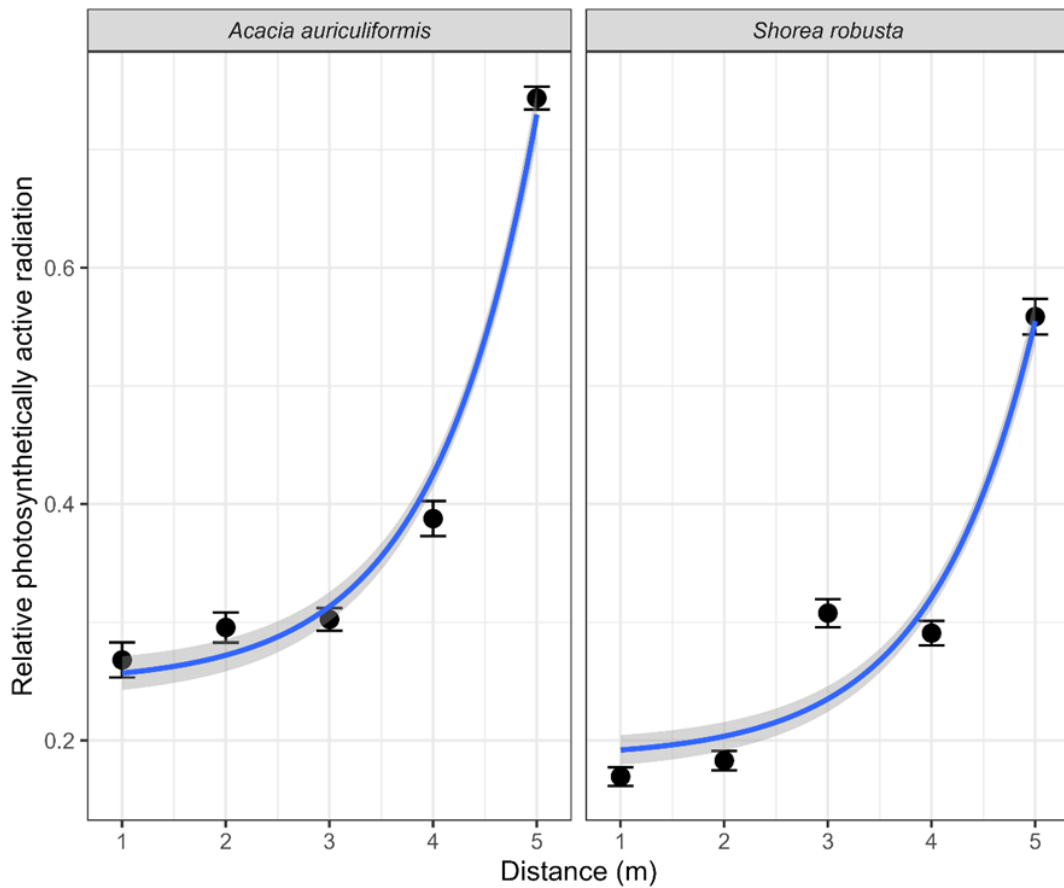


Figure 7. Relationship of RPAR to distance, where X-axis denotes the distance from tree, Y-axis denotes the RPAR

auriculiformis than the *S. robusta* (< 0.29) of having lower aboveground biomass (Figure 8).

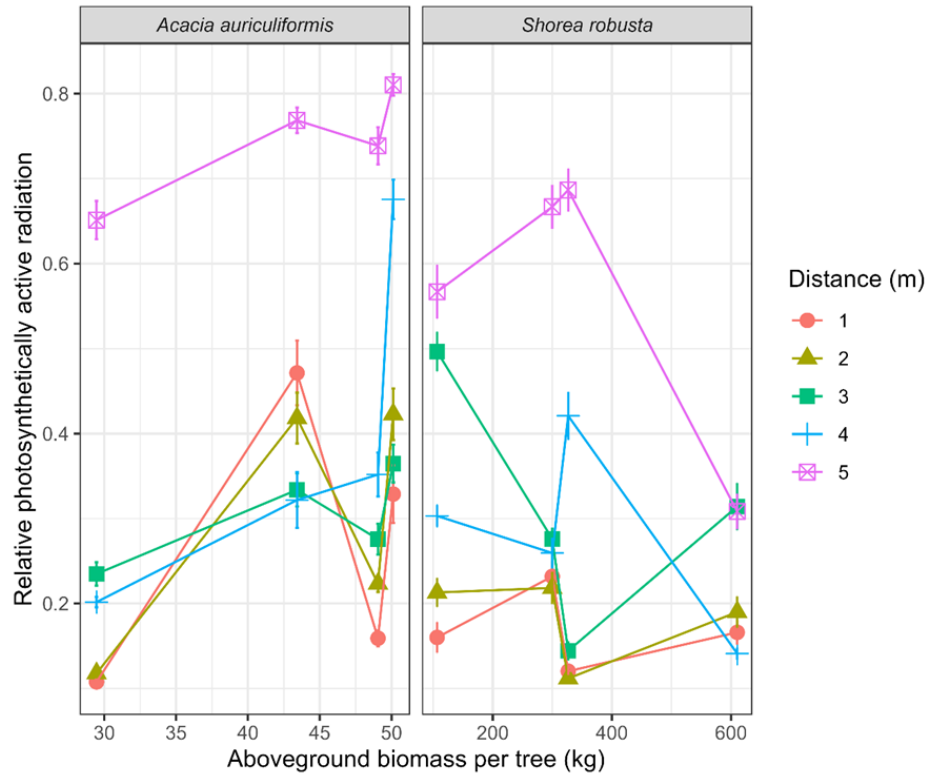


Figure 8. Relationship of RPAR to aboveground biomass per tree at variable distance in *Shorea robusta* and *Acacia auriculiformis*, X-axis denotes the biomass from tree, Y-axis denotes the RPAR, and five colors denote the distance (m) from tree

Relationship of RPAR to Crown Volume with Different Distance

The crown volume and height from ground had significant effect on RPAR of both trees. The RPAR (>0.2) sharply decrease with increase the crown volume at 3 m and 2 m distance from tree for both *Shorea robusta* and *Acacia auriculiformis* species (Figure 9). But RPAR showed increasing manner with crown volume at 5m distance from tree for *S. robusta* (>0.5) but decreasing for *A. auriculiformis* (>0.6) and the value was above 0.5 for both species (Figure 9). Also found that for 1 m and 4 m distance from tree the RPAR fluctuate with increase the crown volume for both species. The average RPAR was below 0.2 for both tree with 1m distance and above 0.3 for both tree with 4 m distance from the tree. Most of the cases *A. auriculiformis* showed the higher value (>0.35) of average relative photosynthetically active radiation (RPAR) than the *S. robusta* (<0.28) because of having lower crown volume.

DISCUSSION

Light distribution in an agroforestry plot plays vital role in the growth of crops. Tree density, size and shape effects the light interception. The leaves and canopy size of tree mainly regulates the light interception (Trápani et al. 1992; Cohen et al. 1997; Schleppei et al. 2007; Suwa 2011; Klančnik & Gaberščik 2015) and tree shading of an agroforestry system depends on the amount of leaf area per tree and crown size (Wang & Jarvis 1990; Duursma & Mäkelä 2007; Sinoquet et al. 2007). In an agroforestry system, the amount of incoming photosynthetically active radiation (PAR) to agroforestry crops is reduced by tree shading, which affects the growth and development of the production (Li et al. 2008). But we found

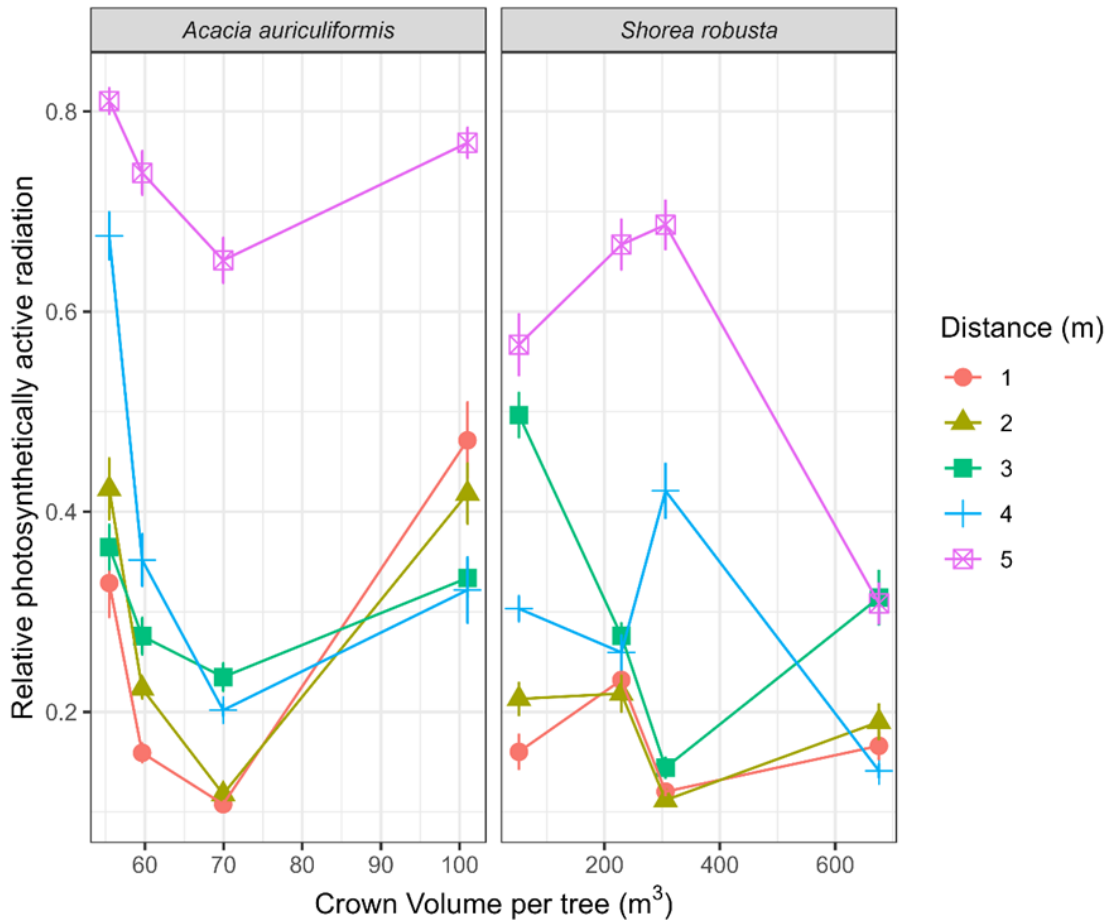


Figure 9. Relationship of RPAR to crown volume per tree at variable distance in *Shorea robusta* and *Acacia auriculiformis*, X-axis denotes the crown volume of trees, Y-axis denotes the RPAR, and five colors denote the distance (m) from ground

that, the average light environment of two examined stands was quite similar while some other stand variables were varied. Generally, it is believed that the canopy shape and size, significantly affect the light interception as well as the growth and development of understory crops in agroforestry practices (Horn 1971; Khan et al. 2004; Sinoquet et al. 2007). The above ground biomass is also positively effect on the light intensity of agroforestry stand. The mean RPAR of *Shorea robusta* with *Ananas comosus*, and *Acacia auriculiformis* with *Ananas comosus* in our study were 0.171 and 0.177 respectively.

Light availability is significantly altered in agroforestry systems (Rivest et al. 2009) and light interception is a driving variable for many key ecosystem processes in forests and agroforestry areas (Mariscal et al. 2004). In every agroforestry system, the tree canopy lessens the incident radiation for the crop (Dufour et al. 2013). The shade of the trees induces stress conditions for the harvest (Dufour et al. 2013). Lack of sufficient incident light boosted the changes in microclimate modification which hampers the potential growth and yield of crops under the trees in the agroforestry system (Alam et al. 2018). In the two study sites, the average height of *Ananas comosus* was quite similar because of the similar light interception of the two tree species. Rahaman et al. (2020) found 42 species of 26 families in natural *Shorea robusta* forest and 15 species of 13 families in *Acacia auriculiformis* plantations in the study area. Besides, Uddin et al. (2021) found 21 species of 18 families in the study area. More research trial of agroforestry system with other tree species found in the natural forest would be sought to contribute to the restoration process in

the area.

Strong correlations ($P < 0.01$) were found among the dbh, height, aboveground biomass, crown size, distance from individual trees etc. (Figure 4). It was found that the value of RPAR was not significant ($P > 0.05$) among the four directions of individual trees in *Shorea robusta* while *Acacia auriculiformis* showed a significant difference ($P < 0.001$) (Table 1). The average relative photosynthetically active radiation (RPAR) was found below 0.2 from the tree to 3 meters in the distance for *Shorea robusta* in most of the cases. In *Acacia auriculiformis*, the average RPAR was found below 0.2 from the tree to 2 meters in the distance. The understory light environment of a tree is affected by the canopy of the tree (Nicotra et al. 1999; Denslow & Guzman 2000; Montgomery & Chazdon 2001). Tree shading significantly reduced the amount of incoming photosynthetically active radiation (PAR) (Li et al. 2008). Crown structure and crown volume are essential determinants of light capture (Horn 1971; Khan et al. 2004; Duursma & Mäkelä 2007; Sinoquet et al. 2007).

In most cases, *Acacia auriculiformis* showed a higher value of average relative photosynthetically active radiation (RPAR) than the *Shorea robusta* because of having a lower crown volume. The crown shape and size of trees are responsible for this kind of light interception. It found that the crown shape of *Shorea robusta* was more than the *Acacia auriculiformis*, which was the cause of the light interception probably by *Shorea robusta* was more than *Acacia auriculiformis*. The total amount of light decreased with increasing crown volume. However, the *Acacia auriculiformis* is growing faster than *Shorea robusta* and the economic returns from *Acacia auriculiformis* agroforestry system is quicker. Because of the quick economic returns, people adjacent to Sal (*Shorea robusta*) forest desired *Acacia auriculiformis* as cover crop in Agroforestry. However, Nurunnahar et al. (2020) found various agroforestry systems with various trees (*Artocarpus heterophyllus*, *Areca catechu*, *Cocos nucifera*, *Swietenia macrophylla*, *Phoenix dactylifera*, *Moringa oleifera*, *Syzygium cumini*, *Borassus flabellifer*, *Azadirachta indica* etc.) and crops (*Oryza sativa*, *Colocasia esculenta*, *Curcuma longa*, *Kaempferia galangal*, *Musa paradisiaca*, *Solanum lycopersicum*, *Capsicum spp.*, *Brassica oleracea*, etc.) in Bangladesh. So, to select the appropriate crop-combination, we need extensive research with various crops. The light environment of various trees should be identified and also measure the light demand of various agriculture crops.

CONCLUSION

In sustainable agroforestry practice, selecting crops and their composition is vital to get more yields. The effects of species, distance from the tree, above-ground biomass, and canopy size and shape were significant on RPAR for both *Shorea robusta* and *Acacia auriculiformis*. Although both species gave similar RPAR at the stand level, there were some differences between individual tree levels. It can be claimed that enough light can penetrate in both tree species (*Shorea robusta* and *Acacia auriculiformis*) in agroforestry stands explored. The results support us to get an idea about the light environment in the agroforestry system in relation to distance from trees. The results of this have implications on conservation of *S. robusta* cover in sal (*Shorea robusta*) forest if the species is considered a candidate tree species for a medium term rotation species in agroforestry practice in the area.

AUTHOR CONTRIBUTION

A.F.I. and N.I.K. designed the research, A.F.I. collected the data, A.F.I.

and N.I.K. analyzed the data, M.N.S. and A.F.I. wrote the manuscript. All authors revised and approved the manuscript.

ACKNOWLEDGEMENTS

The authors are grateful to Forestry and Wood Technology Discipline, Khulna University, Bangladesh for providing logistic support in field data acquisition. This research did not receive any specific grant from any aid agencies.

CONFLICT OF INTEREST

There is no competing interests.

REFERENCES

- A.K.M. Azad, A.K., Pitol, M.N.S. & Hara, Y., 2021. The role of Rubber (*Hevea brasiliensis*) plantation in carbon storage at Bandarbands Hill Tract, Bangladesh. *Int. J of Curr. Res*, 13, (05), pp.17373-17377. doi: 10.24941/ijcr.41365.05.2021
- Alam, B. et al., 2018. Different genotypes of *Dalbergia sissoo* trees modified microclimate dynamics differently on understory crop cowpea (*Vigna unguiculata*) as assessed through ecophysiological and spectral traits in agroforestry system. *Agricultural and Forest Meteorology*, 249, pp.138-148. doi: 10.1016/j.agrformet.2017.11.031
- Branca, G. et al., 2013. Food security, climate change, and sustainable land management. A review. *Agron. Sustain. Dev*, 33, pp.635-650. doi: 10.1007/s13593-013-0133-1
- Ceotto, E. et al., 2013. Comparing solar radiation interception and use efficiency for the energy crops giant reed (*Arundo donax* L.) and sweet sorghum (*Sorghum bicolor* L. Moench). *Field Crops Research*, 149, pp.159-166. doi: 10.1016/j.fcr.2013.05.002
- Chave, J. et al., 2005. Tree allometry and improved estimation of carbon stocks and balance in tropical forests. *Oecologia*, 145, pp.87-99. doi: 10.1007/s00442-005-0100-x
- Chave, J. et al., 2009. Towards a worldwide wood economics spectrum. *Ecology letters*, 12(4), pp.351-366. doi: 10.1111/j.1461-0248.2009.01285.x
- Cohen, S. et al., 1997. Response of citrus trees to modified radiation regime in semi-arid conditions. *Journal of Experimental Botany*, 48(1), pp.35-44. doi: 10.1093/jxb/48.1.35
- Denslow, J.S. & Guzman, S., 2000. Variation in stand structure, light and seedling abundance across a tropical moist forest chronosequence, Panama. *Journal of Vegetation Science*, 11, pp.201-212. doi: 10.2307/3236800
- Du, X. et al., 2015. Effect of cropping system on radiation use efficiency in double-cropped wheat-cotton. *Field Crops Research*, 170, pp.21-31. doi: 10.1016/j.fcr.2014.09.013
- Dufour, L. et al., 2013. Assessing light competition for cereal production in temperate agroforestry systems using experimentation and crop modelling. *Journal of agronomy and crop science*, 199(3), pp.217-227. doi: 10.1111/jac.12008
- Duursma, R. A. & Mäkelä, A., 2007. Summary models for light interception and light-use efficiency of non-homogeneous canopies. *Tree physiology*, 27(6), pp.859-870. doi: 10.1093 treephys/27.6.859
- Fageria, N.K., Baligar, V.C. & Jones, C.A., 2011. Growth and mineral nutrition of field crops, 3rd ed. Boca Raton, FL, USA: CRC Press

- FAO., 2006. World agriculture: towards 2030/2050 prospects for food, nutrition, agriculture and major commodity groups. Rome: FAO. <https://www.fao.org/3/ap106e/ap106e.pdf>
- Foley, J.A. et al., 2011. Solutions for a cultivated planet. *Nature*, 478 (7369), pp.337-342. doi: 10.1038/nature10452
- Forrester, D.I., 2014. A stand-level light interception model for horizontally and vertically heterogeneous canopies. *Ecological Modelling*, 276, pp.14-22. doi: 10.1016/j.ecolmodel.2013.12.021
- Gao, Y. et al., 2010. Distribution and use efficiency of photosynthetically active radiation in strip intercropping of maize and soybean. *Agronomy journal*, 102(4), pp.1149-1157. doi: 10.2134/agronj2009.0409
- George, S.J. et al., 2013. A sustainable agricultural landscape for Australia: a review of interlacing carbon sequestration, biodiversity and salinity management in agroforestry systems. *Agric. Ecosyst. Environ*, 163, pp.28-36. doi: 10.1016/j.agee.2012.06.022
- Gold, M.A., 2017. Agroforestry. *Encyclopedia Britannica*, inc. <https://www.britannica.com/science/agroforestry>
- Horn, H.S., 1971. The adaptive geometry of trees (No. 3). Princeton University Press.
- Khan, M.N.I. et al., 2004. Interception of photosynthetic photon flux density in a mangrove stand of *Kandelia candel* (L.) Druce. *Journal of forest research*, 9(3), pp.205-210. doi: 10.1007/s10310-003-0074-7
- Klančnik, K. & Gaberščik, A., 2015. Leaf spectral signatures differ in plant species colonizing habitats along a hydrological gradient. *J. Plant. Ecol.*, 9, pp.442-450. doi: 10.1093/jpe/rtv068
- Li, F. et al., 2008. Light distribution, photosynthetic rate and yield in a Paulownia-wheat intercropping system in China. *Agroforestry Systems*, 74, pp.163-172. doi: 10.1007/s10457-008-9122-9
- Licker, R. et al., 2010. Mind the gap: how do climate and agricultural management explain the 'yield gap' of croplands around the world? *Global ecology and biogeography*, 19(6), pp.769-782. doi: 10.1111/j.1466-8238.2010.00563.x
- Liu, S. et al., 2021. Importance of the description of light interception in crop growth models. *Plant Physiology*, 186(2), pp.977-997. doi: 10.1093/plphys/kiab113
- Mariscal, M.J. et al., 2004. Light-transmission profiles in an old-growth forest canopy: simulations of photosynthetically active radiation by using spatially explicit radiative transfer models. *Ecosystems*, 7, pp.454-467. doi: 10.1007/s10021-004-0137-4
- Marshall, B. & Willey, R.W., 1983. Radiation interception and growth in an intercrop of pearl millet/groundnut. *Field Crops Res.*, 7(83), pp.141-160. doi: 10.1016/0378-4290(83)90018-7
- Montgomery, R.A. & Chazdon, R.L., 2001. Forest structure, canopy architecture, and light transmittance in tropical wet forests. *Ecology*, 82, pp.2707-2718. doi: 10.2307/2679955
- Mondol, M.A., Wadud, M.A. & Rahman, G.M.M., 2021. Soil, Plant Species and Encroachment Status of Sal Forest in Bangladesh. *European Journal of Applied Sciences*, 9(4), pp.154-171. doi:10.14738/aivp.94.10691
- Munz, S. et al., 2014. Modeling light availability for a subordinate crop within a strip-intercropping system. *Field Crops Res.*, 155, pp.77-89. doi: 10.1016/j.fcr.2013.09.020
- Nair, P.K.R., Kumar, B.M. & Nair, V.D., 2009. Agroforestry as a strategy for carbon sequestration. *J. Soil Sci. Plant Nut.*, 172(1), pp.10-23. doi: 10.1002/jpln.200800030

- Nicotra, A.B., Chazdon, R.L. & Iriarte, S.V., 1999. Spatial heterogeneity of light and woody seedling regeneration in tropical wet forests. *Ecology*, 80, pp.1908-1926. doi: 10.1890/0012-9658(1999)080 [1908:SHOLAW]2.0.CO;2
- Nishat, A. et al., 2002. Bio-ecological zones of Bangladesh. Dhaka (Bangladesh): IUCN Bangladesh Country Office. pp.54–55.
- Nurunnahar., Pitol, M.N.S. & Sharmin, A., 2020. Status and Prospects of Agroforestry at Kaligonj Upazila in Satkhira District. *European Journal of Agriculture and Food Sciences*, 2(6). doi: 10.24018/ejfood.2020.2.6.186
- Orchard, A.E. & Wilson, A.J.G., 2001. Flora of Australia: Vol. 11b, *Mimosaceae, Acacia* part 2, Melbourne, AU: ABRIS, Canberra/CSIRO Publishing.
- Pitol, M.N.S. & Mian, M.B., 2023. High carbon storage and oxygen (O₂) release potential of Mahagony (*Swietenia macrophylla*) woodlot plantation in Bangladesh. *Saudi Journal of Biological Sciences*, 30(1), 103498. doi: 10.1016/j.sjbs.2022.103498
- Pitol, M.N.S., Khan, M.Z. & Khatun, R., 2019. Assessment of Total Carbon Stock in *Swietenia macrophylla* Woodlot at Jhenaidah District in Bangladesh. *Asian Journal of Research in Agriculture and Forestry*, 2 (3), 1-10. doi: 10.9734/AJRAF/2018/46922
- R Core Team., 2021. R: A language and environment for statistical computing. R Foundation for Statistical Computing, Vienna, Austria. <https://www.R-project.org/>.
- Rahaman, M.T., Gurung, D.B. & Pitol, M.N.S., 2020. Comparative Study of Understorey between Exotic Monoculture Plantation (*Acacia* Sp.) and Adjacent Natural Sal (*Shorea Robusta*) Forest. *European Journal of Agriculture and Food Sciences*, 2(6), pp.1-9 doi: 10.24018/ejfood.2020.2.6.204
- Rahman, M.R., Hossain, M.K. & Hossain, M.A., 2019. Diversity and composition of tree species in Madhupur national park, tangail, Bangladesh. *Journal of forest and environmental science*, 35(3), pp.159-172. doi: 10.7747/JFES.2019.35.3.159
- Rahman, M., Nishat, A. & Vacik, H., 2009. Anthropogenic disturbances and plant diversity of the Madhupur Sal forests (*Shorea robusta* C.F. Gaertn) of Bangladesh. *International Journal of Biodiversity Science & Management*, 5, pp.162-173. doi: 10.1080/17451590903236741
- Rahman, M.R. et al., 2017. Floristic composition of Madhupur National Park (MNP), Tangail, Bangladesh. *Bangladesh Agriculture*, 7(10), pp.27-45.
- Rivest, D. et al., 2009. Production of soybean associated with different hybrid poplar clones in a tree-based intercropping system in southwestern Québec, Canada. *Agriculture, ecosystems & environment*, 131, pp.51-60. doi: 10.1016/j.agee.2008.08.011
- Safa, M.S., 2004. The effect of participatory forest management on the livelihood and poverty of settlers in a rehabilitation program of degraded forest in Bangladesh. *Small-scale Forest Economics, Management and Policy*, 3, pp.223-238. doi: 10.1007/s11842-004-0016-z
- Schleppi, P. et al., 2007. Correcting non-linearity and slope effects in the estimation of the leaf area index of forests from hemispherical photographs. *Agricultural and Forest Meteorology*, 144(3-4), pp.236-242. doi: 10.1016/j.agrformet.2007.02.004

- Schroth, G. and da Mota, M.D.S.S., 2013. Technical and institutional innovation in agroforestry for protected areas management in the Brazilian Amazon: opportunities and limitations. *Environmental management*, 52(2), pp.427-440. doi: 10.1007/s00267-013-0049-1
- Sharma, M. et al., 2019. Morphological anomaly in *Shorea robusta* Gaertn. Seeds in Uttarakhand, India. *Indian Forester*, 145(5), pp.492-493. doi: 10.36808/if/2019/v145i5/145690
- Sinoquet, H. et al., 2007. Simple equations to estimate light interception by isolated trees from canopy structure features: assessment with three-dimensional digitized apple trees. *New Phytologist*, 175(1), pp.94-106. doi: 10.1111/j.1469-8137.2007.02088.x
- Suwa, R., 2011. Canopy photosynthesis in a mangrove considering vertical changes in light-extinction coefficients for leaves and woody organs. *J. For. Res.*, 16(1), pp.26-34. doi: 10.1007/s10310-010-0203-z
- Tilman, D. et al., 2001. Forecasting agriculturally driven global environmental change. *Science*, 292(5515), pp.281-284. doi: 10.1126/science.1057544
- Trápani, N. et al., 1992. Ontogenetic changes in radiation use efficiency of sunflower (*Helianthus annuus* L.) crops. *Field Crops Research*, 29(4), pp.301-316. doi: 10.1016/0378-4290(92)90032-5
- Udawatta, R.P. et al., 2008. Agroforestry and grass buffer effects on pore characteristics measured by high-resolution x-ray computed tomography. *Soil Science Society of America Journal*, 72(2), pp.295-304. doi: 10.2136/sssaj2007.0057
- Uddin, M.S., Pitol, M.N.S. & Feroz, S.M., 2021. Floristic composition and woody species diversity in national park of Madhupur tract under Tangail north forest division, Bangladesh. *Journal of Forests*, 8(1), pp.99-108. doi: 10.18488/journal.101.2021.81.99.108
- Wang, Y. & Jarvis, P., 1990. Influence of crown structural properties on PAR absorption, photosynthesis, and transpiration in Sitka spruce: application of a model (MAESTRO). *Tree physiology*, 7, pp.297-316. doi: 10.1093/treephys/7.1-2-3-4.297
- Wang, Z. et al., 2015. Radiation interception and utilization by wheat/maize strip intercropping systems. *Agric. For. Meteorol.*, 204, pp.58-66. doi:10.1016/j.agrformet.2015.02.004
- Whiting, D., 2011. Plant growth factors: light. *CMG Garden notes 142*, pp.1-4. <https://cmg.extension.colostate.edu/Gardennotes/142.pdf>
- Willson, K., 1999. Coffee, cocoa and tea. CAB International. <https://www.cabdirect.org/cabdirect/abstract/19990303788>
- Zanne, A.E. et al., 2009. Data from: Towards a worldwide wood economics spectrum. Dryad Data Repository.

Research Article

The Status, Trends, and Limitations of Philippine Mollusk Production and Trade Based on Available Databases and Publications

John Alberto H. Ordinario^{1,2*}, Jonathan A. Anticamara¹

1)UP Diliman Invertebrate Museum, Institute of Biology, National Science Complex, University of the Philippines-Diliman, Diliman, Quezon City, Philippines 1101

2)Institute of Environmental Science and Meteorology, University of the Philippines, 1101 Quezon City, Philippines

* Corresponding author, email: albertoordinario@gmail.com

Keywords:

mollusk fishery
molluscan management
mollusk trade
shell industry

Submitted:

28 February 2022

Accepted:

11 May 2023

Published:

18 September 2023

Editor:

Miftahul Ilmi

ABSTRACT

Mollusk trade is vital in many coastal areas and island communities throughout the Philippines because it provides livelihoods, food, and incomes to millions of Filipinos via fisheries (e.g., shellfish fishing and gleaning), shell craft, arts, shell trading and collections, and aquaculture. However, the assessments of the national trends and status of mollusc production and trade in the Philippines are largely non-existent in peer-reviewed literature. The main purpose of this paper is to present and evaluate the status and trends of traded Mollusks in the Philippines based on available online databases and a systematic review of published literature. To date, available databases on Philippine mollusk trade showed an initial increase in traded volume (the 1970s to 2006), but decreased afterward. In contrast, the traded mollusk value continued to generally increase over time (albeit the observed decrease between 2011 and 2016), indicating value increase as mollusk volume decreased. However, there is a great need to (1) resolve many of the obvious inconsistencies in data entries across all the available mollusk trade databases (BFAR, PSA, and CITES) and (2) provide field assessment of the Philippine mollusk trade and the conservation status of all traded mollusk taxa in the country.

Copyright: © 2023, J. Tropical Biodiversity Biotechnology (CC BY-SA 4.0)

INTRODUCTION

The trade of aquatic products such as mollusks can significantly contribute to the economic development of the country (Kartika 2014; Jing et al. 2018; Mohsin et al. 2017). In 2018, the global contribution of mollusks and other aquatic invertebrates was around 12% in fish trade in terms of value (FAO 2020). These include Cephalopods, Bivalves, and other shelled mollusks. China is the leading producer with 14.4 million Metric Tons (MT) of the 2018 marine and coastal aquaculture of mollusks and the Philippines ranked 14th with 55,000 MT (FAO 2020). Mollusk trade is very important in many coastal areas and island communities throughout the Philippines. It provides livelihoods, food, and incomes to millions of Filipinos via fisheries (e.g., shellfish fishing and gleaning), shell craft and arts, shell trading and collections, and aquaculture (Salamanca & Pajaro 1996; Salayo 2000; Floren 2003; De Guzman et al. 2020). However, the assessments of the national trends and status of Philippine mollusk production and trade are largely non-existent in peer-reviewed literature.

To date, few outdated and limited scopes of assessment have evalu-

ated the mollusk trade in the Philippines, and they all indicated that this industry is largely ignored in terms of scientific assessments. The International Trade Patterns and Trade Policies in the Philippine Fisheries by Salayo (2000) provided recent accounts of Philippine mollusk trade, albeit over two decades old (Salayo 2000). However, this analysis is aggregated and mixed with crustaceans, making it difficult to accurately assess the status and trend of mollusks trade in the Philippines. Floren (2003) analysed the shell trade industry, but was limited to analyses of Cebu, Philippines data from 1985 to 2002. Moreover, he reported that the shell industry is a significant income earner, but there is a decline in the export volume of shelled mollusks due to the low supply, highlighting the concern of insufficient biological data of the species harvested and poor management. Besides shelled mollusks, there is also a decline in octopus harvests and exports in the Philippines, although catch per unit effort data and population stock analyses for octopuses are largely unknown in the Philippines (Monterey Bay Aquarium 2017). The declining volume of exports and incomplete assessment of the mollusk trade show a strong need to assess the mollusk trade systematically and comprehensively.

A systematic compilation of published literature on mollusk trade was done using SCOPUS to assess the published trends and gaps in mollusk production and trade globally and in the Philippines. A total of 196 papers were reviewed, but few (12 publications) appeared relevant to this paper. Unfortunately, even for the 12 publications, the values were incomparable to the data and analyses provided in this paper. We, nonetheless, used the insights from these 12 publications in our discussion of key results.

Although databases on the national mollusk trade exist, they remained un-evaluated in terms of the status and trends of the trade and the quality of the datasets available in online national and international databases. The main purpose of this paper is to present and evaluate the status, trends, and limitations of traded mollusks in the Philippines based on available online databases. Here, we ask the following questions: (1) What are the status and trends of mollusk trade based on the Bureau of Fisheries and Aquatic Resources (BFAR) annual reporting; (2) What are the status and trends of mollusk trade based on Philippine Statistics Authority (PSA) data; (3) What are the status and trends of Philippine mollusk trade based on the Convention on International Trade in Endangered Species of Wild Flora and Fauna (CITES); and (4) How limited are available information on the status and trends of mollusk Trade based on published literature compared to our analyses.

MATERIALS AND METHODS

Data Compilation

To assess the mollusk trade in the Philippines, three online databases and published literature were compiled, processed, and analysed.

The first dataset compiled was from the Bureau of Fisheries and Aquatic Resources (BFAR) Annual Fisheries Report from 1977 to 2018 (accessible at <https://www.bfar.da.gov.ph/publication>, accessed 25 May 2020). The BFAR Annual Reports presented annual Fisheries data for the entire country by Sector and Region (e.g., Marine Fisheries, Inland Fisheries, and Aquaculture) (Anticamara & Go 2016). However, the BFAR Annual Report for mollusks only provides the National Total Volume (Metric Ton MT) and Value (Philippine Pesos PHP) without regional breakdown. The BFAR dataset reported different types of mollusk products grouped as follows: (1) Shells and Articles: Shells and By-products, Ornamental Shells, and Shell craft Article. (2) Bivalves: Scallops, Clams, Capiz Shells, and Pearls. (3) Gastropods: Abalone Shells. (4)

Cephalopods: Octopus and Cuttlefish. To date, all BFAR reports and analyses focused only on the annual production or short-term (2-3 years) trend analyses. There are no peer-reviewed publications or scientific analyses that have been done on Philippine mollusk production and trade over the past decades. However, there were two reports on the shell industry in the Philippines, but these mainly focused on Cebu and Zamboanga mollusk trade (Salamanca & Pajaro 1996; Floren 2003).

The second database was accessed from the Philippine Statistics Authority (PSA) 1977 to 2015 Foreign Trade Statistics (FTS) of the Philippines (<https://psa.gov.ph/content/foreign-trade-statistics-fts-philippines>, accessed 25 May 2020). The PSA process and publish all the product trade information in the Philippines containing the volume (Kilograms kg) and value (Philippine Pesos PHP and US dollars USD) of mollusk products. In connection with BFAR, both local institutions produce data for mollusk products, but the BFAR data mainly focuses on Fisheries and Aquatic Resources (seaweed, fish, mollusks, squids). Meanwhile, PSA represents the whole foreign and local trade product industry in the Philippines. The PSA dataset was used to check the consistency of trends of the BFAR because of its data similarity. The dataset from PSA provided different mollusk products, but was grouped the same way as the BFAR dataset: Shells and Articles, Bivalves, Gastropods, and Cephalopods.

The third database analysed was taken from the CITES. The data obtained was from 1983 to 2018 CITES Philippine trade database (<https://trade.cites.org>, accessed 25 May 2020). CITES is a non-government organization with a multilateral treaty that protects the survival of plants and animals. It provides an online international database that records and regulates the trade of plants and animals. It presents the trading countries, quantity, purpose, and mollusk taxa traded – i.e., exported from and imported into the Philippines.

Lastly, we systematically compiled published literature on mollusk trade using SCOPUS to assess the published trends and gaps in mollusk trade globally and in the Philippines. We compiled and organized the published literature by compiling the following: (1) Country/Countries where the study was conducted, (2) objectives of the study or their major questions, (3) the methods used to answer the questions, (4) the key findings in terms of mollusk production and trade per unit area and time, by taxa or broader categorizations (e.g., shells and articles), and (5) the major knowledge gaps identified by the paper.

Data Analysis

To show the status and trends of Mollusk Trade of BFAR annual reports over time, the following were performed: (1) We computed the total mean over time of each category of Volume and Values; (2) then plotted the annual time series of the total exported Volume (Metric Ton MT) and Value (Philippine Pesos PHP, with USD conversions; conversion rate was 49.45 PHP = 1 USD as of 10 July 2020); (3) We then presented the Mean traded Volume and Values (\pm standard error SE) to show the magnitude changes over time; (4) Lastly, we presented a time series of mollusk Volume and Values by Categories with Standard Error (i.e., Cephalopods, Shells and Articles, Bivalves, and Gastropods).

The PSA dataset were also analysed to show the status and trends of the mollusk trade in the Philippines. Before plotting the data, the volume data from PSA was converted from kg to MT (1 kg = 0.001 MT) to match the units with the BFAR dataset. The total volume, value, and categories were analysed using the same framework analysis implemented with the BFAR dataset.

The CITES dataset primarily focused on the trend of mollusk production and trade in the Philippines. Based on the different reported unit of measurement from the database, the unit with the least data gaps was the number of individuals or pieces. Using the CITES database, the following were done: (1) annual amount of trade per country was plotted; (2) mean average of each country every five years was computed from the total sum of each country; and (3) we then presented a series of world maps indicating the volume traded over time.

To assess the conservation status and list of species traded in the Philippines, a list of species was obtained from the CITES database, then checked for their conservation status using the IUCN online website (<https://www.iucnredlist.org/>).

To systematically evaluate the published peer-reviewed journals on mollusk production and trade, the keywords ‘Mollusk + Trade’ were used in the Scopus search (www.scopus.com; 26 June 2020). We only focused on studies assessing the trends and gaps in mollusk production and trade. As a result, there were 196 publications, and each was reviewed to find if there is information on mollusk production and trade (such as Geographical Scale-Global/National/Local, Temporal Scale-Years Covered, Species/Taxa Traded, Volume, and Value of Trade). Only 12 publications contained the information needed as specified above. However, the 12 publications are not comparable to our analyses, but we used the information in our discussion of key results.

RESULTS AND DISCUSSION

Status and Trends of Mollusk Trade Based on BFAR and PSA Data

Mollusk Trade Volume

Based on the BFAR Annual Fisheries Report, the trend of mollusk trade from BFAR showed an overall increasing trend. The mean annual exported mollusk volume increased from 1986 to 2006, then decreased until 2016, followed by an increase until 2018 (Figure 1). We used mean annual volume for every five years because annual volume shows a fluctuating pattern (Figure A1). The lowest export volume was in 1986 with 4,237 MT. Its peak was in 2006 with 18,526 MT. (Figure 1; Appendix A1). Afterward, the average export volume decreased from 2007 until 2016 from 14,716 MT to 12,716 MT. Followed by an increase in 2018 with 17,692 MT.

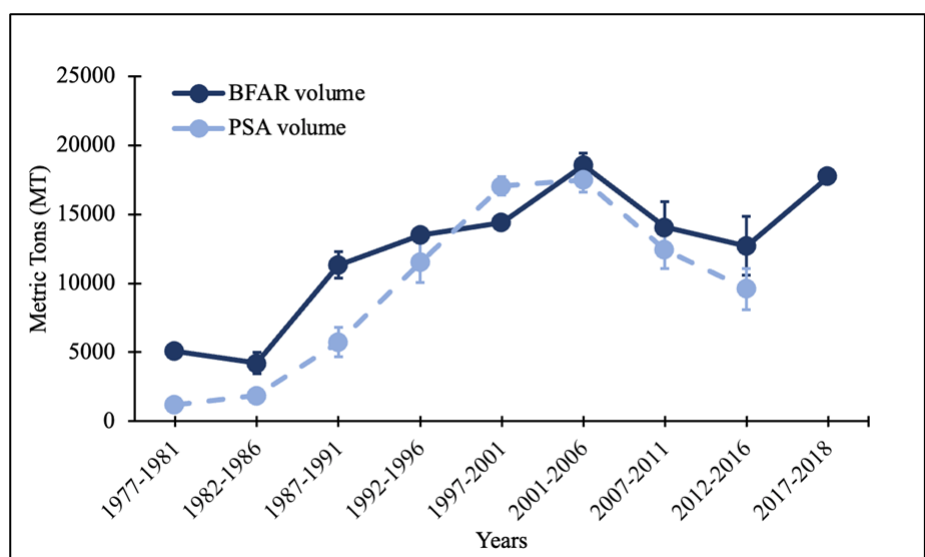


Figure 1. Mean annual volume for every five years of mollusk export trade in the Philippines from 1977 to 2018 based on the BFAR annual Fisheries Report and PSA Foreign Trade Statistics.

In comparison, the PSA Foreign Trade showed a similar trend. The average annual exported volume increased from 1977 until 2006, then decreased afterward. The lowest export volume was in 1977 with 1,205 MT. Its peak was in 2006 with 17,494 MT (Figure 1; Appendix B1).

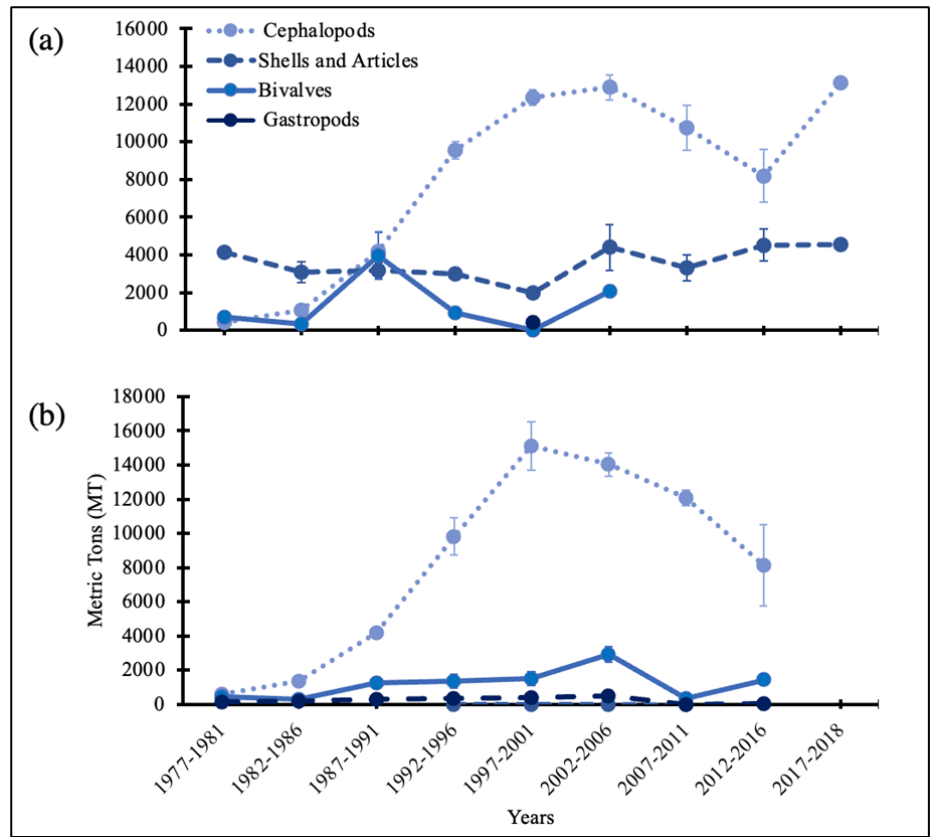


Figure 2. Mean annual volume for every five years of each group on mollusk export trade in the Philippines. Dataset is from (a) 1977 to 2018 BFAR Annual Fisheries Report and (b) 1977 to 2015 PSA Foreign Trade Statistics.

Among the mollusk products that were specified or categorized, the BFAR database indicates that Cephalopods export volume trade increased from 1977 to 2006, but continually decreased from 2007 until 2016, followed by an increase in 2018 (Figure 2a; Appendix A2). Cephalopods were the highest contributor to the Philippine mollusk export trade, with a total volume of 332,978 MT by 2018 (Appendix A3). Shells and Articles initially decreased from 1977 to 2001, followed by an increase in 2006. After 2011 the Shells and Articles trade stabilized until 2018. The total Shell and Article export volume was 147,216 MT by 2018 (Appendix A3). The volume trade of Bivalves fluctuated from 1977 to 2006, having a total volume export of 34,011 MT by 2005. Gastropods were only reported in 1998, with a total amount of 416 MT.

The categorized mollusk products in the PSA database show that the volume from Cephalopods increased from 1977 until 2006, but decreased afterward from 2006 until 2015 (Figure 2b; Appendix B2). Cephalopods are the highest contributor in volume trade, with 318,648 MT by 2015 (Appendix B3). Bivalves continuously increased from 1982 until 2006, then decreased in 2011, followed by an increase in 2015. Bivalves were the second-highest contributor, with a total volume of 46,554 MT. Meanwhile, Gastropods remained unchanged from 1977 to 2015. It is ranked third with 9,770 MT by 2015. Shells and Articles export volume slightly increased from 1992 to 2006. The data reports for Shell and Article were only from 1996 until 2010, with a total volume trade of 68 MT, making it the lowest contributor.

Mollusk Trade Value

In the BFAR database, the average export value trade of mollusks increased from 1977 to 2006, but it decreased from 2006 until 2016, followed by an increase until 2018 (Figure 3). In 1977, the average export value was 115 million PHP (2.33 million USD), which was its lowest value recorded, and then it continuously increased in 2006 to 2.95 billion PHP (59.7 million USD) (Figure 3; Appendix A1). However, after 2007, the value decreased to 1.77 billion PHP (35.8 million USD), then it increased again in 2018 with 3.4 billion PHP (68.9 million USD), its highest peak mean value (Figure 3; Appendix A1).

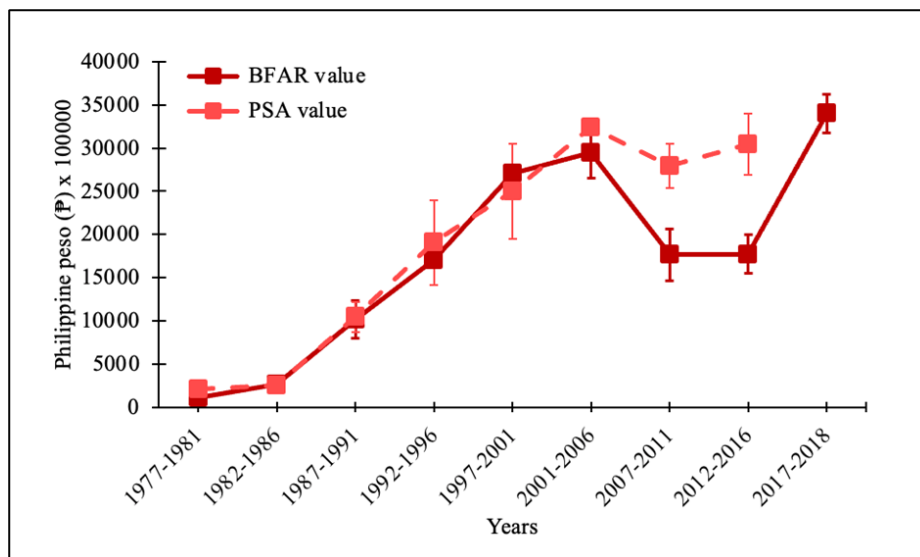


Figure 3. Mean annual value for every five years of mollusk export trade in the Philippines from 1977 to 2018 based on the BFAR annual Fisheries Report and PSA Foreign Trade Statistics.

In comparison, the PSA mean export value increased from 1977 to 2006 and then decreased from 2006 until 2010, followed by an increase until 2015 (Figure 3). In 1977, it reached its lowest value trade of 215 million PHP (4.36 million USD), then it increased to 3.24 billion PHP (65.6 million USD) in 2006 (Figure 3; Appendix B1). Afterward, the value decreased from 2007 to 2011 to 2.79 billion PHP (56.5 million USD), but it again increased to 3.04 billion PHP (61.5 million USD) by 2015, its highest peak mean value.

The categorized mollusk products in BFAR show that the trend of the average value export trade on Cephalopods increased from 1977 to 2006, then decreased from 2007 to 2016, and was followed by an increase in 2018 (Figure 4a). The total Cephalopod trade value from 1977 to 2018 reached around 44.7 billion PHP (904.3 million USD) (Appendix A5). The Shells and Articles trade value initially increased from 1977 to 2005, but decreased from 2006 until 2015 (Figure 4a). The Shells and Articles export value yielded an amount of 16.6 billion PHP (335.2 million USD) by 2018 (Appendix A5). The average trade value of Bivalves initially increased from 1977 to 1986, then slightly decreased in 1996. Afterward, it continuously increases from 1987 to 2006 with a total value of 6 billion PHP (120.3 million USD) (Figure 4a; Appendix A5). The Gastropods reported an export value of 139 million PHP (2.81 million USD) in 1998 (Appendix A5).

In contrast, the PSA dataset shows that the Cephalopod trade value increased from 1977 to 2007, then decreased from 2007 to 2015 (Figure 4b). In the PSA dataset, Cephalopods were the highest contributor for value trading, with a total amount of 48 billion PHP (970.4 million USD)

by 2015 (Appendix B5). The Bivalve export value decreased from 1977 to 1986, but continuously increased from 1987 until 2006, then stabilized afterwards. Yielding a total export value of 21.4 billion PHP (970 million USD) by 2015 (Figure 4b; Appendix B5). Gastropods remained unchanged from 1977 until 2015, with a total value of 2.6 billion PHP (51.7 million USD) by 2015. Lastly, the Shells and Articles export value also remained unchanged from 1996 to 2010, with a total value of 24 million PHP (489.6 USD) by 2010 (Figure 4b; Appendix B5).

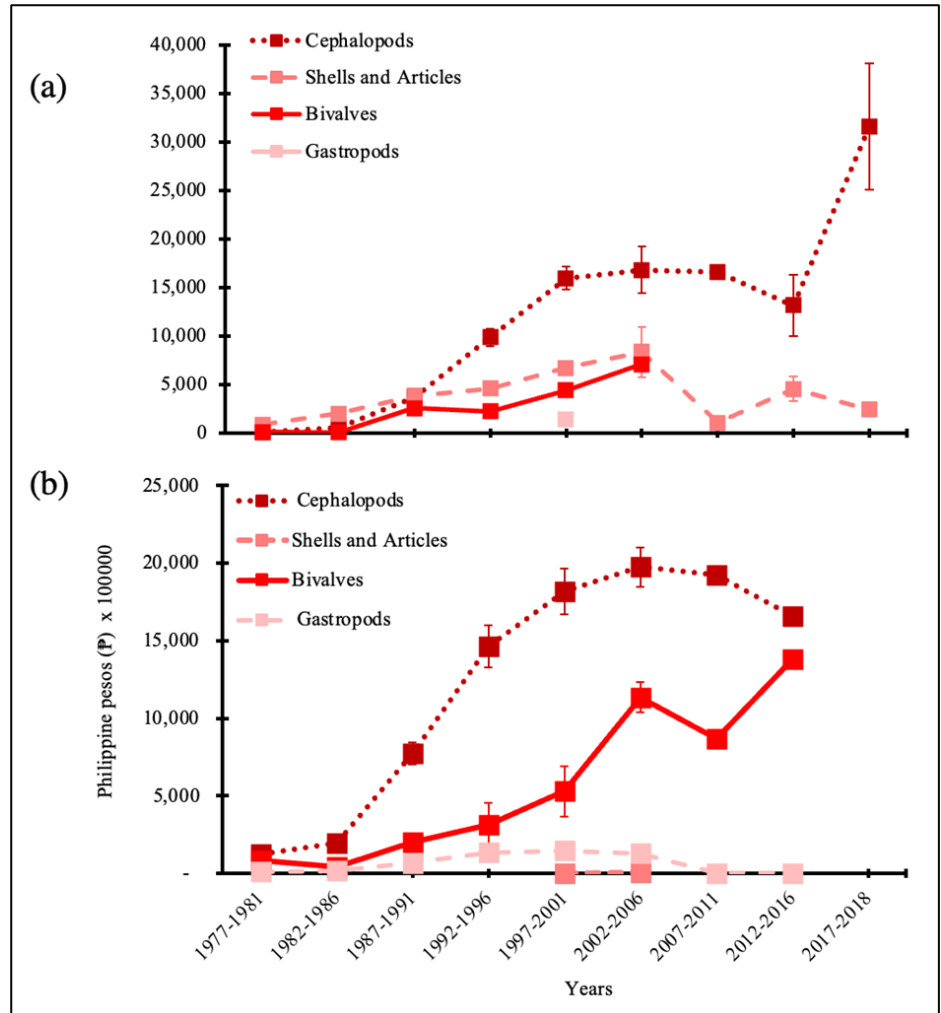


Figure 4. Mean annual value for every five years of each group on mollusk export trade in the Philippines. Dataset is from (a) 1977 to 2018 BFAR Annual Fisheries Report and (b) 1977 to 2015 PSA Foreign Trade Statistics.

Status and Trends of Mollusk Trade based on CITES data.

Based on the CITES dataset, export countries and the pieces of Philippine mollusk exported to them increased from 1984 to 1987 and continuously decreased from 1988 to 2003, but then stabilized afterward (Figure 5). In the CITES dataset, the Philippines recorded its highest amount of mollusk exported in 1989, with 26,788 pieces, while the lowest was in 2009, with 102 pieces (Appendix C1). In 1989, the Philippines exported mollusk to 31 countries - the highest mean mollusk exported was to the United States of America (USA) with 357,388 pieces, while the lowest was to Thailand with 16 Pieces (Figure 5a; Table S1). In 2009, the Philippines exported mollusk to seven countries, with the highest amount sent to Malaysia with 500 Pieces, while the lowest was sent to the Republic of Korea with four Pieces (Figure 5f; Table S1). Due to the small coverage of the country, the colour highlighted may not be observed in the figures presented (Figure 5-6).



Figure 5. Series of maps showing the amount of export trade per Piece for every five years from 1984-2018 CITES Database. The standardized amount per time frame is 0 to 376,095. (a) 1984-1988, (b) 1994-1998, (c) 1999-2003, (d) 2004-2008, (e) 2004-2008, (f) 2009-2013, and (g) 2014-2018.

Meanwhile, the number of countries where the Philippines imported mollusk (and the volume of imports) increased from 1984 until 1998, but decreased from 1999 until 2013, followed by an increase on its way to 2018 (Figure 6). The highest total amount of mollusk imported by the Philippines was in 2004, with 16,181 Pieces, while the lowest was in 2009, with two Pieces (Appendix B2). A total of two countries served as the major source of Philippine mollusk import: the USA, with 17,362 Pieces imported by the Philippines, while the lowest was Nicaragua, with 15,000 Pieces imported by the Philippines (Figure 6c; Table S2). In 2009, the Philippines imported mollusk from two countries: the USA and Palau imported two Pieces each (Figure 6f; Table S2).

The CITES dataset were provided the species name of the traded mollusk. Based on the list of taxa obtained from the CITES dataset, a total of 17 species were reported for the Philippine mollusk trade. Most species belong to Bivalves, with 12 species, while the lowest was from Gastropods, with two species. Meanwhile, the conservation status of the taxa reported seven species as Not Assessed, while two species each are Critically Endangered and Vulnerable (Table 1).

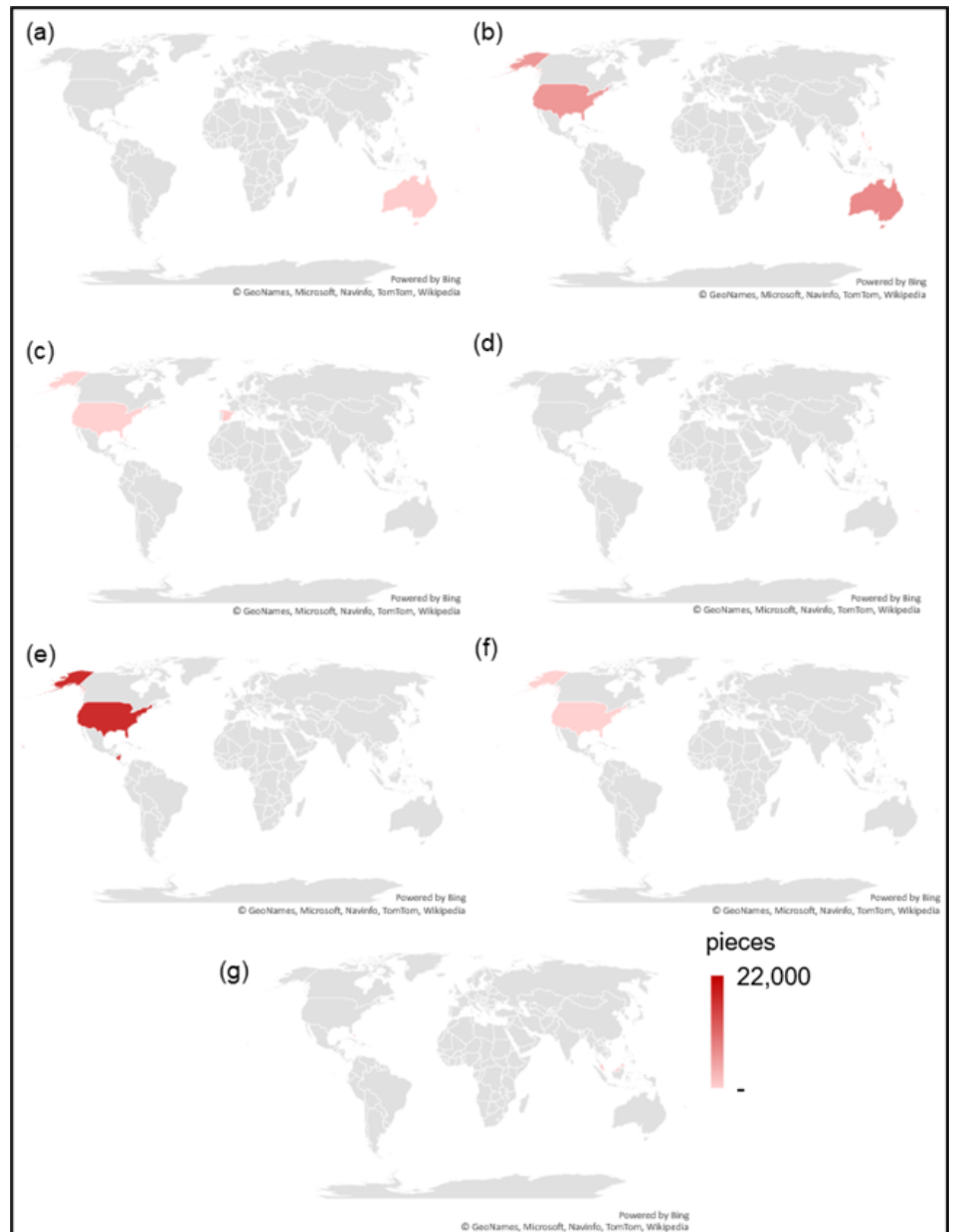


Figure 6. Series of maps showing the volume of mollusk import trade per Piece for every five years from 1984–2018 CITES database. The standardized range of volume per Piece for all time frames is between 0 to 22,000. (a) 1984–1988, (b) 1989–1993, (c) 1994–1998, (d) 1999–2003, (e) 2004–2008, (f) 2009–2013, and (g) 2014–2018.

Volume of Philippine Mollusk trade

The BFAR and PSA database general trend of mollusk trade volume in the Philippines is either stabilizing or declining. The initial increase followed by a decline in mollusk volume exported has a similar pattern to the findings of the Philippine fisheries reports (Salayo 2000; Floren 2003; Anticamara & Go 2016). Although, this is not entirely comparable since they do not have the same scale and variables used in this study. The general trend is most likely true since the Philippines has poor enforcement of fisheries management against overfishing and destructive fishing practices that have led to the fishery species decrease (Alcala & Russ 2002; Muallil et al. 2014). Gleaning of invertebrates in the shallow reef flats is a common activity by women and children living in the coastal area (Ciasico et al. 2008). The Philippines is an archipelagic country with thousands of islands that can provide aid in household income and food (De Guzman et al. 2020). However, gleaning can be destructive and cause environmental impacts. Ciasico (2008) reported that despite the concern-

Table 1. Conservation status of species on Mollusk Traded from the Philippines based on CITES database from 1984–2018.

Species	IUCN status
Bivalves	
<i>Dromus dromas</i> (I. Lea, 1834)	Critically endangered
<i>Epioblasma rangiana</i> (I. Lea, 1838)	Critically endangered
<i>Hippopus hippopus</i> (Linnaeus, 1758)	Lower Risk, conservation dependent
<i>Hippopus</i> spp.	Not assessed
<i>Lampsilis brevicula</i> (I. Lea, 1852)	Near Threatened
<i>Tridacna crocea</i> (Lamarck, 1819)	Least Concerned
<i>Tridacna derasa</i> (Röding, 1798)	Vulnerable
<i>Tridacna gigas</i> (Linnaeus, 1758)	Vulnerable
<i>Tridacna maxima</i> (Röding, 1798)	Lower Risk, conservation dependent
<i>Tridacna</i> spp.	Not assessed
<i>Tridacna squamosa</i> (Lamarck, 1819)	Lower Risk, conservation dependent
<i>Tridacnidae</i> spp.	Not assessed
Gastropods	
<i>Haliotis midae</i> (Linnaeus, 1758)	Not assessed
<i>Strombus gigas</i> (Linnaeus, 1758)	Not assessed
Cephalopods	
<i>Nautilidae</i> spp.	Not assessed
<i>Nautilus pompilius</i> (Linnaeus, 1758)	Not assessed
<i>Nautilus</i> spp.	Not assessed

ing extraction of Conch in Eastern Samar, there are no regulations existing for the conservation of resources. A decline in populations of mollusks in their area occurs when there is unsustainable management, no control in fishing, and overfishing (Galeana-Rebolledo et al. 2018; Alati et al. 2020). Unregulated harvesting of invertebrates leads to a sharp decline in abundance over a relatively short period because the maximum sustainable yield exceeds the time for mollusks to recover (Fröcklin et al. 2014).

The databases used in this study do not entirely reflect the same trends and magnitudes. The volume reported between PSA and BFAR showed a similar trends, but with slight differences. Floren (2003) discovered that the BFAR data for Shell and shell by-products in Cebu, Philippines is not reflective of the reports from PSA (Floren 2003). The highest volume exported of mollusk products in the Philippines was from 2001 to 2005, with 17,710 MT in BFAR database and 17,923 MT in the PSA database (Table 2). In the global context, FAO (2020) reported that mollusk production via aquaculture continuously increased from 4 million MT in 1990 to 17.7 million MT in 2018, but with reports of slow increase and decrease of supply from other countries (FAO 2020). The highest producer is China with 14.4 million MT, and the Philippines ranked at 14 with 55,000 MT of world marine and coastal aquaculture of mollusks by major producers in 2018 (FAO 2020). It is far off from our findings since the volume of mollusk exported of BFAR in 2018 was 15,699 MT, and PSA no data for 2018 (Table 2). On the other hand, CITES volume data used Pieces as their measurement for volume trade. This limitation has led to CITES data being incomparable to other databases. Although, the CITES data import and export volume per Piece showed a fluctuating pattern, which is not reflective of the BFAR and PSA trend pattern. The CITES database shows sudden declines of 26,788 Pieces of mollusks to 2 pieces. This pattern can be a result of inconsistency and unreported trade data. The Philippines needs to consolidate CITES records of animal trade in the Philippines and the local institu-

Table 2. Comparison of volume (Metric Tons / MT) export from BFAR and PSA database showing the mean volume with \pm Standard Deviation from 1977 until 2018. (-) no available data.

Year	BFAR Export Volume	PSA Export Volume
1977-1981	5,074 \pm 331	1,209 \pm 197
1982-1986	4,237 \pm 772	1,889 \pm 322
1987-1991	11,328 \pm 960	5,737 \pm 1076
1992-1996	13,487 \pm 473	11,514 \pm 1445
1997-2001	14,406 \pm 446	17,055 \pm 685
2001-2006	18,526 \pm 901	17,494 \pm 888
2007-2011	14,074 \pm 1853	12,441 \pm 1382
2012-2016	12,716 \pm 2130	9,588 \pm 1477
2017-2018	17,692 \pm 280	-

tions (Cruz & Lagunzad 2021). Blundell and Mascia (2005) and Russo (2015) discovered that the CITES database in their country is unreliable because their findings show a high level of discrepancies and inaccuracy in the reported volume of wildlife trade (Blundell & Mascia 2005; Russo 2015; Robinson & Sinovas 2018). To better understand this issue, further investigation is needed in the future.

The top exported volume category were Cephalopods from both BFAR and PSA databases, with an initial increase then decrease in the recent years of Cephalopods exported. This trend is similar to the global and national analysis available. The global trend of Cephalopod catches declining since 2013, with the prices and volume increasing (Ospina-Alvarez et al. 2022). The trend pattern of Octopus trade in the Philippines in our analysis is very similar to the findings of Monterey Bay Aquarium (2017) indicating the decline of the trend over the past decades is due to the shortage of supply and smaller catch sizes for exportation (Monterey Bay Aquarium 2017). The growing global demand for Cephalopods in the market can significantly contribute to the income and food of families around the world (Monterey Bay Aquarium 2017; Ospina-Alvarez et al. 2022). Furthermore, most commercial cephalopod species are short-lived and quick to reproduce, making them a target for intensive harvesting, that if not carefully assessed and monitored can actually be unsustainable (Rodhouse et al. 2014; Clark 2019).

The lowest exported category was Gastropods in the BFAR database, while Shells and Articles were in the PSA database. Gastropods, Shells and Articles, and Bivalves are shelled mollusk has a lower export volume than Cephalopods. These groups of invertebrates are used for food, Shell craft, handicraft, ornaments, souvenirs, jewellery, and many more (Floren 2003; Alves et al. 2018). The shell industry involves about 5,000 species of Gastropods and Bivalves worldwide, with the Indo-Pacific region having the rarest and most beautiful shells (Dias et al. 2011). Floren (2003) reported 32 species of mollusks (Gastropods and Bivalves) involved in the Philippine Shell Industry (Floren 2003), with multiple reports of overharvesting of gastropods and bivalves in the Philippines (Floren 2003; Tabugo et al. 2013; Abarquez et al. 2019; Vito 2019). Most of the species reported are easily gleaned, which can contribute to the declining trend and low volume export.

Value of Philippine Mollusk trade

The value trade of exported mollusks in the Philippines from the BFAR and PSA database shows a general increase in time. This growth in value over the years can reflect inflation of food prices or an increase in price value due to scarcity of supply with increasing demand (Anticamara & Go 2016; Mohsin et al. 2017; Galeana-Rebolledo et al. 2018). Floren (2003) reported that when the supply for shells decreased, the prices of

Table 3. Comparison of value export in PHP from BFAR and PSA database showing the mean volume with \pm Standard Deviation from 1977 until 2018. (-) no available data.

Year	BFAR Export		PSA Export	
1977-1981	115,251,600	\pm 3,136,989	215,208,790	\pm 100,819,738
1982-1986	262,036,000	\pm 56,902,542	244,338,097	\pm 28,825,912
1987-1991	1,015,861,200	\pm 215,327,730	757,232,401	\pm 396,445,788
1992-1996	1,702,066,400	\pm 65,612,685	1,642,559,229	\pm 1,094,601,010
1997-2001	2,710,587,200	\pm 78,828,845	2,585,368,703	\pm 1,232,135,404
2001-2006	2,946,631,200	\pm 293,675,364	3,173,784,343	\pm 225,714,746
2007-2011	1,766,467,021	\pm 299,448,817	2,622,468,203	\pm 583,560,577
2012-2016	1,773,339,600	\pm 227,368,461	3,199,358,064	\pm 705,401,342
2017-2018	3,402,231,000	\pm 221,595,000	-	-

the shell increased over time. At the same time, the increase in prices can be attributed to the increase in fishing efforts (Anticamara & Go 2016). Fishers tend to spend more resources to harvest more, while fish stocks are decreasing. This entails, increase consumption of gas fuel, new fishing technology, and more time.

The BFAR and PSA database export value trade show slight differences in exported value, while CITES has no data available for traded value. In the global context, the 2020 State of world fisheries and aquaculture report of FAO indicates that the share in value of mollusk exported worldwide in 2018 is 12% with an amount of 34.6 billion USD (FAO 2020). The average peak value of mollusk exported in the Philippines was 3.10 billion PHP (62.8 million USD) from 2016 to 2018 in the BFAR database and 3.20 billion PHP from 2011 to 2015 (64.7 million USD) (Table 3). Our comparison is limited because we were not able to see the breakdown of value production of each country in the 2020 State of world fisheries and aquaculture report of FAO.

The highest value exported category is Cephalopods in both PSA and BFAR databases. Cephalopod industry is a multi-billion-dollar industry that the world participates in (Ospina-Alvarez et al. 2022). The high volume traded and increasing demand for Cephalopods products by the food community has made this the highest value exported mollusk category in the Philippines (Monterey Bay Aquarium 2017). Furthermore, Cephalopods such as squids are economically important in the Philippines, but highly susceptible to overfishing (Hernando & Flores 1981; Monterey Bay Aquarium 2017). Based on our findings, Cephalopod's export value generally continued to increase despite the decrease in volume.

The lowest exported value categories are Gastropods in the BFAR database and Shells and Articles in the PSA database. The explanation of the value trend for shelled mollusks is the same as previously mentioned. The shelled mollusks, such as gastropods and Shells and Articles have low value because of the low volume exported and low supply with reports indicating shelled mollusk populations are declining in the Philippines due to overharvesting and exploitation. These shelled mollusks are highly vulnerable to gleaners since gleaning is easily accessible in coastal areas in the Philippines and the weak enforcement of fishery management.

Caveats and ways forward

One of the caveats of this paper is the lack of taxonomic resolution of mollusk trade in the Philippines. The databases are fragmented and highly variable when categorizing and organizing mollusks trade data. There were no available data from BFAR and PSA showing the volume and value of traded mollusk species. Thus, making it difficult to properly assess and manage mollusk trade in the Philippines and their populations.

Moreover, a multispecies approach was used when recording the data on both BFAR and PSA databases, which was also observed in the assessment of Octopus trade assessment by [Monterey Bay Aquarium \(2017\)](#). The use of multiple species approach or lumping of multiple species in one common name or taxa has important consequences for the conservation status of the mollusks. One is that this can prevent consumers from making informed decisions whether the species is sustainably caught or overfished. Another consequence is that this can bring taxonomic confusion, making it difficult to determine the status of a concerned mollusk. This event of mislabelling and taxonomic confusion has brought the decline of population and risk of extinction to the European Common skate (*Dipturus batis*) ([Iglésias et al. 2010](#)). Hence the use of the scientific name is crucial to properly support the assessment of the conservation status of traded mollusk and reveal whether it is sustainable or not ([Logan et al. 2008](#)). Species-level identification of each mollusk traded enables us to understand the trend and magnitude of mollusks.

Another caveat is that the BFAR, PSA, and CITES data are presented at a highly aggregated level with no regional or local production volume and value information. This limitation inhibits us from accurately reflecting the true extent of mollusk declines in source fishing grounds and can mask the true declines ([Anticamara & Go 2016](#)). This challenge along with poor enforcement of fisheries management hinders us to distinguish the actual pattern of decline in local fishing and the source grounds (e.g., increase in fishing effort sustaining same production volume or serial depletion) ([Cardinale et al. 2011](#)). Furthermore, we also suspect that the current volume and value reported in BFAR and PSA data are underestimated. It does not reflect many other mollusk categories, considering that there is a wide range of mollusk being locally consumed and exploited in the Philippines ([Salamanca & Pajaro 1996](#); [Rodhouse et al. 2014](#); [del Norte-Campos et al. 2019](#)) and that some categories (e.g., Gastropods and Bivalves) only appeared in the reports in few periods and in recent times.

Lastly, the lack of available information about the fishing effort, catch information, and separation of production between local fishers and commercial fishers contributes to the obscurity of the true trends, magnitudes, and impacts of actual mollusk fisheries in the Philippines. This limitation is also observed by Monterey Aquarium when assessing the Cephalopod trade in the Philippines ([Monterey Bay Aquarium 2017](#)). This is the first paper that provides a comprehensive and systematic analysis of the mollusk trade. Other reports about the mollusk trade in the Philippines do not accurately represent the mollusk trade in the Philippines because it only represents a portion of the mollusk trade ([Salayo 2000](#); [Floren 2003](#); [Monterey Bay Aquarium 2017](#)). This paper can also be used for future detailed analyses of Philippine mollusk fisheries and trade. Therefore, we recommend field survey data to obtain the data from each region in the Philippines. This will allow us to better examine the trend of the populations of the species and verify if the decline of mollusk trade volume is due to overfishing. Furthermore, this will allow us to correlate the coastal community activities and population with the trend respective to its region. For example, where there is an increasing trend of mollusc population decline and tourism activity in the region, we can infer that this anthropogenic activity can affect the decline of mollusc species, and can investigate such case in details.

CONCLUSIONS

To date, available databases on Philippine mollusk trade showed an initial increase in traded volume (1970s to 2005), but indicated stagnantly

or decrease trends and magnitudes in recent decades. In contrast, the traded mollusk value generally continued to increase over time (albeit observed decreases from 2007 to 2016), indicating value increase as mollusk volume decreased. Alarmingly, we have observed that the databases used are inconsistent, highly variable, and incomplete. This limitation inhibited us from accurately assessing the true extent of the trend, magnitude, and impact of the mollusk trade in the Philippines. The BFAR and PSA database shows similar results, but have slight differences, while CITES was incomparable because the metric used in its recording was Pieces and not Metric Tons, unlike the BFAR and PSA database.

This is the first paper that provides a comprehensive and systematic assessment of the Philippine mollusk trade. We observed that there is a great need to resolve and field validate the inconsistencies in the data entries across all the available mollusk trade databases (BFAR, PSA, and CITES). Furthermore, we recommend that conducting a comprehensive field assessment is needed in improving our understanding of the Philippine Mollusk trade status, trends and conservation status. Such study can also improve the estimation and monitoring of the economic benefits that Filipinos derived from the mollusk trade.

AUTHOR CONTRIBUTION

This study was conducted and conceptualized by JA. He participated in data gathering, analysis, and write-up. JO did the data gathering, processing, analysis, and write-up.

ACKNOWLEDGMENT

We thank the Office of the Vice-Chancellor for Research and Development of the University of the Philippines (UP-OVCRD) for providing funds to conduct studies on mollusk fisheries of the Philippines via Source of Solutions Grant (SOS 181823).

CONFLICT OF INTEREST

The authors declare that the research was conducted in the absence of any commercial or financial relationships that could be construed as a potential conflict of interest.

ADDITIONAL INFORMATION

The mean volume of each country for CITES export and import dataset can be accessed as supplementary information (Table S1 & S2).

REFERENCES

- Abarquez, V., Mendez, N. & Galan, G., 2019. Preliminary study on diversity of intertidal gastropods in Barangay Day-asán, Surigao City, Philippines. *Ruhuna Journal of Science*, 10, pp.18–31. doi: 10.4038/rjs.v10i1.54.
- Alati et al., 2020. Mollusc shell fisheries in coastal Kenya: Local ecological knowledge reveals overfishing. *Ocean and Coastal Management*, 195, 105285. doi: 10.1016/j.ocecoaman.2020.105285.
- Alcala, A.C. & Russ, G.R., 2002. Status of Philippine Coral Reef Fisheries. *Asian Fisheries Science*, 15(2), pp.177–192.
- Alves, R., Mota, E. & Dias, T., 2018. Use and Commercialization of Animals as Decoration. In *Ethnozoology*. pp.261–275. doi: 10.1016/B978-0-12-809913-1.00014-4.

- Anticamara, J.A. & Go, K.T.B., 2016. Spatio-Temporal Declines in Philippine Fisheries and its Implications to Coastal Municipal Fishers' Catch and Income. *Frontiers in Marine Science*, 3, 21. doi: 10.3389/fmars.2016.00021.
- Blundell, A.G. & Mascia, M.B., 2005. Discrepancies in Reported Levels of International Wildlife Trade. *Conservation Biology*, 19(6), pp.2020–2025. doi: 10.1111/j.1523-1739.2005.00253.x.
- Bureau of Fisheries and Aquatic Resources (BFAR), 2018. 'Philippine Fisheries Profile 2018', viewed 25 May 2020, from <https://www.bfar.da.gov.ph/publication>.
- Cardinale, M., Nugroho, D. & Jonson, P., 2011. Serial depletion of fishing grounds in an unregulated, open access fishery. *Fisheries Research*, 108, pp.106–111. doi: 10.1016/j.fishres.2010.12.007.
- Ciasico et al., 2008. Initial stock assessment of four *Strombus* species [Mollusca: Gastropoda] in Eastern Samar (Central Philippines) with notes on their fishery. *The Philippine Scientist*, 43, pp.52-68. doi: 10.3860/psci.v43i0.371.
- Clark, C., 2019. *A Review of the Global Commercial Cephalopod Fishery, with a Focus on Apparent Expansion, Changing Environments, and Management*. Nova Southeastern University.
- Convention on International Trade in Endangered Species (CITES) of Wild Fauna and Flora, 2019. 'CITES Trade Database', viewed 25 May 2020, from <https://trade.cites.org/>.
- Cruz, R.A.L. & Lagunzad, C.G.B., 2021. The big picture: Consolidating national government and CITES records of animal trade in the Philippines from 1975 to 2019. *Philippine Science Letters*, 14, pp.79-100. <https://www.philsciletters.net/2021-79/>.
- De Guzman et al., 2020. Contribution of Gleaning Fisheries to Food Security and Nutrition of Poor Coastal Communities in the Philippines. *Journal of Environmental Science and Management*, SI-1, 58-71. doi: 10.47125/jesam/2019_sp1/06.
- Dias, T., Neto, N. & Alves, R., 2011. Molluscs in the marine curio and souvenir trade in NE Brazil: Species composition and implications for their conservation and management. *Biodiversity and Conservation*, 20, pp.2393–2405. doi: 10.1007/s10531-011-9991-5.
- Floren, A., 2003. The Philippine Shell Industry with Special Focus on Mactan, Cebu.
- Food and Agriculture Organization (FAO), 2020. The State of World Fisheries and Aquaculture 2020, FAO. doi: 10.4060/ca9229en.
- Fröcklin et al., 2014. Towards Improved Management of Tropical Invertebrate Fisheries: Including Time Series and Gender. *PLoS ONE*, 9 (3), e91161. doi: 10.1371/journal.pone.0091161.
- Galeana-Rebolledo et al., 2018. Socioeconomic Aspects for Coastal Mollusk Commercial Fishing in Costa Chica, Guerrero, México. *Natural Resources*, 9, pp.229–241. doi: 10.4236/nr.2018.96015.
- Hernando, A.M. & Flores, E.E.C., 1981. The Philippines Squid Fishery: A Review. *Marine Fisheries Review*, p.8.
- Iglésias, S.P., Toulhoat, L. & Sellos, D.Y., 2010. Taxonomic confusion and market mislabelling of threatened skates: important consequences for their conservation status. *Aquatic Conservation: Marine and Freshwater Ecosystems*, 20(3), pp.319–333. doi: <https://doi.org/10.1002/aqc.1083>.
- Jing, D., Mu, Y.T. & Mohsin, M., 2018. Evaluation of international competitiveness of China's marine mollusca trade. *Indian Journal of Geo-Marine Sciences*, 47(04), p.7.

- Kartika, S., 2014. A Study on Indonesian Mollusk Fishery and its Prospect for Economy. *International Journal of Marine Science*, 4. doi: 10.5376/ijms.2014.04.0005.
- Logan et al., 2008. An impediment to consumer choice: Overfished species are sold as Pacific red snapper. *Biological Conservation*, 141(6), 1591–1599. doi: 10.1016/j.biocon.2008.04.007 10.1016.
- Mohsin et al., 2017. Molluscan fisheries in Pakistan: Trends in capture production, utilization, and trade. *Indian Journal of Geo-Marine Sciences*, 46, 929–935.
- Monterey Bay Aquarium, 2017. ‘Common octopus and Big blue octopus’, in *Monterey Bay Aquarium Seafood Watch*, viewed 25 May 2020, from https://www.seafoodwatch.org/globalassets/sfw-data-blocks/reports/o/mba_seafoodwatch_big_blue_common_octopus_philippines.pdf.
- Muallil et al., 2014. Status, trends, and challenges in the sustainability of small-scale fisheries in the Philippines: Insights from FISHDA (Fishing Industries’ Support in Handling Decisions Application) model. *Marine Policy*, 44, pp.212–221. doi: 10.1016/j.marpol.2013.08.0
- del Norte-Campos, A., Burgos, L. & Villarta, K., 2019. A Ranked Inventory of Commercially-important Mollusks of Panay, West Central Philippines as a Guide to Prioritize Research. *The Philippine Journal of Fisheries*, 26(2), pp.119–136. doi: 10.31398/tpjf/26.2.2019-0004.
- Ospina-Alvarez et al., 2022. A network analysis of global cephalopod trade. *Sci Rep*, 12(1), 322. doi: 10.1038/s41598-021-03777-9.
- Philippine Statistics Authority, 2015. ‘Foreign Trade Statistics (FTS) of the Philippines 2015’, in *Foreign Trade Statistics (FTS) of the Philippines*, viewed 25 May 2020, <https://psa.gov.ph/content/foreign-trade-statistics-fts-philippines>
- Robinson, J.E. & Sinovas, P., 2018. Challenges of analyzing the global trade in CITES-listed wildlife. *Conservation Biology*, 32(5), pp.1203–1206. doi: 10.1111/cobi.13095.
- Rodhouse et al., 2014. Environmental Effects on Cephalopod Population Dynamics: Implications for Management of Fisheries. in EAG Vidal (ed.). *Advances in Cephalopod Science: Biology, Ecology, Cultivation and Fisheries. Advances in Marine Biology*, 67, pp.99–233. doi: 10.1016/B978-0-12-800287-2.00002-0.
- Russo, A., 2015. *The prevalence of documentation discrepancies in CITES (Convention on the International Trade in Endangered Species of Wild Fauna and Flora) trade data for Appendix I and II species exported out of Africa between the years 2003 and 2012*. University of Cape Town.
- Salamanca, A. & Pajaro, M., 1996. The utilization of seashells in the Philippines. *Traffic Bulletin*, 16, pp.61–72.
- Salayo, N.D., 2000. International Trade Patterns and Trade Policies in the Philippine Fisheries. p.44.
- Tabugo et al., 2013. Some economically important bivalves and gastropods found in the Island of Hadji Panglima Tahil, in the province of Sulu, Philippines. *International Research Journal of Biological Sciences*, 2(7), pp.30–36
- Vito, M., 2019. Diversity and abundance of economically important bivalves in north - western Bohol, Philippines. *Journal of Fisheries and Aquatic Science*, 6, pp.44–48.

APPENDICES

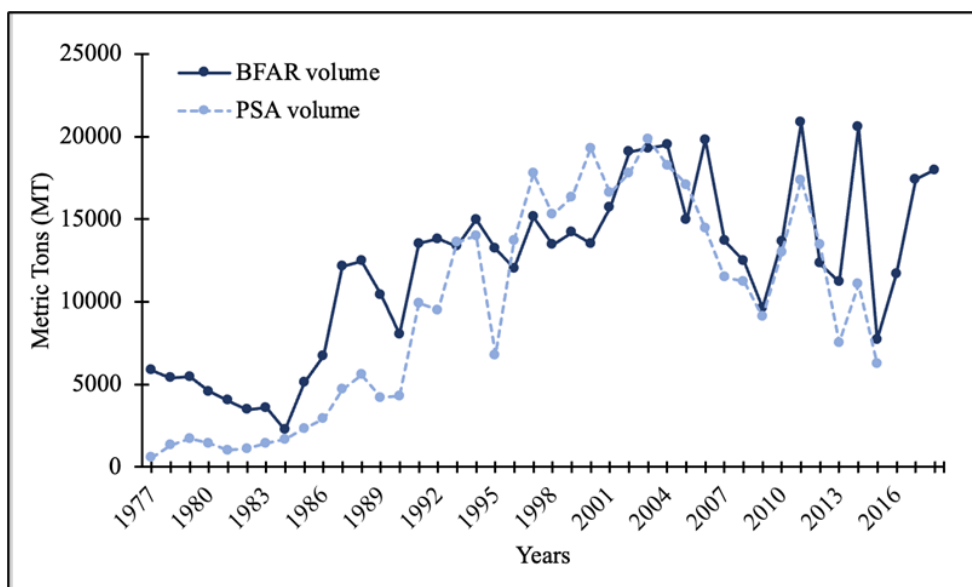


Figure A1. Time-series of total volume of mollusk trade in the Philippines from 1977 to 2018 from BFAR Annual Fisheries Report and PSA Foreign Trade Statistics.

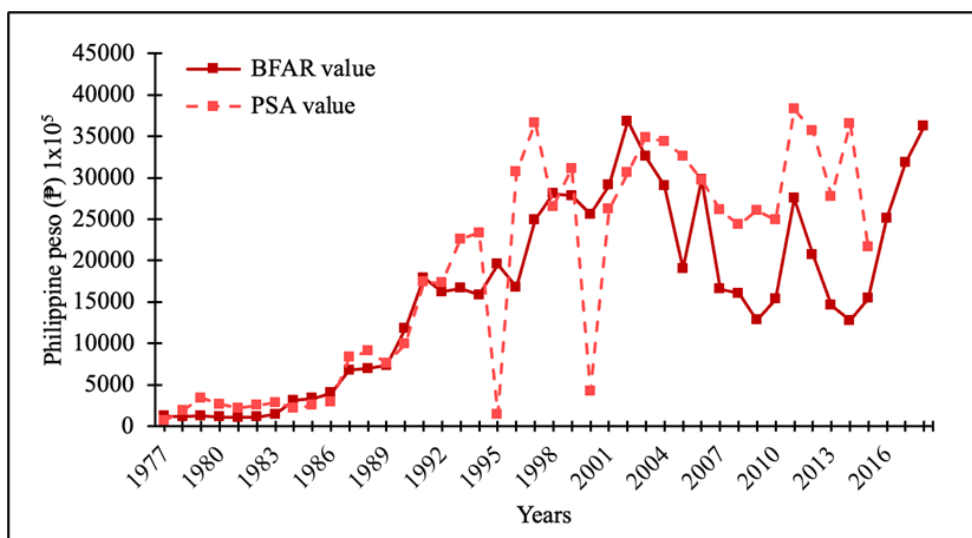


Figure A2. Time-series of total value of mollusk trade in the Philippines from 1977 to 2018 from BFAR Annual Fisheries Report and PSA Foreign Trade Statistics.

Appendix A1. Mean volume (Metric Tons= MT) and Mean Value (Philippine Pesos= PHP) of mollusk trade per five years showing the mean \pm Standard Deviation (SD) from 1977-2018 BFAR Fisheries Annual Report.

Year	Volume	Value
1977-191	5,074 \pm 331	115,251,600 \pm 3,136,989
1982-1986	4,237 \pm 772	262,036,000 \pm 56,902,542
1987-1991	11,328 \pm 960	1,015,861,200 \pm 215,327,730
1992-1996	13,487 \pm 473	1,702,066,400 \pm 65,612,685
1997-2001	14,406 \pm 446	2,710,587,200 \pm 78,828,845
2001-2006	18,526 \pm 901	2,946,631,200 \pm 293,675,364
2007-2011	14,074 \pm 1853	1,766,467,021 \pm 299,448,817
2012-2016	12,716 \pm 2130	1,773,339,600 \pm 227,368,461
2017-2018	17,692 \pm 280	3,402,231,000 \pm 221,595,000

Appendix A2. Mean volume (MT) of each group showing the mean \pm Standard Deviation (SD) from 1977-2018 BFAR Fisheries Annual Report. (-) means no data report.

Year	Shells and Articles		Bivalves		Cephalopods		Gastropods	
1977-1981	4,161	\pm 547	710	\pm 166	432	\pm 42	-	-
1982-1986	3,090	\pm 1,223	356	\pm -	1,075	\pm 626	-	-
1987-1991	3,167	\pm 954	3,978	\pm 2,759	4,182	\pm 2,374	-	-
1992-1996	2,985	\pm 745	942	\pm 458	9,560	\pm 1,059	-	-
1997-2001	1,969	\pm 261	1	\pm 0	12,353	\pm 939	416	\pm -
2002-2006	4,400	\pm 2,717	2,070	\pm 428	12,884	\pm 1,511	-	-
2007-2011	3,314	\pm 1,511	-	-	10,760	\pm 2,681	-	-
2012-2016	4,526	\pm 1,918	-	-	8,190	\pm 3,108	-	-
2017-2018	4,576	\pm 371	-	-	13,116	\pm 25	-	-

Appendix A3. Annual export volume of mollusk trade per category in the Philippines from 1977 to 2018 BFAR Annual Fisheries Report. (-) means no data report.

Year	Shells and Articles	Bivalves	Cephalopods	Gastropods
1977	5,015	845	-	-
1978	4,179	763	464	-
1979	4,242	764	470	-
1980	3,735	468	382	-
1981	3,632	-	411	-
1982	2,568	356	558	-
1983	2,804	-	786	-
1984	1,494	-	761	-
1985	3,982	-	1141	-
1986	4,603	-	2130	-
1987	3,747	5,523	2886	-
1988	2,228	7,096	3158	-
1989	2,163	5,043	3221	-
1990	4,341	480	3225	-
1991	3,357	1,750	8422	-
1992	4,141	1,585	8088	-
1993	2,818	1,189	9361	-
1994	3,250	900	10824	-
1995	2,387	537	10311	-
1996	2,329	498	9215	-
1997	2,226	-	12910	-
1998	1,978	-	11060	416
1999	1,765	1	12437	-
2000	1,654	2	11865	-
2001	2,223	1	13493	-
2002	2,714	2,123	14240	-
2003	3,224	1,618	14462	-
2004	5,478	2,469	11552	-
2005	1,933	-	13019	-
2006	8,650	-	11147	-
2007	3,554	-	10146.87	-
2008	2,430	-	10051	-
2009	1,552	-	8086	-
2010	3,449	-	10233	-
2011	5,587	-	15281	-
2012	3,622	-	8717	-
2013	5,273	-	5945	-
2014	7,388	-	13217	-
2015	2,308	-	5398	-
2016	4,041	-	7673	-
2017	4,314	-	13098	-
2018	4,838	-	13133	-
Total	147,216	34,011	322,978	416

Appendix A4. Mean value (₱) of each group showing the mean ± Standard Deviation (SD) from 1977-2018 BFAR Fisheries Annual Report. (-) means no data report.

Year	Shells and Articles		Bivalves	
1977-1981	90,414,250	± 5,180,783	15,900,250	± 2,511,799
1982-1986	164,089,600	± 75,234,482	10,696,000	± 0
1987-1991	336,458,000	± 138,508,564	198,983,000	± 138,990,284
1992-1996	487,785,600	± 52,058,498	300,899,400	± 124,897,024
1997-2001	622,762,600	± 115,625,365	351,804,000	± 46,610,858
2002-2006	696,944,200	± 581,153,731	631,695,750	± 236,173,291
2007-2011	346,324,083	± 59,087,522	-	-
2012-2016	306,718,600	± 284,181,040	-	-
2017-2018	469,088,667	± 71,841,342	-	-

Year	Cephalopods		Gastropods	
1977-1981	15,000,000	± 1,732,051	-	-
1982-1986	36,496,800	± 25,627,118	-	-
1987-1991	242,013,200	± 92,112,865	-	-
1992-1996	938,944,600	± 205,048,581	-	-
1997-2001	1,424,437,600	± 263,826,463	139,144,000	± 0
2002-2006	1,730,019,200	± 532,776,942	-	-
2007-2011	1,466,157,138	± 149,281,613	-	-
2012-2016	1,514,391,200	± 702,034,596	-	-
2017-2018	2,636,802,000	± 920,088,056	-	-

Appendix A5. Annual export value of mollusk trade per category in the Philippines from 1977 to 2018 BFAR Annual Fisheries Report. (-) means no data report.

Year	Worked Shells and Articles	Bivalves	Cephalopods	Gastropods
1977	99,657,000	19,601,000	-	-
1978	87,000,000	15,000,000	16,000,000	-
1979	92,000,000	15,000,000	16,000,000	-
1980	83,000,000	14,000,000	13,000,000	-
1981	90,000,000	-	16,000,000	-
1982	79,242,000	10,696,000	20,542,000	-
1983	114,849,000	-	30,374,000	-
1984	280,015,000	-	35,328,000	-
1985	256,342,000	-	80,240,000	-
1986	277,466,000	-	125,086,000	-
1987	302,449,000	160,816,000	214,398,000	-
1988	275,557,000	197,610,000	223,546,000	-
1989	275,665,000	188,207,000	269,308,000	-
1990	551,153,000	249,299,000	377,728,000	-
1991	528,718,000	501,404,000	763,448,000	-
1992	498,736,000	421,022,000	702,488,000	-
1993	426,677,000	264,882,000	974,015,000	-
1994	517,417,000	187,361,000	1,059,494,000	-
1995	467,380,000	129,828,000	1,195,278,000	-
1996	400,282,000	115,845,000	1,004,614,000	-
1997	514,298,000	-	1,672,022,000	-
1998	700,389,000	-	1,543,186,000	139,144,000
1999	762,754,000	456,574,000	1,563,735,000	-
2000	736,090,000	482,993,000	1,338,631,000	-
2001	649,878,000	392,361,000	1,868,337,000	-
2002	952,920,000	616,876,000	2,112,773,000	-
2003	710,861,000	537,264,000	2,009,120,000	-
2004	1,130,127,000	980,282,000	795,266,000	-
2005	40,935,000	-	1,864,600,000	-

Appendix A5. Contd.

Year	Worked Shells and Articles	Bivalves	Cephalopods	Gastropods
2006	1,353,123,000	-	1,629,009,000	-
2007	145,237,417	-	1,512,672,689	-
2008	80,790,000	-	1,525,813,000	-
2009	52,242,000	-	1,229,886,000	-
2010	100,228,000	-	1,433,405,000	-
2011	170,763,000	-	2,581,298,000	-
2012	189,832,000	-	1,882,455,000	-
2013	343,173,000	-	1,115,902,000	-
2014	310,165,000	-	966,921,000	-
2015	519,660,000	-	1,025,380,000	-
2016	920,369,000	-	1,592,841,000	-
2017	192,649,000	-	2,987,987,000	-
2018	294,248,000	-	3,329,578,000	-
total	16,574,336,417	5,956,921,000	44,717,704,689	139,144,000

Appendix B1. volume (MT) and Value (₱) of mollusk trade showing the Mean ± Standard Deviation (SD) from 1977-2015 PSA Foreign Export Trade Report.

Year	Volume			Value		
1977-1981	1,209	±	441	215,208,790	±	100,819,738
1982-1986	1,889	±	719	244,338,097	±	28,825,912
1987-1991	5,737	±	2,406	757,232,401	±	396,445,788
1992-1996	11,514	±	3,231	1,642,559,229	±	1,094,601,010
1997-2001	17,055	±	1,532	2,585,368,703	±	1,232,135,404
2001-2006	17,494	±	1,987	3,173,784,343	±	225,714,746
2007-2011	12,441	±	3,091	2,622,468,203	±	583,560,577
2012-2015	9,588	±	3,302	3,199,358,064	±	705,401,342

Appendix B2. Mean volume (MT) of each category showing the Mean ± Standard Deviation (SD) from 1977-2015 PSA Foreign Export Trade Report. (-) means no data report.

Year	Shells and Articles			Bivalves			Cephalopods			Gastropods		
1977-1981	-			428	±	181	616	±	295	164	±	36
1982-1986	-			314	±	152	1,365	±	605	209	±	53
1987-1991	-			1,270	±	599	4,182	±	465	285	±	86
1992-1996	1	±	1	1,365	±	925	9,823	±	2,404	326	±	247
1997-2001	2	±	2	1,509	±	956	15,128	±	3,167	415	±	238
2002-2006	11	±	11	2,926	±	1,067	14,040	±	1,525	516	±	107
2007-2011	-			350	±	511	12,072	±	1,027	19	±	26
2012-2015	-			1,436	±	462	8,128	±	4,767	25	±	40

Appendix B3. Annual export volume of mollusk trade per category in the Philippines from 1977 to 2015 PSA Foreign Trade Statistics. (-) means no data report.

Year	Shells and Articles			Bivalves			Cephalopods			Gastropods		
1977	-			221			215			127		
1978	-			514			673			127		
1979	-			678			857			187		
1980	-			436			818			175		
1981	-			293			519			205		
1982	-			270			686			159		
1983	-			302			863			273		
1984	-			352			1,091			223		
1985	-			112			2,056			152		
1986	-			534			2,130			240		
1987	-			1,677			2,886			136		
1988	-			2,065			3,158			359		
1989	-			674			3,221			298		

Appendix B3. Contd.

Year	Shells and Articles	Bivalves	Cephalopods	Gastropods
1990	-	746	3,225	313
1991	-	1,186	8,422	319
1992	-	1,113	8,087	300
1993	-	1,670	11,375	548
1994	-	1,404	12,443	145
1995	-	41	6,702	34
1996	1	2,596	10,509	602
1997	2	2,600	14,584	595
1998	5	2,055	12,649	568
1999	4	1,780	14,060	493
2000	-	185	19,091	9
2001	1	926	15,257	409
2002	5	1,180	16,175	436
2003	29	2,862	16,445	529
2004	2	4,008	13,629	634
2005	6	3,465	13,018	600
2006	13	3,118	10,934	380
2007	-	114	11,375	-
2008	-	187	11,036	-
2009	-	38	9,068	1
2010	-	1,258	11,706	43
2011	-	152	17,174	53
2012	-	1,945	11,533	6
2013	-	1,525	6,012	-
2014	-	1,448	9,545	84
2015	-	825	5,420	10
Total	68	46,554	318,648	9,770

Appendix B4. Total value of each taxonomic Class showing the Mean \pm Standard Deviation (SD) from 1977-2015 PSA Foreign Export Trade Report. (-) means no data report.

Year	Shells and Articles		Bivalves	
1977-1981	-	-	82,384,449	\pm 42,466,340
1982-1986	-	-	45,519,876	\pm 25,696,938
1987-1991	-	-	203,072,136	\pm 99,473,830
1992-1996	-	-	311,675,681	\pm 316,747,877
1997-2001	242,459	\pm 205,131	531,403,816	\pm 362,496,209
2002-2006	4,577,771	\pm 2,334,458	1,136,162,682	\pm 220,919,380
2007-2011	-	-	867,144,143	\pm 99,330,534
2012-2015	-	-	1,382,856,572	\pm 198,363,058
Year	Cephalopods		Gastropods	
1977-1981	122,850,643	\pm 10,240,917	10,240,917	\pm 3,847,918
1982-1986	196,066,130	\pm 17,896,992	17,896,992	\pm 4,590,983
1987-1991	774,646,418	\pm 68,815,506	68,815,506	\pm 35,330,200
1992-1996	1,462,447,262	\pm 134,427,285	134,427,285	\pm 109,433,347
1997-2001	1,816,127,767	\pm 148,249,198	148,249,198	\pm 112,308,127
2002-2006	1,974,327,048	\pm 129,058,462	129,058,462	\pm 30,151,018
2007-2011	1,924,612,165	\pm 1,638,539	1,638,539	\pm 2,087,393
2012-2015	1,657,485,938	\pm 1,739,975	1,739,975	\pm 1,827,422

Appendix B5. Annual export value of mollusk trade per category in the Philippines from 1977 to 2015 PSA Foreign Trade Statistics. (-) means no data report.

Year	Shells and Articles	Bivalves	Cephalopods	Gastropods
1977	-	23,522,268	34,758,187	6,789,306
1978	-	75,098,154	111,408,461	6,772,312
1979	-	140,055,478	187,271,944	11,535,966
1980	-	99,542,781	148,044,969	16,035,334
1981	-	73,703,565	132,769,656	10,071,668

Appendix B5. Contd.

Year	Shells and Articles	Bivalves	Cephalopods	Gastropods
1982	-	54,947,508	180,248,130	14,747,995
1983	-	72,270,534	186,602,157	24,550,265
1984	-	14,796,777	187,879,019	17,861,870
1985	-	21,839,189	216,711,589	12,690,560
1986	-	63,745,373	208,889,755	19,634,267
1987	-	285,317,523	526,152,649	21,655,959
1988	-	308,741,856	534,950,013	65,062,323
1989	-	77,232,715	625,484,292	57,552,298
1990	-	127,946,186	782,534,664	81,262,134
1991	-	216,122,402	1,404,110,470	118,544,817
1992	-	210,368,927	1,392,274,025	127,623,661
1993	-	272,185,581	1,795,222,775	193,549,975
1994	-	224,073,138	2,046,240,278	66,563,667
1995	-	4,130,790	140,359,939	1,425,697
1996	113,695	847,619,967	1,938,139,294	282,973,423
1997	56,647	531,021,550	2,835,235,295	300,247,419
1998	442,447	458,898,419	1,994,840,385	201,017,440
1999	423,498	1,020,450,518	1,945,292,946	143,880,519
2000	-	11,398,040	413,995,246	796,766
2001	289,701	635,250,551	1,891,274,963	95,303,847
2002	5,303,102	867,188,419	2,047,100,910	141,286,893
2003	7,715,157	927,015,360	2,412,659,046	138,343,911
2004	1,223,924	1,251,367,692	2,030,137,319	157,684,266
2005	4,162,545	1,319,251,874	1,806,642,790	129,719,446
2006	4,484,129	1,315,990,064	1,575,095,177	78,257,793
2007	-	996,132,394	1,616,143,526	-
2008	-	735,806,457	1,699,282,327	-
2009	-	814,796,379	1,788,474,475	587,724
2010	-	920,401,074	1,563,978,549	2,910,949
2011	-	868,584,412	2,955,181,948	4,694,023
2012	-	1,404,170,891	2,163,412,235	2,542,594
2013	-	1,516,912,323	1,258,104,038	-
2014	-	1,514,394,545	2,137,773,497	3,927,284
2015	-	1,095,948,529	1,070,653,982	490,021
Total	24,214,845	21,418,240,203	47,985,330,921	2,558,594,394

Appendix C1. Mean annual exported volume per piece of mollusk products showing the mean and standard deviation from the Philippines from 1983 to 2019 CITES database.

Year	Exported Mollusks
1984-1988	19,213 ± 66,153
1989-1993	26,788 ± 66,041
1994-1998	3,784 ± 8,755
1999-2003	407 ± 421
2004-2008	2,216 ± 5,308
2009-2013	102 ± 183
2014-2018	4,605 ± 7,271

Appendix C2. Mean annual imported volume per piece of mollusk products showing the Mean ± Standard deviation in the Philippines from 1983 to 2019 CITES database.

Year	Imported Mollusks
1984-1988	500 ± 0
1989-1993	4,620 ± 3,765
1994-1998	7,502 ± 12,558
1999-2003	40 ± 0
2004-2008	16,181 ± 1,670
2009-2013	2 ± 0
2014-2018	10,100 ± 14,001

Supplementary Table 1. Mean exported mollusk per piece from the Philippines 1984 to 2018 CITES database.

Year	Argentina	Australia	Austria	Bahamas
1984-1988	538 ± -	13,521 ± 19,502	-	-
1989-1993	-	9,462 ± 9,041	-	500 ± -
1994-1998	-	105 ± 134	100 ± -	-
1999-2003	-	247 ± -	7 ± -	-
2004-2008	-	-	-	-
2009-2013	-	-	-	-
2014-2018	-	-	-	-
Year	Belgium	Brazil	Canada	China
1984-1988	14,334 ± 10,686	-	8,753 ± 7,928	6,606 ± -
1989-1993	30,220 ± 35,153	52 ± -	7,808 ± 11,606	-
1994-1998	300 ± -	-	1,164 ± 819	-
1999-2003	-	-	-	-
2004-2008	-	-	-	-
2009-2013	-	-	-	-
2014-2018	-	-	-	-
Year	Cyprus	Czech Republic	Denmark	Fiji
1984-1988	-	-	2,769 ± 3,153	718 ± -
1989-1993	212 ± 285	-	306 ± 36	310 ± -
1994-1998	-	150 ± -	747 ± 261	-
1999-2003	-	50 ± -	-	-
2004-2008	-	-	-	-
2009-2013	-	-	-	-
2014-2018	-	-	-	-
Year	Former Pacific Trust Territory	France	French Polynesia	Germany
1984-1988	218 ± -	8,985 ± 14,083	-	27,275 ± 13,649
1989-1993	-	74,580 ± 45,128	2,653 ± 2,899	63,276 ± 63,258
1994-1998	-	500 ± 141	-	22,806 ± 15,103
1999-2003	-	-	-	-
2004-2008	-	-	-	-
2009-2013	-	-	-	-
2014-2018	-	-	-	-
Year	Greece	Guam	Hong Kong	Iceland
1984-1988	829 ± -	29 ± 17	4,865 ± 4,448	577 ± -
1989-1993	2,696 ± 2,779	-	6,452 ± 4,367	-
1994-1998	-	-	40 ± 14	-
1999-2003	-	-	-	-
2004-2008	-	-	-	-
2009-2013	10 ± -	-	-	-
2014-2018	4 ± -	309 ± -	-	-
Year	India	Israel	Italy	Japan
1984-1988	1,400 ± -	-	16,126 ± 16,136	52,896 ± 54,742
1989-1993	-	3,499 ± 3,615	19,712 ± 8,861	66,404 ± 71,809
1994-1998	-	200 ± -	-	8,804 ± 7,528
1999-2003	-	-	-	267 ± 157
2004-2008	-	-	-	300 ± -
2009-2013	-	-	-	-
2014-2018	-	-	- ± 40	-

Supplementary Table 1. Contd.

Year	Korea, Republic of	Luxembourg	Malaysia	Malta
1984-1988	5,330 ± -	-	-	-
1989-1993	50 ± 54	-	-	100 ± -
1994-1998	830 ± 269	50 ± -	150 ± -	-
1999-2003	-	-	-	-
2004-2008	-	-	115 ± -	-
2009-2013	4 ± -	-	500 ± -	-
2014-2018	-	-	153 ± -	-
Year	Mauritius	Morocco	Netherlands	New Caledonia
1984-1988	256 ± -	4,107 ± -	27,188 ± 19,011	-
1989-1993	7,828 ± -	-	53,996 ± 39,013	1,100 ± -
1994-1998	-	-	7,072 ± 8,497	-
1999-2003	-	-	-	-
2004-2008	-	-	-	-
2009-2013	-	-	-	-
2014-2018	-	-	-	-
Year	New Zealand	Norway	Poland	Portugal
1984-1988	100 ± -	2 ± -	-	1,500 ± -
1989-1993	55 ± 64	-	-	1,100 ± -
1994-1998	15 ± 12	-	-	-
1999-2003	10 ± 3	-	-	-
2004-2008	16 ± 1	-	636 ± -	-
2009-2013	-	-	8 ± 4	-
2014-2018	-	-	17,128 ± -	-
Year	Saudi Arabia	Singapore	Spain	Sweden
1984-1988	1,420 ± 618	270 ± 307	1,210 ± 1,119	39 ± -
1989-1993	-	1,701 ± 2,410	50,261 ± 54,337	1,537 ± -
1994-1998	-	-	4,359 ± 2,716	80 ± -
1999-2003	-	900 ± -	739 ± 493	-
2004-2008	-	200 ± -	2 ± -	-
2009-2013	-	42 ± 25	6 ± -	-
2014-2018	-	-	-	-
Year	Switzerland	Taiwan, Province of China	Thailand	United Kingdom of Great Britain
1984-1988	4,384 ± 4,574	-	-	27,756 ± 29,157
1989-1993	100 ± -	1,066 ± 972	16 ± 21	65,980 ± 73,548
1994-1998	248 ± 342	163 ± 53	100 ± -	2,436 ± 902
1999-2003	-	-	-	-
2004-2008	-	-	-	-
2009-2013	-	-	-	-
2014-2018	-	-	-	-
Year	United States of America		Unknown	
1984-1988	376,095 ±	289,679	4,722 ±	3,298
1989-1993	357,388 ±	250,876	-	-
1994-1998	36,606 ±	44,313	-	-
1999-2003	1,039 ±	2,069	-	-
2004-2008	14,245 ±	11,325	-	-
2009-2013	144 ±	198	-	-
2014-2018	9,903 ±	13,497	-	-

Supplementary Table 2. Mean imported mollusk per piece to the Philippines from 1984 to 2018 CITES database.

Years	Australia	Bahamas	Malay- sia	New Caledo- nia	Nicara- gua	Pa- lau	Philip- pines	Spain	United States of America
1984- 1988	500	-	-	-	-	-	-	-	-
1989- 1993	15,000	-	-	-	-	-	360	-	6,000
1994- 1998		22,000	-	-	-	-	-	475	30
1999- 2003	-	-	-	40	-	-	-	-	-
2004- 2008	-	-	-	-	15,000	-	-	-	17,362
2009- 2013	-	-	-	-	-	3	-	-	2
2014- 2018	-	20,000	200	-	-	-	-	-	-

Research Article

Region of Nuclear Ribosomal DNA (*ITS2*) and Chloroplast DNA (*rbcL* and *trnL-F*) as A Suitable DNA Barcode for Identification of *Zingiber loerzingii* Valetton From North Sumatera, Indonesia

Eko Prasetya^{1*}, Lazuardi¹, Fauziyah Harahap¹, Yuanita Rachmawati², Yusnaeni Yusuf³, Said Iskandar Al Idrus⁴, Puji Prastowo¹

1) Department of Biology, Faculty of Mathematics and Natural Sciences, Universitas Negeri Medan, Medan, 20221, North Sumatera, Indonesia

2) Department of Biology, Faculty of Sciences and Technology, Islamic State University Sunan Ampel Surabaya, Surabaya, 60237, East Java, Indonesia

3) Department of Biology, Faculty of Mathematics and Natural Sciences, Universitas Negeri Makasar, Makasar, Indonesia, 90224, South Sulawesi, Indonesia

4) Department of Mathematics, Faculty of Mathematics and Natural Sciences, Universitas Negeri Medan, Medan, 20221, North Sumatera, Indonesia

* Corresponding author, email: ekoprasetya.biologi@gmail.com

Keywords:

chloroplast DNA
DNA barcode
North Sumatera
nuclear DNA
Zingiber loerzingii

Submitted:

09 August 2022

Accepted:

16 May 2023

Published:

22 September 2023

Editor:

Furzani Binti Pa'ee

ABSTRACT

Zingiber loerzingii Valetton is one of the species in the Zingiberaceae family found throughout Aceh and North Sumatera, Indonesia, with slimy flowers, yellowish white color, and dark orange stamens. *Z. loerzingii* is endemic in North Sumatera with a very limited distribution. The International Union for Conservation of Nature and Natural Resources classifies this plant into the vulnerable ones category. This study aims to examine the potential of DNA barcoding from nuclear DNA (*ITS2*) and DNA chloroplasts (*rbcL* and *trnL-F*) to identify *Z. loerzingii* plants. The research sample was obtained from two main distribution areas of *Z. loerzingii* in North Sumatera, Indonesia, namely Sibolangit Nature Reserve and Tangkahan Conservation Forest. The results showed that all the DNA barcode markers used were able to classify *Z. loerzingii* into the same group in the phylogenetic analysis. *ITS* marker is the most effective marker for classifying Zingiberaceae species compared to *rbcL* and *trnL-F* markers. The *ITS2* marker has the lowest level of intraspecific and intraspecific genetic distance overlap compared to the *rbcL* and *trnL-F* markers. This research is expected to provide information related to the DNA barcode of *Z. loerzingii* in an effort to conserve this rare plant.

Copyright: © 2023, J. Tropical Biodiversity Biotechnology (CC BY-SA 4.0)

INTRODUCTION

Zingiberaceae is a family of plants with the largest amount of members of the order Zingiberales (Kress et al. 2002; Pedersen 2004) spread throughout the Indo-Malay region and consist of about 52 genera and 1200 species (Sabu 2006). Most members of this family are used in spices, vegetables, nutraceuticals, and traditional medicine (Kala 2005; Tushar et al. 2010; Zakaria et al. 2011). Identification of the Zingiberaceae family is very difficult because of the narrow differences in morphological characteristics between species and the high degree of phenotypic plasticity (Kress et al. 2002; Vinitha et al. 2014).

The *Zingiber* genus is one of the genera in the Zingiberaceae family (Miller 1754). It is distributed throughout the tropical rainforests of Asia with the highest diversity level in the forests of Southeast Asia (Theilade 1999). Most species in the *Zingiber* genus are rare and endangered plants, and their habitat is notoriously difficult to access, complicating efforts to collect and study them (Tushar et al. 2010). *Zingiber loerzingii* is a species of the genus *Zingiber* and Zingiberaceae family (Valeton 1918) with characteristics which consist of slimy flowers, dark orange-colored stamens, and yellowish-white flowers found in Aceh and North Sumatra, Indonesia (Rugayah et al. 2017). *Z. loerzingii* is listed as vulnerable on the IUCN Red List (Nurainas & Ardiyani 2019). This plant is difficult to find in nature because of its endemic nature, its limited distribution area, and its rarity in Indonesia (Rugayah et al. 2017). Due to the decreasing population of this plant, an appropriate and fast identification method is needed for the conservation needs of this plant.

DNA barcoding is a method for species-level identification using short DNA segments (Kress et al. 2005; Hollingsworth et al. 2009). The DNA barcode used must be conserved among taxa and have sufficient polymorphism to discriminate (Chase et al. 2007; Kress et al. 2015). Commonly used plant DNA barcodes include RuBisCo (*rbcL*) and maturase K (*matK*), nuclear-encoded ribosomal internal transcribed spacer (*ITS*), and *ITS* shorter fragment *ITS2* (Ratnasingham & Hebert 2007; Hollingsworth et al. 2009). DNA barcodes cannot be used indiscriminately for all plants – each has a different advantage in identifying plants, even in some types of plants, but the three markers can be very useful.

ITS2 markers can classify genera in the Zingiberaceae family into different groups through phylogenetic analysis (Shi et al. 2011; Ren et al. 2019). The *ITS2* marker is also reported to be able to identify species in the genus *Alpinia* originating from Peninsular Malaysia with a success rate of up to 96.97% (Tan et al. 2020). The its sequence (*ITS* 1, 5.8S, *ITS* 2) was able to classify 18 species of the *Zingiber* genus from species in other genera in the Zingiberaceae family. (Theerakulpisut et al. 2012). *ITS2* markers, *trnH-psbA*, *matK*, *rbcL*, and *trnL-F* were reported to be able to group genera and species in the *Zingiberaceae* family (Shi et al. 2011; Chen et al. 2014; Vinitha et al. 2014). The markers *trnL-F*, *matK*, and *ITS* showed greater intraspecific differences than interspecific differences in *Curcuma* (Zingiberaceae) (Záveská et al. 2012).

One of the difficulties in identifying species in the Zingiberaceae family is that there is no one effective marker for all species in this family, therefore it is necessary to test the ability of each marker in each genus or species to determine *ITS* effectiveness. The *matK* or *rbcL* plastid loci have been reported to exhibit paraphyla results in *Hedychium coccineum* and *Hedychium flavescens* (Vinitha et al. 2014). The *matK*, *rbcL*, *trnH-psbA*, and *trnL-F* markers did not show any barcode gaps in the *Curcuma* genus. Barcoding gaps are very important to show the success of using DNA barcodes in the observed samples (Hebert et al. 2003; Theodoridis et al. 2012; Pino-Bodas et al. 2013). The *rbcL* marker has no genetic variation and *matK* is relatively difficult to amplify and is sequencing in the *Roscoea* genus (Zingiberaceae) (Zhang et al. 2014).

The use of DNA barcodes in plants does have limitations, including difficulties in DNA amplification due to degraded DNA (Särkinen et al. 2012), attachment location mismatch like *matK* (Piredda et al. 2011; Kool et al. 2012), and low levels of discrimination such as *rbcL* (Stoeckle et al. 2011; Newmaster et al. 2013). This study aims to examine the potential of DNA barcoding *trnL-F*, *rbcL*, and *ITS2* in identifying the *Z. loerzingii* rare plant from North Sumatra Indonesia, and is expected to provide im-

portant information related to DNA barcoding in *Z. loerzingii* rare plant from North Sumatra.

MATERIALS AND METHODS

Sample Collection and DNA Extraction

A total of 5 samples of fresh *Z. loerzingii* were collected from Sibolangit Nature Reserve (4 samples) and Tangkahan Conservation Forest North Sumatra (1 sample), Indonesia. Fresh leaf samples were stored in a freezer at -20°C for long-term storage. DNA isolation was performed using the GeneJet Plant Genomic DNA Purification Kit (Thermo Fisher Scientific, Waltham, MA, USA) following the manufacturer's recommended protocol. The results of DNA isolation were tested qualitatively using gel electrophoresis and visualised using gel documentation (Bio-Rad Laboratories, Hercules, CA, USA).

Amplification and Sequencing

The *ITS2*, *rbcl*, and *trnL-F* DNA regions were amplified using polymerase chain reaction (PCR) in a thermocycler (LabCycler SensoQuest PCR, SensoQuest, Germany) with a total volume of 25 µL [2.5 µL of reverse primer, 2.5 µL of forward primer; 5 µL of distilled water; 2.5 µL of DNA template; 12.5 µL of PCR mix (MyTaq HS Red Mix, Bioline, USA)]. The primer used for *rbcl* sequence is *rbcl* a_f (5'- ATG TCA CCA CAA ACA GAG ACT AAA GC-3') dan *rbcl* a_rev (5'-GTA AAA TCA AGT CCA CCR CG-3') (Costion et al. 2011), whereas the primers for the *trnL-F* sequence are *trnL-F* F (5'-GGT TCA AGT TCT ATC CCC CC-3') and *trnL-F* R (5'-ATT TGA GAC ACG AG ACT GGT-3') (Taberlet et al. 1991), and the primers for the *ITS2* sequence are *ITS2-S2F* (5'-ATG CGA TAC TTG GTG TGA AT-3') and *ITS2-S3R* (5'-GAC GCT TCT CCA GAC TAC AAT-3') (Yao et al. 2010). Amplification was carried out with a pre-denaturation program at 97°C for 4 minutes, denaturation at 94°C for 45 seconds, annealing at 52°C for 50 seconds and extension at 72°C for 1 minute. PCR products were visualized using 1% agarose gel with SYBR Safe DNA gel stain (Invitrogen, USA). PCR products with positive results (DNA bands are clearly visible) will be sent to the First Base DNA Sequencing Service in Singapore for sequencing.

Data Analysis

The results of the *ITS2*, *rbcl*, and *trnL-F* sequences were analysed using the Bioedit 7.2.5 application (Hall 1999) to determine the consensus sequence. Nucleotide composition, genetic distance, and phylogenetic tree were constructed using MEGA (Molecular Evolutionary Genetics Analysis) version 11 (Tamura et al. 2021) based on alignment of sequence data. The method used for phylogenetic tree analysis is Neighbor Joining and Maximum Parsimony with 1000 bootstrap replicates.

RESULTS AND DISCUSSION

All samples in this study were successfully amplified using 3 main markers (*ITS2*, *rbcl*, and *trnL-F*). The results of the visualisation of the PCR product showed presence of a single band, which means the sequence was successfully amplified. The alignment analysis of the sequencing results shows that the length of the sequence consists of ± 492 bp (*ITS2*), ± 577 bp (*rbcl*), and ± 397 bp (*trnL-F*). The results of the analysis using BLAST software at the National Center for Biotechnology Information (NCBI) resulted in a homology level of *ITS2* sequences in *Z. loerzingii* of 99.73%. There is only one *ITS2* sequence data for *Z. loerzingii* in NCBI, while the *rbcl* and *trnL-F* markers have not been found in the NCBI da-

tabase so that the level of homology with the database cannot be measured. The nucleotide composition of *Z. loerzingii* using three barcode markers is presented in Table 1.

The length of the DNA barcode sequencing results varies greatly in each Zingiberaceae species (Kress et al. 2002; Shi et al. 2011; Vinitha et al. 2014; Ounjai et al. 2016; Saha et al. 2020). The average GC content that has been reported in Zingiberaceae with the *ITS2* marker is in the *Alpinia* genus (59.35%) (Tan et al. 2020), *Plagiostachys* (58,60%) (Julius & Suleiman 2008), *Myxochlamys* (Takano & Nagamasu 2007), and *Globba* (52.2%) (Williams et al. 2004). *ITS2* data on *Z. loerzingii* (59.2%) is still unpublished. The average GC content that has been reported in the *rbcL* marker is in the genus *Alpinia* (43.0%) (Davis et al. 2004), *Amomum* (42.9%) (Li et al. 2011), *Curcuma* (42.7%) (Kress & Erickson 2007), *Globba* (42.8%) (Kress et al. 2001), *Hedychium* (42.8%) (Vinitha et al. 2014), *Re-nealmia* (43.1%) (Givnish et al. 2010), and *Zingiber* (43.1%) (Smith et al. 1993). The GC content of the *trnL-F* barcode sequence in Zingiberaceae has not been reported. The only data reported is the *trnL-F* sequence in the Zingiberaceae tribe from the sample obtained from the Royal Botanic Garden of Edinburgh with GC content ranging from 31.5%-33.41% and an average of 32.78% (Ngamriabsakul et al. 2004).

The features of the three barcode markers (*ITS2*, *rbcL*, and *trnL-F*) on *Z. loerzingii* are presented in Table 2. All three show high levels of conserved sites. Variable sites are only visible on the *ITS2* marker. Due to the absence of *rbcL* and *trnL-F* *Z. loerzingii* sequence data on NCBI, intraspecific analysis of these markers did not use external comparisons, but only used study samples. The results showed that conserved sites on the *ITS2* marker were 97.97%, *rbcL* was 100%, and *trnL-F* was 100%. DNA barcode features on Zingiberaceae species in India showed that the conserved sites level on the *rbcL* marker was 88.91%, *trnL-F* was 82.93%, and *ITS2* was 48.33% (Vinitha et al. 2014).

Table 1. Nucleotide composition, AT content, and GC content using three main markers (*ITS2*, *rbcL*, and *trnL-F*) in *Z. loerzingii*.

Sample	Collection site	Barcode	Composition (%)				Content (%)		Total (bp)
			A	C	G	T	A/T	G/C	
<i>Z. loerzingii</i>	SNR T1	<i>ITS2</i>	20.5	24.4	32.7	22.4	42.9	57.1	492
<i>Z. loerzingii</i>	SNR T2	<i>ITS2</i>	20.2	24.6	32.6	22.3	42.7	57.3	484
<i>Z. loerzingii</i>	SNR T3	<i>ITS2</i>	20.2	24.6	32.6	22.5	42.8	57.2	484
<i>Z. loerzingii</i>	SNR T4	<i>ITS2</i>	20.2	24.8	32.6	22.3	42.6	57.4	484
<i>Z. loerzingii</i>	TCF T5	<i>ITS2</i>	20.3	24.8	32.6	22.0	42.5	57.5	472
<i>Z. loerzingii</i>	*NCBI (MN803334.1)	<i>ITS2</i>	17.1	25.5	33.7	22.6	40.8	59.2	368
<i>Z. loerzingii</i>	SNR R1	<i>rbcL</i>	27.8	19.8	23.1	29.3	57.1	42.9	576
<i>Z. loerzingii</i>	SNR R2	<i>rbcL</i>	27.9	19.8	23.1	29.3	57.2	42.8	577
<i>Z. loerzingii</i>	SNR R3	<i>rbcL</i>	27.9	19.8	23.1	29.3	57.2	42.8	577
<i>Z. loerzingii</i>	SNR R4	<i>rbcL</i>	27.8	19.8	23.1	29.3	57.1	42.9	576
<i>Z. loerzingii</i>	TCF R5	<i>rbcL</i>	27.9	19.8	23.1	29.3	57.2	42.8	577
<i>Z. loerzingii</i>	SNR L1	<i>trnL-F</i>	33.4	11.1	22.8	32.2	65.9	34.1	395
<i>Z. loerzingii</i>	SNR L2	<i>trnL-F</i>	33.2	11.6	22.9	32.2	65.5	34.5	388
<i>Z. loerzingii</i>	SNR L3	<i>trnL-F</i>	33.4	11.4	22.8	32.2	65.7	34.3	395
<i>Z. loerzingii</i>	SNR L4	<i>trnL-F</i>	33.2	11.3	22.9	32.0	65.6	34.4	397
<i>Z. loerzingii</i>	TCF L5	<i>trnL-F</i>	32.8	12.5	22.2	32.2	65.2	34.8	329

SNR: Sibolangit Nature Reserve; TCF: Tangkahan Conservation Forest

*Data obtained from National Center for Biotechnology Information

Table 2. Features of three barcoding markers (*ITS2*, *rbcl*, and *trnL-F*) of *Z. loerzingii*.

Locus	<i>ITS2</i>	<i>rbcl</i>	<i>trnL-F</i>
Total number of sites (bp)	6	5	5
Conserved sites (bp)	482	577	395
Variable sites (bp)	2	0	0
Parsimony Informative sites (bp)	0	0	0
Singleton sites (bp)	2	0	0

Different base substitutions in the analysis region were evaluated for all codon positions and are shown in Table 3. In general, the transitional substitution was higher in the *ITS2* region, lower in the *trnL-F* region, and the same as the transversional substitution in the *rbcl* region. The transitional and transversional substitution values tend to be the same because the *ITS2*, *rbcl*, and *trnL-F* sequences are highly conserved in *Z. loerzingii*. A small difference only occurred in the *trnL-F* marker with a difference in value of only 0.01%. Relative rates of synonymous substitution in most chloroplast DNA are more conserved (Muse 2000). The results of a comparative study of Ginger (*Zingiber officinale*) in the Zingiberaceae family using a complete chloroplast genome showed that the inverted repeat region (including *matK* and *rbcl*) experienced slow nucleotide substitution (Cui et al. 2019). The rate of insertion and deletion of *ITS* markers is more frequent than substitution (Elbadri et al. 2002).

The relative distribution of interspecific and intraspecific variation is presented in Figure 1. The results showed that the three barcode markers used had a high intraspecific distribution at a smaller genetic distance than the interspecific distribution. Discrimination in the distribution of intraspecific and interspecific distances was clearly seen in the *ITS2* marker which was indicated by the small degree of overlap compared to the *rbcl* and *trnL-F* markers (Figure 1A). This indicates that the *ITS2* marker is more effective when used as DNA barcode to identify *Z. loerzingii*. The barcode markers *rbcl* and *trnL-F* showed a high intraspecific distribution at a smaller genetic distance, but the interspecific distribution showed high overlap with the intraspecific distribution. It also shows that there is no barcode gap between the *rbcl* and *trnL-F* barcode markers (Figure 1B, Figure 1C).

Barcoding gap is generated by plotting differences between the mean intraspecific and interspecific distances (Meyer & Paulay 2005; Bhagwat et al. 2015). Barcode gap shows no overlapping area between interspecific and intraspecific distances (Hebert et al. 2003; Pino-Bodas et al. 2013; Chen et al. 2015). In this study, there was an overlap between the intraspecific and interspecific distances in the *ITS2*, *rbcl*, and *trnL-F* markers. However, the smallest overlapping level was found in the *ITS2* marker. Analysis of *ITS2* sequences as DNA barcodes in Zingiberaceae in E'mei region, Sichuan province, China, showed a clear barcode gap (Ren et al. 2019). Several studies showed that there is no barcoding gap according to observations using the *rbcl*, *ITS*, and *ITS2* markers (Ferguson 2002; Meier et al. 2006; Shearer & Coffroth 2008; Hollingsworth et al. 2009). Research on closely related plants also did not show any barcoding gap using *rbcl* and *matK* markers (Lahaye et al. 2008; Bhagwat et al. 2015).

Based on the phylogenetic tree analysis constructed using the Maximum Parsimony method, the three barcode markers used seemed to be able to include *Z. loerzingii* samples in the same group. However, only marker *ITS2* showed the highest level of species and genus discrimination (Figure 2A) compared to markers *rbcl* and *trnL-F*. The markers *rbcl*

Table 3. Pattern of Nucleotide Substitution of *ITS2*, *rbcl*, and *trnL-F* regions in *Z. loerzingii* (%)

DNA Barcodes	<i>ITS2</i>				<i>rbcl</i>				<i>trnL-F</i>				
	Base	A	T	G	C	A	T	G	C	A	T	G	C
A	-	0.00	0.00	25,00	25,00	-	8,34	8,34	8,34	-	8,34	8,34	8,33
T	0.00	-	25,00	0.00	0.00	8,34	-	8,34	8,34	8,34	-	8,33	8,34
G	0.00	25,00	-	0.00	0.00	8,34	8,34	-	8,34	8,34	8,33	-	8,34
C	25,00	0.00	0.00	-	-	8,34	8,34	8,34	-	8,33	8,34	8,34	-

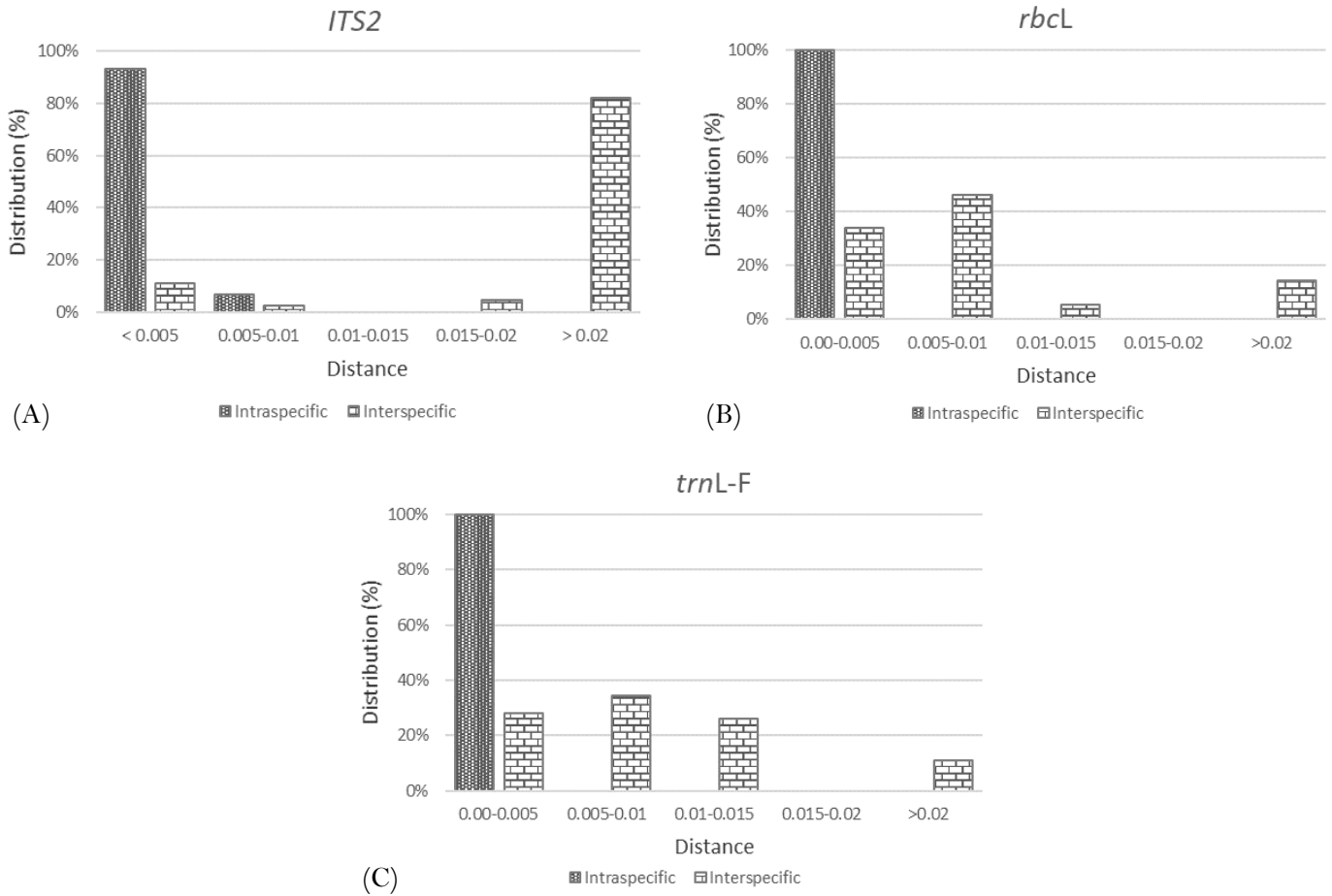


Figure 1. Barcoding gap with the intraspecific and interspecies distances

and *trnL-F* showed discrimination at family level, especially in the Zingiberaceae family (Figure 2B, Figure 2C), but were unable to classify genera or species therein.

DNA barcoding research on Zingiberaceae species in India showed that *rbcl* and *matK* markers are more recommended as DNA barcodes for Zingiberaceae species, and highlighted the low ability of *ITS* and *ITS2* as barcoding markers for this family (Vinitha et al. 2014). This is different from the results of this study which showed that the *ITS2* marker is more effective in classifying genera and species in the Zingiberaceae family, especially *Z. loerzingii* species. In the genus *Curcuma*, it was reported that barcode markers with high success rates were *rbcl* and *trnH-psbA* (100%), *trnL-F* (95.7%), *matK* (89.7%), and *ITS2* (82.6%) (Chen et al. 2015). Research related to DNA barcoding Zingiberaceae from North-East India shows that the *ycf1b* region is the region with the highest conserved sites, while the *ITS* region is the lowest (Saha et al. 2020). The *ycf1* gene is the most promising DNA plastid barcode for land plants (Dong et al. 2015).

The effectiveness of using DNA barcode markers on species in the Zingiberaceae family shows variations. According to our observations, species and geography factors are important in determining the effective

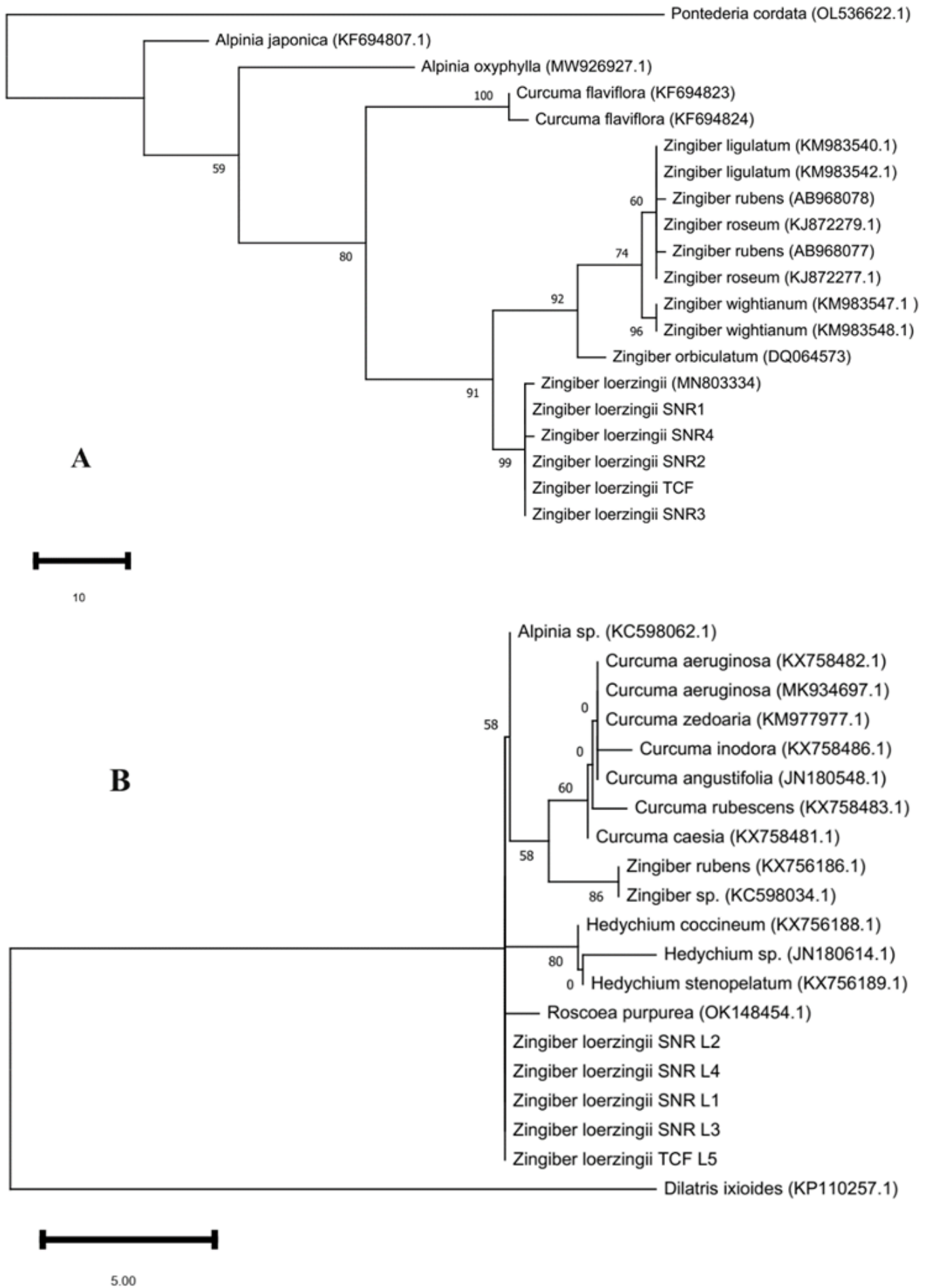


Figure 2. Maximum Parsimony tree for *Z. loerzingii*, closely related family Zingiberaceae and outgroup (*Dilatriis ixioides* or *Pontederia cordata*) using *ITS2* (A), *rbcL* (B), and *trnL-F* (C) barcode.

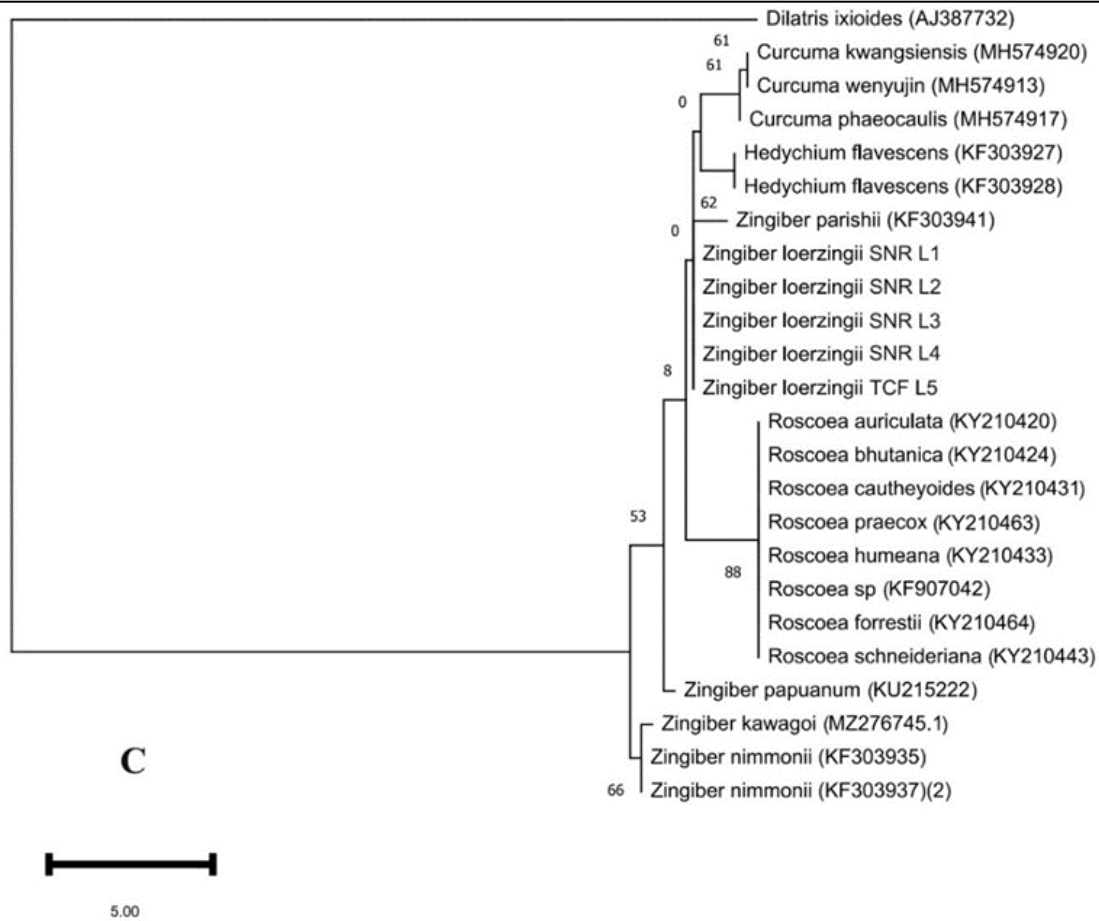


Figure 2. Contd.

DNA barcode markers to use. *ITS* markers are generally ineffective (25%) when used in Zingiberaceae species in India (Vinita et al. 2014), while in the genus *Curcuma* (Zingiberaceae) obtained from the South China Botanical Garden and the US National herbarium, the marker showed effectiveness up to 82.6% (Chen et al. 2014). Barcode marker *ITS2* is a marker that has the highest discrimination ability at the genus (99.5%) and species (73.1%) levels in 30 Zingiberaceae genera from China (Shi et al. 2011). The very wide distribution of Zingiberaceae, especially in tropical Asia such as Sumatra, Borneo, and the Malayan Peninsula, gives rise to high variations due to the adaptation efforts made by the species to geo-ecological conditions (Jatoi et al. 2007). Due to the diversity of geographical areas of distribution, undoubtedly many Zingiberaceae species have not been identified (Larsen et al. 1999).

CONCLUSIONS

The conclusion that can be drawn from this study is that the markers *ITS2*, *rbcL*, and *trnL-F* were able to group *Z. loerzingii* together in the phylogenetic analysis. The *ITS2* marker is especially an effective marker for classifying the Zingiberaceae family based on genus and species compared to *rbcL* and *trnL-F*. Barcoding gap analysis showed that the *ITS2* marker has a small degree of overlap compared to the *rbcL* and *trnL-F* markers in *Z. loerzingii*, and therefore, it is more effective when used as an intraspecific species. The development of DNA barcode markers on Zingiberaceae species must take into account the geographical distribution of samples, so that the results can be more accurate.

AUTHOR CONTRIBUTION

E.P. designed the research and collected data, F.H. and L.L supervised

the entire research process, while Y.R., Y.Y. S.I., and T.H. analysed the research data. All authors were involved in writing and revising the manuscript. .

ACKNOWLEDGMENTS

This research was supported by the PENELITIAN DASAR Scheme from the Institute for Research and Community Service, UNIVERSITAS NEGERI MEDAN in 2022.

CONFLICT OF INTEREST

The authors declare that they have no conflict of interest. The authors are responsible for the content and article writing.

REFERENCES

- Bhagwat, R.M. et al., 2015. Two New Potential Barcodes to Discriminate *Dalbergia* Species. *PLOS ONE*, 10(11), e0142965. doi: 10.1371/journal.pone.0142965.
- Chase, M.W. et al., 2007. A proposal for a standardised protocol to barcode all land plants. *TAXON*, 56(2), pp.295–299. doi: 10.1002/tax.562004.
- Chen, J. et al., 2014. Testing DNA barcodes in closely related species of *Curcuma* (Zingiberaceae) from Myanmar and China. *Molecular Ecology Resources*, 15(2), pp.337–348. doi: 10.1111/1755-0998.12319.
- Chen, J. et al., 2015. Testing DNA barcodes in closely related species of *Curcuma* (Zingiberaceae) from Myanmar and China. *Molecular Ecology Resources*, 15(2), pp.337–348. doi: 10.1111/1755-0998.12319.
- Costion, C. et al., 2011. Plant DNA Barcodes Can Accurately Estimate Species Richness in Poorly Known Floras. *PLoS ONE*, 6(11), e26841. doi: 10.1371/journal.pone.0026841.
- Cui et al., 2019. Comparative and Phylogenetic Analyses of Ginger (*Zingiber officinale*) in the Family Zingiberaceae Based on the Complete Chloroplast Genome. *Plants*, 8(8), 283. doi: 10.3390/plants8080283.
- Davis, J.I. et al., 2004. A Phylogeny of the Monocots, as Inferred from *rbcL* and *atpA* Sequence Variation, and a Comparison of Methods for Calculating Jackknife and Bootstrap Values. *Systematic Botany*, 29(3), pp.467–510. doi: 10.1600/0363644041744365.
- Dong, W. et al., 2015. *ycf1*, the most promising plastid DNA barcode of land plants. *Scientific Reports*, 5(1), p.8348. doi: 10.1038/srep08348.
- Elbadri, G.A.A. et al., 2002. Intraspecific variation in *Radopholus similis* isolates assessed with restriction fragment length polymorphism and DNA sequencing of the internal transcribed spacer region of the ribosomal RNA cistron. *International Journal for Parasitology*, 32(2), pp.199–205. doi: 10.1016/S0020-7519(01)00319-8.
- Ferguson, J.W.H., 2002. On the use of genetic divergence for identifying species. *Biological Journal of the Linnean Society*, 75(4), pp.509–516. doi: 10.1046/j.1095-8312.2002.00042.x.
- Givnish, T.J. et al., 2010. Assembling the Tree of the Monocotyledons: Plastome Sequence Phylogeny and Evolution of Poales 1. *Annals of the Missouri Botanical Garden*, 97(4), pp.584–616. doi: 10.3417/2010023.
- Hall, T.A., 1999. BioEdit: a user-friendly biological sequence alignment editor and analysis program for Windows 95/98/NT. *Nucleic acids symposium series*, 41(41), pp.95–98.

- Hebert, P.D.N. et al., 2003. Biological identifications through DNA barcodes. *Proceedings of the Royal Society of London. Series B: Biological Sciences*, 270(1512), pp.313–321. doi: 10.1098/rspb.2002.2218.
- Hollingsworth, M.L. et al., 2009. Selecting barcoding loci for plants: evaluation of seven candidate loci with species-level sampling in three divergent groups of land plants. *Molecular Ecology Resources*, 9(2), pp.439–457. doi: 10.1111/j.1755-0998.2008.02439.x.
- Jatoi, S.A., Kikuchi, A. & Watanabe, K.N., 2007. Genetic diversity, cytology, and systematic and phylogenetic studies in Zingiberaceae. *Genes, Genomes and Genomics*, 1(1), pp.56–62.
- Julius, A. & Suleiman, M., 2008. Preliminary molecular phylogeny of Bornean Plagiostachys (Zingiberaceae) based on DNA sequence data of internal transcribed spacer (ITS). *Journal of Tropical Biology and Conservation*, 4(1), pp.67–80.
- Kala, C.P., 2005. Ethnomedicinal botany of the Apatani in the Eastern Himalayan region of India. *Journal of Ethnobiology and Ethnomedicine*, 1. doi: 10.1186/1746-4269-1-11.
- Kool, A. et al., 2012. Molecular Identification of Commercialized Medicinal Plants in Southern Morocco. *PLoS ONE*, 7(6), e39459. doi: 10.1371/journal.pone.0039459.
- Kress, W.J. et al., 2001. Unraveling the Evolutionary Radiation of the Families of the Zingiberales Using Morphological and Molecular Evidence R. Olmstead, ed. *Systematic Biology*, 50(6), pp.926–944. doi: 10.1080/106351501753462885.
- Kress, W.J., Prince, L.M. & Williams, K.J., 2002. The phylogeny and a new classification of the gingers (Zingiberaceae): evidence from molecular data. *American Journal of Botany*, 89(10), pp.1682–1696. doi: 10.3732/ajb.89.10.1682.
- Kress, W.J. et al., 2005. Use of DNA barcodes to identify flowering plants. *Proceedings of the National Academy of Sciences*, 102(23), pp.8369–8374. doi: 10.1073/pnas.0503123102.
- Kress, W.J. & Erickson, D.L., 2007. A Two-Locus Global DNA Barcode for Land Plants: The Coding rbcL Gene Complements the Non-Coding trnH-psbA Spacer Region. *PLoS ONE*, 2(6), e508. doi: 10.1371/journal.pone.0000508.
- Kress, W.J. et al., 2015. DNA barcodes for ecology, evolution, and conservation. *Trends in Ecology & Evolution*, 30(1), pp.25–35. doi: 10.1016/j.tree.2014.10.008.
- Lahaye, R. et al., 2008. DNA barcoding the floras of biodiversity hotspots. *Proceedings of the National Academy of Sciences*, 105(8), pp.2923–2928. doi: 10.1073/pnas.0709936105.
- Larsen, K. et al., 1999. *Gingers of Peninsular Malaysia and Singapore*, Borneo: Natural History Publications.
- Li, D.-Z. et al., 2011. Comparative analysis of a large dataset indicates that internal transcribed spacer (ITS) should be incorporated into the core barcode for seed plants. *Proceedings of the National Academy of Sciences*, 108(49), pp.19641–19646. doi: 10.1073/pnas.1104551108.
- Meier, R. et al., 2006. DNA Barcoding and Taxonomy in Diptera: A Tale of High Intraspecific Variability and Low Identification Success. *Systematic Biology*, 55(5), pp.715–728. doi: 10.1080/10635150600969864.
- Meyer, C.P. & Paulay, G., 2005. DNA Barcoding: Error Rates Based on Comprehensive Sampling. *PLoS Biology*, 3(12), p.e422. doi: 10.1371/journal.pbio.0030422.
- Miller, P., 1754. *The Gardeners Dictionary*, London: Rivington.

- Muse, S. V, 2000. Examining rates and patterns of nucleotide substitution in plants. *Plant Molecular Biology*, 42, pp.25–43. doi: <https://doi.org/10.1023/A:1006319803002>.
- Newmaster, S.G. et al., 2013. DNA barcoding detects contamination and substitution in North American herbal products. *BMC Medicine*, 11 (1), 222. doi: 10.1186/1741-7015-11-222.
- Ngamriabsakul, C., Newman, M.F. & Cronk, Q.C.B., 2004. The Phylogeny of Tribe Zingibereae (Zingiberaceae) Based on ITS (nrDNA) and trnL-F (cpDNA) Sequences. *Edinburgh Journal of Botany*, 60(3), pp.483–507. doi: 10.1017/S0960428603000362.
- Nurainas & Ardiyani, M., 2019. Zingiber loerzingii. *The IUCN Red List of Threatened Species 2019*, e.T117465518A124284822. doi: 10.2305/IUCN.UK.2019-2.RLTS.T117465518A124284822.en.
- Ounjai, S. et al., 2016. Multi Chloroplast Genes for Species Identification in Bar-HRM Analysis of Taxonomical Complex Medicinal Plants Group (Zingiberaceae). *Chiang Mai Journal of Science*, 44(4), pp.1311–1321.
- Pedersen, L.B., 2004. Phylogenetic analysis of the subfamily Alpinioideae (Zingiberaceae), particularly Etlingera Giseke, based on nuclear and plastid DNA. *Plant Systematics and Evolution*, 245(3–4), pp.239–258. doi: 10.1007/s00606-004-0126-2.
- Pino-Bodas, R. et al., 2013. Species delimitation in Cladonia (Ascomycota): a challenge to the DNA barcoding philosophy. *Molecular Ecology Resources*, 13(6), pp.1058–1068. doi: 10.1111/1755-0998.12086.
- Piredda, R. et al., 2011. Prospects of barcoding the Italian wild dendroflora: oaks reveal severe limitations to tracking species identity. *Molecular Ecology Resources*, 11(1), pp.72–83. doi: 10.1111/j.1755-0998.2010.02900.x.
- Ratnasingham, S. & Hebert, P.D.N., 2007. BARCODING: bold: The Barcode of Life Data System (<http://www.barcodinglife.org>). *Molecular Ecology Notes*, 7(3), pp.355–364. doi: 10.1111/j.1471-8286.2007.01678.x.
- Ren, Y. et al., 2019. Analysis of Zingiberaceae in E'mei Area Using ITS2 Sequences. *Chinese Journal of Experimental Traditional Medical Formulae*, 24, pp.217–223.
- Rugayah, R. et al., 2017. *Tumbuhan Langka Indonesia : 50 Jenis Tumbuhan Terancam Punah*, Jakarta: LIPI Press.
- Sabu, M., 2006. *Zingiberaceae and Costaceae of South India*, Kerala, India: Indian Association for Angiosperm Taxonomy.
- Saha, K. et al., 2020. DNA barcoding of selected Zingiberaceae species from North-East India. *Journal of Plant Biochemistry and Biotechnology*, 29(3), pp.494–502. doi: 10.1007/s13562-020-00563-y.
- Särkinen, T. et al., 2012. How to Open the Treasure Chest? Optimising DNA Extraction from Herbarium Specimens. *PLoS ONE*, 7(8), e43808. doi: 10.1371/journal.pone.0043808.
- Shearer, T.L. & Coffroth, M.A., 2008. DNA BARCODING: Barcoding corals: limited by interspecific divergence, not intraspecific variation. *Molecular Ecology Resources*, 8(2), pp.247–255. doi: 10.1111/j.1471-8286.2007.01996.x.
- Shi, L.-C. et al., 2011. Testing the potential of proposed DNA barcodes for species identification of Zingiberaceae. *Journal of Systematics and Evolution*, 49(3), pp.261–266. doi: 10.1111/j.1759-6831.2011.00133.x.

- Smith, J.F., Kress, W.J. & Zimmer, E.A., 1993. Phylogenetic Analysis of the Zingiberales Based on rbcL Sequences. *Annals of the Missouri Botanical Garden*, 80(3), p.620. doi: 10.2307/2399850.
- Stoeckle, M.Y. et al., 2011. Commercial Teas Highlight Plant DNA Barcode Identification Successes and Obstacles. *Scientific Reports*, 1(1), p.42. doi: 10.1038/srep00042.
- Taberlet, P. et al., 1991. Universal primers for amplification of three non-coding regions of chloroplast DNA. *Plant Molecular Biology*, 17(5), pp.1105–1109. doi: 10.1007/BF00037152.
- Takano, A. & Nagamasu, H., 2007. Myxochlamys (Zingiberaceae), a new genus from Borneo. *Acta Phytotaxonomica et Geobotanica*, 58(1), pp.19–32. doi: <https://doi.org/10.18942/apg.KJ00004609388>.
- Tamura, K., Stecher, G. & Kumar, S., 2021. MEGA11: Molecular Evolutionary Genetics Analysis Version 11 F. U. Battistuzzi, ed. *Molecular Biology and Evolution*, 38(7), pp.3022–3027. doi: 10.1093/molbev/msab120.
- Tan, W.H., Chai, L.C. & Chin, C.F., 2020. Efficacy of DNA barcode internal transcribed spacer 2 (ITS 2) in phylogenetic study of *Alpinia* species from Peninsular Malaysia. *Physiology and Molecular Biology of Plants*, 26(9), pp.1889–1896. doi: 10.1007/s12298-020-00868-1.
- Theerakulpisut, P. et al., 2012. Phylogeny of the genus *Zingiber* (Zingiberaceae) based on nuclear ITS sequence data. *Kew Bulletin*, 67(3), pp.389–395. doi: 10.1007/s12225-012-9368-2.
- Theilade, I., 1999. A synopsis of the genus *Zingiber* (Zingiberaceae) in Thailand. *Nordic Journal of Botany*, 19(4), pp.389–410. doi: 10.1111/j.1756-1051.1999.tb01220.x.
- Theodoridis, S. et al., 2012. DNA barcoding in native plants of the Labiatae (Lamiaceae) family from Chios Island (Greece) and the adjacent Çeşme-Karaburun Peninsula (Turkey). *Molecular Ecology Resources*, 12(4), pp.620–633. doi: 10.1111/j.1755-0998.2012.03129.x.
- Tushar et al., 2010. Ethnomedical uses of Zingiberaceous plants of Northeast India. *Journal of Ethnopharmacology*, 132(1), pp.286–296. doi: 10.1016/J.JEP.2010.08.032.
- Valeton, T., 1918. *Zingiber loerzingii*. *Bulletin du Jardin Botanique de Buitenzorg II*, 27, p.146.
- Vinitha, M.R. et al., 2014. Prospects for discriminating Zingiberaceae species in India using DNA barcodes. *Journal of Integrative Plant Biology*, 56(8), pp.760–773. doi: 10.1111/jipb.12189.
- Williams, K.J., Kress, W.J. & Manos, P.S., 2004. The phylogeny, evolution, and classification of the genus *Globba* and tribe Globbeae (Zingiberaceae): appendages do matter. *American Journal of Botany*, 91(1), pp.100–114. doi: 10.3732/ajb.91.1.100.
- Yao, H. et al., 2010. Use of ITS2 Region as the Universal DNA Barcode for Plants and Animals B. Hansson, ed. *PLoS ONE*, 5(10), p.e13102. doi: 10.1371/journal.pone.0013102.
- Zakaria, Z.A. et al., 2011. *Zingiber zerumbet* (L.) Smith: A review of its ethnomedicinal, chemical, and pharmacological uses. *Evidence-based Complementary and Alternative Medicine*, 2011. doi: 10.1155/2011/543216.
- Záveská, E. et al., 2012. Phylogeny of *Curcuma* (Zingiberaceae) based on plastid and nuclear sequences: Proposal of the new subgenus *Ecomata*. *TAXON*, 61(4), pp.747–763. doi: 10.1002/tax.614004.
- Zhang, D., Duan, L. & Zhou, N., 2014. Application of DNA barcoding in *Roscoea* (Zingiberaceae) and a primary discussion on taxonomic status of *Roscoea cautleoides* var. *pubescens*. *Biochemical Systematics and Ecology*, 52, pp.14–19. doi: 10.1016/j.bse.2013.10.004.

Research Article

Herbaceous Diversity in the *Gumuk* Ecosystem in Ledokombo District-Jember Regency with Varied Land Use Type

Wiwin Maisyaroh^{1,2,*}, Luchman Hakim³, Sudarto⁴, Jati Batoro³

1)Departement of Biology Education, FTIK UIN KHAS Jember, Jl. Mataram 01 Mangli Jember 68136, East Java Indonesia.

2)Doctoral Program Biology Departement, Faculty of Mathematics and Natural Sciences, Brawijaya University. Jl. Veteran Ketawanggede Lowokwaru Malang 65145, East Java, Indonesia.

3)Biology Departement, Faculty of Mathematics and Natural Sciences, Brawijaya University. Jl. Veteran Ketawanggede Lowokwaru Malang 65145, East Java, Indonesia.

4)Departement of Soil Science, Faculty of Agriculture, Brawijaya University. Jl. Veteran Ketawanggede Lowokwaru Malang 65145, East Java, Indonesia.

*Corresponding author, email: mynajla11@gmail.com

Keywords:

herbaceous,
diversity

Gumuk ecosystem
landscape unique.

Submitted:

21 September 2022

Accepted:

19 May 2023

Published:

27 September 2023

Editor:

Ardaning Nuriliani

ABSTRACT

Gumuk is a unique landscape in Jember Regency resulting from the eruption of Mount Raung that can provide ecosystem services through its ecological functions. Increased mining activity in *Gumuk* and land-use changes can lead to a decline in biodiversity and affect ecosystem services. This study aims to determine the diversity of herbaceous in the *Gumuk* ecosystem. Conducted in January - March 2021 in Ledokombo District, Jember Regency. The spatial distribution of *Gumuk* was carried out using GIS. Herbaceous sampling was carried out using 2x2 plots on three types of *Gumuk* utilisation, namely mixed gardens, sand mining, and stone mining. The results showed that there were 136 *Gumuk* in Ledokombo District. One hundred twenty herbaceous species (49 families) were found in all types of *Gumuk*. Mixed gardens have the highest species diversity (109 species, 49 families) compared to other types. *Digitaria sanguinalis* (L.) Scop. has high dominance in all types. Species dominance showed a moderate category for all types of *Gumuk* ($D = 0.07$). Community complexity in all types was in the high class ($D' = 0.90$) and species diversity was in the high class ($H' = 3.25$). Evenness index ϵ was different in the three types of *Gumuk*; in mixed gardens, the evenness of species was lower (0.23) than the other two types.

Copyright: © 2023, J. Tropical Biodiversity Biotechnology (CC BY-SA 4.0)

INTRODUCTION

Landscape changes can impact ecological communities (Turner et al. 2001), such as the loss of natural ecosystems that can cause vulnerability to some species, especially those who are sensitive to change (Gustafson 2002). The exposure to biodiversity can occur due to changes in the interrelationships between landscape elements and could lead to biodiversity extinction in a long run (Indrawan et al. 2007; Horvath 2019). The effects to ecosystem services are due to differences in agricultural production and hydrological systems, and changes in soil properties (Hasan et al. 2020).

Jember Regency, East Java, has a unique landscape including thou-

sands of small hills (hillocks) as a geological phenomenon, resulted from Mount Raung activities. This small hill is called *Gumuk* by the local community and spread across all sub-districts in Jember, particularly in the Ledokombo district. The height of *Gumuk* is less than 60 meters (Bemmelen 1949) and this is in line with the classification of landforms as wavy topography/sloping hill or small hill (Zuidam & Cancelado 1979). Geologically, *Gumuk* is an example of the ruins of a young volcanic cone on the western side of a volcano that is less stable (Bemmelen 1949). It has economic, social, cultural, and ecological values for a geological formation. Moreover, *Gumuk* also plays a role as habitat for various types of plants and feeding ground for birds as well as corridor in migration. The study of bird diversity in the *Gumuk* ecosystem shows a moderate level (Maisyaroh et al. 2021), indicating that the *Gumuk* ecosystem has potential as a bird habitat even though it has a low diversity of trees.

Currently, the exploitation of *Gumuk* in Jember for mining is increasing. The sand and stone of *Gumuk* are mined for the community's economy activities (Bemmelen 1949). Unfortunately, most mining activities are illegal. This is related to the private ownership status of *Gumuk* and some even become a joint ownership. *Gumuk* can become a source of local wealth for both economic and ecological interests. However, high exploitation is unavoidable, so in the long term, the loss of *Gumuk* and the change of land use will have ecological impact (Hasan et al. 2020), including the decrease in biodiversity. As we know, each species has a different response to disturbance (Newbold et al. 2020). Landscape changes due to mining activities can affect vegetation and hydrogeology (Ikhsan et al. 2019). In addition, the land conversion also contributes to the reduction of green open space which can affect the microclimate (Indrawan et al. 2007).

The diversity of herbaceous in a habitat can be used as an indicator of disturbance. Each herb species has a different tolerance level to changes in environmental conditions (da Silva et al. 2020; Jhariya & Singh 2021). Herbs can also play an essential role in an area because they can increase biomass (Khan et al. 2020). Furthermore, some species have the potential for phytoremediation (da Silva et al. 2020). Many herbaceous species also have high potential as sources of food and medicine for the community (Hakim 2015; La Rosa et al. 2021), as biopesticides (Saripah et al. 2020), as refugia (Maisyaroh 2014; Sutriyono et al. 2019; Abidin et al. 2020), and as exotic plants (Khan et al. 2020). Herbs can also be used as alternative plants for reforestation other than trees (Khan et al. 2020). Herb abundance correlates with higher biomass, carbon storage, and CO₂ mitigation (Khan et al. 2020). The number of *Gumuk* scattered randomly in Jember makes it possible to have a relatively complex diversity of herbs.

This study aims to explore the potential of herbs in the *Gumuk* ecosystem. This study begins with mapping the spatial distribution of *Gumuk* in the Ledokombo district to see the number and distribution of *Gumuk*. The spatial distribution of *Gumuk* then used as the basis for sampling herbs. The areas were grouped into three sampling areas based on the type of land use, namely mixed gardens, sand mining, and stone mining. The diversity of herbs was analysed for each kind of land use to see the dynamics of biodiversity in the changing landscape of *Gumuk*.

MATERIALS AND METHODS

Study Site

This research was conducted from January to March 2021 in the Ledokombo District, Jember Regency, East Java. This district has an area

of 57.03 km² and consists of 10 villages. Ledokombo is one of the districts in Jember which is close to Mount Raung, so the distribution of *Gumuk* in this area is quite large. Ledokombo has an altitude of 370 m above sea level (8°07'54.2" S 113°52'42.5" E) and the average rainfall is 254 mm per year. In Ledokombo District, various land- use types represented all *Gumuk* land uses in Jember Regency. Community empowerment activities in the social and economic have been productive in the last ten years. The Ledokombo community declared their territory as the *Ledokombo Learning Tourism Village* (Hang 2020) to pioneer *Gumuk* conservation efforts.

Distribution and Determination of Gumuk, Sampling Area, and Vegetation Survey

Manuscript is divided using the numbered sections. Authors should divide the manuscript into clearly defined and numbered sections. Second level section numbering is done automatically; following the upper level's number. Use this numbering also for internal cross-referencing: do not just refer to the text. Any subsection should be given a brief heading.

The distribution of the *Gumuk* was mapped using SAGA GIS (Conrad et al. 2015) and ArcGIS (Esri, USA). The determination of the *Gumuk* was conducted by classifying the landform using the TPI (Topographic Position Index) method, which measures the difference elevation at the midpoint and the average height of the surroundings at a certain radius. Moreover, the determination was continued according to the classification of Van Zuidam (Zuidam & Cancelado 1979), that the topography with a slope level of 8 -13% and a height difference of 25-75 m is a category of undulating land topography/sloping hills. Based on that determination, the type of the *Gumuk* ranged from 10-50 m in height, and the area is >1 ha.

The *Gumuk* distribution map was then used as a reference in vegetation sampling. The sampling area is divided into three land-use locations: mixed garden, sand mining, and stone mining. *Gumuk* with diverse garden is *Gumuk* that is currently used for plantations, dominated by certain types of plantation crops, and some are interspersed with seasonal crops. *Gumuk* with sand mining is *Gumuk* which is presently used for sand and gravel mining. Moreover, *Gumuk* with stone mining is *Gumuk* used for block stones and stone plates mining. The vegetation survey was carried out by making plots 2x2 m (Wijana 2014). Each plot counts the species found and records the abiotic parameters. The Sampling point of *Gumuk* was determined by purposive sampling according to the number of village representation and the type of land use. Fifty *Gumuk* became the sampling area, the number was more than 30% of the total samples. Thirty samples of *Gumuk* for a mixed garden, ten for sand mining, and ten for stone mining. The total number of plots is 100, wherein each *Gumuk* two plots are assigned. Species found in sample plots were identified using Flora of Java (Becker & Brink 1965) and The Mountain Flora of Java (Van Steenis 2006).

Data Analysis

The analysis of the *Gumuk* distribution map is carried out by counting the number of *Gumuk* in each village. The Important Value Index (IVI) is calculated from the sum of the Relative Density (KR) and Relative Frequency (FR) (Mueller-Dombois & Ellenberg 1974). Dominance Index (D), Simpson's Index (D'), Shannon Wiener Diversity Index (H'), and Index of Evenness (E) were analyzed using PAST (Paleontological Statistics), ver. 3.22 (Hammer 2001). Vegetation data from three sam-

pling areas were then compared.

RESULTS AND DISCUSSION

Gumuk Distribution in Ledokombo District

The GIS mapping showed 136 *Gumuk* in Ledokombo district and spread over ten villages (Figure 1).

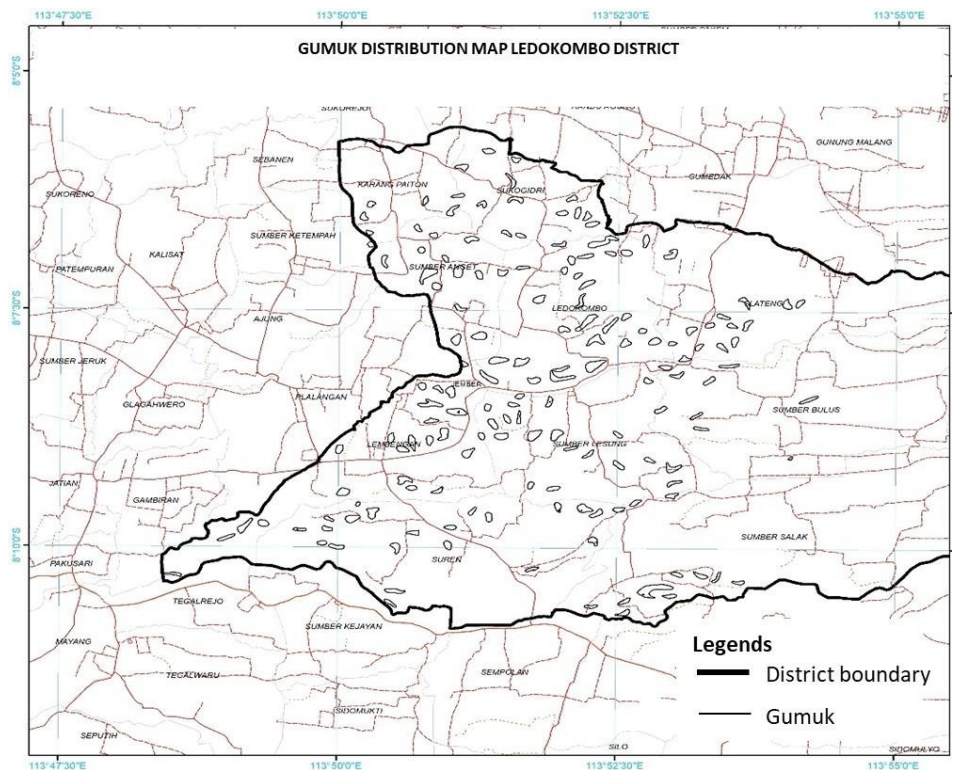


Figure 1. *Gumuk* distribution map in Ledokombo District.

The total area of those *Gumuk* was 222.80 ha. A total of 50 *Gumuk* were used as sampling areas. The villages with the highest *Gumuk* distributions and the highest area were Ledokombo village, Lembengan village, and Suren village (Figure 2).

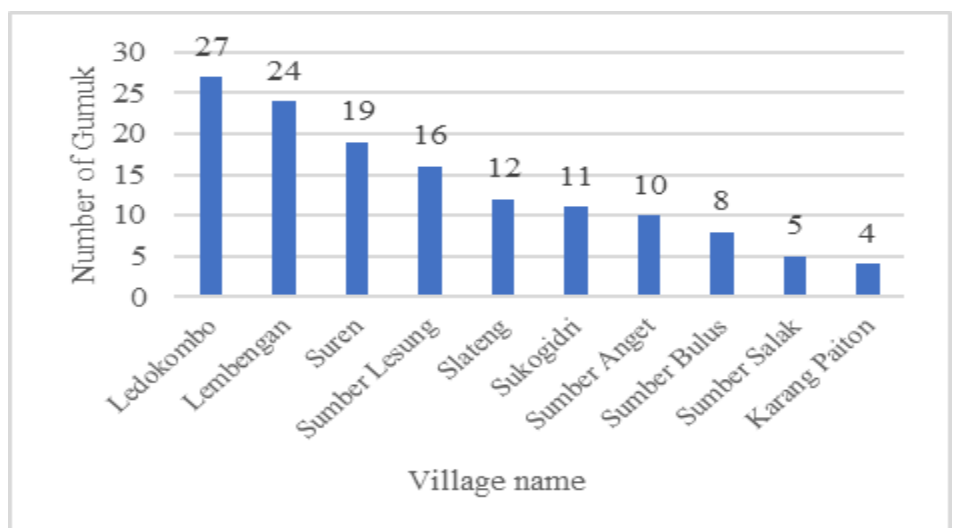


Figure 2. Number of *Gumuk* in each village in Ledokombo District.

The land use of *Gumuk* in Ledokombo village and Lembengan village was dominated by the mixed garden with various plantation commodities, such as Sengon (*Albizia chinensis*), Mahogany (*Swietenia ma-*

hagoni), Papaya (*Carica papaya*), Banana (*Musa* sp.), White Teak (*Gmelina arborea*), Balsa (*Ochroma lagopus*), Bamboo (*Bambusa* sp.), and Coffee (*Coffea* sp.). Several *Gumuk* in these two villages are also used for sand mining; some showed intense mining activities with a large mining area. Sand mining activities use heavy and large-scale equipment and employ many workers. The use of these heavy equipments accelerate the process of land degradation and loss of vegetation. *Gumuk* in Suren Village is dominated by stone mining, namely stone blocks and stone slabs. Suren village is famous for having the best slab mining products compared to other areas in Jember Regency. Stone mining activities are still carried out traditionally. The distribution of *Gumuk* by land use type is shown in Figure 3.

Herbaceous Diversity in Ledokombo District

A total of 120 herbs consisting of 49 families were found in all types of *Gumuk*. The ten most commonly found families are Asteraceae (14 species), Poaceae (10 species), Lamiaceae (9 species), Cyperaceae (6 species), Rubiaceae (5 species), Amaranthaceae (5 species), Pteridaceae (4 species), Zingiberaceae (4 species), Commelinaceae (3 species), and Oxalidaceae (3 species). Asteraceae is a family that has a high species diversity that can live in various habitats; this family has essential benefits as food providers, medicine, and ornamental plants, as well as the Lamiaceae family (Michel et al. 2020; Saini et al. 2020; Garcia-Oliveira 2021; Kurniawan et al. 2022). Even some Asteraceae have a high potential for new functional foods (Garcia-Oliveira 2021; Kurniawan et al. 2022). Asteraceae dominance was also reported on herbaceous dynamics in urban areas in India (Khan 2020), also became the family with the highest IVI value

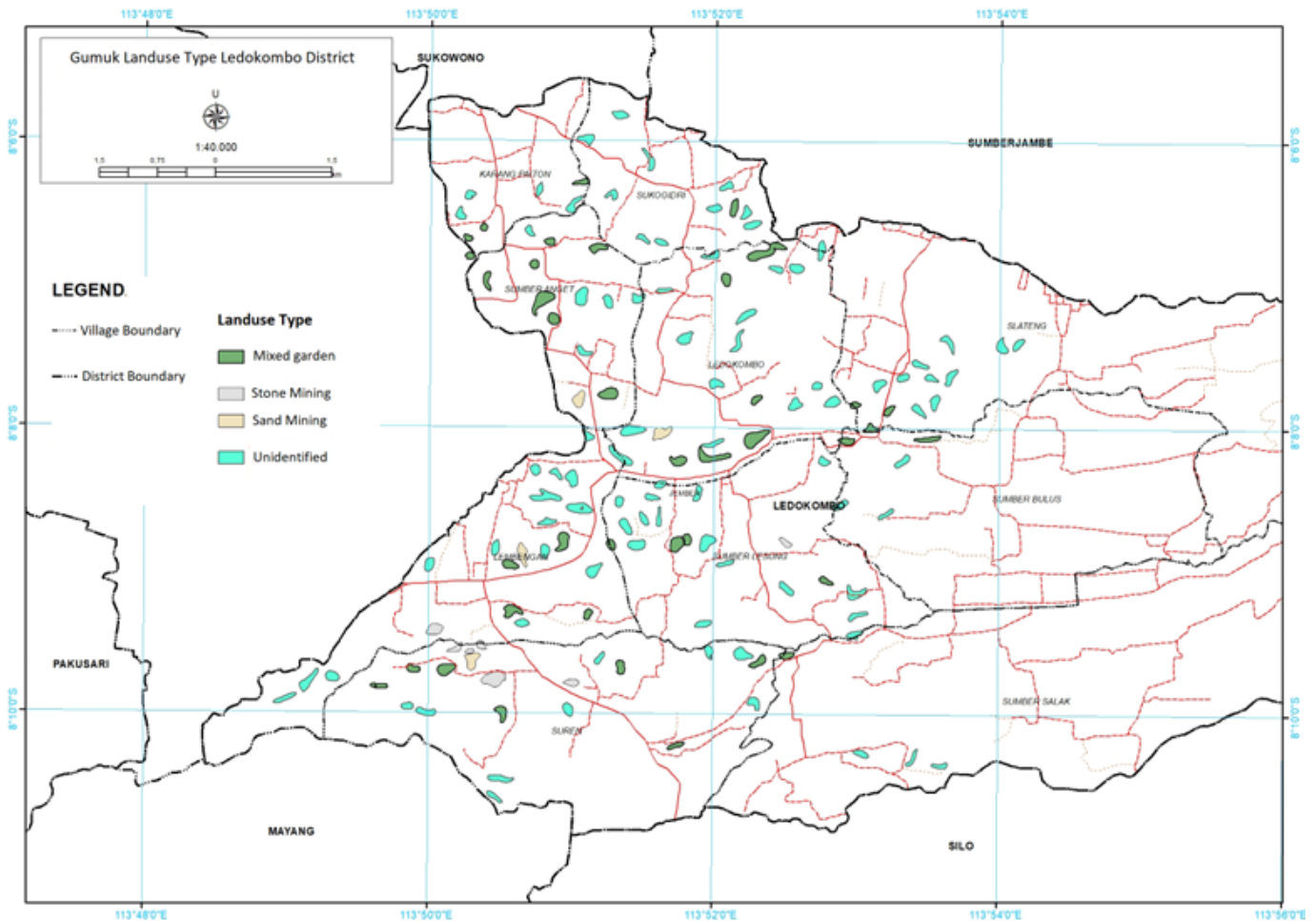


Figure 3. Distribution of *Gumuk* by land use type in each village in Ledokombo District.

in the Savannas in Padar and Komodo Islands (Sutomo 2020). This weed dispersal strategy is strongly influenced by geographical conditions (Dematteis et al. 2019), natural seed dispersal by wind also contributes to the breeding and spread of this weed at the landscape level (Mao et al. 2022).

Based on land use type, *Gumuk* with mixed gardens showed the highest species diversity (109 species, 49 families) compared to sand mining (46 species, 27 families) and stone mining (48 species, 25 families) (Figure 4). There is a significant difference in species diversity between mixed gardens and the other two types of land use. In the mining area, sand and rock excavation show almost the same diversity of species and families. However, the *Gumuk* material in the two mining areas are quite different; artificial influences are more dominant in the presence of plants. Landscape changes tend to be dominated by disturbances caused by human activities. It is clear that land cover changes are mainly caused by direct human use through agriculture, grazing, forestry, and development (Indrawan et al. 2007; Pearson 2022).

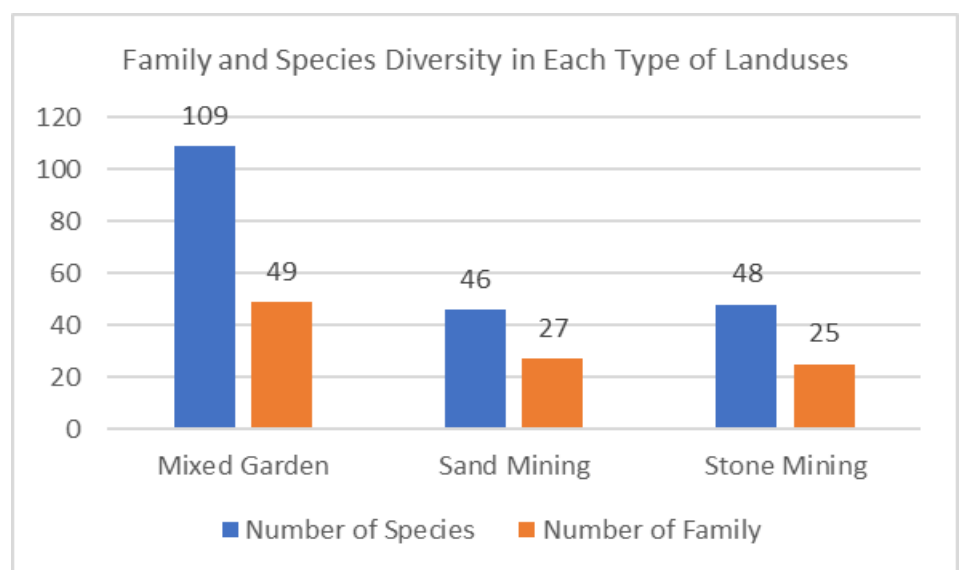


Figure 4. Family and species diversity in each type of land uses in Ledokombo District.

The highest Important Value Index (IVI) in the mixed garden was *Digitaria sanguinalis* (L.) Scop. (26.54%), *Commelina erecta* (14.72%), and *Oplismenus undulatifolius* (10.40%). While in sand mining, the species with the highest Important Value Index (IVI) was *C. erecta* (17.56%), *D. sanguinalis* (L.) Scop. (13.95%), and *Drymaria cordata* (13.34%). Furthermore, the highest Important Value Index (IVI) in stone mining was *D. sanguinalis* (L.) Scop. (20.74 %), *Alternanthera sessilis* (L.) R. Br. ex D (12.57%), and *Chromolaena odorata* (12.36%) (Table 1). The IVI can describe the role of a species in the ecosystem; the high IVI indicates that the species greatly affects the stability of the ecosystem (Fachrul 2007; Wijana 2014).

The *D. sanguinalis* (L.) Scop. was a species that have high dominance in all types of land use. This species belongs to the Poaceae family, which has a high tolerance for disturbance, is resistant to dry, hot, and highly competitive conditions, also known as an agricultural weed (Jones 2021; Kanupriya 2021). Dominance of *D. sanguinalis* (L.) Scop. was also reported in Wonogiri Indonesia (Solikhatun et al. 2019). This species contains phytotoxic substances that exhibit several types of bioactivities such as anti-inflammatory and antifungal (Kanupriya et al. 2021). Its

Table 1. The Five Highest Important Value Index (IVI) for each land-use type in Ledokombo District.

Landuse Type	Species	IVI (%)
Mixed Garden	<i>Digitaria sanguinalis</i> (L.) Scop.	26.54
	<i>Commelina erecta</i>	14.72
	<i>Oplismenus undulatifolius</i>	10.4
	<i>Synedrella nodiflora</i>	9.28
	<i>Peperomia pellucida</i>	8.00
Sand Mining	<i>Commelina erecta</i>	17.56
	<i>Digitaria sanguinalis</i> (L.) Scop.	13.95
	<i>Drymaria cordata</i>	13.34
	<i>Eleusine indica</i>	12.19
	<i>Perilla frutescen</i>	10.49
Stone Mining	<i>Digitaria sanguinalis</i> (L.) Scop.	20.74
	<i>Alternanthera sessilis</i> (L.) R. Br. ex D	12.57
	<i>Chromolaena odorata</i>	12.36
	<i>Tithonia diversifolia</i>	10.4
	<i>Commelina erecta</i>	9.3

high distribution and abundance could be utilized to explore its benefit and reduce its role as a weed. Meanwhile, *C. erecta* has the highest IVI in sand mining and ranks second in mixed gardens. This species also has a high adaptability and can be used as an environmental parameter to see the level of pollution (Tongo et al. 2021).

In addition to *D. sanguinalis* (L.) Scop and *C. erecta*, the species with the highest IVI values in the three landuses were quite varied, landuse differences being the main factor. However, other species that have a high IVI are dominated by Asteraceae, such as *Synedrella nodiflora*, *Chromolaena odorata*, *Tithonia diversifolia*, these three species were found in all types of landuse. Asteraceae is known as a family that has a high variety of species and spreads in almost every type of habitat.

The Dominance index (D) in mixed gardens, sand mining, and stone mining shows almost similar values (0.07, 0.07, and 0.07) (Table 2). The dominance index ranges from 0 – 1; the smaller the value indicates the absence of a dominating species, while the closer to 1 indicates the dominance of certain species in an ecosystem (Odum 1971). The three land-use types show species dominance in the low category, which means that no particular species dominate in the three land-use types.

The Simpson Index (D') in three types of *Gumuk* land use showed the same value (0.92) (Table 2). This indicates that the complexity of the community in the *Gumuk* ecosystem is relatively high (Odum 1971). Likewise, the Shannon Wiener index (H') showed the same value for the three types of *Gumuk* (>3) (Table 1), which indicates that the species diversity of herb in the *Gumuk* ecosystem is in the high category (Odum 1971). The difference in land use types does not affect the diversity of herbaceous species; even though the ecosystem is disturbed, it still has a relatively wide variety of species. This is also supported by another report that the stability of herb composition was shown to be related to species richness before disturbance (Kermavnar et al. 2021). Before the disturbance, *Gumuk* was initially used for plantations and the plant diversity was quite complex. Even though there are mining activities, it is possible that the plant species could still survive.

Abiotic parameters (Table 3) in each land use type also show slight differences; the difference is quite visible in light intensity. In mixed gardens, the light intensity is lower due to the tree stands. Soil humidity in mixed gardens is higher than the two landuses, this soil moisture will determine the availability of water in the soil for plant growth. Several

Table 2. Diversity index for each type of land use in Ledokombo District.

Diversity Index	Mixed Garden	Sand Mining	Stone Mining
Dominance (D)	0.07	0.07	0.07
Simpson_(1-D)	0.92	0.92	0.93
Shannon (H)	3.25	3.03	3.18
Evenness (eH/S)	0.23	0.45	0.50

Table 3. Abiotic parameters in each type of land use in Ledokombo District.

Abiotic Parameters	Mixed Garden	Sand Mining	Stone Mining
Temperature (°C)	29.09 ± 2.76	26.68 ± 3.04	29.29 ± 2.20
Humidity (%)	78.58 ± 6.50	80.40 ± 4.16	74.71 ± 5.99
Soil pH	6.30 ± 0.35	6.43 ± 0.49	6.76 ± 0.16
Soil Moisture (%)	69.77 ± 14.06	53.00 ± 23.35	45.57 ± 21.66
Light Intensity (Lux)	5737.60 ± 5502.44	12390.00 ± 6606.24	11147.14 ± 5727.46

families were noted to have significance on soil moisture and pH (Irakiza et al. 2022). The large number of stands in the mixed garden causes low light intensity, this makes the high soil moisture in this area higher than the others. These abiotic parameters were taken from each observation plot in the morning, afternoon, and evening.

Evenness index (E) showed different values in the three types of land use. The mixed garden was 0.23, sand mining was 0.45, and stone mining was 0.50. The evenness of species was in a low category in the diverse park, while in sand mining and stone mining, the evenness of species is in the moderate category. Evenness index value (E) ranged between 0 – 1. The value closer to 1 indicates that all species have an even abundance (Odum 1971; Magurran 1988).

CONCLUSIONS

There are 136 *Gumuk* in Ledokombo District; Ledokombo, Lembengan, and Suren villages have 51% of the total *Gumuk* in Ledokombo District. In mixed gardens, 109 species were found, indicating that herb diversity was twice as great as that of sand mining (46 species) and rock mining (48 species). The *D. sanguinalis* (L.) Scop. has highest IVI value in two types of *Gumuk*, including mixed gardens (26.54%) and stone mining (20.74%). While in sand mining, the highest IVI is *C. erecta* (17.56%). The Dominance index in the three types of *Gumuk* showed low category. The complexity of the herb community in the *Gumuk* ecosystem can be categorized as high ($D' = 0.9$), as well as the level of species diversity ($H' > 3$). Meanwhile, the evenness level of herbaceous species in the mixed gardens ($E = 0.2$) was lower than in sand mining ($E = 0.4$) and stone mining ($E = 0.5$). It is essential to continuously observe changes in vegetation composition to identify demographic patterns and impacts of changes to the *Gumuk* landscape.

AUTHOR CONTRIBUTION

WM, LH, JB, and SDT drafted the concept and developed the methodology; WM and LH collected the data; WM, LH, and JB were responsible for vegetation analysis and species verification; SDT was responsible for analysing and reviewing maps; WM wrote and edit the manuscripts; LH, JB, and SDT finalised the manuscripts.

ACKNOWLEDGMENTS

We are thankful to The Indonesian Ministry of Religion that supported this study through the 5000 Doctoral Program (SK PPK No. 4832 30 August 2019).

CONFLICT OF INTEREST

This research was conducted as an effort to conserve *Gumuk*, but to develop a strategy for *Gumuk* conservation one has to deal with the personal interests of the local community as the owner of *Gumuk*.

REFERENCES

- Abidin, Z. et al., 2020. Refugia effect on arthropods in an organic paddy field in Malang District East Java Indonesia. *Biodiversitas*, 21(4), pp.1415-1421. doi: 10.13057/biodiv/d210420
- Becker, C.A. & Brink, B., 1965. *Flora of Java (Spermatophytes only) Volume II*. Groningen, Nordhoff.
- Bemmelen, R.W.V., 1949. *The Geology of Indonesia Vol. IA: General Geology of Indonesia and Adjacent Archipelagos*. Government Printing Office, The Hague, pp.545-657.
- Conrad, O. et al., 2015. System for Automated Geoscientific Analyses (SAGA) v. 2.1.4. *Geoscientific Model Development*, 8, pp.1991-2007. doi: 10.5194/gmd-8-1991-2015
- da Silva, I.C.B. et al., 2020. Spatial variation of herbaceous cover species community in Cu-contaminated vineyards in Pampa biome. *Environmental Science and Pollution Research International*, 27(12), pp.13348-13359. doi: 10.1007/s11356-020-07851-zs
- Dematteis, B., Maria, S.P. & Juan, P.C., 2019. The Evolution of dispersal traits based on diaspore features in South American populations of *Senecio madagascariensis* (Asteraceae). *Australian Journal of Botany*, 67(4), pp.358-366. doi: 10.1071/BT18177
- Fachrul, M.F., 2007. *Metode sampling bioekologi*. Bumi Aksara, Jakarta.
- Garcia-Oliveira P. et al., 2021. Traditional plants from Asteraceae family as potential candidates for functional food industry. *Food & Function*, 12(7), pp.2850-2873. doi: 10.1039/d0fo03433a
- Gustafson, E.J., 2002. *Simulating Changes in Landscape Pattern*, in: S.E. Gergel and M.G. Turner (Eds.), *Learning Landscape Ecology: a Practical Guide to Concept and Techniques*. Springer, Chapter 5. pp. 49-61
- Hakim, L., 2015. *Rempah dan herba kebun pekarangan rumah masyarakat: Keragaman, Sumber Fitofarmaka dan Wisata Kesehatan-kebugaran*. Dandra Pustaka Indonesia, Yogyakarta.
- Hammer, Ø., Harper, D.A.T. & Ryan, P.D., 2001. PAST: paleontological statistics software package for education and data analysis. http://palaeo-electronica.org/2001_1/past/issue1_01.htm
- Hang, L., 2020. Melihat Kembali Strategi Komunitas Tanoker. *Buletin Tanoker*, VI edition, Jember.
- Hasan, S.S. et al., 2020. Impact of land-use change on ecosystem services: A review. *Environmental Development*, 34, 100527. doi: 10.1016/j.envdev.2020.100527.
- Horvath, Z., 2019. Habitat Loss Over Six Decades Accelerates Regional and Local Biodiversity Loss Via Changing Landscape Connectance. *Ecology Letters*, 22, pp.1019-1027. doi: 10.1111/ele.13260
- Ikhsan, F.A. et al., 2019. The hazard of change landscape and hydrogeology zone south karst mountain impact natural and human activity in Region Jember. *IOP Conference Series: Earth and Environment Science*, 243, 012036. doi: 10.1088/1755-1315/243/1/012036
- Indrawan, M., Primack, R.B., Supriatna, J., 2007. *Biologi Konservasi*. Yayasan Obor Indonesia, Jakarta.
- Irakiza, R. et al., 2022. Environmental and Management Factors That Influence Commelina Species in Selected Agro-Ecological Zones in Western Kenya. *American Journal of Plant Sciences*, 13, pp.884-911. doi: 10.4236/ajps.2022.136059

- Jhariya, M.K. & Singh L., 2021. Herbaceous diversity and biomass under different fire regimes in a seasonally dry forest ecosystem. *Environment, Development and Sustainability*, Springer, 23, 2021, pp.6800–6818. doi: 10.1007/s10668-020-00892-x
- Jones, E.A.L., Contreras, D.J. & Everman, W.J., 2021. Chapter 9 - *Digitaria ciliaris*, *Digitaria ischaemum*, and *Digitaria sanguinalis*, In: Chauhan BS (Ed.). *Biology and Management of Problematic crop weed species*, pp.173–195. doi: 10.1016/B978-0-12-822917-0.00014-8
- Kanupriya et al., 2021. Medicinal potential of *Digitaria*: an overview. *Journal of Pharmacognosy and Phytochemistry*, 10(1), pp.1717–1719.
- Kermavnar, J. et al., 2021. Post-harvest forest herb layer demography: general patterns are driven by pre-disturbance conditions. *Forest Ecology and Management*, 491, 119121. doi: 10.1016/j.foreco.2021.119121
- Khan, N. et al., 2020. Herbaceous dynamics and CO₂ mitigation in an urban setup—a case study from Chhattisgarh India. *Environmental Science and Pollution Research*, 27, pp.2881–2897. doi: 10.1007/s11356-019-07182-8
- Kurniawan, B., Purnomo & R.S. Kasiamdari, 2022. Diversity, Abundance, and Traditional Uses of Asteraceae Species in Mount Bisma, Dieng Plateau, keajar Wonosobo Central Java. *Journal of Tropical Biodiversity and Biotechnology*, 7(1), jtbb66953. doi: 10.22146/jtbb.66953.
- La Rosa, A. et al., 2021. Ethnobotany of the Aegadian Islands: safeguarding biocultural refugia in the Mediterranean. *Journal of Ethnobiology and Ethnomedicine*, 17, 47. doi: 10.1186/s13002-021-00470-z
- Magurran, A.E., 1988. *Ecological Diversity and Its Measurement*. Princeton University Press, New Jersey, 1988, pp.1–47.
- Maisyaroh, W., 2014. *Pemanfaatan tumbuhan liar dalam pengendalian hayati*. UB Press, 2014.
- Maisyaroh, W. et al., 2021. Bird Diversity in the Gumuk Ecosystem in Jember. *IOP Conference Series: Earth and Environmental Science*, 886, 012046. doi: 10.1088/1755-1315/886/1/012046
- Mao, R. et al., 2022. Wind dispersal of seeds of *Parthenium hysterophorus* L. (Asteraceae) contributes to its steady invasion and spread. *Austral Ecology: A Journal of Ecology in the Southern Hemisphere*, 47 (4), pp.791–803. doi: 10.1111/aec.13159
- Michel, J., Abd Rani, N.Z. & Husain, K., 2020. A review on the potential use medicinal plant from Asteraceae and Lamiaceae plant family in cardiovascular diseases. *Frontiers in Pharmacology*, 11, 852. doi: 10.3389/fphar.2020.00852
- Mueller-Dombois, D. & Ellenberg, H., 1974. *Aims and Methods of Vegetation Ecology*. John Wiley and Sons, New York.
- Newbold, T. et al., 2020. Global effects of land use on biodiversity differ among functional groups. *Functional Ecology*, 34(3), pp.684–693. doi: 10.1111/1365-2435.13500
- Odum, E.P., 1971. *Fundamental of Ecology*, Ed. 3. Oxford University Press, New York.
- Pearson, S.C., 2022. *Landscape patterns from organism-based perspectives*, In: Gergel SE, Turner MG (Eds.). *Learning Landscape Ecology (A Practical Guide to Concepts and Technique)*. Springer-Verlag, New York. pp.187–198.
- Saini, I., Chauhan, J. & Kaushik, P., 2020. Medicinal value of domiciliary ornamental plants of the Asteraceae family. *Journal of Young Pharmacists*, 12(1), pp.3–10. doi: 10.5530/jyp.2020.12.2

- Saripah, B. et al., 2020. Zingiberaceae essential oils as a potential biopesticide for cocoa pod borer, *Conopomorpha cramerella* Snellen, In: Niogret J, Sanchez V, Marelli J-P (Eds.). *Proceedings of an Asia-Pacific Regional Cocoa IPM Symposium, Australian Centre for International Agricultural Research*, Canberra, pp.35-40.
- Solikhatun, I., Maridi & Budiastuti S., 2019. Analisis vegetasi penutup lantai (Lower Crop Community- LCC) di kawasan sabuk hijau Waduk Serbaguna Wonogiri. *Seminar Nasional Pendidikan Biologi dan Saintek (SNPBS) ke-IV*, pp.354-363.
- Sutomo, S., 2020. Vegetation Composition of Savanna Ecosystem as a Habitat for The Komodo Dragon (*Varanus komodoensis*) on Padar and Komodo Islands, Flores East Nusa Tenggara Indonesia. *Journal of Tropical Biodiversity and Biotechnology*, 5(1), pp.10-15. doi: 10.22146/jtbb.48280.
- Sutriono, Purba E. & Marheni, 2019. Insect management with refugia plant in upland rice (*Oryza sativa* L.). *IOP Conference Series: Earth and Environmental Science*, 260, p. 012138. doi: 10.1088/1755-1315/260/1/012138
- Tongo, I., et al., 2021. Levels, bioaccumulation and biomagnification of pesticide residues in a tropical freshwater food web. *International Journal of Environmental Science and Technology*, 19(3), pp.1467-1482. doi: 10.1007/s13762-021-03212-6
- Turner, M.G., Robert, H.G. & Robert, V.O., 2001. *Landscape Ecology in Theory and Practice: Pattern and Process*. Springer-Verlag: New York.
- Van Steenis, C.G.G.J., 2006. *Flora Pegunungan Jawa*. LIPI Press, Jakarta.
- Wijana, N., 2014. *Metode analisis vegetasi*. Plantaxia, Yogyakarta.
- Zuidam, R.A.V. & Cancelado, F.I.V.Z., 1979. *ITC Textbook of Photo-Interpretation, Vol. VII, Use of Aerial Detection in Geomorphology and Geographical Landscape Analysis, Chapter 6, in Terrain Analysis and Classification Using Aerial Photographs: a Geomorphological Approach*. International Institute for Aerial Survei and Earth Science (ITC).

Research Article

In Silico Approach for DNA Barcoding using Phylogenetic Analysis of *Coelogyne* spp. based on the *matK*, *rpoC1*, *rbcl* and nrDNA Markers

Apriliana Pratiwi^{1,2}, Anggiresti Kinasih^{1,2}, Maura Indria Meidianing^{1,2}, Febri Yuda Kurniawan^{1,3}, Endang Semiarti^{2*}

1)Biology Orchid Study Club (BiOSC), Faculty of Biology, Universitas Gadjah Mada, 55281 Yogyakarta, Indonesia

2)Department of Tropical Biology, Faculty of Biology, Universitas Gadjah Mada, 55281 Yogyakarta, Indonesia

3)Study Program of Biotechnology, Graduate School, Universitas Gadjah Mada, 55281 Yogyakarta, Indonesia

*Corresponding author, email: endsemi@ugm.ac.id

Keywords:

Coelogyne
conservation
DNA barcoding
in silico
phylogenetic analysis

Submitted:

18 February 2022

Accepted:

19 May 2023

Published:

02 October 2023

Editor:

Furzani Binti Pa'ee

ABSTRACT

In silico biology is considered as an effective and applicable approach to initiate various research, such as biodiversity taxonomical conservation. Phylogenetic analysis using *in silico* taxonomy method for orchid species can provide data on genetic diversity and evolutionary relationships. One particular method that can be used to evaluate specific targets of gene loci in the taxonomic study is DNA barcoding. This research was conducted to determine the specific target locus gene using *matK*, *rbcl*, *rpoC1*, and nrDNA markers for DNA barcoding of the *Coelogyne* genus with *in silico* approach using phylogenetic analysis. All marker sequences were collected from the NCBI website and analysed using several softwares and methods, namely Clustal X for sample sequence alignment and MEGA 11 for phylogenetic tree construction and analysis. The results showed that the gene locus in *Coelogyne* recommended was the nrDNA gene locus. Phylogenetic analysis revealed that the use of the nrDNA gene locus was able to separate 17 *Coelogyne* species with two outgroup species, namely *Cymbidium* and *Vanilla*, then followed with ribulose-1,5-bisphosphate carboxylase/oxygenase large subunit (*rbcl*) while the other gene loci, namely maturase K (*matK*) and polymerase beta' subunit (*rpoC1*) provided a visual phylogenetic tree in which the two outgroup species entered into the same clade as the *Coelogyne* species. Thus, the results of this study can be used as a reference to support the *Coelogyne* breeding and conservation program.

Copyright: © 2023, J. Tropical Biodiversity Biotechnology (CC BY-SA 4.0)

INTRODUCTION

Orchids (Orchidaceae) are herbaceous plants that have the potential to be used as research objects because of their large diversity. Orchid plant taxonomy is important for the plant classification, and various researchers can easily describe and identify variations and relationships between one species and another. *Coelogyne* is a genus of orchids with about 200 species spread throughout Asia (Chase et al. 2015), including India, China, Philippines, Pacific Indonesia, and Fiji Islands (Singh & Kumaria 2020). In Indonesia, most *Coelogyne* species are found in dense tropical forests, especially in Kalimantan, Sumatra, and Sulawesi, and several species have not been identified. One of Indonesia's endemic species is *Coelogyne pandurata*, or black orchid found in East Kalimantan (Hartati &

Muliawati 2020) The IUCN's ecological conservation status of *Coelogyne* is least concerned in CITES (Convention on International Trade in Endangered Species of Fauna and Flora), *Coelogyne pandurata* is classified as Appendices II. Identification of *Coelogyne* species in Indonesia based on morphological characterisation was already done in previous research using phenetic taxonomy. The study found that *C. pandurata* from East Kalimantan has high morphological similarities with *C. rumphii* from South Sulawesi, and *C. mayeriana* from Kalimantan has high similarity with *C. asperata* from West Kalimantan (Hartati et al. 2019). However, the combination of homologous and non-homologous data becomes biased and the evolutionary relationship was not given as information in phenetic taxonomy.

Advances in the field of science strongly support the development of a classification system, namely phylogenetic taxonomy (Haider 2018). Phylogenetic taxonomic studies produce classification data for species collection and provide information about the relationship between species (Rivero 2016) because the data used include DNA sequence data (Nauheimer et al. 2018; Zhang et al. 2021). The phylogenetic analysis system can also contribute to the conservation of orchid plants such as *Coelogyne*. The taxonomic status of *Coelogyne* can be clarified through phylogenetic analysis so that conservation priorities are known (Li et al. 2018). Unique evolutionary lineages of *Coelogyne* can also be identified to compare rare and widespread species. The nucleotide sequence of a standard genome region is needed as a tool for species identification to produce a phylogenetic tree with a higher level of discrimination. This process can be achieved by determining DNA barcodes. DNA barcoding method is currently known as one aspect of genetic conservation managements (Kim et al. 2014). DNA barcoding is now widely practiced and often used because it can support various studies, such as complementing information in plant classification and increasing authentication and identification of medicinal plants (Mishra et al. 2016; Parveen et al. 2016).

Research on DNA barcoding in *Coelogyne* has been carried out previously in India. Still, this study only used the *rbcl* gene and *Coelogyne* species in India, so there is no information about *C. pandurata* (Ramudu & Khasim 2016). The previous research also conducted phylogenetic analysis but it only focused on the relationship between *C. fimbriata* and *C. ovalis* using a combination of chloroplast fragments and *matK*. Still, *matK* phylogenetic tree has low bootstrap results (Jiang et al. 2020). A comparison of five different loci, such as *rbcl*, *rpoB*, *rpoC1*, *matK*, and *ITS* has been done and shown that *ITS* is the most efficacy barcode that can be used for discriminate 47 genera of Indian Orchid then, followed by *matK* (Parveen et al. 2017). Based on genetic distance, phylogenetic tree, and similarity of 94 genera of five subfamilies of medicinal Orchidaceae from Asia, a single barcode region such as *ITS* then *matK* has higher species discrimination capability than the combination of two barcode region (Raskoti & Ale 2021). It also has similarities with the jewel orchids in Vietnam, where multi-locus barcodes cannot improve resolution for species classification (Ho et al. 2021). The results of DNA barcoding in the genera level, infrageneric rank, and species level may have a different result, such as in *Euphrasia* where *ITS* barcoding cannot provide a clear resolution of species-level separation (Wang et al. 2018). In some arid plant, *rbcl* (88%) have a higher success amplification rate than *matK* as a barcode (Bafeel et al. 2011). Previous study showed that *matK* have high resolution in discriminate orchid in intergeneric level of family Orchidaceae, but not a good barcode to resolve phylogeny at intrageneric of *Dendrobium* (Chattopadhyay et al. 2017).

In this study, a phylogenetic analysis is conducted on intrageneric level in *Coelogyne* genera using the *in silico* method, through DNA barcode of *matK*, *rbcl* and *rpoC*. In this research, *ITS* region was not included because the data was not available in the Gene Bank. Instead, nuclear ribosomal DNA (nrDNA) that consists of *ITS1-5,85S-ITS2* region was used. The use of DNA barcodes is based on various aspects, such as the type of living thing itself. The Plant Working Group Consortium for the Barcode of Life (CBOL) recommends the use of *rbcl* + *matK* as the core barcode in plant phylogenetic analysis (CBOL Plant Working Group 2009). In addition to the use of these two types of barcodes, it is highly recommended to carry out additional analysis using other types of barcodes (Hollingsworth et al. 2011). In various studies in the genetics of orchids and plants, *rpoC1* is one of the chloroplast genes often used (Parveen et al. 2016; Kim et al. 2020) which belongs to the *Coelogyne* genus (Singh & Kumaria 2020). In this research, *rpoC1* was present as an additional barcode to enhance the carried-out analysis and to compare the exact resolution between three loci that had better results. This research aim was to determine the specific target locus gene using *matK*, *rbcl*, and *rpoC1* markers for DNA barcoding of each species in *Coelogyne* genus with *in silico* approach using phylogenetic analysis.

MATERIALS AND METHODS

Materials

The research was carried out by accessing the DNA sequences of the *Coelogyne* genus from the *matK*, *rbcl*, *rpoC1* and nrDNA gene loci as the sample. Currently, research has found out that *Coelogyne* species with the *matK* gene locus have DNA sequence lengths up to 500-900 base pairs, *rpoC1* gene locus has up to 400-550 DNA base pairs, *rbcl* gene locus has ± 600 DNA base pairs, and nrDNA has 600-800 base pair. All DNA sequences belonging to Asian *Coelogyne* species were accessed via the nucleotide database at The European Bioinformatics Institute (EBI) (<https://www.ebi.ac.uk/>) and National Center for Biotechnology Information (NCBI) GenBank (www.ncbi.nlm.nih.org/nucleotide) (Vu et al. 2018). Based on NCBI, there were 21 sequences and 19 sequences collected from EBI which had *matK*, *rbcl*, *rpoC1* and nrDNA gene loci. Gene loci with unverified names were not used and removed from the data. Each sequence was selected into a separate gene locus and was selected based on the specifications of the nucleotide base length of each locus. The final 19 loci were used for analysis in this study (Table 1).

Methods

The sequences of each species that have been found were then collected in FASTA format. The alignment of the collected sequences was performed using the CLUSTAL X software program, and the .aln output format was predefined. The .aln output of the CLUSTAL X software program was processed with MEGA 11 and then saved in MEGA format for phylogenetic tree analysis (Hall 2013). The best model for constructing a phylogenetic tree for each data set is determined in advance in the program. The phylogenetic tree construction method used in this study is Neighbor-Joining with 1000 bootstrap based on the best model tamura-3-parameter (Ho & Nguyen 2020).

Data analysis was performed from the most representative gene locus for phylogenetic analysis using MEGA 11 and DNAsp. Genetic variation was observed to learn about the polymorphic data that represent the mutation of each nucleotide. The genetic distance matrix was conducted to determine the divergence between each species in the *Coelo-*

Table 1. The *matK*, *rpoC1*, *rbcL* and nrDNA sequences of 19 species of *Coelogyne* and 2 outgroup species of *Cymbidium* and *Vanilla* used in the study.

Orchid Species	Accession Number			
	<i>matK</i>	<i>rbcL</i>	<i>rpoC1</i>	nrDNA
<i>Coelogyne asperata</i>	KU877844	KU877824	KX037361	AF281128
<i>Coelogyne mayeriana</i>	MN400412	MN400420	-	AF281129
<i>Coelogyne pandurata</i>	KU877841	MN416671	KU219954	AF281130
<i>Coelogyne trinervis</i>	KF974497	JN005393	KP662087	AF302744
<i>Coelogyne rochussenii</i>	MK398201	MN416673	KP662089	MK356175
<i>Coelogyne cumingii</i>	MK398200	MN400414	KP662086	MK356172
<i>Coelogyne verrucosa</i>	AY003884	-	-	AF281131
<i>Coelogyne ovalis</i>	MN416677	MN416668	MT067929	KY966509
<i>Coelogyne fimbriata</i>	KR905392	KU219968	KP662093	EU441205
<i>Coelogyne nitida</i>	JN004370	MK155298	KP662088	HQ130496
<i>Coelogyne schilleriana</i>	KU877839	KU219970	KU219952	-
<i>Coelogyne pachystachya</i>	KU877838	KU219969	KU219951	-
<i>Coelogyne barbata</i>	KX298581	KU219960	KP662085	AF302755
<i>Coelogyne velutina</i>	KU877840	MN416675	KU219953	AF302753
<i>Coelogyne xyrekes</i>	MK398225	KU219966	KP662092	MK356198
<i>Coelogyne pulverula</i>	KU877846	KU877826	KX037358	MK356157
<i>Coelogyne viscosa</i>	KX298597	KU219955	KP662080	MK356152
<i>Coelogyne fuscescens</i>	KF974501	KU219959	KP662084	KF866234
<i>Coelogyne eberhardtii</i>	MN400408	MN400416	KP662091	AF302754
<i>Cymbidium aloifolium</i>	KX298600	JN005425	HM053600	JF729014
<i>Vanilla planifolia</i>	MF349972	JN005701	JN005354	AF030049

gyne genus. Haplotype was determined to learn about the location of inherited allele groups from a single parent using DNA sp, and a haplotype map was constructed using Network. GC content and nucleotide diversity were determined to ensure the data is valid for *Coelogyne* genus.

RESULTS AND DISCUSSION

This research was conducted using the NCBI website to search for *Coelogyne* DNA barcodes consisting of three 4 gene loci, namely *matK*, *rpoC1*, *rbcL*, and nrDNA. Based on result given in the Table 2, *matK* locus have the lowest G+C content and nrDNA has the highest G+C content. Moderate amount of G+C content about 29.48% for *matK*, 44.12% for *rpoC1*, 42.18% for *rbcL* and 57.27% for nrDNA . Based on (Wu et al. 2020) the overall G+C content of *Coelogyne* is 43.3%, so the most representative data for G+C content was *rpoC1* and *rbcL*. The result is similar with previous study that stated *rbcL* and *rpoC1* has good quality of sequence compared to other locus (Parveen et al. 2016; Hosein et al. 2017; El-Sherif & Ibrahim 2020).

However, based on examination using DNAsp (Table 3), *rbcL* and *rpoC1* has lowest parsimony, also *rbcL* shown lowest polymorphic, number of mutation, nucleotide diversity, and gaps compared to another locus. The *rbcL* gene encodes the formation of rubisco enzyme to fixation of carbon dioxide in light independent photosynthetic reactions, therefore, *rbcL* is important to maintain, so mutations are rare (Rajaram et al. 2019).

High number of mutation and haplotype diversity is shown in nrDNA that consists of internal transcriber spacer that located between small-subunit of ribosomal DNA. The pattern of high haplotype diversity (Hd:1.00) corresponds to relatively low nucleotide diversity (Pi:0.096)

Table 2. GC content of *Coelogyne* species based *matK*, *rpoC1*, *rbcL*, nrDNA gene locus.

Species	Guanin and Cytosin (G + C) content (%)			
	<i>matK</i>	<i>rpoC1</i>	<i>rbcL</i>	nrDNA
<i>Coelogyne pulverula</i>	28.04	44.27	42.19	55.64
<i>Coelogyne pandurata</i>	27.10	44.27	41.69	55.90
<i>Coelogyne rochussenii</i>	32.50	44.27	42.02	56.47
<i>Coelogyne asperata</i>	27.10	45.29	41.86	56.75
<i>Coelogyne xyrekes</i>	32.14	44.27	42.02	56.81
<i>Coelogyne viscosa</i>	28.97	44.27	42.19	56.99
<i>Coelogyne velutina</i>	28.50	44.52	42.19	57.08
<i>Coelogyne nitida</i>	28.50	44.27	42.69	57.30
<i>Coelogyne fuscescens</i>	28.97	44.27	42.52	57.39
<i>Coelogyne fimbriata</i>	27.10	44.27	42.19	57.41
<i>Coelogyne ovalis</i>	32.14	41.33	42.35	57.50
<i>Coelogyne eberhardtii</i>	31.79	44.27	42.35	57.69
<i>Coelogyne cumingii</i>	32.14	44.27	42.35	57.75
<i>Coelogyne trinervis</i>	28.97	44.02	42.19	57.96
<i>Coelogyne mayeriana</i>	32.50	-	41.86	58.02
<i>Coelogyne verrucosa</i>	27.10	-	-	58.06
<i>Coelogyne barbata</i>	27.57	44.02	42.19	58.81
<i>Cymbidium aloifolium</i>	32.24	42.96	42.02	68.27
<i>Vanilla planifolia</i>	30.48	42.74	43.02	53.87

indicating that the *Coelogyne* population has experienced rapid growth and expansion over time (Yun et al. 2020). The evolutionary processes can occur in an organism because of genetic mutations and or recombinant processes which then form new species (Dharmayanti 2011). The results in this study were a phylogenetic tree of the species collected and constructed using the MEGA 11 program. The formation of the clade represents the genetic relationship between the *Coelogyne* species. In the phylogenetic tree, *Cymbidium* and *Vanilla* used as a correction factor, because both were very distantly and far related from other *Coelogyne* species as can be seen in the values.

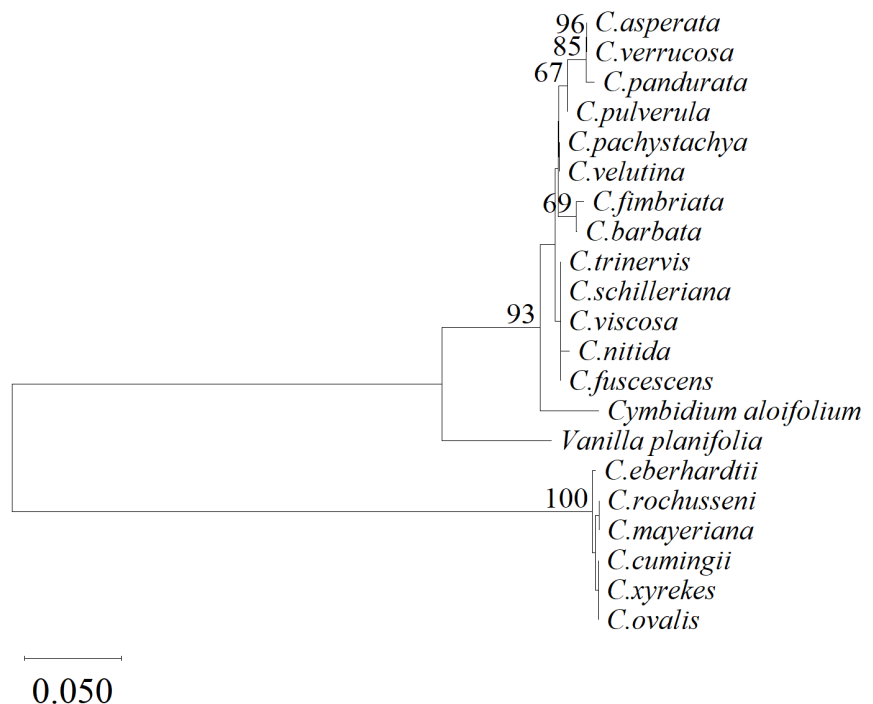


Figure 1. *Coelogyne* phylogenetic tree using the maturase K barcode (*matK*).

Table 3. Examination using DNAsp.

Data	<i>matK</i>	<i>rpoC1</i>	<i>rbcL</i>	nrDNA
Number of sites	290	1040	602	363
Gaps/missing data	86	651	0	70
Parsimony informative site	85	7	7	52
Variable polymorphic site	95	161	43	135
Total number of mutation	102	165	44	175
Nucleotide diversity (Pi)	0.18490	0.04627	0.0097	0.09602
Haplotype diversity (Hd)	0.914	0.784	0.9316	1.000
Number of haplotype (h)	12	10	13	19

Utilisation of the *matK* gene locus in the phylogenetic tree showed that *Coelogyne* was divided into 2 clades, where *Cymbidium* and *Vanilla planifolia* join the first clade of *Coelogyne* species (Figure 1). From the first clade, *C. pandurata*, *C. asperata* and *C. verrucosa* have a close evolutionary relationship. The second clade consists of *C. eberhardtii*, *C. rochussenii*, *C. cumingii*, *C. mayeriana*, *C. ovalis* and *C. xyrekes* (Figure 1). This indicated that *matK* gene locus showed inconsistent results due to the presence of *Cymbidium* and *Vanilla* in the same clade as several *Coelogyne* genera and *C. mayeriana* that located far away from another Indonesian orchid. This result is similar with previous research, barcode of *matK* showed the putative incongruence, therefore, it is non-functional for phylogenetic analysis of Orchidaceae. Many closely related species of Indian orchid cannot be discriminated by *matK* based on genetic distance, blast, and tree building method (Srivastava & Manjunath 2020).

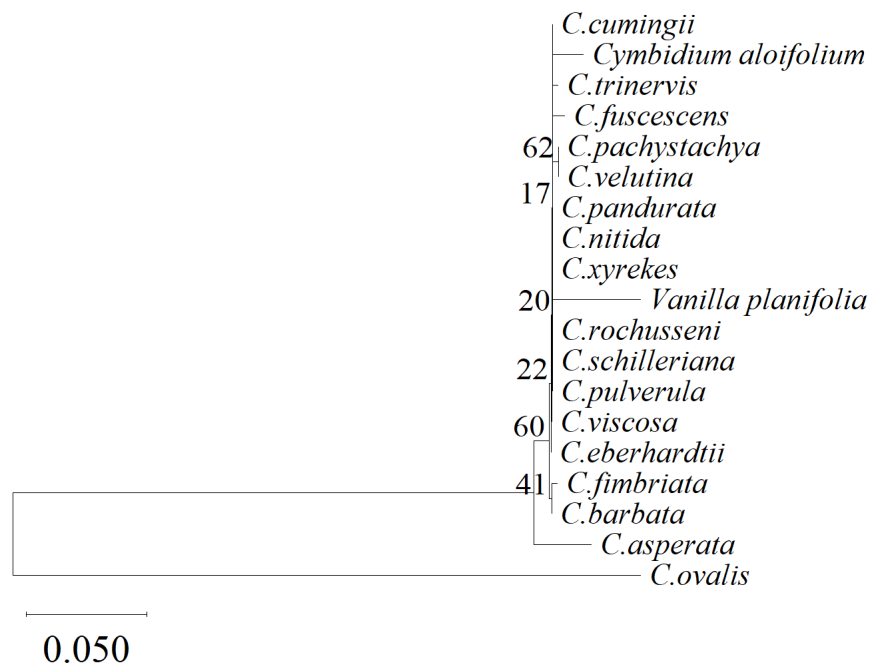


Figure 2. *Coelogyne* phylogenetic tree using RNA barcode of polymerase beta' subunit (*rpoC1*).

The result of phylogenetic tree construction using the *rpoC1* gene locus (Figure 2) cannot discriminate species in different genus and has low bootstrap value. *Cymbidium* and *Vanilla* should not be in the same clade as *Coelogyne* because it has a different genus. Species *Coelogyne* from Indonesia such as *C. pandurata*, *C. mayeriana* and *C. asperata* also located far apart. This indicated that the use of the *rpoC1* and *matK* gene locus was not effective as a basis or material for phylogenetic analysis in *Coelogyne*. The *rpoC1* locus is not recommended to be used in DNA barcoding

because it exhibits low polymorphism data compared to *matK* locus (Hosein et al. 2017). Locus gene of *rpoC1* showed low power in distinguishing genetic variability between some species compared to *rbcL* (El-Sherif & Ibrahim 2020). Species discrimination rates of *rpoC1* is the lowest compared to *rbcL*, *matK*, and *ITS* based on genetic distance, phylogenetic tree, and blast method after calculated using Kimura-2-parameter model (Parveen et al. 2017).

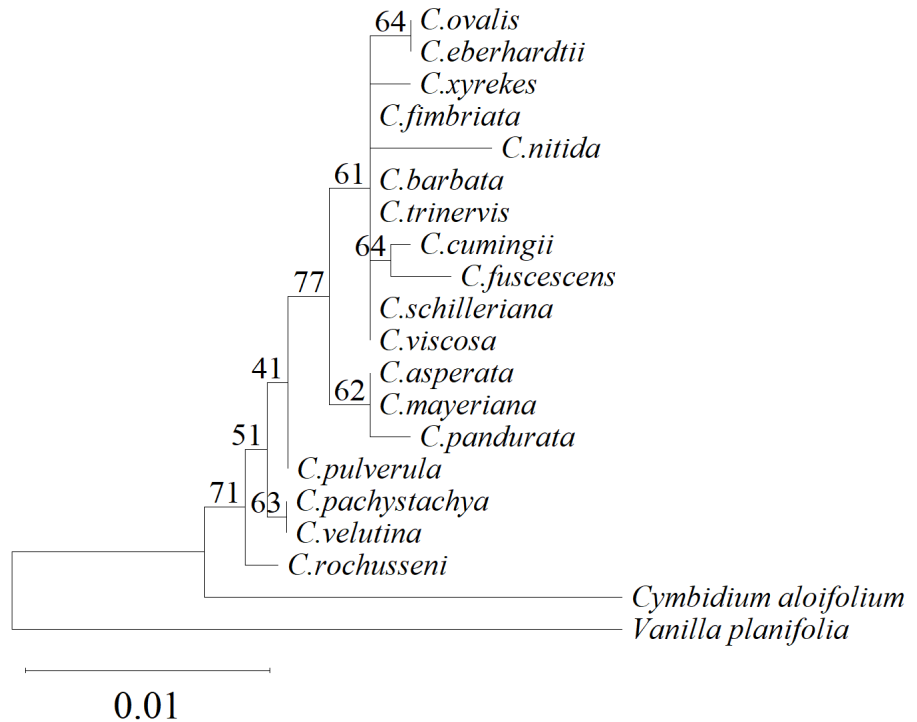


Figure 3. *Coelogyne* phylogenetic tree using the barcode of ribulose-1,5-bisphosphate carboxylase/oxygenase large subunit (*rbcL*).

The use of the *rbcL* gene locus in the phylogenetic tree (Figure 3) gave representative results as the basis for *Coelogyne* phylogenetic analysis because *Cymbidium* was in a separate clade with another 19 *Coelogyne* species. This result was also supported by (Ho et al. 2021), *rbcL* shown the best result as a DNA barcoding marker than *matK* for distinguishing some jewel orchid species. Gene locus of *rbcL* is the best for phylogenetic analysis compared to another plastid chloroplast regions. Discriminatory power of *rbcL* is higher than *matK* because it has good sequence quality, recoverability, and universality (Maloukh et al. 2017). The *rbcL* locus is a plastid gene in the chloroplast genome that encodes rubisco, considered sufficient and suitable for discrimination of Orchidaceae at the generic and species level (Ramudu & Khasim 2016). The visualisation of the phylogenetic tree shows that *Vanilla* lies on a different evolutionary path from other species. This showed that there is a close relationship between *Coelogyne* and *Cymbidium*, but *Coelogyne* has a distant evolutionary relationship with *Vanilla*.

The phylogenetic tree (Figure 3) also showed that all *Coelogyne* from Indonesia such as *C. mayeriana* from Kalimantan, *C. asperata* from West Kalimantan have close evolutionary relationship then followed with *C. pandurata* from East Kalimantan that classified in the same subclade. This result is in agreement with phenetic taxonomy that has been done previously in morphology comparison of each species from Indonesia (Hartati et al. 2019; Hartati & Muliawati 2020). However, the tree are not representative for the separation of orchids originating from Asia, such as *C. fimbriata* and *C. ovalis* which should have close relationship

(Jiang et al. 2020) but located far apart in the phylogenetic tree constructed with *rbcL*. The ability of *rbcL* to discriminate each genus within the same family was higher than *matK*, but both were less effective at differentiating species within the same genus. The discrimination power of *rbcL* in the intrageneric group is low compared to other locus (Chattopadhyay et al. 2017). Although having high quality sequence, *rbcL* species resolution was inferior, when using BLASTn and Neighbor-joining method tree, *rbcL* was unable to discriminate species in the same *Phaphiopedilum* genus (Rajaram et al. 2019). Discrimination rate and resolution of *rbcL* used to distinguish each *Coelogyne* species from India was 36.36% based distance method, 72.72% based on phylogenetic tree Kimura-2-parameter, 44.44% based on cluster and all of that considered as low (Ramudu & Khasim 2016).

In contrast, phylogenetic tree constructed with nrDNA locus (Figure 4) have high separation and discrimination power, this is related to *Cymbidium* and *Vanilla* that are already located as outgroup. Some of species already resolved into some different subclades and the evolutionary relationship can be distinguished. High bootstrap values are also shown in the branches which represent the close evolutionary relationship between *C. fimbriata* and *C. ovalis*. Orchid species from Indonesia, such as *C. asperata*, *C. pandurata*, *C. mayeriana*, also showed a close evolutionary relationship. *C. asperata* was closer to *C. verrucosa* compared to other species, it was relevant with previous research (Jiang et al. 2020). The phylogenetic tree constructed by nrDNA demonstrated high resolution and promising discrimination between intrageneric group of *Dendrobium* groups compared to *matK* and *rbcL* (Chattopadhyay et al. 2017). The reason nrDNA shows the best phylogenetic results is because 5,8S comprises conserved sequence and *ITS* generally carries variation among closely related genera. The phylogenetic tree constructed by maximum-likelihood method using *ITS* region showed high resolution and discrimination compared to *matK* and *rbcL* on 7 genera Indian endemic orchid (Srivastava & Manjunath 2020). Higher mutation rate obviously represent in *ITS* and *ITS2*, so it has great potential in systematic study and species identification (Duan et al. 2019).

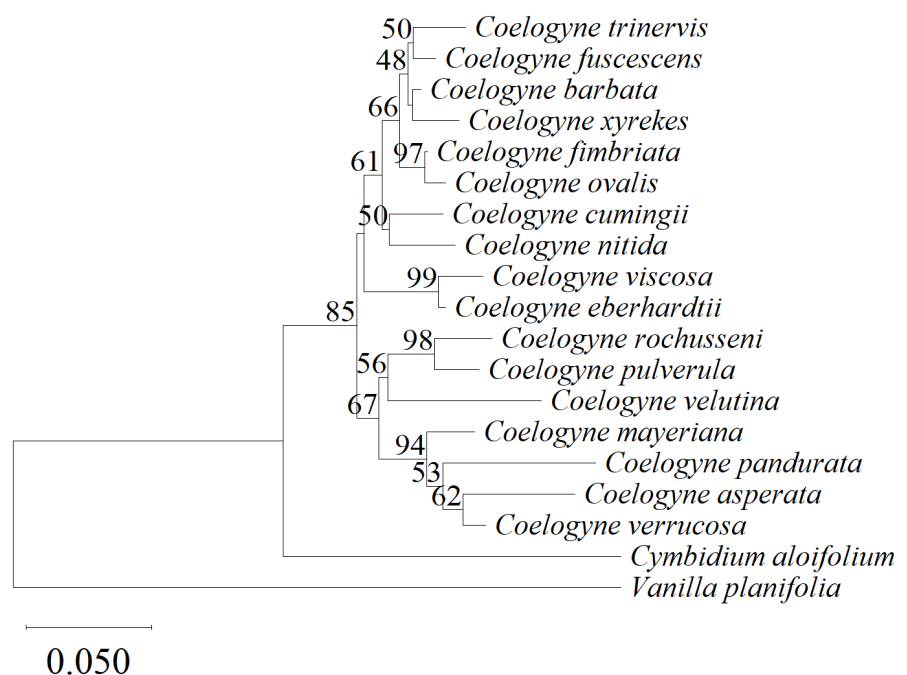


Figure 4. *Coelogyne* phylogenetic tree using the barcode of nrDNA (*ITS1+5,8S+ITS2*).

Total genetic distance shown in Table 4, for *rbcl* after generate using Tamura-3-parameter model shown the low value at 0.002–0.012. Some of species like *C.mayeriana*, *C.asperata*, *C.viscosa*, *C.schilleriana*, *C.trinervis*, *C.barbata*, *C.fimbriata* have the same pattern of genetic distance at 0.007. This result is in accordance with previous research that generate average interspecific distance 0.007 using Kimura-2-parameter model in some of *Coelogyne* species (Ramudu & Khasim 2016). This proves that *rbcl* is the most conserved one because it displays the lowest genetic sequence divergence value (Raskoti & Ale 2021).

Total genetic distance of nrDNA that consist of *ITS* region has highest value compared to *rbcl*. This result shown in Table 5, related to previous research that stated intraspecific genetic distance and interspecific variation in *ITS* ranged as highest followed by *ITS2* then the lowest is *rbcl* (Raskoti & Ale 2021). The genetic distance pattern of *C. mayeriana*, *C. pandurata*, and *C. asperata* which are considered as endemic orchid from Indonesia was distinct from other species due to differences in the origin of geographical population growth and evolutionary sources based on previous research (Yun et al. 2020).

There are 13 different haplotypes in total were observed in *rbcl* (Figure 5a). Based on *rbcl* haplotype distribution (Table 6), *C.viscosa*, *C.barbata*, *C.schilleriana*, *C.fimbriata*, and *C.trinervis* shared the same haplotype at H4. Species *C.pachystachya* and *C.velutina* also share the same haplotype at H9. *C.ovalis* and *C.eberhardtii* share same haplotype at H1. The frequency of H4 is 5 meanwhile frequency of H1, H2, and H7 is 2. Based on *rbcl* haplotype map (Figure 5a), H4 individu is the source of evolutionary formation of H1, H9, H6, H11 with low mutation line, and H7 with more mutation line. This is in accordance to each species such as *C. fimbriata* with H4 that has close evolutionary relationship with *C. ovalis* with H1. Indonesian orchid species, *C. asperata*, and *C.mayeriana* share the same haplotype in H2 and evolutionarily develop into H3 which consist of *C. pandurata*. Meanwhile, the form haplotype map that builds using nrDNA (Figure 5b), *C. pandurata* has H2 that develop from *C. mayeriana* with H16, then both evolved from *C. verrucosa* with H19, then all of them evolved from *C. asperata* with H17. Meanwhile *C. fimbriata* (H1) and *C. ovalis* (H18) join in the same median vectors, *Cymbidium* (H14) shows many mutation lines that developed from *C. fimbriata*.

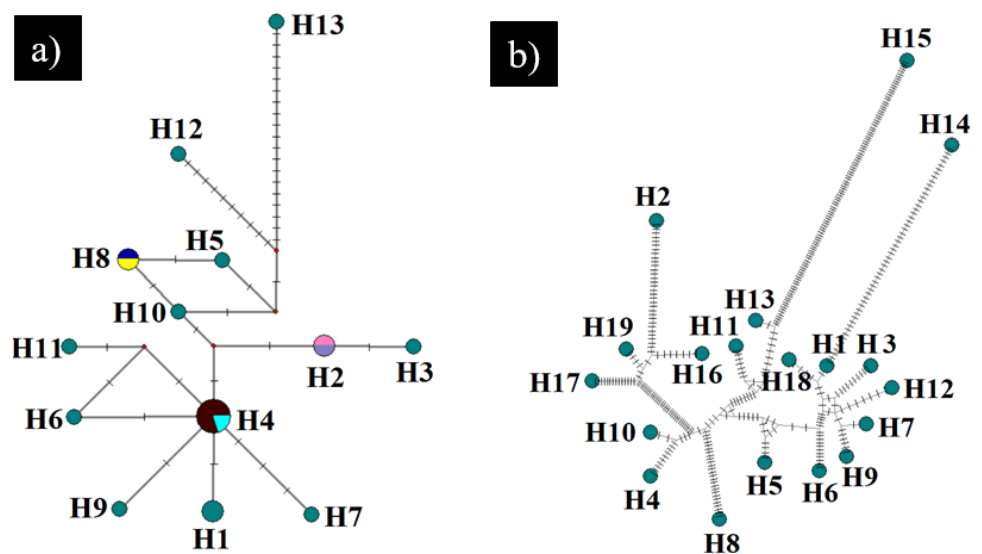


Figure 5. Haplotype map of a) *rbcl* loci gene and b) nrDNA loci gene of *Coelogyne*

Table 4. Total genetic distance between *Coelogyne* species using *rbcL*

	1	2	3	4	5	6	7	8	9	10	11	12	13	14	15	16	17	18	19	20
<i>C.rochussenii</i>	-	-	-	-	-	-	-	-	-	-	-	-	-	-	-	-	-	-	-	-
<i>C.velutina</i>	0.002	-	-	-	-	-	-	-	-	-	-	-	-	-	-	-	-	-	-	-
<i>C.pachystachya</i>	0.002	0.000	-	-	-	-	-	-	-	-	-	-	-	-	-	-	-	-	-	-
<i>C.pulverula</i>	0.003	0.002	0.002	-	-	-	-	-	-	-	-	-	-	-	-	-	-	-	-	-
<i>C.mayeriana</i>	0.007	0.005	0.005	0.003	-	-	-	-	-	-	-	-	-	-	-	-	-	-	-	-
<i>C.asperata</i>	0.007	0.005	0.005	0.003	0.000	-	-	-	-	-	-	-	-	-	-	-	-	-	-	-
<i>C.viscosa</i>	0.007	0.005	0.005	0.003	0.003	0.003	-	-	-	-	-	-	-	-	-	-	-	-	-	-
<i>C.schilleriana</i>	0.007	0.005	0.005	0.003	0.003	0.003	0.000	-	-	-	-	-	-	-	-	-	-	-	-	-
<i>C.trinervis</i>	0.007	0.005	0.005	0.003	0.003	0.003	0.000	0.000	-	-	-	-	-	-	-	-	-	-	-	-
<i>C.barbata</i>	0.007	0.005	0.005	0.003	0.003	0.003	0.000	0.000	0.000	-	-	-	-	-	-	-	-	-	-	-
<i>C.fimbriata</i>	0.007	0.005	0.005	0.003	0.003	0.003	0.000	0.000	0.000	0.000	-	-	-	-	-	-	-	-	-	-
<i>C.pandurata</i>	0.008	0.007	0.007	0.005	0.002	0.002	0.005	0.005	0.005	0.005	0.005	-	-	-	-	-	-	-	-	-
<i>C.eberhardtii</i>	0.008	0.007	0.007	0.005	0.005	0.005	0.002	0.002	0.002	0.002	0.002	0.007	-	-	-	-	-	-	-	-
<i>C.ovalis</i>	0.008	0.007	0.007	0.005	0.005	0.005	0.002	0.002	0.002	0.002	0.002	0.007	0.000	-	-	-	-	-	-	-
<i>C.cumingii</i>	0.008	0.007	0.007	0.005	0.005	0.005	0.002	0.002	0.002	0.002	0.002	0.007	0.003	0.003	-	-	-	-	-	-
<i>C.xyrekes</i>	0.008	0.007	0.007	0.005	0.005	0.005	0.002	0.002	0.002	0.002	0.002	0.007	0.003	0.003	0.003	-	-	-	-	-
<i>C.fuscescens</i>	0.010	0.008	0.008	0.007	0.007	0.007	0.003	0.003	0.003	0.003	0.003	0.008	0.005	0.005	0.005	0.005	-	-	-	-
<i>C.nitida</i>	0.012	0.010	0.010	0.008	0.008	0.008	0.005	0.005	0.005	0.005	0.005	0.010	0.007	0.007	0.007	0.007	0.008	-	-	-
<i>Cymbidium</i>	0.020	0.022	0.022	0.020	0.024	0.024	0.024	0.024	0.024	0.024	0.024	0.025	0.025	0.025	0.025	0.025	0.027	0.029	-	-
<i>Vanilla</i>	0.036	0.038	0.038	0.036	0.039	0.039	0.039	0.039	0.039	0.039	0.039	0.041	0.041	0.041	0.041	0.041	0.043	0.045	0.050	-

Table 5. Total genetic distance between *Coelogyne* species using nrDNA

Species	1	2	3	4	5	6	7	8	9	10	11	12	13	14	15	16	17	18	19	
<i>C.viscosa</i>	-	-	-	-	-	-	-	-	-	-	-	-	-	-	-	-	-	-	-	-
<i>C.eberhardtii</i>	0.02	-	-	-	-	-	-	-	-	-	-	-	-	-	-	-	-	-	-	-
<i>C.fimbriata</i>	0.07	0.06	-	-	-	-	-	-	-	-	-	-	-	-	-	-	-	-	-	-
<i>C.ovalis</i>	0.07	0.06	0.01	-	-	-	-	-	-	-	-	-	-	-	-	-	-	-	-	-
<i>C.cumingii</i>	0.07	0.06	0.05	0.05	-	-	-	-	-	-	-	-	-	-	-	-	-	-	-	-
<i>C.nitida</i>	0.08	0.06	0.05	0.05	0.04	-	-	-	-	-	-	-	-	-	-	-	-	-	-	-
<i>C.barbata</i>	0.08	0.06	0.02	0.03	0.04	0.04	-	-	-	-	-	-	-	-	-	-	-	-	-	-
<i>C.trinervis</i>	0.08	0.07	0.04	0.05	0.06	0.06	0.03	-	-	-	-	-	-	-	-	-	-	-	-	-
<i>C.fuscescens</i>	0.08	0.07	0.02	0.03	0.05	0.05	0.02	0.03	-	-	-	-	-	-	-	-	-	-	-	-
<i>C.xyrekes</i>	0.09	0.08	0.04	0.04	0.05	0.05	0.02	0.04	0.03	-	-	-	-	-	-	-	-	-	-	-
<i>C.pulverula</i>	0.10	0.09	0.08	0.08	0.07	0.08	0.08	0.09	0.09	0.09	-	-	-	-	-	-	-	-	-	-
<i>C.mayeriana</i>	0.10	0.08	0.08	0.08	0.08	0.09	0.07	0.08	0.08	0.08	0.08	-	-	-	-	-	-	-	-	-
<i>C.rochussenii</i>	0.10	0.09	0.08	0.08	0.08	0.09	0.08	0.10	0.09	0.10	0.04	0.09	-	-	-	-	-	-	-	-
<i>C.verrucosa</i>	0.11	0.10	0.08	0.08	0.09	0.09	0.08	0.09	0.07	0.09	0.08	0.04	0.09	-	-	-	-	-	-	-
<i>C.velutina</i>	0.13	0.10	0.10	0.11	0.11	0.11	0.10	0.11	0.10	0.11	0.10	0.10	0.11	0.12	-	-	-	-	-	-
<i>C.pandurata</i>	0.14	0.13	0.13	0.14	0.13	0.13	0.12	0.13	0.13	0.13	0.11	0.09	0.13	0.09	0.15	-	-	-	-	-
<i>C.asperata</i>	0.15	0.14	0.12	0.12	0.12	0.12	0.11	0.13	0.13	0.12	0.10	0.07	0.12	0.06	0.16	0.10	-	-	-	-
<i>Cymbidium</i>	0.21	0.19	0.19	0.20	0.21	0.22	0.19	0.20	0.19	0.20	0.23	0.20	0.20	0.18	0.25	0.26	0.27	-	-	-
<i>Vanilla</i>	0.43	0.42	0.40	0.41	0.41	0.43	0.40	0.40	0.41	0.41	0.44	0.43	0.45	0.44	0.46	0.46	0.47	0.49	-	-

Table 6. Haplotype distribution of *Coelogyne* and outgroup species using *rbcl* and nrDNA loci gene

Hap	Distribution of <i>Coelogyne</i> species based on loci gene	
	<i>rbcl</i>	nrDNA
H1	<i>C.ovalis</i> , <i>C.eberhardtii</i>	<i>C.fimbriata</i>
H2	<i>C.asperata</i> , <i>C.mayeriana</i>	<i>C.pandurata</i>
H3	<i>C.pandurata</i>	<i>C.trinervis</i>
H4	<i>C.trinervis</i> , <i>C.fimbriata</i> , <i>C.schilleriana</i> <i>C.barbata</i> , <i>C.viscosa</i>	<i>C.rochussenii</i>
H5	<i>C.rochussenii</i>	<i>C.cumingii</i>
H6	<i>C.rochussenii</i>	<i>C.nitida</i>
H7	<i>C.nitida</i>	<i>C.barbata</i>
H8	<i>C.pachystachya</i> , <i>C.velutina</i>	<i>C.velutina</i>
H9	<i>C.xyrekes</i>	<i>C.xyrekes</i>
H10	<i>C.pulverula</i>	<i>C.pulverula</i>
H11	<i>C.fuscescens</i>	<i>C.viscosa</i>
H12	<i>Cymbidium aloifolium</i>	<i>C.fuscescens</i>
H13	<i>Vanilla planifolia</i>	<i>C.eberhardtii</i>
H14	ND	<i>Cymbidium aloifolium</i>
H15	ND	<i>Vanilla planifolia</i>
H16	ND	<i>C.mayeriana</i>
H17	ND	<i>C.asperata</i>
H18	ND	<i>C.ovalis</i>
H19	ND	<i>C.verrucosa</i>

Abbreviation : Hap = haplotype, H = number of haplotype, ND = not detected

CONCLUSIONS

The research shows that the use of the nrDNA which consist of *ITS* gene region is more recommended in phylogenetic analysis among species in the *Coelogyne* genus then followed by *rbcl*. Based on phylogenetic tree and haplotype map constructed with nrDNA, all *Coelogyne* species from Indonesia have close evolutionary relationship, *C. pandurata* (H2) evolved from *C. mayeriana* (H16), then both evolved from *C. verrucosa* (H19), then all of them evolved from *C. asperata* (H17). In addition, it is necessary to improve the DNA barcode data from the *Coelogyne* genus thus phylogenetic analysis carried out can represent a more significant number of species so that the research results obtained will be more accurate.

AUTHORS CONTRIBUTION

AP as first author did phylogenetic analysis, full paper writing, reviewing and editing, AK did nucleotide data analysis using DNAsp, haplotype map construction, full paper writing, reviewing and editing, MIM did full paper writing and editing, FYK reviewing and editing, ES reviewing and editing.

ACKNOWLEDGMENTS

The authors would like to thank the Biology Orchid Study Club (BiOSC) members who have helped in the collection and data collection of orchid samples.

CONFLICT OF INTEREST

There is no any conflict of interest regarding the research or the funding.

REFERENCES

- Bafeel, S.O. et al., 2011. Comparative evaluation of PCR success with universal primers of maturase K (matK) and ribulose-1, 5-bisphosphate carboxylase oxygenase large subunit (rbcL) for barcoding of some arid plants. *Plant Omics*, 4, pp.195-198.
- CBOL Plant Working Group, 2009. A DNA barcode for land plants. In *Proceedings of the National Academy of Sciences*, 106. pp. 12794–12797.
- Chase, M.W. et al., 2015. An updated classification of Orchidaceae. *Botanical Journal of the Linnean Society*, 177(2), pp.151–174. doi: 10.1111/boj.12234.
- Chattopadhyay, P., Banerjee, G. & Banerjee, N., 2017. Distinguishing Orchid Species by DNA Barcoding: Increasing the Resolution of Population Studies in Plant Biology. *OMICS: A Journal of Integrative Biology*, 21(12), pp.711–720. doi: 10.1089/omi.2017.0131.
- Duan, H. et al., 2019. The screening and identification of DNA barcode sequences for *Rehmannia*. *Scientific Reports*, 9, 17295. doi: 10.1038/s41598-019-53752-8.
- El-Sherif, N. & Ibrahim, M., 2020. Implications of rbcL and rpoC1 DNA Barcoding in Phylogenetic Relationships of some Egyptian *Medicago sativa* L. Cultivars. *Egyptian Journal of Botany*, 60(12), pp.451–460. doi: 10.21608/ejbo.2020.20028.1399.
- Haider, N., 2018. A Brief Review on Plant Taxonomy and its Components. *Jour Pl Sci Res*, 34(2), pp.275–290.
- Hall, B.G., 2013. Building Phylogenetic Trees from Molecular Data with MEGA. *Molecular Biology and Evolution*, 30(5), pp.1229–1235. doi: 10.1093/molbev/mst012.
- Hartati, S. et al., 2019. Morphological characterization of *Coelogyne* spp for germplasm conservation of orchids. *Revista Ceres*, 66(4), pp.265–270. doi: 10.1590/0034-737x201966040004.
- Hartati, S. & Muliawati, E.S., 2020. Short Communication: Genetic variation of *Coelogyne pandurata*, *C. rumphii* and their hybrids based on RAPD markers. *Biodiversitas Journal of Biological Diversity*, 21(10), pp.4709-4713. doi: 10.13057/biodiv/d211033.
- Ho, V.T. et al., 2021. Comparison of matK and rbcL DNA barcodes for genetic classification of jewel orchid accessions in Vietnam. *Journal of Genetic Engineering and Biotechnology*, 19(1), 93. doi: 10.1186/s43141-021-00188-1.
- Ho, V.T. & Nguyen, M.P., 2020. An in silico approach for evaluation of rbcL and matK loci for DNA barcoding of Cucurbitaceae family. *Biodiversitas Journal of Biological Diversity*, 21(8), pp.3879-3885. doi: 10.13057/biodiv/d210858.
- Hollingsworth, P.M., Graham, S.W. & Little, D.P., 2011. Choosing and Using a Plant DNA Barcode. *PLoS ONE*, 6(5), e19254. doi: 10.1371/journal.pone.0019254.
- Hosein, F.N. et al., 2017. Utility of DNA barcoding to identify rare endemic vascular plant species in Trinidad. *Ecology and Evolution*. *Ecology and Evolution*, 7(18), pp.7311–7333. doi: 10.1002/ece3.3220.
- Dharmayanti, N.L.P.I., 2011. Molecular phylogenetic: organism taxonomy method based on evolution history. *Wartazoa*, 21(1), pp.1–5.
- Jiang, K. et al., 2020. Chloroplast Genome Analysis of Two Medicinal *Coelogyne* spp. (Orchidaceae) Shed Light on the Genetic Information, Comparative Genomics, and Species Identification. *Plants*, 9 (10), 1332. doi: 10.3390/plants9101332.

- Kim, H.M. et al., 2014. DNA barcoding of Orchidaceae in Korea. *Molecular Ecology Resources*, 14(3), pp.499–507. doi: 10.1111/1755-0998.12207.
- Kim, Y.-K. et al., 2020. Plastome Evolution and Phylogeny of Orchidaceae, With 24 New Sequences. *Frontiers in Plant Science*, 11, 22. doi: 10.3389/fpls.2020.00022.
- Li, J. et al., 2018. Prioritizing the orchids of a biodiversity hotspot for conservation based on phylogenetic history and extinction risk. *Botanical Journal of the Linnean Society*, 186(4), pp.473–497. doi: 10.1093/botlinnean/box084.
- Maloukh, L. et al., 2017. Discriminatory power of rbcL barcode locus for authentication of some of United Arab Emirates (UAE) native plants. *3 Biotech*, 7(2), 144. doi: 10.1007/s13205-017-0746-1.
- Mishra, P. et al., 2016. DNA barcoding: an efficient tool to overcome authentication challenges in the herbal market. *Plant Biotechnology Journal*, 14(1), pp.8–21. doi: 10.1111/pbi.12419.
- Nauheimer, L. et al., 2018. Australasian orchid biogeography at continental scale: Molecular phylogenetic insights from the Sun Orchids (Thelymitra, Orchidaceae). *Molecular Phylogenetics and Evolution*, 127, pp.304–319. doi: 10.1016/j.ympev.2018.05.031.
- Parveen, I. et al., 2016. DNA Barcoding for the Identification of Botanicals in Herbal Medicine and Dietary Supplements: Strengths and Limitations. *Planta Medica*, 82(14), pp.1225–1235. doi: 10.1055/s-0042-111208.
- Parveen, I. et al., 2017. Evaluating five different loci (rbcL, rpoB, rpoC1, matK, and ITS) for DNA barcoding of Indian orchids. *Genome*, 60(8), pp.665–671. doi: 10.1139/gen-2016-0215.
- Rajaram, M.C. et al., 2019. DNA Barcoding of Endangered Paphiopedilum species (Orchidaceae) of Peninsular Malaysia. *Phytotaxa*, 387(2), pp.94–104. doi: 10.11646/phytotaxa.387.2.2.
- Ramudu, J. & Khasim, S.M., 2016. DNA Barcoding of some Indian Coelogyne (Epidendroideae, Orchidaceae). *J. Orchid Soc. India*, 30, pp.65–73.
- Raskoti, B.B. & Ale, R., 2021. DNA barcoding of medicinal orchids in Asia. *Scientific Reports*, 11(1), 23651. doi: 10.1038/s41598-021-03025-0.
- Rivero, D.G., 2016. Darwinian Archaeology and Cultural Phylogenetics. *In Cultural Phylogenetics Springer*, pp.43–72. doi: 10.1007/978-3-319-25928-4_3.
- Singh, N. & Kumaria, S., 2020. A Combinational Phytomolecular-Mediated Assessment in Micropropagated Plantlets of Coelogyne ovalis Lindl.: A Horticultural and Medicinal Orchid. *Proceedings of the National Academy of Sciences, India Section B: Biological Sciences*, 90(2), pp.455–466. doi: 10.1007/s40011-019-01118-5.
- Srivastava, D. & Manjunath, K., 2020. DNA barcoding of endemic and endangered orchids of India: A molecular method of species identification. *Pharmacognosy Magazine*, 16(70), pp.290–299. doi: 10.4103/pm.pm_574_19.
- Vu, H.-T. et al., 2018. In Silico Study on Molecular Sequences for Identification of Paphiopedilum Species. *Evolutionary Bioinformatics*, 14, 117693431877454. doi: 10.1177/1176934318774542.
- Wang, X. et al., 2018. DNA barcoding a taxonomically complex hemiparasitic genus reveals deep divergence between ploidy levels but lack of species-level resolution. *AoB PLANTS*, 10(3). doi: 10.1093/aobpla/ply026.

- Wu, Q.-P. et al., 2020. Characterization of the complete chloroplast genome of *Coelogyne fimbriata* (Orchidaceae). *Mitochondrial DNA Part B*, 5(3), pp.3507–3509. doi: 10.1080/23802359.2020.1827058.
- Yun, S.A. et al., 2020. Genetic diversity and population structure of the endangered orchid *Pelatantheria scolopendrifolia* (Orchidaceae) in Korea. *PLOS ONE*, 15(8), e0237546. doi: 10.1371/journal.pone.0237546.
- Zhang, G.-Q. et al., 2021. Phylogenetic incongruence in *Cymbidium* orchids. *Plant Diversity*, 43(6), pp.452–461. doi: 10.1016/j.pld.2021.08.002.

Research Article

Birds Species on Vertical Stratification of Mangrove Vegetation Nusa Lembongan, Bali Indonesia

I Ketut Ginantra^{1*}, I Ketut Muksin¹, Martin Joni¹

1)Biology Study Program, Faculty of Mathematics and Natural Sciences, Udayana University, Bali

*Corresponding author, email: ketut_ginantra@unud.ac.id

Keywords:

Nusa Lembongan mangrove
vegetation strata
bird species
pure mangrove vegetation
mixed mangrove and dry vege-
tation

Submitted:

15 October 2022

Accepted:

03 July 2023

Published:

06 October 2023

Editor:

Ardaning Nuriliani

ABSTRACT

This study aims to determine the use of vertical stratification of mangrove vegetation by bird species in the mangrove ecosystem of Nusa Lembongan. The study was conducted at seven mangrove ecosystem sites, in April-July 2021. Observation of the number of birds in each vegetation strata was carried out using the point count method. The association of the use of vegetation strata by bird species was carried out by *Detrended correspondence analysis* (DCA) statistical test. The results showed that total of 32 species are found in the mangrove ecosystem of Nusa Lembongan which belong to 26 families. There is a strong association between bird species and the vertical strata of vegetation. The species of birds associated with pure mangrove vegetation are; strata I, namely *Amaurornis phoenicurus* (Pennant,1769), *Ardea purpurea* Linnaeus, 1766, *Sterna bergii* M.H.K.Lichtenstein, 1823, *Passer domesticus* (Linnaeus, 1758), and *Pycnonotus aurigaster* (Vieillot, 1818); strata II are *Todiramphus chloris* (Boddaert,1783), *Todiramphus sanctus* (Vigors and Horsfield,1827), *Alcedo coerulescens* Vieillot,1818 and *Butorides striata* (Linnaeus,1758); strata III are *Hypothymis azurea* (Boddaert, 1783), *Lanius schach* Linnaeus,1758, *Merops philippinus* Linnaeus,1767, *Nectarinia jugularis* Linnaeus,1766 and *Gerygone sulphurea* Wallace, 1864; strata IV are *Collocalia linchi* Horsfield & F.Moore,1854, *Oriolus chinensis* Linnaeus, 1766, *Hirundo tahitica* Gmelin,1789 and *Pycnonotus goiaver* (Scopoli, 1786). The bird species associated with mixed mangrove and dryland vegetation are strata I, namely species *Turnix suscitator* (J.F.Gmelin,1789), *Acridotheres javanicus* Cabanis,1851, *Anthreptes malacensis* (Scopoli, 1786), *Passer domesticus* (Linnaeus,1758), *Pycnonotus aurigaster* (Vieillot,1818), *Spilopelia chinensis* (Scopoli,1786)and *Geopelia striata* (Linnaeus,1766); strata II, namely *Alcedo coerulescens* Vieillot,1818, *Zosterops chloris* Bonaparte, 1850, *Todiramphus sanctus* (Vigors and Horsfield,1827) and *Todiramphus chloris* (Boddaert,1783); strata III, namely *Anthreptes malacensis* (Scopoli,1786), *Cacomantis merulinus* (Scopoli,1786), *Hypothymis azurea* (Boddaert,1783), *Copsychus saularis* (Linnaeus,1758), *Nectarinia jugularis* Linnaeus,1766, *Gerygone sulphurea* Wallace,1864 and *Merops philippinus* Linnaeus,1767; strata IV, namely *Collocalia linchi* Horsfield & F.Moore,1854, *Hirundo tahitica* Gmelin,1789 and *Corvus* sp. Factors influencing strata preference by birds are resources, both food and space, as well as the bioecological characteristics of the birds themselves.

Copyright: © 2023, J. Tropical Biodiversity Biotechnology (CC BY-SA 4.0)

INTRODUCTION

Mangrove forest on the coast of Nusa Lembongan, which covers an area of 202 ha, has an important role physically, biologically, ecologically, and

economically. Physical roles include maintaining a stable coastline from abrasion, controlling seawater intrusion into groundwater, protecting the area behind the mangroves from waves. Economic functions include the development of mangrove ecotourism and source of livelihood for fishermen. Biological/ecological functions include a feeding ground, a spawning ground and a nursery ground for various types of fish, crustaceans, mollusks, and birds. It is even stated that mangroves are habitat for about 13% of Indonesian avifauna and mangroves play an important role for migratory waterbirds. Bird diversity is also an indicator of the health condition of mangroves (Negelkerken et al. 2008; Setiawan et al. 2012; Salahuddin et al. 2021; Wetland International 2022).

Birds use mangrove vegetation for foraging, nesting, perching, attracting mates, playing, breeding, and sheltering. Bird species that utilise mangrove habitats are generally from groups of water birds, but also terrestrial birds. The use of vegetation by birds is closely related to the vertical stratification of mangrove vegetation. Certain types make use of the bottom layer/mud flat, mangrove root layer, canopy layer or the top of the vegetation. Bibby et al. (2000) stated that the selection of strata by birds is determined because birds also have micro-habitat needs. Many species of birds live in the upper canopy layer, so it is difficult to find the birds (especially because they move quickly). However, there are also bird species that do not occupy canopy in the vegetation, but prefer shrub habitats which are usually under stands. The choice of bush habitat is also due to the fact that the habitat is suitable and able to meet their needs.

Several studies related to bird associations in the vertical stratification of mangrove forests found that each layer of habitat/vegetation found variations in bird richness. For example, in the *Avicennia alba* strata vegetation the most widely used by birds is the top layer of vegetation and in the *Rhizophora mucronata* strata vegetation the most common bird is the middle layer of vegetation (Pradana et al. 2022). Hernowo (2016) found that the middle vegetation strata of mangrove vegetation in Batu Ampar, Kubu Raya District, West Kalimantan Province, were mostly used by birds. The Nusa Lembongan mangroves also show vertical stratification related to the use of bird diversity. There are birds that use the bottom layer/mud/water level, root layer, canopy layer and top layer of mangrove vegetation in Nusa Lembongan. Thus, the purpose of this study was to determine the use of vertical stratification of mangrove vegetation by bird species in the mangrove ecosystem of Nusa Lembongan.

MATERIAL AND METHODS

Study Site

The study was conducted in 7 locations of the Nusa Lembongan mangrove forest (Figure 1). The geographical position of the mangrove ecosystem of Nusa Lembongan is at 8° 40'00,22" S and 115° 28'02,99" E. The research was conducted on two vegetation groups, namely pure mangrove vegetation and mixed mangrove vegetation with dry vegetation. Pure mangrove vegetation is vegetation composed of true mangrove species and associated species, while mixed vegetation is vegetation consisting of mangrove plant species and dry vegetation around the mangroves. The research was carried out for 4 months from April to July 2021.

Research Procedure

Identification of bird species is done directly from field observations with the help of binoculars. The birds found were photographed with a digital camera. Identification of bird species based on morphological characters



Figure 1. Maps of Research Locations.

(including the shape of the legs, feathers, feather colour, wings, wing colour, beak). Identification refers to the Java, Bali, and Sumatra bird field guide series (MacKinnon et al. 2010).

Observation of bird abundance were carried out by using the point count method (Bibby et al. 2000). Counting points were done at 7 sites of the mangrove ecosystem, at each site 3 counting points were carried out. At each point, observations were carried out for 15 minutes with a distance of 150 meters between points. Surveys for the presence of bird species were conducted based on the vertical stratification of mangrove habitats. The parameters observed at each point of count were the species and the number of individual birds.

Based on the results of observations on the use of pure mangrove vegetation and mixed mangrove with dry vegetation by bird species in the field, the stratification of mangrove habitat is divided into 4 strata. The four strata are stratum I which is the vegetation floor (mud/sand/water average); stratum II is mangrove root layer; stratum III is the canopy layer and stratum IV is the top surface layer of the canopy to the top of the vegetation (up to a distance of 5 meters above the surface of the vegetation canopy) (Figure 2).

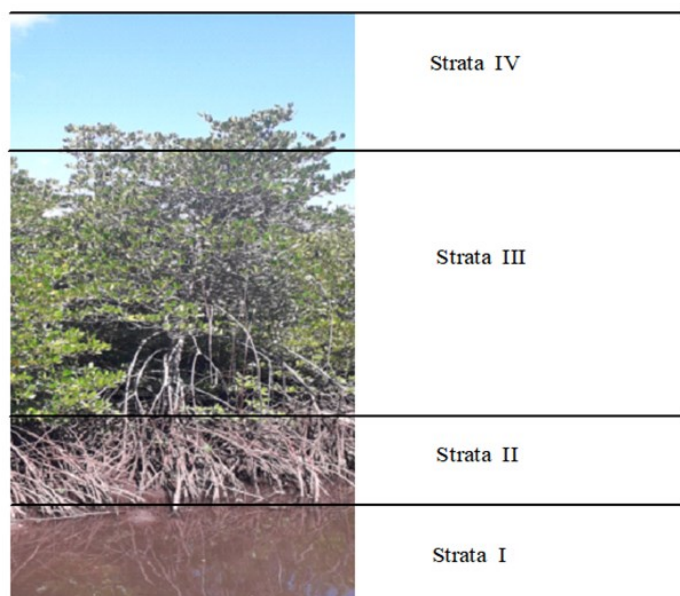


Figure 2. Strata category of the use of vegetation by birds in the mangroves of Nusa Lembongan.

Data Analysis

Data on the species and number of individuals of each bird were analysed in descriptive quantitative method by describing the analysis of the list of species and the number of birds in each category of vertical mangrove strata. Association of vegetation strata utilisation by bird species was tested for DCA correspondence (Detrended Correspondence Analysis) using SPSS version 24.

RESULTS AND DISCUSSION

Mangrove Vegetation Vertical Strata

The vertical stratification of mangroves related to the use of birds is divided into four strata. Strata I is part of the forest floor; in this strata, it can be flat mud, rocky sand, water, or sandy soil with undergrowth; strata II is the root part of mangrove vegetation (support roots, knee roots, breath roots); strata III is the main part of the vegetation canopy; strata IV is the part of the canopy surface above the vegetation to a height of 5 meters. Several researchers determined the vertical structure of mangroves based on the height from the ground to the top of the mangrove canopy (Hernowo 2016; Kusmana & Azizah 2022; Pradana et al. 2022).

At the seven observation sites, there were variations in each strata (especially in strata I, II and III) based on the main species of mangrove constituents, the presence of coastal vegetation or species of mangrove associations and the zoning of mangrove areas. Mangrove vegetation in Nusa Lembongan related to its use by birds, is divided into two groups, namely pure mangrove vegetation and mixed mangrove vegetation and dryland vegetation.

Pure mangrove vegetation

Pure mangrove vegetation was represented by site 1, site 3, site 5 and site 7. The plant species in pure mangrove vegetation consisted of *Rhizophora mucronata*, *Rhizophora stylosa*, *Rhizophora apiculata*, *Sonneratia alba*, as well as several species of *Excoecaria agalloca*, *Lumnitzera racemosa* and *Bruguiera gymnorhiza*. Some associated plants including *Pandanus tectorius*, *Hibiscus sinensis*, *Thespesia populnea*, *Terminalia cattapa*, and *Guettarda speciosa*. Strata I is part of the mangrove forest floor, which can be rocky sand, sand, mud flats, sea water when high tides and only some parts have mangrove plants association. Strata II is dominated by the mangrove root system (stilt roots and pneumatophore). Strata III is the main layer of the mangrove canopy and stratum IV is the canopy surface up to 5 meters above the canopy (Figure 3).

Mixed vegetation of mangrove and dry land vegetation

Mixed mangrove vegetation was represented by site 2, site 4 and site 6. The plant species in mixed mangrove vegetation were dominated by *Sonneratia alba*, *Avicennia marina*, *Avicennia alba*, *Lumnitzera racemosa*, some *Rhizophora stylosa*, *Rhizophora apiculata*, and several associated plant species mangroves, namely *Opuntia* sp., *Salicornia* sp., *Pandanus tectorius*. Strata I is the ground floor of the mangrove forest and the ground floor of dry land, can be sandy soil, flat mud and dry soil with some undergrowth (grass). Strata II is dominated by the mangrove root system. This site is bordered by several land plant trees including *Acacia auriculiformis*, *Acacia leucophloea*, *Borreria flabelifer*, *Leucaena leucocephala*, *Cocos nucifera* and *Terminalia cattapa*, as well as dry vegetation including *Manihot utilissima*, *Gliricidia sepium*, *Ficus glabera*, *Cassia fistula*, *Ziziphus mauritiana*, *Antidesma bunius*, *Hibiscus sinensis*, *Tectona grandis*, *Lannea grandis*, *Azadirachta indica*, *Manilkara kauki*, *Schleichera oleosa*, as well as lower



Figure 3. Pure mangrove vegetation structure in the Nusa Lembongan mangrove ecosystem.

vegetation including grass *Adropogon aciculatus*, *Cyperus barbatus*, *Eragrostis* sp., and *Imperata cylindrica*. Strata III in this site is composed of a canopy layer of mangrove vegetation and tree vegetation of land plants. Strata IV of mixed mangrove vegetation is the surface layer to the top of the mangrove canopy and land plant canopy.



Figure 4. Mixed mangrove vegetation structure in the Nusa Lembongan mangrove ecosystem.

Birds in the vegetation strata

In the mangrove ecosystem of Nusa Lembongan, 32 species of birds that were found belong to 26 families. The number of bird species found in pure mangrove vegetation was 20 species and in mixed mangrove vegetation (mangrove and dry land vegetation) as many as 28 species. In pure mangrove vegetation, 20 species of birds were found, 13 species of the birds are terrestrial bird groups and 7 species are water birds. Terrestrial bird species found in mangrove vegetation are nectar-eating birds (nectarivore), fruit-eating (frugivore) and grain-eating (granivore) and insectivorous or small reptiles (Table 1). Flowers from many types of mangrove plants produce nectar, which can be used by nectarivore birds.

Insects and small reptiles associated with mangrove plants serve as food for insectivorous birds. [Kartijono et al. \(2010\)](#) and [Pradana et al. \(2022\)](#) also found that many nectar-eating and insectivorous birds used mangrove vegetation on Mosquito Island and Wonorejo mangroves. Water bird species that were found are fish-eating birds, crustaceans, sea worms and mollusks. This faunal fauna is common in mangrove habitats.

The number of water birds found in the mangroves of Nusa Lemongan is relatively lesser than water birds in other mangrove ecosystems. Among them are the number of water birds in the mangroves of the Bali Island of Serangan as many as 24 species ([Sumardika et al. 2017](#)), 15 species of water birds in the Pejarakan mangroves ([Ginatra et al. 2020](#)) and the number of water birds in the mangrove area of the south

Table 1. Bird species in pure mangrove vegetation.

No	Scientific name	Common name	Number individual in vegetation strata				Main feeding guilds (birds group)	
			I	II	III	IV		
1	<i>Amaurornis phoenicurus</i> (Pennant,1769)	white breasted waterhen	4				Carnivore (Water bird)	
2	<i>Alcedo coerulescens</i> Vieillot,1818	Small blue kingfisher		5	5		Carnivore (Water bird)	
3	<i>Ardea purpurea</i> Linnaeus, 1766	Purple heron	3		5	4	Carnivore (Water bird)	
4	<i>Butorides striata</i> (Linnaeus,1758)	Striated heron	3	5			Carnivore (Water bird)	
5	<i>Collocalia linchi</i> Horsfield & F. Moore,1854	Cave swiftlet				20	Insectivore (Terrestrial bird)	
6	<i>Gerygone sulphurea</i> Wallace, 1864	Golden-bellied gerygone			6	3	Insectivore (Terrestrial bird)	
7	<i>Hirundo tahitica</i> Gmelin,1789	Pacific Swallow			6	7	Insectivore (Terrestrial bird)	
8	<i>Hypothymis azurea</i> (Boddaert,1783)	Black-naped monarch				3	Insectivore (Terrestrial bird)	
9	<i>Lanius schach</i> Linnaeus,1758	Long-tailed Shrike				3	Insectivore (Terrestrial bird)	
10	<i>Merops philippinus</i> Linnaeus,1767	Blue-tailed bee-eater				3	Insectivore (Terrestrial bird)	
11	<i>Nectarinia jugularis</i> Linnaeus,1767	Olive-backed sunbird				18	3	Nectarivore (Terrestrial bird)
12	<i>Oriolus chinensis</i> Linnaeus,1767	Back naped oriale				4	3	Frugivora (Terrestrial bird)
13	<i>Pachycephala grisola</i> (Blyth, 1843)	Mangrove whistler		2	2			Insectivore (Terrestrial bird)
14	<i>Passer domesticus</i> (Linnaeus,1758)	House sparrow	7				2	Granivore (Terrestrial bird)
15	<i>Pycnonotus aurigaster</i> (Vieillot,1818)	Sooty-headed Bulbul	12			28		Frugivora (Terrestrial bird)
16	<i>Pycnonotus goiaver</i> (Scopoli, 1786)	Yellow vented bulbul					4	Frugivora (Terrestrial bird)
17	<i>Sterna bergii</i> M.H.K.Lichtenstein,1823	Greater Crested Tern	5				2	Carnivore (Water bird)
18	<i>Spilopelia chinensis</i> (Scopoli, 1786)	Spotted dove	5			21	7	Frugivora (Terrestrial bird)
19	<i>Todiramphus chloris</i> (Boddaert,1783)	Collared kingfisher		8	9			Carnivore (Water bird)
20	<i>Todiramphus sanctus</i> (Vigors and Horsfield,1827)	Sacred kingfisher		3	3			Carnivore (Water bird)

coast of Bangkalan, Madura Island as many as 15 species (Ramadhani et al. 2022).

Utilization of birds in mangrove vegetation strata is divided into 4 strata. The division of these strata is slightly different from what were found by Hernowo (2016) who divides 3 strata on the utilization of mangrove vegetation in Batu Ampar. In the Batu Ampar mangrove, the mud average and the mangrove root system become one strata, namely strata C. While the Nusa Lembongan mangroves, the lowest stratum is divided into two, namely the average mud, water or substrate is strata I and strata II are the root part of the mangrove. Birds use stratum 3 (the main part of the mangrove canopy) which is 48.7% and stratum IV (the surface to the top of the mangrove canopy) which is 25.0% compared to stratum I which is 17.1% and stratum II is 9.2%. Hernowo (2016), Kartijono et al. (2010), and Pradana et al. (2022) also found that the main stratum of the mangrove canopy was mostly used by birds. The association of the use of bird species in pure mangrove vegetation strata is presented through a biplot correspondence analysis (Figure 5).

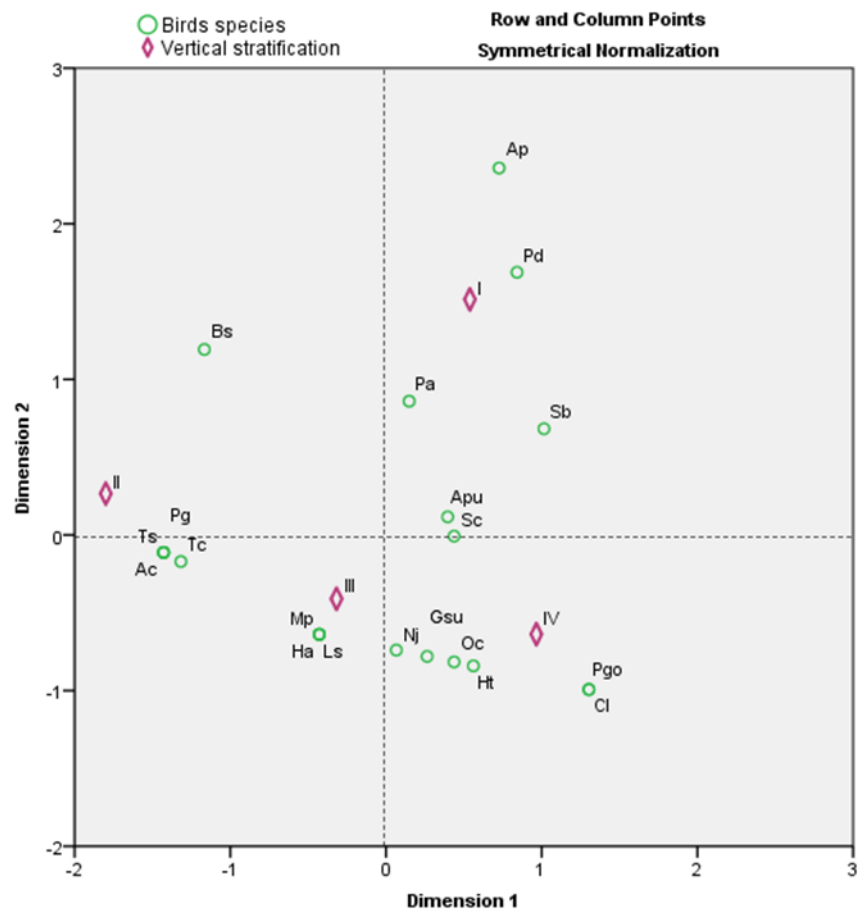


Figure 5. Biplot correspondence analysis of birds on pure vegetation of mangroves. (Birds species code; **Ap:** *Amaurornis phoenicurus*; **Apu:** *Ardea purpurea*; **Bs:** *Butorides striatus*; **Pd:** *Passer domesticus*; **Pa:** *Pycnonotus aurigaster*; **Sc:** *Spilopelia chinensis*; **Sb:** *Sterna bergii*; **Ac:** *Alcedo caerulescens*; **Pg:** *Pachycephala grisola*; **Tc:** *Todiramphus chloris*; **Ts:** *Todirhamphus sanctus*; **Gsu:** *Gerygone sulphurea*; **Ht:** *Hirundo tahitica*; **Ha:** *Hypothymis azurea*; **Ls:** *Lanius shcach*; **Mp:** *Merops philippinus*; **Nj:** *Nectarinia jugularis*; **Oc:** *Oriolus chinensis*; **Cl:** *Collocalia linchi*; **Pgo:** *Pycnonotus goiaver*)

Common bird species associated in strata I and strata II include collared kingfisher (*Todiramphus chloris*), purple heron (*Ardea purpurea*), sacred kingfisher (*Todirhamphus sanctus*), mangrove whistler (*Pachycephala grisola*), white breasted waterhen (*Amaurornis phoenicurus*), small blue

kingfisher (*Alcedo caerulescens*), greater Crested Tern (*Sterna bergii*), and striated heron (*Butorides striatus*). The species of birds that use strata I and II are fish-eating birds, crustaceans and mollusks associated with mangrove habitats. In feeding activities, these birds are generally silent and perched first on the mangrove roots to wait for their prey in the water or in the mud. As soon as the prey is seen in the water or in the mud, it immediately flies into the water or mud to catch the prey. There were also birds observed, namely striated heron and purple heron pecking mollusks in the mangrove roots. White breasted waterhen and purple heron were observed walking along the mangrove mud mudflat while pecking on crustaceans and mollusks. Sutopo et al. (2017), Hernowo, (2016) and MacKinnon et al. (2010), stated that in terms of bird bioecology, the presence of birds in strata I and strata II is related to the habits of these birds in foraging for food.

In strata III, associated birds include blue-tailed bee-eater (*Merops philippinus*), black-naped monarch (*Hypothymis azurea*), golden-bellied gerygone (*Gerygone sulphurea*), long-tailed shrike (*Lanius shcach*), back-naped oriale (*Oriolus chinensis*), sooty-headed bulbul (*Pycnonotus aurigaste*), spotted dove (*Spilopelia chinensis*), and olive-backed sunbird (*Nectarinia jugularis*). The types of birds in strata III are seed/fruit-eating, insect-eating and nectar-eating birds. Mangrove stratum III is more utilized by bird species, this is because this strata provides more resources for bird life, both as a food source, perch, resting place, mating and nesting activities. Pradana et al. (2022), Cita and Budiman. (2019), Mancini et al. (2018), and Hernowo, (2016) stated that the complexity, structural heterogeneity and productivity of mangrove vegetation are important factors for the diversity of bird species.

Species of birds in strata IV include cave swiftlet (*Collocalia linchi*), yellow vented bulbul (*Pycnonotus goiaver*), and pacific swallow (*Hirundo tahitica*), is a type of bird that is able to eat insects that fly above the canopy or insects that perch on the surface of the mangrove canopy. Cave swiftlets is generally observed to catch insects while flying over vegetation. Kopij (2000) has previously observed *Collocalia linchi* and *Apus pacificus* to be flying in large numbers around mangrove forests, both of which flying round and round to hunt down insects. Cave swiftlet (*Collocalia linchi*) is quite high in population in the mangrove ecosystem of Nusa Lembongan. MacKinnon et al. (2010) stated that *Collocalia linchi* and *Apus pacificus* are species of birds that have a wide distribution and are very common worldwide from the lowlands to the highlands. They show flocking behaviour.

The choice of stratification of mangrove vegetation is more related to the bird's preference for the necessities of life provided by each vegetation stratum, whether food, resting place, perching while making sounds, playing, or taking shelter. During our research, we did not find any birds using mangrove vegetation for nesting. Some bird researchers also state that the presence of birds in vegetation stratification is more closely related to vegetation productivity, fulfilment of micro habitat needs, these habitats are suitable and able to meet the needs of certain bird species (Bibby et al. 2000; Nagelkerken et al. 2008; Wisnubudi 2009; Cita & Budiman 2019).

Table 2 shows the species of birds that use mixed vegetation of mangroves and dry vegetation. 28 bird species were found utilizing mixed mangrove and dry vegetation. In this type of vegetation, there are also more groups of terrestrial birds, which are 24 species, compared to water birds, which are 4 species.

Table 2. Bird species in mixed mangrove and dry vegetation.

No	Scientific name	Common name	Number individual in vegetation strata				Feeding guilds (birds group)	
			I	II	III	IV		
1	<i>Acridotheres javanicus</i> Cabanis, 1851	Javan myna	4			2	Insectivore (Terrestrial bird)	
2	<i>Alcedo coerulescens</i> Vieillot, 1818	Small blue kingfisher	2	5	2		Carnivore (Water bird)	
3	<i>Amaurornis phoenicurus</i> (Pennant, 1769)	white breasted water-hen	4				Carnivore (Water bird)	
4	<i>Anthreptes malacensis</i> (Scopoli, 1786)	Brown-throated sun-bird				5	Nectarivore (Terrestrial bird)	
5	<i>Cacomantis merulinus</i> (Scopoli, 1786)	Plaintive cuckoo				4	Insectivore (Terrestrial bird)	
6	<i>Collocalia linchi</i> Horsfield & F. Moore, 1854	Cave swiftlet				13	Insectivore (Terrestrial bird)	
7	<i>Copsychus saularis</i> (Linnaeus, 1758)	Oriental magpie-robin				4	Insectivore (Terrestrial bird)	
8	<i>Corvus</i> sp.	Crow				3	3	Carnivore (Terrestrial bird)
9	<i>Geopelia striata</i> (Linnaeus, 1766)	Zebra dove	5			9	4	Granivore (Terrestrial bird)
10	<i>Gerygone sulphurea</i> Wallace, 1864	Golden-bellied gerygone				6	3	Insectivore (Terrestrial bird)
11	<i>Hirundo tahitica</i> Gmelin, 1789	Pacific Swallow				6	7	Insectivore (Terrestrial bird)
12	<i>Hypothymis azurea</i> (Boddaert, 1783)	Black-naped monarch				6		Insectivore (Terrestrial bird)
13	<i>Lalage sueurii</i> (Vieillot, 1818)	White shouldered triller				3		Insectivore (Terrestrial bird)
14	<i>Lanius schach</i> Linnaeus, 1758	Long-tailed Shrike				5		Insectivore (Terrestrial bird)
15	<i>Lonchura molucca</i> (Linnaeus, 1766)	Black faced munia				3		Granivore (Terrestrial bird)
16	<i>Merops philippinus</i> Linnaeus, 1767	Blue-tailed bee-eater				5	4	Insectivore (Terrestrial bird)
17	<i>Nectarinia jugularis</i> Linnaeus, 1766	Olive-backed sunbird				11	3	Nectarivore (Terrestrial bird)
18	<i>Oriolus chinensis</i> Linnaeus, 1766	Black naped oriole				2	3	Frugivora (Terrestrial bird)
19	<i>Passer domesticus</i> (Linnaeus, 1758)	House sparrow	6			3		Granivore (Terrestrial bird)
20	<i>Psilopogon haemacephalus</i> (P.L.S. Müller, 1776)	Coppersmith Barbet				3		Frugivora (Terrestrial bird)
21	<i>Pycnonotus aurigaster</i> (Vieillot, 1818)	Sooty-headed Bulbul	9	4	24			Frugivora (Terrestrial bird)
22	<i>Pycnonotus goiaver</i> (Scopoli, 1786)	Yellow vented bulbul				3	3	Frugivora (Terrestrial bird)
23	<i>Spilopelia chinensis</i> (Scopoli, 1786)	Spotted dove	12			4	3	Frugivora (Terrestrial bird)
24	<i>Todiramphus chloris</i> Boddaert, 1783	Collared kingfisher	5	6	3	3		Carnivore (Water bird)
25	<i>Todiramphus sanctus</i> (Vigors and Horsfield, 1827)	Sacred kingfisher		4	2			Carnivore (Water bird)
26	<i>Treron vernans</i> (Linnaeus, 1771)	Pink-necked green pigeon				5		Frugivora (Terrestrial bird)
27	<i>Turnix suscitator</i> (J.F. Gmelin, 1789)	Barred buttonquail	4					Granivore (Terrestrial bird)
28	<i>Turnix suscitator</i> (J.F. Gmelin, 1789)	Lemon-bellied white-eye		3	5			Insectivore (Terrestrial bird)

In strata III (main part of the vegetation canopy) the richest bird species are 55.9%, strata IV is 17.3%, strata I is 18.9% and strata II is 7.9%. The species of birds associated in strata I and strata II were actually more terrestrial birds, compared to water bird species. Terrestrial bird species include barred buttonquail (*Turnix suscitator*), javan myna (*Acridotheres javanicus*), brown-throated sunbird (*Anthreptes malacensis*), house sparrow (*Passer domesticus*), spotted dove (*Spilopelia chinensis*), sooty-headed bulbul (*Pycnonotus aurigaster*). Barred buttonquail, spotted dove, sooty-headed bulbul are typical birds whose activities are mostly in bushes, soil, around grass on the beach or in fields (Mackinon 2010). Types of water birds in strata I and II include Small blue kingfisher (*Alcedo caeruleus*) and collared kingfisher (*Todiramphus chloris*). In strata III, the species richness is higher in mixed mangrove and dry vegetation types than in pure mangrove vegetation types, especially terrestrial bird species.

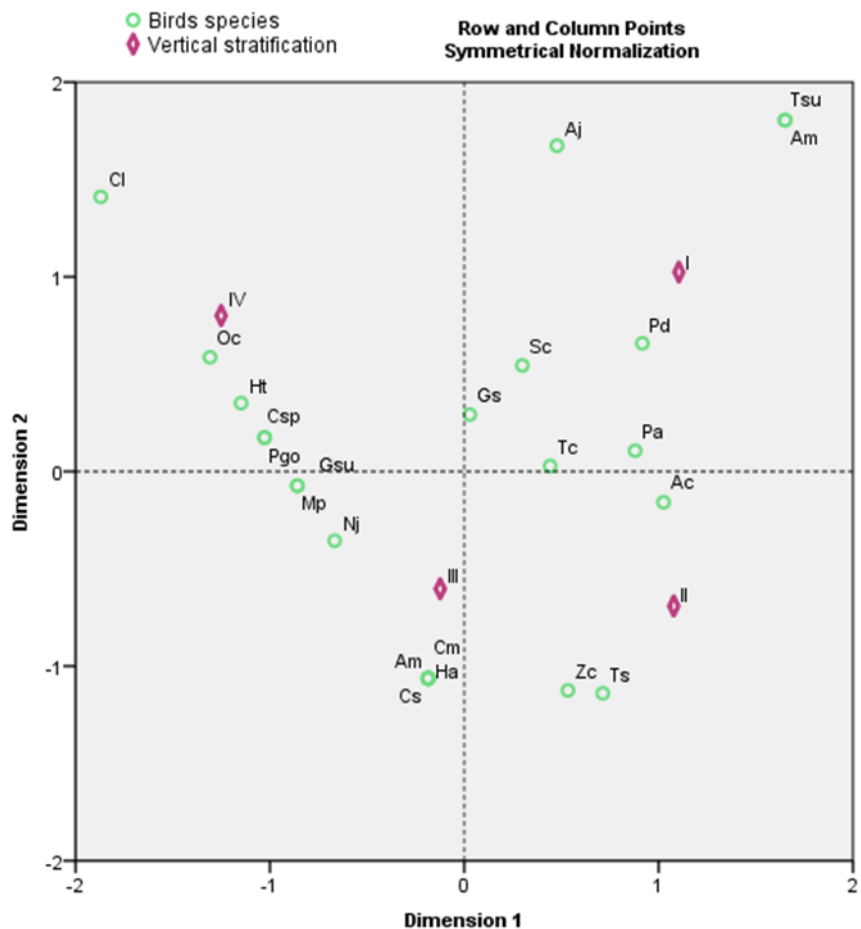


Figure 6. Biplot correspondence analysis of birds on mixed vegetation of mangroves and dry land. (Birds species code: **Aj**:*Acridotheres javanicus*; **Ac**:*Alcedo caeruleus*; **Ap**:*Amaurornis phoenicurus*; **Gs**: *Geopelia striata*; **Pd**: *Passer domesticus*; **Pa**: *Pycnonotus aurigaster*; **Sc**: *Spilopelia chinensis*; **Tc**:*Todiramphus chloris*; **Tsu**:*Turnix suscitator*; **Ts**:*Todiramphus sanctus*; **Zc**:*Zosterops chloris*; **Am**:*Anthreptes malacensis*; **Cm**:*Cacomantis merulinus*; **Cs**:*Copsychus saularis*; **Csp**:*Corvus sp.*; **Gsu**:*Gerygone sulphurea*; **Ht**:*Hirundo tahitica*; **Ha**:*Hypothymis azurea*; **Lsu**:*Lalage sueurii*; **Ls**:*Lanius shcach*; **Lm**:*Lonchura molucca*; **Mp**:*Merops philippinus*; **Nj**:*Nectarinia jugularis*; **Oc**:*Oriolus chinensis*; **Ph**:*Psilopogon haemacephala*; **Pgo**:*Pycnonotus goiaver*; **Tv**:*Treron vernans*; **Cl**:*Collocalia linchi*)

Bird species associated with strata IV include cave swiftlet (*Collocalia linchi*), back naped oriale (*Oriolus chinensis*), pacific swallow (*Hirundo tahitica*), and yellow vented bulbul (*Pycnonotus goiaver*). These

types of birds carry out the activity of catching insects while flying, some are perched on the top of the canopy while catching insects or small reptiles, some are perched while making sounds and some are flying over the canopy. Association for the use of bird species in mixed vegetation strata of mangroves and dry land, presented through biplot correspondence analysis (Figure 6).

In general, the factors that influence strata preference by birds are resources, both food and space to rest, perches, mating activities, nesting places, shelter from heat, shelter from predators, play, and the bioecological characteristics of the birds themselves. (Mackinon, 2010; Mohd-Azlan et al. 2015; Iswandaru et al. 2020; Safe'i et al. 2021; Pradana et al. 2022). For example, striated heron and purple heron are commonly found in strata I and II, namely the mangrove roots, mud flats or in water. This is related to the bird's habit of foraging for food, such as fish eaters or aquatic vertebrates. So, they will perch in areas close to the water to be able to keep an eye on their prey.

CONCLUSION

The use of mangrove vegetation strata by birds in the Nusa Lembongan mangrove ecosystem is divided into 4 vertical strata. There is a strong association between bird species and the vertical strata of vegetation. In pure mangrove vegetation, the number of bird species that are strongly associated with strata I is 5 species; strata II as many as 4 species; strata III is 5 species, and stratum IV is 4 species. In the mixed vegetation of mangroves and dry vegetation, there were 7 species of birds that had a strong association in strata I; strata II is 4 species; strata III as many as 7 species and strata IV is 3 species.

AUTHOR CONTRIBUTION

I.K.G. is the main author who design research, browse related literature, analyze data and write articles. I.K.M is responsible for collecting data in the field, tabulating data, and checking draft articles. M.J. assisting in data collection in the field, data tabulation, checking the English language of the manuscript.

ACKNOWLEDGMENTS

We would like to thank the Institute for Research and Community Service, Dean of the Faculty of Mathematics and Natural Sciences, Udayana University for facilitating research funding through the PUPS scheme. Thanks to Made Oka Vidyawidanta and Egmont Congdenjit, who have helped in the field.

CONFLICT OF INTEREST

We certify that there is no conflict of interest in the research or funding of this manuscript

REFERENCES

- Bibby, C.J. et al., 2000. *Bird Census Techniques*. 2nd edition. Academic Press, London.
- Cita, K.D. & Budiman, M.A.K. 2019. Bird Diversity and Its Association in Mangrove Habitats of Teluk Bintuni Regency, West Papua. *IOP Conference Series: Earth Environmental Sciences*, 394, 012006. doi: 10.1088/1755-1315/394/1/012006.

- Ginantra, I.K. et al., 2020. Diversity of Birds for Ecotourism Attractions in the Mangrove Ecosystem of Nature Conservation Forum Putri Menjangan. *Journal of Environmental Management and Tourism*, 11 (1), pp.54-64.
- Hernowo, J.B. 2016. Birds Communities at Mangrove of Batu Ampar, Kubu Raya District, West Kalimantan Province. *JMHT*, 22(2), pp.138-148.
- Iswandaru, D. et al., 2020. Bird community structure of small islands: a case study on the Pahawang Island, Lampung Province, Indonesia. *Silva Balcanica*, 21(2), pp.5-18. doi: 10.3897/silvabalcanica.21.e56108.
- Kartijono, N.E. et al., 2010. Vegetation Species Diversity and Bird Habitat Profile of Pulau Nyamuk Mangrove Forest of Karimunjawa National Park. *Biosaintifika*, 2(1), pp.27-39.
- Kitamura, S. et al., 1998. Handbook of Mangroves in Indonesia. Bali and Lombok. The International Society For Mangrove Ecosystem (ISME).
- Kusmana, C. & Azizah, N.A., 2022. Species composition and Vegetation Structure of Mangrove Forest in Pulau Rambut Wildlife Reserve, Kepulauan Seribu, DKI Jakarta. *IOP Conf. Series: Earth and Environmental Science*, 950, 012020.
- Kopij, G. 2000. Diet of Swifts (Apodidae) and Swallows (Hirundinidae) During the Breeding Season in South African Grassland. *ACTA ORNITHOLOGICA.*, Vol. 35 (2000) No. 2: 202-206
- Mancini, P.L. et al., 2018. Differences in diversity and habitat use of avifauna in distinct mangrove areas in São Sebastião, São Paulo, Brazil. *Ocean & Coastal Management*, 164, pp.79-91. <https://doi.org/10.1016/j.ocecoaman.2018.02.002>.
- MacKinnon, J. et al., 2010. *Birds of Sumatra, Java, Bali and Kalimantan (Including Sabah, Sarawak and Brunei Darussalam)* [LIPI-Field Guide Series]. Bogor: Puslitbang Biologi-LIPI.
- Mohd-Azlan, J. et al., 2015. The Role of Habitat Heterogeneity in Structuring Mangrove Bird Assemblages. *Diversity*, 7(2), pp.118-136. doi: 10.3390/d7020118
- Nagelkerken, I. et al., 2008. The habitat function of mangroves for terrestrial and marine fauna: A review. *Aquatic Botany*, 89(2), pp.155-185. doi: 10.1016/j.aquabot.2007.12.007
- Pradana, F.E. et al., 2022. Utilization of Mangrove Vegetation Vertical Strata by Bird in Wonorejo, Surabaya. Copyright © 2022 ADOC.PUB. Available at: <https://adoc.pub/queue/pemanfaatan-strata-vertikal-vegetasi-mangrove-oleh-burung-di.html>
- Ramadhani, A. et al., 2022. Diversity and abundance of water birds in the mangrove area of south coast of Bangkalan, Madura Island, Indonesia. *BIODIVERSITAS*, 23(6), pp.3277-3284. doi: 10.13057/biodiv/d230657
- Safe'i, R. et al., 2021. Biodiversity and Site Quality as Indicators of Mangrove Forest Health Pasir Sakti, Indonesia. *Annals of R.S.C.B.*, 25 (2), pp.4400- 4410.
- Salahuddin, M.A.A. et al., 2021. Species Diversity of Birds as Bioindicators for Mangroves Damage at Special Economic Zones (SEZ) Mandalika in Central of Lombok, Indonesia. *IOP Conf. Series: Earth and Environmental Science*, 913, 012058. doi: 10.1088/1755-1315/913/1/012058

- Sutopo, N. et al., 2017. Spatial and Time Pattern Distribution of Water Birds Community at Mangrove Ecosystem of Bengawan Solo Estuary - Gresik Regency). *Media Konservasi*, 22(2), pp.129-137. doi: 10.29244/medkon.22.2.129-137
- Sumardika, I.P.A. et al. 2017. Bird Species Richness In Serangan Island, Bali. *Jurnal Biologi Udayana*, 21(2), pp.64 -70. doi: 10.24843/JBIOUNUD.2017.vol21.i02.p04
- Setiawan F. et al., 2012. Mapping of Mangrove Forest Density Area as a Marine Conservation Area in Nusa Lembongan, Bali Using Alos Satellite Imagery. (Research Report). Universitas Padjadjaran.
- Wetland International, 2022. Wetlands International-Indonesia Programme. Available at : <https://indonesia.wetlands.org/id/>
- Wisnubudi, G. 2009. Use of Vegetation Strates By Bird In The Area Tourism Mountain Halimun-Salak National Park. *VIS VITALIS*, 2 (2), pp.41-49.

Research Article

Induction of Synthetic Polyploids of Porang (*Amorphophallus muelerri* Blume) and Assessment of Its Genetic Variability Using Morphological Data and RAPD Molecular Marker

Suyono¹, Imey Tamara Indivia², Ruri Siti Resmisari², Fitriyah², Didik Wahyudi^{1*}

1) Plant Physiology Laboratory, Biology Department, Science and Technology Faculty Universitas Islam Negeri Maulana Malik Ibrahim Malang, Jl. Gajayana No.50, Kota Malang, Jawa Timur 65144, Indonesia.

2) Plant Tissue Culture, Biology Department, Science and Technology Faculty Universitas Islam Negeri Maulana Malik Ibrahim Malang, Jl. Gajayana No.50, Kota Malang, Jawa Timur 65144, Indonesia.

3) Biology Molecular Laboratory, Biology Department, Science and Technology Faculty Universitas Islam Negeri Maulana Malik Ibrahim Malang, Jl. Gajayana No.50, Kota Malang, Jawa Timur 65144, Indonesia.

*Corresponding author, email: didik_wahyudi@bio.uin-malang.ac.id

Keywords:

Genetically modified organisms
iles-iles
molecular marker
porang mutant
suweg

Submitted:

11 February 2023

Accepted:

16 June 2023

Published:

11 October 2023

Editor:

Furzani Binti Pa'ee

ABSTRACT

This study uses morphological characteristics and RAPD markers to evaluate the polyploidization of synthetic porang. Seeds of triploid porang ($2n=2x=26$) were soaked in the different colchicine concentrations for 24 hours. After colchicine treatment, the porang seeds were planted to an MS medium that contained 2.2 μM of 6-benzylaminopurine (BAP), then, 40 days after planting in the MS media, the morphology and molecular of synthetic polyploid porang were characterized. For DNA extraction, a total of 100 mg of young leaves of porang plantlet was collected. One way Anova followed by the Duncan test (95%) was performed for phenotypic characterization. The number of different alleles, number of effective alleles, Shannon's information index, diversity, and unbiased diversity were assessed for genetic diversity. Synthetic polyploid porang has a higher total shoot, root, and wider leaves than normal porang. Polyploidy induction also successfully increased the genetic diversity of porang, and the genetic diversity will increase porang adaptability and sustainability of porang cultivation.

Copyright: © 2023, J. Tropical Biodiversity Biotechnology (CC BY-SA 4.0)

INTRODUCTION

Porang (*Amorphophallus muelerri*) known as tuberous plant is a member of the *Araceae* family. (Wahyudi et al. 2013). Porang tuber contains the highest glucomannan compared to the other genus in family of *Araceae* (Ekowati et al. 2015). Glucomannan is a hemicellulose that is hydrocolloid and easily soluble in water (Nurlela et al. 2021), so it is widely used for food ingredients (Tester & Al-Ghazzewi 2017) and emulsifier in the industrial product (Li et al. 2018). Furthermore, glucomannan is also beneficial in the food sector as used as an ingredient for shirataki, konnyaku, edible film, and artificial rice (Tester & Al-Ghazzewi 2017). In the industrial sector, glucomannan is widely used as material for immobilization, fixation support, and encapsulation (Yang et al. 2017). Because of its many benefits, making porang a major export commodity in Indonesia

(Atase Perdagangan KBRI Tokyo 2021).

Through the Ministry of Agriculture, the Indonesian government has instructed to cultivate porang throughout the archipelago. However, most farmers have cultivated the porang vegetatively using bulbils and tubers recently. Unfortunately, these types of cultivation cause porang in Indonesia to have a low genetic variation (Wahyudi et al. 2013; Nikmah et al. 2016). Alternatively, porang farmers use seeds as a seedling. Still, because porang seeds are apomixis, the resulting plants are either genetically similar to their parents or have a limited range of traits. That will have an impact on the sustainability of porang cultivation in Indonesia. Therefore, efforts to increase porang genetic variation either through polyploidy induction (Touchel et al. 2020) or mutation induction are urgently needed.

Naturally, over the course of their evolutionary history, the majority of Angiosperms double their genomes once or more (Aversano et al. 2012). However, polyploidy can be synthetically triggered with the aid of colchicine, oryzalin, and trifluralin (Touchel et al. 2020). Still, polyploid induction with colchicine was more successful than with oryzalin and trifluralin (Talebi et al. 2017). Colchicine is an alkaloid that causes mutations and doubles plant chromosomes (Alkadi et al. 2018) by inhibiting the anaphase stage. Inhibition of anaphase causes spindle fibers to bind to tubulin, resulting in the chromosomes not being separated, which eventually causes cells to contain multiple chromosomes (polyploidy) (Miri 2020). Colchicine has been frequently used as a chemical agent to induce polyploidy and has succeeded in increasing the productivity of flowering plants (Manzoor et al. 2019), herbal plants (Madani et al. 2019) and horticultural plants (Eng & Ho 2019)

According to a report, after polyploidization, synthetic polyploids displayed quick alterations in the genomic organization and gene activity (Song & Chen 2015). Polyploid plants' genotypes can alter as a result of epigenetic and genetic interactions, heterozygosity, gene silence, and gene dosage effects (Miri 2020). Losing duplicated genes, DNA sequence changes, rearrangements of the structural chromosome, and gene conversion are some examples of genomic modifications after polyploidy induction (Ding & Chen 2018). Some morphological characteristics including plant height, leaf and stomata morphology, flowering time, biomass, and tuber size are also the affected trait after polyploidy induction (Sattler et al. 2016).

The detection of polyploidy level is categorized as direct (Miri 2020) and indirect method (Wibisono et al. 2021). The direct method, which counts the total of chromosomes during metaphase of cell division using cytogenetic techniques, is frequently time-consuming and requires quite specific procedures for every species (Sattler et al. 2016). In addition, high chromosome number and small chromosome size are also a shortcoming of direct method by using cytogenetic (Guo et al. 2016). Indirect methods like morphological, physiological, and molecular markers are additional methods of addressing the direct method's shortcomings in detecting polyploidization in the plant (Sattler et al. 2016). Normally, the morphological assessment considers the quantity, total, and size of leaves and shoots (Salma et al. 2017). The polyploid synthetic plant commonly has a bigger flower, larger fruit, and tuber and ticker leaf than the normal plant (Zang et al. 2018).

Advances in molecular technologies have opened a new perspective for determining polyploidization. For example, Guo et al. (2016) have succeeded in developing 10 single copies of fully informative SSRs for detecting ploidy levels in polyploid willow. With the help of this analytical tools, polyploids plant may be promptly screened, and precise ploidy

levels can be efficiently confirmed by flow cytometry (FCM). Also, [Aliyev et al. \(2007\)](#) used random amplified polymorphic DNA (RAPD) to detect diploid and tetraploid wheat. Furthermore, [Wahyudi et al. \(2020\)](#) successfully used the RAPD marker to detect mutant soybean after being induced by ethyl methyl sulfonate (EMS). Gene redundancy after polyploid induction may be the reason why dominant molecular markers like RAPD is widely used for polyploidy detection ([Aversano et al. 2012](#)). Therefore, the current study aims to assess the polyploidization of synthetic porang by using morphological character and RAPD marker.

MATERIALS AND METHODS

Plant Material, polyploidy induction, and in vitro propagation

Six treatments with four replications, and a completely randomized design were used in this study. Seeds of triploid porang ($2n=2x=26$) were used for chromosome duplication. Total of 72 of porang seeds were soaked in the variation of colchicine concentration, including 0, 0.05, 0.1, 0.15, 0.2, and 0.25 ppm for twenty hours in dark condition. After colchicine treatment, porang seed was transferred to an MS medium supplemented with 2.2 μ M of 6-benzylaminopurine (BAP). All cultures were preserved at $25\pm 2^{\circ}\text{C}$ under 24-hour white illumination (1,500 lux) for 40 days. After 40 days in MS medium plantlets were ready for analysis.

Phenotypic characterization

Forty days after planting in the MS media, the morphology of synthetic polyploid porang was characterized. The total root and shoot, the height of shoot, and the length and width of leaves were calculated to compare normal and synthetic porang. The height of shoot was measured with the ruler from the shoot base to the highest of shoot. The length of leaves was measured with the ruler from the base to the tip of leaves whereas the width of leaves was measured from the widest side of the leaves. Young leaves were then stored for DNA isolation.

DNA Extraction and PCR RAPD

100 mg of young leaves of porang plantlet was collected for DNA isolation. The DNA was extracted using The Wizard® Genomic DNA Purification Kit Promega following the manufacturer's guidelines for plants. The quality of total DNA was then assessed by electrophoresis on 1% agarose gel for DNA isolation and 1.5 % for PCR RAPD and ladder 1-Kb (Thermo Scientific) was used as a marker.

PCR-RAPD was carried out with PCR Thermocycler (BIORAD) using 17 OPA (Operon Technology Ltd) primers (OPA 1 -17). PCR reaction contains 10 μ l mixtures consisting of 3 μ l double distilled water (ddH₂O), 1 μ l primers of OPA 1-18 (10 pmol), 5 μ l MyTaq HSRed Mix and 1 μ l DNA template (20 ng/ μ l). The temperature profile of PCR consists of one cycle at 94 °C for 4 minutes, followed by 45 cycles of amplification. Each amplification cycle had denaturing step at 94 °C for 30 seconds, an annealing (the temperatures of OPA 1-17 were followed the research of [Probojati et al. \(2019\)](#)) for 30 seconds and terminated with extension step at 72 °C for 5 minutes. The final extension was performed at 72 °C for 7 minutes. The PCR products were then examined by gel electrophoresis (1.5%) followed by Sybr green staining, with a DNA ladder 100 bp (NexView) for marker. DNA bands were photographed under a UV transilluminator (BioRAD).

Data analysis

One-way Anova followed by the Duncan test (95%) was performed for

phenotypic characterization. The presence or absence of a certain DNA fragment was indicated by a score of 1 or 0 on the RAPD bands. To create the data matrix, only amplification bands that were repeatable and clear were rated. The matrix data (score 0 and 1) was then used to detect the genetic diversity of normal and synthetic polyploid porang. Genetic diversity was analyzed using GenAEx 6.5 software (Peakall & Smouse 2012). The genetic diversity was assessed based on N_a = No. of Different Alleles, N_e = No. of Effective Allele, I = Information Index, h = Diversity, and u_h = Unbiased Diversity. Furthermore, the data matrix was also used to cluster normal and synthetic polyploid porang. Unweighted pair group method with an arithmetic mean (UPGMA) algorithm followed by Jaccard's coefficient similarity (Hammer et al. 2001) was used for clustering analysis. Clustering analysis was performed in PAST (Paleontological Statistics) software. The percentage of polymorphism was determined by dividing the polymorphic bands of each primer by the sum of the scored bands x 100. The polyploidy was also assessed by comparing the band thickness of each primer and the presence of a band between normal and synthetic polyploidy of porang.

RESULTS AND DISCUSSION

Effect of colchicine on the morphology of synthetic polyploids of porang

The application of colchicine with different concentrations affects the growth of porang, especially the number of roots and shoots, shoots height and length, and width of leaves (Table 1). The most roots, as well as the longest and widest leaves in synthetic polyploids of porang showed at a concentration of 0.1 ppm, whereas the highest number and height of shoot was observed at a concentration of 0.15 ppm (Table 1). Applying colchicine above 0.1 ppm reduces the number of roots and length and width of leaves, whereas the concentration of colchicine above 0.15 ppm reduces the total and height of shoots (Table 1).

The increasing number of roots and shoots of the synthetic polyploid plant was also observed in *Dracocephalum kotschyi* Boiss (Zahedi et al. 2014) and *Sphagneticola calendulacea* (L.) (Kundu et al. 2018), where Tetraploid plants had much more roots than diploid plants. However, applying colchicine at high concentrations will negatively impact the plants because it will inhibit root growth (Manzoor et al. 2019) and reduce the percentage of root formation (Miri 2020). This phenomenon was also observed in this study, where the concentration of colchicine above 0.1 ppm decreased the formation of roots (Table 1).

Moreover, the length and width of leaves are also impacted by colchicine treatment (Table 1) (Figure 1). Talei et al. (2020) also stated a similar result on polyploid induction of *Stevia rebaudiana*. Different colchicine concentrations significantly affected to the total and length of leaves of *Stevia rebaudiana*. The increasing number of leaves will increase the stomata size and density, providing more efficient water use or transpiration rates (Wei et al. 2019).

Table 1. Colchicine's effect on the growth of synthetic polyploid porang.

Concentration	Roots number	Shoots number	Shoot height	leaf length	leaf width
0 ppm	1.875a	4.6625a	1.93a	1.2875a	0.8125a
0.05 ppm	3ab	4.745a	3.6075ab	3.425ab	2.1626ab
0.1 ppm	5.1650b	7.9975ab	6.315bc	5.655b	4.03b
0.15 ppm	3.9575ab	10.9950b	9.6425c	4.9325b	3.3b
0.2 ppm	2.665a	6.83ab	5.175ab	3.9ab	2.5ab
0.25 ppm	2a	4.58a	3.2925ab	3.2125ab	2.425ab

Note: Different letters indicate significantly different based on the 5% Duncan's test

Some polyploids are well-known for producing larger organs such as flowers, fruits, and especially the leaves (Eng & Ho 2019). This phenomenon, known as the "Giga" effect, causes cell size to increase as a result of the chromosome duplication (Sattler et al. 2016). As a result, the farmers will invest less in resources (such as fertilizer and plant growth regulators) to generate a larger crop, which can help reduce dangerous chemical residues (Manzoor et al. 2019). As a result, polyploidization could be advantageous for the agronomically-intensive industries of pomiculture, floriculture, and horticulture (Eng & Ho 2019). Likewise, in this study, increasing the number of roots, the size of the leaves, and the height of the shoots are expected to increase the porang tubers' sizes, so the results of this study will be very beneficial for farmers.

Natural and synthetic polyploid plants are thought to respond to environmental change more effectively than diploid ones. Nonetheless, specific reactions are more typical than predicted tendencies (Mtileni et al. 2021). Notably, polyploid plants are frequently more resistant to stressors such as drought (Li et al. 2021) and salinity (Chao et al. 2013). As a result, chromosome doubling induction is a common technique for increasing both phenotype and genotype traits (Breseghello et al. 2013). Polyploidy induction has been utilized with a variety of plants *Agastache foeniculum* (Talebi et al. 2017), *Musa* spp. (Khamrit & Jongrungrklang 2022), *Physalis peruviana* (Comlekcioglu & Ozden 2019), and *Capsicum annum* (Tammu et al. 2021) and proven to improve their agronomic value.

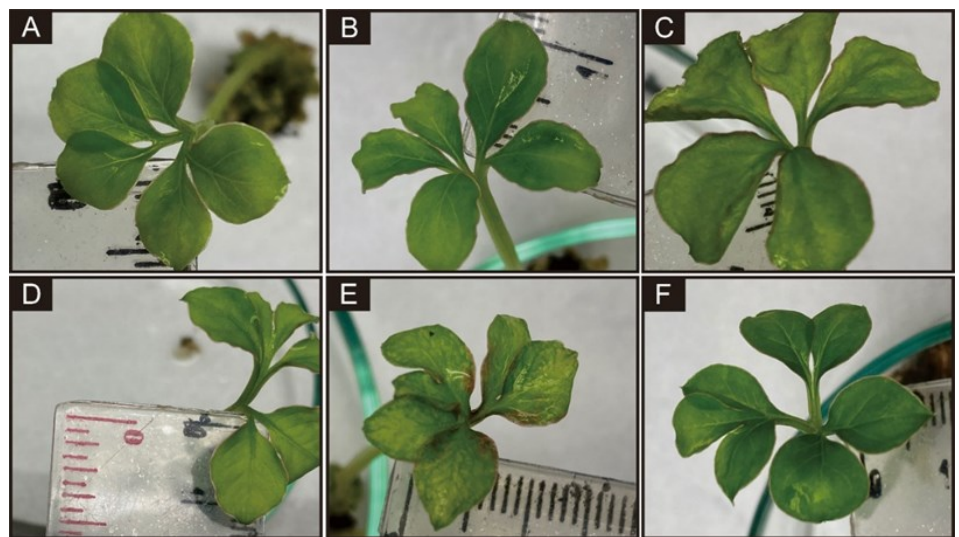


Figure 1. Effect of various concentrations of colchicine on length and width of leaves. a. 0 ppm b. 0.05 ppm c. 0.1 ppm d. 0.15 ppm e. 0.2 ppm f. 0.25 ppm.

Colchicine application also affects the number and height of shoots (Table 1) (Figure 2). However, colchicine application of more than 0.15 ppm decreased shoot formation and height of the shoot. Differences in shoot growth in synthetic polyploids of porang may be caused by the reorganization and restructuring of the polyploid plant genomes, resulting in alteration in genes activation (Soltis et al. 2015). The increased cell dimensions after genome duplication can be described as a sequence of downstream effects (Ruiz et al. 2020). However, it is yet unknown whether these cellular modification affect the overall phenotype and function of the organism (Madani et al. 2021).

Polyploid is a natural phenomenon and has long been acknowledged as an important factor in the diversification of Angiospermae (Soltis et al. 2015). The more genetic variation present in a single polyploid individual than in their diploid ancestors is frequently cited as the

reason for polyploids' "success" (Soltis et al. 2014). Moreover, this genetic diversity might result in novel biochemical, physiological, morphological, and ecological traits, giving polyploids an advantage over their diploid parents in the short term (Mtileni et al. 2021).

Polyploidy is an essential tool in plant breeding and has been commonly used by breeders to increase agronomic interest (Julião et al. 2020). The increase of agronomic interest was signed by the change in plant's morphological characteristics that can be accomplished by modification both chromosome and gene numbers in a cell. Polyploidy is a common phenomenon that is found in over 80% of plants and contributes for 2–4% in flowering plants speciation (Madani et al. 2021).



Figure 2. Effect of various concentrations of colchicine on the number and length of the shoot. a. 0 ppm b. 0.05 ppm c. 0.1 ppm d. 0.15 ppm e. 0.2 ppm f. 0.25 ppm.

There are three principal advantages of polyploidy induction, including heterosis (Bansal et al. 2012), gene redundancy (Roulin et al. 2013), and asexual reproduction (Manzoor et al. 2019). In contrast to their diploid parents, heterosis on synthetic polyploids produces robust polyploid plants (Bansal et al. 2012). Gene redundancy, on the other hand, preserves polyploid synthetic plants from the harmful effects of mutation. However, the induction of polyploid plants has a disadvantage, including the interrupting effects of nuclear and cell enlargement, the epigenetic instability that leads to gene regulation changes, and meiotic errors (Madani et al. 2021).

Polyploidy induction using colchicine increase genetic diversity of synthetic polyploids of Porang

A total of 36 loci were successfully amplified using 16 RAPD primers. OPA 15 produced the fewest band (1 band), and OPA 11 produced the most bands (4 bands) (Figure 3). The distinctive band between normal and synthetic polyploid porang was observed in OPA 7 (600 and 700 bp) and OPA 13 (1000 bp) (Figure 3). The appearance of a new band (new

allele) in synthetic polyploids of porang was detected in OPA 11 (600 bp) (Figure 3). The thickening band between normal and synthetic polyploid porang was also detected (600 and 700 bp in OPA 7 and 13) (Figure 3).

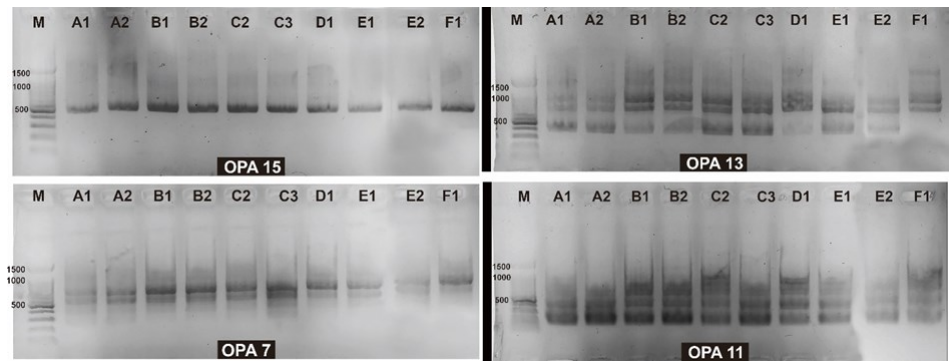


Figure 3. RAPD amplification profile of normal and synthetic polyploid porang. A1 and A2: 0 ppm, B1 and B2: 0.05 ppm, C1 and C2: 0.1 ppm, D1 and D2: 0.15 ppm, E1 and E2: 0.2 ppm and F1: 0.25 ppm.

Polyploids are able to be identified based on characteristic of morphology (Miri 2020) and physiology (Fu et al. 2021) with limited precision. Otherwise, we can count the chromosome number under a microscope to directly identify polyploids (Moghbel et al. 2015) or use a flow cytometer to assess DNA concentration (Guo et al. 2016). However, these procedures are laborious and time-consuming, especially when working with many samples. In contrast to these traditional methods, molecular markers offer a highly effective and trustworthy way to select polyploids on a wide scale from natural stands (Aversano et al. 2012).

The emergence of the new allele in synthetic polyploid was also detected in *Lippia alba* (Julião et al. 2020) and *Glycine max* L (Roulin et al. 2013). Genome duplication or redundancy, that enables one of the copies of a chromosome to accumulate mutations (del Pozo & Ramirez-Parra 2015), might explain why synthetic polyploid porang has a new allele and thickening band. In addition, of course, these genetic and epigenetic changes result in the evolution of novel features, which boosts adaptability (Roulin et al. 2013).

A total of 36 loci were then used to detect the genetic diversity of normal and synthetic polyploid (mutant) porang. The Gene diversity index and the percentage of polymorphic loci are general parameters used as indicators of the genetic richness of the taxa. Synthetic polyploid porang has a higher Shannon index value and a percentage of polymorphic loci than normal porang (Table 2). Furthermore, synthetic polyploid porang also has higher diversity and unbiased diversity value than normal porang (Table 2). This result indicated that polyploid induction using colchicine successfully increases the genetic diversity of porang.

Polyploidy induction has been shown to promote genetic diversity by establishing breeding lines in short order and rehabilitating hybrid fertility (Pereira et al. 2014). The increasing genetic diversity after polyploid induction seems to be a general phenomenon that has also been observed in *Lippia alba* (Julião et al. 2020), *Gerbera hybrida* (Bhattarai et al. 2021) and *Pogostemon Cablin* (Afifah et al. 2020). Increasing genetic diversity will bring several benefits and improvements in various contexts, including plant adaptability, disease resistant and increasing productivity and yield.

Three main clusters were divided into normal porang and induced polyploid porang (Figure 4). The first cluster comprises normal porang (control), whereas the second and third clusters contain induced poly-

Table 1. Colchicine's effect on the growth of synthetic polyploid porang.

Parameter	Normal porang	Synthetic polyploid porang
P (%)	27.78	88.89
Na (mean ± SE)	1.278 ± 0.076	2.167 ± 0.102
Ne (mean ± SE)	1.278 ± 0.076	1.846 ± 0.083
I (mean ± SE)	0.193 ± 0.052	0.635 ± 0.049
He (mean ± SE)	0.139 ± 0.038	0.413 ± 0.030
uHe (mean ± SE)	0.278 ± 0.076	0.472 ± 0.035

polyploid porang (Figure 4). The second cluster consists of induced polyploid porang with a concentration (0.05-0.15 ppm) and is observed to be morphologically different compared to normal porang (control) (Figure 1). This result indicated the RAPD marker's capability for genotyping synthetic polyploid plants. This result also recommends using 0.05-0.15 ppm of colchicine when inducing polyploid in porang.

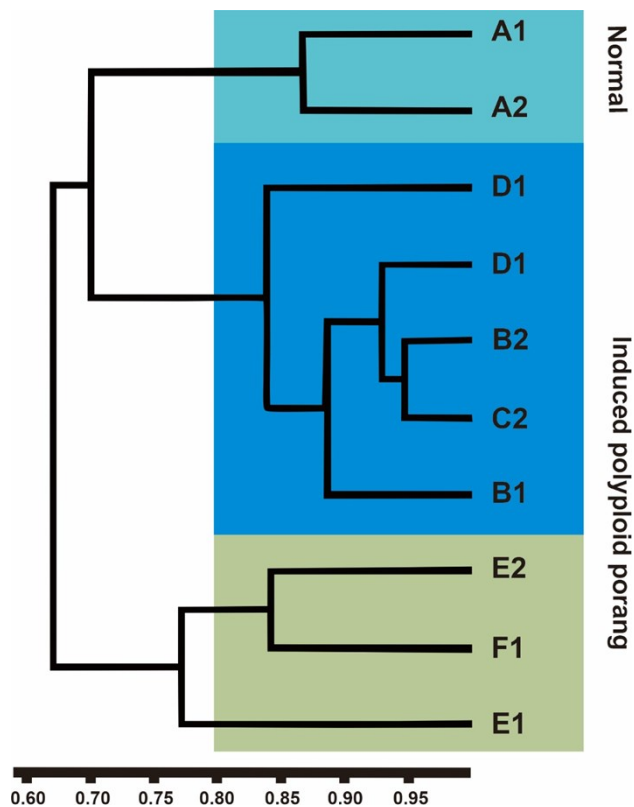


Figure 4. Clustering analysis of normal and synthetic polyploid porang. A1 and A2: 0 ppm, B1 and B2: 0.05 ppm, C1 and C2: 0.1 ppm, D1 and D2 0.15 ppm, E1 and E2: 0.2 ppm and F1: 0.25 ppm. Note: Number below the scale shows the similarity value.

Clustering analysis (Figure 4) strengthens the finding that polyploidy induction is proven to increase genetic diversity (Table 2). This is undoubtedly profitable for porang cultivation since porang cultivation has recently been practised by most vegetative farmers using tuber and bulbils (Lontoh et al. 2019), so porang has low genetic diversity (Wahyudi et al. 2013). In addition, although porang produces seed, the seed is apomixis which causes porang seedlings to have the same character as their parent. Therefore, polyploidization is the only way to enhance the genetic diversity of porang.

CONCLUSIONS

In conclusion, polyploidy induction is successfully achieved in porang, resulting in porang with a higher total shoot, root, and wider leaves.

However, a colchicine concentration above 0.1 decreases the productivity of porang. Polyploidy induction also successfully increased the genetic diversity of porang; of course, the genetic diversity will improve porang adaptability and support the sustainability of porang cultivation. In addition, RAPD is a reliable marker capable of determining the polyploid on porang.

AUTHOR CONTRIBUTION

S., D.W., and R.S.R. conceived the presented idea, developed the theory, and performed the computations. I.T.I. and F. contribute in practical lab and data collection. All authors discussed the results and contributed to the final manuscript.

ACKNOWLEDGMENTS

This research was funded by Universitas Islam Negeri Maulana Malik Ibrahim Malang through bantuan penelitian pengembangan pendidikan tinggi with number DIPA BLU- DIPA 025.04.2.423812/2022. The authors are also thankful to porang group research of Biology Department Fakultas Saintek Universitas Islam Negeri Maulana Malik Ibrahim Malang.

CONFLICT OF INTEREST

No Conflict of interest

REFERENCES

- Afifah, U.A.N., Wiendi, N.M.A. & Maharijaya A. 2020. In vitro polyploidy Induction of patchouli (*Pogostemon Cablin* Benth.) by colchicine. *Journal of Tropical Crop Science*, 7(1), pp.37-44. doi: 10.29244/jtcs.7.01.37-44
- Aliyev, R.T., Abbasov, M.A. & Mammadov, A.C., 2007. Genetic identification of diploid and tetraploid wheat species with RAPD markers. *Turkish Journal of Biology*, 31, pp.173-180.
- Alkadi, H., Khubeiz, M. & Jbeily, R., 2018. Colchicine : A Review on Chemical Structure and Clinical Usage. *Infectious Disorders - Drug Targets*, 18(2), pp.105-121. doi: 10.2174/1871526517666171017114901
- Atase Perdagangan KBRI Tokyo., 2021. *Laporan Analisis Intelijen Bisnis Porang HS: 071440*. Atase Perdagangan KBRI Tokyo 2021.
- Aversano et al., 2012. Molecular tools for exploring polyploid genomes in plants. *International Journal of Molecular Sciences*, 13(8), pp. 0316-10335. doi: 10.3390/ijms130810316
- Bansa, P., Banga, S. & Banga, S.S., 2012. Heterosis as investigated in terms of polyploidy and genetic diversity using designed *Brassica juncea* amphiploid and its progenitor diploid species. *Plosone*, 7(2), p.e29607. doi: 10.1371/journal.pone.0029607.
- Bhatarai, K., Kareem, A. & Deng, Z., 2021. In vivo induction and characterization of polyploids in gerbera daisy. *Scientia Horticulturae*, 282, pp.1-8. doi: 10.1016/j.scienta.2021.110054
- Breseghello, F. & Coelho, A.S.G., 2013. Traditional and modern plant breeding methods with examples in rice (*Oryza sativa* L.). *Journal of Agricultural and Food Chemistry*, 61, pp. 8277-8286. doi: 10.1021/jf305531j
- Chao et al., 2013. Polyploids exhibit higher potassium uptake and salinity tolerance in arabidopsis. *Science*, 341, pp. 658-659. doi: 10.1126/science.1240561

- Comlekcioglu, N. & Ozden, M., 2019. Polyploidy induction by colchicine treatment in golden berry (*Physalis peruviana*), and effects of polyploidy on some traits. *Journal of Animal and Plant Sciences*, 29(5), pp.1336-134.
- del Pozo, J.C. & Ramirez-Parra, E. 2020., Whole genome duplications in plants: an overview from Arabidopsis. *Journal of Experimental Botany*, 66(22), pp.6991–7003. doi: 10.1093/jxb/erv432
- Ding, M. & Chen, Z.J., 2018. Epigenetic perspectives on the evolution and domestication of polyploid plant and crops. *Current Opinion in Plant Biology*, 42, pp.37-48.
- Eng, W.H. & Ho, W.S., 2019. Polyploidization using colchicine in horticultural plants: A review. *Scientia Horticulturae*, 246, pp.604-617. doi: 10.1016/j.scienta.2018.11.010
- Ekowati, G., Yanuwadi, B. & Azrianingsih R., 2015. Sumber glukomanan dari edible Araceae di Jawa Timur. *Jurnal Pembanginan dan alam Lestasi*, 6(1), pp.32-41.
- Fu et al., 2021. Physiological characteristics and genetic diversity of *Lilium distichum* Nakai autotetraploids. *Scientia Horticulturae*, 282, p.110012. doi: 10.1016/j.scienta.2021.110012
- Guo et al., 2016. An analytical toolkit for polyploid willow discrimination. *Scientific Reports*, 6, pp.1-8. doi: 10.1038/srep37702
- Hammer, O., Harper, D.A.T. & Ryan, P.D., 2001. Past: Paleontological statistics software package for education and data analysis. *Palaeontologia Electronica*, 4, pp.1-9.
- Julião et al., 2020. Induction of synthetic polyploids and assessment of genomic stability in *Lippia alba*. *Frontiers in Plant Science*, 11(292), pp.1-11. doi: 10.3389/fpls.2020.00292
- Khamrit, R. & Jongrungklang, N., 2022. In vitro tissue culture techniques and colchicine-induced polyploidy in banana (*Musa*, AA Group)' Kluai Khai. *Asian Journal of Plant Sciences*, 21(1), pp.111-118. doi: 10.3923/ajps.2022.111.118
- Kundu et al., 2018. In vitro tetraploidization for the augmentation of wedelolactone in *Sphagneticola calendulacea* (L.) Pruski. *Acta Physiologiae Plantarum*, 40(12), pp.1–11. doi: 10.1007/s11738-018-2786-5
- Li et al., 2018. Konjac glucomannan octenyl succinate (KGOS) as an emulsifier for lipophilic bioactive nutrient encapsulation. *Journal of the Science of Food and Agriculture*, 98(15), pp.5742-5749. doi: 10.1002/jsfa.9122
- Li et al., 2021. Multiple responses contribute to the enhanced drought tolerance of the autotetraploid *Ziziphus jujuba* Mill. var. *spinosa*. *Cell & Bioscience*, 11(119), pp.2-10. doi: 10.1186/s13578-021-00633-1
- Lontoh et al., 2019. Yield evaluation of selected clones apomictic iles-iles (*Amorphophallus muelleri* Blume) on second growing period. *Indonesian Journal of Agronomy*, 47(2), pp.171-179. doi: 10.24831/jai.v47i2.19445
- Madani et al., 2021. Effect of polyploidy induction on natural metabolite production in medicinal plants. *Biomolecules*, 11(6), p.899. doi: 10.3390/biom11060899
- Manzoor et al., 2019. Studies on colchicine induced chromosome doubling for enhancement of quality traits in ornamental plants. *Plants*, 8(194), pp.2-16. doi:10.3390/plants8070194
- Miri, S.M., 2020. Artificial polyploidy in the improvement of horticultural crops. *Journal of Plant Physiology and Breeding*, 10(1), pp.1-28.

- Mtileni, M.P., Venter, N. & Glennon, K.L., 2021. Ploidy differences affect leaf functional traits, but not water stress responses in a mountain endemic plant population. *South African Journal of Botany*, 138, pp.76-83. doi: 10.1016/j.sajb.2020.11.029
- Moghbel, N., Borujeni, M.K. & Bernard, F., 2015. Colchicine effect on the DNA content and stomata size of *Glycyrrhiza glabra* var.glandulifera and *Carthamus tinctorius* L. cultured in vitro. *Journal of Genetic Engineering and Biotechnology*, 13(1), pp.1-6. doi: 10.1016/j.jgeb.2015.02.002
- Nurlela et al., 2021. Characterization of glucomannan extracted from fresh porang tubers using ethanol technical grade. *Molecule*, 16(1), pp.1-8. doi: 10.20884/1.jm.2021.16.1.632
- Nikmah, I.A., Azrianingsih, R. & Wahyudi, D., 2016. Genetic diversity of porang populations (*Amorphophallus muelleri* Blume) in Central Java and West Java based on LEAFY second intron marker. *Journal of Tropical Life Science*, 6(1), pp.23-27. doi: 10.11594/jtls.06.01.05
- Peakall, R. & Smouse, P.E., 2012. GenALEX 6.5: genetic analysis in Excel. Population genetic software for teaching and research-an update. *Bioinformatics*, 28, pp.2537-2539.
- Pereira et al., 2014. Chromosome duplication in *Lolium multiflorum* Lam. *Crop Breeding and Applied Biotechnology*, 14, pp.251-255. doi:1590/1984-70332014v14n4n39
- Probojati, RT., Wahyudi, D., & Hapsari, L. 2019. Clustering analysis and genome inference of pisang raja local cultivars (*Musa* Spp.) from Java Island by random amplified polymorphic DNA (RAPD) marker. *Journal of Tropical Biodiversity and Biotechnology*, 4(2), pp.42-53. doi: 10.22146/jtbb.44047
- Roulin et al., 2013. The fate of duplicated genes in a polyploid plant genome. *The Plant Journal*, 73(1), 143-153. doi: 10.1111/tpj.12026
- Ruiz et al., 2020. Synthetic polyploidy in grafted crops. *Frontiers in Plant Science*, 11, p.540894. doi: 10.3389/fpls.2020.540894
- Salma, U., Kundu, S. & Mandal, N., 2017. Artificial polyploidy in medicinal plants: advancement in the last two decades and impending prospects. *Journal of Crop Science and Biotechnology*, 20(1), 9-19. doi: 10.1007/s12892-016-0080-1
- Sattler, M.C., Carvalho, C.R. & Clarindo, W.R., 2016. The polyploidy and its key role in plant breeding. *Planta*, 243, pp.281-296.
- Soltis et al., 2014. Polyploidy and novelty: Gottlieb's legacy. *Philosophical Transactions of the Royal Society B*, 369, pp.20130351. doi: 10.1098/rstb.2013.0351
- Soltis et al., 2015. Polyploidy and genome evolution in plants. *Current Opinion in Genetics & Development*, 35, pp.119-125. doi: 10.1016/j.pbi.2005.01.001
- Song, Q. & Chen, J., 2015. Epigenetic and developmental regulation in plant polyploids. *Current Opinion in Plant Biology*, 24, pp.101-109. doi: 10.1016/j.pbi.2015.02.007
- Talebi et al., 2017. Effect of different antimitotic agents on polyploid induction of anise hyssop (*Agastache foeniculum* L.). *Caryologia*, 70, pp.184-193. doi: 10.1080/00087114.2017.1318502
- Talei et al., 2020. Improving productivity of steviol glycosides in *Stevia rebaudiana* via induced polyploidy. *Journal of Crop Science and Biotechnology*, 23(4), pp.301-309. doi: 10.1007/s12892-020-00038-5

- Tammu, R.M., Nuringtyas, T.R. & Daryono, B.S., 2021. Colchicine effects on the ploidy level and morphological characters of Katokkon pepper (*Capsicum annuum* L.) from North Toraja, Indonesia. *Journal of Genetic Engineering and Biotechnology*, 19(31), pp.2-8. doi: 10.1186/s43141-021-00131-4
- Tester, R.F. & Al-Ghazzawi, F.H., 2013. Mannans dan health, with a special focus on glucomannans. *Food Research International*, 50, pp.384-391. doi: 10.1016/j.foodres.2012.10.037
- Touchell, D.H., Palmer, I.E. & Ranney, T.G., 2020. In vitro ploidy manipulation for crop improvement. *Frontiers in Plant Science*, 11, p.722. doi: 10.3389/fpls.2020.00722
- Wahyudi, D., Azrianingsih, R. & Mastuti R., 2013. Genetic variability of porang populations (*Amorphophallus muelleri*) in West Java and Central Java based on trnL intron sequences. *Journal of Biodiversity and Environmental Science*, 3(9), pp.31-41.
- Wahyudi, D., Hapsari, L. & Sundari., 2020. RAPD analysis for genetic variability detection of mutant Soybean (*Glycine max* (L.) Merr). *Journal of Tropical Biodiversity and Biotechnology*, 5(1), pp.68-77. doi: 10.22146/jtbb.53653
- Wibisono et al., 2021. Performance of putative mutants and genetic parameters of *Plectranthus amboinicus* (L.) through mutation induction with colchicine. *AGROSAINSTEK: Jurnal Ilmu dan Teknologi Pertanian*, 5(2), pp.89-99.
- Wei et al., 2019. Functional trait divergence and trait plasticity confer polyploid advantage in heterogeneous environments. *New Phytologist*, 221, pp. 2286–2297.
- Yang et al., 2017. A review on konjac glucomannan gels: microstructure and application. *International Journal of Molecular Sciences*, 18(11), pp.2250. doi: 10.3390/ijms18112250
- Zahedi et al., 2014. Overproduction of valuable methoxylated flavones in induced tetraploid plants of *Dracocephalum kotschy* Boiss. *Botanical Studies*, 55(22), pp.1-10
- Zhang et al., 2018. Induction, identification and characterization of polyploidy in *Stevia rebaudiana* Bertoni. *Plant Biotechnology*, 35, pp. 81-86.

Research Article

In Silico Analysis of *Phalaenopsis Orchid Homeobox1* (*POH1*) Functional Gene for Shoot Development in *Phalaenopsis Orchid*

Nuzlan Rasjid¹, Febri Yuda Kurniawan², Saifa Usni Putri¹, Aviesta Linggabuwana¹, Ireneus Seno Prasajo¹, Endang Semiarti^{1*}

1)Department of Tropical Biology. Faculty of Biology, Universitas Gadjah Mada. Sleman, D.I. Yogyakarta 55281, Republic of Indonesia.

2)Study Program of Biotechnology, Graduate School, Universitas Gadjah Mada. Sleman, D.I. Yogyakarta 55281, Republic of Indonesia.

* Corresponding author, email: endsemi@ugm.ac.id

Keywords:

POH1

Conserved Domain

Transcription Factor

Protein Modelling

Phalaenopsis

Submitted:

17 April 2023

Accepted:

26 June 2023

Published:

16 October 2023

Editor:

Furzani Binti Pa'ee

ABSTRACT

The most favorite ornamental crop in Indonesia is orchid which benefited as floriculture. Therefore, the quality of this crop must be improved. Biotechnology is appropriate to be used to improve the quality and quantity of orchid plants. To conduct this method, researchers must know what genes function in plant development. In *Phalaenopsis* orchids, the gene has been identified as homeobox genes called *Phalaenopsis Orchid Homeobox1* (*POH1*). This research aims to conduct *in silico* analysis of the gene. The materials were retrieved from mRNA and amino acid databases. Then, the materials are aligned, visualized, motif location analysis, motif function discovery, phylogenetic construction, and protein 3D structural modelling. Based on mRNA and amino acid alignment, there are 4 domain regions that are conserved in *POH1* and other homologous genes, such as KNOX1, KNOX2, ELK Domain, and Homeobox KN Domain, which roles as a transcription factor involved in plant development. SWISS-MODEL and ColabFold were used in protein modelling of the protein. By ColabFold modelling, the modelling prediction uses 325 residues, higher than SWISS-MODEL in 59 residues. ColabFold validation by Ramachandra Plot depicts having the most favourite regions is 68.6%, while SWISS-MODEL is 92.3%. Another validation parameter is overall quality factor and QMEAN Score. Protein modelling by ColabFold has overall quality factor 89.252 and QMEAN Score 0.41 ± 0.05. However, SWISS-MODEL 3D prediction has overall quality factor 98.039 and QMEAN score of 0.71 ± 0.11.

Copyright: © 2023, J. Tropical Biodiversity Biotechnology (CC BY-SA 4.0)

INTRODUCTION

Orchids are the most favourite ornamental crops in Indonesia. Approximately, there are 5,000 orchids out of 30,000 orchids found throughout the world's third-largest area of tropical rainforest (Semiarti et al. 2015). They have been used in the floriculture trade, e.g. cut flowers and potted plants (Chandra De et al. 2014). Furthermore, the quality of the crops should be improved by biotechnology methods. To use this method, we must have a comprehensive understanding of orchid development (Hossain et al. 2013).

All plants during their life cycle will grow into three phases, name-

ly, the embryogenic phase, the vegetative phase, and the generative phase (Howell 1998). Each phase is characterised by phenotypic change as effect of the expression of functional genes. These genes interact with each other and one of them is the key gene that will drive into the next phase (Howell 1998; Moore 2013). These are called homeobox genes that function in developmental transcription factors and are identified in plants and animals (Holland 2013; Viola & Gonzalez 2016).

In plants, there are 14 classes that are classified as homeobox genes and one of the genes is the class-1 *KNOTTED1-like homeobox* (*KNOX1*) gene. It is identified as transcriptional factor for maintaining the Shoot Apical Meristem (SAM) (Scofield et al. 2008). The SAM in plants comprises indeterminate cells that continually regenerate and then form structures above ground. In the next step, it contributes to the formation of plant shoots (Howell 1998). In orchids, there are two growth habits that are known as sympodial and monopodial. *Phalaenopsis* orchids have monopodial growth habit that depicts from one stem and grows pointedly upward (Zahara & Win 2019). A gene that has been identified in *Phalaenopsis* orchids called *Phalaenopsis Orchid Homeobox1* (*POH1*), which is *KNOX1* homologous gene (Semiarti et al. 2008). The gene affects shoot formation of orchid in earlier stages of plant development, mainly in 4-16 weeks and after 48 weeks development, based on its expression analysis (Semiarti et al. 2016). This article intends to perform *in silico* analysis of the genes.

MATERIALS AND METHODS

Materials

The research was conducted from December 2022 to March 2023. The materials were retrieved from mRNA and amino acid databases. Then, they would be analysed by bioinformatic tools. The mRNA and amino acid sequence had been obtained from the NCBI database (<https://www.ncbi.nlm.nih.gov/>) and OrchidBase 6.0 (<https://cosbi.ee.ncku.edu.tw/orchidbase6/>).

Methods

The obtained sequences were aligned and visualized by Multalin on <http://multalin.toulouse.inra.fr/multalin/> (Corpet 1988). Motif location analysis use MEME Suite (<https://meme-suite.org/meme/tools/meme>) (Bailey et al. 2015) and motif function analysis use InterPro (<https://www.ebi.ac.uk/interpro/about/interproscan/>) (Paysan-Lafosse et al. 2023). Then, the phylogenetic tree of mRNA was constructed using the Maximum Likelihood approach with bootstrapping 1000 repeats, Kimura 2-parameter model with 2 Gamma distribution model and amino acid sequence using JTT (Jones Taylor Thornton) with 2 gamma distribution model, by MEGA 11 (Tamura et al. 2021). To carry out protein 3-dimensional structural prediction, ColabFold (Goddard et al. 2018; Mirdita et al. 2022) and SWISS-MODEL web server (<https://swissmodel.expasy.org/>) were used (Arnold et al. 2006). The prediction structure was validated with Ramachandran Plot on PROCHECK (Laskowski et al. 2013), Overall Quality Factor on ERRAT (Colovos & Yeates 1993), and protein model quality estimation on QMEAN (Benkert et al. 2009). To evaluate the modelled structure, benchmarking to AlphaFold database (<https://www.ebi.ac.uk/Tools/sss/fast/>) was conducted.

RESULTS AND DISCUSSION

The Results of *POH1* gene Alignment

According to alignment analysis of *POH1* gene shows polymorphism at the nucleotide level. Through the analysis, it was seen that there are mutations and deletions in this alignment. Figure 1 shows coding sequences that would be translated into four domain regions, such as KNOX1, KNOX2, ELK domain and Homeobox KN Domain. The domain is categorized as Three Amino-Acid Loop Extension (TALE) family homeoproteins that are involved in plant growth and development. The gene structure of this gene is highly identical between species (Razzaq et al. 2020). In this case, *POH1* gene with other homologous genes is highly identical, it comprises around 900-1400 bp for each species.

The Analysis of Amino Acid Sequence

The *POH1* Protein sequence analysis shows a conserved amino acid sequence. Protein motif analysis and its location describe conserved regions on plants. It means that homeobox genes can be found in different species (Holland 2013). Its roles as a transcription factor that regulates gene function to enhance and repress certain genes (Gao et al. 2014; Yuan et al. 2018). Highly conserved amino acids are coloured in red and blue colours, meanwhile non-conserved amino acids are black colours (Figure 2). Motif locations at amino acid sequence indicated that there are 4 important domains to regulate plant development (Figure 3, Table 1). Each domain has specific roles in plant development. KNOX1 function correlates to tissue proliferation and maintains potential meristematic of flowering plant and moss sporophytes, while the function of KNOX2 is to regulate the alternation of generations by suppressing the haploid body plan in the diploid phase, which causes morphological transition to the land plants. Besides, KNOX1 modulation activity is involved in contributing to leaf shape diversity of flowering plants (Sakakibara et al. 2013; Furumizu et al. 2015). Moreover, KNOX2 also acts as negative regulator of secondary cell wall biosynthesis (Wang et al. 2020). ELK Domain acts as a signal for nuclear localization and is included in protein-protein interaction (Nagasaki et al. 2001; Ito et al. 2002; Nookaraju et al. 2022). Homeobox KN Domain acts as transcription factor that is conserved in different plants, which also affects in leaf shape elaboration (Wang & Jiao 2020; Zhang et al. 2022).

Phylogenetic Analysis of *POH1* Gene with Other Homologous Genes

The *POH1* phylogenetic analysis was performed by mRNA and amino acid sequences. In mRNA sequence phylogenetic construction, there are 2 clades and 1 outgroup. The gene sequence has highly similarities with *DOH1* gene from *Dendrobium* orchid. Moreover, phylogenetic construction by using amino acid sequence reveals that *POH1* gene still highly has similarities with *DOH1* from *Dendrobium* orchid (Figure 4a; b, respectively).

Protein Modelling of *POH1* Protein and Its Domain Function

The three-dimensional structural prediction was performed by 2 web servers, ColabFold (Figure 5a) and SWISS-MODEL (Figure 5b). Based on the Ramachandran plot, ColabFold structural prediction has residues in most favoured regions accounting for 68.6%, meanwhile, SWISS-MODEL has 92.3%. However, SWISS-MODEL modelling uses 59 residues, compared to ColabFold which uses 325 residues, all the translated amino acids. These results are correlated to algorithms that use in the

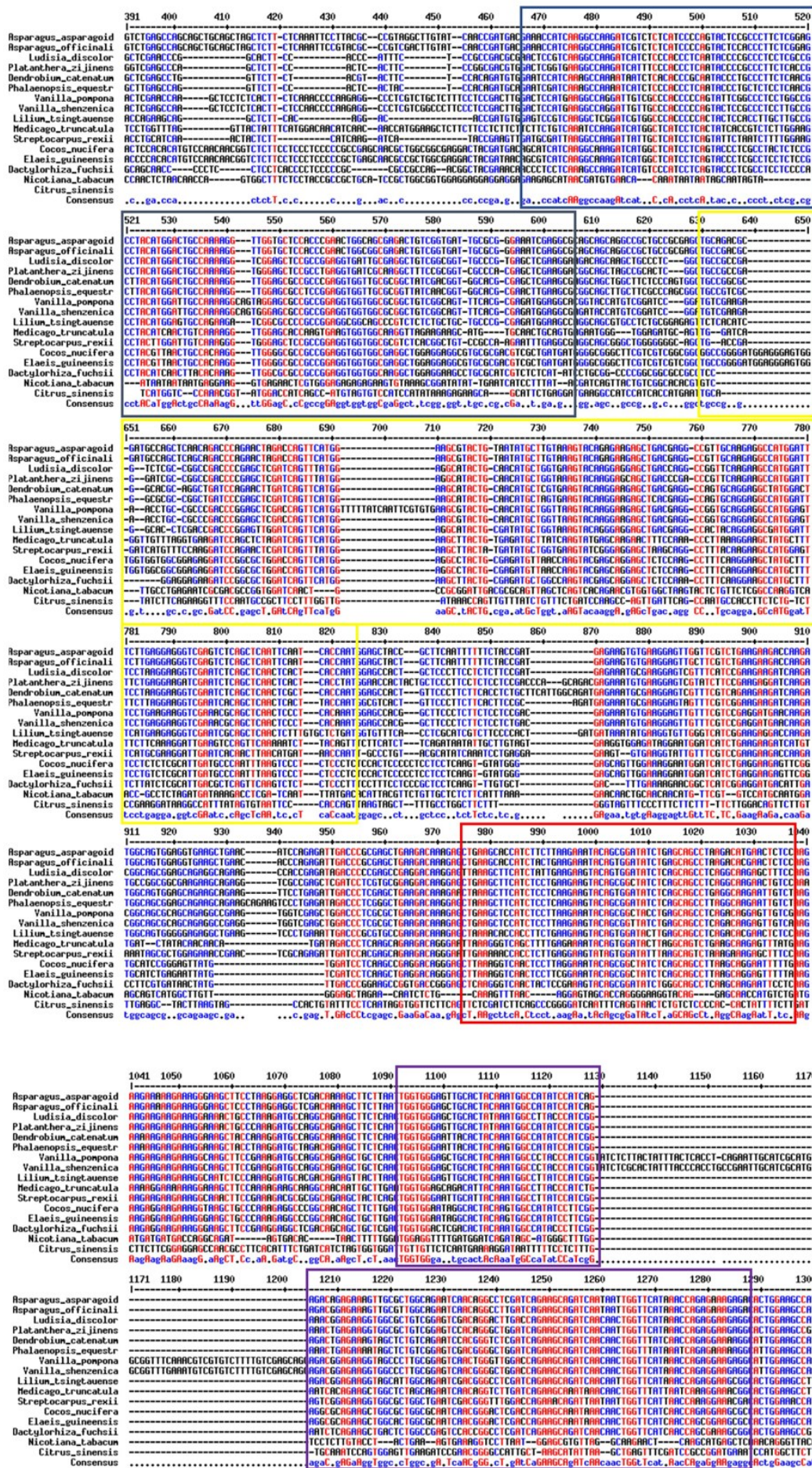


Figure 1. The result of *POHI* gene alignment with other homologous genes. Different colours of the box described different domains; = KNOX1; = KNOX2; = ELK Domain; and = Homeobox KN Domain.

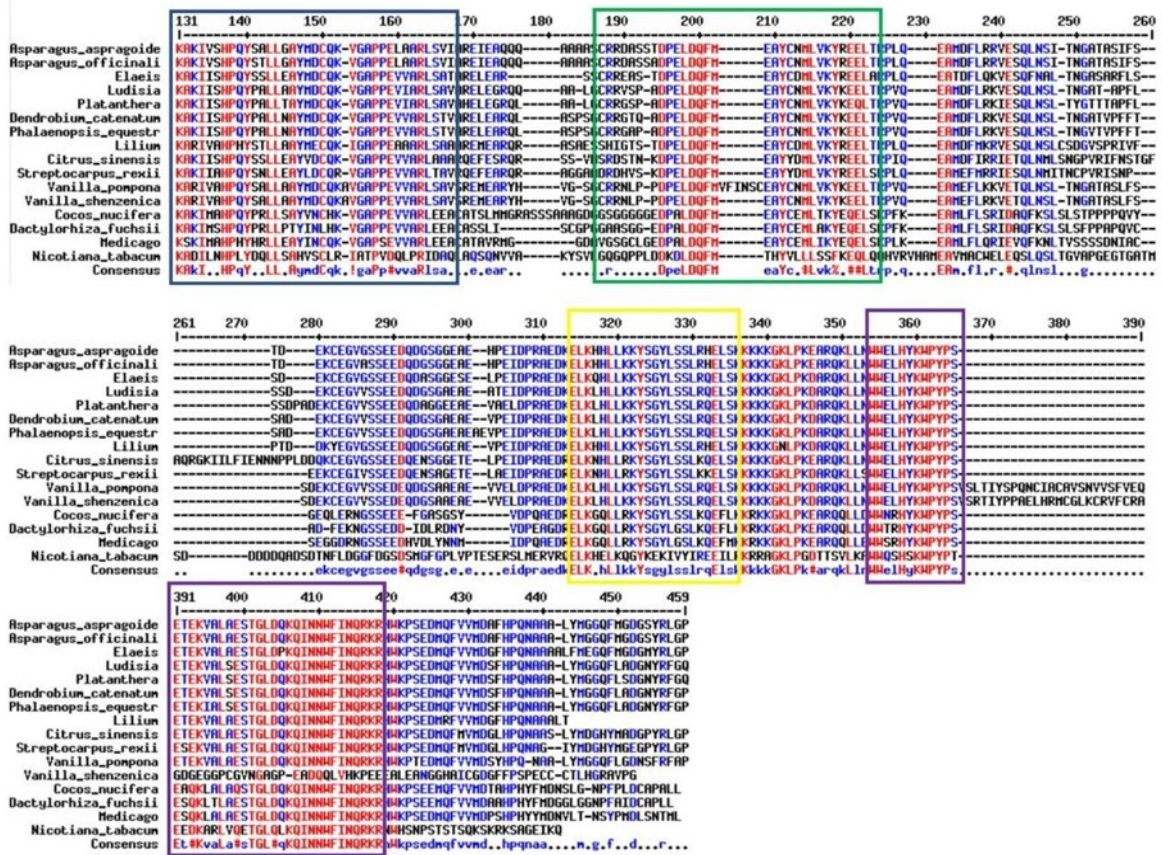


Figure 2. The result of POH1 protein alignment with other homologous genes. Different colours of the box described different domains; ■ = KNOX1; ■ = KNOX2; ■ = ELK Domain; and ■ = Homeobox KN Domain.

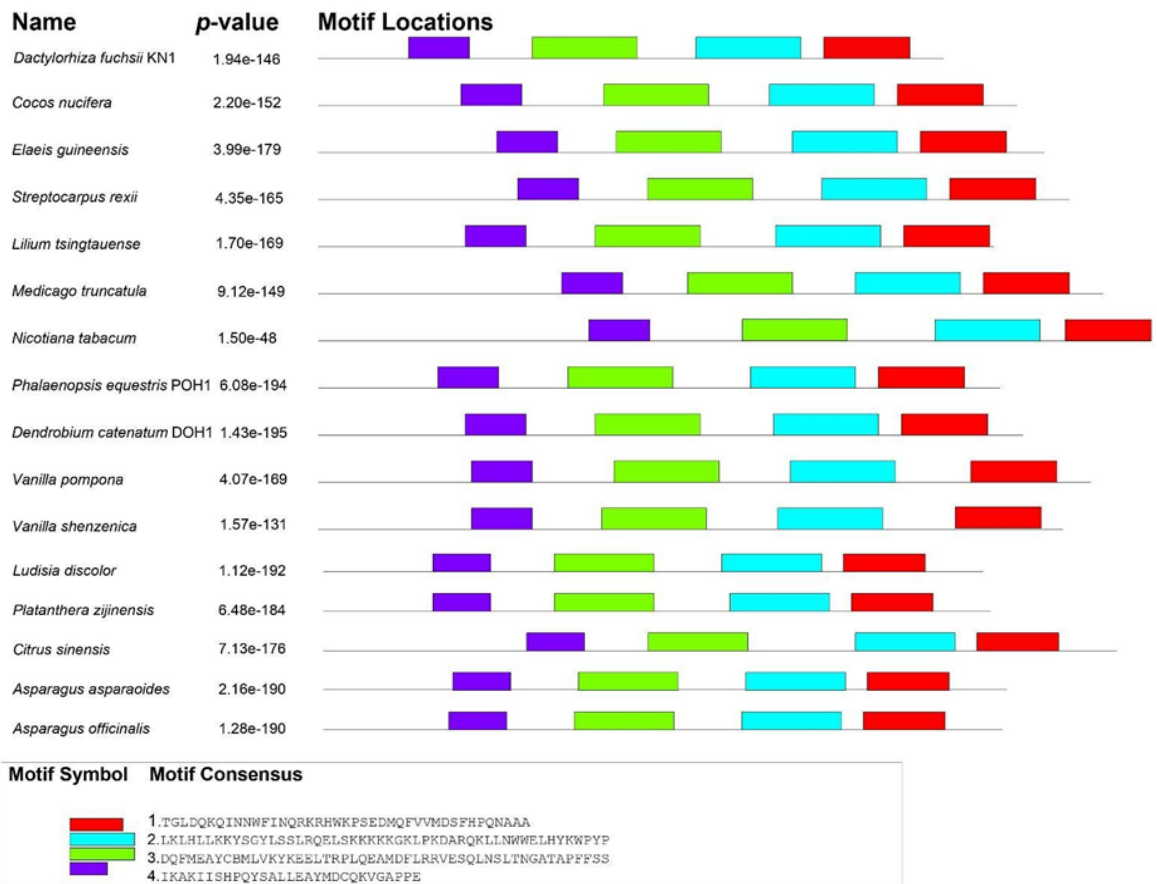






Figure 3. Domain location in amino acid sequence.

Table 1. The Function of Each Domain.

No	Domain	Domain Name	Function	Reference
1		Homeobox KN domain	Regulation DNA-templated transcription	(Hirayama et al. 2007; Mukherjee et al. 2010)
2		ELK domain	Nuclear localization signal; protein-protein interaction domain	(Nagasaki et al. 2001; Ito et al. 2002; Nookaraju et al. 2022)
3		<i>KNOX2</i>	DNA- binding	(Nagasaki et al. 2001)
4		<i>KNOX1</i>	DNA- binding	(Nagasaki et al. 2001)

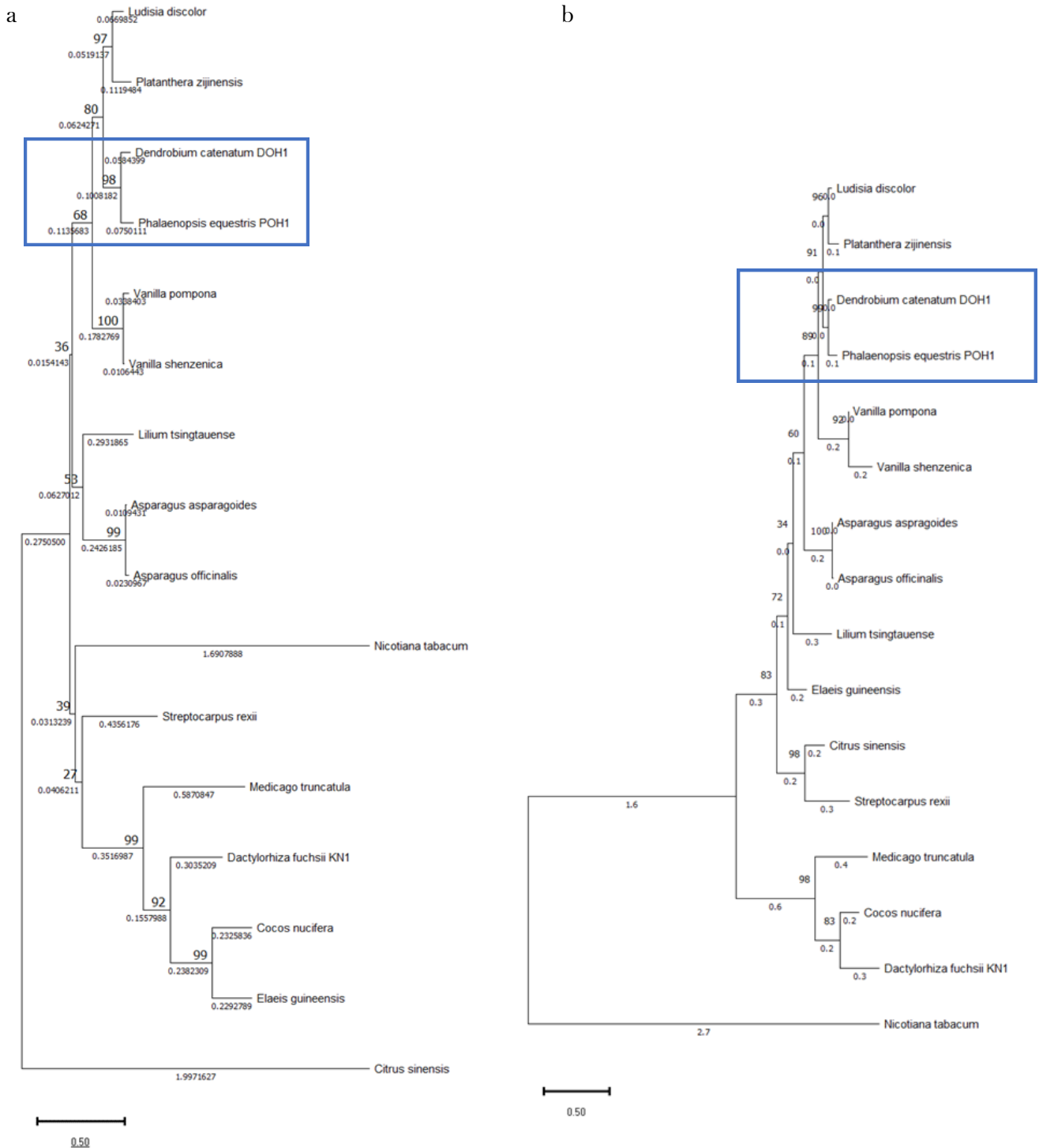


Figure 4. Phylogenetic analysis of *POH1* gene sequence with other homologous genes. (Construction by using: a. mRNA and b. amino acid sequences).

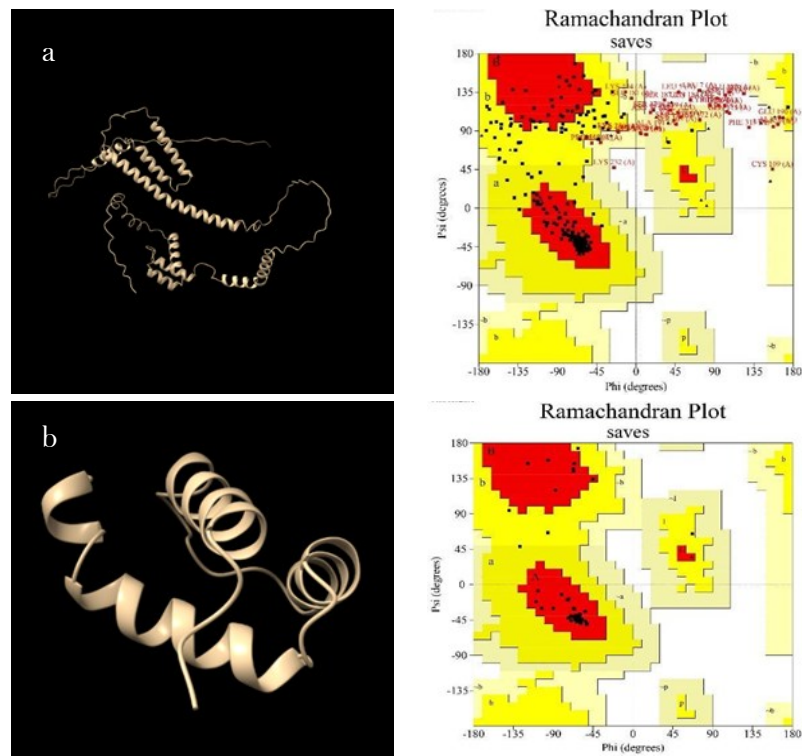


Figure 5. Three-Dimensional Structural Prediction. (a = ColabFold Modelling; b = SWISS-MODEL modelling).

WEB-SERVERS. ColabFold modelling focus on physical interactions or the evolutionary history (Jumper et al. 2021), meanwhile SWISS-MODEL build a model from templates in their database (Arnold et al. 2006). Moreover, other ways to validate protein modelling are overall quality factor and QMEAN score. Overall quality factor of these structures is 89.252 (ColabFold modelling) and 98.039 (SWISS-MODEL modelling) (Figure 6). According to QMEAN scores, SWISS-MODEL modelling has higher score than ColabFold, 0.71 ± 0.11 to 0.41 ± 0.05 (Figure 6 a; b, respectively). Moreover, benchmarking effort to AlphaFold database shows that the modelled protein has 50 proteins that are homolog. In the database, the homologous proteins comprise around 300-400 amino acids. The highest relationship of this modelled protein in structural AlphaFold database found on Homeobox Protein Knotted-1-like 2 in *Dendrobium catenatum* (AlphaFoldDB: A0A2I0XDV6). Based on ColabFold modelling, we investigate the location of domain, which is KNOX1, KNOX2, ELK Domain and Homeobox KN Domain in 3D structural prediction (Figure 7). KNOX1 and KNOX2 domains are formed into MEINOX domain which is separated by a poorly conserved linker sequence (Nookaraju et al. 2022).

MEINOX Domain that is located in N-terminus will interact with POX domain from BEL protein (Zhang et al. 2021). The interaction between POX and MEINOX is hydrophobic (Ezura et al. 2022). The interaction of them affects phytohormone regulation that is related to plant development (Niu & Fu 2022). The heterodimer modulates phytohormone by activating cytokinin and repressing gibberellin (Tadege 2013; Testone et al. 2015; Marsch-Martínez & de Folter 2016), which correlates to shoot development (Wybouw & De Rybel 2019; Arro et al. 2019). Not only for shoot development, but also KNOX protein linked up to the lignification process in dicot and monocot plants (Townsend et al. 2013; Xu et al. 2019), the diversity of leaf shape (Gao et al. 2015; Wang et al. 2022), and a necessary role in starchy storage organs (Dong et al. 2019; Rüscher et al. 2021). Moreover, it involves to environmental response because of high temperature and humidity stress (Shu et al. 2015). To

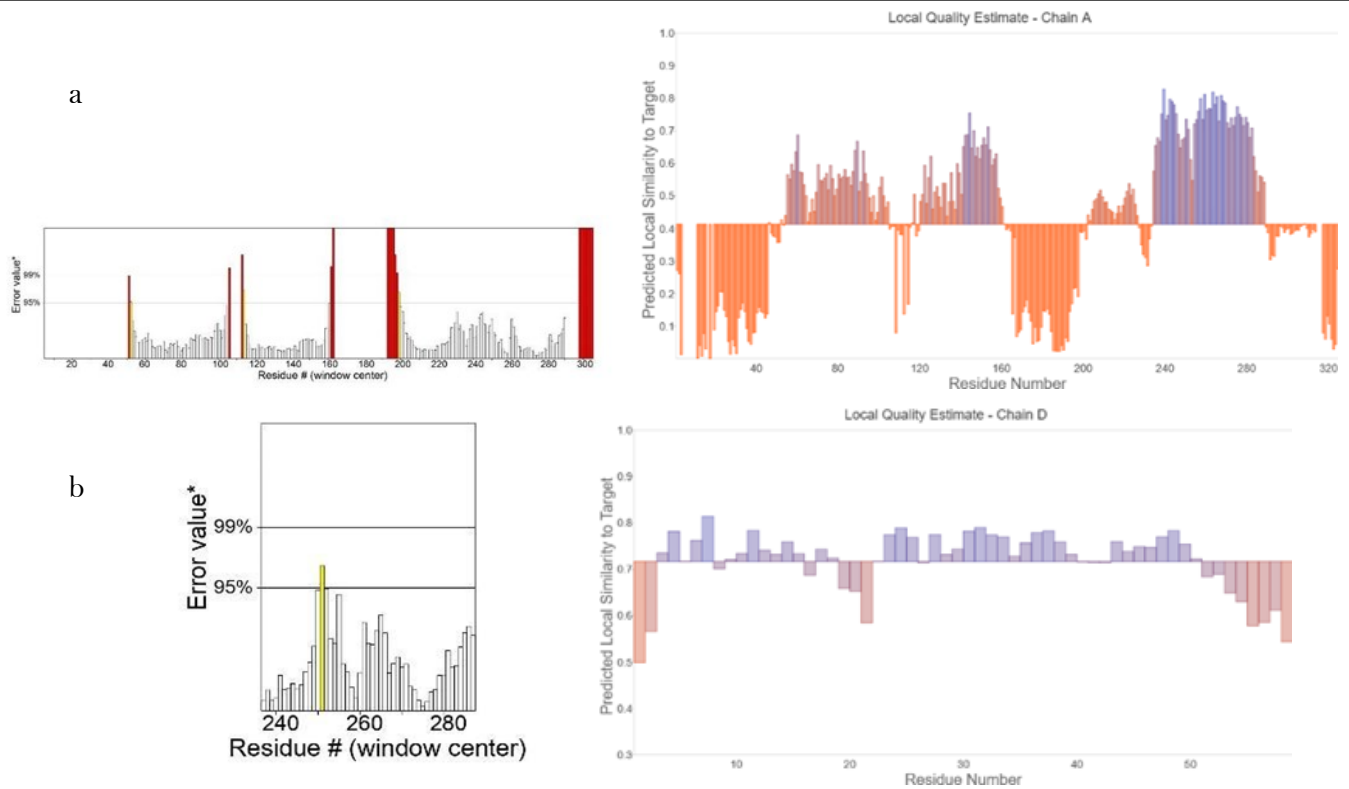


Figure 6. Protein Modelling Validation by Overall Quality Factor and QMEAN Score. (a = ColabFold Modelling; b = SWISS-MODEL Modelling).



Figure 7. The location of domain in 3D structural prediction. KNOX1, KNOX2, ELK, and homeobox KN domains are in green, yellow, blue, and red, respectively.

conclude this paragraph, the research on different functions of *POH1* gene, KNOX1 homologous gene in *Phalaenopsis* orchids, has to be broadened to reveal its functions.

CONCLUSIONS

POH1 gene is a gene that contributes to shoot formation in *Phalaenopsis* orchids and has four domains as transcription factors, such as KNOX1, KNOX2, ELK Domain, and Homeobox KN Domain. Three-dimensional structure modelling is performed by SWISS-MODEL and ColabFold. In SWISS-MODEL modelling use 59 residues with the percentage of most favoured regions of 92.3%, overall quality factor of 98.039, and QMEAN score 0.71 ± 0.11 , while ColabFold uses 325 residues with a percentage of most favoured regions accounting for 68.6%, overall quality factor 89.252, and QMEAN scores 0.41 ± 0.05 .

AUTHOR CONTRIBUTION

ES designed and controlled the research. NR conducted the data retrieval of mRNA and amino acid sequence and data analysis and wrote the manuscript. FYK, SUP, AL, and ISP conducted data and manuscript proof-reading.

ACKNOWLEDGMENTS

This research was supported by Universitas Gadjah Mada RTA (Rekognisi Tugas Akhir) 2022, Contract No: 3550/UN.1.P.III.Dit-Lit/PT.01.05/2022 that was given to ES as principal investigator.

CONFLICT OF INTEREST

The authors declare that there is no conflict of interest in this research.

REFERENCES

- Arnold, K. et al., 2006. The SWISS-MODEL workspace: a web-based environment for protein structure homology modelling. *Bioinformatics*, 22(2), pp.195–201. doi: 10.1093/bioinformatics/bti770.
- Arro, J. et al., 2019. RNA-Seq reveals new DELLA targets and regulation in transgenic GA-insensitive grapevines. *BMC Plant Biology*, 19(1), p.80. doi: 10.1186/s12870-019-1675-4.
- Bailey, T.L. et al., 2015. The MEME suite. *Nucleic acids research*, 43(W1), pp.W39–W49. doi: 10.1093/nar/gkv416.
- Benkert, P., Künzli, M. & Schwede, T., 2009. QMEAN server for protein model quality estimation. *Nucleic acids research*, 37 (suppl_2), pp.W510–W514. doi: 10.1093/nar/gkp322.
- Chandra De, L. et al., 2014. *Commercial orchids*, De Gruyter Open.
- Colovos, C. & Yeates, T.O., 1993. Verification of protein structures: patterns of nonbonded atomic interactions. *Protein science*, 2(9), pp.1511–1519. doi: 10.1002/pro.5560020916.
- Corpet, F., 1988. Multiple sequence alignment with hierarchical clustering. *Nucleic acids research*, 16(22), pp.10881–10890. doi: 10.1093/nar/16.22.10881.
- Dong, T. et al., 2019. RNA-Seq and iTRAQ reveal multiple pathways involved in storage root formation and development in sweet potato (*Ipomoea batatas* L.). *BMC plant biology*, 19(1), pp.1–16.
- Ezura, K., Nakamura, A. & Mitsuda, N., 2022. Genome-wide characterization of the TALE homeodomain family and the *KNOX-BLH* interaction network in tomato. *Plant Molecular Biology*, 109(6), pp.799–821. doi: 10.1007/s11103-022-01277-6.
- Furumizu, C. et al., 2015. Antagonistic roles for *KNOX1* and *KNOX2* genes in patterning the land plant body plan following an ancient gene duplication. *PLoS Genetics*, 11(2), e1004980. doi: 10.1371/journal.pgen.1004980.
- Gao, J. et al., 2015. Evolution, diversification, and expression of KNOX proteins in plants. *Frontiers in plant science*, 6, p.882. doi: 10.3389/fpls.2015.00882.
- Gao, J. et al., 2014. Molecular phylogenetic characterization and analysis of the WRKY transcription factor family responsive to *Rhizoctonia solani* in maize. *Maydica*, 59(1), pp.32–41.
- Goddard, T.D. et al., 2018. UCSF ChimeraX: Meeting modern challenges in visualization and analysis. *Protein Science*, 27(1), pp.14–25. doi: 10.1002/pro.3235.

- Hirayama, Y. et al., 2007. Expression patterns of class I *KNOX* and *TAB-BY* genes in *Ruscus aculeatus* (Asparagaceae) with implications for phylloclade homology. *Development Genes and Evolution*, 217(5), pp.363–372. doi: 10.1007/s00427-007-0149-0.
- Holland, P.W.H., 2013. Evolution of homeobox genes. *Wiley Interdisciplinary Reviews: Developmental Biology*, 2(1), pp.31–45. doi: 10.1002/wdev.78.
- Hossain, M.M. et al., 2013. The application of biotechnology to orchids. *Critical Reviews in Plant Sciences*, 32(2), pp.69–139. doi: 10.1080/07352689.2012.715984.
- Howell, S.H., 1998. *Molecular Genetics of Plant Development*, Cambridge: Cambridge University Press.
- Ito, Y., Hirochika, H. & Kurata, N., 2002. Organ-specific alternative transcripts of *KNOX* family class 2 homeobox genes of rice. *Gene*, 288 (1), pp.41–47. doi: [https://doi.org/10.1016/S0378-1119\(02\)00460-2](https://doi.org/10.1016/S0378-1119(02)00460-2).
- Jumper, J. et al., 2021. Highly accurate protein structure prediction with AlphaFold. *Nature*, 596(7873), pp.583–589. doi: 10.1038/s41586-021-03819-2.
- Laskowski, R.A., Furnham, N. & Thornton, J.M., 2013. The Ramachandran plot and protein structure validation. In *Biomolecular forms and functions: a celebration of 50 years of the ramachandran map*. World Scientific, pp.62–75. doi: 10.1142/9789814449144_0005.
- Marsch-Martínez, N. & de Folter, S., 2016. Hormonal control of the development of the gynoecium. *Current Opinion in Plant Biology*, 29, pp.104–114. doi: <https://doi.org/10.1016/j.pbi.2015.12.006>.
- Mirdita, M. et al., 2022. ColabFold: making protein folding accessible to all. *Nature Methods*, 19(6), pp.679–682. doi: 10.1038/s41592-022-01488-1.
- Moore, J.H., 2013. Gene Interaction. In *Brenner's Encyclopedia of Genetics: Second Edition*. Elsevier Inc., pp. 200–201. doi: 10.1016/B978-0-12-374984-0.00592-1.
- Mukherjee, K. & Brocchieri, L., 2010. Evolution of Plant Homeobox Genes. In *eLS*. Wiley. doi: 10.1002/9780470015902.a0022865.
- Nagasaki, H. et al., 2001. Functional analysis of the conserved domains of a rice *KNOX* homeodomain protein, OSH15. *The Plant cell*, 13(9), pp.2085–2098. doi: 10.1105/tpc.010113.
- Niu, X. & Fu, D., 2022. The roles of BLH transcription factors in plant development and environmental response. *International Journal of Molecular Sciences*, 23(7), 3731. doi: 10.3390/ijms23073731.
- Nookaraju, A. et al., 2022. Understanding the Modus Operandi of Class II *KNOX* Transcription Factors in Secondary Cell Wall Biosynthesis. *Plants*, 11(4), 493. doi: 10.3390/plants11040493.
- Paysan-Lafosse, T. et al., 2023. InterPro in 2022. *Nucleic Acids Research*, 51(D1), pp.D418–D427.
- Razzaq, A. et al., 2020. In silico analyses of TALE transcription factors revealed its potential role for organ development and abiotic stress tolerance in Cotton. *Int. J. Agric. Biol*, 23, pp.1083–1094. doi: 10.17957/IJAB/15.1389.
- Rüscher, D. et al., 2021. Auxin signaling and vascular cambium formation enable storage metabolism in cassava tuberous roots. *Journal of Experimental Botany*, 72(10), pp.3688–3703. doi: 10.1093/jxb/erab106.
- Sakakibara, K. et al., 2013. *KNOX2* genes regulate the haploid-to-diploid morphological transition in land plants. *Science*, 339(6123), pp.1067–1070. doi: 10.1126/science.1230082.

- Scofield, S., Dewitte, W. & Murray, J.A.H., 2008. A model for Arabidopsis class-1 KNOX gene function. *Plant Signaling & Behavior*, 3(4), pp.257–259. doi: 10.4161/psb.3.4.5194.
- Semiarti, E. et al., 2008. Isolation and characterization of *Phalaenopsis Orchid Homeobox1 (POH1)* cDNAs, knotted1-like homeobox family of genes in *Phalaenopsis amabilis* orchid. In *Proceedings of The 2nd International Conference on Mathematics and Natural Sciences (ICMNS) ITB, Bandung, Indonesia*. pp. 28–30.
- Semiarti, E. et al., 2015. Induction of In Vitro Flowering of Indonesian Wild Orchid, *Phalaenopsis amabilis* (L.) Blume. *KnE Life Sciences*, 2 (1), 398. doi: 10.18502/cls.v2i1.182.
- Semiarti, E. et al., 2016. Dynamic expression of *POH1* gene in shoot development during in vitro culture of *Phalaenopsis* orchid. *AIP Conference Proceedings*, 1744, 020019.. doi: 10.1063/1.4953493.
- Shu, Y. et al., 2015. GmSBH1, a homeobox transcription factor gene, relates to growth and development and involves in response to high temperature and humidity stress in soybean. *Plant Cell Reports*, 34 (11), pp.1927–1937. doi: 10.1007/s00299-015-1840-7.
- Tadege, M., 2013. Molecular insight into polarity-mediated lamina outgrowth. *International Journal of Plant Biology and Research*, 1(1), 1005.
- Tamura, K., Stecher, G. & Kumar, S., 2021. MEGA11: molecular evolutionary genetics analysis version 11. *Molecular biology and evolution*, 38(7), pp.3022–3027. doi: 10.1093/molbev/msab120.
- Testone, G. et al., 2015. The *KNOTTED-like* genes of peach (*Prunus persica* L. Batsch) are differentially expressed during drupe growth and the class 1 KNOPE1 contributes to mesocarp development. *Plant Science*, 237, pp.69–79. doi: 10.1016/j.plantsci.2015.05.005.
- Townsley, B.T., Sinha, N.R. & Kang, J., 2013. *KNOX1* genes regulate lignin deposition and composition in monocots and dicots. *Frontiers in Plant Science*, 4, 121. doi: 10.3389/fpls.2013.00121.
- Viola, I.L. & Gonzalez, D.H., 2016. Structure and evolution of plant homeobox genes. In *Plant Transcription Factors*. Elsevier, pp.101–112. doi: 10.1016/B978-0-12-800854-6.00006-3.
- Wang, S. et al., 2020. The Class II *KNOX* genes *KNAT3* and *KNAT7* work cooperatively to influence deposition of secondary cell walls that provide mechanical support to Arabidopsis stems. *The Plant Journal*, 101(2), pp.293–309. doi: 10.1111/tpj.14541.
- Wang, Y. et al., 2022. The cellular basis for synergy between *RCO* and *KNOX1* homeobox genes in leaf shape diversity. *Current Biology*, 32 (17), pp.3773–3784. doi: 10.1016/j.cub.2022.08.020.
- Wang, Y. & Jiao, Y., 2020. Keeping leaves in shape. *Nature Plants*, 6(5), pp.436–437. doi: 10.1038/s41477-020-0660-0.
- Wybouw, B. & De Rybel, B., 2019. Cytokinin – A Developing Story. *Trends in Plant Science*, 24(2), pp.177–185. doi: 10.1016/j.tplants.2018.10.012.
- Xu, X. et al., 2019. Identification of homeobox genes associated with lignification and their expression patterns in bamboo shoots. *Biomolecules*, 9(12), 862. doi: 10.3390/biom9120862.
- Yuan, Q. et al., 2018. A genome-wide analysis of GATA transcription factor family in tomato and analysis of expression patterns. *International Journal of Agriculture and Biology*, 20(6), pp.1274–1282. doi: 10.17957/IJAB/15.0626.
- Zahara, M. & Win, C.C., 2019. Morphological and stomatal characteristics of two Indonesian local orchids. *Journal of Tropical Horticulture*, 2(2), pp.65–69.

- Zhang, X. et al., 2022. Identification and responding to exogenous hormone of *HB-KNOX* family based on transcriptome data of Caucasian clover. *Gene*, 828, 146469. doi: <https://doi.org/10.1016/j.gene.2022.146469>.
- Zhang, Y. et al., 2021. Hormonal regulatory patterns of laknoxs and label1 transcription factors reveal their potential role in stem bulblet formation in LA hybrid lily. *International Journal of Molecular Sciences*, 22(24), 13502. doi: 10.3390/ijms222413502

Research Article

In silico Screening of Potential Antidiabetic Phenolic Compounds from Banana (*Musa* spp.) Peel Against PTP1B Protein

Rico Alexander Pratama¹, Junaida Astina¹, Arli Aditya Parikesit^{2*}

1)Department of Food Science and Nutrition, School of Life Sciences, Indonesia International Institute for Life Sciences (i3L), Jalan Pulomas Barat Kav 88, East Jakarta 13210, Indonesia

2)Department of Bioinformatics, School of Life Sciences, Indonesia International Institute for Life Sciences (i3L), Jalan Pulomas Barat Kav 88, East Jakarta 13210, Indonesia

* Corresponding author, email: arli.parikesit@i3l.ac.id

Keywords:

antidiabetic
banana peel
diabetes mellitus
in silico
phenolic compound
PTP1B

Submitted:

15 March 2023

Accepted:

11 July 2023

Published:

25 October 2023

Editor:

Ardaning Nuriliani

ABSTRACT

Type 2 diabetes mellitus (T2DM) is a global problem with increasing prevalence. The current treatments have made an immense progress with some side effects, such as drug resistance, acute kidney toxicity, and increased risk of heart attack. Banana (*Musa* spp.) peel comprises 40% of banana fruit contains high phenolic compounds whilst some studies have suggested a correlation between phenolic compounds and antidiabetic activity. One of the novel protein targets that has been identified as a potential anti-diabetic treatment is PTP1B (PDB ID:2NT7). Therefore, this study aimed to screen the potential PTP1B inhibitor for antidiabetic treatment from phenolic compounds in banana peel. QSAR, molecular docking, ADME-Tox, and molecular dynamics analysis were deployed to examine forty-three phenolic compounds in banana peel. Eighteen ligands were screened by QSAR analysis and eight of them had a lower binding energy than the standard (ertiprotafib) in molecular docking, with urolithin A and chrysin were the lowest. Both passed Lipinski's rule of five, had a good intestinal absorption, and no blood-brain barrier penetration, however, their mutagenicity, carcinogenicity, and irritation to the skin and eyes were still in questions. Molecular dynamics analysis found both of them were in a stable conformation with PTP1B. This study suggested a potential of urolithin A and chrysin as PTP1B inhibitor for antidiabetic treatment. Additionally, further experimentation is required to validate this finding.

Copyright: © 2023, J. Tropical Biodiversity Biotechnology (CC BY-SA 4.0)

INTRODUCTION

Type 2 Diabetes mellitus (T2DM) is a metabolic disease characterized by elevation of blood glucose level caused by a complex pathophysiology (Galicia-Garcia et al. 2020). Diabetes affects 415 million people globally and T2DM encompasses 90% of the patients (Chatterjee et al. 2017). Pathophysiology of T2DM includes initial insulin resistance which is compensated by an increase in insulin secretion to maintain glucose homeostasis, yet over time failure in β -cell occurs and insulin secretion is diminished, causing hyperglycemia (Goyal & Jialal 2020).

Current treatment of T2DM is focused on disease management, including diet, exercise, and blood glucose monitoring as well as pharmacological treatment (Goyal & Jialal 2020). In general, common targets for

antidiabetic drugs are categorized into insulin secretagogues, mimickers, and sensitizer, as well as starch and sugar blockers (Kanwal et al. 2022). Food and Drugs Administrative (FDA) has approved 59 antidiabetic drugs (36 mono- and combinatorial therapies) (Dahlén et al. 2022). However, this pharmacological treatment poses adverse effects, including drug resistance, acute kidney toxicity, and increased risk of heart attack (Salehi et al. 2019). Therefore, it is necessary to find a new therapeutic agent with less adverse effects, yet with better efficacy as a means to manage T2DM.

Approximately a hundred of new antidiabetic drugs are being developed in more than three hundreds clinical trials (Dahlén et al. 2022). Interestingly, 40% of these new drugs target novel therapeutic targets. One of the promising target for the antidiabetic treatment is Protein Tyrosine Phosphatase 1B (PTP1B) (Eleftheriou et al. 2019). PTP1B is known as a negative regulator in the insulin signalling pathway, in which it dephosphorylates insulin receptor and its substrate that eventually desensitize insulin action (Tautz et al. 2013; Eleftheriou et al. 2019; Liu et al. 2022). Interestingly, in a study of PTP1B knock-out mice exhibited better glucose control and insulin sensitivity (Haj et al. 2005). Therefore, its inhibition is thought to be a promising target for T2DM.

With a production of 120 tonnes annually, banana is the most produced fruit in the world, with India as the biggest producers, followed by China, Indonesia, and Uganda (Food and Agriculture Organization of the United Nations 2022). Comprising 40% of the fruit, banana peel is a major fruit waste (Sharma et al. 2016). This results in an enormous volume of waste being sent to the landfill or incinerator, which, if handled improperly, would later result in the emission of greenhouse gases and the generation of harmful incomplete combustion materials, among other environmental problems. On the other hand, banana peel is a good source of phytochemicals, including phenolic compounds (Acevedo et al. 2021). Therefore, it is important to identify alternate uses for banana peel.

In recent years, there has been growing interest in phenolic compounds due to their abundance in plants as secondary metabolites and their potential health-promoting roles, including as antioxidants, anti-cancer agents, anti-diabetic agents, inhibitors of adipogenesis, regulators of blood pressure, and suppressors of inflammatory genes (Gutiérrez-Grijalva et al. 2016). Specifically, the anti-diabetic effects of phenolic compounds have been extensively studied in animal and in limited human models, showing a decrease in blood glucose and improvement of insulin secretion and sensitivity (Aryaeian et al. 2017; Naz et al. 2019). Research has also shown that phenolic extracts from certain plants, such as persimmon, finger millet, raspberry, cumin, and fig, exhibit antidiabetic properties by inhibiting enzymes such as α -amylase and α -glucosidase (Asgar 2013; Wojdyło et al. 2016; Praparatana et al. 2022). *In silico* studies have also shown that phenolic compounds in anthocyanins, flavanols, flavonoids, and proanthocyanidins have the highest potential for antidiabetic effects (Asgar 2013; Damián-Medina et al. 2020; Mudunuri et al. 2022). Specifically, few studies have also predicted the potential inhibition of PTP1B by some phenolic compounds (Damián-Medina et al. 2020; Rath et al. 2022). However, despite extensive research, there is still a lack of understanding about the antidiabetic potential of phenolic compounds from banana peel.

Therefore, this study aimed to screen potential phenolic compounds in banana peel on antidiabetic property against PTP1B protein using an *in silico* approach, including Quantitative Structure-Activity Analysis (QSAR), molecular docking and visualization, Absorption, Distribution,

Metabolism, Excretion, and Toxicity (ADME-Tox) prediction, and molecular dynamics simulation, which further can be used as a new candidate for diabetes treatment.

MATERIALS AND METHODS

Materials

Structures of forty-three phenolic compounds in banana peel and ertiprotafib (CID: 157049) as standard were retrieved from PubChem Database (<https://pubchem.ncbi.nlm.nih.gov/>) (Kim et al. 2021). PTP1B protein (PDB ID: 2NT7) was retrieved from Protein Data Bank (<https://www.rcsb.org/>) (Burley et al. 2021).

Methods

The workflow of this study includes structure retrieval and preparation, QSAR analysis, molecular docking and visualization, ADME-Tox prediction, and molecular dynamics simulation (Wijaya et al. 2021; Wisnumurti et al. 2022).

Structure Retrieval and Preparation

Phenolic compounds in banana peel were reviewed from literature (Aboul-Enein et al. 2016; Suleria et al. 2020; Bashmil et al. 2021), retrieved from PubChem Database, and used as ligands. Ertiprotafib, which is a PTP1B inhibitor that has passed phase II clinical trial was used as standard in this study and its structure was retrieved from PubChem Database as well (Liu et al. 2022). The ligands and standard were retrieved in SMILES (simplified molecular input line entry system) format for QSAR and ADME-Tox analysis, and .sdf format for molecular docking and molecular dynamics simulation (Aurora et al. 2022). Their energy was minimized prior to docking and converted to .pdbqt format using OpenBabel wizard in PyRx (Wicaksono et al. 2022).

Structure of PTP1B protein (PDB ID: 2NT7) was retrieved from Protein Data Bank (<https://www.rcsb.org/>) (Burley et al. 2021). PyMol was used to remove unnecessary residues (water and innate ligand) attached to the retrieved structure.

QSAR Analysis

The QSAR analysis was used to predict and initially screen the potential ligand based on the relationship between chemical structure and biological activity with known compounds. PASS online (<http://www.way2drug.com/passonline/>) is an online software used for QSAR analysis (Filimonov et al. 2014). SMILES of the ligands were inputted into the server and the results were shown in probability of activity (Pa) and probability of inactivity (Pi). Having $P_a > P_i$ suggests the activity to be possible (Hussain et al. 2016).

Molecular Docking Validation

Re-docking was performed before the study to validate the procedure. A native inhibitor (PDB Chem ID: 902) was removed from crystallised structure of PTP1B (PDB ID: 2NT7) and re-docked against the protein using Vina wizard in PyRx. The re-docking followed the same protocol to ensure that the docking protocol is capable to precisely dock the ligands into the protein, reflected by the less deviation of the re-docked native ligand from the original co-crystallized position calculated in RMSD (root-mean-square deviation) value using Discovery Studio. RMSD of $< 2 \text{ \AA}$ is regarded sufficient to validate the docking protocol (Pratama et al. 2021).

Molecular Docking and Visualization

Molecular docking was performed to the selected ligands towards PTP1B using Autodock Vina wizard (Eberhardt et al. 2021) in PyRx (Dallakyan & Olson 2015). In addition, a standard was docked towards PTP1B to compare and determine the similarity of the interaction between the ligands and standard. The results of molecular docking were in the form of binding energy scores (kcal/mol) with a more negative value means a higher affinity. Docking grid was set to the whole protein, with the centre of X:44.2, Y:16.8, and Z:15.1, and dimensions of X:62.9, Y:53.3, and Z:42.7. The interaction between amino acid residues of PTP1B and ligands were illustrated by 2D visualization using BIOVIA Discovery Studio (BIOVIA Systèmes Dassault 2019).

ADME-Tox Prediction

The ADME-Tox analysis was used to predict the pharmacokinetics and toxicity of the ligands when used as drugs. ADMETlab 2.0, a webserver ADME-Tox software which is able to predict ADME-related, toxicity, and medicinal properties, was used for this analysis (Xiong et al. 2021). SMILES of the selected ligands were inputted into the server and several parameters were analysed, including Lipinski's Rule of Five, human intestinal absorption (HIA), blood-brain barrier (BBB), Ames toxicity, carcinogenicity, skin sensitization, eye irritation, LC₅₀ of fathead minnow and *Daphnia magna*.

Molecular Dynamics Simulation

The selected ligands in the complexes with PTP1B were subjected to molecular dynamics simulation to analyse conformational changes and stability of the complex in a dynamic model. Online server CABS-Flex 2.0 is a webserver to conduct a molecular dynamics simulation in a low computational cost yet with an accurate result used in this study (Kuriata et al. 2018). Selected ligands-protein complexes were subjected to this analysis and inputted into the server in .pdb format and the other parameters were left default.

RESULTS AND DISCUSSION

Quantitative Structure-Activity Relationship Analysis

Initially, forty-three phenolic compounds from banana peel were reviewed from the literature (Table 1). All of them were subjected to QSAR analysis using PASS online for antidiabetic and PTP1B inhibitory activity. Antidiabetic activity refers to the ability to reduce blood glucose level which occurs through several means, including insulin secretion, as well as promoting and inhibiting diabetes-related protein (Kanwal et al. 2022). In order to narrow down the selection, PTP1B inhibitory activity was also analysed.

Pa is the probability of being active while, contrary, Pi is the probability of being inactive, therefore, by default, only $P_a > P_i$ is considered possible for a biological activity (Filimonov et al. 2014). A total of 18 phenolic compounds were selected based on the parameter above (Table 2). In regards to the Pa, a threshold of $P_a > 0.7$ indicates a highly significant activity, $P_a = 0.3 - 0.7$ indicates moderate activity, while $P_a < 0.3$ indicates a low activity (Parikesit & Nurdiansyah 2021). However, low Pa value does not certainly mean that they have low activity, because studies of the similar compounds are limited, hence the low probability (Kusuma et al. 2022). In fact, if it would be experimentally confirmed, the compound might happen to be a new structurally active compound (Hussain et al. 2016). Therefore, they were subjected to further analysis in molecular docking.

Molecular Docking Validation

Using the same docking protocol, the native ligand was re-docked against the protein to retrieve the predicted binding conformation. Subsequently, the re-docked ligand was compared to its co-crystallised struc-

Table 1. Phenolic compounds from banana peel.

Compounds	Class	Banana Species
Caffeic acid	Phenolic Acids	MP
Chlorogenic acid		MAC
Ferulic acid	Phenolic Acids	MAC
Gallic acid		MAC
Protocatechuic acid 4-O-glucoside		MAC
2-Hydroxybenzoic acid	Hydroxybenzoic Acid	MAC
3,4-O-Dimethylgallic acid		MAL
Caffeoyl glucose		MAC
Cinnamic acid	Hydroxycinnamic Acid	MP, MAC
m-coumaric acid		MAC
3-Hydroxyphenylpropionic acid		MAC
p-Coumaroyl glycolic acid	Hydroxyphenylpropanoic Acids	MAC, MAD, MAL, MAR, MP,
3,4-Dihydroxyphenylacetic acid	Hydroxyphenylacetic Acids	MAC, MAR
Urolithin A		MAC
Scopoletin	Hydroxycoumarins	MP
Umbelliferone		MAM
Cyanidin 3,5-O-diglucoside		MAR
Delphinidin 3-O-(6"-acetyl-galactoside)	Anthocyanins	MP, MAC, MAM
Malvidin 3-O-(6"-acetyl-glucoside)		MAR
Chrysin		MP
Gardenin B		MAC
Cirsilineol	Flavones	MAC
Chrysoeriol 7-O-glucoside		MAC
6-Hydroxyluteolin 7-rhamnoside		MAC
Hesperetin 3'-O-glucuronide		MAC
Naringenin	Flavanones	MAC
Neeriocitrin		MAR
3-Methoxysinensetin		MAC
Isorhamnetin 3-O-glucoside 7-O-rhamnoside		MAC
Myricetin 3-O-galactoside		MAC
Myricetin 3-O-rhamnoside		MAC
Myricetin 3-O-rutinoside	Flavonols	MAC
Patuletin 3-O-glucosyl-(1->6)- [apiosyl(1->2)]-glucoside		MAR
Quercetin 3-O-xylosyl-glucuronide		MAC
Rutin		MAC
5,6,7,3',4'-Pentahydroxyisoflavone	Isoflavonoids	MAC
Isoquercitrin		MAC
4-Hydroxybenzaldehyde	Hydroxybenzaldehydes	MAC
Demethoxycurcumin	Curcuminoids	MAC
Isopimpinellin	Furanocoumarins	MAC
Carnosic acid	Phenolic Terpenes	MAC
Schisantherin A	Lignans	MAC
Salvianolic acid B	Other Polyphenols	MAC

Note: MP: *Musa paradisiaca*, MAC: *Musa acuminata* Canvendish, MAD: *Musa acuminata* Ducasse, MAL: *Musa acuminata* Ladyfinger, MAR: *Musa acuminata* Red Dacca, MAM: *Musa acuminata* Monkey. Adapted from [Suleria et al. \(2020\)](#), [Bashmil et al. \(2021\)](#), and [Aboul-Enein et al. \(2016\)](#).

Table 2. PASS Online Prediction Results.

Compounds	Antidiabetic		PTP1B Inhibitor	
	Pa	Pi	Pa	Pi
Ertiprotafib (standard)	0,925	0,004	0,700	0.002
Caffeic acid	0.385	0.048	0,188	0,014
Ferulic acid	0,274	0,098	0,228	0,009
Gallic acid	0,317	0,073	0,167	0,018
3,4-O-Dimethylgallic acid	0,510	0,022	0,159	0,019
p-Coumaroyl glycolic acid	0,443	0,033	0,278	0,006
3,4-Dihydroxyphenylacetic acid	0,510	0,022	0,159	0,019
Urolithin A	0,251	0,074	0,171	0,017
Scopoletin	0,172	0,031	0,071	0,062
Umbelliferone	0,241	0,008	0,106	0,039
Chrysin	0,317	0,031	0,174	0,016
Gardenin B	0,326	0,027	0,106	0,039
Cirsilineol	0,300	0,039	0,116	0,033
Hesperetin 3'-O-glucuronide	0,504	0,023	0,071	0,062
Naringenin	0,229	0,132	0,171	0,017
3-Methoxysinensetin	0,381	0,015	0,139	0,024
5,6,7,3',4'-Pentahydroxyisoflavone	0,305	0,037	0,086	0,051
Carnosic acid	0,223	0,050	0,132	0,026
Salvianolic acid B	0,572	0,015	0,149	0,022

ture by measuring the RMSD value. RMSD value between re-docked ligand and co-crystallized ligand was 1.254 Å (Figure 1A). Both results showed the same orientation with only a slight shifted position around the rotatable bond. The re-docked ligand showed a binding energy value of -9.3 kcal/mol and the interactions with amino acid residues is depicted in Figure 1B.

Molecular Docking and Visualisation

Molecular docking analysis was carried out to predict both the structural conformation of the ligands necessary to bind with PTP1B as well as the

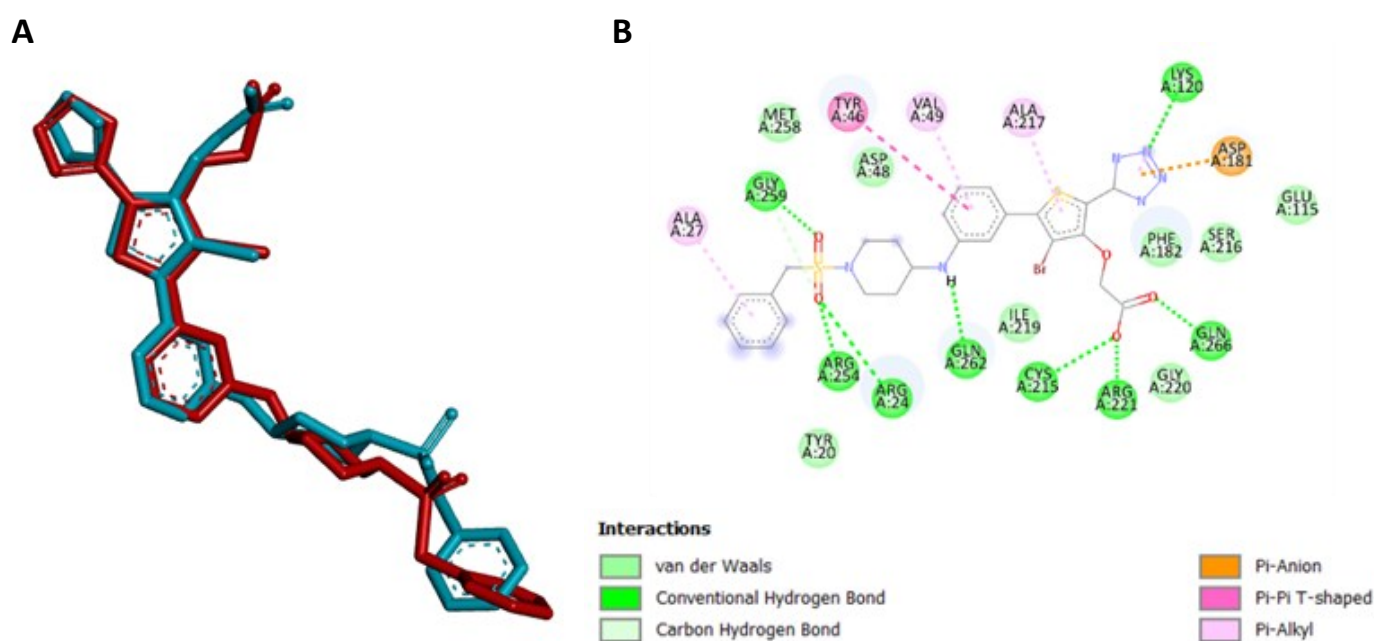


Figure 1. Molecular docking validation. Superimposed re-docked ligand (blue) to co-crystallized ligand (red) (A). Interactions of re-docked ligand with amino acid residues (B).

strength of binding reflected by their binding energy. Binding energy is integral to the inhibitory effect since the inhibition of the biological activity is the results of ligand binding to the protein target (Lopina 2017). The interaction between ligands and PTP1B could be analysed based on the binding energy. The lower the binding energy, the more stable is the ligands since they require smaller energy to bind with the protein binding site.

Binding energy of the ligands with PTP1B is depicted in Table 3. It showed that 8 ligands had binding energy lower than the standard (-7.4 kcal.mol). In that regard, it implied that they could form a stronger, more efficient complexes with PTP1B. The lead ligands which inhibited PTP1B, therefore, are urolithin A and chrysin, since both of them had a better binding energy score than the standard and other ligands, with a binding energy of -8.8 kcal/mol.

Discovery Studio used for the visualization is not only able to predict the favourable bonds, namely charged, halogen, hydrophobic, and hydrogen bonds, but also the unfavourable bonds, including steric bumps, charge repulsion, acceptor-acceptor and donor-donor clashes (Biovia 2019). Favorable bonds are responsible for increasing binding affinity due to intermolecular attraction, including hydrogen bonds, covalent bond, Van der Waals interaction, electrostatic force, and coordination bond (Chen & Krugan 2009). On the other hand, unfavourable bonds dictate the repulsion in the ligand-protein binding, hence lowering the binding affinity. Formed favourable and unfavourable bonds were used to correlate the binding affinity scores and how they achieved those. Additionally, presence of unfavourable bonds also affects the stability of ligand-protein complex due to repulsion (Dhorajiwala et al. 2019).

Figure 2 depicts the interactions between ligands and amino acid residues in PTP1B. Urolithin A showed interactions with residue Tyr46, Val49, Phe182, Ala217, and Arg221, while chrysin with Val49, Ala217,

Table 3. Molecular Docking Results.

Compounds	Class	Binding Energy (kcal/mol)
Ertiprotafib (standard)	-	-7.4
Caffeic acid	Phenolic acids	-6.7
Ferulic acid		-5.5
Gallic acid		-6.2
3,4-O-Dimethylgallic acid		-6.5
p-Coumaroyl glycolic acid	Hydroxyphenyl-propanoic acids	-6.9
3,4-Dihydroxyphenylacetic acid	Hydroxyphenyl-acetic acids	-6.5
Urolithin A*	Hydroxycoumarins	-8.8
Scopoletin		-7.2
Umbelliferone		-6.3
Chrysin*		-8.8
Gardenin B	Flavones	-6.4
Cirsilineol		-7.6
Hesperetin 3'-O-glucuronide	Flavanones	-8.4
Naringenin		-8.5
3-Methoxysinensetin	Flavonols	-6.2
5,6,7,3',4'-Pentahydroxyisoflavone	Isoflavonoids	-7.6
Carnosic acid	Phenolic terpenes	-7.5
Salvianolic acid B	Other polyphenols	-7.9

Gly220, and Arg221. However, unfavourable bonds between urolithin A and Gln266, and between chrysin and Phe182 and Tyr46 were present, depicted in red in Figure 2. These unfavourable bonds might have affected the ligand-protein binding due to repulsive interaction (Dhorajiwala et al. 2019). Unfavourable bonds were also present in the other ligand-protein complexes, except in cirsilineol, 5,6,7,3',4'-pentahydroxyisoflavone, and salvianolic acid, although having higher binding energy. The fact that ligands with low binding energy had unfavourable bonds indicated the possibility that repulsion effect was nullified by other types of interaction, as the attractive forces from favourable bonds were much stronger, hence low binding energy (Kukic & Nielsen 2010). However, unfavourable bonds might still impact the complex stability, thus should be interpreted along with molecular dynamics results.

All the eight lead ligands with promising binding energy bound with PTP1B at the same site and can be seen by the sharing of some residue interactions. The interactions mainly involved the catalytic binding site A and D (Liu et al. 2022). A site is the main catalytic site in PTP1B and the most accessible pocket, that contains a catalytic Cys215 and other residues, including Tyr46, Asp48, Val49, Phe182, Ala217, Ile219, and Gln262 (Liu et al. 2022). Because of its primary catalytic role, inhibition targeting this site is of high interest. However, targeting solely site A lacks of specificity since this site is highly conserved among other PTPs. On the other hand, D site is a narrow small pocket located near A site. D site does not have any biological implication in the insulin signalling pathway, yet targeting this site along with other sites may improve the specificity (Liu et al. 2022). It mainly involves Try46, Glu115, Lys120, Asp181, Phe182, Ser216, and Arg221 (Liu et al. 2022). With regards to these catalytic binding sites, it was shown in a study that PTP1B targeting site A and D, along with site C was the most promising among other catalytic inhibitors (Zhang & Du 2018).

Additionally, two hydroxide groups as good hydrogen donors and with aromatic rings that help stabilising their conjugated base that makes them even more superior donors. One hydroxide group bound with Arg221 via hydrogen bond, however, it clashed with Gln266 which also acted as a hydrogen donor. The hydroxide group and Phe182 in the chrysin showed hydrogen clash, and the ketone group and Tyr46, which are hydrogen acceptors, showed repulsion. The other interactions were brought about by the interaction of the π - π and π - σ orbitals between the ligands and amino acid residues, as well as by the presence of the phenolic aromatic rings.

Inhibition of PTP1B would help manage T2DM since it prevents the down-regulation of insulin signalling cascade which causes insulin resistance (Tautz et al. 2013; Liu et al. 2022). This investigation suggests that some phenolic compounds found in banana peel can bind to PTP1B and may potentially have an inhibitory effect. Their inhibitory effect towards PTP1B has not been extensively researched. However, the ability of several phenolic compounds to bind with PTP1B has been predicted by some *in silico* studies (Damián-Medina et al. 2020; Mechchate et al. 2021; Rath et al. 2022). This current work also found that the majority of the promising ligands were in the class of polyphenols, including flavones, flavanones, and isoflavonoids. With regards to that, Rath et al. (2022) also concluded the potential of several polyphenols as PTP1B inhibitors. Similarly, an *in vivo* investigation also revealed that an extract from *Cudrania tricuspidate* leaves high in polyphenols had a potent inhibitory effect on PTP1B (Kim et al. 2016).

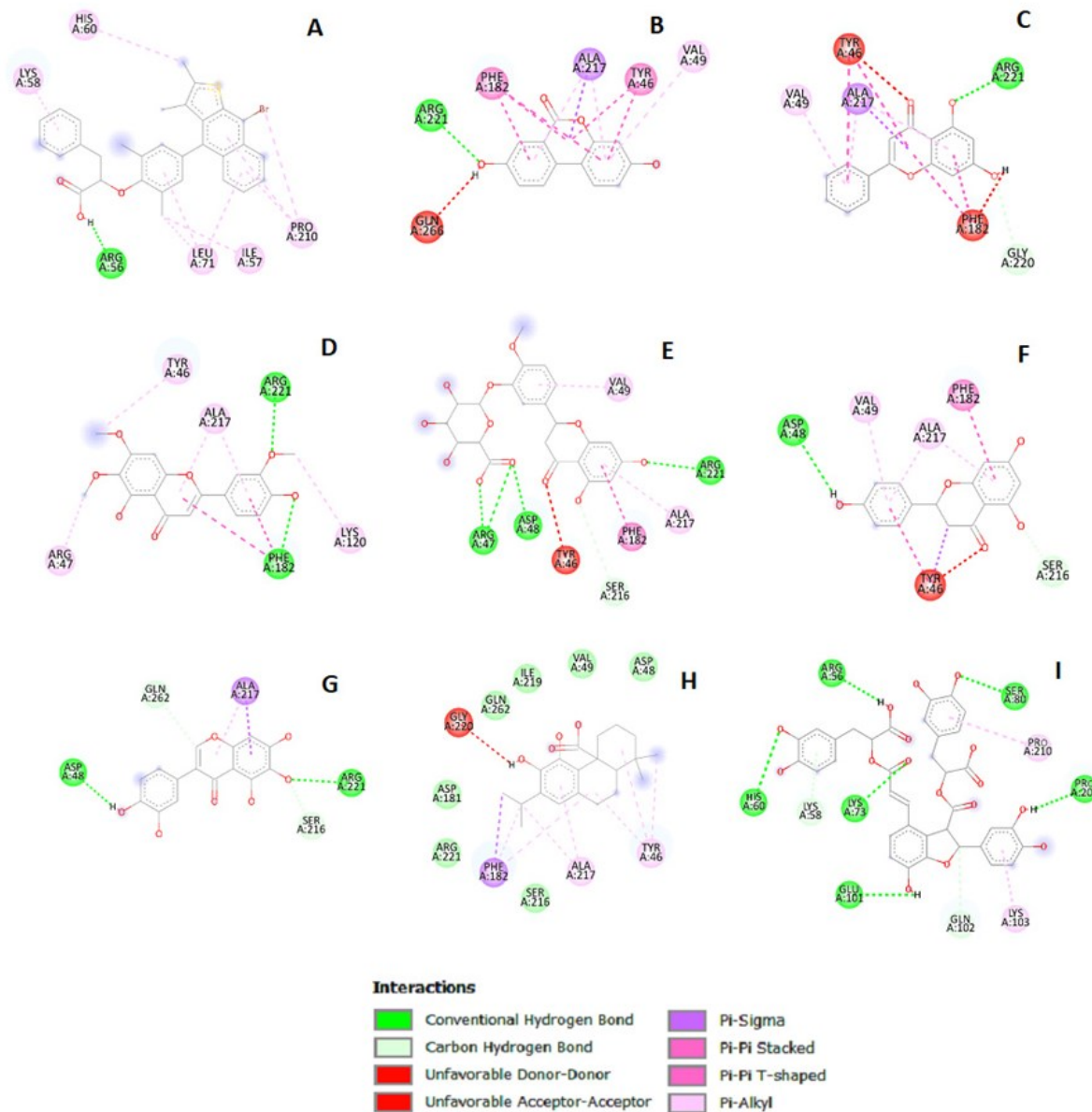


Figure 2. Visualisation of the interactions between ligands and amino acid residues of PTP1B. Interaction with ertiprotafib (A), urolithin A (B), chrysin (C), Cirsilineol (D), hesperetin 3'-O-glucuronide (E), naringenin (F), 5,6,7,3',4'-pentahydroxyisoflavone (G), carnosic acid (H), and salvianolic acid (I).

Absorption, Digestion, Metabolism, Excretion, and Toxicity (ADME-Tox) Analysis

Using ADMETlab 2.0 online program, drug-likeness according to Lipinski's Ro5 and other ADME-Tox criteria was predicted, as shown in Table 4. Drug-likeness is useful criterion for a new drug discovery because safe and approved medications have a window range of physico-chemical properties that will display typical molecular behavior *in vivo* (Bickerton et al. 2012). Typically, Lipinski's Rule of Five is used to assess drug-likeness for oral bioavailability. If a compound violates no more than one rule, it is considered as a strong candidate. All of the potential leads passed Lipinski's Rule of Five, with the exception of hesperetin 3'-O-glucuronide. This indicates that hesperetin 3'-O-glucuronide may have low absorbability or permeability, making it an unsuitable option for an oral medication.

Almost all ligands had a good HIA and absent from BBB. A good HIA is needed since an orally administered drugs need to be absorbed through the intestinal lumen. The inability of the ligands to cross BBB

Table 4. ADMET-Tox Prediction of the Ligands.

Compounds	Lipinski's Rule Violation ^a	HIA ^b	BBB Penetration ^c	Ames Toxicity ^d	Carcinogenicity ^e	Skin Sensitivity	Eye Irritation ^g	LC ₅₀ FM ^h	LC ₅₀ DM ^f
Ertiprotafib	2	---	---	---	-	+++	--	6.490	6.261
Urolithin A	0	---	---	---	+	+++	+++	4.890	5.129
Chrysin	0	---	---	+	-	+++	+++	5.066	5.220
Cirsilineol	0	---	---	-	---	+	++	5.120	6.587
Hesperetin 3'-O-glucuronide	2	+	---	---	---	--	---	4.790	5.404
Naringenin	0	---	---	---	+	+++	+++	6.692	6.410
5,6,7,3',4'-Pentahydroxyisoflavone	0	--	---	+	---	+++	+++	5.033	6.006
Carnosic acid	0	---	-	---	---	+++	++	4.573	5.604
Salvianolic acid B	1	---	---	---	-	--	-	7.044	7.223

Note: The prediction probability values are depicted into 6 symbols: 0 - 0.1 (---), 0.1 - 0.3 (--), 0.3 - 0.5 (-), 0.5 - 0.7 (+), 0.7 - 0.9 (++), and 0.9 - 1 (+++). HIA: Human Intestinal Absorption, BBB: Blood-Brain Barrier. ^a: accepted if no more than 1 violation exist; ^b: HIA+ = <30%, HIA- ≥30% absorption, value is probability being HIA+; ^c: probability of BBB+; ^d: probability of being toxic; ^e: probability of being toxic; ^f: probability of being sensitizer; ^g: probability of being irritants; ^h: 96-h lethal concentration to kill 50% of fathead minnow in $-\log[(\text{mg/L})/(1000 \times \text{MW})]$; ⁱ: 46-h lethal concentration to kill 50% *Daphnia magna* in $-\log[(\text{mg/L})/(1000 \times \text{MW})]$.

showed low indication of toxicity to the brain. Interestingly, Ames test showed a positive result for chrysin and 5,6,7,3',4'-pentahydroxyisoflavone, but not in naringenin and urolithin A, and *vice versa* in carcinogenicity test. In this regard, Ames test mutagenicity and carcinogenicity should have a high correlation. However, mutagen in Ames test does not certain the carcinogenicity in human (Föllmann et al. 2013). Furthermore, almost all of them were irritants to the eyes and skin. Lastly, the environmental toxicity towards fathead minnow and *Daphnia magna* were comparable to the control.

Molecular Dynamics Simulation Analysis

Figure 3 shows the RMSF (root mean squared fluctuation) in the fluctuation plot of the complex between PTP1B and standard, urolithin A, and chrysin. As seen in the figure, the fluctuation of the amino acids still fell in the range of 1-3 Å, which is considered stable (Parikesit & Nurdiansyah 2021). However, some residues of PTP1B complex with both urolithin A and chrysin fluctuate significantly. The PTP1B-urolithin A complex had significant fluctuation in Arg43, Glu62, Asp63, Asn90, and Glu207, while in PTP1B-chrysin complex in Asp298. Differences in RMSF fluctuation between complexed with urolithin A and chrysin indicated that the ligand conformations affected the complex stability (Parikesit & Nurdiansyah 2021).

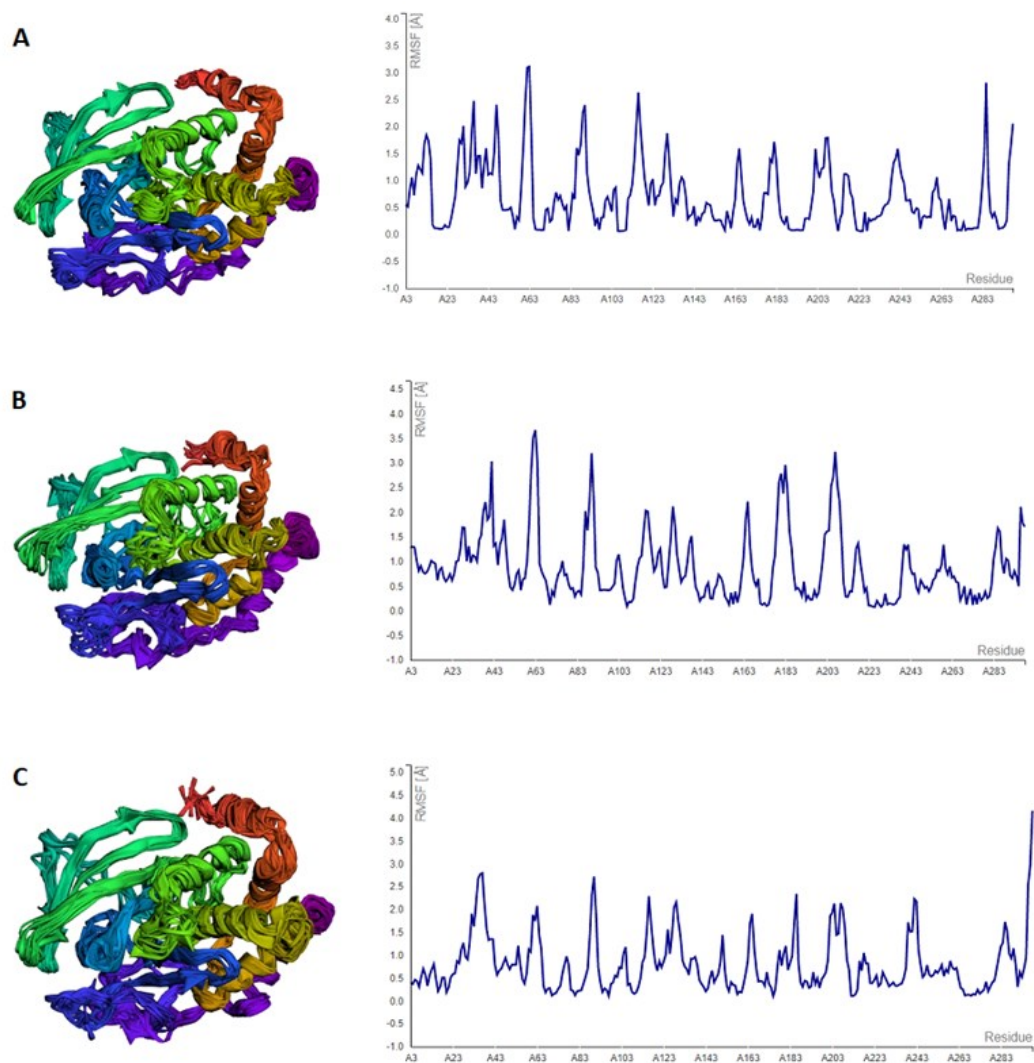


Figure 3. RMSF Fluctuation Plot. Ensemble of protein models are depicted on the left and fluctuation plot on the right for PTP1B complexes with (A) ertiprotafib (standard), (B) urolithin A, and (C) chrysin.

CONCLUSION

Forty-three phenolic compounds from banana peel have successfully been screened for their potential to inhibit PTP1B, a novel anti-diabetic target for the treatment of T2DM. Using PASS online, the potential ligands were converged down into 18 ligands that specifically inhibit PTP1B. Eight ligands with favorable binding energy were identified using molecular docking, with urolithin A and chrysin as the most favourable. Although they both met Lipinski's Rule of Five, had good HIAs, and lacked BBB penetration, their potential for mutagenicity, carcinogenicity, and skin and ocular sensitivity remained in questions. Both Urolithin A and Chrysin displayed a stable conformation with PTP1B in a molecular dynamic simulation. Hence, the current research suggests that urolithin A and chrysin are potential PTP1B inhibitors. Lastly, experimental *in vitro* and *in vivo* studies are required to validate the findings of this investigation.

AUTHORS CONTRIBUTION

R.A.P. conducted this research and wrote the original manuscript. A.A.P. conceptualised research idea, validated, and supervised this research. J.A. reviewed the manuscript and supervised this research.

ACKNOWLEDGMENTS

The authors would like to thank the Department of Research and Community Service of Indonesia International Institute for Life Sciences (RCS i3L) for their heartfelt support.

CONFLICT OF INTEREST

The authors declare no conflict of interest.

REFERENCES

- Aboul-Enein, A.M. et al., 2016. Identification of phenolic compounds from banana peel (*Musa paradaisica* L.) as antioxidant and antimicrobial agents. *Journal of Chemical and Pharmaceutical Research*, 8(4), pp.46–55.
- Acevedo, S.A. et al., 2021. Recovery of Banana Waste-Loss from Production and Processing: A Contribution to a Circular Economy. *Molecules (Basel, Switzerland)*, 26(17), 5282. doi: 10.3390/molecules26175282.
- Aryaeian, N., Sedehi, S.K. & Arablou, T., 2017. Polyphenols and their effects on diabetes management: A review. *Medical journal of the Islamic Republic of Iran*, 31(1), pp.886–892. doi: 10.14196/MJIRI.31.134.
- Asgar, A., 2013. Anti-diabetic potential of phenolic compounds: A review. *International Journal of Food Properties*, 16(1), pp.91–103. doi: 10.1080/10942912.2011.595864.
- Aurora, Y. et al., 2022. Identification of Flavonoids of *Kalanchoe Pinnata* as Candidate Drugs for COVID-19 Gamma-Variant Treatment. *Malaysian Journal of Fundamental and Applied Sciences*, 18(6), pp.630–643. doi: 10.11113/MJFAS.V18N6.2594
- Bashmil, Y.M. et al., 2021. Screening and Characterization of Phenolic Compounds from Australian Grown Bananas and Their Antioxidant Capacity. *Antioxidants*, 10(10), 1521. doi: 10.3390/ANTIOX10101521.
- Bickerton, G.R. et al., 2012. Quantifying the chemical beauty of drugs. *Nature Chemistry*, 4(2), pp.90–98. doi: 10.1038/nchem.1243.

- BIOVIA Systèmes Dassault, 2019. BIOVIA Discovery Studio.
- Burley, S.K. et al., 2021. RCSB Protein Data Bank: powerful new tools for exploring 3D structures of biological macromolecules for basic and applied research and education in fundamental biology, biomedicine, biotechnology, bioengineering and energy sciences. *Nucleic Acids Research*, 49(D1), pp.D437–D451. doi: 10.1093/NAR/GKAA1038.
- Chatterjee, S., Khunti, K. & Davies, M.J., 2017. Type 2 diabetes. *The Lancet*, 389(10085), pp.2239–2251. doi: 10.1016/S0140-6736(17)30058-2.
- Chen et al., 2009. Investigation of atomic level patterns in protein—small ligand interactions. *PLoS ONE*, 4(2), e4473. doi: 10.1371/journal.pone.0004473
- Dahlén, A.D. et al., 2022. Trends in Antidiabetic Drug Discovery: FDA Approved Drugs, New Drugs in Clinical Trials and Global Sales. *Frontiers in Pharmacology*, 12, 4119. doi: 10.3389/FPHAR.2021.807548/BIBTEX.
- Dallakyan, S. & Olson, A.J., 2015. Small-molecule library screening by docking with PyRx. *Methods in Molecular Biology*, 1263, pp.243–250. doi: 10.1007/978-1-4939-2269-7_19/COVER.
- Damián-Medina, K. et al., 2020. In silico analysis of antidiabetic potential of phenolic compounds from blue corn (*Zea mays* L.) and black bean (*Phaseolus vulgaris* L.). *Heliyon*, 6(3), e03632. doi: 10.1016/J.HELIYON.2020.E03632.
- Dhorajiwala, T.M., Halder, S.T. & Samant, L., 2019. Comparative In Silico Molecular Docking Analysis of L-Threonine-3-Dehydrogenase, a Protein Target Against African Trypanosomiasis Using Selected Phytochemicals. *Journal of Applied Biotechnology Reports*, 6(3), pp.101–108. doi: 10.29252/JABR.06.03.04.
- Eberhardt, J. et al., 2021. AutoDock Vina 1.2.0: New Docking Methods, Expanded Force Field, and Python Bindings. *Journal of Chemical Information and Modeling*, 61(8), pp.3891–3898. doi: 10.1021/ACS.JCIM.1C00203/SUPPL_FILE/CI1C00203_SI_002.ZIP.
- Eleftheriou, P., Geronikaki, A. & Petrou, A., 2019. PTP1b Inhibition, A Promising Approach for the Treatment of Diabetes Type II. *Current topics in medicinal chemistry*, 19(4), pp.246–263. doi: 10.2174/1568026619666190201152153.
- Filimonov, D.A. et al., 2014. Prediction of the biological activity spectra of organic compounds using the pass online web resource. *Chemistry of Heterocyclic Compounds*, 50(3), pp.444–457. doi: 10.1007/S10593-014-1496-1/METRICS.
- Föllmann, W. et al., 2013. Ames Test. In *Brenner's Encyclopedia of Genetics: Second Edition*. Academic Press, pp.104–107. doi: 10.1016/B978-0-12-374984-0.00048-6.
- Food and Agriculture Organization of the United Nations, 2022, 'FAOSTAT' in *Food and Agriculture Organization of the United Nations*, viewed 16 February 2023, from <https://www.fao.org/>
- Galicia-Garcia, U. et al., 2020. Pathophysiology of Type 2 Diabetes Mellitus. *International Journal of Molecular Sciences*, 21(17), pp.1–34. doi: 10.3390/IJMS21176275.
- Goyal, R. & Jialal, I., 2020, 'Diabetes Mellitus Type 2' in StatPearls, viewed 5 February 2023, from <https://www.ncbi.nlm.nih.gov/books/NBK513253/?report=classic>
- Gutiérrez-Grijalva, E.P. et al., 2016. Review: dietary phenolic compounds, health benefits and bioaccessibility. *Archivos Latinoamericanos de Nutrición*, 66(2).

- Haj, F.G. et al., 2005. Liver-specific protein-tyrosine phosphatase 1B (PTP1B) re-expression alters glucose homeostasis of PTP1B^{-/-} mice. *Journal of Biological Chemistry*, 280(15), pp.15038–15046. doi: 10.1074/jbc.M413240200.
- Hussain, S.M. et al., 2016. Characterization of isolated bioactive phytoconstituents from *Flacourtia indica* as potential phytopharmaceuticals-An in silico perspective. *Journal of Pharmacognosy and Phytochemistry*, 5(6), pp.323-331.
- Kanwal, A. et al., 2022. Exploring New Drug Targets for Type 2 Diabetes: Success, Challenges and Opportunities. *Biomedicines*, 10(2), 331. doi: 10.3390/BIOMEDICINES10020331.
- Kim, D.H. et al., 2016. Antiobesity and Antidiabetes Effects of a *Cudrania tricuspidata* Hydrophilic Extract Presenting PTP1B Inhibitory Potential. *BioMed research international*, 2016, 8432759. doi: 10.1155/2016/8432759.
- Kim, S. et al., 2021. PubChem in 2021: new data content and improved web interfaces. *Nucleic Acids Research*, 49(D1), pp.D1388–D1395. doi: 10.1093/NAR/GKAA971.
- Kukic, P. & Nielsen, J.E., 2010. Electrostatics in proteins and protein–ligand complexes. *Future Medicinal Chemistry*, 2(4), pp.647-66. doi: 10.4155/fmc.10.6
- Kuriata, A. et al., 2018. CABS-flex 2.0: a web server for fast simulations of flexibility of protein structures. *Nucleic Acids Research*, 46(W1), pp.W338–W343. doi: 10.1093/NAR/GKY356.
- Kusuma, S.M.W., Utomo, D.H. & Susanti, R., 2022. Molecular Mechanism of Inhibition of Cell Proliferation: An In Silico Study of the Active Compounds in *Curcuma longa* as an Anticancer. *Journal of Tropical Biodiversity and Biotechnology*, 7(3), 74905. doi: <https://doi.org/10.22146/jtbb.74905>
- Liu, R. et al., 2022. Human Protein Tyrosine Phosphatase 1B (PTP1B): From Structure to Clinical Inhibitor Perspectives. *International Journal of Molecular Sciences*, 23(13), 7027. doi: 10.3390/IJMS23137027.
- Lopina, O.D., 2017. Enzyme Inhibitors and Activators. *InTech*. doi: 10.5772/67248.
- Mechchate, H. et al., 2021. Insight into Gentisic Acid Antidiabetic Potential Using In Vitro and In Silico Approaches. *Molecules*, 26(7), 1932. doi: 10.3390/MOLECULES26071932.
- Mudunuri, G.R. et al., 2022. Novel In Silico and In Vivo Insights of Flavonoids as Anti-Diabetic and Anti-Oxidant in Rodent Models. *Indian Journal of Pharmaceutical Sciences*, 84(4), pp.1041–1050. doi: 10.36468/PHARMACEUTICAL-SCIENCES.998.
- Naz, D. et al., 2019. In vitro and in vivo Antidiabetic Properties of Phenolic Antioxidants From *Sedum adenotrichum*. *Frontiers in Nutrition*, 6, 177. doi: 10.3389/fnut.2019.00177
- Parikesit, A.A. & Nurdiansyah, R., 2021. Virtual screening of lead compounds for SARS-CoV-2. *J Pharm Pharmacogn Res*, 9(5), pp.730-745.
- Praparatana, R. et al., 2022. Flavonoids and Phenols, the Potential Anti-Diabetic Compounds from *Bauhinia strychnifolia* Craib. *Stem. Molecules*, 27(8), 2393. doi: 10.3390/MOLECULES27082393.
- Pratama, M.R.F. et al., 2022. Introducing a Two-Dimensional Graph of Docking Score Difference vs. Similarity of Ligand-Receptor Interactions. *Indonesian Journal of Biotechnology*, 26(1), pp.54-60. doi: 10.22146/ijbiotech.62194

- Rath, P. et al., 2022. Potential Therapeutic Target Protein Tyrosine Phosphatase-1B for Modulation of Insulin Resistance with Polyphenols and Its Quantitative Structure–Activity Relationship. *Molecules*, 27(7), 2212. doi: 10.3390/MOLECULES27072212.
- Salehi, B. et al., 2019. Antidiabetic Potential of Medicinal Plants and Their Active Components. *Biomolecules*, 9(10), 551. doi: 10.3390/BIOM9100551.
- Sharma, R., Oberoi, H.S. & Dhillon, G.S., 2016. Fruit and Vegetable Processing Waste: Renewable Feed Stocks for Enzyme Production. *Agro-Industrial Wastes as Feedstock for Enzyme Production: Apply and Exploit the Emerging and Valuable Use Options of Waste Biomass*, pp.23–59. doi: 10.1016/B978-0-12-802392-1.00002-2.
- Suleria, H.A.R., Barrow, C.J. & Dunshea, F.R., 2020. Screening and Characterization of Phenolic Compounds and Their Antioxidant Capacity in Different Fruit Peels. *Foods* 9(9), 1206. doi: 10.3390/FOODS9091206.
- Tautz, L., Critton, D.A. & Grotegut, S., 2013. Protein tyrosine phosphatases: Structure, function, and implication in human disease. *Methods in Molecular Biology*, 1053, pp.179–221. doi: 10.1007/978-1-62703-562-0_13/COVER.
- Wicaksono, A. et al., 2022. Screening Rafflesia and Sapria Metabolites Using a Bioinformatics Approach to Assess Their Potential as Drugs. *Philippine Journal of Science*, 151(5), pp.1771–1791. doi: 10.56899/151.05.20.
- Wijaya, R.M. et al., 2021. Covid-19 in silico drug with zingiber officinale natural product compound library targeting the mpro protein. *Makara Journal of Science*, 25(3), pp.162–171. doi: 10.7454/mss.v25i3.1244.
- Wisnumurti, R.F., Aslanzadeh, S. & Aditya Parikesit, A., 2022. Computational examination of flavonoid compounds: Utilization of molecular simulation to discover drug candidates for Covid-19. *Rasayan J. Chem*, 15(2), pp.1132–1136. doi: 10.31788/RJC.2022.1526877.
- Wojdyło, A. et al., 2016. Phenolic compounds, antioxidant and antidiabetic activity of different cultivars of Ficus carica L. fruits. *Journal of Functional Foods*, 25, pp.421–432. doi: 10.1016/J.JFF.2016.06.015.
- Xiong, G. et al., 2021. ADMETlab 2.0: an integrated online platform for accurate and comprehensive predictions of ADMET properties. *Nucleic Acids Research*, 49(W1), pp.W5–W14. doi: 10.1093/NAR/GKAB255.
- Zhang, Y. & Du, Y., 2018. The development of protein tyrosine phosphatase1B inhibitors defined by binding sites in crystalline complexes. *Future Med. Chem.*, 10(19), pp.2345–2367. doi: 10.4155/FMC-2018-0089.

Research Article

Cobalamin and Thiamine Effect on Microalgae Biomass Production in the Glagah Consortium

Tri Wahyu Setyaningrum^{1,4}, Arief Budiman^{2,3}, Eko Agus Suyono^{1,3*}

1)Department of Tropical Biology, Faculty of Biology, Universitas Gadjah Mada, Yogyakarta 55281, Indonesia

2)Department of Chemical Engineering, Faculty of Engineering, Universitas Gadjah Mada, Yogyakarta 55281, Indonesia

3)Center for Energy Studies, Universitas Gadjah Mada, Yogyakarta 55281, Indonesia

4)Department of Biology, Faculty of Mathematics and Natural Science, Universitas Mataram, Mataram 83125, Indonesia

*Corresponding author, email: eko_suyono@ugm.ac.id

Keywords:

biomass
cobalamin
microalgae-bacteria interaction
thiamine

Submitted:

01 February 2023

Accepted:

15 April 2023

Published:

30 October 2023

Editor:

Miftahul Ilmi

ABSTRACT

The Glagah consortium is a mixed culture of various microalgae and bacteria isolated from Glagah Beach, Yogyakarta. Cobalamin and thiamine, which are given by symbiotic bacteria, are assumed will increase biomass. This study aimed to determine the effect of cobalamin and thiamine on microalgae biomass production in the Glagah consortium. The microalgae of Glagah consortium were cultivated for 10 days with vancomycin and gentamicin antibiotic as treatment and without antibiotics as a control. The parameters measured included the number of bacterial colonies, cobalamin and thiamine levels measured by LC-MS, chlorophyll a and b levels, cell density of microalgae and dry biomass. The highest level of cobalamin and thiamine was in the Glagah consortium without antibiotics. Cobalamin and thiamine increased in the exponential phase along with the increasing *Staphylococcus* sp. colonies. The Quantity of *Staphylococcus* sp. colonies in the exponential phase was 62.10^5 (cfu/mL). The level of cobalamin in the exponential phase was 2.33 µg/L and the level of thiamine in the exponential phase was 49.71 µg/L. The highest productivity dried weight biomass was 0.0134 g/L/day in the day-6th on the Glagah consortium without antibiotics. This result showed that microalgae and bacterial interaction was mutualism symbiosis involving cobalamin and thiamine that increased in the exponential phase along with the increasing *Staphylococcus* sp. colonies. This interaction was able to increase biomass microalgae.

Copyright: © 2023, J. Tropical Biodiversity Biotechnology (CC BY-SA 4.0)

INTRODUCTION

Microalga is a micro-sized algae which produces very useful biomass and it was utilized to fulfil human's needs in their daily lives, such as biofuel, the pharmaceutical industries, and the supplement of food. Biomass produced by microalga consortium which involves the interaction of microalgae and bacteria has not been well researched. The beneficial interaction between microalgae and bacteria is assumed to improve the production of biomass. One natural example of how microalgae and bacteria interact is the Glagah consortium isolated from Glagah beach, Yogyakarta. The consortium of Glagah is a mixed culture consisting of various species of microalgae and some symbiotic bacteria. Suyono et al. (2018) reported that the mixed culture of Glagah consortium which consists of *Cyclotella polymorpha*, *Cylindrospermopsis raciborskii*, *Golenkinia radiata*, *Sy-*

racosphaera pirus, *Corethron criophilum*, *Cochliopodium vestitum* and *Chlamydomonas* sp. have a mutualism symbiosis with symbiotic bacteria.

The association of symbiotic bacteria and microalgae in the consortium of Glagah is a mutualism symbiosis where microalgae and bacteria support each other for their growths (Suyono et al. 2018). Generally, microalgae as a photoautotroph organism which is able to use the energy of the light in changing an inorganic carbon becomes an organic carbon, expanding the source of carbon to support the growth of bacteria and used for the synthesis of DNA, and improving bacteria's biofilm (Matsui et al. 2003). In that kind of symbiosis, as the reciprocal relation, bacteria support the growth of microalgae by producing CO₂ and use the excess of oxygen produced by microalgae, so it can prevent the photorespiration which is harmful for the microalgae also the inorganic nutrition and the growth factor which is needed (Amin et al. 2015; Wang et al. 2016)

Based on the analysis of the type of microalgae in the consortium of Glagah, cobalamin (B12) and thiamine (B1) are vitamins B which are expected to be significantly involved in the relation of mutualism symbiosis between microalgae consortium of Glagah and its symbiotic bacteria. Some kinds of microalgae consortium of Glagah are indicated to need the cobalamin and thiamine, but they are unable to synthesise themselves (auxotroph). According to Croft et al. (2006), the auxotroph microalgae to cobalamin and thiamine are in the group of Chlorophyta and Haptophyta. *Golenkinia radiata* and *Chlamydomonas* sp. which are microalgae in the consortium of Glagah include the group of Chlorophyta. *Syracosphaera pirus* is microalgae in the consortium of Glagah which is auxotroph to the cobalamin and thiamine and both of those vitamins obtained from their symbiosis. Microalgae auxotroph to the cobalamin and thiamine need the cobalamin and thiamine from another microbes. Cobalamin and thiamine are vitamins B that are only produced by prokaryotic organisms, especially bacteria (Warren et al. 2002)

Cobalamin and thiamine given by symbiotic bacteria are assumed to be able to support the growth of microalgae due to the function of these two vitamins. Cobalamin which plays an important role in protein synthesis, and thiamine which plays an important role in the formation of amino acids and carbohydrates can increase cell growth and division because cell growth is controlled by these compounds (Konopka et al. 2015; Rosnow et al. 2018). So, the presence of bacteria is assumed to be able to increase microalgae cell density and its biomass. Therefore, the research about the interaction of bacteria and microalgae in the Glagah consortium to increase biomass is needed to prove this.

The goal of this research was to determine the effect of cobalamin and thiamine on microalgae biomass levels in the Glagah consortium. The interaction of microalgae and symbiotic bacteria in the Glagah consortium involving cobalamin and thiamine in the production of microalgae biomass was studied by analysing the number of bacteria colonies, the level of cobalamin, thiamine, chlorophyll a, b and dry biomass in Glagah consortium without antibiotics and with antibiotics. The antibiotics used are Vancomycin and Gentamicin to inhibit the growth of positive gram bacteria and the negative gram bacteria in the consortium of Glagah (Li et al. 2011; Grenni et al. 2018)

MATERIALS AND METHODS

Materials

The materials of this research included microalgae consortium of Glagah isolated from the Glagah beach, Yogyakarta, gentamicin and vancomycin antibiotics, BBM (Bold Basal Medium) for cultivation, NA (Nutrient

Agar) medium, methanol, the vitamin standard of cobalamin and thiamine.

Methods

This research consisted of three treatments. The first treatment was the Glagah consortium given 25 ppm Gentamicin and 100 ppm Vancomycin antibiotics. In the treatment 2, the antibiotic dosage used was 50 ppm Gentamicin and 200 ppm Vancomycin. In the treatment 3, the dosage of antibiotic used was 100 ppm Gentamicin and 400 ppm Vancomycin. The control in this research was the consortium of Glagah without antibiotics. Every treatment consisted of three repetitions.

The cultivation of the Glagah Consortium

First, 250 mL of the consortium of Glagah was mixed into the 250 mL BBM (Bold Basal Medium) in the 1000 mL culture bottle. After that, it was given some serials of treatment for 10 days. In the treatment 1, the dosage of antibiotic used was 25 ppm of Gentamicin and 100 ppm of Vancomycin. In the treatment 2, the dosage of antibiotic used was 50 ppm of Gentamicin and 200 ppm of Vancomycin. In the treatment 3, the dosage of antibiotic used was 100 ppm Gentamicin and 400 ppm Vancomycin. A control in this study was microalgae consortium of Glagah without antibiotics. Each treatment needed 3 culture bottles as the repetition. The lighting was conducted by using TL lamp continuously, cool white fluorescent and was continuously given an aeration.

The Calculation of Microalgae Cell

The calculation of microalgae cells was conducted every day from the day -0 until the day-10th by using a microscope set by Opti Lab and Haemocytometer Neubauer. The sample used was 1 mL then it was entered into the tube 2 mL, then it was counted using a microscope. The calculation was conducted by counting the cell at the two view fields (5 sides) at Haemocytometer Neubauer. The formulation of the cell density as follow:

Cell density (the quantity of cell/mL) = (the quantity of counted cell)/64 x 160 x 10⁴ x 1.25

The Calculation of the Number of Bacterial Colonies

Calculation of the number of bacterial colonies was done by the spread plate method. The medium used was NA (Nutrient Agar) medium with pH 6-7. The liquid NA medium was poured into the petri dish aseptically and waited for it to dry. After drying, 6 dilutions of the Glagah consortium culture sample were carried out by mixing 0.1 mL of the sample with 0.9 BBM medium for 10⁻¹ dilution, then 0.1 mL of the mixture was taken and mixed with 0.9 BBM medium for dilution 10⁻² and so on until dilution 10⁻⁶. The 10⁻⁴, 10⁻⁵ and 10⁻⁶ dilutions were poured into each NA medium then were flatten with driglaski. Spread plates were calculated at early, log, and stationary phase. After 48 hours incubation at room temperature, the colon counted with a hand counter. The Total Plate Count was calculated according to SNI 2897: 2008 concerning the method of testing microbial contamination in meat, eggs and milk, and its processed products.

The Calculation of Dry Biomass

The calculation of the dry biomass was conducted every day from day-0 until day 10th. First, 2 mL of the sample was entered into the tube, then it was centrifuged with the speed 8000 rpm for 15 minutes. Supernatant was excluded and left the pellet by filtering with the filter paper. The re-

sult of the filter was wrapped with the filter paper, then it was entered into the oven for 15 minutes in 70°C.

The Calculation of Chlorophyll a and b

2 mL of sample was centrifuged at a speed of 12000 rpm for 10 minutes, then pellet was added by 1 mL of methanol, then it was centrifuged at a speed of 12000 rpm for 10 minutes (J. Cheng et al. 2016). The sample poured into a glass cuvette and the absorbance was calculated at wavelengths of 480, 652 and 665 nm in the spectrophotometer. Chlorophyll a and b levels were calculated using the following equation.

$$\text{Chlorophyll a (mg/L)} = 16.5169 \times A_{665} - 8.0962 \times A_{652}$$

$$\text{Chlorophyll b (mg/L)} = 27.4405 \times A_{652} - 12.1688 \times A_{665}$$

The Calculation of Cobalamin and Thiamine

The level of cobalamin (Vitamin B12) and thiamine (Vitamin B1) were counted by using LC-MS. The sample taken was 10 mL and was obtained from three phases of the growth of microalgae that was early, log and stationary phase. First, the preparation of the sample was conducted by filtering the sample with millex 0.22 µM, afterwards injected 2 µL to the LCMSMS. Second, vitamin standard was made by weighing the vitamin standard of B1 and vitamin B12 1000 ppm for each, then made the standard of the mixture containing 500 ppm, made the standard of mixture series of 25 ppb, made the standard of mixture series of 2 ppb afterwards injected 2 µL to LCMSMS duplo.

RESULTS AND DISCUSSION

The consortium of Glagah was a mixture culture isolated from Glagah Beach, Special Region of Yogyakarta which consisted of various species of microalgae and symbiotic bacteria. Suyono et al. (2018) reported that the mixture culture of microalgae Glagah consisted of *Cylindrospermopsis raciborskii*, *Syracosphaera pirus*, *Corethron criophilum*, *Golenkinia radiate*, *Cochliopodium vestitu*, *Cyclotella polymorpha* and *Chlamydomonas* sp. had a relation of mutualism symbiosis with the symbiotic bacteria. The symbiotic bacteria successfully cultured in this research were 4 species, they were: *Clostridium* sp., *Streptococcus* sp., *Veillonella* sp., dan *Staphylococcus* sp.

The injection of Vancomycin and Gentamicin antibiotics was able to decrease the quantity of the bacteria's colony which had symbiosis with microalgae. It could be seen from the calculation of the quantity of the colony of 4 species bacteria observed at the 3 points of the growth phase of microalgae, those were early, log, and stationary phase (Table 1).

Table 1. The quantity of bacteria's colony at the growth of microalgae Glagah consortium phase in every treatment.

The Quantity of Bacteria's Colony (cfu/mL)	Control (Without Antibiotic)		Treatment 1 (100 ppm Vancomycin, 25 ppm Gentamicin)			Treatment 2 (200 ppm Vancomycin, 50 ppm Gentamicin)			Treatment 3 (400 ppm Vancomycin, 100 ppm Gentamicin)			
	Early	Log	End	Early	Log	End	Early	Log	End	Early	Log	End
<i>Staphylococcus</i> sp	34. 10 ⁵	62. 10 ⁵	44. 10 ⁵	22. 10 ⁵	16. 10 ⁵	<100	1,7. 10 ⁵	<100	<100	2,3. 10 ⁵	<100	<100
<i>Streptococcus</i> sp.	300. 10 ⁵	194. 10 ⁵	505,6. 10 ⁵	14. 10 ⁵	<100	<100	40. 10 ⁵	<100	<100	<100	<100	<100
<i>Clostridium</i> sp.	41. 10 ⁵	1,85. 10 ⁵	4. 10 ⁵	22. 10 ⁵	16. 10 ⁵	<100	1,7. 10 ⁵	<100	<100	<100	<100	<100
<i>Veillonella</i> sp.	4,5. 10 ⁵	3. 10 ⁵	4. 10 ⁵	2. 10 ⁵	<100	<100	80. 10 ⁵	<100	<100	<100	<100	<100

Based on the analysis of the species of bacteria, only *Staphylococcus* sp. was able to produce cobalamin and thiamine. *Staphylococcus* sp. efficiently gave cobalamin and thiamine in the exponential phase of the growth of microalgae in the culture of Glagah consortium without the antibiotic. In the exponential phase, the number of *Staphylococcus* sp. colony was increasing and in the stationary phase was decreasing (Table 1). It was in line with the level of thiamine which was increasing in the exponential phase whereas in the stationary phase was decreasing (Table 2). Table 2 showed that in the control, the level of thiamine was increasing from 0.41 µg/L in the early phase to 49.71 µg/L in the exponential phase, whereas in the stationary phase it was decreasing to 0.44 µg/L.

Therefore, it was assumed that the *Staphylococcus* sp. affected the increasing of thiamine's quantity. *Staphylococcus* sp. was able to synthesise thiamine because it contained the biosynthesis coded thiamine gene (Müller et al. 2009). The level of cobalamin was also increasing at the exponential phase, that was from 1.21 µg/L at the early phase became 2.33 µg/L (Table 2). Besides affecting the level of thiamine at the exponential phase, *Staphylococcus* sp. also affecting the level of cobalamin. *Staphylococcus* sp. had the enzyme which was involved in the cobalamin's biosynthesis (Leisico et al. 2018).

Staphylococcus sp. as the provider of cobalamin and thiamine was also working together with another bacterium which were *Streptococcus* sp., *Clostridium* sp., and *Veillonella* sp. in supporting the growth of microalgae. The culture of the Glagah consortium without antibiotics had more various quantities of the bacteria's colony than the consortium of Glagah with antibiotics so the growth of microalgae was more efficient as seen from the cell density, chlorophyll a, b and biomass. The *Streptococcus* sp. and *Staphylococcus* sp. were facultative anaerobe produced CO₂ by utilising the excess of oxygen produced by microalgae so it inhibited the photorespiration which harmed the microalgae (Wang et al. 2016). It also provided of nutrition in the form of nitrogen and phosphorus needed for the growth of microalgae (Jiang et al. 2007; Foster et al. 2011; Kazamia et al. 2012; Wang et al. 2016). Bacteria can produce the factors of growth such as chelator, phytohormone (IAA) to support the growth of microalgae (Amin et al. 2015; Wang et al. 2016). *Clostridium* sp. can produce Indoleacetic acid (IAA) which was synthesised from the tryptophan which was produced by microalgae and then that IAA was used by microalgae to support their growth (Whitehead et al. 2008; Cooper & Smith 2015).

The calculation of cell density showed that Glagah consortium culture with the highest quantity of *Staphylococcus* sp. colonies and the highest levels of cobalamin and thiamine had the highest cell density of microalgae (Figure 1). It was because cobalamin functioned as a cofactor at the synthesis of methionine which was the factor of initiation translation/ synthesis of protein so all expressions of gen depended on those

Table 2. The level of cobalamin and thiamine at the phase of microalgae Glagah consortium growth in every treatment.

Measurement	Control (Without Antibiotic)			Treatment 1 (100 ppm Vancomycin, 25 ppm Gentamicin)			Treatment 2 (200 ppm Vancomycin, 50 ppm Gentamicin)			Treatment 3 (400 ppm Vancomycin, 100 ppm Gentamicin)		
	Early	Log	End	Early	Log	End	Early	Log	End	Early	Log	End
The level of thiamine (µg/L)	0.41	49.71	0.44	1.23	1.13	0.43	0.73	0.57	0.39	1	0.78	0.46
The level of cobalamin (µg/L)	1.21	2.33	0.72	1.02	0.94	0.63	1.09	1.02	0.67	1.74	1.08	0.63

vitamins (Croft et al. 2006). Besides that, thiamine was a micronutrient needed as a cofactor of some enzymes which were involved in the central metabolism of the formation of amino acid and carbohydrate that was in the form of glycolysis process, Krebs' cycle, phosphate pentose path, and the Calvin's cycle (Moulin et al. 2013)

The quantity of the highest bacterium's colony in the exponential phase at the control sample caused the high level of cobalamin at that phase. The higher level of cobalamin in the control also affected the level of chlorophyll a and chlorophyll b. Based on the measurement result of chlorophyll level a and b showed that the chlorophyll a and b at the consortium of Glagah without antibiotics (control) was higher than the consortium of Glagah with the antibiotics (treatment) (Table 3,4 and 5). Cobalamin was directly involved in the photosynthesis process because it functioned as a photoreceptor which was able to respond the light for the activation of photosynthetic genes expression (Z. Cheng et al. 2016). The received light converted the form of adenosylcobalamin to OHB12 which then activated photosynthetic gene expression. Besides the function of cobalamin produced by bacteria, bacteria also created good photosynthetic conditions by consuming oxygen produced by microalgae thereby reducing the excess oxygen which prevented photorespiration (Z. Cheng et al. 2016).

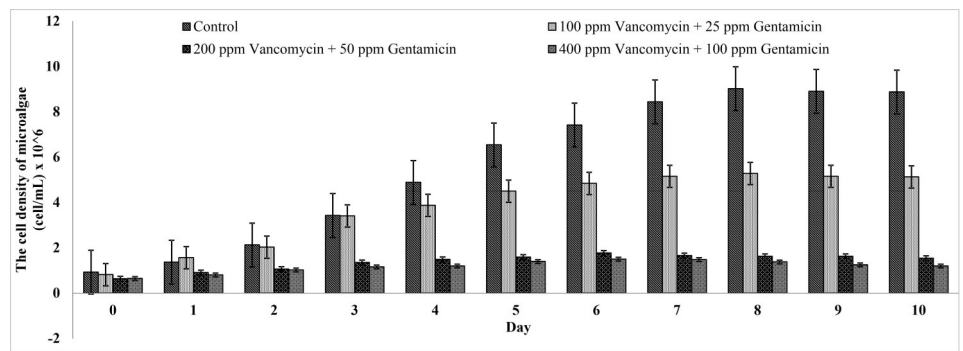


Figure 1. The Cell Density of the Microalgae Glagah Consortium.

The result of the cell density of microalgae was directly proportional with their dry weight (Figure 2). It was because cobalamin played an important role in protein synthesis, and thiamine which played an important role in the formation of amino acids and carbohydrates can increase cell growth and division because cell growth was controlled by these compounds so microalgae biomass (Konopka et al. 2015; Rosnow et al. 2018).

The highest levels of chlorophyll a and b in Glagah consortium was also impacted in their dry biomass. Chlorophyll a and b were photosynthetic pigments that absorb light with certain wavelengths for photosynthesis. Photosynthesis processes that occur properly increased the ability to transform light energy into carbon source for microalgae growth so that biomass increased. The increasing of chlorophyll b also affected the molecular organisation of thylakoid membranes because it functions as an antenna complexes in thylakoid membranes (Voitsekhovskaja & Tyutereva 2015).

The highest peak of the dry biomass was on the day-6th with the highest productivity in the control of 0.01341 g/L (Table 6). The dry biomass showed the quantity of biomass which could be used to fulfil the needs of humans. This research showed that the interaction of the microalgae Glagah consortium with symbiotic bacteria was able to increase the level of cobalamin and thiamine and these vitamins influenced the increasing of chlorophyll a, b and dry biomass level.

Table 3. The level of chlorophyll a, b and in the early phase.

SAMPLE	Chlorophyll a (mg/L)	Chlorophyll b (mg/L)
Control (without antibiotics)	2.590	3.080
Treatment 1 (100 ppm Vancomycin, 25 ppm Gentamicin)	3.084	3.433
Treatment 2 (200 ppm Vancomycin, 50 ppm Gentamicin)	3.172	4.462
Treatment 3 (400 ppm Vancomycin, 100 ppm Gentamicin)	2.486	2.811

Table 4. The level of chlorophyll a, b in the log phase.

SAMPLE	Chlorophyll a (mg/L)	Chlorophyll b (mg/L)
Control (without antibiotics)	17.219	16.721
Treatment 1 (100 ppm Vancomycin, 25 ppm Gentamicin)	15.154	15.675
Treatment 2 (200 ppm Vancomycin, 50 ppm Gentamicin)	7.054	8.332
Treatment 3 (400 ppm Vancomycin, 100 ppm Gentamicin)	5.830	6.350

Table 5. The level of chlorophyll a, b in the stationary phase.

SAMPLE	Chlorophyll a (mg/L)	Chlorophyll b (mg/L)
Control (without antibiotics)	16.242	6.880
Treatment 1 (100 ppm Vancomycin, 25 ppm Gentamicin)	11.824	6.198
Treatment 2 (200 ppm Vancomycin, 50 ppm Gentamicin)	7.443	5.803
Treatment 3 (400 ppm Vancomycin, 100 ppm Gentamicin)	5.748	4.780

Table 6. The productivity of dry weight biomass.

SAMPLE	Productivity of dry weight biomass (g/L/day) x 10 ⁻²
Control (without antibiotics)	1.34
Treatment 1 (100 ppm Vancomycin, 25 ppm Gentamicin)	1.02
Treatment 2 (200 ppm Vancomycin, 50 ppm Gentamicin)	0.92
Treatment 3 (400 ppm Vancomycin, 100 ppm Gentamicin)	0.75

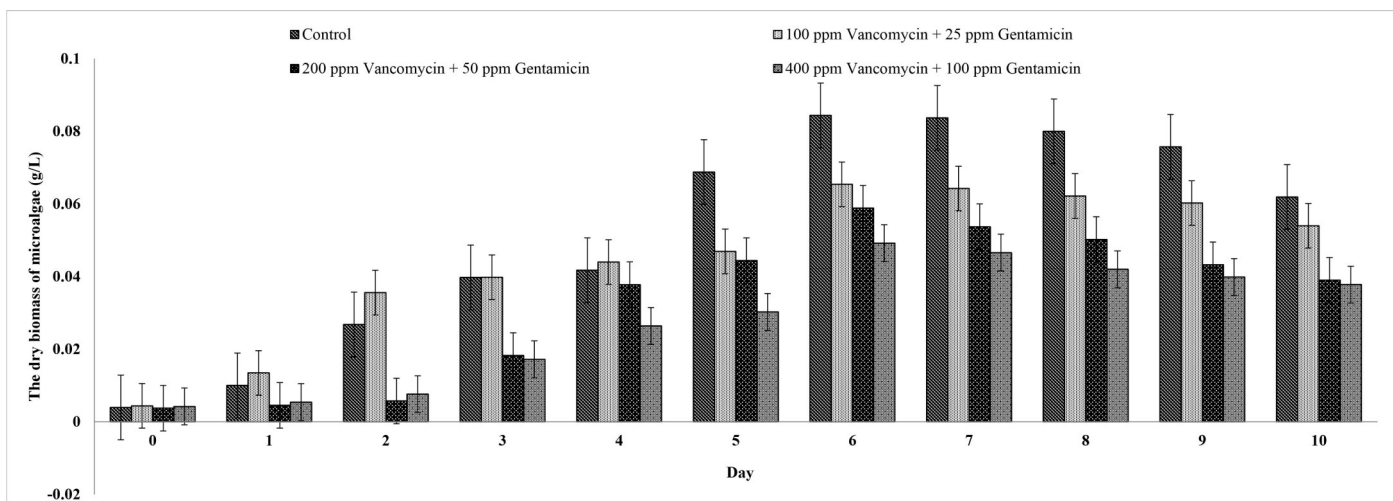


Figure 2. The Dry Biomass of the Microalgae Glagah Consortium.

CONCLUSIONS

This research showed that microalgae Glagah consortium consisting of *Cyclotella polymorpha*, *Cylindrospermopsis raciborskii*, *Golenkinia radiata*, *Syracosphaera pirus*, *Corethron criophilum*, *Cochliopodium vestitum* and *Chlamydomonas* sp. had a mutualism symbiosis with their symbiotic bacteria. Bacteria that were successfully cultured were divided into 4 species, those were: *Clostridium* sp., *Streptococcus* sp., *Veillonella* sp., and *Staphylococcus* sp. It was a mutualism symbiosis involving cobalamin and thiamine. Cobalamin and thiamine increased in the exponential phase along with the increasing quantity of the colony of *Staphylococcus* sp. The interaction of the

microalgae consortium of Glagah with symbiotic bacteria was able to increase the number of microalgae cells, and also chlorophyll a and b levels. Therefore, the biomass level also increased with the increasing quantity of the cell microalgae and chlorophyll a and b level.

AUTHOR CONTRIBUTION

T.W.S. collected, analysed data, and wrote the manuscript. E.A.S designed the research, wrote, and reviewed the manuscript. A.B. wrote and reviewed the manuscript.

ACKNOWLEDGMENTS

The authors would like to acknowledge the financial support from the Ministry of Research and Technology and Higher Education Republic of Indonesia and USAID through the SHERA program Centre for Development of Sustainable Region (CDSR). This manuscript is a part of the first author's thesis.

CONFLICT OF INTEREST

There are no conflicts of interest.

REFERENCES

- Amin, S.A. et al., 2015. Interaction and signalling between a cosmopolitan phytoplankton and associated bacteria. *Nature*, 522, pp.98–101. doi: 10.1038/nature14488.
- Cheng, J. et al., 2016. Enhancing the growth rate and astaxanthin yield of *Haematococcus pluvialis* by nuclear irradiation and high concentration of carbon dioxide stress. *Bioresource Technology*, 204, pp.49–54. doi: 10.1016/j.biortech.2015.12.076
- Cheng, Z., Yamamoto, H. & Bauer, C.E., 2016. Cobalamin's (Vitamin B12) Surprising Function as a Photoreceptor. *Trends Biochem. Sci.*, 41(8), pp.647–650. doi: 10.1016/j.tibs.2016.05.002.
- Cooper, M.B. & Smith, A.G., 2015. Exploring mutualistic interactions between microalgae and bacteria in the omics age. *Curr. Opin. Plant Biol.*, 26, pp.147–153. doi: 10.1016/j.pbi.2015.07.003.
- Croft, M.T., Warren, M.J. & Smith, A.G., 2006. Algae need their vitamins. *Eukaryot. Cell*, 5, pp.1175–1183. doi: 10.1128/EC.00097-06.
- Foster, R.A. et al., 2011. Nitrogen fixation and transfer in open ocean diatom-cyanobacterial symbioses. *The ISME Journal*, 5, pp.1484–1493. doi: 10.1038/ismej.2011.26.
- Grenni, P., Ancona, V. & Barra Caracciolo, A., 2018. Ecological effects of antibiotics on natural ecosystems: A review. *Microchem. J.*, 136, pp.25–39. doi: 10.1016/j.microc.2017.02.006.
- Jiang, L. et al., 2007. Quantitative studies on phosphorus transference occurring between *Microcystis aeruginosa* and its attached bacterium (*Pseudomonas* sp.). *Hydrobiologia*, 581, pp.161–165. doi: 10.1007/s10750-006-0518-0.
- Kazamia, E. et al., 2012. Mutualistic interactions between vitamin B12-dependent algae and heterotrophic bacteria exhibit regulation. *Environ. Microbiol.*, 14, pp.1466–1476. doi: 10.1111/j.1462-2920.2012.02733.x.
- Konopka, A., Lindemann, S. & Fredrickson, J., 2015. Dynamics in microbial communities: Unraveling mechanisms to identify principles. *The ISME Journal*, 9, pp.1488–1495. doi: 10.1038/ismej.2014.251.

- Leisico, F. et al., 2018. First insights of peptidoglycan amidation in Gram -positive bacteria - the high-resolution crystal structure of *Staphylococcus aureus* glutamine amidotransferase GatD. *Scientific Reports*, 5, 5313. doi: 10.1038/s41598-018-22986-3.
- Li, D. et al., 2011. Bacterial community characteristics under long-term antibiotic selection pressures. *Water Res.*, 45(18), pp.6063–6073. doi: 10.1016/j.watres.2011.09.002.
- Matsui, K., Ishii, N. & Kawabata, Z., 2003. Release of extracellular transformable plasmid DNA from *Escherichia coli* cocultivated with algae. *Appl. Environ. Microbiol.*, 69, pp.2399–2404. doi: 10.1128/AEM.69.4.2399-2404.2003.
- Moulin, M. et al., 2013. Analysis of *Chlamydomonas* thiamin metabolism in vivo reveals riboswitch plasticity. *Proc. Natl. Acad. Sci. U. S. A.*, 110(36), pp.14622–14627. doi: 10.1073/pnas.1307741110.
- Müller, I.B. et al., 2009. The Vitamin B1 Metabolism of *Staphylococcus aureus* Is Controlled at Enzymatic and Transcriptional Levels 4. *PLoS One*, 4(11), e7656. doi: 10.1371/journal.pone.0007656.
- Rosnow, J.J. et al., 2018. A cobalamin activity-based probe enables microbial cell growth and finds new cobalamin-protein interactions across domains. *Appl. Environ. Microbiol.*, 84(18), e00955. doi: 10.1128/AEM.00955-18.
- Suyono, E.A., Retnaningrum, E. & Ajjah, N., 2018. Bacterial symbionts isolated from mixed microalgae culture of Glagah strains. *Int. J. Agric. Biol.*, 20(1), pp.33–36. doi: 10.17957/IJAB/15.0326.
- Voitsekhovskaja, O. V. & Tyutereva, E. V., 2015. Chlorophyll b in angiosperms: Functions in photosynthesis, signaling and ontogenetic regulation. *J. Plant Physiol.*, 189, pp.51–64. doi: 10.1016/j.jplph.2015.09.013.
- Wang, H. et al., 2016. Effects of bacterial communities on biofuel-producing microalgae: Stimulation, inhibition and harvesting. *Crit. Rev. Biotechnol.*, 36(2), pp.341–352. doi: 10.3109/07388551.2014.961402.
- Warren, M.J. et al., 2002. The biosynthesis of adenosylcobalamin (vitamin B12). *Nat. Prod. Rep.*, 19(4), pp.390–412. doi: 10.1039/b108967f.
- Whitehead, T.R. et al., 2008. Catabolic pathway for the production of skatole and indoleacetic acid by the acetogen *Clostridium drakei*, *Clostridium scatologenes*, and swine manure. *Appl. Environ. Microbiol.*, 74(6), pp.1950–1953. doi: 10.1128/AEM.02458-07.

Research Article

Spatial Distribution of *Cedrela Odorata* Smaller Trees Affects Forest Regeneration in Exotic Tree Plantations in Central Côte d'Ivoire

Bi Tra Aimé Vroh^{1*}, Abdoulaye Koné²

1)UFR Biosciences, University Félix Houphouët-Boigny, 22 BP 582 Abidjan 22, Côte d'Ivoire

2)Centre d'Excellence Africain sur Changement Climatique, Biodiversité et Agriculture Durable, University Félix Houphouët-Boigny, Abidjan, Côte d'Ivoire

* Corresponding author, email: vrohbitra@gmail.com

Keywords:

forest plantation
invasive alien plant
aggregated distribution
mixed-species forest
timber production

Submitted:

10 May 2023

Accepted:

19 July 2023

Published:

03 November 2023

Editor:

Miftahul Ilmi

ABSTRACT

Cedrela odorata L. was introduced as a possible forest restoration species in classified forests at Côte d'Ivoire. Because of its demonstrated invasive behavior in other tropical forests, this study aimed to assess the impact of *Cedrela odorata* on the regeneration of spontaneous plant species in tree plantations. On the base of *Cedrela odorata* larger tree densities, two types of forest plantation were considered: Type I (240 stems/ha) and Type II (176 stems/ha). In these plantations, plots with 0.25 ha were chosen to locate each tree with dbh ≥ 2.5 cm, in an orthonormal reference. The tree density, the basal area, the species richness, the Shannon diversity index and the rank-abundance curves were determined considering smaller and larger trees. The horizontal spatial arrangement and Ripley's K function were performed to understand the spatial relationship between *Cedrela odorata* smaller trees and those of spontaneous species. The results shown lower spontaneous plant species richness (15-20 species) and diversity (1.15 - 1.43); the dominance of *Cedrela odorata* smaller trees (43.02 - 62.95 % of all stems). The *Cedrela odorata* smaller trees and those of other species have dependent spatial distributions; expressed by a spatial repulsion between the two groups up to a distance of 18 m in the most densified forest plantation. This repulsion was related to an aggregated distribution of *Cedrela odorata* smaller trees in plantation with higher tree density. The study suggests a 170-stems/ha (or lower) of *Cedrela odorata* planting density for biodiversity establishment improvement outcomes in forest plantations.

Copyright: © 2023, J. Tropical Biodiversity Biotechnology (CC BY-SA 4.0)

INTRODUCTION

Cedrela odorata L. (Figure 1) is a native of India and America ([Global Invasive Species Database 2015](#)). It has been introduced to many countries in Pacific Islands and Africa. While the species was listed on the IUCN Red List of Threatened Species in parts of the Americas, this species paradoxically became an invasive species in Pacific Island including Hawaii and the Galapagos, the South Africa and Tanzania ([Pasicznik 2008](#); [Kilawe et al. 2022](#)).

In Côte d'Ivoire (West Africa), *Cedrela odorata* has been introduced as a timber tree and as a possible forest restoration species since the 1920s ([Cintron 1990](#)). This species quickly gained popularity in carrying out industrial reforestation initiatives. The ecological conditions being

important to the extensive growth of the species, it has sometimes spread outside the planted areas, modifying abundantly the existing surrounding flora (Vroh et al. 2022).

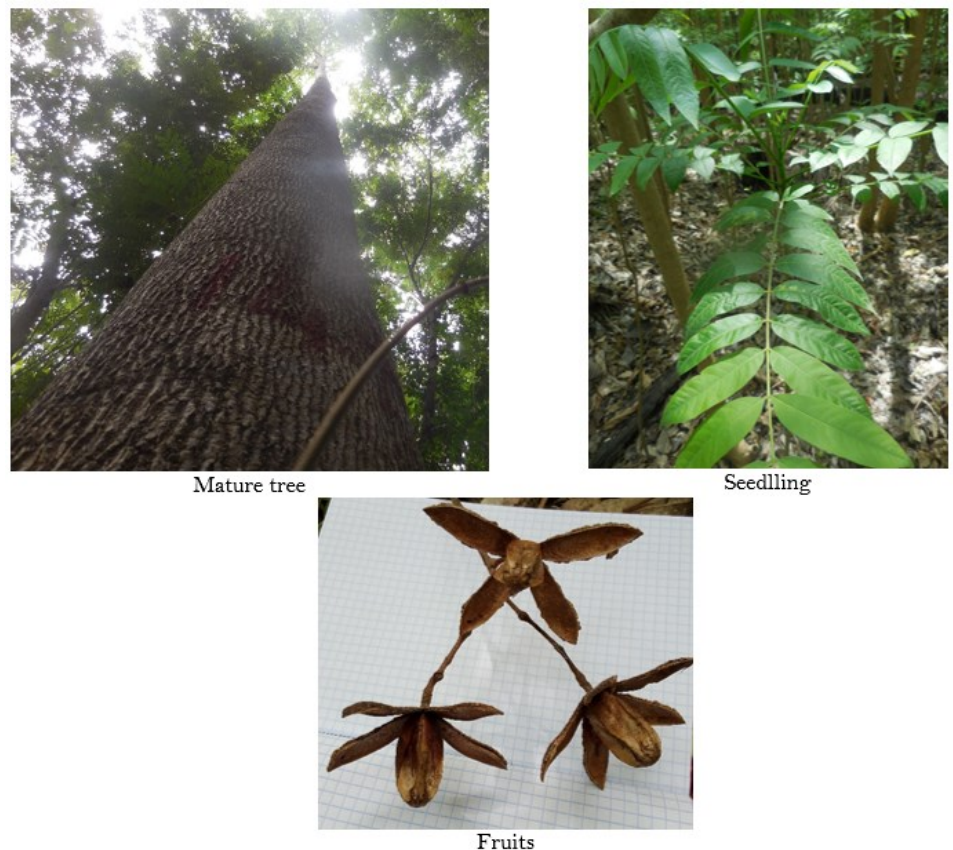


Figure 1. Photographic views of *Cedrela odorata*.

In the country, Classified forests are managed by the government. In this category of protected forest, the forest plantations are authorized for the purpose of reforestation or wood production. Among Ivorian classified forests, the largest areas of the forest plantations are in Téné Classified Forest (TCF). In this area, the exotic species Teck (*Tectona grandis* L.f.), Gmelina (*Gmelina arborea*, Roxb.) and Cedrela (*Cedrela odorata* L.) represented more than 60 % of the reforested area (Eblin & Amani 2015). In the TCF, *Tectona grandis* was many planted as monoculture; while *Cedrela odorata* and *Gmelina arborea* were mostly associated as mixed-species plantations (Sangne 2009). However, in these mixed-species plantations, *Cedrela odorata* smaller trees had more than 50 % of all sapling and seedling tree species occurrences (Koné & Vroh 2021; Vroh et al. 2022). According to Der Meersch et al. (2021) this concurrency is due to the lasting effects of the wildfire which destroyed more than 65 % of this space in 1980-1981. However, more than 30 years later, in Téné forest, published quantitative data demonstrating the positive or negative effects of exotic tree plantations based on *Cedrela odorata*, on plant diversity establishment, is still limited. Yet, these data are critical in deciding whether tree plantations can be a valuable component in the country's indigenous forest rehabilitation and the Reducing Emissions from Deforestation and Forest Degradation (REDD+) programs.

This study presents an overview of the behavior of *Cedrela odorata* as well as its impacts on the establishment of forest regrowths in forest plantations. We hypothesize that in forest plantations based on *Cedrela odorata*, the establishment of forest regrowths are independent of its spatial structure. The study aimed to assess the impacts of *Cedrela odorata* on

the regeneration of spontaneous plant species in tree plantations at Téné Classified Forest. Specifically, the study (1) analyzed the floristic and dendrometric characteristics of the forest plantations, (2) characterized the spatial distribution of *Cedrela odorata* trees, (3) defined the interspecific structuring between *Cedrela odorata* and spontaneous sapling and seedling trees.

MATERIALS AND METHODS

Study Area

The study was conducted in the Téné Classified Forest (TCF) managed by the Government agency (SODEFOR) since 1973. The site (Figure 2) is located in the Oumé department (6°27' - 6°37' N and 5°20' - 5°40' W). The TCF is considered the pioneer in timber production and industrial tree plantation development in the country.

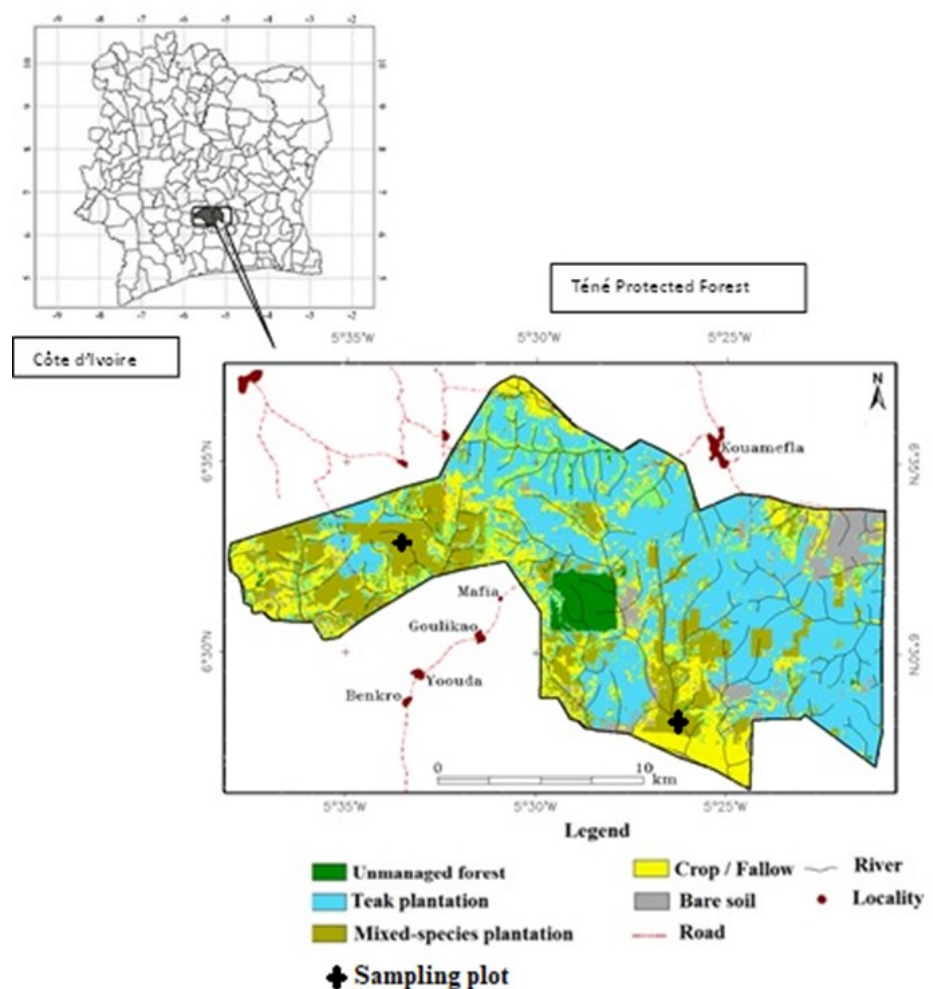


Figure 2. Map of land use type in the Téné Classified Forest in Côte d'Ivoire (Source: Adapted of Sangne 2009).

The mean annual rainfall in Oumé department was 1,200 mm, while the mean annual temperature is 25 °C (Vroh et al. 2022). The vegetation is dominated by semi-deciduous forests characterized by *Celtis* spp. and *Triplochiton scleroxylon* K. Schum.

The TCF covers 29,400 ha, of which 22,000 ha are forest plantations. Currently in the site, there are two forest plantation types: the monospecific *Tectona grandis* forests and the mixed-species tree forests based on *Gmelina arborea* and *Cedrela odorata* (Figure 2). These two tree plantation types are intended especially for commercial use. The planta-

tions under 10 years old (young plantations) are subject to regular cutting operations while in those with more than ten years (10–40 years), thinning and selective tree cutting are done (SODEFOR 2014). For 40 years, awaiting for the timber exploitation, the plantations are abandoned without any cutting operations.

For this study, only mixed-species plantations based on *Cedrela odorata* and *Gmelina arborea*, over 40 years were chosen. Indeed, in these plantations, cutting effects are reduced and natural regeneration is provided without human disturbance.

Two types of mixed-species plantations of more than 40 years were chosen based on botanical inventories carried out by Koné & Vroh (2021) and Vroh et al. (2022) in the Téné Classified Forest. According to these authors, in the TCF, the average density of mature stems (dbh \geq 10 cm in adult plantations) of the target species (*Cedrela odorata*) was 234.95 stems/ha. Thus, for the forest plantation Type I, we selected a plot with 240 stems/ha as planting density of *Cedrela odorata*. This plantation type was considered closer to average across the Téné Classified Forest. For the forest plantation Type II, the planting density of *Cedrela odorata* was 176 stems/ha. This latter type was considered as a plot where the planting density is low compared to the average in the TCF. Also, this density of *Cedrela odorata* in the forest plantation Type II is closer to the standard which is 120–150 stems/ha according to Lemmens (2008). Thus, inventories were carried out in one plot per forest plantation Type.

Sampling Design and Data Collection

The sampling design was adapted from the classic method described by Picard & Gourlet-Fleury (2008). The size of the plots was 2500 m²; i.e. 50 m x 50 m. Many authors have used this plot size (0.25 ha) as observation units in the analysis of spatial patterns (Nicotra 1998; Fonton et al. 2011; Havyarimana et al. 2013). In addition, this plot size significantly reduced the errors accumulation during the distance measurement between trees (Boose et al. 1998).

Each plot was subdivided into four (4) sub-plots of 625 m²; i.e. (25m x 25m). Data collection consisted of locating each individual of *Cedrela odorata* and other tree species in an orthonormal reference (o, i, j). Only trees with at least 2.5 cm diameter at breast height (dbh \geq 2.5 cm) were considered and their cartesian coordinates were read following a grid. In practice, an origin of the axes (x0, y0) has been defined for each plot of 2500 m².

Data Analysis

Firstly, in the identified stand, two size classes of trees were defined: 2.5 cm \leq dbh < 10 cm as smaller trees (sapling and seedling) and dbh \geq 10 cm as larger trees (mature). In each forest plantation type and for each tree size class, the total tree density (N), the basal area, the species richness (S) and the Shannon diversity index (H') were estimated. Also, rank-abundance curves (Kindt & Coe 2005; Marcon 2018) of tree species were constructed to highlight the most abundant species. All these diversity indices permitted to know the quality and the quantity of the forest regrowths affected by *Cedrela odorata* smaller trees.

Secondly, we determined the horizontal spatial arrangement of *Cedrela odorata* (smaller and larger trees) through the distribution maps using the coordinates (xi, yi). Then, Ripley's K function (Ripley 1977) was performed to confirm the distribution mode observed through the maps (He & Duncan 2000; Fonton et al. 2011). This Ripley's function is widely used in spatial pattern analysis and offers the advantage of inte-

grating information on all inter-point distances (Diggle 1983). In application, the Ripley's function $K(r)$ is estimated for an area with circular radius r . However, Kiêu & Mora (1999) demonstrated that the function $K(r)$ is biased for trees located at the border of the plot area. To address this issue, Besag (1977) recommended linearized function $L(r)$. This function is the local bias correction method of Ripley (1981) which yields more robust results and is easier to interpret than $K(r)$.

If $L(r)$ was equal to zero for a given value of r , the null hypothesis was accepted; that meant that the trees have a random distribution. For non-random distributions, a Monte Carlo approach was used with 1,000 random runs for all trees in the plot. A 95% confidence interval was generated for a given value of r , with r increasing from 1 to 25 m in 1-m increments (Diggle 1983). The distance limit of 25 m corresponded to half the observation plot and represented the scale of analysis considered (Ripley 1977). If $L(r)$ was greater than the upper confidence limit (positive) there was an aggregated distribution. In contrast, if $L(r)$ was smaller than the lower confidence limit (negative), there was an overdispersed distribution (Abdourhamane et al. 2017).

Thirdly, Ripley's $L_{12}(r)$ intertype function was used to understand the spatial relationship between *Cedrela odorata* smaller trees (group 1) and those of spontaneous species (group 2). Indeed, the $L_{12}(r)$ function permitted to quantify the degree or type of spatial relationship between the two groups (Haase et al. 1996). The 95% confidence interval for $L_{12}(r)$ was also calculated using a Monte Carlo simulation. In order to understand the establishment of spontaneous species, each simulation consisted of randomly assigning new coordinates to given trees in group 2 while coordinates of group 1 were left unchanged (Goreaud & Péliissier 2003). For this intertype function, the null hypothesis was that groups 1 and 2 have independent spatial distributions. If the value of $L_{12}(r)$ was significantly different from zero up to distance r , this null hypothesis was rejected. When $L_{12}(r)$ was statistically larger than zero, the parameter indicates spatial attraction between the two groups up to distance r . In contrast, when $L_{12}(r)$ was statistically smaller than zero, the parameter indicates spatial repulsion between the two groups up to distance r .

All the horizontal spatial arrangement maps and Ripley's spatial distribution analyses were performed using Programita software (Wiegand & Moloney 2004).

RESULTS AND DISCUSSION

As a reminder, two types of mixed-species forest plantations were chosen based on the density of the larger trees (dbh ≥ 10 cm) of the target species, *Cedrela odorata*: plantation Type I with 240 stems/ha and plantation Type II with 176 stems/ha.

Floristic and Dendrometric Characteristics of The Forest Plantations

From 15 to 20 trees species were recorded per plot (Table 1), with more species represented in smaller trees (13 to 17 species; $2.5 \text{ cm} \leq \text{dbh} < 10 \text{ cm}$) than in larger trees (8 to 9 species; $\text{dbh} \geq 10 \text{ cm}$). The lower richness observed for larger trees could be related to the cutting and thinning activities realized by the SODEFOR agencies until 40 years after the creation of the plantations.

The forest plantation Type I, with 20 species, was the richer than the Type II. The Shannon diversity index values varied from 1.15 (forest plantation Type I) to 1.43 (forest plantation Type II) for all trees, and lower for each category of trees. These results shown that the tree spe-

cies diversity was very low. This reflected a dominance phenomenon of one or a few species (Marcon 2019) in the two forest plantation types.

Overall tree density in the stand varied from 3372 to 4456 stems/ha respectively in forest plantations Type I and Type II; the corresponding densities of smaller trees represented 70.5 – 81.4 %. The basal area in the stand varied from 44.1 m²/ha (forest plantation Type II) to 48.8 m²/ha (forest plantation Type I); the corresponding basal areas of larger trees represented 86.2 – 89.9 % (Table 1). These results shown that the lower density of larger trees in the forest plantation type II, favored a higher density of tree regrowth. Indeed, forest regrowth does not generally tolerate significant shade (Avalos 2019).

In the two forest plantation types, the larger tree class in the stand was dominated by *Gmelina arborea* with 600 stems/ha (Type II) and 724 stems/ha (Type I). The second most abundant species was *Cedrela odorata* with 176 and 240 stems/ha respectively in forest plantations Type II and Type I (Figure 3).

The smaller trees which result in natural forest regrowth, were dominated by *Cedrela odorata* as shown in Figure 4. The density of the species represented 43.02 and 62.95 % of the overall densities respectively in forest plantations Type I and Type II. This means that *Cedrela odorata* had the most represented abundance of the overall species. Also, the abundance of *Cedrela odorata* was higher in forest plantations where the larger trees density was lower. This result is similar to those demonstrated by Muellner et al (2010). According to these authors, the saplings of *Cedrela odorata* do not tolerate heavy shade.

The other species had lower abundances in both forest plantation types (Figure 3). For forest plantation type I, *Newbouldia laevis* with 8 stems/ha in the larger trees class, was represented by 48 stems/ha (2.02 %) in the smaller trees class. This tropical native species, grows usually in Guinean savannas to dense forests and secondary forests areas (Adomou et al. 2018). In many Ivorian ecological areas, this species is well adapted to the highly anthropized habitats like the Téné Classified Forest area.

For forest plantation Type II, *Cassia siamea* is the third most abundant species with 28 (3.4 %) and 596 stems/ha (16,4 %) respectively for larger and smaller trees. This alien species, native to Asia, was introduced into Téné Classified Forest for ornamental and decorative purposes of the forest police camp. However, it spread very quickly in several forest plantations at TCF.

Native species like *Baphia nitida*, *Milicia excelsa*, with a wide range of distribution in Guineo-Congolian area, were less well represented in the two plantation types. This confirms that in previous years, natural stands have faced disturbances either from human-induced or related to competition with planted species (Meyer et al. 2021).

Table 1. Summary of floristic and structural parameters in the two plantation types.

Groups	Density (stems/ha)		Richness		Shannon		Basal area (m ² / ha)	
	Type I	Type II	Type I	Type II	Type I	Type II	Type I	Type II
Larger trees (dbh ≥ 10 cm)	992	828	8	9	0.19	0.18	43.9	38
Smaller trees (2.5 cm ≤ dbh < 10 cm)	2380	3628	17	13	0.88	1.10	4.8	6.1
Total	3372	4456	20	15	1.15	1.43	48.8	44.1

Note: Type I = forest plantation with 240 stems/ha as *Cedrela odorata* density; Type II = forest Plantation with 176 stems/ha as *Cedrela odorata* density.

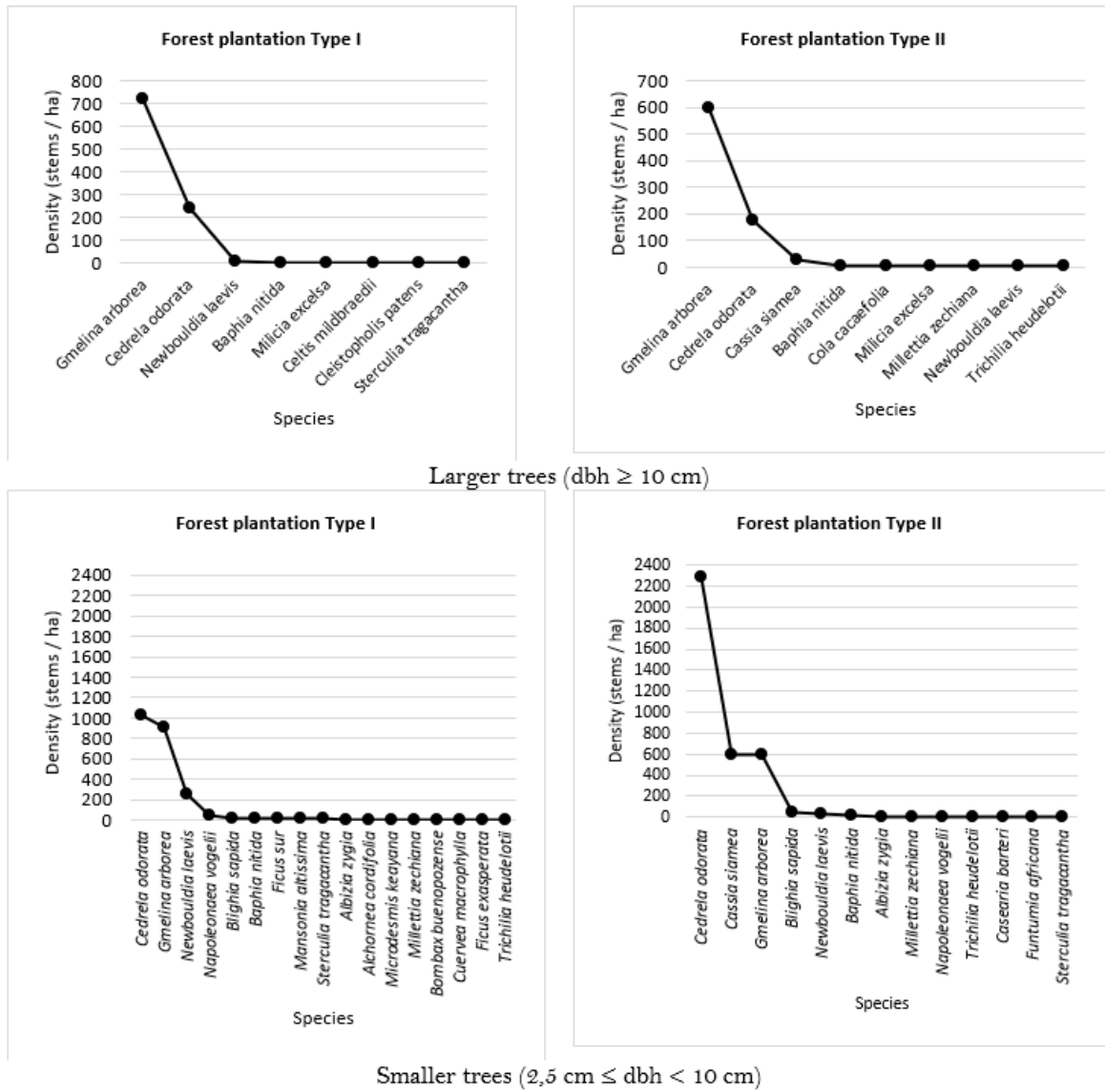


Figure 3. Abundances of recorded species in the two forest plantation types. Type I = forest plantation with 240 stems/ha as *Cedrela odorata* density; Type II = forest Plantation with 176 stems/ha as *Cedrela odorata* density.



Figure 4. A view of *Cedrela odorata* smaller trees abundance level in a forest plantation.

Spatial Structure of *Cedrela Odorata*

The overall spatial distribution of *Cedrela odorata* (larger and smaller trees) presented a significant aggregate radius of more than 24 m in forest plantation Type I (Figure 5). In the forest plantation Type II, the spatial distribution was also, characterized by a significant aggregate radius of 13 m. However, beyond 13 m, the distribution was random in this plantation type. The size of the aggregates is therefore greater for higher plantation density of *Cedrela odorata*. The large size of the aggregates is related to the wind dispersion of *Cedrela odorata* propagules (Muellner et al 2010).

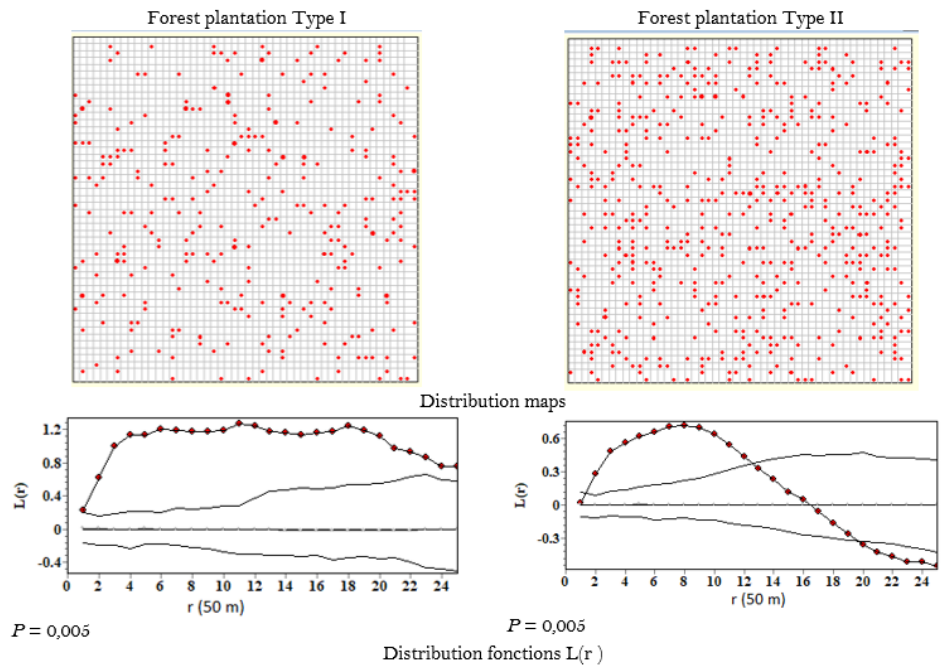


Figure 5. Spatial distribution maps and functions of larger and smaller stems of *Cedrela odorata* in the two forest plantation types. Type I = forest plantation with 240 stems/ha as *Cedrela odorata* density; Type II = forest Plantation with 176 stems/ha as *Cedrela odorata* density.

When the two categories of trees are considered separately, we observed a random distribution of the *Cedrela odorata* larger trees (Figure 6). This distribution attested to the homogeneity of the larger trees; resulting in the history of cutting and thinning activities effects. By contrast, the spatial structure of *Cedrela odorata* smaller trees was characterized by an aggregated distribution in the two forest plantation types (Figure 7). In the forest plantation Type I, the *Cedrela odorata* smaller trees presented a clump of 17 m radius, with two aggregation peaks, at 6 and 24 m. In the forest plantation Type II, the spatial distribution of *Cedrela odorata* smaller trees presented a clump with radius of 13 m.

These results shown that the aggregated distribution of *Cedrela odorata* is due to smaller trees. Also, the clumped radius was greater when the planting density was higher. The standard planting density (120-150 stems/ha) as recommended by Lemmens (2008) could then, reduce the clumped radius of *Cedrela odorata* smaller trees. In the two forest plantation types, the aggregate spatial distributions of *Cedrela odorata* smaller trees can be interpreted as reflecting variations in the characteristics of the environment (Dajoz 2003). The species aggregated in places where environmental conditions are favorable for its development (Thammanu et al. 2021).

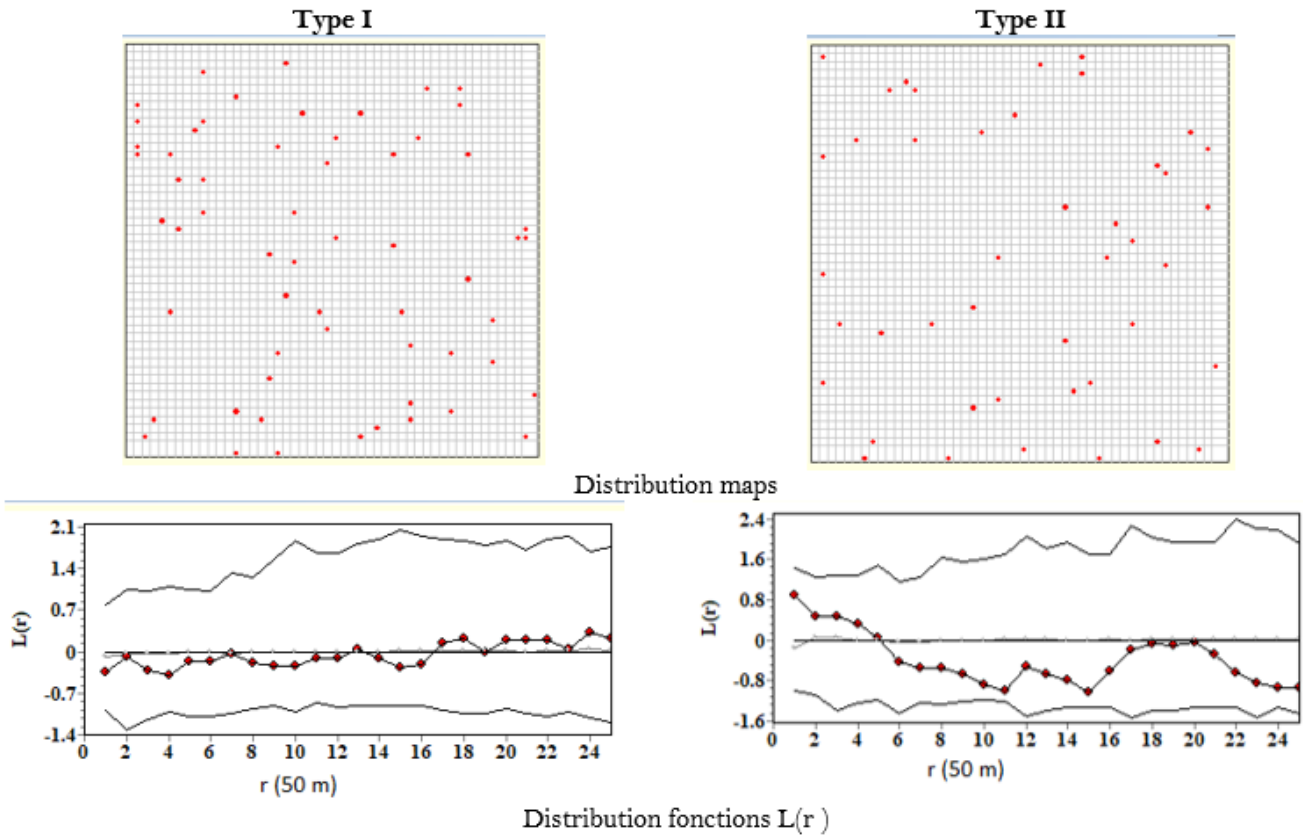


Figure 6. Spatial distribution maps and functions of *Cedrela odorata* larger trees in the two forest plantation types. Type I = forest plantation with 240 stems / ha as *Cedrela odorata* density; Type II = forest Plantation with 176 stems / ha as *Cedrela odorata* density.

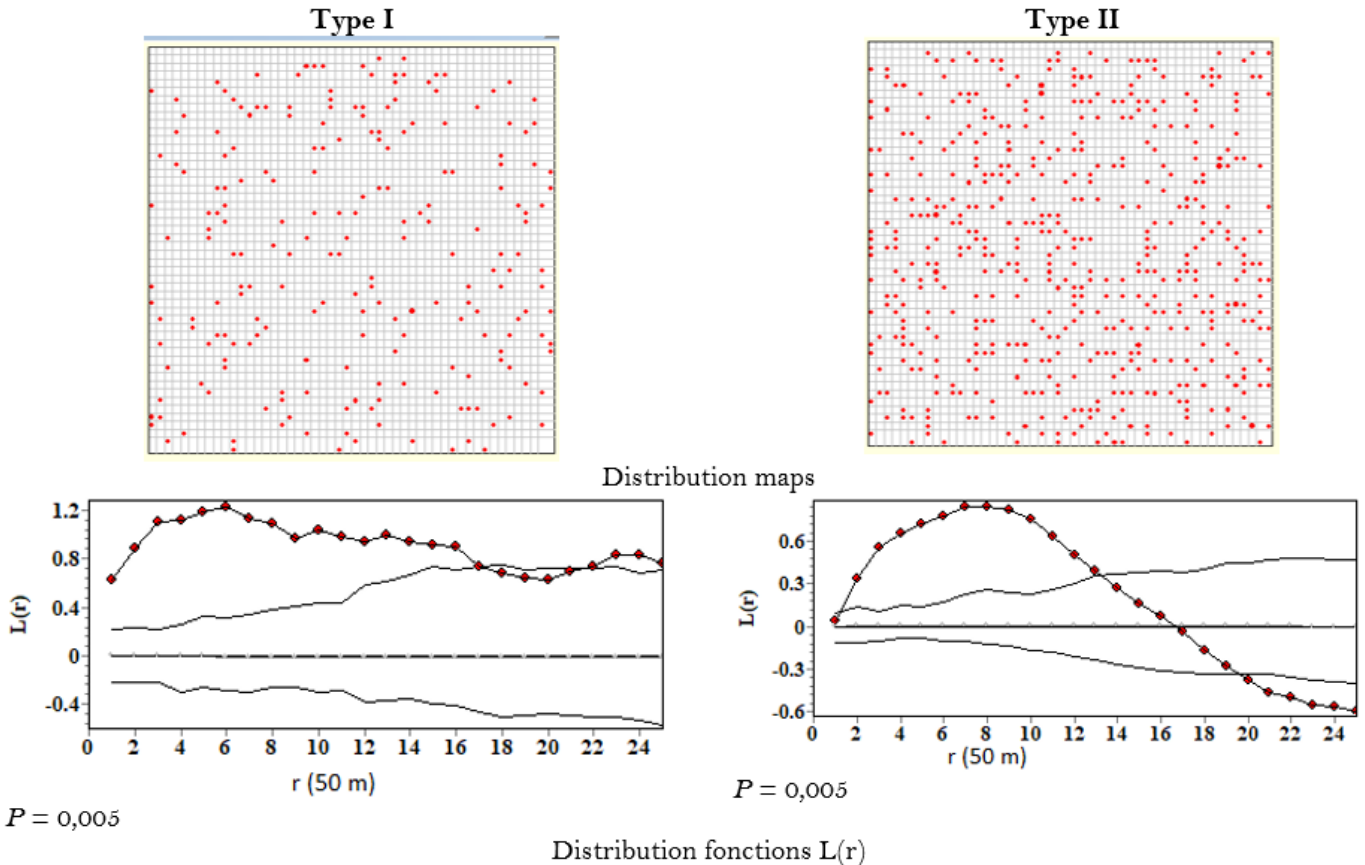


Figure 7. Spatial distribution maps and functions of *Cedrela odorata* smaller trees in the two forest plantation types. Type I = forest plantation with 240 stems/ha as *Cedrela odorata* density; Type II = forest Plantation with 176 stems/ha as *Cedrela odorata* density.

Effect of *Cedrela Odorata* Smaller Trees on Forest Regrowths

The L12 function assessed the spatial association between *Cedrela odorata* and the spontaneous species (Figure 8). In the forest plantation Type I, the value of L12(r) is significantly different from zero up to a distance of 18 m. This meant that, in this plantation type, *Cedrela odorata* smaller trees and those of other species have dependent spatial distributions. Indeed, the L12(r) function is statistically smaller than zero, indicating a spatial repulsion, between the two groups up to distance 18 m. By contrast, the association between these two groups was random for all values of r in plantation Type II (Figure 8). When the larger trees (adults) density was reduced, there was an independent distribution between *Cedrela odorata* smaller trees and those of spontaneous forest regrowth. The observed repulsion of spontaneous species is therefore eliminated when the density of *Cedrela odorata* larger trees is reduced to around 170 stems/ha or lower.

In the plantation type with around 240 stems/ha, the abundance and dominance of *Cedrela odorata* smaller trees could be linked to ecological niche specialization (Stoll & Bergius 2005). As demonstrated by many authors (Le Maître et al. 2011; Pearson et al. 2018; Dydersky & Jagodziński 2020), the spatial repulsion of a species trees can restrict the establishment of spontaneous species and promote changes in species composition and community structure. Indeed, the local dominance expressed by an aggregate distribution of a tree species can reduce the diversity (Havyarimana et al. 2013).

In plantations with more *Cedrela odorata* large trees (Type I), an

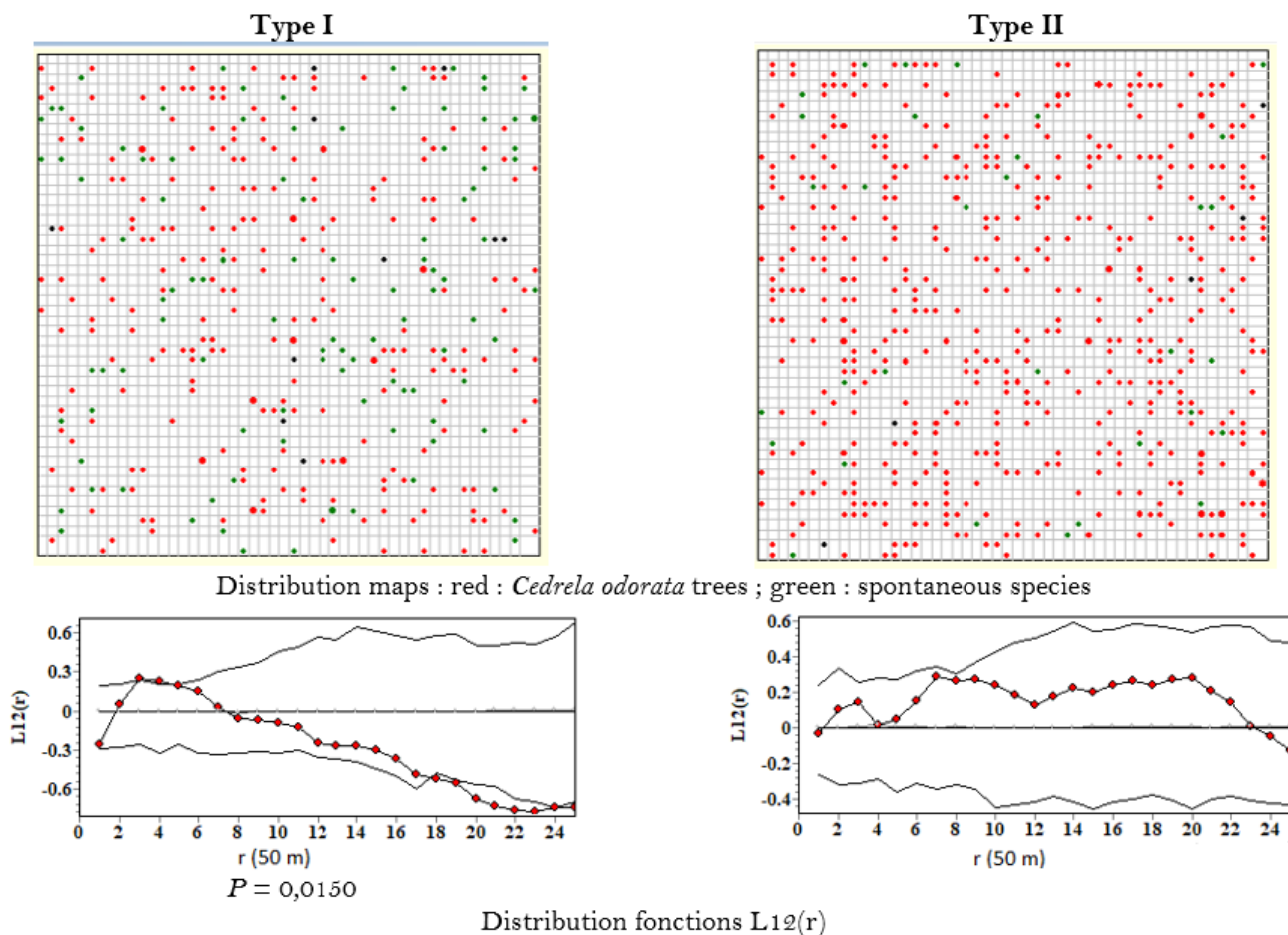


Figure 8. Distribution maps and bivariate functions of spatial association between smaller trees species in the two forest plantation types. Type I = forest plantation with 240 stems/ha as *Cedrela odorata* density; Type II = forest Plantation with 176 stems/ha as *Cedrela odorata* density.

interspecific repulsion was observed, between the two groups of smaller trees, up to a distance of 18 m. To take into account *Cedrela odorata* behavior (repulsion between smaller trees), we suggest to SODEFOR two planting strategies based on this species. If SODEFOR maintains the density of *Cedrela odorata* larger trees around 240 stems/ha (forest plantation type I), then a minimum spacing of 18 m between *Cedrela odorata* smaller trees could be adopted throughout the planting process. With this spacing, spontaneous species could better establish in order to improve plant diversity. But this strategy could evidently demand more labor effort. The second strategy (less costly) would consist to reduce the *Cedrela odorata* larger trees in plantations to 170 stems/ha (or less); which could favor the establishment of spontaneous species. This last management strategy favors a good canopy openness which is an important factor influencing understory richness and light to forest regrowths establishment (Lemenih & Teketay 2005; Carnus et al. 2006).

However, although resulting from the different analyzed processes, the suggested spacing of *Cedrela odorata* smaller trees and density of larger trees may not be optimal for many purposes. Indeed, these suggested spacing and densities may depend on sapling and seedlings mortality rates, ecological zones, given the great climatic variation in Côte d'Ivoire. Other studies could then, take into account more forest plantation sites (based on *Cedrela odorata*) with different biotics and abiotic parameters to confirm and improve the spacing and densities. We must consider also the associated species used for polyculture plantation.

To improve plant species outcomes of plantations established on previously forested lands, the Government Agency SODEFOR could also leave remnant native trees during harvest, managing plantations on longer rotations, avoiding intensive site preparation. Other factors will be necessary: the proximity to native forest (Goldman et al. 2008), the best adaptation of exotic species to increased light (Herault et al. 2004), canopy cover provided (Battles et al. 2001). Further experiment works and field inventories would help to clarify these points.

CONCLUSIONS

This study tested the relationships between forest regrowths distributions in plantations based on *Cedrela odorata*. For ecological characteristics, the main results shown lower native plant species richness and diversity related to the cutting and thinning activities. *Cedrela odorata* smaller trees abundance was higher when the density of the larger trees of the species was lower.

For spatial structure, the results shown an aggregated distribution of *Cedrela odorata* smaller trees. The clumped radius of these smaller trees was greater when the larger trees density was higher. The smaller trees of *Cedrela odorata* and other species have dependent spatial distributions; expressed by a spatial repulsion between the two groups up to a distance of 18 m in forest plantation with higher planting density. To improve biodiversity outcomes of plantations established, we recommend to SODEFOR a 170-stems/ha (or lower) of larger trees density of *Cedrela odorata*; this density will eliminate or reduce the spatial repulsion between the forest regrowths and smaller trees of this species. However, further experiment works and field inventories would help to clarify the suggested *Cedrela odorata* larger trees density.

AUTHOR CONTRIBUTION

V.B.T.A. and K.A. contributed to the study conception and design. Material preparation, data collection and analysis were performed by the two

authors. The first draft of the manuscript was written by V.B.T.A. and commented by K.A. All authors read and approved the final manuscript.

ACKNOWLEDGMENTS

The authors gratefully acknowledge ITTO (International Tropical Timber Organization) towards the financial support of this research through the project number 016/21A. We wish to acknowledge support from Government agency SODEFOR (Côte d'Ivoire) during the field work.

CONFLICT OF INTEREST

The authors have no competing interests to declare that are relevant to the content of this article.

REFERENCES

- Abdourhamane, H. et al., 2017. Structure démographique et répartition spatiale des populations de *Sclerocarya birrea* du secteur sahélien du Niger. *Bois et Forêts Des Tropiques*, 333(3), pp.55-66 doi: 10.19182/bft2017.333.a31468
- Adomou, C.A. et al., 2018. Analyse des connaissances traditionnelles et des déterminants relatifs à l'utilisation de *Newbouldia laevis* (PBeauv) Seemann ex Bureau (Bignoniaceae) au Sud-Bénin. *Afrique SCIENCE*, 14(1), pp.194-205.
- Avalos, G., 2019. Shade tolerance within the context of the successional process in tropical rain forests. *Revista de Biología Tropical*, 67(2), pp .53-77. doi: 10.15517/rbt.v67i2supl.37206
- Battles, J.J. et al., 2001. The effects of forest management on plant species diversity in a Sierran conifer forest. *For Ecol. Manag.*, 146, pp.211-222
- Besag, J., 1977. Contribution to the discussion of Dr. Ripley's paper. *J R Stat Soc B*, 39, pp.193-195
- Boose, E.R., Boose, E.R. & Lezberg, A. 1998. A practical method for mapping trees using distance measurements. *Ecology*, 79(3), pp.819-827.
- Carnus, J.M., Parrotta, J. & Brockerhoff, E., 2006. Planted forests and biodiversity. *Journal of Forestry Research*, 104, pp.65-77.
- Cintron, B.B., 1990. *Cedrela odorata* L. Cedro, Spanish Cedar. In *Silvics of North America: 2. Hardwoods*. Washington DC: Agriculture Handbook 654, Department of Agriculture, Forest Service. pp.128-134.
- Dajoz, R., 2003. *Précis d'écologie*. Paris, France.
- der Meersch, V.V. et al., 2020. Causes and consequences of *Cedrela odorata* invasion in West African semi-deciduous tropical forests. *Biological Invasions*, 23, pp.537-552. doi: 10.1007/s10530-020-02381-8
- Diggle, J.P., 1983. *Statistical analysis of spatial point patterns. Applications to Economical, Biomedical and Ecological Data*. New York, USA: Academic Press.
- Dyderski, M.K. & Jagodziński, A.M., 2020. Impact of invasive tree species on natural regeneration species composition, diversity, and density. *Forests*, 11(4), 456. doi: 10.3390/F11040456
- Eblin, M.O. & Amani, Y.C., 2015. Déforestation et politique de reboisement dans les forêts classées : cas de la forêt de la Téné (Centre-ouest de la Côte d'Ivoire). *European Scientific Journal*, 11(26), pp.110-127.
- Fonton, N.H. et al., 2011. Plot size for modelling the spatial structure of Sudanian woodland trees. *Annals of Forest Science*, 68, pp.1315-1321. doi: 10.1007/s13595-011-0111-1

- Global Invasive Species Database GISD, 2015, 'Species profile Cedrela odorata', in *IUCN GISD Database*, viewed 28 February 2021, from <http://www.iucngisd.org/gisd/species>.
- Goldman, R.L., Goldstein, L.P. & Daily, G.C., 2008. Assessing the conservation value of a human-dominated island landscape: plant diversity in Hawaii. *Biodivers Conserv.*, 17, pp.1765–1781
- Goreaud, F. & Péliissier, R. 2003. Avoiding misinterpretation of biotic interactions with the intertype K12-function: population independence vs. random labelling hypotheses. *J Veg Sci*, 14, pp.681–692
- Haase, P. et al., 1996. Spatial patterns in two-tiered semiarid shrubland in southeastern Spain. *J. Veg. Sci.*, 7, pp.527–534.
- Havyarimana, F. et al., 2013. Impact de la structure spatiale de *Strombosia scheffleri* Engl. et *Xymalos monospora* (Harv.) Baill. sur la régénération naturelle et la coexistence des espèces arborescentes dans la réserve naturelle forestière de Bururi, Burundi. *Bois et Forêt des Tropiques*, 316(2), pp.49–61. doi: 10.19182/bft2013.316.a20530
- He, F. & Duncan, R.P., 2000. Density-dependent effects on tree survival in an old-growth Douglas fir forest. *J Ecol*, 88, pp.676–688
- Herault, B., Bouxin, G. & Thoen, D., 2004. Comparison of the regeneration patterns of woody species between Norway spruce plantations and deciduous forests on alluvial soils. *Belg J Bot*, 137, pp.36–46
- Kiêu, K. & Mora, M., 1999. Estimating the reduced moments of a random measure. *Adv App Prob*, 31, pp.48–62
- Kilawe; C.J., Mchelu, H.A. & Emily, C.J., 2022. The impact of the invasive tree *Cedrela odorata* on the Electric Blue Gecko (*Lygodactylus williamsi*) and its habitat (*Pandanus rabaiensis*) in Kimboza Forest Reserve, Tanzania. *Global Ecology and Conservation*, 38, e02225. doi: 10.1016/j.gecco.2022.e02225
- Kindt, R. & Coe, R., 2005. *Tree diversity analysis. A manual and software for common statistical methods for ecological and biodiversity studies*. Nairobi: World Agroforestry Centre (ICRAF).
- Kone, Y. & Vroh, B.T.A., 2021. Diversité de la régénération des ligneux dans les plantations forestières au centre de la Côte d'Ivoire. *Biotechnol. Agron. Soc. Environ.*, 25(4), pp.253–266
- Le Maître, D.C. et al., 2011. Impacts of invasive Australian acacias: implications for management and restoration. *Diversity and Distributions*, 17(5), pp.1015–1029. doi: 10.1111/j.1472-4642.2011.00816.x
- Lemenih, M. & Teketay, D., 2005. Effect of prior land use on the recolonization of native woody species under plantation forests in the highlands of Ethiopia. *For Ecol Manag*, 218, pp.60–73
- Lemmens, R.H.M.J., 2008. *Cedrela odorata* L. In *PROTA (Plant Resources of Tropical Africa / Ressources végétales de l'Afrique tropicale)*. Wageningen, Netherlands: PROTA Network Office Europe, Wageningen University, pp. 103–134
- Marcon, E., 2019. Mesure de la biodiversité et de la structuration spatiale de l'activité économique par l'entropie. *Revue économique*, 70(3), pp.305–326
- Marcon, E., 2018. *Mesures de la Biodiversité*. Kourou, France: Master, UMR Écologie des forêts de Guyane (ECOFOG).
- Meyer, S.E. et al., 2021. Invasive Species Response to Natural and Anthropogenic Disturbance. In *Invasive Species in Forests and Rangelands of the United States*. Springer, Cham. doi: 10.1007/978-3-030-45367-1_5
- Muellner, A.N. et al., 2010. Biogeography of *Cedrela* (Meliaceae, Sapindales) in Central and South America. *American Journal of Botany*, 97(3), pp.511–518.

- Nicotra, A.B., 1998. Sex ratio variation and spatial distribution of *Siparuna grandiflora*, a dioecious shrub. *Æcologia*, 115, pp.102-113.
- Pasiecznik, N., 2008. *Cedrela odorata* (Spanish cedar). *CABI Compendium*. doi: 10.1079/cabicompendium.11975
- Pearson, D.E. et al., 2018. Community assembly theory as a framework for biological invasions. *Trends Ecol. Evol.*, 33(5), pp.313-325. doi: 10.1016/j.tree.2018.03.002
- Picard, N. & Gourlet-Fleury, S., 2008. *Manuel de référence pour l'installation de dispositifs permanents en forêt de production dans le Bassin du Congo*. Commission des Forêts d'Afrique Centrale (COMIFAC).
- Ripley, B.D., 1977. Modelling spatial patterns. *Journal of the Royal Statistical Society B*, 39, pp.172-212.
- Ripley, B.D., 1981. *Spatial statistics*. New York, USA: Wiley. doi: 10.1002/0471725218
- Sangne, Y.C., 2009. *Dynamique du couvert forestier d'une aire protégée soumise aux pressions anthropiques : cas de la forêt classée de Téné dans le département d'Oumé (Centre-ouest de la côte d'Ivoire)*. Université Félix Houphouët-Boigny, Abidjan.
- SODEFOR, 2014. *Stratégie de lutte contre les défrichements*. Unité de Gestion Forestière Téné, p.40
- Stoll, P. & Bergius, E., 2005. Pattern and process: competition causes regular spacing of individuals within plant populations. *J Ecol*, 93, pp.395-403
- Thammanu, S., Marod, D. & Han, H., 2021. The influence of environmental factors on species composition and distribution in a community forest in Northern Thailand. *J. For. Res.*, 32, pp.649-662. doi: 10.1007/s11676-020-01239-y
- Vroh, B.T.A., Koné, Y. & Djongmo, A.V., 2022. Plant species diversity and structure in tree plantations at Téné Protected Forest (Côte d'Ivoire). *Annals of Silvicultural Research*, 47(1), pp.39-47
- Wiegand, T. & Moloney, K.A., 2004. Rings, circles and null-models for point pattern analysis in ecology. *Oikos*, 104, pp.209-229

Research Article

The Diversity of Scarabaeid Beetles (Scarabaeidae: Coleoptera) in The Lowland Rainforest Ecosystem of Sorong Nature Tourism Park, West Papua, Indonesia

La Ode Fitriadiansyah¹, Tri Atmowidi^{2*}, Windra Priawandiputra², Sih Kahono³

1)Student of Animal Biosciences Study Program, Graduate School, IPB University

2)Department of Biology, Faculty of Mathematics and Natural Sciences, IPB University, Campus Dramaga, Bogor 16680

3)Research Centre for Applied Zoology, National Research and Innovation Agency (BRIN), Cibinong 16912, Indonesia

* Corresponding author, email: atmowidi@apps.ipb.ac.id

Keywords:

active sampling
beetle abundance
dung traps
light trap

Submitted:

06 October 2022

Accepted:

06 May 2023

Published:

13 November 2023

Editor:

Ardaning Nuriliani

ABSTRACT

Scarabaeid beetles have an essential role in forest ecosystems, such as nutrient recycling, seed dispersal, forest regeneration, controlling parasite populations, and reducing carbon emissions. This study aims to analyse the diversity of scarabaeid beetles in the lowland rainforest ecosystem of Sorong Nature Tourism Park (SNTTP), West Papua, Indonesia. The purposive sampling method was used to determine the study sites in three habitat types, i.e., rehabilitation zone, conservation zone, and protection zone. Collection of beetles were conducted by baited dung traps (type A, B, and C), light trap, and active sampling. The baits, i.e., cow and human excrements were used and was replaced every 24 hours (68 repetitions for 68 days) in each habitat. Results showed a total of 30 individuals belonging to 13 species of scarabaeid beetles were collected. *Onthophagus* has a highest species richness (5 species) compared to *Aphodius* sp., *Anomala* sp., and *Adoretus* sp. (1 species). The protection zone has a highest diversity index ($H' = 2.09$), followed by conservation zone ($H' = 2$) and rehabilitation zone ($H' = 0.5$). Based on trap type, dung trap collected the most beetle species (9 species), followed by light trap (6 species) and active sampling (2 species). Pearson correlation analysis showed soil pH significantly correlated with beetle abundance. This study was the first report of scarabaeid beetles in West Papua, Indonesia.

Copyright: © 2023, J. Tropical Biodiversity Biotechnology (CC BY-SA 4.0)

INTRODUCTION

Scarabaeid beetles (Scarabaeidae: Coleoptera) have various colours, from brown and black to bright-metallic colour, body size from 1.5 to 160 mm, antennae to sense odours, forelegs to dig, males and sometimes females have prominent horns to fight for mates or food (Arnett et al. 2002; Bouchard et al. 2011). Arnett et al. (2002) reported the scarabaeid beetle consisting of 27.800 species worldwide. Subfamilies, such as Aphodiinae and Scarabaeinae consisting of 6.850 species, while Orphninae, Melolonthinae, Dystinae, Ruthelinae, and Cetoniinae consisting of 20.950 species.

The description and biodiversity of scarabaeid beetle is widely studied in tropical and temperate areas (Allegro & Sciaky 2003; Nichols et al. 2007). Adult Scarabaeid have diverse feed preferences, such as animal manure, carrion, fungi, herbs, pollen, fruit, compost, and plant root. Some scarabaeid live in ant nest (myrmecophiles), termite nests (termitophiles),

and rodent and bird nests (Arnett et al. 2002). Whereas some families of Scarabaeidae, Geotrupidae, and Hybosoridae feed on microbial-rich fluids of mammalian excrement and use them to incubate larvae (Halffter & Edmonds 1982).

Some publications of scarabaeid beetles in Indonesia have been reported previously. Kahono and Setiadi (2007) reported 28 species of dung beetle in mountain forest ecosystem of Pangrango National Park, West Java and the dominant species was *Onthophagus variolaris* Lansb (382 individuals). Priawandiputra et al. (2020) also reported in the lowland forest ecosystem in the Pangandaran Nature Reserve, West Java and the dominant species was *Onthophagus babirusa* Eschscholtz (434 individuals). Dung beetles have also been reported in montane forest of the Harau Valley Nature Reserve, West Sumatra (Putri et al. 2014); Kayan Mentaran National Park, East Kalimantan (Kahono & Ubaidillah 2003); Gunung Palung National Park, West Kalimantan (Malina et al. 2018); and Lambusango Forest, Buton, Sulawesi (Moy et al. 2016). Latifa et al. (2019) reported the diversity and abundance of coprophagous beetles in organic and non-organic farms in West Java consist of 15 species belonging to 2 families i.e Scarabaeidae and Aphodiidae. The dominant species were *Copris reflexus* and *Onthophagus pauper*.

Sorong Nature Tourism Park (SNTP) is a nature conservation area located in West Papua, Indonesia which was established based on the Decree of the Minister of Agriculture No. 397/Kpts/Um/5/1981 with an area of 945.90 ha (MoA 1981; BKSDA 2008). SNTP is a lowland rainforest ecosystem with varied topography, such as flat, wavy, and steep with a slope of 0-15%. Annual rainfall is 3,066 mm, with 193.3 rainy days per year (BKSDA 2008). The tourism park has type A climate and as home of various fauna such as mammals, aves, reptiles, amphibians, and butterflies (BKSDA 2008; Beljai 2017). Compared to other faunas, there is no information regarding scarabaeid beetle diversity in this area. This study aims to analyse the diversity of scarabaeid beetles in the lowland rainforest ecosystem of Sorong Nature Tourism Park, Papua, Indonesia.

MATERIALS AND METHODS

Study Area

The collection of scarabaeid beetles was carried out in three habitats of lowland rainforest ecosystem of SNTP, i.e., rehabilitation zone (RZ) (0°54'35"S 131°20'35"E), conservation zone (CZ) (0°55'02"S 131°20'21"E), and protection zone (PZ) (0°55'56"S 131°20'36"E) (Figure 1). The rehabilitation zone is bordered by community gardens dominated by shrubs and herbaceous plants such as Poaceae and Bromeliaceae. In this zone, some species of mammals were found, such as wild boars (*Sus* sp.) and moles (Geomyidae). The conservation zone has a relatively large canopy and is dominated by shrubs and trees. The protection zone is the most expansive area in the SNTP compared to other zones. This zone has more complex plants, such as merbau (*Insia* spp.), papuan palm (*Sammieria leucophylla*: Palmae), matoa (*Pometia pinnata*: Sapindaceae), rambutan (*Nephelium lappaceum*: Sapindaceae), medang (*Beilshmiadia* sp.: Lauraceae), angšana (Fabaceae), amugia, langsung (*Lansium domesticum*: Meliaceae), cempedak (*Artocarpus integer*: Moraceae), *Araucaria* spp. Some mammals found in this zone, such as wild boar (*Sus* sp.), mole (Geomyidae), ground kangaroo (Macropodidae), and kuskus (Phalangeridae).

Collection of Beetles

Beetles were collected during six months on sunny days for sixty-eight days from August to December 2021 in three zone habitats (rehabilitation, conservation, protection zones) of the SNTP lowland

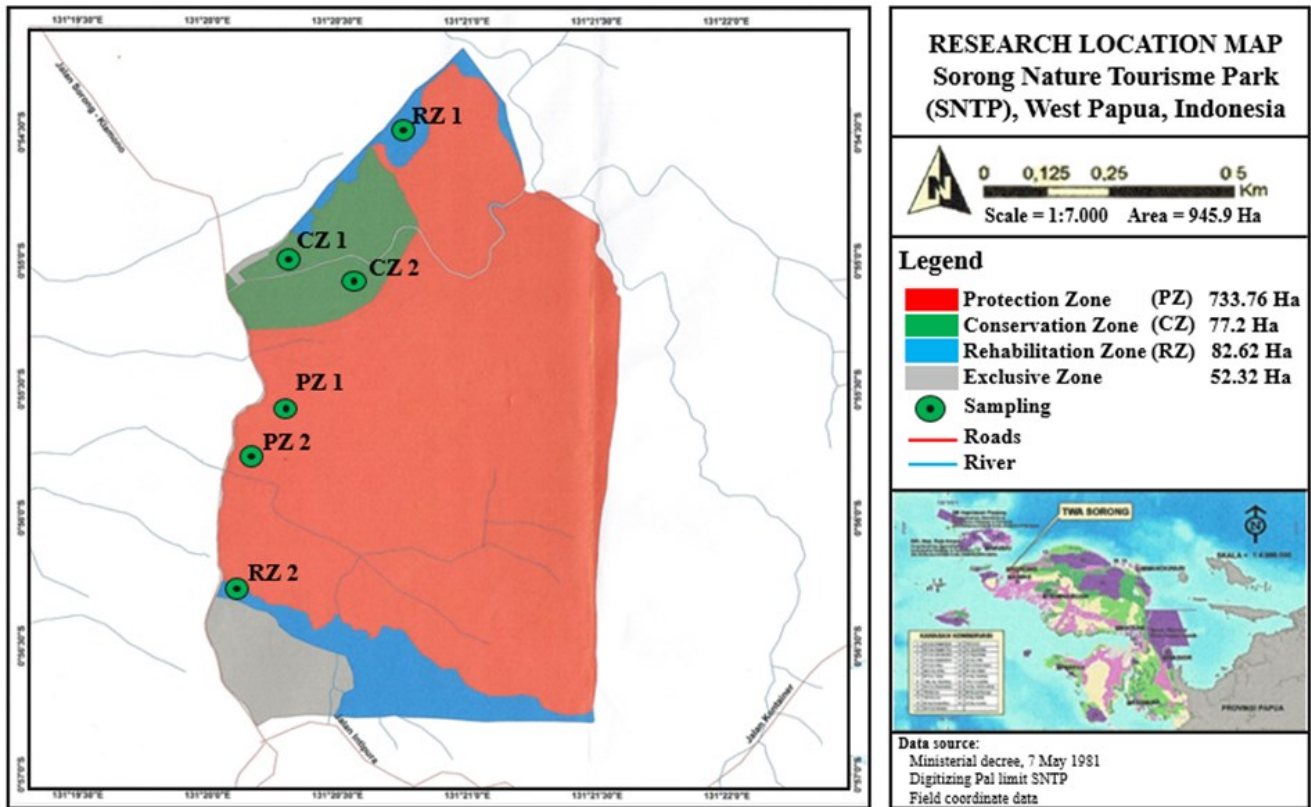


Figure 1. Sampling location of scarabaeid beetles in Sorong Nature Park, West Papua.

rainforest ecosystem. Beetles were collected using dung traps, light trap, and active sampling (Figure 2) (Abot et al. 2012; Milotić et al. 2018; Priawandiputra et al. 2020). Three types of dung traps (type A, B, and C) were used (Milotić et al. 2018). Type A dung trap was made from plastic cups (13 cm in height, 6 cm in bottom diameter, 9 cm in top diameter, and 480 ml in volume). At the top of the trap was hanged with 10 g of excrement and wrapped with gauze. Type B dung trap was made of plastic containers (12 cm in height, 10 cm in bottom diameter, 12 cm in top diameter, and 1000 ml in volume). At the top of the trap was hanged with about 1000 g of mammal dung. Type C dung trap was made of a plastic plate with 1000 g of excrement. In a total, we used 75 dung traps with 25 traps in each zone. The traps were baited with cow excrement (*Bos* sp.) and sometimes were replaced by human excrement because cow excrement was not available continuously. The beetle samples were collected every 24 hours. The excrement was replaced every 24 hours (68 repetitions for 68 days) in each habitat. Two light traps were installed in each zone for 12 hours, from 06.00 pm to 06.00 am. The light trap consists of one set (two 15-watt lamps, a car battery, and a net). Sample of beetles was also collected by using the active sampling method, i.e., collecting by hands along the road (Priawandiputra et al. 2020). Environmental parameters, such as air humidity and temperature, soil moisture and pH, and light intensity were also measured. Vegetation type, altitude and topography of three habitats were also recorded.

Preservation and Identification of Beetle Specimens

Beetle samples were soaked in 70% ethanol and pinned for dry preservation. The beetle body length was also measured. Specimen identification based on Balthasar (1963), Creedy and Mann (2012), and the website (www.boldsystem.org). The beetle specimens were verified with the specimen collection of Bogor Zoological Museum, National Research and Innovation Agency (BRIN), Cibinong, Indonesia.

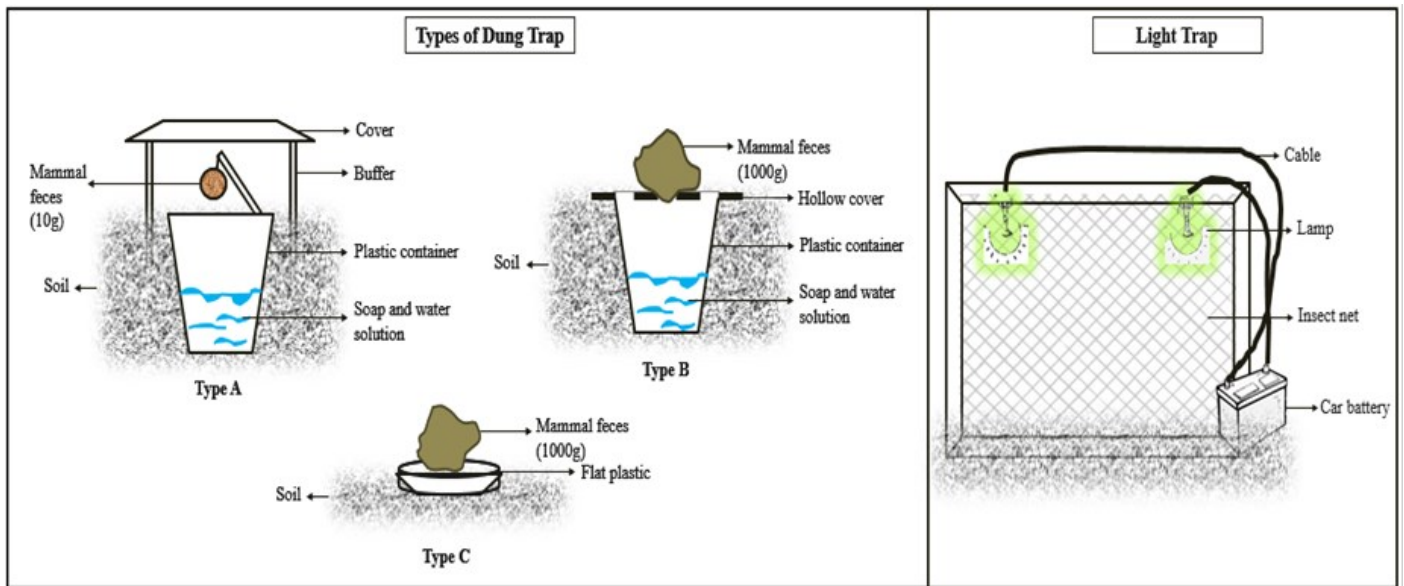


Figure 2. Model of dung trap and light trap used in this research.

Data Analysis

The diversity of beetle species was analysed using the Shannon-Wiener diversity index, evenness index, and Simpson dominance index (Sweke et al. 2013). The t-test was used to analyse the beetle diversity among sites (Hutcheson 1970; Magurran 1988). The analysis of similarity (ANOSIM-SIMPER) was used to show the species composition at each site (Clarke & Ainsworth 1993; Clarke 1993). Statistical analysis was performed using PAST (Paleontological Statistics) software version 3.14 (Hammer et al. 2001).

RESULTS AND DISCUSSION

Abundance, Species Richness and Composition

In this study, 30 individuals belonging to 13 species of scarabaeid beetles were found. Based on body size, *Xylotrupes*, *Holotrichia*, and *Anomala* have a large body sizes (38–50 mm) compared to other species (less than 10 mm) (Figure 3). The scarabaeid beetles found in this study were dominated by small body size. The large beetles are more difficult to survive because they require more food and a longer reproductive time (Slade et al. 2014; Sa'roni et al. 2020).

The accumulated number of beetles fluctuated from August to December 2021. The highest diversity of beetles occurred in October (12 individuals, 8 species), followed by December (9 individuals, 7 species), November (5 individuals, 4 species), and August (4 individuals, 4 species) (Table 1). The beetles were not found in September, may be due to a high rainfall (400–500 mm) and only 5 sunny days (Table 1). Heavy rainfall inhibits the activity of scarabaeid beetles. These results supported Wardhaugh et al. (2018) that stated a high rainfall affected beetle abundance in wet tropics of Queensland (low abundance in September and high in December). In contrast in Java, Indonesia the highest abundance of dung beetles occurred in the rainy season compared to the dry season (Priawandiputra et al. 2020).

Based on sampling coverage ratio, this sampling covered 55.6% of beetle species in SNTP (Table 2). The highest beetle abundance was found in conservation zone (13 individuals), followed by protection zone (12 individuals), and rehabilitation zone (5 individuals). The species richness was also high in conservation and protection zones (9 species), followed by conservation zone (8 species), and rehabilitation zone (2 spe-

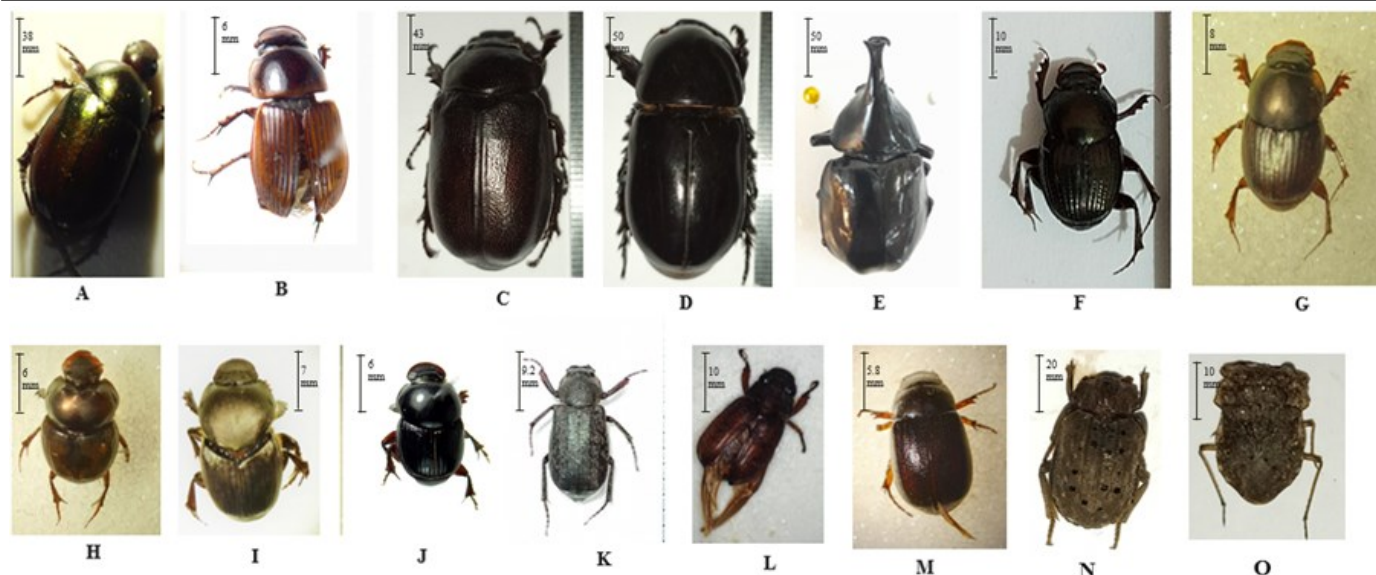


Figure 3. Scarabaeid beetle found at SNTP. A: *Anomala* sp.; B: *Aphodius* sp.; C: *Holotrichia* sp.; D: *Xylotrupes* sp.; E: *Xylotrupes gideon*; F: *Onthophagus* sp1; G: *Onthophagus* sp2; H: *Onthophagus* sp3; I: *Onthophagus* sp4; J: *Onthophagus* sp5; K: *Apogonia* sp1; L: *Adoretus* sp; M: *Apogonia* sp2; N: *Omorgus* sp.; O: *Gelastocoris* sp.

Table 1. The rainfall in August-December 2021 at study site (data from the Meteorology, Climatology and Ge physics Agency at SNTP).

Collection time	Rainfall (mm)	Category	Number of rainy days	Number of days without rain (sampling time)
August	300-400	High	21	10
September	400-500	High	25	5
October	200-300	Medium	9	22
November	300-400	High	19	11
December	200-300	Medium	11	20

cies). Protection zone has a highest diversity index ($H'=2.09$), followed by conservation zone ($H'=2$), and rehabilitation zone ($H'=0.5$). The highest species richness was found in conservation zone ($a=0.91$), followed by protection zone ($a=0.90$) and rehabilitation zone ($a=0.82$) (Table 2).

The high abundance of beetles in the protection and rehabilitation zones may related to the presence of mammals and the complexity of plant species. Similarly, Simba et al. (2022) reported the abundance and species richness of beetles was higher in protected area compared to agricultural area. The abundance of beetles also increases along the number of mammals in the area. The distribution and presence of large mammals that provide manure as a food for beetles and affect their abundance, composition, and diversity (Priawandiputra et al. 2020).

The highest dominance index was found in conservation zone ($D=0.15$), followed by protection zone ($D=0.14$) and rehabilitation zone ($D=0.68$). The results of the ANOSIM-SIMPER multivariate analysis showed differences in species composition of scarabaeid beetle in three habitat types ($p=0.0001$). The species that the most contributed was *Holotrichia* sp. (22.69%), followed by *Apogonia* sp1 (16.33%), *Adoretus* sp. (11.56%), *Apogonia* sp2 (9.97%), *Onthophagus* sp1 (6.57%), *Xylotrupes* sp. (6.35%), *Xylotrupes gideon*, *Onthophagus* sp3, and *Onthophagus* sp5 (3.94%), *Onthophagus* sp2, *Onthophagus* sp4, *Aphodius* sp., and *Anomala* sp. (2.46%).

Four species of beetles (*Anomala* sp., *Aphodius* sp., *Onthophagus* sp2, and *Onthophagus* sp4) were only found in the protection zone. Tsunoda et al. (2017) revealed that *Anomala* is omnivorous, which feeds on roots of various plant species and soil organic matter. Three species of beetles

(*Xylotrupes gideon*, *Onthophagus* sp3, *Onthophagus* sp5) were only found in the conservation zone. While in the rehabilitation zone was only found 1 species (*Xylotrupes* sp.) which was not found in other zones. *Xylotrupes* is a polyphagous, both fruits and leaves (Firake et al. 2013). The species found in three different habitats was *Holotrichia* sp. *Holotrichia* is a herbivore, their larvae and adult eat leaves (Rizwangul et al. 2018). While, *Aphodius* and *Onthophagus* are decomposers that consume the excrement of large mammals (Priawandiputra et al. 2020). The genus with the highest species richness was *Onthophagus*. *Onthophagus* successfully wide dispersed due to its smaller body size, aggressive and competitive behaviour, and high survival in disturbed habitats (Hanski & Cambefort 1991; Muhaimin et al. 2015).

This study showed the diversity of beetles was lower than in previous studies in Kalimantan, Sulawesi, Java, and Sumatera. Moy et al. (2016) reported 1710 individuals belonging to 29 species of scarabaeid beetles were found in the Lambusango forest in Southeast Sulawesi. Meanwhile, 8073 individuals belonging to 65 species were collected in East Kalimantan (Ueda et al. 2017). Priawandiputra et al. (2020) reported in lowland forests of Pangandaran Nature Reserve was collected 853 individuals belonging to 17 species of beetles. While Putri et al. (2014) in the montane forest of the Harau Valley Nature Reserve, West Sumatra collected 539 individuals belonging to 18 species of scarabaeid beetles.

Compared to the beetle of lowland forest in West Java (Priawandiputra et al. 2020), Southeast Sulawesi (Moy et al. 2016), and East Kalimantan (Ueda et al. 2017), the species of beetles collected in this study were different. Results of this study showed some species of beetles attracted to mammal excrement of *Omorgus* sp. and *Gelastocoris* sp. that has not been reported previously. Differences in species composition of beetles between study sites were caused by differences in sampling time,

Table 2. The species and abundance of scarabaeid beetles collected in three zone habitats in SNTP. PZ: protection zone, CZ: conservation zone, RZ: rehabilitation zone.

Species	Collection method	Number of Individuals			Total	Role in the ecosystems
		PZ	CZ	RZ		
<i>Anomala</i> sp.	light trap	1	0	0	1	herbivore
<i>Aphodius</i> sp.	dung trap	1	0	0	1	decomposer
<i>Holotrichia</i> sp.	light trap, dung trap	3	2	4	9	herbivore
<i>Xylotrupes</i> sp.	active sampling	0	0	1	1	herbivore
<i>Xylotrupes gideon</i>	light trap	0	1	0	1	herbivore
<i>Onthophagus</i> sp1	dung trap	1	1	0	2	decomposer
<i>Onthophagus</i> sp2	dung trap	1	0	0	1	decomposer
<i>Onthophagus</i> sp3	dung trap	0	1	0	1	decomposer
<i>Onthophagus</i> sp4	dung trap	1	0	0	1	decomposer
<i>Onthophagus</i> sp5	dung trap	0	1	0	1	decomposer
<i>Apogonia</i> sp1	light trap, dung trap	1	3	0	4	decomposer
<i>Apogonia</i> sp2	light trap, dung trap, active sampling	1	2	0	3	herbivore
<i>Adoretus</i> sp.	light trap	2	2	0	4	herbivore
Number of individuals		12	13	5	30	
Species richness (a)		9	8	2	13	
Chao1 (b)		19.5	9.5	2	27	
Sampling coverage ratio (a/b x 100%)		46.15	84.21	100	55.6	
Shannon-Wiener (H')		2.09	2	0.50	2.2	
Evenness (E)		0.90	0.91	0.82	0.7056	
Dominance (D)		0.138	0.147	0.68	0.148	

bait type, number of traps, sampling area, and biogeographical history (Priawandiputra et al. 2020). Kalimantan and Java islands were fragments of the Sunda continental until they separated in the Eocene, while East Sulawesi including southeast Sulawesi was originally part of Australasia to the early Miocene (Cox et al. 2016). Therefore, Sulawesi has many endemic fauna species including the beetle which is not found on other western islands, including Java and Kalimantan (Balthasar 1963; Shahabuddin 2010).

Papua has a wilderness type with the largest and oldest tropical rainforest in the Asia-Pacific region (Marshall et al. 2011). The Papua Island originates from the Australian tectonic plate which has shifted to the north, forming the central cordillera, and shifting the tip of the island to the north and northwest. The middle cordillera has been formed by the compression of the Australian plate with the Pacific plate, with massive uplift over several million years. Apart from the geological linkages, there are considerable environmental differences between the continents of Australia and New Guinea. Australia is drier and temperate, while Papua is tropical and humid. These two basic differences explain difference biota in the two areas. Climatologically, Papua is one of the cloudiest places on earth stretching the equator to 12 degrees south latitude. Papua's equatorial climate is seasonally dominated by the northwest monsoon and southeast trade winds. In most parts of Papua, the influence of the northwest monsoon brings rain and unpredictable weather, while the southeast trade wind tends to bring cool and dry weather. The large size of the island, its constant climate that supports vegetative growth, rugged topography, and proximity to the source areas of the Asian and Australian continents have made Papua a hyper generator of biodiversity including insects.

Based on the collection method, the highest number of individuals collected was light trap (14 individuals), followed by dung trap (14 individuals), and active sampling (2 individuals) (Figure 4). Light trap is effective for trapping many groups of insects including beetles that are active at night (Garcia-Lopez et al. 2011). Dung trap collected the highest beetle richness (9 species consist of *Aphodius* sp., *Holotrichia* sp., *Onthophagus* sp1, *Onthophagus* sp2, *Onthophagus* sp3, *Onthophagus* sp4, *Onthophagus* sp5, *Apogonia* sp1, *Apogonia* sp2), followed by light trap (6 species consist of *Anomala* sp., *Holotrichia* sp., *Xylotrupes gideon*, *Adoretus* sp., *Apogonia* sp1, *Apogonia* sp2) and active sampling (2 species consist of *Xylotrupes* sp. and *Apogonia* sp2). Dung trap type C collected the highest number of individuals (9 individuals), followed by type B (3 individuals) and type A (2 individuals) (Figure 4). Types B and C dung traps have a high abundance due to the larger bait than type A. This result supported Errouissi et al. (2004) that large baits attract significantly more dung beetles than small baits. Few beetles were attracted to the small dung size of sheep and goats compared to large and bulky cow dung.

Environmental Factors

The environmental parameters measured in each collection zone were different, except for soil pH (Table 3). Based on Pearson correlation, soil pH significantly correlated ($p=0.00$), while air temperature and humidity, light intensity, and soil humidity were not correlated ($p=0.95$, $p=0.84$, $p=0.80$, and $p=0.93$) with beetle abundance (Table 4). Juniarti and Rusniarsyah (2022) reported in the neutral pH of soil, the diversity of insects was high. Wet soil interferes beetle excavation and affects of its larvae (Sowig 1995, 1996; Nichols et al. 2008). Temperature affects beetle reproduction, feeding, and breeding behaviour (Lobo et al. 1998; Chown 2001).

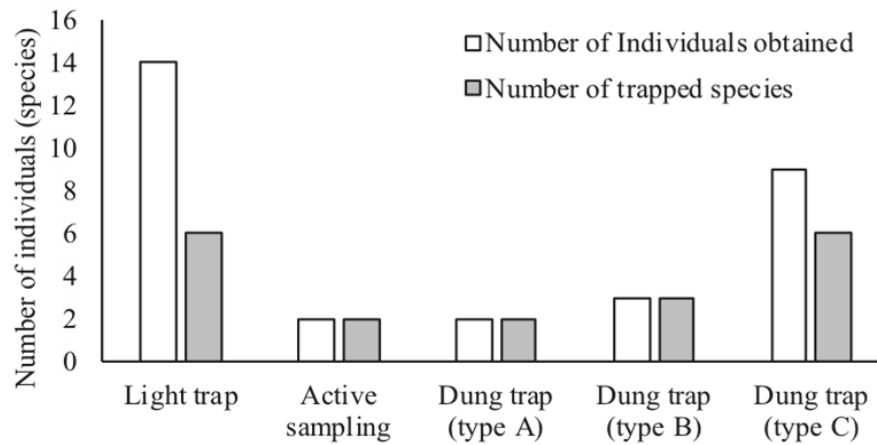


Figure 4. The number of species and individuals of beetles based on the collection method.

Table 3. Environmental factors at three zones of study sites (rehabilitation, conservation, protection) in SNTP (means \pm Standard deviation).

Habitat type (zone)	Air temperature ($^{\circ}$ C)	Air humidity (%)	Soil moisture (%)	Soil pH	Light intensity (lux)
Rehabilitation zone	28 \pm 1.41	82.2 \pm 1.92	84.2 \pm 1.92	7 \pm 0	900 \pm 7.91
Conservation zone	27 \pm 0	88.2 \pm 0.96	88.5 \pm 1.29	7 \pm 0	752 \pm 5.70
Protection zone	27 \pm 0	90.5 \pm 0.71	90.7 \pm 0.58	7 \pm 0	738 \pm 5.70

Table 4. Pearson correlation between environmental parameters and beetle abundance (*=significant).

Environmental parameters	Correlation coefficient (r)	p-value
Air temperature ($^{\circ}$ C)	-0.5	0.95
Air humidity (%)	0.6	0.84
Soil humidity (%)	0.6	0.80
Soil pH	1.0	0.00*
Light intensity	-0.5	0.93

CONCLUSIONS

A total of 30 individuals belonging to 13 species of beetles were collected in SNTP, West Papua, Indonesia. The highest species richness was *Onthophagus*, followed by *Aphodius* sp., *Anomala* sp., *Adoretus* sp., *Apogonia* sp., and *Omorgus* sp. The highest diversity of scarabaeid beetles was found in the protection zone, followed by the conservation zone and rehabilitation zones. Light trap and type C dung trap were effective for collecting scarabaeid beetles compared to others traps.

AUTHOR CONTRIBUTION

L.O.F.: designed of the research, collected and analysed the data, funding acquisition, writing-original draft. T.A., W.P., and S.K.: wrote, reviewed and edited the manuscript. L.O.F. and S.K.: specimen identification of beetles.

ACKNOWLEDGMENTS

We thank the head of the West Papua BKSDA and staff, for granting permission to research at SNTP and for their technical assistance. We also thank to SNTP forest guides, especially Mr. Harry, Mr. Tito, and Mr. Petrus for their access to facilities and assistance during our field-work. Mr. Sarino who has assisted in the specimen identification process.

CONFLICT OF INTEREST

The authors declare no conflict of interests regarding the research or the research funding.

REFERENCES

- Abot, A.R. et al., 2012. Abundance and diversity of coprophagous beetles (Coleoptera: Scarabaeidae) caught with a light trap in a pasture area of the Brazilian Cerrado. *Studies on Neotropical Fauna and Environment*, 47(1), pp.53–60. doi: 10.1080/01650521.2012.662846.
- Allegro, G. & Sciaky, R., 2003. Assessing the potential role of ground beetles as bioindicators. *Forest Ecology and Management*, 175, pp.275–284. doi: 10.1016/S0378-1127(02)00135-4.
- Arnett, J.R.H. et al., 2002. American beetles, volume II: Polyphaga: Scarabaeoidea through Curculionoidea. *CRC Press*. doi: 10.1201/9781420041231.
- Balthasar, V., 1963. Monographie der Scarabaeidae und Aphodiidae der palaearktischen und orientalischen Region. Band 1, 2 und 3, Verlag der Tschechoslowakischen Akademie der Wissenschaften, Prague. doi: 10.4039/Ent97446-4.
- Beljai, M., 2017. Characteristics of Natural Tourism Potential in the Sorong Nature Park Area. *AGRICOLA*, 7(1), pp.68–89. doi: 10.30574/wjarr.2020.6.3.0163.
- BKSDA West Papua, 2008. The KSDA book information field regions I Sorong. Center for the conservation of the resources natural of West Papua. Sorong.
- Bouchard, P. et al., 2011. Family-group names in Coleoptera (Insecta). *ZooKeys*, 88, pp.1–972. doi: 10.3897/zookeys.88.807.
- Chown, S.L., 2001. Physiological variation in insects: hierarchical levels and implications. *J Insect Physiol*, 47, pp.649–60. doi: 10.1016/S0022-1910(00)00163-3.
- Creedy, T.J. & Mann, D.J., 2012. *Identification guide to the Scarabaeinae beetles of Cusuco National Park, Honduras*. UK: Operation Wallacea.
- Clarke, K.R., 1993. Non-parametric multivariate analyses of changes in community structure. *Austral Ecology*, 18(1), pp.117–143. doi: 10.1111/j.1442-9993.1993.tb00438.x.
- Clarke, K. R. & Ainsworth, M., 1993. A method of linking multivariate community structure to environmental variables. *Marine Ecology-Progress Series*, 92, pp.205–205. doi: 10.3354/meps092205.
- Cox, C.B., Moore, P.D. & Ladle, R.J., 2016. *Biogeography: An Ecological and Evolutionary Approach 9th Edition*. New Jersey, US: Wiley-Blackwell.
- Errouissi, F. et al., 2004. Effects of the attractiveness for dung beetles of dung pat origin and size along a climatic gradient. *Environmental Entomology*, 33(1), pp.45–53. doi: 10.1603/0046-225x-33.1.45.
- Firake, D.M. et al., 2013. First report of elephant beetles in the genus *Xylotrupes hope* (Coleoptera: Scarabaeidae) attacking guava. *The Coleopterists Bulletin*, 67(4), pp.608–610. doi: 10.1649/0010-065x-67.4.608.
- Garcia-Lopez, A. et al., 2011. Sampling scarab beetles in tropical forests: The effect of light source and night sampling periods. *Journal of Insect Science*, 11(1), 95. doi: 10.1673/031.011.9501.
- Halffter, G. & Edmonds, W. D., 1982. *The nesting behavior of beetles (Scarabaeinae)-an ecological and evolutive approach*. Mexico D.F: Instituto de Ecologia.
- Hammer, Ø. et al., 2001. PAST: paleontological statistics software package for education and data analysis. *Palaeontologia Electronica*, 4(1).
- Hanski, I. & Cambefort, Y., 1991. Beetles ecology. Princeton University Press,.

- Hutcheson, K., 1970. A test for comparing diversities based on the shannon formula. *J. Theor Biol.*, 29(1), pp.151-154. doi: 10.1016/0022-5193(70)90124-4.
- Juniarti, F. & Rusniarsyah, L., 2022. Diversity of Soil Surface Interface Insects in Three Land Use Types in Sintang District, West Kalimantan. *IOP Conf. Series: Earth and Environmental Science*, 959 012026. doi: 10.1088/1755-1315/959/1/012026.
- Kahono, S. & Ubaidillah, R., 2003. Species Richness of Parasitic Wasp Superfamily Chalcidoidea (Insecta: Hymenoptera) at North Kayan Mentarang National Park, East Kalimantan, Indonesia. In *Joint Biodiversity Expedition in Kayan Mentarang National Park*. Jakarta, IDN: Ministry of Forestry – WWF Indonesia – ITTO.
- Kahono, S. & Setiadi, L. K., 2007. Diversity and Vertical Distribution of Scarabaeidae Stool Weevil (Coleoptera: Scarabaeidae) In Wet Tropical Forest Mountains Gede Pangrango National Park, West Java, Indonesia. *Biodiversitas*, 8(4), pp.118-121. doi: 10.13057/biodiv/d080209.
- Latifa, H., Atmowidi, T. & Noerdjito W.A. 2019. Biodiversity of coprophagous beetles in organic and non-organic farming. *Journal of Biological Resources* 5(2), pp.52-57. doi: 10.29244/jsdh.5.2.52-57.
- Lobo, J.M., Lumaret, J.P. & Jay-Robert P., 1998. Sampling beetles in the French Mediterranean area: effects of abiotic factors and farm practices. *Pedobiologia (Jena)*, 42, pp.252–66.
- Magurran, A., 1988. *Ecological diversity and its measurement*. New Jersey: Princeton University Press. doi: 10.1007/978-94-015-7358-0.
- Malina, V.C. & Junardi, K., 2018. Species of beetles (Coleoptera: Scarabaeidae) in Gunung Palung National Park, West Kalimantan. *Protobiont*, 7(2), pp.47-54. doi: 10.26418/protobiont.v7i2.25301.
- Marshall, A.J. & Beehler, B.M., 2011. *Ecology of Indonesian Papua Part One*. US: Tuttle Publishing
- Milotić, T. et al., 2018. Dung beetle assemblages, dung removal and secondary seed dispersal: data from a large-scale, multi-site experiment in the Western Palaearctic. *Frontiers of Biogeography*, 10, pp.1-2. doi: 10.21425/f5101-237289.
- Ministry of Agriculture [MoA], 1981 Decree of the Ministry of Agriculture No. 397/Kpts/Um/5/1981, 1 February 1981, Ascertainment of Sorong Natural Tourism Park.
- Moy, M.S., Mardiasuti, A. & Kahono, S., 2016. Response of beetle communities (Coleoptera: Scarabaeidae) across gradient of disturbance in the tropical lowland forest of Buton, Sulawesi. *Zoo Indonesia*, 25 (1), pp.58-70. doi: 10.52508/zi.v25i1.3024.
- Muhaimin, A.M.D., Hazmi, I.R. & Yaakov, S., 2015. Colonisation of beetles (Coleoptera: Scarabaeidae) of smaller body size in the Banri Forest Reserve, Selangor, Malaysia: A model sampling site for a secondary forest area. *Pertanika J Trop Agric*, 38(4), pp.531-532.
- Nichols, E. et al., 2007. Global dung beetle response to tropical forest modification and fragmentation: A quantitative literature review and metaanalysis. *Biological conservation*, 137, pp.1-19. doi: 10.1016/j.biocon.2007.01.023.
- Nichols, E. et al., 2008. Ecological functions and ecosystem services provided by Scarabaeinae beetles. *Biol Conserv*, 141, pp.1461– 74. doi: 10.1016/j.biocon.2008.04.011.
- Priawandiputra, W. et al., 2020. Dung beetle assemblages in lowland forests of Pangandaran Nature Reserve, West Java, Indonesia. *Biodiversitas*, 21(2), pp.497-504. doi: 10.13057/biodiv/d210210.

- Putri, R., Dahelmi & Herwina H., 2014. Dung Beetle species (Coleoptera: Scarabaeidae) at Lembah Harau Nature Reserve, West Sumatra. *J Biol UA*, 3(2), pp.35-140. doi: 10.25077/jbioua.3.2.%25p.2014.
- Rizwangul, A. et al., 2018. Feeding preference and taxis behavior of adult *Holotrichia oblita* (Coleoptera: Scarabaeidae) on three plants. *Acta Entomologica Sinica*, 61(5), pp.585-595.
- Sa'roni, S.M. et al., 2020. Diversity of dung beetle (Coleoptera: Scarabaeidae) in oil palm agropasture ecosystem in West Kotawaringin Regency, Central Kalimantan, Indonesia. *IOP Conference Series: Earth and Environmental Science*, 468(1), 12006. doi: 10.1088/1755-1315/468/1/012006.
- Shahabuddin, 2010. Diversity and community structure of beetles (Coleoptera: Scarabaeidae) across a habitat disturbance gradient in Lore Lindu National Park, Central Sulawesi. *Biodiversitas*, 11(1), pp.29-33. doi: 10.13057/biodiv/d110107.
- Simba, L.D. et al., 2022. Interactive effects of rangeland management and rainfall on dung beetle diversity. *Biodiversity and Conservation*, 31, pp.2639-2656. doi: 10.1007/s10531-022-02448-z.
- Slade, E.M. et al., 2014. Can cattle grazing in mature oil palm increase biodiversity and ecosystem service provision?. *The Planter*, 90 (1062), pp.655-665.
- Sowig, P., 1995. Habitat selection and offspring survival rate in three paracoprid beetles: the influence of soil type and soil moisture. *Ecography (Cop)*, 18, pp.147-54. doi: 10.1111/j.1600-0587.1995.tb00335.x.
- Sowig, P., 1996. Brood care in the beetle *Onthophagus vacca* (Coleoptera: Scarabaeidae): the effect of soil moisture on time budget, nest structure, and reproductive success. *Ecography (Cop)*, 19, pp.254-258. doi: 10.1111/j.1600-0587.1996.tb01252.x.
- Sweke, E.A. et al., 2013. Fish diversity and abundance of Lake Tanganyika: comparison between protected area (Mahale Mountains National Park) and unprotected areas. *International Journal of Biodiversity*, 2013(3), pp.516-522. doi: 10.1155/2013/269141.
- Tsunoda, T., Suzuki, J.I. & Kaneko, N., 2017. Fatty acid analyses to detect the larval feeding preferences of an omnivorous soil-dwelling insect, *Anomala cuprea* (Coleoptera: Scarabaeidae). *Applied Soil Ecology*, 109, pp.1-6. doi: 10.1016/j.apsoil.2016.09.020.
- Ueda, A. et al., 2017. List of beetles (Coleoptera: Coprophagous group of Scarabaeoidea) collected in lowland near Balikpapan, East Kalimantan, Indonesia. *Bulletin of FFPRI*, 16(2), pp.109-119.
- Wardhaugh, C.W., Stone, M.J. & Stork, N.E., 2018. Seasonal variation in a diverse beetle assemblage along two elevational gradients in Australian Wet Tropics. *Scientific Reports*, 8(1), 8559. doi: 10.1038/s41598-018-26216-8.

Research Article

Comparison of Soil Arthropod Diversity and Community Structure in Various Types of Land Cover in Malang Region, East Java, Indonesia

Bagyo Yanuwadi^{1*}, Suharjono¹, Nia Kurniawan¹, Muhammad Fathoni¹, Miftah Farid Assidiqy¹, Agus Nurrofik¹, Abdul Mutholib Shahroni¹

¹)Department of Biology, Faculty of Mathematics and Natural Sciences, Brawijaya University, Malang, Indonesia

*Corresponding author, email: yanuwadi@ub.ac.id

Keywords:

Arthropods
diversity
heterogeneity
land cover
Malang

Submitted:

29 November 2022

Accepted:

21 February 2023

Published:

17 November 2023

Editor:

Miftahul Ilmi

ABSTRACT

Land cover heterogeneity can affect the structure of soil arthropod communities that are critical in maintaining the stability of soil ecosystems. This study aimed to understand the effect of land cover variation on the diversity and community structure of soil arthropods. The types of habitats used include urban areas, agroforestry, gardens, and natural forests which are determined in the Malang Region, East Java, Indonesia. Hand sorting and hay-bait traps were applied in this study to obtain a variety of arthropod soils and the Berlese-Tullgren funnel was used to extract them. As a result, there are 25 families from 15 orders collected based on their ecological roles. The abundance of Philoscidae in sites S1 and S2 (urban green space), Talitridae in site S6 (agroforestry), and Isotomidae in sites S3, S4, and S5 (highland mixed forest) was highest and dominant. Site S7 has the highest diversity even though its family richness is lower. The site S3 counter-site had relatively high taxa richness, but low diversity. Mixed forest habitats contain a more complex diversity of soil arthropods, which can serve as a model for improving the fertility of disturbed ecosystems.

Copyright: © 2023, J. Tropical Biodiversity Biotechnology (CC BY-SA 4.0)

INTRODUCTION

Land cover heterogeneity has a close relationship with biodiversity due to its positive effect in providing niche habitats (Katayama et al. 2014). Biodiversity increases due to vegetation heterogeneity which will lead to a series of gradual changes in ecological processes and functions (Tylianakis et al. 2008; Stein et al. 2014). The relationship between diversity and ecosystem stability also depends on the intrinsic response of species to environmental fluctuations, the speed of response from disturbances, and the reduction of competition between species (Loreau & Mazancourt 2013). In terrestrial ecosystems, heterogeneity shows an impact not only on soil arthropod communities but also on their abundance, richness, and diversity (Tao et al. 2019).

The soil arthropod community has a different ecological role in each taxon. Based on their soil characteristics, arthropods are divided into 3 main roles, namely herbivores (leaf chewers & leaf piercers), predators (ambush predators & hunting predators), and detritivores (detritus shredders, bioturbators, and detritus grazers) (McCary & Schmitz 2021). Detritivores are referred to as soil dominant arthropods and are im-

portant in carrying out biogeochemical processes to maintain soil health and nutrient cycling (Joly et al. 2018; Lindsey-Robbins et al. 2019). Because it has a close relationship with soil ecosystems, soil arthropods have the potential to be able to respond sensitively to changes due to a relative decrease in environmental factors from their activities (Coyle et al. 2017). For example, the conversion of conventional land to organic can lead to an increase in the abundance and richness of taxa as a bioindicator response to environmental change (Ghiglieno et al. 2020).

Soil arthropods play an important role in maintaining the stability of terrestrial ecosystems (Bagyaraj et al. 2016). They participate in processing nutrient cycles and energy flows in the soil and participates in terrestrial ecosystem services (Yin et al. 2010). Soil arthropod activity aims to decompose and humify organic matter into fragmented materials (Zan et al. 2022). They break down dead organic matter with endogenic enzymes and facilitate microbes to stimulate nutrient mineralization (Griffiths et al. 2021). This collaborative activity results in soil formation processes, increased nutrition, and biotic regulation, and promotes plant growth (Briones 2018). Soil-digging arthropods such as termites and ants also participate in increasing soil porosity by facilitating aeration, and root penetration, preventing surface crust and erosion of the topsoil (Culliney 2013). Some of the existence of various arthropod soils can provide complex benefits in maintaining the balance of the ecosystem.

This study aims to understand the effect of land cover variations on the diversity and community structure of soil arthropods. The differences in land cover were selected based on the type of habitat, including urban green space, agroforestry, gardens, and natural mixed forests. We hypothesize that areas with preserved ecosystems will have higher soil arthropod diversity than disturbed locations. This ecosystem's high biodiversity can serve as a model for fixing land and making it fertile.

MATERIALS AND METHODS

Study Site

Malang Region is organized by 3 administration areas, consisting of Malang City, Malang Regency, and Batu City. This area has various ecological landscapes from a coastal ecosystem in the lowland to a highland mixture of a forest. Because of that, the types of soil are very different depending on the microclimate they constitute. Sampling sites were determined at as many as 7 location points by differentiating several types of habitats for comparison (Table 1) (Figure 1).

Data Collection

From July to September 2022, three repetitions of soil microarthropod sampling were accomplished at every site. Three plots were chosen via purposive sampling as the sampling sites for each type of site. The samples were taken with hand sorting methods and hay-bait traps. The hand sorting method was conducted at a 3x3 meter area for each plot in site sampling. The sample was collected with a fork to separate rocks or rot-

Table 1. List of sampling sites in Malang region, East Java, Indonesia.

Site	Latitude	Longitude	Elevation (masl)	Description
S1	-7.952354°	112.614273°	495	Urban green space surrounded by buildings.
S2	-7.968484°	112.626708°	465	Urban green space near the urban street
S3	-8.013325°	112.853480°	1254	Highland mixed forest and some vegetable plantations
S4	-7.740722°	112.534447°	1608	Highland mixed forest near some vegetable plantations
S5	-7.991934°	112.823548°	1170	Highland mixture forest
S6	-7.823920°	112.579372°	1262	Dominated by coffee agroforestry plantation
S7	-8.250536°	112.884328°	430	Mixed forest and part of it becomes coffee agroforestry

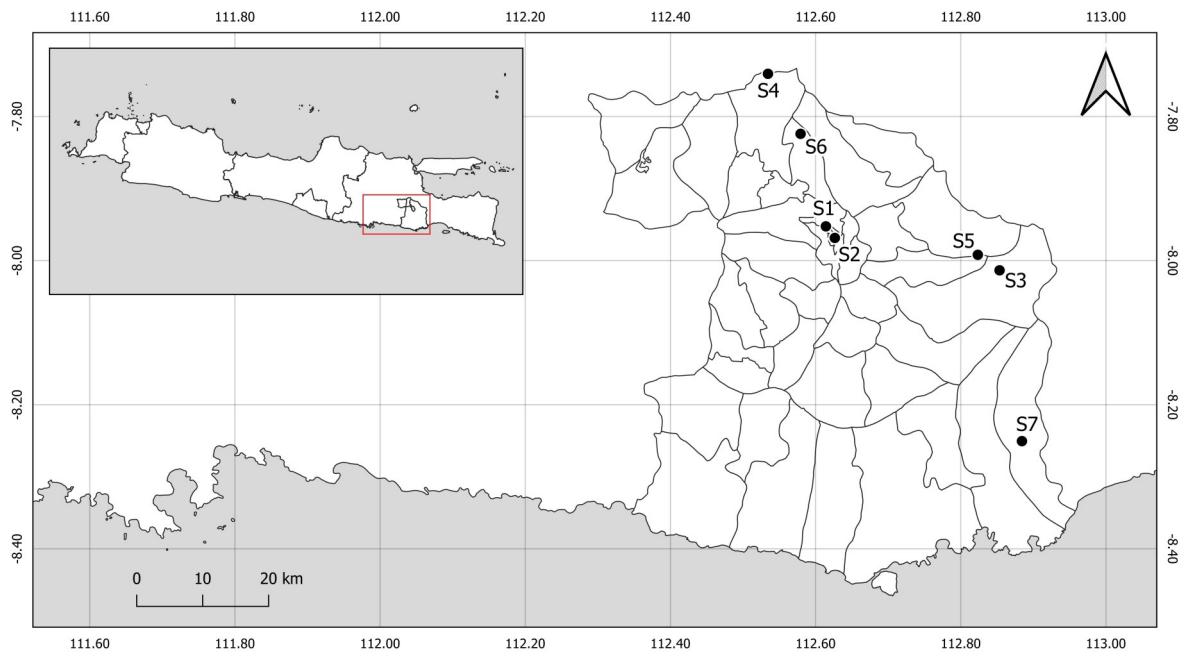


Figure 1. Soil microarthropod sampling sites in Malang Region, East Java, Indonesia.

ten wood, while a shovel took samples of soil for arthropods (Upton & Mantle 2010). This sampling activity will be limited to 15 minutes at each sampling site. All samples were entered into a separate sample bottle of 50 mL which was filled with 70% ethanol for preparation. Then, the sample can be distributed to the laboratory for identification.

Hay-bait trap with modification is made from a mesh plastic container with a height of 10 cm and diameter 8 cm (Tuf et al. 2015). The mesh plastic container was filled with dry leaf litter (*Terminalia cattapa*) and mixed with a pellet. Dried leaf litter soaked for up to 2 days before being installed in the sampling site. A total of 3 traps were used in the study and installed at each site on different land cover types. Its trap is installed around 10 cm into the soil until the mouth container is level with the soil surface. This trap was left for 2 weeks until leaf litter shrank and was filled by soil arthropods. After that, the trap was taken out and placed in a plastic bag to be transported to the laboratory.

Samples from the hay-bait trap were extracted using Berlese-Tullgren funnels for 3 days. The soil arthropods were examined under a stereo microscope Leica MZ75 and isolated and quantified as morphospecies (family level). To identify soil microarthropod samples, soil arthropod identification references were used (Krantz 1971; Gunadi 1994; Schmalfuss 2003; Gibb & Oseto 2006; Decker 2013). The whole process (extraction, observation, and identification) was carried out at the Fauna Diversity Laboratory, Brawijaya University. The coordinates and elevation of each sampling site are determined by GPS (Global Positioning System). Soil samples from where soil arthropods were extracted were processed in the laboratory to determine some edaphic parameters such as soil temperature, soil humidity, and pH. While air parameters were measured as air humidity and air temperature with a thermo-hygrometer.

Data Analysis

One-way analysis of variance (ANOVA) is used to test differences in abundance and diversity at different sites. The diversity differences tested were including, taxa richness (TR), Shannon diversity index (H'), Simpson diversity index ($1-D$), and Pielou's evenness index (J') (Simpson 1949; Hill 1973; Magurran 2004). Then, Tukey's post hoc was used to

compare the significance of the average diversity index values between sampling sites. This test was carried out at a significance level of $\rho \leq 0.05$ using IBM SPSS Statistics (version 26) software (IBM Corp. 2019). The similarity of habitat types at each site was determined by clustering analysis. This analysis is made into a simple tree construction using the UPGMA clustering method based on the Bray-Curtis similarity (Michener & Sokal 1957). Furthermore, Non-Metrix Dimensional Scaling (NMDS) analysis was performed to coordinate the location with environmental factors (soil temperature, air temperature, air humidity, soil humidity, and pH) (Clarke 1993). Ordination between sampling sites and environmental factors based on the abundance of soil arthropods and described by Canonical Correspondence Analysis (CCA) (ter Braak 1986). The clustering analysis and ordination were tested using Paleontological Statistics (PAST) software (Hammer et al. 2001).

RESULTS AND DISCUSSION

Family Diversity and Abundance

The arthropod soils obtained in this study belong to 25 families from 15 different orders (Table 2; Figure 2). Of these taxa, if sorted from the group with the highest composition, namely detritivores (15 families), predators (9 families), and herbivores (4 families). Detritivores are the most dominant group of soil arthropods in composing the composition of soil fauna communities (Lindsey-Robbins et al. 2019). The more detritivores in an environment can indicate that the land has high fertility. This is because their job is to transform dead organic matter into micro-fragments through the process of excretion in the form of faeces. This fragmentation change has a positive effect on the rates of carbon (C) and nitrogen (N) in decomposition. These two contents can increase substantially in biogeochemical cycles and the ratio can vary depending on the type of litter (Joly et al. 2018).

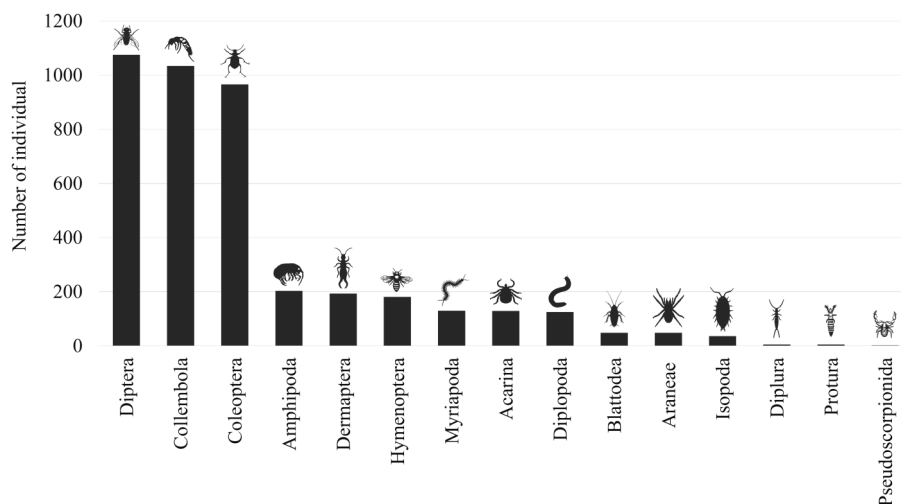


Figure 2. The number of individuals in each order of arthropods.

The highest abundance of soil arthropods was found at sites S1 (596 individuals) and S2 (613 individuals) compared to other sites. The Philoscidae family is very abundant in sites S1 (48.83%) and S2 (76.35%) which are classified as urban green space habitats. The selected site was taken from one of the urban green spaces which are in an area with a high anthropogenic level. Most of the Philoscidae have been identified as having high adaptation to disturbed habitat conditions (Kenne & Araujo 2015). This response also does not indicate any negative impact from the

surrounding human activities. This adaptive condition causes members of the Philoscidae taxa to have cosmopolitan and synanthropic characteristics with a very wide distribution range. The high abundance of species is also supported by the invasion of exotic species with high reproduction rates, but only on a local scale (Karasawa 2022). Meanwhile, terrestrial isopods can also be bioindicators in urban areas because they can accumulate metals (Cd, Cr, Cu, Fe, Pb, and Zn) in their bodies (Gál et al. 2008).

Sites S3 (72.76% individual), S4 (50.64% individual), and S5 (66.47% individual) have the most abundant taxa in the Collembola order of the Isotomidae family (Table 2). Collembola (springtail) as taxa with abundant individuals requires high humidity in the soil ecosystem. This is also supported by the three sites which are classified as highlands with

Table 2. The relative abundance (%) of soil arthropods in each sampling site in Malang Region, East Java, Indonesia.

Taxa	Relative abundance (%)							Guild
	S1	S2	S3	S4	S5	S6	S7	
Acarina								
Macrochelidae	0.17	0.16	0.18	0.64	2.35	0	6.00	P
Tetranychidae	1.01	1.31	1.58	1.29	2.06	1.07	6.00	P
Amphipoda								
Talitridae	0	0.16	0	1.50	0	69.40	0	D
Araneae								
Lycosidae	0.17	0	0	0	0	0	0	P
Lynphiidae	1.34	0.98	0.53	1.50	1.47	1.07	10	P
Blattodea								
Blattellidae	0.67	2.61	0	0.64	0	0	0	H/D
Termitidae	1.85	0	0	0.64	0	0	0	D
Coleoptera								
Carabidae	1.51	0.33	0.18	0.21	2.65	1.78	2.00	H/D
Curculionidae	0	0	0.35	2.79	0	0.71	6.00	H
Collembola								
Tomoceridae	1.17	4.57	7.03	14.38	0	0.71	2.00	D
Isotomidae	1.01	2.12	72.76	50.64	66.47	3.20	4.00	D
Neanuridae	0	0	0	7.30	5.29	2.85	0	D
Dermaptera								
Anisolabididae	21.31	7.34	1.93	0.21	0.59	1.78	4.00	H
Diplopoda								
Harpagophoridae	11.41	1.96	2.28	1.72	4.12	2.14	8.00	D
Diplura								
Japygidae	0.17	0	0.53	0	0	0	2.00	D
Diptera								
Drosophilidae	0.50	0	0	0.43	0.29	0	2.00	D
Chironomidae	0.17	0	0.53	0.21	0	0.36	2.00	D
Cecidomyiidae	0	0	0.35	0.21	0	0.36	2.00	P
Hymenoptera								
Formicidae	6.38	1.47	6.85	7.08	12.35	4.63	14.00	P/D
Isopoda								
Philoscidae	48.83	76.35	2.81	7.73	0	8.90	18.00	D
Armadillidae	0	0	0	0	2.06	0.36	0	D
Myriapoda								
Scolopocryptopidae	1.85	0.16	1.58	0	0	0.36	10	P
Geophilidae	0.17	0.49	0.35	0.64	0	0	0	P
Protura								
Protentomidae	0.34	0	0.18	0.21	0	0	2.00	D
Pseudoscorpionida								
Neobisiidae	0	0	0	0	0.29	0.36	0	P
Number of individuals	596	613	569	466	340	281	50	

Notes: P = predator, H = herbivore, and D = detritivore.

most of them covered in a dense canopy of tree vegetation. The abundant leaf litter from fallen trees facilitates collembola for finding food and shelter. Moreover, the wide leaf area and thick litter also participate in maintaining moisture on the soil surface (Butenschoen et al. 2011). In contrast to site S6 which is more dominated by Terrestrial Amphipod (Amphipod: Talitridae) abundance. Terrestrial Amphipods have high-humidity habitats under litter, weathered logs, or rocks (Gonçalves et al. 2021). In the agroforestry ecosystem at site S6, it has provided a preferred habitat for terrestrial amphipods to become cosmopolitan. They are the most abundant and major detritivores in decomposing leaf litter from agroforestry plants (*Coffea* sp.) at site S6.

Community Structure and Abiotic Correlation

The results of the ecological index calculation show that site S7 has the highest diversity ($H' = 2.56$; $1-D = 0.90$; $J' = 0.76$) compared to other sites, although the family richness is lower. This means that at this site, the food web is still balanced without any species dominating. Fulfilment of niche habitats can be categorized equally between the community structure of the taxa. On the other hand, site S3 has high taxa richness (TR = 17), but low diversity ($H' = 1.02$; $1-D = 0.39$; $J' = 0.16$) (Figure 3).

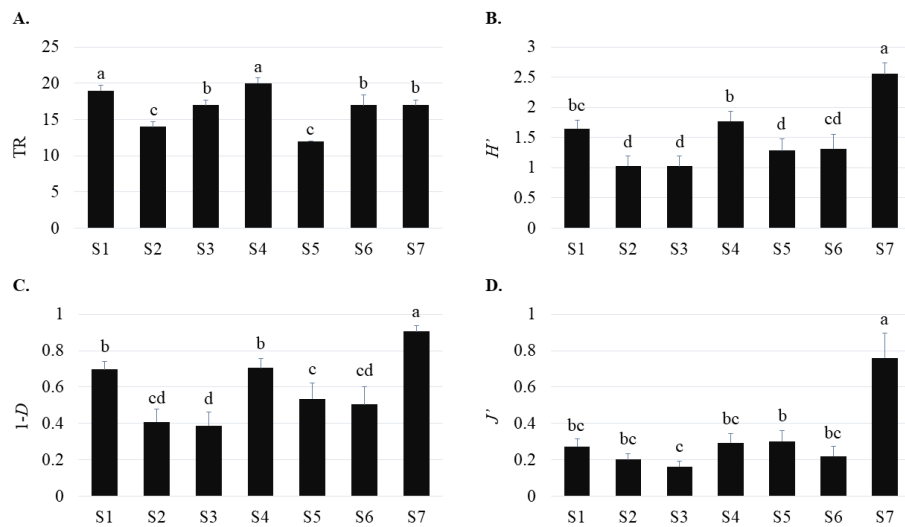


Figure 3. Differences in diversity index values at each site; A. taxa richness (TR), B. Shannon diversity index (H'), C. Simpson diversity index ($1-D$), and D. Pielou's evenness index (J').

Habitat similarity analysis showed the formation of three different groups on the results of clustering (Figure 4) and NMDS ordination (Figure 5). S6 and S7 are grouped into the same habitat type based on the abundance and richness of soil species of arthropods and their environmental factors. Both of these sites have agroforestry land with most of

Table 3. The mean (\pm stdev) value of microclimate and soil physics from the measurement results at each site.

Site	Mean \pm stdev				
	ST ($^{\circ}$ C)	AT ($^{\circ}$ C)	SH (%)	AH (%)	pH
S1	25.28 \pm 1.30	23.75 \pm 0.42	45.17 \pm 20.11	55.83 \pm 2.79	6.98 \pm 0.04
S2	24.50 \pm 0.58	23.33 \pm 0.98	60.00 \pm 29.61	60.50 \pm 3.39	6.65 \pm 0.38
S3	20.43 \pm 0.54	20.83 \pm 2.14	45.67 \pm 26.19	85.33 \pm 6.06	6.68 \pm 0.21
S4	18.10 \pm 0.59	21.00 \pm 2.68	60.00 \pm 23.66	86.83 \pm 7.96	6.80 \pm 0.18
S5	21.50 \pm 0.40	21.67 \pm 1.61	39.40 \pm 5.29	86.00 \pm 6.56	6.97 \pm 0.06
S6	19.32 \pm 0.69	18.67 \pm 1.37	42.33 \pm 14.04	76.33 \pm 7.71	6.57 \pm 0.19
S7	24.12 \pm 1.21	22.17 \pm 1.72	80.17 \pm 25.90	59.83 \pm 4.58	6.07 \pm 0.61

the vegetation in the form of *Coffea* sp. However, site S7 is still classified as an ecotone because it is bordered by natural forest so it can be identified from its high diversity value without any taxa dominating (Figure 3). Ecotone provides a more varied niche that promotes a complicated community structure (Zhu et al. 2011). The uniqueness of this S7 site is its location which is classified as lowland but the vegetation structure is mostly highland plants. This is also supported by the geological structure in the form of a cliff close to the river which forms a waterfall. That way, it is undeniable that S7 has a high diversity value with varied vegetation composition. This heterogeneous vegetation can cause changes in ecological functions toward supporting ecosystem stability (Stein et al. 2014).

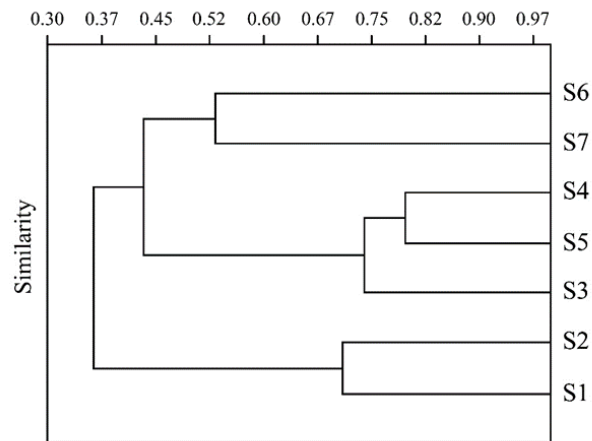


Figure 4. Hierarchical clustering analysis of soil arthropods composition with Bray-Curtis similarity between sites.

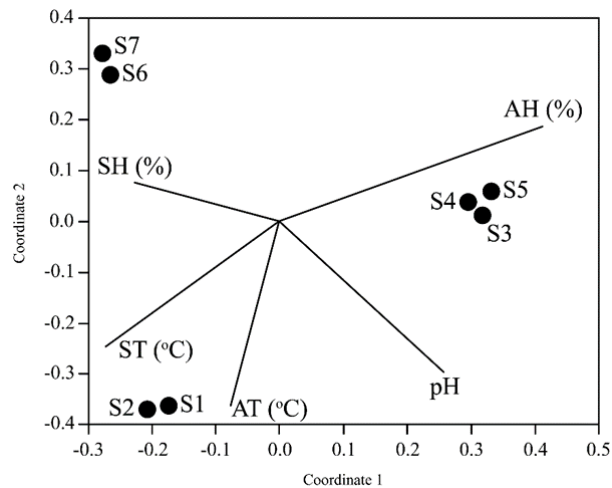


Figure 5. NMDS analysis between sampling sites with abiotic factors and soil arthropods abundance and family richness; SH= soil humidity, AH= air humidity, ST= soil temperature, AT= Air temperature; Stress = 0.092.

In the second grouping which consists of sites S3, S4, and S5, all of them are located in the highlands with most of them being upland forests with several land conversions. The change to a cereal and vegetable garden has changed the landscape structure. Management practices that are still conventional in cultivating land can reduce biodiversity, especially soil animals (Ghiglieno et al. 2020). On the other hand, the three sampling sites have a fairly high percentage of air humidity (S3= $85.33 \pm 6.06\%$; S4= $86.83 \pm 7.96\%$; S5: $86.00 \pm 6.56\%$) (Figure 4; Table 3). So

according to habitat suitability, the dominant taxa are springtails (Collembola: Isotomidae), resulting in a close habitat similarity.

Sites S1 and S2 are grouped in the same cluster based on the soil arthropod community structure. Likewise, the soil temperature (S1= $25.28 \pm 1.30^\circ\text{C}$; S2= $24.50 \pm 0.58^\circ\text{C}$) and air temperature (S1= $23.75 \pm 0.42^\circ\text{C}$; S2= $23.33 \pm 0.98^\circ\text{C}$) are higher than other sites (Figure 5; Table 3). This increase in temperature is possible because landscapes S1 and S2 include urban areas that do not have a wide canopy cover. Smaller and less heterogeneous canopy cover causes a significant increase in temperature in urban areas (Jung et al. 2021). In addition, the influence of residue from vehicle engines near the sampling site also initiates the increase in heat.

All arthropod soils show varying relationships between taxa and environmental variables. There is an inverse relationship between temperature and humidity levels but at different pH variables (Figure 5). The influence of air humidity slightly affects the intensity of pH in the soil. High humidity in a location can initiate wetting of the forest floor. In this way, the nutrients resulting from the decomposition and humification of the detritivore arthropod soil along with the microbes can also be absorbed through the soil porosity. Soil porosity is carried out by soil-digging arthropods, for example, termites (Termitidae) to facilitate aeration and root penetration and prevent surface crust and erosion of the topsoil (Culliney 2013). The absorbed minerals can cause changes in the biochemical content. The biochemical content of the elements carbon (C) and nitrogen (N) in the soil is an important factor in changing the soil pH level (Joly et al. 2018).

Talitridae, Neobisiidae, Cecidomyiidae, Chironomidae, Carabidae, Armadillidae, Curculionidae, and all collembola (Tomoceridae, Isotomidae, and Neanuridae) prefer to avoid habitats with high temperatures. This is related to their habitat preferences by choosing high-humidity habitats. However, terrestrial isopods (Philoscidae), spiders (Lycosidae & Lynphiidae), termites (Termitidae), cockroaches (Blattellidae), and earwigs (Anisolabididae) can still tolerate high ambient temperatures. Some soil arthropods that have a role as predators such as spiders and earwigs are not affected by changes in environmental variables. Based on research showing temperature and humidity do not affect the life history of spi-

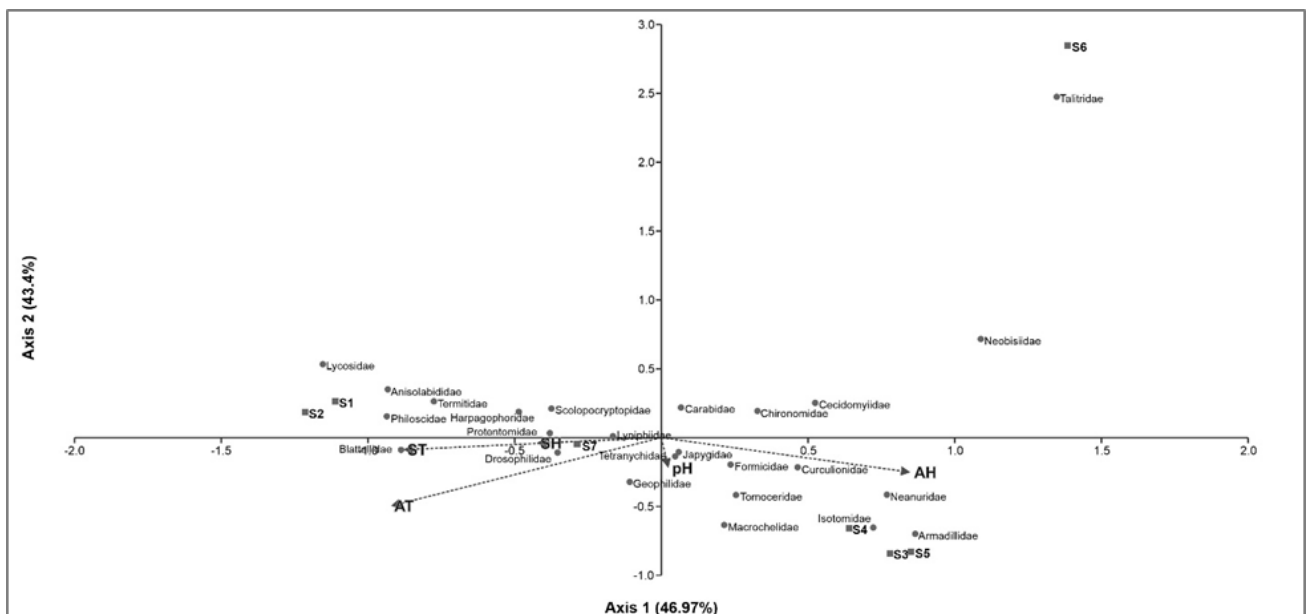


Figure 6. Ordination diagram from Canonical Correspondence Analysis (CCA) showing the relationship between soil arthropods group with abiotic factors.

ders (Steves et al. 2021). They can be dispersed and have a wide hunting range. They can hunt directly to control their prey population in a food web system.

Diversity of soil arthropods shows a variety of ecological roles in positioning themselves in food webs in terrestrial ecosystems. Natural ecosystems without any disturbance from humans lead to stability in abundance, and the richness of taxa, composition, and functional traits are more maintained. The size of the role needed in filling the availability of niches is also a determining factor in the formation of an ecosystem balance.

This research on diversification and community composition may serve as the foundation for a greater understanding of the significance of soil arthropods, particularly in Indonesia. Different subgroups of soil arthropods may be useful in soil restoration. For instance, isopods can boost nitrogen elements, which help to speed up plant growth, by acting as detritus shredders in the decaying soil organic matter (Mc Carry & Schmitz 2021). By using mixed forest floor ecosystems as a model, this potential may be exploited as an experimental object to improve soil fertility in plantation areas.

CONCLUSIONS

The diversity of site S7 is the highest compared to other sites, although the taxa richness is less than S1 and S4. Several taxa dominate them, Philoscidae (Isopoda) in urban green space areas (S1 & S2), Isotomidae (Collembola) in upland forest areas (S3, S4, & S5), and Tallitridae (Amphipoda) in agroforestry (S6 & S7). Several species that dominate this variation of habitat may have the potential to become specific decomposers in improving soil fertility. Measurement of mineral content and classification of litter can also be carried out to compare the results of the decomposition of abundant taxa against the ratio of soil biochemistry.

AUTHOR CONTRIBUTION

The research was designed by A.M.S., M.F.A., and M.F., who also collected and evaluated the data. The initial manuscript was written by B.Y., while S. and A.N. looked over, edited, and proofread the final draft. N.K. supervised the entire procedure.

ACKNOWLEDGMENTS

We gratefully acknowledge to The Directorate of Research and Community Service, Directorate General of Strengthening Research and Development Ministry of Research, Technology and Higher Education of the Republic of Indonesia (Grant number 3110.15/UN10.F09/PN/2022) provided financial support to NK for this work.

CONFLICT OF INTEREST

The authors declare that they have no conflict of interest.

REFERENCES

- Bagyaraj, D.J., Nethravathi, C.J. & Nitin, K.S., 2016. Soil Biodiversity and Arthropods: Role in Soil Fertility. In: Economic and Ecological Significance of Arthropods in Diversified Ecosystems, Springer, pp.17–51. doi: 10.1007/978-981-10-1524-3_2.
- Briones, M. J. I., 2018. The Serendipitous Value of Soil Fauna in Ecosystem Functioning: The Unexplained Explained. *Frontiers in Environmental Science*, 6. doi:10.3389/fenvs.2018.00149.

- Butenschoen, O., Scheu, S. & Eisenhauer, N., 2011. Interactive effects of warming, soil humidity and plant diversity on litter decomposition and microbial activity. *Soil Biology and Biochemistry*, 43(9), pp.1902–1907. doi: 10.1016/j.soilbio.2011.05.011.
- Clarke, K.R., 1993. Non-parametric Multivariate Analysis of Changes in Community Structure. *Austral J Ecol*, 18, pp.117–143.
- Coyle et al., 2017. Soil fauna responses to natural disturbances, invasive species, and global climate change: Current state of the science and a call to action. *Soil Biol. Biochem.*, 110, pp.116–133. doi: 10.1016/j.soilbio.2017.03.008.
- Culliney, T., 2013. Role of Arthropods in Maintaining Soil Fertility. *Agriculture*, 3(4), pp.629–659. doi: 10.3390/agriculture3040629.
- Decker, P., 2013. *Annotated Checklist of The Millipedes (Diplopoda) and Centipedes (Chilopoda) of Singapore*. Raffles Museum of Biodiversity Research.
- Gál et al., 2008. Metal uptake by woodlice in urban soils. *Ecotoxicology and Environmental Safety*, 69(1), pp.139–149. doi: 10.1016/j.ecoenv.2007.01.002.
- Ghiglieno et al., 2020. Response of the Arthropod Community to Soil Characteristics and Management in the Franciacorta Viticultural Area (Lombardy, Italy). *Agronomy*, 10(5), pp.740. doi: 10.3390/agronomy10050740.
- Gibb, T.J. & Oseto, C.Y., 2006. *Arthropod Collection and Identification Field and Laboratory Techniques*. Academic Press.
- Gonçalves et al., 2021. Soil Arthropods in the Douro Demarcated Region Vineyards: General Characteristics and Ecosystem Services Provided. *Sustainability*, 13, pp.7837. doi: 10.3390/su13147837.
- Griffiths et al., 2021. The impact of invertebrate decomposers on plants and soil. *New Phytol*, 231, pp.2142–2149. doi: 10.1111/nph.17553.
- Gunadi, B., 1994. Seasonal Fluctuations of Collembola along The Slope of A Pine Forest Plantation in Central Java. *Acta Zoologica*, 195, pp. 62.
- Hammer, O., Harper, D. & Ryan, P., 2001. PAST: Paleontological Statistics Software Package for Education and Data Analysis. *Palaeontologia Electronica*, 4, pp. 1–9.
- Hill, M.O., 1973. Diversity and Evenness: A Unifying Notation and its Consequences. *Ecology*, 54, pp.427–432.
- IBM Corp., 2019. IBM SPSS Statistics for Windows. Armonk, IBM Corp.
- Joly et al., 2018. Litter conversion into detritivore faeces reshuffles the quality control over C and N dynamics during decomposition. *Funct Ecol*. 32, pp.2605– 2614. doi: 10.1111/1365-2435.13178.
- Jung, M.C., Dyson, K. & Alberti, M., 2021. Urban Landscape Heterogeneity Influences the Relationship between Tree Canopy and Land Surface Temperature. *Urban Forestry & Urban Greening*, 57, pp.126930. doi: 10.1016/j.ufug.2020.126930.
- Karasawa, S., 2022. Comparison of isopod assemblages (Crustacea: Isopoda: Oniscidea) among four different habitats—Evergreen forest, exotic bamboo plantation, grass and urban habitat, *Pedobiologia*, pp.91–92. doi: 10.1016/j.pedobi.2022.150805.
- Katayama et al., 2014. Landscape Heterogeneity–Biodiversity Relationship: Effect of Range Size. *Plos One*, 9(3), e93359. doi: 10.1371/journal.pone.0093359.

- Kenne, D.C. & Araujo, P.B., 2015. *Balloniscus glaber* (Crustacea, Isopoda, Balloniscidae), a habitat specialist species in a disturbed area of Brazil. *Iheringia. Série Zoologia*, 105(4), pp.430–438. doi: 10.1590/1678-476620151054430438.
- Krantz, G.W., 1971. *A Manual of Acarology*. O.S.U. Book Stores.
- Lindsey-Robbins et al., 2019. Effects of Detritivores on Nutrient Dynamics and Corn Biomass in Mesocosms. *Insects*, 10(12), pp.453. doi: 10.3390/insects10120453.
- Loreau, M. & de Mazancourt, C., 2013. Biodiversity and ecosystem stability: a synthesis of underlying mechanisms. *Ecology Letters*, 16, pp.106–115. doi: 10.1111/ele.12073.
- Magurran, A.E., 2004. *Measuring Biological Diversity*. Blackwell Publishing: Oxford.
- McCary, M.A. & Schmitz, O.J., 2021. Invertebrate functional traits and terrestrial nutrient cycling: Insights from a global meta-analysis. *J Anim Ecol.*, 90, pp.1714– 1726. doi: 10.1111/1365-2656.13489.
- Michener, C.D. & Sokal, R.R., 1957. A Quantitative approach to a Problem of Classification. *Evolution*, 11, pp.490–499.
- Schmalzfuss, H., 2003. World Catalog of Terrestrial Isopods (Isopoda: Oniscidea). *Stuttgarter Beiträge zur Naturkunde, Serie A, (Biologie)*, 654, pp. 341.
- Simpson, E.H., 1949. Measurement of Diversity. *Nature*, 163, pp.688. doi: 10.1038/163688a0.
- Stein, A., Gerstner, K. & Kreft, H., 2014. Environmental heterogeneity as a universal driver of species richness across taxa, biomes and spatial scales. *Ecol. Lett.*, 17, pp.866–880. doi: 10.1111/ele.12277.
- Steves, I., Pedro, B. & Berry, P., 2021. Air Temperature and Humidity at the Bottom of Desert Wolf Spider Burrows Are Not Affected by Surface Conditions. *Insects*, 12(10), pp.943. doi: 10.3390/insects12100943.
- Tao et al., 2019. Vegetation Heterogeneity Effects on Soil Macro-Arthropods in an Alpine Tundra of the Changbai Mountains, China. *Plants*, 8(10), pp.418. doi: 10.3390/plants8100418.
- ter Braak, C.J.F., 1986. Canonical Correspondence Analysis: A New Eigenvector Technique for Multivariate Direct Gradient Analysis. *Ecology*, 67, pp.1167–1179. doi: 10.2307/1938672.
- Tuf et al., 2015. Hay-bait Traps are a useful Tool for Sampling of Soil Dwelling Millipedes and Centipedes. *ZooKeys*, 510, pp.197–207. doi:10.3897/zookeys.510.9020.
- Tylianakis et al., 2008. Resource Heterogeneity Moderates the Biodiversity-Function Relationship in Real World Ecosystems . *Plos Biology*, 6(5), e122. doi: 10.1371/journal.pbio.0060122.
- Upton, M.S. & Mantle, B.L., 2010. *Methods for Collecting, Preserving, and Studying Insects and other Terrestrial Arthropods*. The Australian Entomological Society.
- Yin et al., 2010. A review on the ecogeography of soil fauna in China. *J. Geogr. Sci.*, 20, pp.333–346. doi: 10.1007/s11442-010-0333-4.
- Zan, P., Mao, Z. & Sun, T., 2022. Effects of soil fauna on litter decomposition in Chinese forests: a meta-analysis. *PeerJ*, 10, e12747. doi: 10.7717/peerj.12747.
- Zhu, X., Hu, Y. & Gao, B., 2011. Influence of Enviroment of Forest-Steppe Ecotone on Soil Arthropods Community in Northern Hebei, China. *Procedia Environmental Sciences*, 10, pp.1862–1867. doi: 10.1016/j.proenv.2011.09.291.

Research Article

Profiling of Single Garlic Extract Microencapsulation: Characterization, Antioxidant Activity, and Release Kinetic

Sri Rahayu Lestari^{1*}, Abdul Ghofur¹, Siti Imroatul Maslikah¹, Sunaryono², Amalia Nur Rahma¹, Dahniar Nur Aisyah¹, Ikfi Nihayatul Mufidah¹, Nadiya Dini Rifqi¹, Nenes Prastita¹, Dewi Sekar Miasih¹, Alif Rosyidah El Baroroh¹

1)Departement of Biology, Faculty of Mathematics and Natural Sciences, Universitas Negeri Malang, Jl. Semarang 5, Malang 65145, Indonesia

2)Departement of Physics, Faculty of Mathematics and Natural Sciences, Universitas Negeri Malang, Jl. Semarang 5, Malang 65145, Indonesia

* Corresponding author, email: srirahayulestari@um.ac.id

Keywords:

Microencapsulation
Chitosan-alginate
Single garlic extract

Submitted:

10 November 2022

Accepted:

12 June 2023

Published:

23 November 2023

Editor:

Furzani Binti Pa'ee

ABSTRACT

Single garlic is known to have many benefits as an alternative therapy for various types of metabolic syndrome. The bioactive compounds, allicin, and alliin, in garlic are unstable and easily degraded in digestion. Chitosan-alginate microencapsulation is thought to increase stability and protect active compound so its therapeutic effect is more optimal. This study aimed to characterize the microencapsulation chitosan-alginate of single garlic extract (MCA-SGE), as well as to examine the antioxidant activity and kinetic release of MCA-SGE in vitro. The research procedure includes the steps of single garlic extraction, preparation of MCA-SGE, characterization of MCA-SGE (PSA, SEM, and FTIR) as well as biological testing of MCA-SGE through antioxidant activity and kinetic release tests. PSA results showed the mean particle size of MCA-SGE was 439.0 ± 1.9 nm or 0.4 μ m with a polydispersity index (PDI) value of 0.579 ± 0.046 and a zeta potential value of 15.4 ± 0.3 mV. The SEM results showed that the morphology of MCA-SGE was spherical with a smooth surface and a micrometre size of 0.4 - 0.7 μ m. The FTIR results describe a shift in absorption and addition of SGE functional groups after encapsulation. The results of the antioxidant activity test showed the antioxidant activity of MCA-SGE was 65%, while SGE was 55%. The results of the kinetic release showed that more allicin and alliin were released by SGE than MCA-SGE during the 4-hour kinetic release simulation. MCA-SGE has the potential to be used as a drug delivery system with controlled release.

Copyright: © 2023, J. Tropical Biodiversity Biotechnology (CC BY-SA 4.0)

INTRODUCTION

Single garlic (*Allium sativum*) is a type of garlic with one clove (Lestari et al. 2020). Single garlic has various benefits, such as antioxidant, anti-inflammatory, anticancer, antidiabetic, and anti-obesity (Lestari & Rifa'i 2018; Szychowski et al. 2018; Sasi et al. 2021). Single garlic contains various bioactive compounds in the form of organosulfur and phenolic compounds, including *allicin*, *diallyl sulphide*, *diallyl trisulphide*, *diallyl disulfide*, *ajoene*, and *2-vinyldithiins* (Abdel-Gawad et al. 2018; Shang et al. 2019). *Allicin* and *alliin* are the most dominant organosulfur compounds, but both compounds have the disadvantage of being unstable and easily de-

graded due to pH conditions in the gastrointestinal tract (Bhatwalkar et al. 2021). The weakness of the single garlic bioactive compound can reduce its bioavailability and hinder its potential as a therapeutic agent (Kyriakoudi et al. 2021; Lestari et al. 2021). The solution to overcome the weakness of a single important compound of garlic is to encapsulate the compound in a drug delivery system (Akhter et al. 2022).

Microencapsulation is one of the drug delivery systems to protect bioactive compounds in microcapsules, which are characterised by bioactive compounds coated with encapsulating agents (Alencar et al. 2022). Bioactive compounds will be enclosed between the polymer chain bonds so that a microencapsulated structure is formed on a microparticle scale (Pedroso-Santana & Fleitas-Salazar 2020). The size range of the microparticles is 1 to 1000 m (Lengyel et al. 2019a). The advantages of microencapsulation include protecting bioactive compounds from adverse environmental conditions, controlled release of bioactive compounds, and increasing stability and bio-accessibility (Baltrusch et al. 2022). The polymer in the microencapsulation must be inert to bioactive ingredients, easily soluble, allow controlled release, and compatible with processing conditions (pH/temperature) (Pateiro et al. 2021). Chitosan is a polymer derived from crustacean shells, fungal cell walls, or insect cuticles, while alginate is a polymer extracted from brown algae (Katuwavila et al. 2016). Chitosan and alginate are polyelectrolyte polymers with opposite charges, in addition, when combining alginate with chitosan, it can help stabilise unstable alginates (Katuwavila et al. 2016; Sorasitthyanukarn et al. 2018). The advantages of chitosan and alginate are that they have biocompatibility, biodegradability, and are non-toxic (Loquercio et al. 2015). Crosslinker CaCl_2 acts as a crosslinker in strengthening the bonds between polymers (Tao et al. 2021).

Previous studies have stated that encapsulation can improve the stability of bioactive compounds for the better and increase their solubility (Sorasitthyanukarn et al. 2018; Machado et al. 2021). According to the research of (Amiri et al. 2021), encapsulation of garlic oil with chitosan can maintain antioxidant content. Research (Natrajan et al. 2015) showed that the results of an in vitro kinetic release study on nano encapsulated turmeric and citronella oil showed an increased bioavailability of the compounds of turmeric oil and citronella oil. Many studies on encapsulation have been carried out, but encapsulation using a single garlic extract as the microencapsulated content of chitosan-alginate has not been reported. This study was conducted with the aim of characterising and testing the effect of chitosan-alginate microencapsulation on antioxidant activity and the results of in vitro kinetic release studies of single garlic extract.

MATERIALS AND METHODS

Materials

The tools used include analytical balance (OHAUS), dry oven, incubator shaker (Stuart), rotary evaporator (IKA RV 10 digital V-C Rotary Evaporator), magnetic stirrer (Thermoline cimarec), centrifuge (Hettich), sonicator (IWAKI), ultra thurax (IKA-WERKE), pH meter (Hanna), vortex (SIBATA), Scanning Electron Microscopy (SEM) (FEI Quanta FEG 650 type), Malvern Zetasizer (Zetasizer Nano, Version 7.01, Malvern Instruments Ltd.), spectrophotometer (Biochrom Libra S12), IR spectrophotometer (Shimadzu IRSpirit-T), shaker water bath, spatula, stirring rod, beaker glass (Pyrex), micropipette (Thermo), tweezers, syringe (Onemed), volumetric flask (Pyrex), measuring cup (Pyrex), vial, 0.45 μm microfilter (Corning 28 mm Syringe Filter Non-Pyrogenic), stopwatch, and refrigerator (Sharp). The materials used include single garlic from

Sarangan Village, Magetan District, East Java, Indonesia, 70% ethanol (Merck), chitosan (Sigma-Aldrich), alginate (Sigma-Aldrich), Tween-80 (Sigma-Aldrich), acetic acid, 1M NaOH, CaCl₂, Phosphate Buffer Saline (PBS), aquabides (Ikapharmindo), selovan bags, sewing thread, gloves, aluminum foil, and plastic wrap.

Methods

Preparation of Single Garlic Extract (SGE)

A total of 1 kg of crushed garlic was macerated in 70% ethanol (1:3) for 3 x 24 hours. The maceration filtrate was evaporated using a rotary evaporator to obtain liquid SGE. SGE is stored at 4°C (Qadariah et al. 2020).

Preparation of MCA-SGE

The nano encapsulated components consisted of: alginate in 0.5% Tween-80 (0.3 mg/ml), chitosan in 1% acetic acid (0.3 mg/ml; pH 5), and CaCl₂ in aquabides (0.67 mg/ml). MCA-SGE was made by ionic gelation method by gradually mixing each component and homogenizing using a magnetic stirrer, ultra turax and sonification process. The formed MCA-SGE was stored at 4°C (Natrajan et al. 2015).

Characterisation of MCA-SGE

a. Particle Size Analyser (PSA)

The average particle size, polydispersity index (PDI), and zeta potential (ZP) were characterized using PSA Nano-Zetasizer Ver. 7.01 (Malvern Instruments Ltd.) with Dynamic Light Scattering (DLS) technique (Sorasitthyanukarn et al. 2018). MCA-SGE samples that have been diluted with deionized water are placed in a cuvette for analysis at 25°C (Natrajan et al. 2015; Filho et al. 2019).

b. Scanning Electron Microscopy (SEM)

MCA-SGE which has been spray dried was used for this analysis. 0.5 g of MCA-SGE powder was then imaged with Scanning Electron Microscopy (SEM) (Natrajan et al. 2015).

c. Fourier Transform Infrared Spectroscopy (FTIR)

The FTIR test was carried out using a modified research method by Praseptiangga et al. (2020), 2 mg of samples were taken and tested with an IR spectrophotometer Shimadzu IR Spirit-T analysed with Shimadzu LabSolutions IR, the test was carried out with a scan number of 10, and a resolution of 4 cm⁻¹.

MCA-SGE Biological Test

a. Antioxidant Activity Test

Antioxidant activity test can with DPPH (1,1-diphenyl-2-picrylhydrazyl) test. Testing of antioxidant activity using the procedure of (Rajasree et al. 2021), with modifications. DPPH solution (50 mM) was mixed in samples (5:1) of various concentrations (including 3000 ppm, 6000 ppm, 12000 ppm, 24000 ppm), and 1 ml of DPPH solution (50 μM) for control. Then it was incubated for 30 minutes at room temperature in the dark, absorbance was measured in a spectrophotometer at 517 nm, and the results are used to calculate the percentage of antioxidants (%) through the formula in equation (1).

$$\% \text{ Antioxidants} = \frac{A_0 - A_1}{A_0} \times 100 \quad (1)$$

Information:

A0 = control absorbance

A1 = sample absorbance

In-vitro Kinetic Release Test

A total of 3 ml of MCA-SGE solution in PBS was put into a cellophane bag and immersed in 25 ml of PBS solution containing 20% ethanol at pH 1.5 as the release medium. The study was started by gently stirring at 37°C for a time of 4 hours. Then HPLC was analysed to determine the levels of the active compounds allicin and alliin. The percentage of kinetic release was calculated using the formula in equation (2).

$$\text{Kinetic Release Percentage (\%)} = \frac{\text{levels of active compounds after}}{\text{levels of active compounds before}} \times 100 \quad (2)$$

RESULTS AND DISCUSSION

Characterisation of MCA-SGE

Based on the results of the MCA-SGE Z-Average characterization, the particle size is 439.0 ± 1.9 nm and SGE is 350.67 ± 2.14 nm (Table 1). Z-Average uses the principle of dynamic light scattering, so it has a larger average particle diameter size than measurements with a regular microscope. Particle size is caused by the concentration of the constituent components of the nanoparticle (Chopra et al. 2012). The addition of chitosan and CaCl₂ increases the average particle size (Yousefi et al. 2020). According to Fei et al. (2015) the pH factor and the ability of kinetic reactions between material particles also affect the size in the formation of microencapsulation. The ionic interaction between chitosan and alginate forms an electrostatic bond which also gives rise to an increase in particle size because it includes a polyelectrolyte membrane on the surface of the microcapsule. Microcapsule particle size > 200 μm has a higher control release (Dima et al. 2013).

Table 1. Characterisation of PSA MCA- SGE.

Characterisation of PSA	MCA-SGE	SGE
Particle size/ Z-average (nm)	439.0 ± 1.9	350.67 ± 2.14
Polydispersity Index	0.579 ± 0.046	0.75 ± 0.01
Zeta Potential (mV)	-15.4 ± 0.3	not analysed

The Z-Average value is used to determine the average size of MCA-SGE and SGE particles, while the PDI value of MCA-SGE and SGE is used to determine the homogeneity distribution of particles. The PDI value is used to determine the distribution of particle homogeneity. A good PDI value or indicating homogeneous particles is less than 0.500 or close to 0 (Aleksandra Zielińska et al. 2020). A graph of the MCA-SGE and SGE particle size distribution can be seen in Figure 1.

The results of the characterisation of PDI MCA-SGE are 0.579 ± 0.046 and SGE are 0.75 ± 0.01 (Table 1). A PDI value close to 0 indicates that the distribution of particle homogeneity is high (mono dispersity), while a higher PDI value (close to 1) indicates that the particles are widely distributed (polydispersity) or heterogeneous (Danaei et al. 2018). Research by Wang et al. (2016) reported that the PDI value of MCA ranged from 0.340 ± 0.040 so the particles were said to be homogeneous. The PDI value of MCA-SGE and SGE was higher than 0.500 so both of them were categorised as heterogeneous because most of the MCA-SGE and SGE particles were not formed, and the resulting sizes varied. The high value of PDI also occurs due to weak ionic interactions between the constituent components which result in particle aggregation or clumping (Loquercio et al. 2015).

The zeta potential value indicates the stability of a microencapsulated suspension. The zeta potential value of MCA-SGE is -15.4 ± 0.4 mV (Table 1). The zeta potential value of microencapsulation is affected

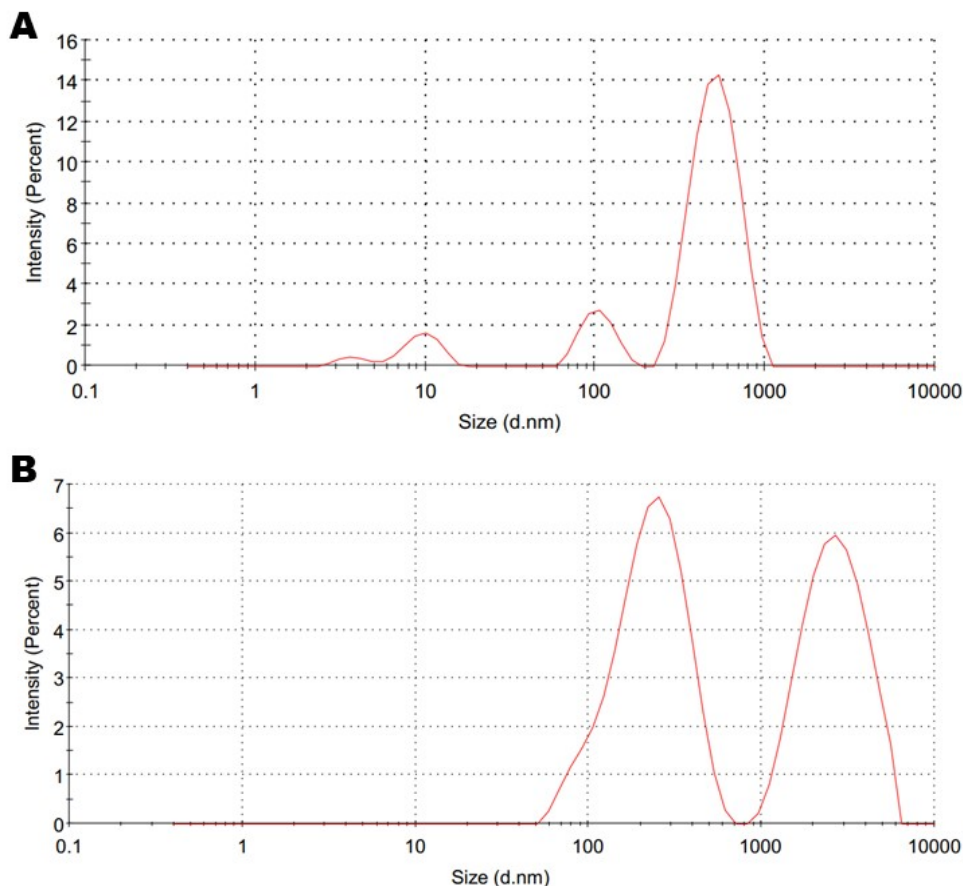


Figure 1. Profile of particle size distribution by intensity. (A) Particle size distribution of MCA-SGE. (B) Particle size distribution SGE.

by surface chemistry, particle concentration, size of particle, pH of the medium, temperature, solvent, and ionic strength (dos Santos et al. 2015; Mudalige et al. 2018). Zeta potential is important to know because it can affect the stability of colloidal systems, the interaction of nanoparticles with other charged molecules, and the efficiency of drug delivery (Kyzioł et al. 2017). The zeta potential value of MCA-SGE (Table 1) is in the range of ± 10.0 mV to ± 30.0 mV, where the particles are classified as less stable (Aziz et al. 2013). The colloidal system will tend to agglomerate (aggregate) because the repulsion between the particles is low (Zhou et al. 2018). This negative MCA-SGE zeta potential could be due to the high concentration of alginate (Krisanti et al. 2017). This is following (Wang et al. 2016) who reported that a higher alginate ratio resulted in more anions in the system or in other words the amount of NH_3^+ chitosan charge was lower than the COO^- -alginate charge, thus causing the zeta potential value of the system to be less positive. Microparticles are said to have good mucoadhesive if they have a zeta potential value between 20-50 mV (Krisanti et al. 2017).

Scanning Electron Microscopy (SEM)

The results of the morphological characterization of MCA-SGE using SEM are shown in Figure 2A shows MCA-SGE (100x) which is shaped like a lump of agglomerated particles. Figure 2B shows the MCA-SGE (1000 x) particles of non-uniform size. Figure 2C (10,000x) shows the spherical morphology of MCA-SGE with sizes in the micrometre range, i.e. $0.422 - 0.719 \mu\text{m}$, and has a smooth surface of microparticles.

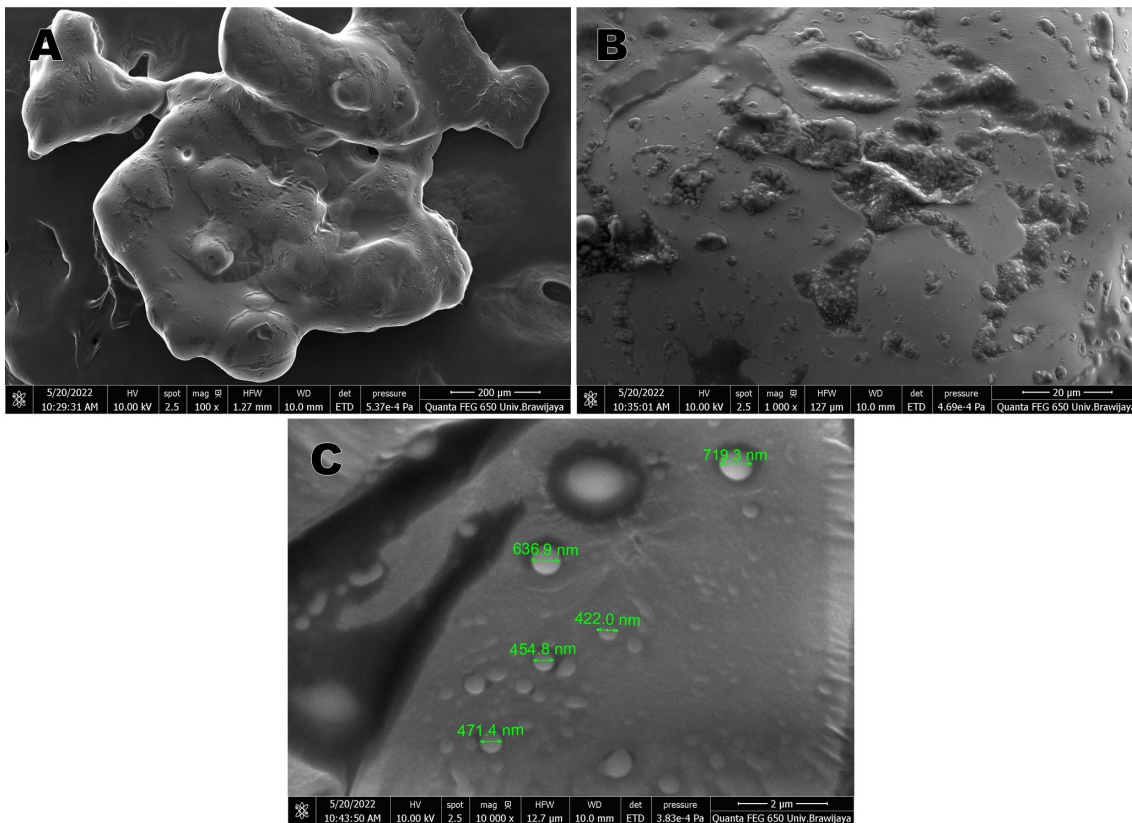


Figure 2. Morphology of MCA-EBT by scanning electron microscopy observation.

The morphology of MCA-SGE with a magnification of 100 x looks like a lump of agglomerated particles. This indicates that an agglomeration has formed. There are two causes of agglomeration, Brown agglomeration occurs when particles collide and stick together as a result of random Brownian motion, while gravitational agglomeration occurs when slowly settling particles are caught by faster settling particles, leading to the formation of lumps (Singer et al. 2018). The morphology of MCA-SGE with 10,000x magnification shows that the formed MCA-SGE particles are not uniform or different. The morphology of MCA-SGE with a magnification of 10,000x shows that MCA-SGE is round in shape with different sizes, which are in the range of 422 - 719 nm, and has a smooth surface of microparticles. Based on this size range, MCA-SGE is categorized as microparticles. Microparticles have particle sizes in the range of 1 to 1000 nm (Lengyel et al. 2019b). MCA-SGE sizes in the range < 500 nm (422 nm, 455 nm, and 471 nm) are more easily absorbed by cells when in the body (Pudlarz & Szymraj 2018). The results of different sizes can be caused by particle aggregation (Michen et al. 2015). According to the research results of Natrajan et al. (2015), the morphology of the turmeric and lemongrass oil nanoencapsulation is also round but has an average size below 300 nm (Natrajan et al. 2015). Research by Buanasari et al. (2021) reported that plant extract microcapsules using chitosan were round with a smooth surface. However, sometimes capsules may also develop roughness on their surface during spray drying. And such imperfections are developed when the film formation process during drying of atomised droplets slow down. In a similar way, the internal morphology was analysed and it was observed that the microcapsules obtained were hollow and the core material was stuck onto the surface, which is also a particle characteristic obtained using spray drying. Differences in wall material also affected the topography of the microcapsules formed (Choudhury et al. 2021).

Fourier Transform Infrared Spectroscopy (FTIR)

The infrared (IR) graph of SGE is presented in Figure 3, while the IR graph of MCA-SGE is presented in Figure 4. Functional groups that appear in the two samples include amine and hydroxyl strains (N-H and O-H) indicated by the presence of absorption at 3344.47 cm⁻¹ IR SGE. and absorption at 3343.04 cm⁻¹ IR MCA-SGE; alkane group (C-H) indicated by the absorption at 2936.57 cm⁻¹ IR SGE and absorption at 2928.01 cm⁻¹ IR MCA-SGE; alkyl groups (C-H) were indicated by the presence of absorption at 1454.74 cm⁻¹ IR SGE and IR MCA-SGE; aromatic amine group (C-N) was indicated by the absorption at 1279.31 cm⁻¹ IR SGE and absorption at 1283.59 cm⁻¹ IR MCA-SGE; cyclohexane compound (C-H) was indicated by the absorption at 934.17 cm⁻¹ IR SGE and absorption at 935.59 cm⁻¹ IR MCA-SGE; aromatic compounds (C-H) were indicated by the absorption at 818.65 cm⁻¹ IR SGE and absorption at 821.50 cm⁻¹ IR MCA-SGE; disulfide group (C-S) was indicated by the absorption at 599.01 cm⁻¹ IR SGE and absorption at 600.44 cm⁻¹ IR MCA-SGE. A number of other uptakes showing different functional groups at IR SGE and IR MCA-SGE are presented in Table 2 and Table 3.

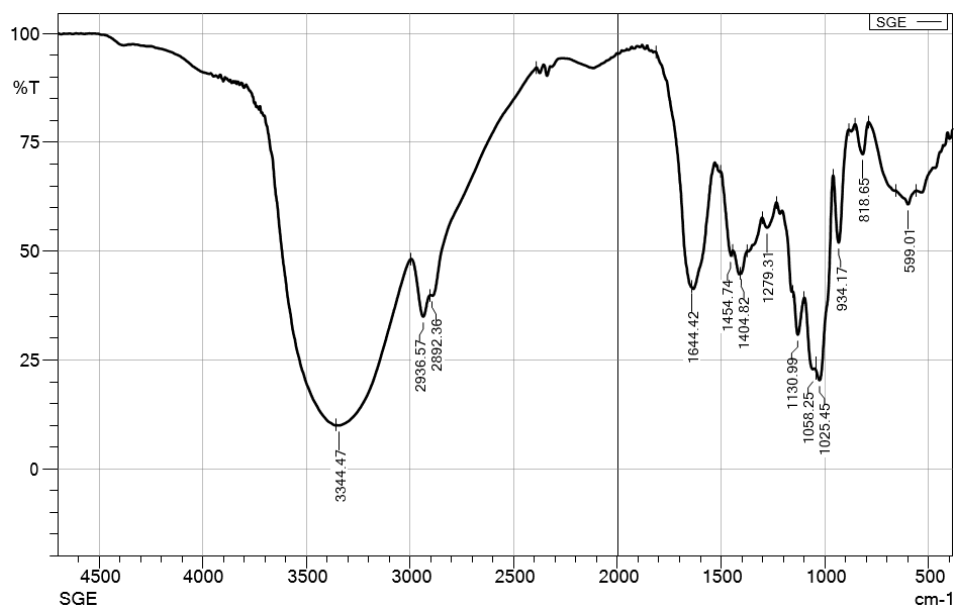


Figure 3. IR Graph Profile of SGE.

Table 2. List of IR SGE Absorption and Functional Groups.

Absorbance (cm ⁻¹)	Bond Type	Functional groups	Reference
599.01	C-S	Disulfide	
818.65	C-H 1,4 (para)	Aromatic compounds	
934.17	C-H	cyclohexane	
1025.45	C-F	Aromatic fluoro compounds	(Nandiyanto et al. 2019)
1058.25	C-O	Ether	
1130.99	C-N	Amine	
1279.31	C-N	Aromatic amine	
1404.82	O-H	Carboxylic acid	(Merck 2022)
1454.74	C-H	Alkyl	
1644.42	N-H	Amine	(Nandiyanto et al. 2019)
2892.36	C-H	Metin	
2936.57	C-H	Alkanes	(Merck 2022)
3344.47	N-H & O-H	Amines and Hydroxyl	(Nandiyanto et al. 2019; Merck 2022)

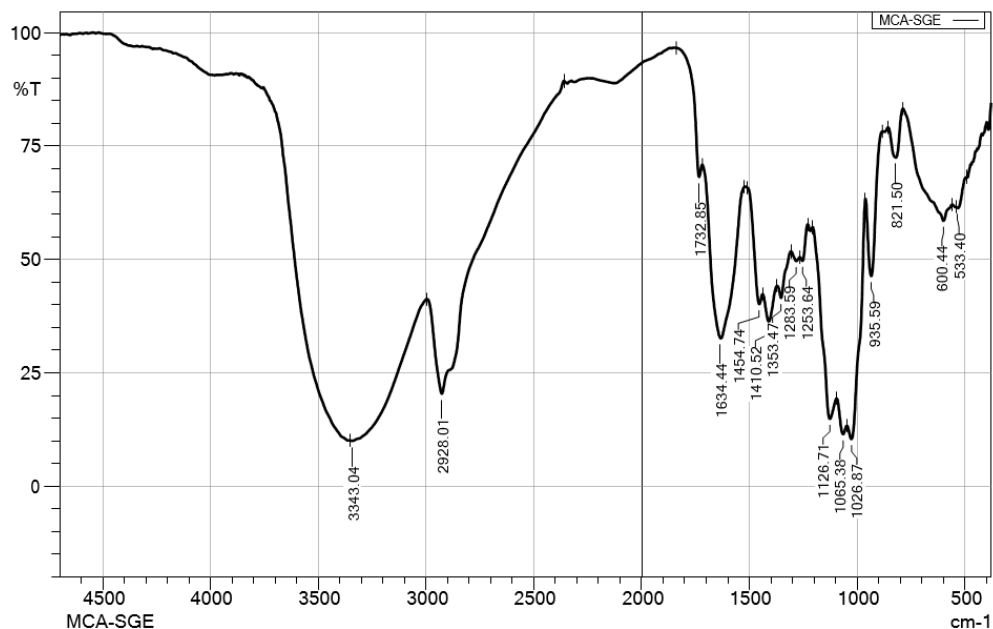


Figure 4. IR Graph Profile of MCA-SGE.

Table 3. List of MCA-SGE IR Absorption and Functional Groups.

Absorbance (cm ⁻¹)	Bond Type	Functional groups	Reference
533.40	C-I	Aliphatic iodo compounds	
600.44	C-I	Aliphatic iodo compounds	(Nandiyanto et al. 2019)
821.50	C-H 1,4 (para)	Aromatic compounds	
935.59	C-H	cyclohexane	
1026.87	C-N	Amine	(Merck 2022)
1065.38	C-N	Amine	
1126.71	C-O	Alcohol	(Nandiyanto et al. 2019)
1253.64	-O	Aromatic ether	
1283.59	C-N	Aromatic amine	
1353.47	O-H	Alcohol	(Merck 2022)
1410.52	-COO-	Carboxylate	(Nandiyanto et al. 2019)
1454.74	C-H	Alkyl	
1634.44	C=O	Amide I	(Nandiyanto et al. 2019; Merck 2022)
1732.85	C=O	Esther	
2928.01	C-H	Alkanes	(Merck 2022)
3343.04	N-H & O-H	Amine	(Nandiyanto et al. 2019; Merck 2022)

Absorption of 3344.47 cm⁻¹, 1644.42 cm⁻¹, 1279.31 cm⁻¹, and 1130.99 cm⁻¹ on SGE indicated an amine compound. The number of amine groups that are read on SGE indicates the presence of alliin and alliin content (Borlinghaus et al. 2014). The IR SGE graph also shows the presence of carbonyl, carboxylate and aromatic compounds (Table 2). Carbonyl compounds, carboxylate compounds and aromatic compounds were visible in the FTIR results of garlic methanol extract (Divya et al. 2017).

The MCA-SGE graph shows some additional absorptions that provide information on the functional groups of the encapsulated material. Chitosan gives rise to absorption at 1634.44 cm⁻¹ which is the am-

ide I functional group (Filho et al. 2019). Another material that gives rise to absorption at 1732.85 cm^{-1} is an ester group that can be found in sodium alginate (Szabó et al. 2020). Some absorptions at 1065.38 cm^{-1} , 1410.52 cm^{-1} , 1634.44 cm^{-1} , and 3343.04 cm^{-1} respectively were amine (C-N), carboxylate (COO-), amide (N-H) and amine and hydroxyl (N-H) strains. and O-H). These four functional groups appear when the combination of chitosan-alginate material is used in encapsulation (Ahmad et al. 2022). Other absorptions such as at 1025.45 cm^{-1} (aliphatic compound) IR SGE shifted at 1026.87 cm^{-1} at IR MCA-SGE. Absorption at 1130.99 cm^{-1} (amine) IR SGE shifted at 1126.71 cm^{-1} at IR MCA-SGE. The absorption at 1279.31 (aromatic amine) IR SGE shifted at 1283.59 cm^{-1} IR MCA-SGE. The absorption at 1454.74 cm^{-1} (alkyl) IR SGE shifted at 1454.74 cm^{-1} IR MCA-SGE. The shift in the absorption value that occurs indicates an interaction in the form of an electrostatic force between SGE and the encapsulation constituent materials.

Antioxidant Activity

Antioxidants play an important role in protecting the body from the influence of free radicals and oxidative damage, so the presence of antioxidants in the body is important (Kurnia et al. 2021) Antioxidants react with DPPH through very fast electron transfer and with slow transfer of hydrogen atoms, this reaction causes antioxidant compounds to inhibit the action of free radicals (Schaich et al. 2015; Abbaspour-Gilandeh et al. 2021).

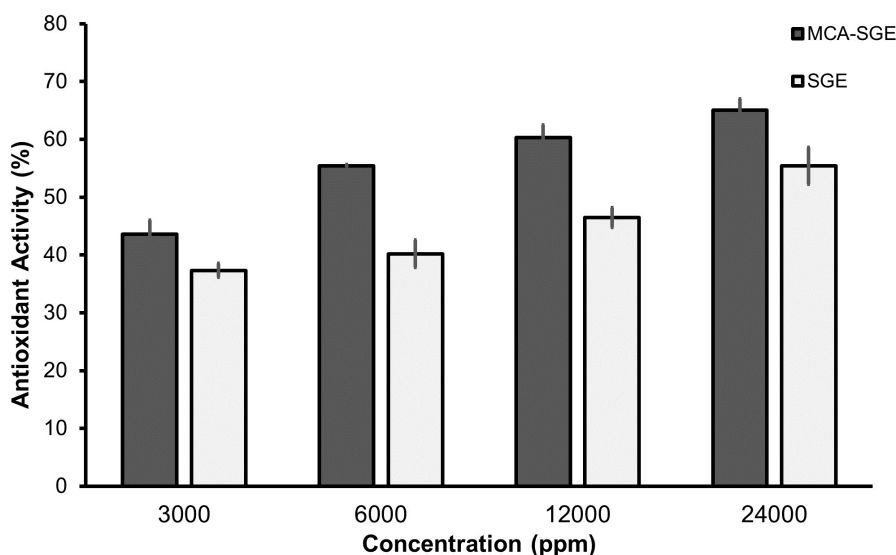


Figure 5. Antioxidant Activity of SGE and MCA-SGE.

Data from the DPPH test results showed (Figure 5) there was an increase in the percentage of antioxidants with an increase in the concentration level of SGE and MCA-SGE. MCA-SGE tends to have higher antioxidants than SGE. The higher antioxidants of MCA-SGE compared to SGE may be due to additional antioxidant components from the ingredients used in microencapsulated formulations. It is mentioned that alginate oligosaccharides have antioxidant activity (Zhang et al. 2020) In addition, chitosan also has radical damping activity from the hydroxyl group and the amino group (Avelelas et al. 2019) This result is supported by the previous research that the encapsulation of garlic oil with chitosan polymer increases antioxidant activity (Amiri et al. 2021). Other studies also describe a similar thing that one of the main aspects of microencap-

sulation is to improve

bioavailability of food antioxidants (Ozkan et al. 2019). Microencapsulation protects bioactive compounds (mainly antioxidant compounds) effectively against destructive environmental conditions, in addition to providing physical stability, improved bio-accessibility, as well as controlled release over time (Mohammadalinejad & Kurek 2021). High concentration will be more effective in becoming a better pro-oxidant (Bagheri et al. 2016)

Release Kinetic (RK) in vitro

The kinetic release test results of *allicin* and *alliin* compounds in single garlic extract chitosan-alginate microencapsulation (MCA-SGE) were carried out in the gastric environment (pH 1.5). The significance value in the T-paired Test between the levels of *allicin* and *alliin* compounds in SGE and MCA-SGE shows a signification of < 0.05 so that there is an average difference between the levels of *allicin* and *alliin* compounds SGE and MCA-SGE before the kinetic release test. Decreasing of active compounds after kinetic release tests also occur in MCA-SGE (Table 4).

The percentage of kinetic release of *allicin* and *alliin* compounds in SGE is greater with a percentage value of 86% than that of MCA-SGE which is in the range of values of 64.58% in *allicin* and 58.81 % in *alliin*. Microencapsulation has the potential to reduce the release of a single garlic active compound from the low pH of the gastric gastrointestinal fluid. It is reported that chitosan and alginate used can control the release of encapsulated compounds (Park et al. 2022; Waqas et al. 2022). Controlled drug delivery systems have been developed to improve the next staging of the drug in the body with two main purposes, to reduce the number of single doses per day improving patient compliance of treatments and to decrease the fluctuations of plasma levels, in order to obtain better therapeutic efficacy and lower toxicity (Saha & Das 2015). Previous research showed that during a span of 4 hours, when it was at pH 1.5 the kinetic release results of turmeric oil and citronella oil encapsulated with chitosan-alginate were about 35% and 5%, respectively (Natrajan et al. 2015).

The release of the drug has a sensitivity to pH, alginate is less easily soluble in low pH than chitosan. The interaction of encapsulated materials at a low pH will further help the release of active compounds when exposed to blood pH (pH 7.4). This causes more bioactive ingredients to be absorbed into the blood system and later the bioactive ingredients are transported in the circulatory system (Patel et al. 2013).

Table 4. Results of In-vitro Kinetic Release Test of SGE and MCA-SGE.

Sample	Pre-RK levels (µg/ml)		Levels after RK (µg/ml)		Percentage Release Kinetic (%)	
	<i>Allicin</i>	<i>Alliin</i>	<i>Allicin</i>	<i>Alliin</i>	<i>Allicin</i>	<i>Alliin</i>
SGE	52090.57 ± 4025.62	31080.76 ± 2403.78	44872.23 ± 5486.90	26770.54 ± 3276.35	86.16 ± 8.58	86.15 ± 8.59
MCA-SGE	102150.72 ± 12067.78	64868.34 ± 7665.89	62215.23 ± 5598.78	35973.41 ± 3239.49	64.58 ± 4.07	58.81 ± 3.71

CONCLUSIONS

MCA-SGE is efficient as a drug delivery agent for SGE based on characterisation (PSA, SEM, and FTIR analysis), antioxidant activity, and kinetic release. The MCA-SGE based on PSA analysis were successfully prepared and showed good characteristics in range micrometer. FTIR study reported a shift in absorption and addition of SGE functional groups after encapsulation. The results of the antioxidant activity test showed that the antioxidant activity of MCA-SGE was higher than SGE and could be used as a drug delivery system with controlled release.

AUTHOR CONTRIBUTION

S.R.L., A.G., S.I.M. and S. designed the research and supervised the process. A.N.R, D.N.A, I.N.M, and N.D.R prepared the MCA-SGE formulation, and collected the data. N.P., D.S.M and A.R.E.B collected, to analyse the data and prepared the manuscript.

ACKNOWLEDGMENTS

This research was funded by Directorate of Research, Technology, and Community Service, The Ministry of Education, Culture, Research, and Technology Republic Indonesia, the Fundamental Research Scheme – National Competition Research with contract number 20.06.38/UN32.20.1/LT/2023.

CONFLICT OF INTEREST

The authors declare that they do not have a conflict of interest.

REFERENCES

- Abbaspour-Gilandeh, Y. et al., 2021. Combined hot air, microwave, and infrared drying of hawthorn fruit: Effects of ultrasonic pretreatment on drying time, energy, qualitative, and bioactive compounds' properties. *Foods*, 10(5). doi: 10.3390/foods10051006.
- Abdel-Gawad, M. et al., 2018. in Vitro Antioxidant, Total Phenolic and Flavonoid Contents of Six Allium Species Growing in Egypt. *Journal of Microbiology, Biotechnology and Food Sciences*, 8(2), pp.343–346.
- Ahmad, R.M. et al., 2022. Preparation and Characterization of Blank and Nerolidol-Loaded Chitosan–Alginate Nanoparticles. *Nanomaterials*, 12(7), 1183. doi: 10.3390/nano12071183
- Akhter, M.H. et al., 2022. Drug Delivery Challenges and Current Progress in Nanocarrier-Based Ocular Therapeutic System. *Gels*, 8(2). doi: 10.3390/gels8020082.
- Aleksandra Zielińska et al., 2020. Polymeric Nanoparticles: Production, Characterization, Toxicology and Ecotoxicology. *Molecules*, 25, p.3731. doi: 10.3390/molecules25163731
- Alencar, D.D. de O. et al., 2022. Microencapsulation of Cymbopogon citratus D.C. Stapf Essential Oil with Spray Drying: Development, Characterization, and Antioxidant and Antibacterial Activities. *Foods*, 11(8). doi: 10.3390/foods11081111.
- Amiri, N. et al., 2021. Nanoencapsulation (in vitro and in vivo) as an efficient technology to boost the potential of garlic essential oil as alternatives for antibiotics in broiler nutrition. *Animal*, 15(1), 100022. doi: 10.1016/j.animal.2020.100022.
- Avelelas, F. et al., 2019. Antifungal and antioxidant properties of chitosan polymers obtained from nontraditional Polybius henslowii sources. *Marine Drugs*, 17(4), pp.1–15. doi: 10.3390/md17040239.

- Aziz, S.A.A. et al., 2013. Effect of Zeta Potential of Stanum Oxide (SnO₂) on Electrophoretic Deposition (EPD) on Porous Alumina. *Advanced Materials Research*, 795, pp.334–337. doi: 10.4028/www.scientific.net/AMR.795.334.
- Bagheri, R. et al., 2016. Comparing the effect of encapsulated and unencapsulated fennel extracts on the shelf life of minced common kilka (*Clupeonella cultriventris caspia*) and *Pseudomonas aeruginosa* inoculated in the mince. *Food Science and Nutrition*, 4(2), pp.216–222. doi: 10.1002/fsn3.275.
- Baltrusch, K.L. et al., 2022. Spray-drying microencapsulation of tea extracts using green starch, alginate or carrageenan as carrier materials. *International Journal of Biological Macromolecules*, 203, pp.417–429. doi: 10.1016/j.ijbiomac.2022.01.129.
- Bhatwalkar, S.B. et al., 2021. Antibacterial Properties of Organosulfur Compounds of Garlic (*Allium sativum*). *Frontiers in Microbiology*, 12 (July), pp.1–20. doi: 10.3389/fmicb.2021.613077.
- Borlinghaus, J. et al., 2014. Allicin: chemistry and biological properties. *Molecules (Basel, Switzerland)*, 19(8), pp.12591–12618. doi: 10.3390/molecules190812591.
- Buanasari, Sugiyo, W. & Rustaman, H., 2021. Preparation and evaluation of plant extract microcapsules using Chitosan. *IOP Conference Series: Earth and Environmental Science*, 755(1). doi: 10.1088/1755-1315/755/1/012063.
- Chopra, M. et al., 2012. Synthesis and Optimization of Streptomycin Loaded Chitosan-Alginate Nanoparticles. *International Journal of Scientific & Technology Research*, 1(10), pp.31–34.
- Choudhury, N., Meghwal, M. & Das, K., 2021. Microencapsulation: An overview on concepts, methods, properties and applications in foods. *Food Frontiers*, 2(4), pp.426–442. doi: 10.1002/fft2.94.
- Danaei, M. et al., 2018. Impact of Particle Size and Polydispersity Index on the Clinical Applications of Lipidic Nanocarrier Systems. *Pharmaceutics*, 10(2), 57. doi: 10.3390/pharmaceutics10020057.
- Dima, C. et al., 2013. Microencapsulation of coriander oil using complex coacervation method. *Scientific Study and Research: Chemistry and Chemical Engineering, Biotechnology, Food Industry*, 14(3), pp.155–162.
- Divya, B. et al., 2017. A Study on Phytochemicals, Functional Groups and Mineral Composition of *Allium sativum* (Garlic) Cloves. doi: 10.22159/ijcpr.2017v9i3.18888.
- Fei, X. et al., 2015. Microencapsulation mechanism and size control of fragrance microcapsules with melamine resin shell. *Colloids and Surfaces A: Physicochemical and Engineering Aspects*, 469, pp.300–306. doi: 10.1016/j.colsurfa.2015.01.033.
- Filho, J.C.P. et al., 2019. Design of chitosan-alginate core-shell nanoparticles loaded with anacardic acid and cardol for drug delivery. *Polymeros*, 29(4), pp.1–10. doi: 10.1590/0104-1428.08118.
- Katuwavila, N.P. et al., 2016. Chitosan-Alginate Nanoparticle System Efficiently Delivers Doxorubicin to MCF-7 Cells. *Journal of Nanomaterials*, 2016. doi: 10.1155/2016/3178904.
- Krisanti, E., Aryani, S.D. & Mulia, K., 2017. Effect of chitosan molecular weight and composition on mucoadhesive properties of mangostin-loaded chitosan-alginate microparticles. *AIP Conference Proceedings*, 1817. doi: 10.1063/1.4976766.
- Kurnia, D. et al., 2021. Antioxidant properties and structure-antioxidant activity relationship of allium species leaves. *Molecules*, 26(23), pp.1–28. doi: 10.3390/molecules26237175.

- Kyriakoudi, A. et al., 2021. Innovative delivery systems loaded with plant bioactive ingredients: Formulation approaches and applications. *Plants*, 10(6), pp.1–56. doi: 10.3390/plants10061238.
- Kyzioł, A. et al., 2017. Preparation and characterization of alginate/chitosan formulations for ciprofloxacin-controlled delivery. *Journal of Biomaterials Applications*, 32(2), pp.162–174. doi: 10.1177/0885328217714352.
- Lengyel, M. et al., 2019a. Microparticles, microspheres, and microcapsules for advanced drug delivery. *Scientia Pharmaceutica*, 87(3). doi: 10.3390/scipharm87030020.
- Lengyel, M. et al., 2019b. Microparticles, Microspheres, and Microcapsules for Advanced Drug Delivery. *Scientia Pharmaceutica*, 87(3), pp.1–31.
- Lestari, S.R. & Rifa'i, M., 2018. Regulatory T cells and anti-inflammatory cytokine profile of mice fed a high-fat diet after single-bulb garlic (*Allium sativum* L.) oil treatment. *Tropical Journal of Pharmaceutical Research*, 17(11), pp.2157–2162. doi: 10.4314/tjpr.v17i11.7.
- Lestari, S.R. et al., 2020. Single Garlic Oil Modulates T Cells Activation and Proinflammatory Cytokine in Mice with High Fat Diet. *Journal of Ayurveda and Integrative Medicine*, 11(4), pp.414–420. doi: 10.1016/j.jaim.2020.06.009.
- Lestari, S.R. et al., 2021. Self-nanoemulsifying drug delivery system (SNEEDS) for improved bioavailability of active compound on single clove garlic: Optimization of PEG 400 and glycerol as co-surfactant. *AIP Conference Proceedings*, 2353. doi: 10.1063/5.0052638.
- Loquercio, A. et al., 2015. Preparation of Chitosan-Alginate Nanoparticles for Trans-cinnamaldehyde Entrapment. *Journal of Food Science*, 80(10), pp.N2305–N2315. doi: 10.1111/1750-3841.12997.
- Machado, N.D. et al., 2021. Preservation of the antioxidant capacity of resveratrol via encapsulation in niosomes. *Foods*, 10(5), pp.1–12. doi: 10.3390/foods10050988.
- Merck, 2022. IR Spectrum Table & Chart.
- Michen, B. et al., 2015. Avoiding drying-artifacts in transmission electron microscopy: Characterizing the size and colloidal state of nanoparticles. *Scientific Reports*, 5. doi: 10.1038/srep09793.
- Mohammadlinejhad, S. & Kurek, M.A., 2021. Applsci-11-03936.Pdf. *Applied Sciences*.
- Mudalige, T. et al., 2018. Characterization of Nanomaterials: Tools and Challenges. In *Micro and Nano Technologies, Nanomaterials for Food Applications*. Elsevier Inc. pp.313-353. doi: 10.1016/B978-0-12-814130-4.00011-7.
- Nandiyanto, A.B.D., Oktiani, R. & Ragadhita, R., 2019. How to read and interpret ftir spectroscopy of organic material. *Indonesian Journal of Science and Technology*, 4(1), pp.97–118. doi: 10.17509/ijost.v4i1.15806.
- Natrajan, D. et al., 2015. Formulation of essential oil-loaded chitosan-alginate nanocapsules. *Journal of Food and Drug Analysis*, 23(3), pp.560–568. doi: 10.1016/j.jfda.2015.01.001.
- Ozkan, G. et al., 2019. A review of microencapsulation methods for food antioxidants: Principles, advantages, drawbacks and applications. *Food Chemistry*, 272(August 2018), pp.494–506. doi: 10.1016/j.foodchem.2018.07.205.
- Park, K.H. et al., 2022. Controlled Drug Release Using Chitosan-Alginate-Gentamicin Multi-Component Beads. , pp.1–13.

- Pateiro, M. et al., 2021. Nanoencapsulation of promising bioactive compounds to improve their absorption, stability, functionality and the appearance of the final food products. *Molecules*, 26(6). doi: 10.3390/molecules26061547.
- Patel, B.K., Parikh, R.H. & Aboti, P.S., 2013. Development of Oral Sustained Release Rifampicin Loaded Chitosan Nanoparticles by Design of Experiment. *Journal of Drug Delivery*, 2013, pp.1–10. doi: 10.1155/2013/370938.
- Pedroso-Santana, S. & Fleitas-Salazar, N., 2020. Ionotropic gelation method in the synthesis of nanoparticles/microparticles for biomedical purposes. *Polymer International*, 69(5), pp.443–447. doi: 10.1002/pi.5970.
- Praseptianga, D. et al., 2021. Preparation and FTIR spectroscopic studies of SiO₂-ZnO nanoparticles suspension for the development of carrageenan-based bio-nanocomposite film. *AIP Conf. Proc.*, 2219, 100005. doi: 10.1063/5.0003434
- Pudlarz, A. & Szemraj, J., 2018. Nanoparticles as carriers of proteins, peptides and other therapeutic molecules. *Open Life Sciences*, 13(1), pp.285–298. doi: 10.1515/biol-2018-0035.
- Qadariah, N., Lestari, S.R. & Rohman, F., 2020. Single Bulb Garlic (*Allium Sativum*) Extract Improve Sperm Quality in Hyperlipidemia Male Mice Model. *Jurnal Kedokteran Hewan - Indonesian Journal of Veterinary Sciences*, 14(1), pp.7–11. doi: 10.21157/j.ked.hewan.v14i1.13562.
- Rajasree, R.S. et al., 2021. An evaluation of the antioxidant activity of a methanolic extract of cucumis melo l. Fruit (f1 hybrid). *Separations*, 8(8), pp.1–15. doi: 10.3390/separations8080123.
- Saha, P. & Das, P.S., 2015. Advances in Controlled Release Technology in Pharmaceuticals: A Review. *World journal of pharmacy and pharmaceutical sciences*, 6(9), pp.2070–2084. doi: 10.20959/wjpps20179-10194.
- dos Santos, P.P. et al., 2015. Development of lycopene-loaded lipid-core nanocapsules: physicochemical characterization and stability study. *Journal of Nanoparticle Research*, 17(2). doi: 10.1007/s11051-015-2917-5.
- Sasi, M. et al., 2021. Garlic (*Allium sativum* L.) bioactives and its role in alleviating oral pathologies. *Antioxidants*, 10(11). doi: 10.3390/antiox10111847.
- Schaich, K.M., Tian, X. & Xie, J., 2015. Hurdles and pitfalls in measuring antioxidant efficacy: A critical evaluation of ABTS, DPPH, and ORAC assays. *Journal of Functional Foods*, 14, pp.111–125. doi: 10.1016/j.jff.2015.01.043.
- Shang, A. et al., 2019. Bioactive compounds and biological functions of garlic (*allium sativum* L.). *Foods*, 8(7), pp.1–31. doi: 10.3390/foods8070246.
- Singer, A. et al., 2018. Nanoscale Drug-Delivery Systems: In Vitro and In Vivo Characterization. *Nanocarriers for Drug Delivery: Nanoscience and Nanotechnology in Drug Delivery*, pp.395–419. doi: 10.1016/B978-0-12-814033-8.00013-8.
- Sorasitthyanukarn, F.N. et al., 2018. Chitosan/alginate nanoparticles as a promising approach for oral delivery of curcumin diglutamic acid for cancer treatment. *Materials Science and Engineering C*, 93(July), pp.178–190. doi: 10.1016/j.msec.2018.07.069.

- Szabó, L., Gerber-Lemaire, S. & Wandrey, C., 2020. Strategies to functionalize the anionic biopolymer na-alginate without restricting its polyelectrolyte properties. *Polymers*, 12(4). doi: 10.3390/POLYM12040919.
- Szychowski, K.A. et al., 2018. Characterization of Active Compounds of Different Garlic (*Allium sativum* L.) Cultivars. *Polish Journal of Food and Nutrition Sciences*, 68(1), pp.73–81. doi: 10.1515/pjfn-2017-0005.
- Tao, Q. et al., 2021. Ionic and enzymatic multiple-crosslinked nanogels for drug delivery. *Polymers*, 13(20). doi: 10.3390/polym13203565.
- Wang, F. et al., 2016. Effective method of chitosan-coated alginate nanoparticles for target drug delivery applications. *Journal of Biomaterials Applications*, 31(1), pp.3–12. doi: 10.1177/0885328216648478.
- Waqas, M.K. et al., 2022. Alginate-coated chitosan nanoparticles for pH-dependent release of tamoxifen citrate. *Journal of Experimental Nanoscience*, 17(1), pp.522–534. doi: 10.1080/17458080.2022.2112919.
- Yousefi, M. et al., 2020. Development, characterization and in vitro antioxidant activity of chitosan-coated alginate microcapsules entrapping *Viola odorata* Linn. extract. *International Journal of Biological Macromolecules*, 163, pp.44–54. doi: 10.1016/j.ijbiomac.2020.06.250.
- Zhang, Y.H. et al., 2020. Characterization and Application of an Alginate Lyase, Aly1281 from Marine Bacterium *Pseudoalteromonas carrageenovora* ASY5. *Marine Drugs*, 18(2). doi: 10.3390/md18020095.
- Zhou, P. et al., 2018. Loading BMP-2 on nanostructured hydroxyapatite microspheres for rapid bone regeneration. *International Journal of Nanomedicine*, 13, pp.4083–4092. doi: 10.2147/IJN.S158280.

Research Article

Maturation of Female Yellow Rasbora (*Rasbora Lateristriata* Bleeker, 1854) Using Oodev at Different Doses in Feed

Juniman Rey¹, Slamet Widiyanto^{1*}, Bambang Retnoaji¹

¹)Faculty of Biology, Universitas Gadjah Mada. Jl. Teknik Selatan, Sekip Utara, Yogyakarta 55281, Indonesia

* Corresponding author, email: slametbio@ugm.ac.id

Keywords:

Gonadal maturation
hormone
Oodev
reproduction
Rasbora lateristriata

Submitted:

11 July 2022

Accepted:

05 May 2023

Published:

01 December 2023

Editor:

Ardaning Nuriliani

ABSTRACT

The current high demand for Yellow rasbora (*Rasbora lateristriata*) is not supported by the availability of captured Yellow rasbora in nature. Aquaculture is the most rational way of utilizing biological natural resources. In intensive aquaculture, it is necessary to optimize all processes that occur in aquaculture, including hatchery. However, the common problem that often happens in hatchery activities is spawning which depends on the season. The hormonal manipulation technique is an appropriate way to stimulate gonadal maturation. Oodev is a hormonal combination of pregnant mare serum gonadotropin and anti-dopamine to stimulate gonadal maturation. The purpose of this study was to determine the effectiveness of using the Oodev with different doses in feed to accelerate gonad maturation of female Yellow rasbora. The study was carried out with four treatments and three replications in 21 days with different doses of Oodev, such as; A (Feed without Oodev), B (0.5 mL/kg feed), C (1 mL/kg feed) and D (2 mL/kg feed). The parameters observed in this study were gonad maturity level, histological structure of ovary, gonadosomatic index, fecundity, and diameter of eggs. The results showed that the dose of Oodev at 1.0 mL/kg feed was an effective dose to optimize the gonad maturity of female Yellow rasbora. This is proven by the highest results shown on all parameters, such as; the maturity level in the IV phase, histological structure of the ovary which showed the dominance of the oocyte maturation phase, gonadosomatic index of 14.014%, the fecundity of 721 eggs, and egg diameter of 0.865 mm. In conclusion, using Oodev in feed at a dose of 1.0 ml/kg of feed for 21 days is an effective dose to optimize the maturation of female Yellow rasbora.

Copyright: © 2023, J. Tropical Biodiversity Biotechnology (CC BY-SA 4.0)

INTRODUCTION

Yellow rasbora (*Rasbora lateristriata*) is a fish favored by consumers because it has a distinctive taste. The high demand for Yellow rasbora fish is not supported by their availability due to the catches from nature are still limited (Zulfadhli 2015; Puspitasari 2016). Aquaculture is the most rational way of utilizing biological natural resources. Retnoaji et al. (2017) succeeded in aquaculture and conducting conservation through empowering aquaculture groups in Yogyakarta, Indonesia. In intensive aquaculture, it is necessary to optimize all processes that occur in aquaculture, including hatchery breeding which highly determines the number of productions. However, a common problem that is often occurred in

hatchery activities is the aquaculture environment which is sometimes not suitable for stimulating spawning, and the spawning depends on the season (Alavi et al. 2009). In the tropics, changes in water temperature and the amplitude of the air surface elevation caused by changing seasons can be a trigger for spawning (Hutagalung 2015).

The hormonal manipulation technique is an appropriate way to stimulate gonadal maturation in fish. Hormonal engineering to induce gonadal maturation uses a combination of several hormones (Putra et al. 2017). One of the commercial products that contain many alternative hormones is Oodev. Oodev is an innovation trademark developed by the Fish Reproduction and Genetics Laboratory of IPB University, Indonesia. Oodev is a hormonal induction material that is able to accelerate the maturation and re-maturation of the gonad in fish. Oodev is a combination of Pregnant Mare Serum Gonadotropin (PMSG) and anti-dopamine (AD) (Nugraha 2014).

PMSG is a complex glycoprotein obtained from the serum of pregnant horses and, acts similarly like luteinizing hormone (LH) and follicle-stimulating hormone (FSH) (Gallego et al. 2012). The effect of PMSG as FSH is more dominant than LH. The half-life of PMSG is quite long when compared to other gonadotropin hormones. This is because PMSG has a high carbohydrate content, especially in the cyclic acid group. The function of AD in the Oodev hormone is to block dopamine to prevent pituitary gonadotropin secretion from being inhibited (Arfah 2018). Inhibition of dopamine activity can stimulate LH synthesis and its secretion in the hypothalamus (Natalia 2018). LH plays a role in the final egg maturity process. Therefore, dopamine needs to be inhibited using anti-dopamine (Pamungkas et al. 2019).

The use of hormones in fish is usually done by intramuscular injection however, due to several considerations, such as the size of the fish are the reason for the ineffectiveness and inefficient use of hormones by injection. Another alternative method is the use of hormones through oral administration in feed. Research on the use of Oodev hormone through oral administration for gonad maturation of cultured fish has been carried out in several species, including *Chromobotia macracanthus* (Setiowibowo 2019), (*Helostoma teminkii*) (Farida et al. 2019), *Amphiprion clarkia* (Tomasoa et al. 2018), *Pangasianodon hypophthalmus* (Nugraha 2014.; Arfah 2018) but never been done in Yellow rasbora. The purpose of this study was to determine the effectiveness of the Oodev through oral administration in feed to accelerate gonad maturation of female Yellow rasbora.

MATERIALS AND METHODS

Materials

Yellow rasbora broodstocks used in this study were 6-month-old with an average body weight of 5.6 grams obtained from Cangkringan Fisheries Technology Development Center, Sleman, Yogyakarta. This study used a completely randomized design (CRD) with four treatments and three replications with different doses of Oodev, such as; A (Feed without Oodev), B (0.5 mL/kg feed), C (1.0 mL/kg feed), and D (2.0 mL/kg feed).

The tank used in this study was 2 fiber cubes (1.0 m x 0.80 m x 0.60 m). Each cube contains 6 happa nets with a size of 40 cm³. To support growth and maintenance feasibility according to the research by Zulfandi (2015), the appropriate stocking density of broodstock is 10-15 fish/liter. Furthermore, the broodstocks were acclimatized for one week and then selected. Broodstock selection is the main key before spawning. The selection of broodstock aims to ensure uniformity of brood fish, re-

lated to uniform body weight, body shape is not deformed, and in the same reproductive phase that is not present in the gonad maturity phase.

Methods

The supplementation of feed with Oodev uses a coating method that begins with mixing Oodev in feed with a dose according to the treatment applied in this study (Nugraha 2014). The feed coating method begins with the addition of egg white as a binder into the aquades which is then sprayed onto the feed. The feed used was the floating-type pellet (crude protein 31-33%). The frequency of feeding was three times a day for 21 days with a feeding ratio of 3-5% of body weight. The parameters used in this study are described as follows:

Gonad Maturity Level (GML)

After 21 days of treatment, 2-3 fish in each treatment group will be dissected to obtain gonads for determination of GML based on the morphological characteristics of the gonads according to Effendie (1997) which are listed in Table 1.

Table 1. The Characteristics of Gonad Maturity Level.

GML	Female Gonad Morphology
I Immature	The ovary is like a thread. The eggs are not yet distinguishable. The length of the gonads varies between 1/3-1/2 on the length of the body cavity.
II Maturing	There is a milky white tissue, the eggs are still fused and cannot be separated. The length of the gonads varies between 1/3-2/3 on the length of the body cavity.
III Maturing ripe	Larger size, widened anteriorly, and tapered posteriorly, the eggs can be separated, and darker in color. The length of the gonads varies between 1/3-2/3 of the length of the body cavity.
IV Ripe	The egg diameter is getting bigger and visible under the microscope. The eggs are yellow. The length of the gonads varies between 2/3-3/4 of the length of the body cavity.
V Spent	Crimped ovaries, leftover eggs in the posterior. Ovaries are reddish.

Histological structure of the ovary

Development of fish reproductive organs identified morphologically and histologically. Histological observation is the most accurate method and yields the most detailed information because the observations are carried out at the tissue level (Zulfadhli 2015; Suryanti et al. 2015). GML is determined based on morphological characteristics, then it is continued with the histological preparation using the paraffin method. The thickness of the slice on the microtome was adjusted to 5 µm and then Hematoxylin Eosin (HE) staining was performed to identify the different stages of the oocyte formation histologically more accurately. The development of fish reproductive organs can be identified by morphological and histological structures. The terminology in determining the phase of each oocyte development refers to Costa (2015) who suggests an analysis of the histological sections on the ovaries of all species into ten stages of oocyte development with three main phases, namely pre-vitellogenic oocyte growth, vitellogenic oocyte growth, and oocyte maturation.

Gonadosomatic Index (GSI)

Gonadosomatic index is calculated by the following formula (Dadzie & Wangila 1980):

$$GSI = \frac{\text{Weight of Gonad}}{\text{Weight of Fish}} \times 100\%$$

Fecundity

Fecundity is assumed as the number of eggs contained in the ovaries that have reached GML III and IV. The total fecundity was calculated using the sub-sample method of gonadal weight or the gravimetric method with the following formula (Effendie 1997):

$$F = \frac{\text{Total Weight of Gonad}}{\text{Sample Weight of Gonad}} \times \text{total of gonad in sample}$$

Eggs Diameter

The measurement of egg diameter was carried out using ImageJ software developed by the National Institutes of Health and the Laboratory for Optical and Computational Instrumentation. The number of eggs measured was 20 eggs for each treatment group.

Data analysis

Data on gonadosomatic index, fecundity, and egg diameter were analyzed by one-way ANOVA and followed by Tukey test using IBM SPSS version 25. The differences between each sample were considered significant at $p < 0.05$ (Gomez & Gomez 1995). Histological observation of the stages of gonad development was done microscopically using the descriptive comparative method. The advantages of histological observations can provide accurate and detailed information at the tissue level (Zulfadhli 2015).

RESULTS AND DISCUSSION

Gonad Maturation Level (GML)

The level of gonad maturity in broodstock can be seen morphologically with several characteristics that indicate that the broodstock has matured gonads, the most common characteristic of which is the enlarged abdomen towards the anus (Susilo et al. 2019). In female Yellow rasbora, it could be seen that there were differences between the treatments from the morphological characteristics based on Figure 1)

In treatment A (Feed without Oodev) and D (2 mL/kg feed), it's seen that the abdomen of fish was smaller when compared to treatment B (0.5 mL/kg feed) and C (1 mL/kg feed). In treatment C, the abdomen is bigger and fulfilled the abdominal cavity more than in treatment B. Treatment C has shown a different morphological characteristic than the other treatments. The abdominal cavity in treatment C seems to have a lot of volumes. After the morphological characteristics of the fish body shows a difference, surgery was carried out to identify the morphology of the gonads.

Figure 1 shows that treatment C is clearly different from the other treatments. Based on the morphological characteristics of the gonads, according to Effendie (1997), treatment C was in the GML IV category, the which the eggs are yellowish-orange color and occupy 2/3 to 3/4 part of the abdominal cavity. On the other hand, the other treatments did not show the same gonadal morphology as shown by the treatment C. This shows that the treatment C with a dose of Oodev hormone of 1.0 mL/kg of feed is the best treatment. The accuracy of the GML will then be confirmed by the histology of the ovary and GSI results.

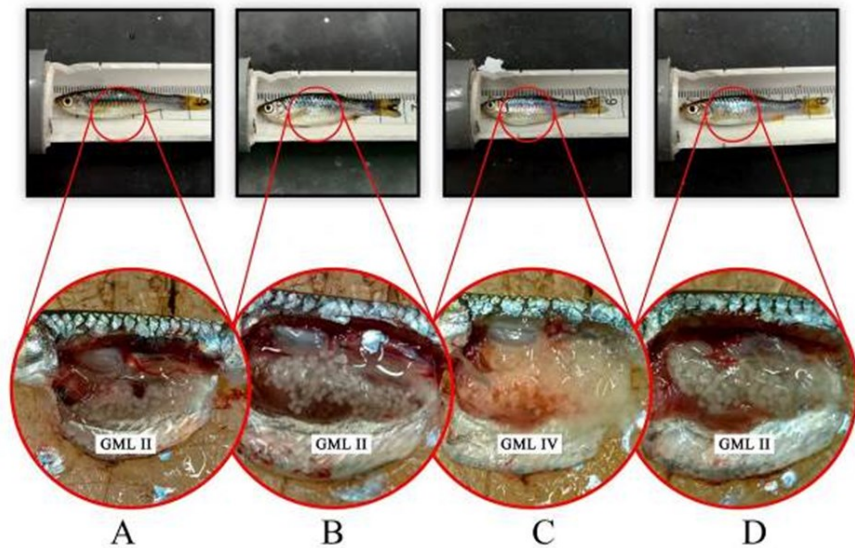


Figure 1. Gonad maturity level (GML) of Yellow rasbora, *Rasbora lateristriata* in Oodev treatments: A. Feed without Oodev; B. 0.5 mL/kg feed; C. 1.0 mL/kg feed; and D. 2.0 mL/kg feed.

Histological Structure of Ovary

According to Zulfadhli et al. (2016), the terminology and features used to differentiate and identify the different stages of oocyte formation histologically may vary according to the researcher and the species. The analysis of the histological section of the ovary according to Costa (2015) is the basis for the terminology guidelines to identify and classify the oocyte phase based on the histological results of the ovaries in each treatment. The results of this histological structure also support a more accurate GML by determining each oocyte phase. Figure 2 shows the histological results of the Yellow rasbora ovary in each treatment and gives a clear illustration that each treatment has different phase dominance.

It is seen in treatment A that the histological results showed several phases of oocyte development including pre-vitellogenic and vitellogenic phases. Treatment A was dominated by pre-vitellogenic, especially in the early primary growth phase with a percentage of 1.75%, late primary growth of 45.61%, and cortical alveolar of 14.04%. The vitellogenic phase was also identified in treatment A with the percentage of primary vitellogenesis was 22.81%, secondary vitellogenesis at 3.51%, and quaternary vitellogenesis at 12.28% (Figure 4).

The late primary growth phase that dominated treatment A was characterized by basophilic cytoplasm stained with hematoxylin and a nucleus showing nucleoli arranged on the periphery. Based on research by Johnson and Braunbeck (2009) and Erkmen and Kirankaya (2016), this phase is also called the perinucleolar oocyte phase. This phase is characterized by the growth of the oocyte, the nucleus (germinal vesicle) increases in size and many nucleoli appear at the periphery of the nucleus. The cytoplasm is darker in color, although late perinucleolar oocytes may have small well-defined, or amphophilic vacuoles in the cytoplasm (Figure 3).

Based on Figure 4, treatment D is like treatment A and B, which were dominated by the pre-vitellogenic phase with a larger portion, namely in the late primary growth phase of 79.75% and cortical alveolar of 10.13%. In the cortical alveolar phase, the diameter is generally larger than the perinuclear phase and characterized by the appearance of cortical alveoli (yolk vesicles) inside the ooplasm.

Treatment B was also identified as being in the vitellogenic phase.

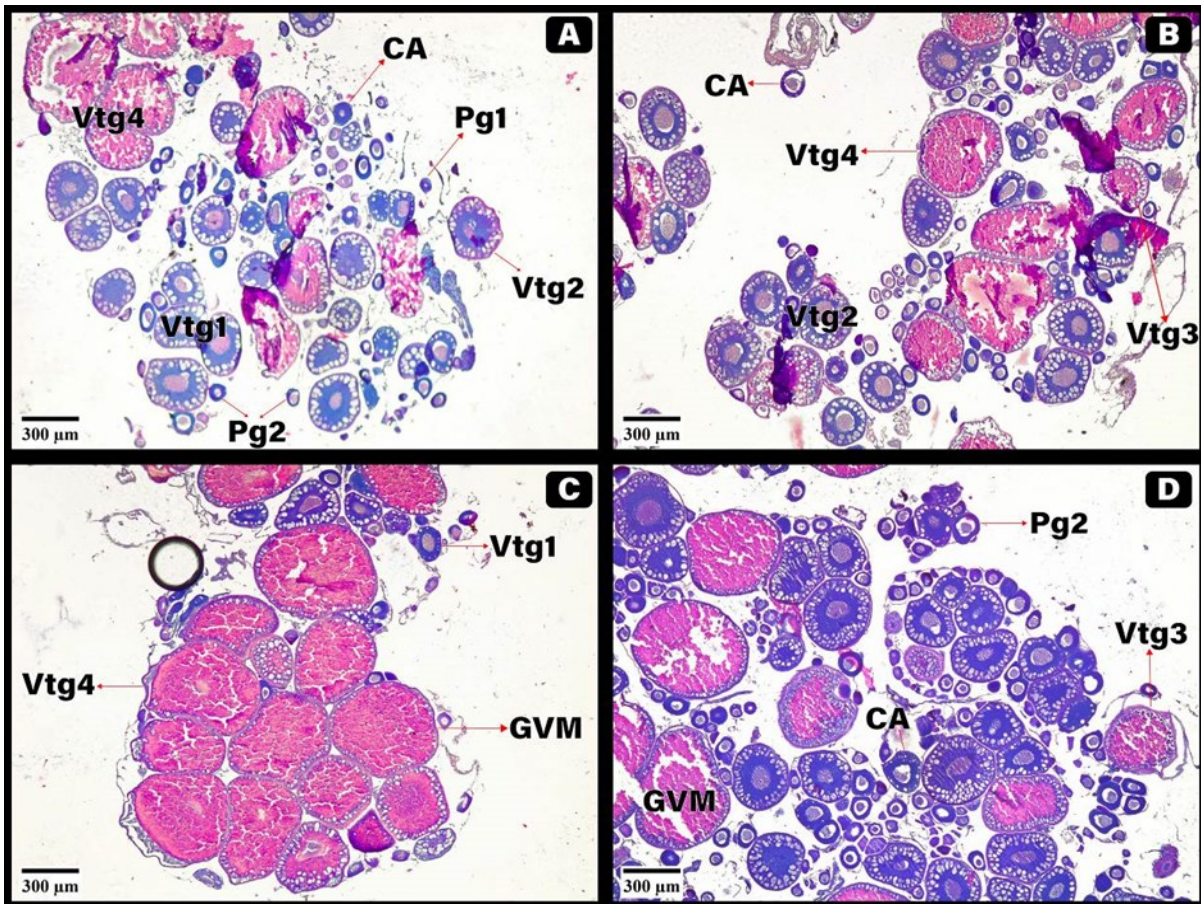


Figure 2. Ovary's histological structure of Yellow rasbora (*Rasbora lateristriata*) in Oodev treatments: A. Feed without Oodev; B. 0.5 mL/kg feed; C. 1.0 mL/kg feed; and D. 2.0 mL/kg feed. *Pre-vitellogenic oocyte growth*: early primary growth (Pg1), late primary growth (Pg2), cortical alveolar (CA); *Vitellogenic oocyte growth*; primary vitellogenesis (Vtg1), secondary vitellogenesis (Vtg2), tertiary vitellogenesis (Vtg3), quaternary vitellogenesis (Vtg4); *Oocyte maturation*: germinal vesicle migration (GVM). Hematoxylin-Eosin staining; 4×10 magnification.

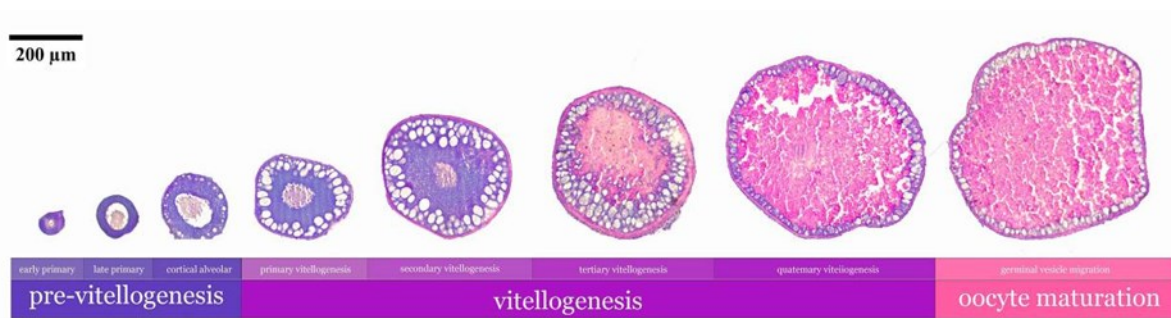


Figure 3. Oocyte stages of development of Yellow rasbora (*Rasbora lateristriata*); *Pre-vitellogenic oocyte growth*: early primary growth (Pg1), late primary growth (Pg2), cortical alveolar (CA); *Vitellogenic oocyte growth*; primary vitellogenesis (Vtg1), secondary vitellogenesis (Vtg2), tertiary vitellogenesis (Vtg3), quaternary vitellogenesis (Vtg4); *Oocyte maturation*: germinal vesicle migration (GVM). Hematoxylin-Eosin Staining; 10×10 magnification.

According to Costa (2015), this phase is divided into; primary vitellogenesis, secondary vitellogenesis, tertiary vitellogenesis, and quaternary vitellogenesis. Primary vitellogenesis is eosinophilic protein granules that are stained pink in hematoxylin-eosin staining, starting to slightly fill the cytoplasm, and more small-sized oil droplets and cortical alveoli can be seen arranged in the periphery of the oocyte. Secondary vitellogenesis (Vtg2) showed regular granules surrounding the cytoplasm and oil droplets began to appear and were located around the nucleus. In tertiary vitellogenesis (Vtg3), yolk granules multiply and fill the cytoplasm. Oil droplets increase in size and are distributed around the nucleus. In qua-

ternary vitellogenesis (Vtg4), the cytoplasm is filled with yolk granules and many oil droplets arranged around the nucleus.

Treatment C as shown in Figure 4, resulted in quaternary vitellogenesis of 20% and an oocyte maturation phase of 32%. This shows that treatment C is the best treatment with oocyte dominance in the late vitellogenesis and oocyte maturation phase. According to Johnson and Braunbeck (2009), in the oocyte maturation phase the cells become larger and hydrated, the nucleus has migrated towards the cell periphery and its size decreased in the periphery making it difficult to identify. The zona radiata will be divided into two layers, including a thick and hollow internal layer and a thinner, noncellular external layer. (Erkmen & Kirankaya 2016) explained that there is a vitelline layer composed of follicular cells that are cuboidal in shape with a large, rounded nucleus which is clearly visible as the outer layer. On the outside, the follicular layer contains a basal lamina and a theca layer (Menke et al. 2011). Histological results in treatment C also supported the previous parameters in this study regarding GML, namely the GML IV phase. This result is like (Prakasa 2020) which states that female Yellow rasbora with GML IV will be dominated by the matured oocyte. This shows that the administration of Oodev at a dose of 1.0 ml/kg of feed is the best dose to make matured oocyte dominated the ovaries.

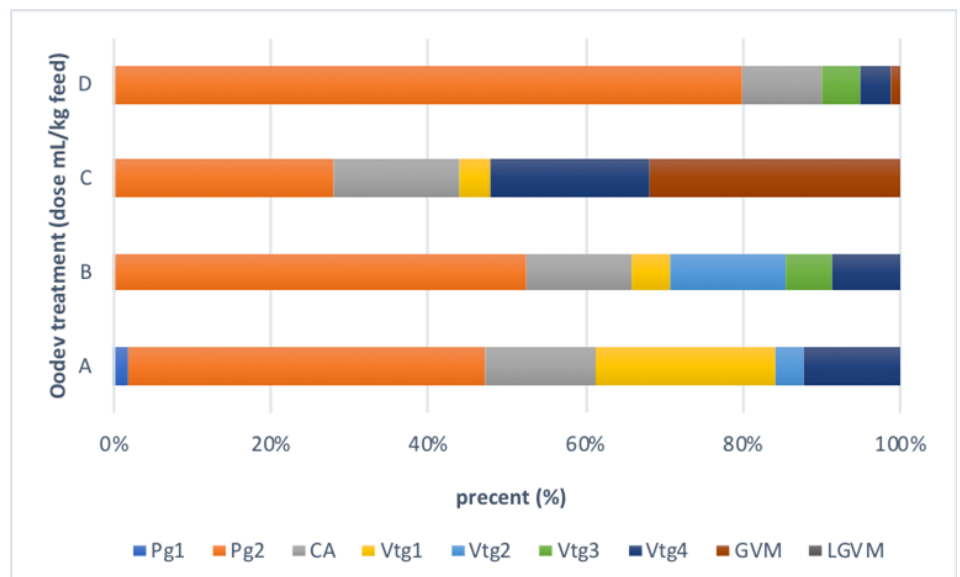


Figure 4. Percentage oocyte stages of development of Yellow rasbora, *Rasbora lateristriata*; *Pre-vitellogenic oocyte growth*: early primary growth (Pg1), late primary growth (Pg2), cortical alveolar (CA); *Vitellogenic oocyte growth*: primary vitellogenesis (Vtg1), secondary vitellogenesis (Vtg2), tertiary vitellogenesis (Vtg3), quaternary vitellogenesis (Vtg4); *Oocyte maturation*: germinal vesicle migration (GVM). Oodev treatments: A. Feed without Oodev; B. 0.5 mL/kg feed; C. 1.0 mL/kg feed; and D. 2.0 mL/kg feed.

Gonadosomatic Index (GSI)

Figure 5 shows the results of the analysis of variance (ANOVA) test on the administration of Oodev through oral administration with different doses on female Yellow rasbora fish which showed significant differences between treatments. The highest average GSI value was obtained from treatment C (1.0 mL/kg feed), which shows values of 14.01%, followed by treatment B (7.84%) and treatment D (7.77%), The lowest GSI value was obtained from treatment A which showed a value of 7.22%.

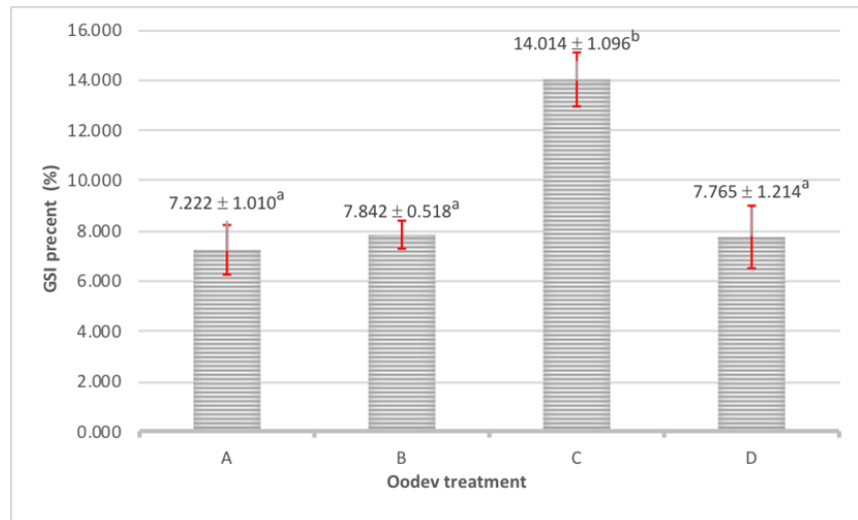


Figure 5. Gonadosomatic index (GSI) value of Yellow rasbora (*Rasbora lateristriata*) in Oodev treatments: A. Feed without Oodev; B. 0.5 mL/kg feed; C. 1.0 mL/kg feed; and D. 2.0 mL/kg feed. Notes: The means ± SD on the bars graph with different superscripts letters are significantly different ($p < 0.05$).

It is assumed that the supplementation of Oodev with a higher dose of more than 1.0 mL/kg feed does not affect the increase in gonadal development. This is due to an excess concentration of FSH in the blood because of the large doses of PMSG given (Nur et al. 2017). The increase in GSI values was related to the increase in gonad size due to the increase in oocyte size and the number of yolk granules during the vitellogenesis process (Susilo et al. 2019; Mellisa et al. 2022).

The Fecundity

The results of the analysis of variance (ANOVA) test on Oodev hormone through oral administration with different doses in female Yellow rasbora showed no significant difference in fecundity values. The value of fecundity obtained varied between each treatment. Figure 6 shows the difference in the average fecundity of female Yellow rasbora in each treatment due to different doses of Oodev administration. Administration of Oodev at a dose of 1.0 mL/kg of feed-in treatment C resulted in the highest average value of fecundity of 721 eggs. In treatments A, B, and D, the fecundity values were 465, 496, and 476 eggs, respectively. Therefore, treatment C is said as the best dose for the effectiveness of the Oodev on fecundity, compared to other treatments. Treatment A, B, and D the difference is not significantly different from each other in the average value. There was a difference of 31 eggs between treatments A and B, 20 eggs between treatments B and D and a difference of only 11 eggs between treatment A and D. Treatment A (Feed without Oodev) was the treatment with the lowest fecundity value.

According to Hutagalung (2015), the administration of Oodev containing PMSG in fish influences earlier egg maturation. Administration of Oodev will increase the accumulation of GtH in fish so that the gonads of fish are stimulated to carry out a faster egg formation process even though environmental conditions are not suitable. In another study, it was explained that the administration of Oodev to improve reproductive performance in fish through oral administration in feed or the intramuscular injection method influenced fish fecundity (Darliansyah et al. 2017).

Egg Diameter

The effect of Oodev in feed through oral administration on Yellow rasbora egg diameter is seen in Figure 7. In this study, the results of the analy-

sis of variance (ANOVA) test showed significantly different results between treatments.

Treatment C showed a significantly different from other treatments with an average egg diameter 0.865 mm. While treatment A, B, and D are not significantly different with an average egg diameter where the treatment are A 0.349 mm, treatment B 0.485 mm, and treatment D 0.416 mm, respectively. It is seen that treatment A has the lowest egg diameter and is assumed due to no PMSG administration.

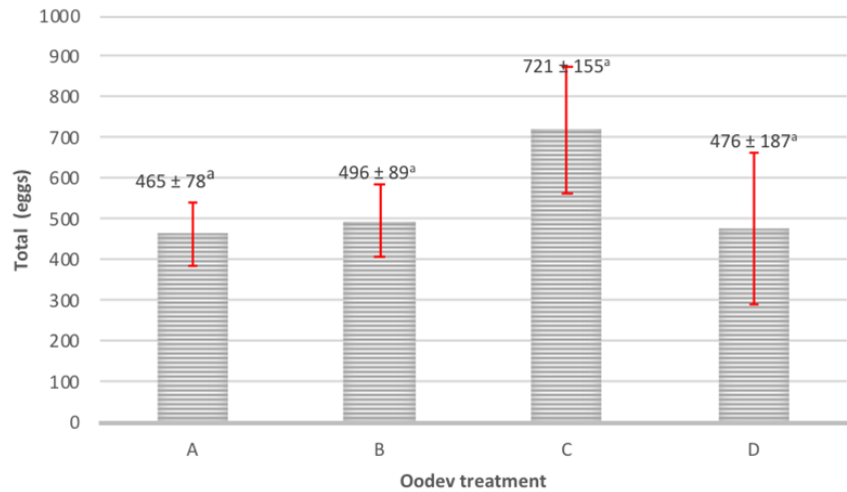


Figure 6. The fecundity of Yellow rasbora (*Rasbora lateristriata*) in Oodev treatments: A. Feed without Oodev; B. 0.5 mL/kg feed; C. 1.0 mL/kg feed; and D. 2.0 mL/kg feed. Notes: The means ± SD on the bars graph with different superscripts letter were significantly different ($p < 0.05$).

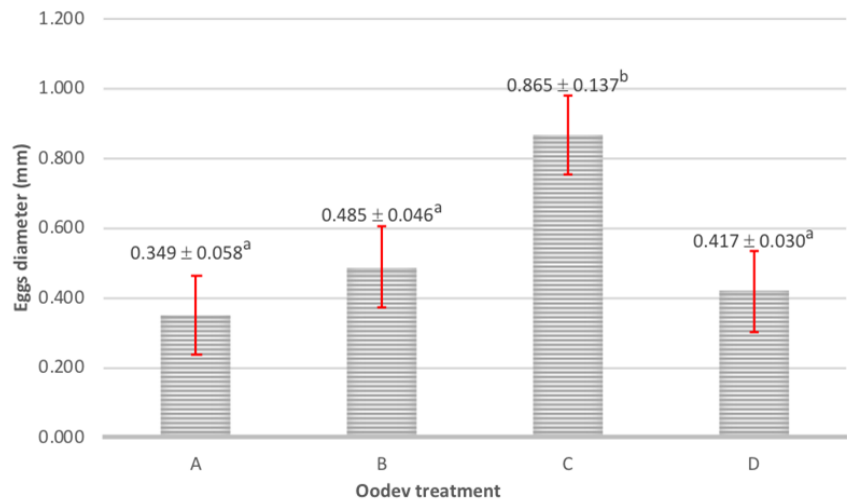


Figure 7. Diameter of Yellow rasbora (*Rasbora lateristriata*) eggs in Oodev treatments: A. Feed without Oodev; B. 0.5 mL/kg feed; C. 1.0 mL/kg feed; and D. 2.0 mL/kg feed. Notes: The means ± SD on the bars graph with different superscripts letter were significantly different ($p < 0.05$).

Treatment D with a higher dose than other treatments also did not show a higher mean diameter of egg. It was assumed that the administration of Oodev with a higher dose did not affect the higher increase in gonad development. This may be due to an excess concentration of FSH in the blood because of high doses of PMSG (Nur et al. 2017). Dhewantara and Rahmatia (2017) revealed that the PMSG hormone affects the development of fish egg diameter due to the increase of the vitellogenin content in eggs. PMSG has a role in stimulating the formation of follicles

because it contains a higher level of FSH and a little bit of LH. The role of FSH in the gonadotropin hormone will stimulate the egg maturation process in fish. Figure 8, it is seen that the variation in egg diameter was obtained in female Yellow rasbora administered with Oodev in feed with different doses.

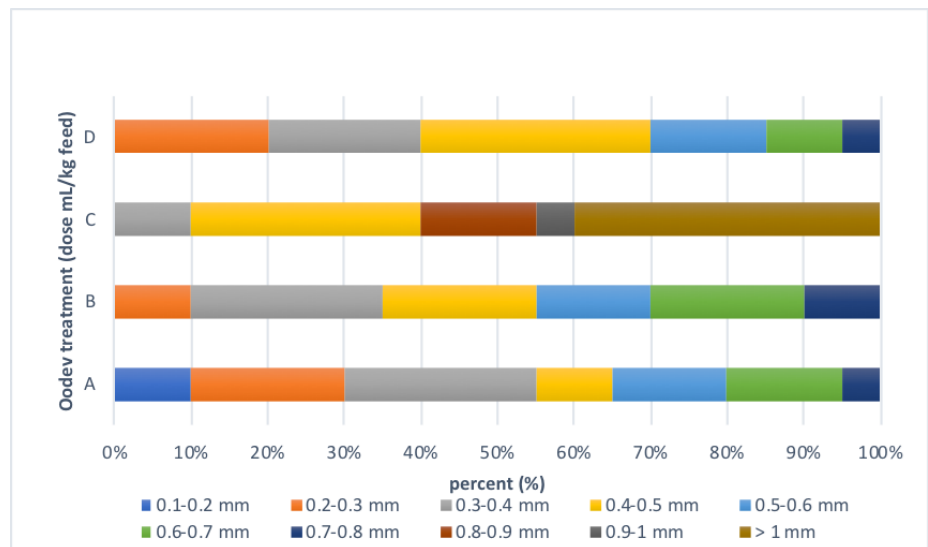


Figure 8. Percentage diameter of Yellow rasbora (*Rasbora lateristriata*) eggs in Oodev treatments: A. Feed without Oodev; B. 0.5 mL/kg feed; C. 1.0 mL/kg feed; and D. 2.0 mL/kg feed.

Figure 8 shows the percentage of egg diameter measurement in treatment C with a diameter of > 0.8 mm which is 60% and the percentage of egg diameter < 0.5 mm is 40%. In treatment B there were no eggs measuring > 0.8 mm, only 10% in this treatment had egg diameters ranging from 0.7 to 0.8 mm, and 55% with a measured diameter of < 0.5 mm. The same results were shown in treatments A and D, that is, there were no eggs with a size > 0.8 mm and only 5% of eggs with a diameter of 0.7–0.8 mm. It is shown that egg diameter in treatment C is proportional to the previously confirmed GML, GSI, and fecundity values obtained in this study. This is also relevant to Farida et al. (2019) that confirm the higher the level of gonad maturity, the larger the diameter of the eggs in the ovaries of *Helostoma teminckii*.

CONCLUSIONS

Administration of Oodev can accelerate the gonad maturation process for female Yellow rasbora (*Rasbora lateristriata*) and improve reproductive performance. Administration of Oodev at a dose of 1.0 mL/kg of feed is the most effective dose for optimizing gonadal maturity, this is evidenced by the highest results for all parameters, namely: gonads in GML IV phase, histological structure of the ovary showing dominance in the oocyte maturation phase, gonadosomatic index (GSI) 14.01%, 721 egg fecundity and an average egg diameter of 0.865 mm.

AUTHOR CONTRIBUTION

All authors have equal contributions to the research and publication. J.R., S.W., and B.R. wrote the manuscript. J.R. designed the study, observed, and collected broodstock of the research samples from the Center Development of Fisheries Technology, Cangkringan, Sleman Jogjakarta. S.W. and B.R. supervised all the processes from the field work to laboratory analysis.

ACKNOWLEDGMENTS

First, the author would like to thank to Gadjah Mada University, Faculty of Biology, Laboratory of Animal Structure and Development for assisting the facilities belonging to this research. Secondly, thank the Center Development of Fisheries Technology, Cangkringan, Sleman Jogjakarta for providing the broodstock in this research. This manuscript is part of Juniman Rey's thesis for the Biology Master's Program, Faculty of Biology, Gadjah Mada University.

CONFLICT OF INTEREST

The authors state that they do not have any conflicts of interest from this manuscript. The authors are solely responsible for the article content and writing.

REFERENCES

- Alavi, S.M.H. et al., 2009. Sperm quality in male *Barbus barbus* L. fed different diets during the spawning season. *Fish Physiol Biochem*, 35 (4), pp.683–693. doi: 10.1007/s10695-009-9325-7.
- Arfah, H., 2018. Perbaikan Kinerja Reproduksi Ikan Patin (*Pangasianodon Hypophthalmus*) Dengan Pemberian Kombinasi Hormon Pmsg + Antidopamin, Vitamin E, Dan Kunyit (*Curcuma Longa*) Melalui Pakan. *Institut Pertanian Bogor*.
- Costa, E.F.D.S., 2015. Reproductive Strategies of Marine Fishes From the Southwest Atlantic Ocean : Application of. *Uni*.
- Dadzie, S & Wangila, B.C.C., 1980. Reproductive biology, length-weight relationship and relative condition of pond raised *Tilapia zilli* (Gervais). *Journal of fish Biology*, 17(3), pp.243–253. doi: 10.1111/j.1095-8649.1980.tb02758.x.
- Darliansyah, R., Rahimi, S.A. & Hasri, I., 2017. Induksi Hormon Pregnant Mare Serumgonadotropin (Pmsg) Dengan Dosis Yang Berbeda Terhadap Pematangan Gonad Ikan Peres (*Osteochilus kapeni*). *Jurnal Ilmiah Mahasiswa Kelautan dan Perikanan Insyiah*, 2(2), pp.286–294.
- Dhewantara, Y.L. & Rahmatia, F., 2017. Rekayasa Maturasi Menggunakan Hormon Oodev Terhadap Ikan *Synodontis* (*Synodontis* Sp). *Akuatika Indonesia*, 2(1), 35. doi: 10.24198/jaki.v2i1.23409.
- Effendie, M.I., 1997. *Metode biologi perikanan*, Yayasan Pustaka Nusantara, Yogyakarta.
- Erkmen, B. & Kirankaya, Ş.G., 2016. A preliminary histological study on ovarium development in mirror carp and scaled carp (*Cyprinus carpio* L., 1758) introduced into gelingüllü reservoir, turkey. *Journal of Aquaculture Engineering and Fisheries Research*, 2(4), pp.185–192. doi: 10.3153/JAEFR16020.
- Farida et al., 2019. Addition of fertilize flour and Oodev in feed to prove gonad parking of fish biawan (*Helostoma temminkii*). *Jurnal Ruaya : Jurnal Penelitian dan Kajian Ilmu Perikanan dan Kelautan*, 7(1), pp.17–27. doi: 10.29406/jr.v7i1.1314.
- Gallego, V. et al., 2012. Study of the effects of thermal regime and alternative hormonal treatments on the reproductive performance of European eel males (*Anguilla anguilla*) during induced sexual maturation. *Aquaculture*, 354–355, pp.7–16. doi: 10.1016/j.aquaculture.2012.04.041.
- Gomez, A. A., & Gomez, K.A., 1995. *Prosedur statistik untuk penelitian pertanian*, Jakarta: UI Press.

- Hutagalung, R.A., 2015. Effectiveness of PMSG against reproduction status of parent female snakehead fish (*Channa Striata*). *Universitas Brawijaya, Malang*.
- Johnson, R.W.J. & Braunbeck, T., 2009. OECD Guidance document for the diagnosis of endocrine-related histopathology of fish gonads. *OECD Environment, Health and Safety Publications, Series on Testing and Assessment*, 123, pp.1–42.
- Mellisa, S., Hasri, I. & Ramdayani, K., 2022. Induction of oocyte developer hormones (oodev) on the maturity of *Poropuntius tawarensis*. *E3S Web of Conferences*, 339, 01009.
- Menke, A.L. et al., 2011. Normal Anatomy and Histology of the Adult Zebrafish. *Toxicologic Pathology*, 0192623311, pp.759–775. doi: 10.1177/0192623311409597.
- Natalia, D., 2018. Analisis Hormon Estradiol dan Fekunditas Ikan Wader Pari (*Rasbora Lateristriata* Bleeker, 1854) Yang Dipelihara Pada Kondisi Lingkungan Berbeda. *Universitas Gadjah Mada*.
- Nugraha, A.D., 2014. Induksi Pematangan Gonad Ikan Patin Siam Pangasianodon Hypophthalmus Secara Hormonal Menggunakan Oodev Melalui Pakan Selama 4 Minggu. *Institut Pertanian Bogor*.
- Nur, B., Cindelaras, S. & Meilisza, N., 2017. Induced maturation of chocolate gourami (*Sphaerichthys osphromenoides* Canestrini, 1860) using pregnant mare serum gonadotropin (PMSG) and antidopamin hormones. *Jurnal Riset Akuakultur*, 12(1), pp.69–76. doi: 10.15578/jra.12.1.2017.69-76.
- Pamungkas, W. et al., 2019. Induction of ovarian rematuration in striped catfish (*Pangasianodon hypophthalmus*) using pregnant mare serum gonadotropin hormone in out-of spawning season. *AACL Bioflux*, 12(3), pp.767–776.
- Prakasa, B.L., 2020. Pengaruh Amputasi Berulang dan Perlakuan Suhu Terhadap Regenerasi Sirip Kaudal dan Kematangan Gonad Ikan Wader Pari (*Rasbora Lateristriata* Bleeker, 1854). *Universitas Gadjah Mada*.
- Puspitasari, C.D., 2016. Perkembangan Gonad Ikan Wader Pari (*Rasbora Lateristriata* Bleeker, 1854). *Universitas Gadjah Mada*.
- Putra, W.K.A., Handrianto, R. & Razai, T.S., 2017. Maturasi Gonad Bawal Bintang (*Trachinotus blochii*) dengan Induksi Hormon Human Chorionic Gonadotropin (hCG) dan Pregnant Mare Serum Gonadotropin (PMSG) Maturation of the Silver Pompano (*Trachinotus blochii*) Gonad by Hormon Human Chorionic Gonadotr. *Jurnal Perikanan Universitas Gadjah Mada*, 19(2), pp.75–78. doi: doi.org/10.22146/jfs.28790.
- Rahmawati, S., 2014. Indeks gonadosomatik dan struktur histologis gonad ikan wader pari (*Rasbora lateristriata* Bleeker, 1854) pada tahap perkembangan pra dewasa dan dewasa. *Universitas Gadjah Mada*.
- Retnoaji, B., Nurhidayat, L. & Husni, A., 2017. Cultivation and Conservation of Indonesian Native Fish (*Rasbora lateristriata*) Through Fish Farmer Group Empowerment in Yogyakarta. *Proceeding of the 1st International Conference on Tropical Agriculture, Springer, Cham.*, pp.475–482. doi: 10.1007/978-3-319-60363-6_50
- Rey, J., 2022. Status Reproduksi Induk Betina Ikan Wader Pari (*Rasbora Lateristriata* Bleeker, 1854) Setelah Pemberian Oodev Melalui Pakan. *Universitas Gadjah Mada*.
- Setiowibowo, C., 2019. Kombinasi Induksi Hormon PMSG, Antidopamin, Kunyit dan Kuda Laut Pada Pakan Terhadap Reproduksi Ikan *Botia Chromobotia Macracantus*. *Institut Pertanian Bogor*.

- Suryanti, A. et al., 2015. Reproductive Biology of Female Bilih Fish (*Mystacoleucus padangensis* Bleeker 1852) in Naborsahan River Toba Lake, North Sumatera, Indonesia. *Asian Journal of Developmental Biology*, 8(1–3), pp.1–10. doi: 10.3923/ajdb.2016.1.10.
- Susilo, W., Farida & Lestari, T.P., 2019. Effects of addition of Oodev in feed to the diameter of the eggs and pregnancy rates on the parent fish biawan (*Helostoma temminckii*). *Jurnal Borneo Akuatika*, 1 (April), pp.7–17.
- Tomasoa, A.M., Azhari, D. & Balansa, W., 2018. Growth, survival and development of the ovaries of Yellow rasbora pari fish (*Rasbora lateristriata* Bleeker, 1854) in different stocking densities. *Jurnal Teknologi Perikanan dan Kelautan*, 9(2), pp.163–168. doi: 10.24319/jtpk.9.163-168.
- Zulfadhli, Wijayanti, N. & Retnoaji, B., 2016. The development of ovarian Yellow rasbora pari fish (*Rasbora lateristriata* Bleeker, 1854): histological approach. *Jurnal Perikanan Tropis*, 3(1), pp.32–39. doi: 10.35308/jpt.v3i1.34.
- Zulfadhli, 2015. Pertumbuhan, Sintasan dan Perkembangan Ovarium Ikan Wader Pari (*Rasbora Lateristriata* Bleeker, 1854) Pada Padat Tebar Berbeda. *Universitas Gadjah Mada*.

Research Article

Bioremediation of Mercury- Polluted Water in Free Water Surface-Constructed Wetland System by *Euglena* sp. and *Echinodorus palifolius* (Nees & Mart.) J.F. Macbr.

Dwi Umi Siswanti¹, Budi Setiadi Daryono¹, Himawan Tri Bayu Murti Petrus², Eko Agus Suyono^{1*}

1)Department of Tropical Biology, Faculty of Biology, Universitas Gadjah Mada, Jl. Teknika Selatan Sekip Utara, Yogyakarta 55281, Indonesia

2)Department of Chemical Engineering (Sustainable Mineral Processing Research Group), Faculty of Engineering, Universitas Gadjah Mada, Jalan Grafika No. 2, Yogyakarta 55281, Indonesia

* Corresponding author, email: eko_suyono@ugm.ac.id

Keywords:

Anatomy

Euglena

Echinodorus palifolius

FWS-CW

growth

Submitted:

19 August 2023

Accepted:

30 November 2023

Published:

13 December 2023

Editor:

Furzani Binti Pa' ee

ABSTRACT

Mercury accumulation in the aquatic environment can be highly harmful. The body takes mercury vapor through the lungs, then absorbs mercury metal through the digestive system, and then the blood carries the metal to the brain. Bioremediation is the process of breaking down or converting harmful compounds into non-toxic forms, which can be accomplished through phytoremediation or phycoremediation. The goal of this study was to examine the growth and anatomy of *Euglena* sp. after being cultured in the mercury-containing FWS-CW waste treatment system. The ability of *Euglena* sp. and *Echinodorus palifolius* to bioremediate mercury at different concentration as well as association and non-association treatments. This study was carried out in a bioreactor known as FSW-CW (Free Water Surface-Constructed Wetlands). Plant growth (plant height and number of leaves), chlorophyll content, diameter of root and petiole, metaxylem diameter of root, petiole, and leaves, cortical thickness of root and leaves, and petiole anatomy were all measured. Water temperature, pH, salinity, and light intensity were all measured as environmental parameters. Mercury treatment reduced *Euglena* density (183.5 cells. mL⁻¹10³ in control and 12.6 cells. mL⁻¹10³ in 100 ppm mercury treatment) and number of *E. palifolius* leaves, but not plant height and chlorophyll. Root and petiole diameters were affected by the mercury treatment, petiole diameter decreased unless the concentration was 100 ppm, whereas root diameter actually increased. The diameter of the root metaxylem increased, but the petioles and leaves, as well as the thickness of the root cortex, did not provide a significant response. The growth of *E. palifolius* was still optimal in the presence of *Euglena* in mercury-containing medium.

Copyright: © 2023, J. Tropical Biodiversity Biotechnology (CC BY-SA 4.0)

INTRODUCTION

Heavy metals and metalloids including mercury are known to be extremely poisonous and carcinogenic, which puts human health and ecological variety at serious risk (Leong & Chang 2020; Tripathi & Poluri 2021) Hg metal will accumulate in the environment and can precipitate and form complex compounds with organic and inorganic materials. Mercury can accumulate in the environment and contribute to global mercury pollution (Al-Sulaiti et al. 2022). Humans are exposed to mercu-

ry both directly and indirectly. Direct exposure occurs when mercury vapor (HgO) oxidises in the atmosphere or when mercury metal (MeHg^+) forms. Inorganic mercury ions (Hg^{3+}) are another kind of mercury exposure. The body takes mercury vapor through the lungs, then it absorbs mercury metal through the digestive system and then the blood, which carries the metal to the brain. One effort to overcome mercury pollution is phytoremediation (Ekawanti & Krisnayanti 2015; Abad et al 2016; Krisnayanti & Probiyantono 2020). Heavy metals will be degraded in plant tissue (Dixit et al. 2015) or evaporates through the transpiration process into the atmosphere (Kumar et al. 2023). Phytoremediation using the constructed wetlands method which utilises media and plants as a way to reduce pollutant levels is an alternative for dealing with environmental pollution (Metcalf 2003; Bilgaiyan 2023). Prasetya et al. (2020) showed a decrease in mercury in the water media given by *E. palifolius* and zeolite in the SSF-CW (Subsurface-Constructed Wetlands) waste treatment system. *E. palifolius* or water jasmine is an ornamental plant that can live in various seasons and is able to act as a pollutant reducer by expanding the area of microorganisms on the roots and forming an oxygen-rich rhizosphere zone (Sari et al. 2018). *E. palifolius* can reduce the phosphate content by 93.81% in the Free Water Surface-Constructed Wetlands (FWS-CW) system (Prasetya et al. 2020). FWS-CW system utilises surface water flow and interactions between vegetation and bio-film bonds in the water phase through microbial degradation, filtration, and sedimentation. The Subsurface Flow System drains wastewater horizontally through granular media and passes through contact with aerobic, anoxic, and anaerobic zones on the surface (Knight et al. 2000; Vymazal 2013; Stefanakis et al. 2014).

As of now, thermal treatment and capping and dredging have been used to reduce mercury levels in the environment, which is the best method for minimising mercury contamination in aquatic systems (Wang et al. 2004; Kumar et al. 2023). However, these methods are quite expensive. Solitary algae and *Cryrtomium macrophyllum*, which have high resistance to mercury are still being used in efforts to develop mercury clean up agents. No species that can behave as hyperaccumulators have been discovered, despite efforts to improve Hg solubility by adding chelators like potassium iodide, sodium thiosulfate, and ammonium thiocyanate (Xun et al. 2017). Due to low biomass, delayed phytoremediation processes, and slow plant development, heavy metal hyperaccumulators are hard to detect (Singh et al. 2021).

Algae can regenerate quickly and high biomass (Devars et al. 2000; Majid et al. 2014). *Euglena* can convert Hg^{2+} to Hg^0 with mercury reductase activity. Estimates of the biological evaporation rate of Hg^{2+} range from 0.7 to 4 nmol (10^6 cells/hour) (Rodriguez-Zavala et al. 2007). *E. gracilis* wild type (Z-strain) and *E. gracilis* var. saccharophila (B-strain) tolerates and accumulates heavy metals up to 1000 ppm Pb, 600 ppm Cd, and 80 ppm Hg. The mechanism of *E. gracilis* to tolerate and to absorb heavy metals involves the adsorption of metal ions to the cell wall or intracellular binding to thiol compounds and finally accumulating in chloroplasts, mitochondria, and cytoplasm for detoxification (Moreno-Sanches et al. 2017). Algae have a significant contribution in removing heavy metals from solution (Danouche et al. 2021). Microalgae can also be used as a potential reservoir for removing toxic heavy metals such as lead (Pb), mercury (Hg), cadmium (Cd) and arsenic (As) (Kumar et al. 2018). Bioremediation using mercury (Hg)-volatilising and immobilising bacteria is an eco-friendly and cost-effective strategy for Hg-polluted farmland (Chang et al. 2022)

Plants can reduce metal uptake by exuding organic acids such as citric, malic and oxalic exudate which chelate metal ions in the soil. Water-soluble mercury (Hg^+ , Hg^{2+}) is often retained by cell wall components. In root apoplastic transport, Hg^{2+} can bind to oxygen-containing molecules, such as organic acids or sulphur-rich proteins in the cell wall, such as extension and expansions (Shah et al. 2021). This study is innovative in the way it employs groups of higher plants (*E. palifolius*) and algae (*Euglena* sp.) to remove mercury from the Free Water Surface-Constructed Wetlands (FWS-CW) waste treatment system. The strain of *Euglena* utilised is IDN 28. *Euglena* sp. solitary has been proven to remediate mercury, as has *E. palifolius*. These two types of living creatures are associated with reducing the concentration level of mercury in water. *E. palifolius* can chelate toxicants, while algae can absorb metals (Ubando et al. 2021). So, the association of the two is expected to have a better impact on heavy metal remediation. The purpose of this study was to analyse the growth of *Euglena* sp. and anatomy of leaves, petiole and roots of *E. palifolius* after being grown in the mercury-containing FWS-CW waste management system and mercury content in chloroplasts of *Euglena* sp.

MATERIALS AND METHODS

Materials

Materials used in this research were *Euglena* culture, *E. palifolius*, *Euglena* sp. strain IDN 28 mono-culture obtained from Nogotirto Algae Park (microalgae cultivation at Yogyakarta, Indonesia) while *E. palifolius* was obtained from rice fields in Bantul, Yogyakarta, Indonesia which had been acclimatised before treatment.

Methods

Medium preparation and mercury treatments

Euglena sp. was cultivated in regular mass cultivation medium with 5 salinity treatments for 18 days. The mercury level used in the study was 0, 25, 50, 75 and 100 ppm, respectively. The justification of mercury was carried out by Hg_2Cl addition. Before cultivating *Euglena* sp., CM medium was made into 1 liter of distilled water. Composition of CM medium was : $(\text{NH}_4)_2\text{SO}_4$, KH_2PO_4 , $\text{MgSO}_4 \cdot 7\text{H}_2\text{O}$, $\text{CaCl}_2 \cdot 2\text{H}_2\text{O}$, $\text{Fe}_2(\text{SO}_4)_3 \cdot 7\text{H}_2\text{O}$, $\text{MnCl}_2 \cdot 4\text{H}_2\text{O}$, $\text{CaSO}_4 \cdot 7\text{H}_2\text{O}$, $\text{ZnSO}_4 \cdot 7\text{H}_2\text{O}$, $\text{CuSO}_4 \cdot 7\text{H}_2\text{O}$, $\text{Na}_2\text{MoO}_4 \cdot 2\text{H}_2\text{O}$, Vitamin B1, Vitamin B12, H_2SO_4 . *Euglena* sp. grown in CM medium under light intensity conditions of 2000 lux (Khatiwada et al. 2020). The culture was placed at a temperature of 25°C, and aerator circulation was carried out at a speed of 150 rpm.

The treatment used in the study were E1 (*Euglena* sp. with 0 ppm mercury), E2 (*Euglena* sp. with 25 ppm mercury), E3 (*Euglena* sp. with 50 ppm mercury), E4 (*Euglena* sp. with 75 ppm mercury), E5 (*Euglena* sp. with 100 ppm mercury), P1 (*Euglena* sp. and *E. palifolius* with 0 ppm mercury), P2 (*Euglena* sp. and *E. palifolius* with 25 ppm mercury), P3 (*Euglena* sp. and *E. palifolius* with 50 ppm mercury), P4 (*Euglena* sp. and *E. palifolius* with 75 ppm mercury), and P5 (*Euglena* sp. and *E. palifolius* with 100 ppm mercury) based on previous study.

Growth measurement

The number of *Euglena* sp. was counted using a manual cell counting method with a modified haemocytometer (Suyono et al. 2015). *Euglena* sp. cell culture was homogenised and then taken as much as 900 microliters. The sample was then put into a 2 mL microtube and added with 100 microliters of 70% alcohol. The sample was then placed on a 1mm

Neubauer haemocytometer and observed under a light microscope, then the image in the microscope was observed with Optilab. After the image from the optilab was saved, the number of cells in the sample was counted. The cells counted were in the five medium boxes in the large box in the middle of the haemocytometer section. The parts of the medium box that were measured are the top right and left corners, the bottom right and left corners, and the middle. After obtaining the calculation results, they were then entered into the formula. Measurements were taken on day 9th. The calculation of specific growth rate of *Euglena* sp. was using specific growth rate formula:

Number of cells (cells/mL) = the measurement result x 5 x 10⁴ sel/mL (Suyono et al. 2015). During treatment, measurements of the plant's height of *E. palifolius*, number of leaves were taken on day 18th.

Anatomy Measurements

Anatomical preparations were made using the paraffin method using Johansen's protocol (1940). Samples were sliced with a rotary microtome with a thickness of 6-12µm. The preparations were dried on a hot plate at 45°C until Canada balsam was dry. Observations made with the aid of an optilab-equipped light microscope. Measurements were made with the Image Ruster application. The parameters measured were root, petiole and leaf metaxylem diameters, root and petiole diameters and root and leaf cortex thickness.

ANOVA was used to assess growth data for *Euglena* sp. and *E. palaeifolius* with a 95% confidence level, followed by the DMRT test (for quantitative data) with software IBM SPSS 2.0 and Graphpad Prims 10.

RESULTS AND DISCUSSION

The Environment Parameter

Environmental parameters measured include temperature, salinity, pH and light intensity. The average daily temperature is 32.4°C (Table 1 and 2) The average intensity of sunlight is 3,568 lux taken at 10.00 am. All treatment has not significantly different temperature and intensity of light.

The salinity of treatment E1 (control treatment *Euglena* sp.) was quite high and differ from E2, E3, E4 and E5. (p < 0.05) (Table 2) Meanwhile, the association *Euglena* sp. and *E. palifolius* for mercury in P1, P2 and P3 treatments showed almost the same salinity but not in P4 and P5. The pH of the water in all treatments showed acidic conditions or low pH, both remediation with *Euglena* alone and the association of *Euglena* with *E. paleifolius*. All treatment has not significantly different pH. This means that the optimum pH for the life of *Euglena* sp. fulfilled. In con-

Table 1. The environment parameter in FWS-CW reactor with *Euglena* sp.

Concentrations of HgCl ₂ treatment	E1	E2	E3	E4	E5
Water temperature (°C)	31.7 ^a ±2	32.4 ^a ±1.5	32.7 ^a ±1.5	32.6 ^a ±1.5	32.5 ^a ±1.5
Salinity (ppm)	1149 ^b ±325	660 ^a ±299	438 ^a ±228	601 ^a ±43	650 ^a ± 77
pH	1.5 ^a ±0.5	1.8 ^a ±0.2	1.9 ^a ±0.2	1.9 ^a ±0.2	1.8 ^a ±0.5
Light intensity (lux)	3355 ^a ±1,958	2646 ^a ±756	2750 ^a ±964	3064 ^a ±1,060	3468 ^a ±1,457

Note: E1, E2, E3, E4, and E5 please see Method section, medium preparation and mercury treatments. Different superscript letters above number indicate significant (p<0.05) difference.

Table 2. The environment parameter in FWS-CW reactor with *E. palifolius* and *Euglena* sp.

Concentrations of HgCl ₂ treatment	P1	P2	P3	P4	P5
Water temperature (°C)	32.2 ^a ±1.7	32.6 ^a ±1.6	32.6 ^a ±1.6	32.4 ^a ±1.6	32.8 ^a ±1.8
Salinity (ppm)	652 ^a ±85	599 ^a ±172	650 ^a ±275	1025 ^b ±68	1128 ^b ±273
pH	1.9 ^a ±0.7	2 ^a ±0.8	2.3 ^a ±1.05	1.6 ^a ±0.4	1.5 ^a ±0.04
Light intensity (lux)	3884 ^a ±2728	2967 ^a ±1,516	3449 ^a ± 1,560	3752 ^a ±1658	3752 ^a ± 2767

Note: P1, P2, P3, P4, and P5 please see Method section, medium preparation and mercury treatments. Different superscript letters above number indicate significant (p<0.05) difference.

trast to the other pH settings, *Euglena* sp. exhibited the maximum growth rate at pH 3.5 (Nurafifah et al. 2023).

The growth rate of *Euglena*

The growth pattern of *Euglena* sp. in the mercury treatments of 0 ppm, 25 ppm, 50 ppm, 75 ppm and 100 ppm is presented in Figure 1.

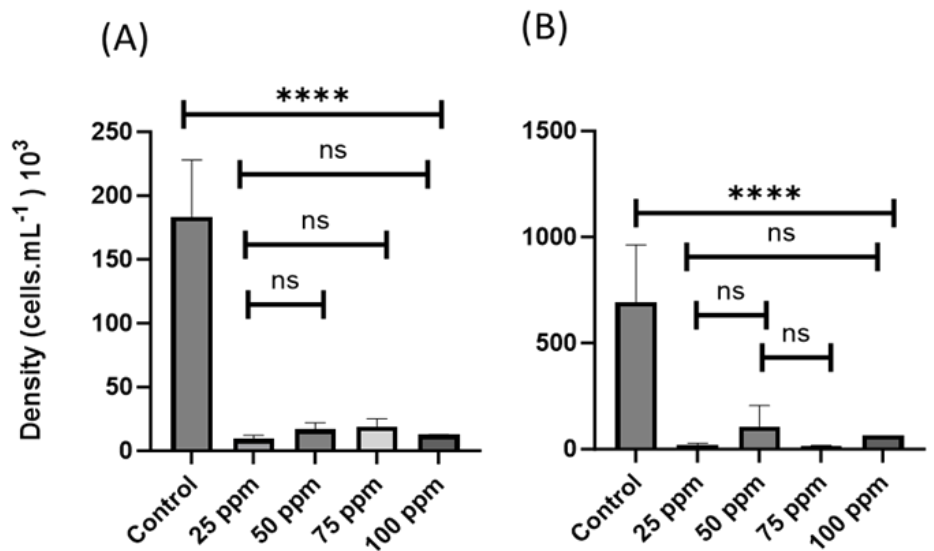


Figure 1. Density of *Euglena* sp. (A) and density of *Euglena* sp. in association with *E. palifolius* (B) in FWS-CW reactor on day 9th. Note: ****= significant (p<0.05) difference. Ns= no significant difference.

Euglena's density was highest in control *Euglena* and *Euglena* association with *E. palifolius*. However, the density of *Euglena* in the P4 treatment (75% mercury treatment in the *Euglena* and *E. palifolius* association) was higher than the other mercury treatments).

Based on Figure 1B. *Euglena*'s density was highest in controls (P1) and P3 showed the highest density among other mercury treatments. This shows that *Euglena* is able to survive in high concentrations of mercury with the association of *E. palifolius*. This is possible because *Euglena* is able to convert Hg²⁺ to Hg⁰ with mercury reductase activity (Khatiwada et al. 2020). The estimation of the biological evaporation rate of Hg²⁺, range from 0.7 to 4 nmol (10⁶ cells/hour) (Rodriguez-Zavala et al. 2007). *E. gracilis* wild type (Z-strain) and *E. gracilis* var. saccharophila (B-strain) tolerates and accumulates beat metals up to 1,000 ppm Pb, 600 ppm Cd and 80 ppm Hg. The mechanism of *E. gracilis* to tolerate and absorb heavy metals involves adsorption of metal ions to the cell wall or intracellular binding to thiol compounds and finally accumu-

lation in chloroplasts, mitochondria and cytoplasm for detoxification. (Moreno-Sanches et al. 2017; Hader & Hemmersbach 2022). Algae have a significant contribution in removing heavy metals from solution (Danouche et al. 2021). Carboxyl, hydroxyl, sulphate and amino groups containing elements O, N, S, P, play a direct role in the binding of heavy metal ions (Rangabhashiyam & Balasubra-Manian 2019; Danouche et al. 2021). The ability to photosynthesise, motility abilities, and stress-sensitive *Euglena* pigments (heavy metals, salinity and toxins) are the reasons for the ease of bioassay measurements on algae (Ahmed & Hader 2010). The IAA hormone synthesised from the roots of *E. palifolius* can influence the growth of *Euglena* (Hakim et al. 2023).

The addition of mercury treatment aims to determine whether the microalgae can be resistant to the stress in their surroundings. Heavy metals such as mercury are one of the heavy metals that are produced by human activities today. Microalgae are very sensitive to this substance, and their growth rates and biological macromolecules will undergo physiological and biochemical changes due to the influence of heavy metals. Based on the hormesis phenomenon, low mercury concentrations can stimulate the growth and metabolism of microalgae. That way even though there is exposure to heavy metals, microalgae can still grow but with a note that heavy metals are used on a small scale (Abdelfattah et al. 2023). The ability of algae to grow and develop under stressful conditions has also been reported by Rangkuti et al. (2023) that under salinity stress conditions of 10 ppm, *Spirulina* grew after the 10th day.

The Growth of *E. palifolius*

The number of leaves (Figure 2A) of *E. palifolius* control remained the highest. Meanwhile, all mercury treatments showed no significant difference in the number of leaves. This indicates a substantial effect of mercury stress on the number of *E. palifolius* leaves within 18 days of treatment. The plant height of *E. palifolius* (Figure 2B) at 25 and 50 ppm mercury treatment was not significantly different with control but not with the 75 and 100 ppm treatments. This shows that the high growth of *E. palifolius* is still tolerant to mercury at concentrations of 25 and 50 ppm. This is possible because *E. palifolius* can neutralise mercury from water. One of the biological mechanisms of metal hyperaccumulation is through the interaction of the rhizosphere, namely the process of interaction of plant roots with the planting medium (soil and water). Hyperaccumulator plants can dissolve metal elements in the rhizosphere and absorb metals, so that the absorption of metals by hyperaccumulator plants exceeds that of normal plants (McGrath et al. 1997; Fu et al. 2021; Shah et al. 2021).

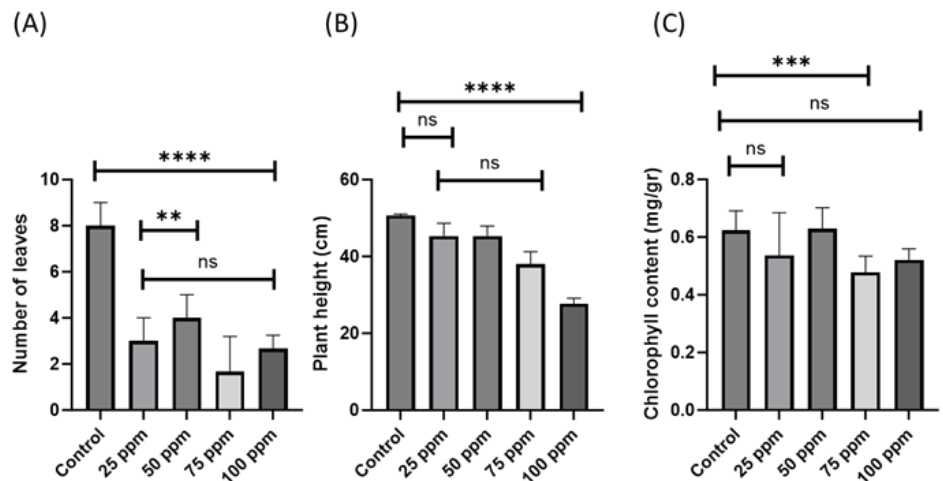


Figure 2. Number of leaves (A), plant height (B), and chlorophyll content of *E. palifolius* in mercury treatments on day 18th (C). Note: ****= significant ($p < 0.05$) difference. Ns= no significant difference.

There is no significant difference in the total chlorophyll content in *E. palifolius* (Figure 2C) in treatment and control. Evidence that the chlorophyll content was not significantly different between the control and the treatment showed no effect of mercury treatment on the chlorophyll content of *E. palifolius* leaves. The heavy metal stress can substitute Mg ions inside the chlorophyll structure. (Yan & Hao 2018). Unlike carotenoids, the emphasis on the excess antioxidant capacity of carotenoids can cause a decrease in carotenoids. It can cause the carotenoid structure to be damaged by toxic ion pressure (Zamani-Ahmadmahmoodi et al. 2020; Indahsari et al. 2022). However, in contrast to *Spirulina*, carotenoids increased at a salinity of 10‰-30‰ (Rangkuti et al. 2023). The contents of carotenoid were higher than total chlorophyll (Gojkovic et al. 2022).

The diameter of petiole (Figure 3A) of *E. palifolius* in the 100 ppm mercury treatment actually had the largest diameter (0.15 μm), while control had 0.08 μm and treatment 25 ppm mercury had 0.1 μm diameter of petiole. The diameter of the petiole in the 100 ppm treatment was not significantly different from the control but significantly different from the other treatments. This shows that the 100 ppm treatment encouraged *E. palifolius* plants to spread their petioles. Figure 4 clearly shows the petiole aerenchyma treated at 100 ppm broader. This aerenchyma is used by plants in addition to being able to stay afloat and provide air supply for respiration; it is also used to store mercury that plants have absorbed.

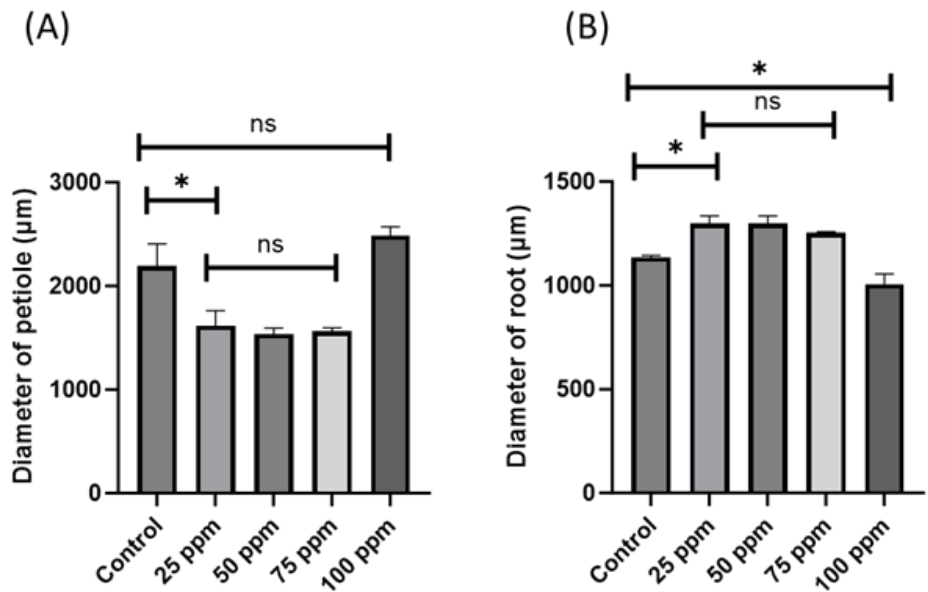


Figure 3. Diameter of petiole (A) and diameter of root of *E. palifolius* in mercury treatments on day 18th (B). Note: *= significant ($p < 0.05$) difference. Ns= no significant difference.

The diameter of root (Figure 3B) in the 25, 50, and 75 ppm of mercury treatments was larger than the control (*Euglena* and *E. palifolius* association). There is a kind of root mechanism to counteract the pollutant in the form of mercury, so that at high concentrations the roots grow stretched rapidly as happened with transgenic tobacco (Hussein et al. 2007) and stem of *E. palifolius* (Wardana et al. 2023).

Anatomy of the rhizome of *Echinodorus* sp. those grown in aquatic systems showed vascular cylinders containing xylem and phloem cells. In contrast, those produced in terrestrial systems showed cortex with air gaps and amyloplasts with parenchyma cells in the cortex and the centre cylinder. Anatomy of the trunk of *Echinodorus* sp. those that grow on the ground are very similar to *Echinodorus* sp. those that grow in water. The rhizome has a cortex formed by aerenchyma with little space between cells. The central cylinder is of the atactostele type, transport bundles distributed randomly on the stele (Claro et al. 2009).

The petiole anatomy of *E. palifolius* in media containing 25, 50, 75, and 100 ppm of mercury appeared to have an anomaly, there is an accumulation of mercury inside the epidermis and around the metaxylem (Figure 4). It can be seen that the cells that make up the transport bundles in the control treatment are much larger and rounder than the other treatments, whereas in the P5 treatment, the cells that make up the transport bundles are smaller.

The root diameter (Figure 3A) corresponds to the root metaxylem diameter, indicating that metaxylem growth promotes root diameter enlargement. The diameter of the roots of *E. palifolius* in the treatment of mercury 25.50 and 75 decreased but increased again at a high concentration of 100 ppm. The high mercury concentration encourages metaxylem to increase in diameter to absorb mercury and store it in cell organelles (Marrugo-Negrete et al. 2015).

The petiole diameter (Figure 3A) decreased at concentrations of 25, 50, and 75 and increased at a concentration of 100 ppm, which was inconsistent with the metaxylem petiole diameter because the petiole diameter was supported by the growth of aerenchyma used as a mercury reservoir (Figure 5). Plants that are submerged and in anoxic environments will change in terms of morphology and anatomy. They will, specifically, have a lot of aerenchyma (Yuan et al. 2022).

Under stress conditions on heavy metals, aquatic plants such as *E. palifolius* will experience anatomical changes, mainly in the roots. This condition is due to the role of the heart of the first gate of defence against pollutants. This anatomical difference can be seen in the diameter of the metaxylem and the thickness of the cortex. The cortical cells of stressed aquatic plants will show an increase. The aerenchyma of aquatic plant roots experienced a significant increase in heavy metal stress and metaxylem. This condition is an attempt by plants to accumulate heavy metals, so they do not enter further and become toxic to plants (Batool et al. 2014; Napaldet et al. 2019; Li et al. 2023).

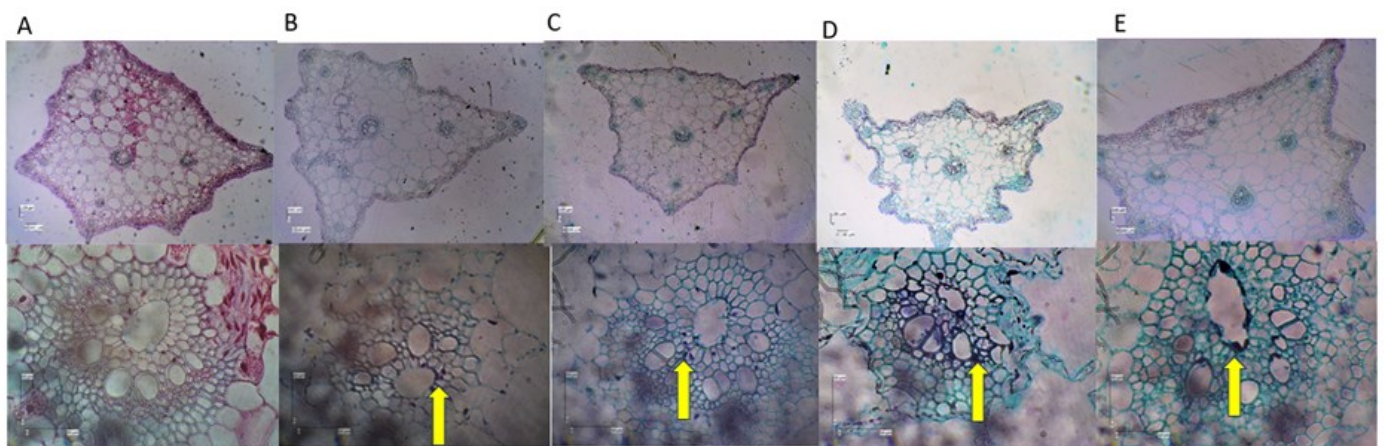


Figure 4. Anatomy of petiole (upper) and petiole metaxylem (lower) of *E. palifolius* after being exposed to mercury for 18 days Notes: (A)=control, (B) = 25 ppm, (C) = 50 ppm, (D) = 75 ppm, (E) 100 ppm (100 times magnification).

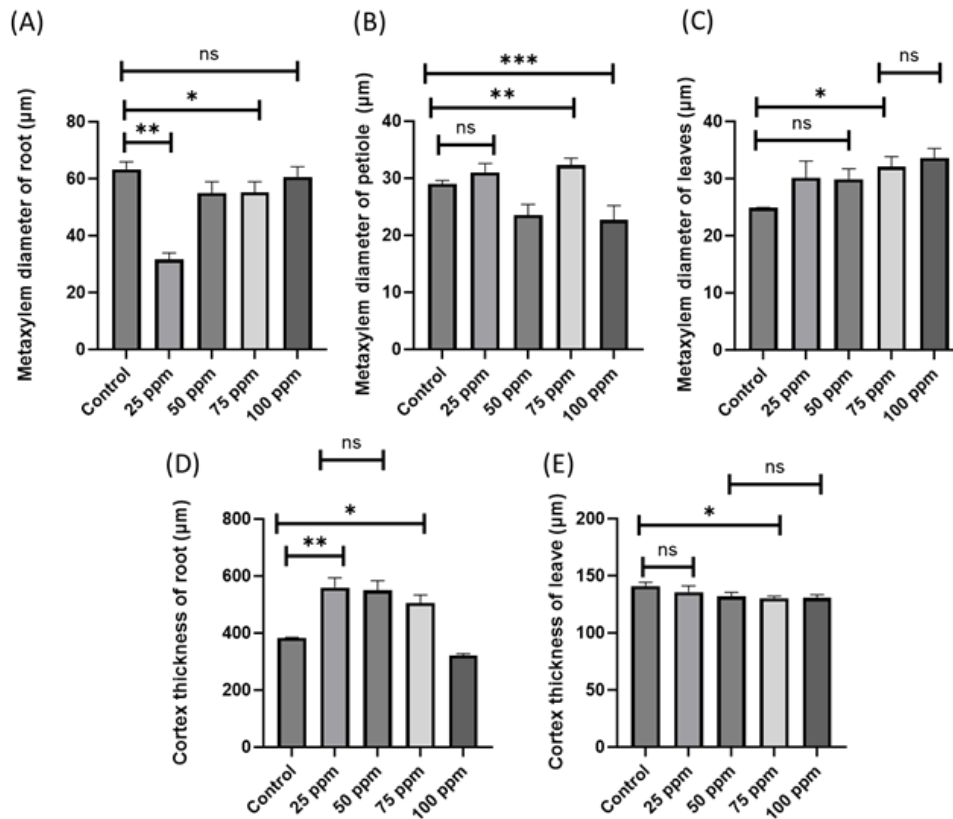


Figure 5. Metaxylem diameter of root (A), petiole (B), leaves (C), cortex thickness of root (D) and cortex thickness of leaf (E) *E. palifolius* in mercury treatments on day 18th. Note: *= significant ($p < 0.05$) difference. Ns= no significant difference.

CONCLUSION

Mercury treatment reduced *Euglena* sp. density and number of *E. palifolius* leaves, but not plant height and chlorophyll. Root and petiole diameters were affected by the mercury treatment, petiole diameter decreased unless the concentration was 100 ppm, whereas root diameter actually increased. The diameter of the root metaxylem increased, but the petioles and leaves, as well as the thickness of the root cortex, did not provide a significant response. Growth of *E. palifolius* was still able to grow optimally on condition of association with *Euglena* sp. in media containing mercury.

AUTHORS CONTRIBUTION

The contribution of each author in this research is D.U.S. prepared, created and wrote the initial draft; B.S.D developed and designed the methodology and reviewed the manuscript; H.T.B.M.P verified the research output and reviewed the manuscript, E.A.S designed the research and coordinated the responsibility for the research activity planning.

ACKNOWLEDGMENTS

This study was a part of a first author dissertation. The Ministry of Research and Technology/National Research and Innovation Agency of the Republic of Indonesia has funded this research with PDD (*Penelitian Disertasi Doktor*) grant scheme (033/E5/PG.02.00/2022).

CONFLICT OF INTEREST

There is no conflict of interest in this study.

REFERENCES

- Abad, S.Q., Rodriguez-Gonzales, P. & Lonso, J.I.G., 2016. Evidence of the direct adsorption of mercury in human hair during occupational exposure to mercury vapour. *Journal of Trace Elements in Medicine and Biology*, 36, pp. 16-21. doi: 10.1016/j.jtemb.2016.03.012.
- Abdelfattah, A. et al., 2023. Microalgae-based wastewater treatment: Mechanisms, challenges, recent advances, and future prospects. *Environmental Science Ecotechnology*, 13, 100205. doi: 10.1016/j.ese.2022.100205.
- Ahmed, H. & Hader, D., 2010. A Fast Algae Bioassay for Assessment of Copper Toxicity in Water using *Euglena gracilis*. *Journal Applied Phycology*, 22, pp. 785-792. doi: 10.1007/s10811-010-9520-z.
- Al-Sulaiti, M.M., Soubra, L. & Al-Ghouti, M.A., 2022. The Causes and Effect of Mercury and Methylmercury Contamination in the Marine Environment: A Review. *Current Pollution reports*, 8, pp. 249-272. doi: 10.1007/s40726-022-00226-7.
- Bilgaiyan, P. et al., 2023. Phytoremediation of Wastewater through Implemented Wetland-A Review. *E3S Web of Conferences*, 405, 04026. doi: 10.1051/e3sconf/202340504026.
- Batool, R. et al., 2014. Structural and functional response to metal toxicity in aquatic *Cyperus alopecuroides* Rottb. *Limnologica*, 48, pp. 46-56. doi: 10.1016/j.limno.2014.06.002.
- Chang, J. et al., 2022. Mechanism controlling the transformation and resistance to mercury (II) for a plant-associated *Pseudomonas* sp. strain, AN-B15. *Journal of Hazardous Materials*, 5(432), pp. 127948. doi: 10.1016/j.jhazmat.2021.127948.
- Claro, K. C., Oliveira, P.S. & Rico-Gray, V., 2009. *Tropical Biology and Conservation Management-Volume V: Ecology*, EOLSS Publications.
- Danouche, M., Ghachtouli, NE. & Arroussi H.E., 2021. Phycoremediation Mechanisms of Heavy Metals Using Living Green Microalgae: Physicochemical and Molecular Approaches for Enhancing Selectivity and Removal Capacity. *Heliyon*, 7(7), e07609. doi: 10.1016/j.heliyon.2021.e07609.
- Devars, S. et al., 2000. Mercury uptake and removal by *Euglena gracilis*. *Archieve of Microbiology*, 174, pp.175-180. doi: 10.1007/s002030000193.
- Dixit, R. et al., 2015. Bioremediation of Heavy Metals from Soil and Aquatic Environment: An Overview of Principles and Criteria of Fundamental Processes. *Sustainability*, 7, pp. 2128-2212. doi: 10.3390/su7022189.
- Ekawanti, A. & Krisnayanti, B.D., 2015. Effect of Mercury Exposure on Renal Function and Hematological parameters among Artisanal and Small-scale Gold Miners at Sekotong, West Lombok, Indonesia. *Journal of Health and Pollution*, 5(9), pp.25-32. doi: 10.5696/2156-9614-5-9.25.
- Fu, Y., You, S. & Luo, X., 2021. A review on the status and development of hyperaccumulator harvest treatment technology. *IOP Conf. Series: Earth and Environmental Science*, 642, 012113. doi: 10.1088/1755-1315/642/1/012113.
- Gojkovic, Z. et al., 2022. The Role of Microalgae in the Biogeochemical Cycling of Methylmercury (MeHg) in Aquatic Environments. *Phycology*, 2(3), pp.344-362. doi: 10.3390/phyco2030019.

- Hader, D.P. & Hammersbach, R., 2022. Euglena, a Gravitactic Flagellata of Multiple Usages. *Life*, 12(10), 1522. doi: 10.3390/life12101522.
- Hakim, W.H.A. et al., 2023. The Effect of IAA Phytohormone 9Indole-3-Acetic Acid) on the Growth, Lipid, Protein, Carbohydrate, and Pigment Content in *Euglena* sp. *Malaysian Journal of Fundamental and Applied Science*, 19, pp.513-524. doi: 10.11113/mjfas.v19n4.2884.
- Hussein, H.S. et al., 2007. Phytoremediation of Mercury and Organomercurial in Chloroplast Transgenic Plants: Enhanced Root Uptake, Translocation to Shoots, and Volatilization. *Environmental Science & Technology*, 41(24), pp.8439-8446. doi: 10.1021/es070908q.
- Indahsari, H.S. et al., 2022. Effect of Salinity and Bioflocculation during *Euglena* sp. Harvest on the Production of Lipid, Chlorophyll, and Carotenoid with *Skeletonema* sp. as a Bioflocculant. *Journal of Pure and Applied Microbiology*, 16(4), pp. 2901-2911. doi : 10.22207/JPAM.16.4.65.
- Khatiwada, B. et al., 2020. Proteomic Response of *Euglena gracilis* to Heavy Metal Exposure – Identification of Key Proteins Involved in Heavy Metal Tolerance and Accumulation. *Algal Research*, 45, pp. 101764. doi: 10.1016/j.algal.2019.101764.
- Knight, R. et al., 2000. *Constructed wetland for Pollution Control*, IWA Publishing.
- Krisnayanti, B.D & Probiyantono, A.S., 2020. *Dampak Merkuri pada Kesehatan manusia di Sektor Pertambangan Emas Skala Kecil*. Global Opportunities for Long-term Development of Artisanal and Small Scale Gold Mining (ASGM).
- Kumar, P.K. et al., 2018. Phycoremediation of Sewage Wastewater and Industrial Flue Gases for Biomass Generation from Microalgae. *South African Journal of Chemical Engineering*, 25, pp.133-146. doi: 10.1016/j.sajce.2018.04.006.
- Kumar, V. et al., 2023. A review on clean-up technologies for heavy metal ions contaminated soil samples. *Heliyon*, 9, e15472. doi: 10.1016/j.heliyon.2023.e15472.
- Li, S. et al., 2023. A review: Responses of Physiological, Morphological and Anatomical Traits to Abiotic Stress in Woody Plants. *Forest*, 14, pp. 1784. doi: 10.3390/f14091784.
- Leong, Y.K. & Chang, Jo-Shu, 2020. Bioremediation of Heavy Metals Using Microalgae: Recent Advances and Mechanisms. *Bioresour Technology*, 303, 122886. doi: 10.1016/j.biortech.2020.122886.
- Majid, M. et al., 2014. Production of Algal Biomass. *Biomass and Bioenergy*. Springer, Cham. doi: 10.1007/978-3-319-07641-6_13.
- Marrugo-Negrete, J. et al., 2015. Phytoremediation of mercury-contaminated soils by *Jatropha curcas*. *Chemosphere*, 127, pp.58-63. doi: 1016/j.chemosphere.2014.12.073.
- McGrath, S.P., Shen, Z.G. & Zhao, F. J., 1997. Heavy Metal Uptake and Chemical Changes in The Rhizosphere of *Thlaspi caerulescens* and *Thlaspi ochroleucum* Grown in Contaminated Soils. *Plant Soil*, 180, pp.153–159. doi: 10.1023/A:1004248123948.
- Metcalf, E., 2003. *Wastewater Engineering: Treatment, Disposal, and Reuse*, New York: Mc Graw Hill Inc.
- Moreno-Sanches, R. et al., 2017. Biochemistry and Physiology of Heavy Metal Resistance and Accumulation in *Euglena*. *Biochemistry, Cell and Molecular Biology*, pp 91-121. doi: 10.1007/978-3-319-54910-1_6.
- Napaldet, J.T. et al., 2019. Effect of phytoremediation on morpho-anatomical characters of some aquatic macrophytes. *Biodiversitas*, 20(5), pp. 1289-1302. doi: 10.13057/biodiv/d200519.

- Nurafifah, I. et al., 2023. The Effect of Acidic pH on Growth Kinetics, Biomass Productivity, and Primary Metabolite Content of *Euglena* sp. *Makara Journal of Science*, 27(2), pp.97-105. doi: 10.7454/mss.v27i2.1506.
- Prasetya, A. et al., 2020. Characteristic of Hg removal using zeolite adsorption and *Echinodorus palifolius* phytoremediation in subsurface flow constructed wetland (SSF-CW) model. *Journal of Environmental Chemical Engineering*, 8(3), 103781. doi: 10.1016/j.jece.2020.103781.
- Rangabhashiyam, S. & Balasubramanian-Manian, P., 2019. Characteristic, performance, equilibrium and kinetic modeling aspect of heavy metal removal using algae. *Bioresource Technology report*, 5, pp.261-279. doi : 10.1016/j.biteb.2018.07.009.
- Rangkuti, P.M., Siswanti, D.U. & Suyono, E.A., 2023. Salinity Treatment as Bacterial Control and Its Impact on Growth and Nutritional Value of *Spirulina* (*Arthospora platensis*) Culture in Open Pond System. *Journa of Fisheries and Environment*, 47(1), pp.63-74.
- Rodriguez-Zavala, J.S. et al., 2007. Molecular Mechanism od Resistance to heavy Metals in Protist *Euglena gracilis*. *Journal of Environmental Science and Health*, 42. doi : 10.1080/10934520701480326.
- Sari, E. et al., 2018. The Effectiveness of Filter Media and *Echinodorus palaeifolius* on Phytoremediation of Leachate. *IOP Conference Series Earth and Environmental Science*, 175(1), 012096. doi: 10.1088/1755-1315/175/1/012096.
- Shah, V. et al., 2021. Improved Mechanistic Model of the Atmospheric redox Chemistry of Mercury. *Environmental Science & Technology*, 55(21), pp.14445-14456. doi: 10.1021/acs.est.1c03160.
- Singh, A., 2021. Studies on Zero-Cost Algae Based Phytoremediation of Dye and Heavy Metal from Simulated Wastewater. *Bioresource Technology*, 342. doi: 10.1016/j.biortech.2021.125971.
- Stefanakis, A.I., Akrotos, C.S. & Tsihrintzis, V.A., 2014. *Constructed Wetlands Classification*. Elsevier Publisher. doi: 10.1016/B978-0-12-404612-2-00002-7.
- Suyono, E.A., 2015. The Effect of Nitrogen Excess in Medium on Carotenoid and Chlorophyll Content of *Chlorella Zofingiensis* Donz Culture. *UAJY Int Smnr*.
- Tripathi, S. & Poluri, K.M., 2023. Heavy metal detoxification mechanisms by microalgae: Insight from transcriptomic analysis. *Environmental Pollution*, 285, 117443. doi: 10.1016/j.envpol.2021.117443.
- Ubando, A.T. et al., 2021. Microalgal biosorption of heavy metal: A comprehensive bibliometric review. *Journal of Hazardous Materials*, 404, 123431. doi: 10.1016/j.jhazmat.2020.123431.
- Vymazal, J. et al., 2013. Emergent plants used in free water surface constructed wetlands: A review. *Ecological Engineering*, 61B, pp.582-592. doi: 10.1016/j.ecoleng.2013.06.023.
- Wang, Q. et al., 2004. Source and remediation for mercury contamination in aquatic system-a literature review. *Environmental Pollution*, 131, pp.323-336. doi: 10.1016/j.envpol.2004.01.010.
- Wardana, W.E. et al., 2023. Effect of Mercury Stress on The Growth and Lipid Content of *Euglena* sp. and *Echinodorus palaeifolius*. *Jurnal Biodjati*, 8(1), pp.172-179. doi: 10.15575/biodjati.v8i1.23764.
- Xun, Y. et al., 2017. Mercury accumulation plant *Cyrtomium macrophyllum* and its potential for phytoremediation of mercury polluted sites. *Chemosphere*, 189, pp.161-170. doi: 10.1016/j.chemosphere.2017.09.055.

- Yan, B. & Hou, Y., 2018. Effect of Soil Magnesium of Plants: a Review. 2nd International Symposium of Resource Exploration and Environmental Science. *IOP Conf.Series: Earth and Environmental Science*, 170, 022168. doi. 10.1088/1775-1315/170/2/022168
- Yuan, Z. et al., 2022. Effect of different water conditions on the biomass, root morphology and aerenchyma formation in bermudagrass (*Chynodon dactylon* (L.) Pers). *BMC Plant Biology*, 22(1), 266. doi : 10.1186/s12870-022-03653-2
- Zamani-Ahmadmahmoodi, R. et al., 2020. Aquatic pollution caused by mercury, lead, and cadmium affects cell growth and pigment content of marine microalga, *Nannochloropsis oculata*. *Environmental Monitoring Assessment*, 192, 330. doi: 10.1007/s10661-020-8222.5.

Review Article

Advancement in Plant Tissue Culture-Based Research for Sustainable Exploitation of Well-Known Medicinal Herb *Bacopa Monnieri*

Abhijith Vinod¹, Shivika Sharma², Vikas Sharma^{1*}

1)Department of Molecular Biology & Genetic Engineering, School of Bioengineering and Biosciences, Lovely Professional University, Phagwara-Jalandhar, India.

2)Biochemical Conversion Division, SSSNIBE-Kapurthala Punjab.

* Corresponding author, email: biotech_vikas@rediffmail.com, vikas.25269@lpu.co.in

Keywords:

Bacopa
Bacoside
callogenesis
micropropagation
PGPRs

Submitted:

27 May 2022

Accepted:

20 April 2023

Published:

13 September 2023

Editor:

Furzani Binti Pa'ee

ABSTRACT

The current review focuses on the plant *Bacopa monnieri*, one of prominent medical herbs in Indian ayurvedic system. The plant is well known for its cognitive and memory enhancing capabilities. The plant contains many useful alkaloids and secondary metabolites. Studies have shown that it has various promising pharmacological properties which have the potential to treat many illnesses and disorders such as asthma, bronchitis, rheumatism also in for renal disease, water retention, blood cleaning etc. This leads to the over exploitation of the plant which puts a stress on the naturally available stock of the plant, therefore, it becomes a necessity to find optimum methods for mass production of the plant and its important secondary metabolites. This review attempts to compile and to discuss the advancements in methods and techniques including type of culture vessels, plant growth regulators (PGRs), effect of stress, plant growth promoting rhizobacteria (PGPRs) interactions; for *in vitro* propagation of *Bacopa monnieri* and the enhanced production of its important bioactive (bacoside) for its sustainable exploitation.

Copyright: © 2023, J. Tropical Biodiversity Biotechnology (CC BY-SA 4.0)

INTRODUCTION

The *Bacopa*, also commonly referred to Water hyssop or the Brahmi plant, is a creeping herb mostly found in wetlands and muddy regions. Belonging to the *Scrophulariaceae* family, it is a key component in many Ayurvedic medicines. The plant leaves are thick and succulent in nature, flower's small and white. The entire plant is medically useful (Bone 1996). It is a perennial plant and distributed among tropical and subtropical regions such as India, China, Nepal, Pakistan, Viet Nam and Sri Lanka. Also, its occurrence has been reported in Florida, some states of USA, and Hawaii. Its presence has also been noted in the Mediterranean basin. The areas of the Arabian Peninsula where this plant has been observed include: Kuwait, UAE, Saudi Arabia, southern and northern parts of Oman, Yemen, Bahrain, and Socotra. Additionally, reports of its presence throughout the western and southern Peninsula have also been recorded. In India, the *Bacopa* plant has been found in many states including Delhi, Andhra Pradesh, Kerala, Goa, Assam, Orissa, Bihar, Gujarat, Andaman, Karnataka, Tamil Nadu, Manipur, West Bengal, Punjab, and Rajasthan.

Since ancient times, the *Bacopa* has been utilised in many Ayurvedic treatments. It has been valued as an important herb in many literatures since about 800 BC, one of its treatments for mental ailments has been documented in the text *Charaka Samhita* (Singh & Dhawan 1997). It is primarily used to improve cerebral capacities, but there are several reports where it has been used against inflammatory diseases including asthma, bronchitis, rheumatism and for treating of numerous kidney disorders like blood purification, water retention etc. (Singh & Dhawan 1982; Channa et al. 2006; Rao et al. 2012).

The presence of several compounds like alkaloids (nicotine and herpestine), flavonoids (apigenin and luteolin), glycosides (thanakunide, asiaticoside), and phytochemicals like wogonin, betulinic acid, β -sitosterol, betulinic acid, stigmaterol, oroxindin and brahmie acid, brahmoside, iso-brahmie acid, brahminoside, vallerine, volatile oil, pectic acid, ascorbic acid, fatty acids, asiatic acid, tannins, thanakunide acid etc. has been documented by (Chopra et al. 1956; Sivaramakrishna et al. 2005; Mathew et al. 2010). Of these, Bacoside-A (3-(α -L-arabinopyranosyl)-O- β -D-glucopyranoside-10, 20-dihydroxy-16-keto-dammar-24-ene) is thought to be the key active compound which helps in assisting memory (Chatterji et al. 1965).

The *Bacopa* plant has been ranked second on the importance for its commercial worth, therapeutic value, and potential for future research and development, based on a study undertaken by The Export-Import Bank of India. Therefore, the estimated annual dry weight demand for the plant is about 12.700 tons, which is around Rs 15 billion (Ahmed 1993). Almost the entirety of this need is satisfied by the existing natural stock or by traditional methods of propagation.

This present study focuses on the effectiveness of secondary metabolites production from *Bacopa monnieri* using various *in-vitro* propagation methods.

The whole *B. monnieri* plant is medically significant (Bone 1996). Plants collected from wild, greenhouses or *in vitro* grown plantlets have been used for micropropagation. Stem, shoot tips, nodal and internodal segments from mature plants as well as from plantlets cultured in *in-vitro* has been used for the micropropagation of *Bacopa monnieri*. Even though different culture medias can be used for micropropagation, a comparative study between Murashige and Skoog (MS (Murashige & Skoog 1962)) and Gamborg's (B₅) media, where no additional plant growth regulators (PGR) were used, showed that MS media is better suited for *B. monnieri* plant for both shoot and leaf multiplication *in vitro* (Koul et al. 2014).

The most widely used plant parts for *B. monnieri* clonal growth are shoot tips and nodes, which are generated from *ex-vitro* (~45% of reports) and *in-vitro* cultivated plants (~16% of reports), amongst which the nodal explants were reported to yield better results for enhanced *in-vitro* callusogenesis (Saha et al. 2020).

Impact of explant size has also been evaluated in one study where explants of size 0.5 cm and 20 explant/40 millimetre (1 explant/2 millimetre) yielded the best explant response in terms of number of shoots per explants regenerated and shoot length. Also, increase in size of explant did not make for an increment in the number of shoots in the same proportion (Jain et al. 2012).

***In-vitro* Callusogenesis**

The induction of callus using leaf explants on semi-solid MS basal media supplemented with various concentrations of Kinetin (Kn) or 6-Benzylaminopurine (BAP) alone; as well as varied quantities of 1-

Naphthaleneacetic acid (NAA) or Indoleacetic acid (IAA) in combination with BAP were tried by (Rout et al. 2011) in which it was observed that a combination of BAP (2.0 mgL^{-1}) with NAA (0.5 mgL^{-1}) gave maximum callusing rate of $71 \pm 2.2\%$. Callus of 1-2 cm in diameter were suitable for organogenesis after sub-culturing in the same media (Sheikh et al. 2015). The impact of growth regulators; cytokinin and auxin, when coconut milk was used as an adjuvant was studied by (Kumari 2019).

The callus obtained from explants (leaf and stem) were pale, with soft surfaces, curled to compact, and turned green when exposed to light. Maximum calli development was obtained from 1-Naphthaleneacetic acid (2.5 mg^{-1}) which gave a (94.22 %) of calli formation in leaf explants; and from nodal explants 2,4-D showed maximum calli formation (of 71.41 %) on 2.5 mg^{-1} and internodal explants on 2,4-D showed 65.21% on 2.5 mg^{-1} (Ali et al. 2020).

According to (Patra et al. 2018) leaf explants grown on MS medium + 0.5 mg L^{-1} 1-Naphthaleneacetic acid + 0.1 mg L^{-1} 6-Benzylaminopurine showed the fastest growth in green callus of $01.83 \pm 0.23 \text{ g/L}$ biomass (on the basis of dry cell weight) in less than two weeks (12 days).

Regeneration by Nodal Segment

Multiple shoot proliferations by using varied intensities of 6-Benzylaminopurine and Kinetin alone or with combination of Indoleacetic acid were demonstrated by (Sape et al. 2020). When shoot bud induction was tested on nodal explants cultured in MS media fortified with N^6 -benzyl adenine (BA), it resulted in gradual swelling of the base and the emergence of multiple shoot buds from both above and below the medium, though only a small number of the shoot buds located above the medium was able to elongate in it. (Behera et al. 2015).

In an assessment conducted by (Chaudhry et al. 2019) with different concentrations of MS media and combinations BAP and NAA, it was reported that the use of MS basal media at full strength was able to produce 100% bud break after 3-4 days of culture. In addition, a maximum number of 12-13 shoots were produced per culture.

The BAP and NAA also were seen to be a crucial factor as 0.5 mg L^{-1} of BAP gave good results (10.2 ± 0.1 shoots per culture), but bud break and shoot regeneration decreased as BAP increased (Dixit & Thakur 2017; Chaudhry et al. 2019). Higher concentrations of NAA (1 mg L^{-1}) caused callus induction. Maximum shoot elongation is more than any other culture and combination in the study took place in simple MS basal media with full strength, where it produced a maximum shoot elongation of 9 cm and 12.0 ± 0.2 shoots per culture, after 4 weeks of culturing and sub-culturing in the same media composition (Chaudhry et al. 2019). The combination of BAP, Kn and NAA, each 1 mg./l , also proved as very effective in obtaining a maximum mean number (18.4 ± 0.8) of shoots per explant (Pandiyani & Selvaraj 2012).

Direct Regeneration by Leaf Explant

Direct regeneration has had the most succeed, as plants grown using direct organogenesis are significantly more stable than those grown through indirect organogenesis (callus) (Kamenickà & Rypák 1989). Based on a study conducted by (Nagella et al. 2009), leaf explants, although they were able to successfully regenerate shoot buds in culture, required a two-stage culture setup. In which the first stage involved growth of the explants in a static medium and in the second stage, they were transferred from the static to liquid medium. Here, the leaf explants

produced shoot buds which were too small and made it impossible to be counted and took longer time in becoming shoots.

There are existing numerous records by which successful leaf explant cultures have been established on different media, as well as with different media composition (Joshi et al. 2010; Koul et al. 2014; Umesh et al. 2014; Rahe et al. 2020) etc.

Leaf explants cultured in full strength MS basal media showed shoot bud break and shoot bud proliferation (90%) in 10 days along the leaf margins. As seen in the case of nodal explants, higher concentrations of NAA induced callus formation. Yellowing of shoot buds were observed in two-week-old cultures composed of MS medium + BAP + NAA combinations. Maximum number of shoots were observed full strength MS basal media with 4 weeks of culture, (10.9 ± 0.3). After 3 weeks of sub culture, maximum shoot elongation of 8.5 ± 0.11 was observed in full strength MS media (Chaudhry et al. 2019) (Table 1).

In vitro Rhizogenesis

Root induction was carried out by using different concentrations of Indole-3-butyric acid (IBA) and MS media (Jain et al. 2013; Dixit & Thakur 2017; Ali et al. 2020), of which half strength MS with 0.2 mgL^{-1} IBA showed maximum root formation with an average of 10.2 roots, with an average length root length of 4.2 cm in four days from shoot inoculation (Behera et al. 2015). When in IBA concentration was increased to 0.3 mg L^{-1} , it produced short and thick roots (Dixit & Thakur 2017).

Hardening and Acclimatization

Plantlets grown *in vitro* via tissue culture cannot be planted directly into the field as they are grown in controlled environmental conditions and therefore, they need to be acclimatized, as to reduce the overall mortality rate (Chaudhry et al. 2019). This can be achieved by a number of means. The type of potting mixture used always serve as a vital component of this process. Several potting mixtures like sand, soil, cocopeat, cow dung, vermiculite, farmyard manure, soilrite, peatmoss etc. have been used in different ratios and combinations resulting in the hardening and acclimatization process of *B. monnieri* (Joshi et al. 2010; Rout et al. 2011; Bhusari et al. 2013; Umesh et al. 2014; Naik et al. 2014; Hegazi 2016; Sharma et al. 2018; Chaudhry et al. 2019) (Table 1).

Rooted shoots after sufficient period of culturing, has to be transferred to pots for hardening. These plantlets have to be carefully detached from their *in vitro* culture media. This is followed by thoroughly cleaning the roots with sterile distilled water under lab conditions, to remove any media remains attached to the roots. These washed plantlets are then transferred to small containers such as plastic cups with potting mixture composed of uncontaminated soil and vermiculture in the ratio (2:1 vol./vol.). They are maintained under (16/8 hr Light/Dark) photoperiods. Primary hardening is done in laboratory conditions by regularly pouring salt solution of half strength MS media. Hardened plantlets were initially encased in polythene bags to maintain a sufficient high humidity of 80%. In two weeks, the polythene covers were removed and direct light exposure was given to these potted plants. Sterile distilled water was used to water the plants under these conditions. A survivability rate of 100% was reported for these plants under glass house conditions (Sharma et al. 2016; Ali et al. 2020).

Bacoside Production

By using the Plackett-Burman (PB) method of study, four factors essen-

Table 1. Some methods used in micropropagation of *Bacopa monnieri*

Explant-source/Type	Observation	Media (shoot induction/multiplication)	Rooting Media	Acclimatization	Reference
Leaf explant (<i>ex vitro</i>)	Multiple shoot formations; rooting.	MS+6.0µM BAP+3% sucrose.	Half Strength MS +1% sucrose+ 2.0 µM IBA.	Sand: soil (3:1)	(Joshi et al. 2010)
Leaf explant (<i>ex vitro</i>)	Callus induction; multiple shoot formations; rooting. (Mean no. of roots/ shoot 6.8±0.72)	MS + 0.5 mg l ⁻¹ NAA+ 2.0 mg l ⁻¹ BAP.	Half MS + 2.00 mg L ⁻¹ IAA	Mixture of soil: sterilized sand: Powdered dry cow dung (1:1:1) for 1 week. 86% survival.	(Rout et al. 2011)
Stem and leaf explants (<i>ex vitro</i>)	Bioreactor as well as different culture vessels used; Multiple shoot formations; Phenolic determination.	MS+ IAA 00.01 mg l ⁻¹ + BAP 02.5 mg l ⁻¹ + 3 % sucrose.	–	–	(Jain et al. 2012)
Axillary nodes, shoot tips and young leaves (<i>ex vitro</i>)	Cost effective method for some culture components; Multiple shoot formations; rooting.	Half semi solid MS +3.0 mgL ⁻¹ Kn +00.5 mgL ⁻¹ IBA.	Half MS+ NAA 0.5 mgL ⁻¹ + IBA 0.5 mgL ⁻¹	In pots containing soil: farmyard manure: sand (1:1:1).	(Bhusari et al. 2013)
Leaf and nodal explants (<i>ex vitro</i>)	Multiple shoot formations; Bacoside production; detection by HPLC method.	MS + 2.0 mg L ⁻¹ Kn.	MS.	soil rite (Mixture of coco brick, vermiculite and cocopeat perlite).	(Umesh et al. 2014)
Leaf, node and internode segments (<i>ex vitro</i>)	Multiple shoot formations; rooting.	MS + 2.0 mg L ⁻¹ Kn.	MS + 2.0 mg L ⁻¹ Kn	soil rite. 95% survival.	(Naik et al. 2014)
Shoot cultures from nodal segments.	Bioreactor based cultures; Growth index measured in terms of dry wet; Multiple shoot formations; bacoside production. (Maximum GI 5.84)	MS+ 3% sucrose+ 1mg L ⁻¹ BAP	–	–	(Sharma et al. 2015)
Shoot tips (<i>ex vitro</i>) & <i>in-vitro</i> sub-cultured shoot tips (for encapsulation).	synthetic seeds; encapsulation, storage and recovery; rooting.	MS+ 0.1 mg/L myo-inositol+ 3% sucrose+ 00.53 µM NAA + 04.44 µM BAP.	MS.	Peatmoss:sand (1:1) 93% survival.	(Hegazi 2016)
Nodal segments with single axillary buds (<i>ex vitro</i>)	Multiple shoot formations; rooting.	MS + IAA 00.5 mg L ⁻¹ + BAP 1.0 mg L ⁻¹	MS+ 00.2 mg L ⁻¹ IBA	– 70% survival in hardening.	(Dixit & Thakur 2017)

Explant-source/Type	Observation	Media (shoot induction/multiplication)	Rooting Media	Acclimatization	Reference
Nodal segments with axillary buds (<i>ex vitro</i>)	Multiple shoot formations; rooting.	Semi solid MS+ 01.5 mg L ⁻¹ Kn + 02.5 mg L ⁻¹ BAP	Half liquid MS+ IBA 1.0 mg L ⁻¹	Sand + Soil+ FYM (1:1:1). 100% survival	(Sharma et al. 2018)
Leaf explants, nodal segments with axillary buds (<i>ex vitro</i>)	Multiple shoot formations; rooting.	MS	Half MS + 0.5 mg L ⁻¹ IAA	Soil: vermiculite mixture (50:50)	(Chaudhry et al. 2019)

BAP- 6-Benzylaminopurine; FYM- Farm Yard Manure; GI- growth index; IBA- Indole-3-butyric acid; IAA- Indoleacetic acid; Kn- Kinetin; MS- Murashige and Skoog medium; NAA- 1-Naphthaleneacetic acid.

tial for producing secondary metabolites were examined by (Patra et al. 2018). Four main factors: size of the inoculum, NO₃⁻/NH₄⁺ ratio, sucrose concentration, and KH₂PO₄ concentration were studied in high yield producing variety of plants (bacoside-A of content up to 10.0 mg g⁻¹ dry weight in whole plant, obtained from CIMAP- Lucknow, India). Here, as some reports had suggested that one-fourth strength of MS medium was more preferable to half-strength MS media for both bacoside and biomass production, one-sixth strength MS media was optimised optimized and used in this case (Wu et al. 2006; Fadel et al. 2010; Patra & Srivastava 2016). It was found that biomass production was affected by sucrose, KH₂PO₄ and inoculum concentration (Patra et al. 2018). The limited effect of sucrose and KH₂PO₄ on bacoside and biomass was also reported by (Seth et al. 2020).

Biomass production was not affected by NO₃⁻/NH₄⁺ ratio (Patra et al. 2018). The inoculum size had a direct effect on the production of secondary metabolites and its growth rate, as the larger the inoculum size, the higher the production of secondary metabolites and the slower the rate of growth. (Patra et al. 2018). As shown (Trejo-Tapia et al. 2003) in *Lavandula spica*, it also imparted a positive impact on enzymes that regulates metabolic path ways.

The buffering ability of the culture medium determines how much cell biomass can increase, which accounts for the positive effect of KH₂PO₄ (Patra et al. 2018). The positive impact of sucrose, as a crucial factor in biomass development because of how it affects osmo-regularity of the culture, as cell signalling molecule and as a carbon source for biomass production (Weathers et al. 2004; Patra et al. 2018).

To analyse and for the further optimization of the media, response surface methodology (RSM) was applied. In accordance to dry weight, 3.65 g/L of maximum biomass was obtained in one-sixth strength of MS medium + 0.1 mg L⁻¹ BAP + 0.5 mg L⁻¹ NAA with 30 grams per litre sucrose, 1.24 mM KH₂PO₄ and 2.0 g/L inoculum. One—sixth strength of MS medium + 0.1 mg L⁻¹ BAP + 0.5 mg L⁻¹ NAA with 41.92 gram per litre sucrose, 0.22 mM KH₂PO₄ and 2.0 g/L inoculum predicted the highest bacoside yield of 0.49 mg g⁻¹ (Patra et al. 2018). It was also found that as KH₂PO₄ was only suitable for high biomass production and not in production of bacoside-A, as bacoside-A being a secondary metabolite which observes a non-growth associated production kinetics (Patra et al. 2018).

Upscaling Using Bioreactors

Different culture vessels have been used in the micropropagation of the *B. monnieri* plant, large scale cultivation of shoots is possible by using bioreactors. It is one of the best available methods for commercial use, in

the propagation and production of phytomedicines. This method of propagation has been known to increase the rate of multiplication of cultures and thereby making the overall process more costs and the energy becomes efficient. It also reduces labour which makes commercial production using bioreactors a more feasible approach (Bhanja et al. 2007; Khan et al. 2009; Koul et al. 2015). Among which, maximum growth index (GI) on the basis of dry weight was recorded in air lift bioreactor system (5.84), which is followed by Growtek bioreactor (4.22) (Sharma et al. 2015) then by magenta box, 100 ml conical, glass jars, 250 ml conical flask. Variations were observed in the results, in depending on the number of shoots per litre and the type of vessels used (Jain et al. 2012). In which air lift bioreactor system showed an increase in shoot number of ~48.33 to ~443.33, while Growtek bioreactor showed an increment from ~9.00 to ~42.67 (Sharma et al. 2015).

Effect of Plant Growth Promoting Rhizobacteria (PGPRs)

Plant growth promoting rhizobacteria (PGPR) are rhizosphere bacteria helping in the promotion and enhancement of plant growth by the use of different mechanisms like biological nitrogen fixation, phosphate solubilization, phytohormone production, rhizosphere engineering, antifungal activity etc. (Bhattacharyya & Jha 2012). PGPRs can also be inducted into various stages of plant tissue culture such as in hardening and rooting, to increase the overall health, survivability and productivity of the plant (Ahemad & Kibret 2014). When halotolerant species of PGPRs were utilised to observe the effects of salt stress in *B. monnieri* plant, it was found that the rhizobacteria *E. oxidotolerans* (GenBank accession no: JQ804988) produced a higher plant yield and greater bacoside-A content than that of non-inoculated plants (Bharti et al. 2012). Here, primary and secondary salinity stresses were established. The primary salinity was achieved by mixing 4 g of sodium chloride per kg of soil with sterilized field soil, followed by irrigation using non-saline sterilised water. Secondary salinity level was achieved by the by irrigating pots with saline solution. The desired concentration of 4 g of sodium chloride kg⁻¹ soil was achieved by the gradual incrementation of sodium chloride concentration every seven days at a gradient of 50 mM, to avoid osmotic shock (Kohler et al. 2010). A 50% increase in fresh weight was reported in inoculated plants in non-saline (control) conditions in comparison to non-inoculated plants. Plants inoculated with *E. oxidotolerans* when exposed to primary and secondary salinity, gave 109 and 138% better herb yield respectively than non-inoculated plants. Non-salinized *E. oxidotolerans* inoculated plants showed a 36% increase in bacoside-A content. Plants inoculated with *E. oxidotolerans* produced 44 and 76 % more bacoside-A content in salinized plants under primary and secondary salt stress, respectively, while non-inoculated plants had a reduction of 33-50% in bacoside-A content (Bharti et al. 2012).

An increase of 1.5% in bacoside-A production was also reported in bacopa plants treated with chitinolytic microbes namely, *Streptomyces* sp. MTN14 and *Chitinophilus* sp. MTN22 alone or in combination. In plants, that were treated with the microbial combination, its bacoside biosynthetic pathway genes were upregulated, and helped in the plant's defensive mechanism by enhancing chlorophyll-a, and defensive enzymes and phenolic compounds like cinnamic acid, ferulic acid, gallic acid and syringic acid; against the pathogen *Meloidogyne incognita* (Gupta et al. 2017).

PGPR inoculation can have strain-specific impacts on the secondary metabolites production in plants as shown by (Walker et al. 2011) which implies the existence of a fine-tuned interaction mechanism. And

as reported by (Bharti et al. 2012), that PGPR inoculated plants, both under stressed condition (salinity stress) as well as under non-stressed condition (non-saline condition) exhibited a higher level of bacoside-A content, which could mean their potential role in secondary metabolite pathway. The increased bacoside content could also be because of the improved leaf-stem ratio of the inoculated plants (Phrompittayarat et al. 2011).

Effect of Abiotic Stress on *B. monnieri*

The effect of drought (mannitol) and salinity (NaCl) was studied on *B. monnieri* plant, it was found that the growth rate was decreased in cultures under both kind of stress. Also, elevated amount of proline content was found in mannitol induced osmotic stress and in salinity stress. Whereas protein content increase was reported in lower concentration of NaCl and mannitol stress, and a reduction of protein content in higher concentrations of the same (Debnath 2008; Dogan 2020).

According to another study conducted by (Dogan 2020), salt stress also affected callus formation and its density. With increase in salt concentration, callus density decreased and loss in callus colour (browning and yellowing) was also reported. Even though low levels of salt stress did not have much of an effect on *in-vitro* culture, high salinity has had an impact on many physiological and biochemical parameters due to decreased chlorophyll content in shoots from applying salt stress, which lead to conditions like chlorosis, lipid peroxidation, and protein degradation (Ashraf & Bhatti 2000; Dogan 2020). Lipid peroxidation can be caused by the reactive oxygen species found in the cell membrane, which can affect the cell permeability, composition, and structure as well as membrane integrity of the plant (Bose et al. 2014). Chlorosis or reduced chlorophyll content in plants under salt stress is caused by membrane degradation due to lipid peroxidation as well as increased chlorophyllase enzyme activity, which degrades chlorophylls, as well as a decrease in chlorophyll production (Ashraf & Bhatti 2000; Santos 2004). The increase in proline content was thought to be caused by more proline productions or because stress conditions decreased the incorporation of proline into other macro molecules like protein. The increased activity of Pyrroline 5-carboxylate reductase (P5CR), proline oxidase, and ornithine amino transferase (OAT) could also give high proline content (Debnath 2008).

Secondary metabolites production increased gradually when treated with Cd up to 10.0 μM which then showed a decrease at higher concentrations of 50.0 μM and 100.0 μM . It indicates that the abiotic stress, which in this case the Cd treatment, increased the secondary metabolite production to a certain limit and then decreases due to Cd at higher concentrations. Increase in bioactive compounds like bacoside A and toxicity bacoside I in all Cd treated plants were found by the use of TLC fingerprinting (Gupta et al. 2014).

The effect of abiotic stress on bacoside production was studied using abiotic elicitors like salicylic acid (SA), jasmonic acid (JA) and copper sulphate (CuSO_4), which were used in different concentrations, it was found that a maximum concentration in bacoside of 08.73 mg g^{-1} dry weight was given by CuSO_4 (45 mg L^{-1}) in an elicitation period of 6 and 9 days. Both JA and SA produced higher concentration of bacoside than that of control but less than CuSO_4 induced cultures. JA (1 mg L^{-1}) gave a bacoside yield of 08.46 mg g^{-1} DW and SA (50 μM) gave 08.14 mg g^{-1} DW of bacoside yield (Sharma et al. 2014).

Seasonal variation i.e., the influence of temperature on wild varieties of *B. monnieri* plant on bacoside production was estimated by collect-

ed samples from different regions (in India) and growing them in a uniform environment for one year. It was found that even though there were variations due to genotypic differences, the greatest amount of bacoside-A content (6.82 mg/plant) was documented during the summer, when the mean temperatures reached 40.0° C and the lowest values (0.34 mg/plant) during winter which recorded a mean temperature lower than 5.0° C (Bansal et al. 2016).

CONCLUSION

Throughout the years, there has been a significant amount of research done on various parameters of micropropagation of *Bacopa monnieri*. Cultures were mostly set up by extracting explants from *ex vitro* plants rather than from *in vitro* ones. Nodal explants were used more extensively than leaf explants for *in vitro* propagation.

The use of bioreactors as a culture vessel have aided in acquiring increased biomass and bacoside production. Several key factors like size of the inoculum, sucrose concentration, $\text{NO}_3^-/\text{NH}_4^+$ ratio, KH_2PO_4 concentration, PGRs etc. play a significant role in biomass and bacoside production directly or indirectly. Plant growth prompting rhizobacteria's (PGPR) like *E. oxidotolerans*, incorporated plants were able to successfully produce higher results in herb yield and in bacoside production compared to non-inoculated plants. Temperature, salinity, and other abiotic elicitors like Cd, JA, CuSO_4 , SA were also found to have an impact on bacoside production in *in vitro* cultures. Even though some crucial factors and parameters have been identified, further studies are still required so as to incorporate the current research parameters to find optimum requirements to enable the mass production of *Bacopa monnieri* as well as its important secondary metabolites.

AUTHOR CONTRIBUTION

Please list the contribution of each author here, e.g.: A.V. written and prepared the manuscript, S.S. edited and reviewed the manuscript, V.S. designed and conceptualized the research and supervised all the process.

ACKNOWLEDGMENTS

List here those individuals who provided help during the research (e.g., providing language help, writing assistance or proofreading the article, etc.).

CONFLICT OF INTEREST

The authors declare that they have no conflict of interest.

REFERENCE

- Ahemad, M. & Kibret, M., 2014. Mechanisms and applications of plant growth promoting rhizobacteria: Current perspective. *Journal of King Saud University - Science*, 26(1), pp.1-20. doi: 10.1016/j.jksus.2013.05.001
- Ahmed, R., 1993. '*Medicinal Plants Used in SM--Their Procurement, Cultivation, Regeneration, and Import/Export Aspects--A Report*', New Delhi: Today and Tomorrow Publishers and Printer.
- Ali, D., Alarifi, S. & Pandian, A., 2020. Somatic embryogenesis and *in vitro* plant regeneration of *Bacopa monnieri* (Linn.) Wettst., a potential medicinal water hyssop plant. *Saudi Journal of Biological Sciences*, October, 28(1), pp.353-359. doi: 10.1016/j.sjbs.2020.10.013
- Ashraf, M. Y. & Bhatti, A., 2000. Effect of salinity on growth and chlorophyll content of rice. *Pak J Sci Ind Res*, Volume 43, pp. 130-131.

- Bansal, M., Reddy, M.S. & Kumar, A., 2016. Seasonal variations in harvest index and bacoside A contents amongst accessions of *Bacopa monnieri* (L.) Wettst. collected from wild populations. *Physiology and Molecular Biology of Plants*, 22(3), pp. 407-413. doi: 10.1007/s12298-016-0366-y
- Behera, S. et al., 2015. An efficient micropropagation protocol of *Bacopa monnieri* (L.) Pennell through two-stage culture of nodal segments and ex vitro acclimatization. *Journal of Applied Biology & Biotechnology*, 3(03), pp.016-021. doi: 10.7324/JABB.2015.3304
- Bhanja, T. et al., 2007. Comparative profiles of alpha-amylase production in conventional tray reactor and GROWTEK bioreactor. *Bioprocess Biosyst Eng*, 30(5), pp.369-76. doi: 10.1007/s00449-007-0133-0
- Bharti, N. et al., 2012. Exiguobacterium oxidotolerans, a halotolerant plant growth promoting rhizobacteria, improves yield and content of secondary metabolites in *Bacopa monnieri* (L.) Pennell under primary and secondary salt stress. *World J Microbiol Biotechnol*, 29, pp.379-387. doi: 10.1007/s11274-012-1192-1
- Bhattacharyya, P.N. & Jha, D.K., 2012. Plant growth-promoting rhizobacteria (PGPR): emergence in agriculture. *World J Microbiol Biotechnol*, 28(4), pp.1327-50. doi: 10.1007/s11274-011-0979-9
- Bhusari, S., Wanjari, R. & Khobragade, P., 2013. Cost Effective In vitro Clonal propagation of *Bacopa monnieri* L. Pennell. *International Journal of Indigenous Medicinal Plants*, 146(2), pp.1239-1244.
- Bone, K., 1996. *Clinical applications of Ayurvedic and Chinese herbs: monographs for the western herbal practitioner*. Queensland, Australia: Physiotherapy press.
- Bose, J., Bose, J. & Rodrigo-Moreno, A., 2014. ROS homeostasis in halophytes in the context of salinity stress tolerance. *J Exp Bot*, 65, pp.1241-1257. doi: 10.1093/jxb/ert430
- Channa, S. et al., 2006. Anti-inflammatory activity of *Bacopa monnieri* in rodents. *Journal of Ethnopharmacology*, 104(1-2), pp.286-289. doi: 10.1016/j.jep.2005.10.009
- Chatterji, N., Rastogi, R. & Dhar, M., 1965. Chemical examination of *Bacopa monnieri* Wettst: part II—the constitution of bacoside A. *Indian journal of chemistry*, 3, pp.24-30.
- Chaudhry, B. et al., 2019. Micropropagation of a medicinally important plant: *Bacopa monnieri*. *Medicinal Plants- International Journal of Phytomedicines and Related Industries*, 11(2), pp.177-182. doi: 10.5958/0975-6892.2019.00022.4
- Chopra, R.N., Nayar, S.L. & Chopra, I.C., 1956. Glossary of Indian medicinal plants. *Council of Scientific and Industrial Research*, p. 32.
- Debnath, M., 2008. Responses of *Bacopa monnieri* to salinity and drought stress in vitro. *Journal of Medicinal Plant Research*, 2(11), pp.347-351.
- Dixit, H. & Thakur, A., 2017. In vitro propagation of a medicinal important plant *Bacopa monnieri* from nodal explants. *Indian Journal of Research in Pharmacy and Biotechnology*, 5(1), pp.1-4.
- Dogan, M., 2020. Effect of salt stress on in vitro organogenesis from nodal explant of *Limnophila aromatica* (Lamk.) Merr. and *Bacopa monnieri* (L.) Wettst. and their physio-morphological and biochemical responses. *Physiology and Molecular Biology of Plants*, 26(4), pp.803-816. doi: 10.1007/s12298-020-00798-y
- Fadel, D. et al., 2010. Effect of Different Strength of Medium on Organogenesis, Phenolic Accumulation and Antioxidant Activity of Spearmint (*Mentha spicata* L.). *The Open Horticulture Journal*, 3, pp. 31-35. doi: 10.2174/1874840601003010031

- Gupta, P. et al., 2014. Effect of Cadmium on Growth, Bacoside A, and Bacopaside I of Bacopa monnieri (L.), a Memory Enhancing Herb. *Scientific World Journal*, 2014, 824586. doi: 10.1155/2014/824586
- Gupta, et al., 2017. Microbial modulation of bacoside A biosynthetic pathway and systemic defense mechanism in Bacopa monnieri under Meloidogyne incognita stress. *Scientific Reports*, 7(1). doi: 10.1038/srep41867
- Singh, H.K. & Dhawan, B.N., 1982. Effect of Bacopa monniera Linn. (Brāhmi) extract on avoidance responses in rat. *Journal of Ethnopharmacology*, 5(2), pp.205-214. doi: 10.1016/0378-8741(82)90044-7
- Hegazi, G.A.E.M., 2016. In vitro Preservation of Bacopa monnieri (L.) Pennell as a Rare Medicinal Plant in Egypt. *Journal of Basic and Applied Scientific Research*, 6(12), pp. 35-43.
- Jain, N., Sharma, V. & Ramawat, K.G., 2012. Shoot culture of Bacopa monnieri: standardization of explant, vessels and bioreactor for growth and antioxidant capacity. *An International Journal of Functional Plant Biology*, 18(2), pp.185-190. DOI: 10.1007/s12298-012-0103-0
- Jain, R., Prasad, B. & Jain, M., 2013. In- vitro regeneration of Bacopa monnieri (L.): A highly valuable medicinal plant. *Int.J.Curr.Microbiol.App.Sci*, 2(12), pp.198-205.
- Joshi, A.G. et al., 2010. High frequency of shoot regeneration on leaf explants of Bacopa monnieri. *Environmental and Experimental Biology*, Volume 8, pp.81-84.
- Kamenickà, A. & Rypák, M., 1989. The regeneration of Actinidia chinensis Pl. cultured in vitro. *Polnohospodarvo*, Volume 35, pp.811-818.
- Khan, M. Y. et al., 2009. Recent advances in medicinal plant biotechnology. *Indian Journal of Biotechnology*, 08, pp.9-22.
- Kohler, J., Caravaca, F. & Roldán, A., 2010. An AM fungus and a PGPR intensify the adverse effects of salinity on the stability of rhizosphere soil aggregates of Lactuca sativa. *Soil Biology and Biochemistry*, 42(3), pp.429-44. doi: 10.1016/J.SOILBIO.2009.11.021
- Koul, A. et al., 2014. Cost Effective Protocol for Micropropagation of Bacopa Monnieri Using Leaf Explants. *International Journal of Science and Research (IJSR)*, 3(4), pp.210-212.
- Koul, A. et al., 2015. Regenerative potential and phytochemical diversity among five accessions of bacopa monnieri (l.) Wettst. *International journal of pharma and bio sciences*, 6, pp. 746-756.
- Kumari, R., 2019. Induction of callus from different explants of bacopa monnieri and effect of adjuvant on the growth rate of the calli. *Indian Journal of Scientific Research*, 10(1), pp. 113. doi:10.32606/IJSR.V10.I1.00017
- Mathew, J. et al., 2010. Bacopa monnieri and Bacoside-A for ameliorating epilepsy associated behavioral deficits. *Fitoterapia*, 81(5), pp.315-322. doi: 10.1016/j.fitote.2009.11.005
- Murashige, T. & Skoog, F., 1962. A revised medium for rapid growth and bioassays with tobacco tissue culture. *Physiol Plant*, 15, pp.473-497. doi: 10.1111/j.1399-3054.1962.tb08052.x
- Nagella, P. et al., 2009. In vitro regeneration of brahmi shoots using semisolid and liquid cultures and quantitative analysis of bacoside A. *Acta Physiologiae Plantarum*, 31(4), pp.723-728. doi: 10.1007/s11738-009-0284-5
- Naik, P.M. et al., 2014. Rapid one step protocol for in vitro regeneration of bacopa monnieri (L.). *Journal of Cell and Tissue Research*, 14(2), pp.4293-4296.

- Pandiyan, P. & Selvaraj, T., 2012. In vitro multiplication of *Bacopa monnieri* (L.) Pennell from shoot tip and nodal explants. *Journal of Agricultural Technology*, 8(3), pp.1099-1108.
- Patra, N. & Srivastava, A.K., 2016. Artemisinin production by plant hairy root cultures in gas- and liquid-phase bioreactors. *Plant Cell Reports*, 35, pp.143–153. doi: 10.1007/s00299-015-1875-9
- Patra, N. et al., 2018. Statistical optimization for enhanced bacoside A production in plant cell cultures of *Bacopa monnieri*. *Plant Cell Tissue and Organ Culture*, 133, pp.20-214. doi: 10.1007/s11240-017-1373-6
- Phrompittayarat, W. et al., 2011. Influence of seasons, different plant parts, and plant growth stages on saponin quantity and distribution in *Bacopa monnieri*. *Songklanakar J. Sci. Technol.*, 33(2), pp.193-199.
- Rahe, M. A. et al., 2020. In vitro Micropropagation of *Bacopa monnieri* (L.) Penn. - An Important Medicinal Plant. *Plant Tissue Cult. & Biotech.*, 30(1), pp.57-63. doi: 10.3329/ptcb.v30i1.47791
- Rao, R. V. et al., 2012. Ayurvedic medicinal plants for Alzheimer's disease: a review. *Alzheimer's Research &*, 4(3), 22. doi: 10.1186/alzrt125
- Rout, J. R. et al., 2011. Standardization of an efficient protocol for in vitro clonal propagation of *Bacopa monnieri* L. - an important medicinal plant. *Journal of Agricultural Technology*, 7(2), pp. 289-299.
- Saha, P.S. et al., 2020. In Vitro Propagation, Phytochemical and Neuropharmacological Profiles of *Bacopa monnieri* (L.) Wettst.: A Review. *Plants*, 9(4), 411. doi: 10.3390/plants9040411
- Santos, C.V., 2004. Regulation of chlorophyll biosynthesis and degradation by salt stress in sunflower leaves. *Scientia Horticulturae*, 103(1), pp.93-99. doi: 10.1016/j.scienta.2004.04.009
- Sape, S.T., Kandukuri, A.V., Owk, A.K., 2020. Direct axillary shoot regeneration with nodal explants of *Bacopa monnieri* (L.) Pennell – A MULTI MEDICINAL HERB. *Journal of Applied Biological Sciences*, 14(2), pp.190-197.
- Seth, B. et al., 2020. Statistical optimization of bacoside A biosynthesis in plant cell suspension cultures using response surface methodology. *3 Biotech*, 10(6), 264. doi: 10.1007/s13205-020-02258-6
- Sharma, M. et al., 2014. Enhanced bacoside production in shoot cultures of *Bacopa monnieri* under the influence of abiotic elicitors. *Natural Product Research*, 29(8), pp.745-749. doi: 10.1080/14786419.2014.986657
- Sharma, M. et al., 2015. Bacoside biosynthesis during in vitro shoot multiplication in *Bacopa monnieri* (L.) Wettst. grown in Growtek and air lift bioreactor. *Indian Journal of Biotechnology*, 14, pp.547-551.
- Sharma, N., Singh, R. & Pandey, R., 2016. In Vitro Propagation and Conservation of *Bacopa monnieri* L.. In: *Protocols for In vitro Cultures and Secondary Metabolites Analysis of Aromatic and Medicinal Plants*. New York: Springer, pp.153-171. doi: 10.1007/978-1-4939-3332-7
- Sharma, M. et al., 2018. Scaling up of Protocol for in vitro Multiplication and Conservation of Elite Genotype of *Bacopa monnieri* L. Pennell. *International Journal of Current Microbiology and Applied Sciences*, 7 (10), pp.3225-3236. doi: 10.20546/ijcmas.2018.710.374
- Sheikh, S.S., Dakhane, V.P. & Chaudhary, A.D., 2015. Callus Induction in *Bacopa monnieri* (Linn.) Pennell by Nodal, Internodal, Young and Mature Leaf Explants. *International Journal of Research In Biosciences, Agriculture & Technology*, Special Issue 1, pp.101-108.
- Singh, H. & Dhawan, B., 1997. Neuropsychopharmacological effects of

- the Ayurvedic nootropic *Bacopa monniera* Linn. (Brahmi). *Indian J Pharmacol*, 29, pp.359-365.
- Sivaramakrishna, C. et al., 2005. Triterpenoid glycosides from *Bacopa monnieri*. *Phytochemistry*, 66(23), pp.2719-2728. doi: 10.1016/j.phytochem.2005.09.016
- Trejo-Tapia, G., Arias-Castro, C. & Rodríguez-Mendiola, M., 2003. Influence of the culture medium constituents and inoculum size on the accumulation of blue pigment and cell growth of *Lavandula spica*. *Plant Cell, Tissue and Organ Culture*, 72, pp.7-12. doi: 10.1023/A:1021270907918
- Umesh, T.G., Sharma, A. & Rao, N.N., 2014. Regeneration potential and major metabolite analysis in nootropic plant *Bacopa monnieri* (L.) Pennell. *Asian J Pharm Clin Res*, 7(1), pp.134-136.
- Walker, V. et al., 2011. Host plant secondary metabolite profiling shows a complex, strain-dependent response of maize to plant growth-promoting rhizobacteria of the genus *Azospirillum*. *New Phytol*, 189 (2), pp. 494-506. doi: 10.1111/j.1469-8137.2010.03484.x
- Weathers, P.J. et al., 2004. Alteration of biomass and artemisinin production in *Artemisia annua* hairy roots by media sterilization method and sugars. *Plant Cell Reports*, 23(6), pp.414-418.
- Wu, C.H. et al., 2006. Optimization of culturing conditions for the production of biomass and phenolics from adventitious roots of *Echinacea angustifolia*. *Journal of Plant Biology*, 49, pp.193-199. doi: 10.1007/BF03030532

Review Article

Extremophilic Cellulases: A Comprehensive Review

Subham Mohanta¹, Megha Bahuguna¹, John David Baley¹, Shivika Sharma¹, Vikas Sharma^{1*}

¹)Department of Molecular Biology & Genetic Engineering, School of Bioengineering and Biosciences, Lovely Professional University, Phagwara-Jalandhar, Punjab, India.

* Corresponding author, email: vikas.25269@lpu.co.in; biotech_vikas@rediffmail.com

Keywords:

Cellulases
Extremophiles
Extremozymes
Acidophile
Halophiles
Thermophiles

Submitted:

02 June 2022

Accepted:

17 May 2023

Published:

08 November 2023

Editor:

Miftahul Ilmi

ABSTRACT

Microbial cellulases are an important industrial enzyme having diverse applications in biotechnology, environmental challenges, industrial products and processes. Extremophiles like thermophilic bacteria are a good source of industrially important cellulases as these can withstand industrially rigorous procedures like paper deinking, fabric material softening, bio stoning, paper and pulp, biopolishing cloth material, animal feed and juice. Identification of novel cellulases or improving them through biotechnological interventions has remained a challenge for researchers. Genetic manipulation of thermophilic bacteria for increased cellulase production or synthetic biology approaches for cellulase gene/gene cluster extraction from thermophilic bacteria and expression in appropriate hosts for improved cellulase synthesis. The classic and high-throughput technologies like genomics, metagenomics and bioinformatics could be exploited to isolate cellulase genes from a variety of thermophilic bacteria and further processing. Keeping in view the ultimate requirement of extremophilic cellulases in industries, present study is a compilation of various aspects related to extremophilic cellulases their sources, production, biotechnological interventions and challenges.

Copyright: © 2023, J. Tropical Biodiversity Biotechnology (CC BY-SA 4.0)

INTRODUCTION

Bio molecules originating from natural resources are playing an important role in production of everyday items. Enzymes are one of those compounds that are well-known across the world for their numerous industrial uses. For example, they are widely used in dairy products, food and feed, paper and pulp, brewing, pharmaceutical manufacturing, and detergents industry. Cellulase is a widely used enzyme. The need for cellulase enzyme is expanding quickly, according to current worldwide cellulase market study studies. Cellulose, the cellulase substrate, is the most prevalent carbohydrate on the planet. It is the most important element in plant matter. (O'sullivan 1997).

Extremophiles are important research subjects for many scientific disciplines, from adaptation studies to extreme environments to biogeochemical cycles. Extremophiles, especially those that can survive in a variety of extremes, are a key topic of study for many disciplines. Research on extremophiles has an impact on both the study of quest for life origin and extraterrestrial life. In modern times by producing extremozymes, extremophiles are playing an important role in biotechnology sector. The frequent use of extremozymes in industrial production processes and research under extreme conditions (high temperature, high pressure, and

extreme pH ranges) makes them important entities. Present work is a pragmatic approach to discuss current state of "Extremophilic Cellulases" knowledge and applications of extremozymes in many industries, identifying knowledge gaps and potential study areas.

CELLULASES

Cellulose is a biodegradable material found in large quantities in agricultural waste. Microbial cellulases have a significant approach nowadays due to their wide industrial utilization. Also, cellulases are an important part of the second-generation biofuel production as the hydrolytic action of the enzyme converts complex cellulose into simple monomer units (Jayasekara & Ratnayake 2019). The generated reducing sugars are then utilized to make ethanol, which is used as a biofuel. Endoglucanases, cellobiohydrolases or exoglycanases, and alpha glucosidases are the three primary types of cellulases. These enzymes can be found in anaerobic cellulolytic bacteria as single enzymes or as part of a multicomponent enzyme complex (cellulosome). Thermophiles and thermotolerant enzymes have diverse industrial applications.

Cellulose- a linear polymer of D-glucose connected through 1,4-glucosidic linkage is the most common carbohydrate found in nature and an important structural cell wall component of plants. It resists enzymatic breakdown better than other plant cell wall polysaccharides because of its partly crystalline form (Patyshakuliyeva 2016). Cellulases are inducible enzymes generated during the growth of cellulosic materials by a variety of microorganisms, including fungus and bacteria. (Kuhad et al. 2011). There are bacteria that are anaerobic, aerobic, thermophilic, and mesophilic. The most researched cellulase manufacturers include Trichoderma, Cellulomonas, Clostridium, Thermomonospora and Aspergillus (Table 1).

Table 1. Different types of genus and species of micro-organisms involved in the production of cellulases enzyme.

Group	Genus	Species
Fungi	<i>Aspergillus</i>	<i>Aspergillus niger</i> <i>Aspergillus oryzae</i>
	<i>Fusarium</i>	<i>Fusarium solani</i> <i>Fusarium oxysporum</i>
	<i>Trichoderma</i>	<i>Trichoderma Reesei</i> <i>Trichoderma. harzianum</i>
Bacteria	<i>Acidothermus</i> <i>Bacillus</i>	<i>Acidothermus cellulolyticus</i> <i>Bacillus</i> sp. <i>Bacillus subtilis</i>
	<i>Clostridium</i>	<i>C. acetobutylicum</i>
	Actinomycetes	<i>Cellulomonas</i>
<i>Streptomyces</i>		<i>Streptomyces</i> sp.

EXTREMOPHILES- NICHES (HABITATS, ISOLATED)

When it comes to temperature, pH, and salinity, the anthropocentric word "extremophile" was coined more than 30 years ago to characterise a microorganism capable of surviving and thriving under conditions that are extremely harsh and difficult for humans and the majority of known microbes (Canganella & Wiegel 2011) to survive. Extremophiles thrive

in harsh conditions like extremes pH, high salt and temperature, radiation, high metal concentrations and extreme pressures. Extreme pH, temperature, high salinity, radiation acidic and basic, low water activity are only a few of the environmental difficulties for which these bacteria have developed unique systems and molecular responses (Sarmiento et al. 2015). These extremophiles have developed different molecular strategies for survival (Neifar 2015).

Alkalophiles live in very alkaline pH habitats, such as sodic lakes, and thrive in extremely alkaline pH conditions. Other extremophilic forms, known as pollution-loving microorganisms, may live and develop in the presence of high quantities of nuclides, pollutants such as polyhydroxylalkanoates (PAHs), pesticides, and other contaminants.

Acidophiles are microbes in very acidic conditions, often with a pH of 2. Acidophilic bacteria flourish in acidic lakes, certain hydrothermal systems, acid sulphate soils, sulfidic regoliths, and ores, as well as metal and coal mine-affected environments. The oxidation of the metal and other sulfidic minerals produces very acidic conditions that are home to a wide range of prokaryotic and eukaryotic life forms that are acidophilic and acid tolerant.

Halophiles are a type of extremophile that needs a lot of salt to survive and flourish. Halophiles are divided into two types: obligatory halophiles, which require a NaCl content of 3% or above, and halotolerant, which may thrive at both average and higher salt concentrations. Compatible solutes, also known as osmolytes, are metabolites that help cells maintain osmotic equilibrium. Producing or acquiring compatible solutes is a frequent adaptation for living in high-salt habitats (Charlesworth & Burns 2016). Halophilic bacteria are the major microbial communities present in hypersaline environments all over the planet. Halophilic bacteria have low nutritional needs, are resistant to high salt concentrations, and can regulate the osmotic pressure of their surroundings. The salt requirements of halophiles are divided into three categories: low (1-3%), moderate (3-15%), and extreme (3-15%). (15-30 percent). Temperature, pH, and growth media all influence salt requirements.

Adaptations

Extremophiles have developed unique methods to survive in their harsh surroundings by modifying their natural machinery. These methods and mechanisms, on the other hand, are extremely complicated. For example, in extreme alkali concentrations, extremophiles maintain an osmotic balance by enhancing appropriate solutes inside the cells or using ion pumps; in low pH conditions, an adequate pH is maintained by proton pump inside the cell; and in reduced or extreme heats, they change the design of their cytoplasmic membrane.

Exopolysaccharides (EPSs) surrounding most microbial systems in extreme ecosystems like deep-sea hydrothermal vents, Antarctic region, salty lagoons and hot springs constitutes an important component of extracellular polymers. Extremophiles have developed many adaptations to withstand and survive the harshness of extreme conditions, for instance, high temperatures, reduced pH or temperature, extreme salt and radioactivity (Nicolaus 2010).

The cytoplasmic membrane of bacteria determines the makeup of the cytoplasm to a great extent because ion electrochemical gradients across membranes, particularly proton and sodium ion electrochemical gradients, are critical for these microorganism's bioenergetic conditions, techniques to limit ion permeability across their cytoplasmic membrane are required. All biological membranes proton and sodium permeabilities increase as the temperature rises. Psychrophilic (cold-suitable) organisms

populations have potential uses in a broad range of technical, agricultural and therapeutic processes. In order for progress to occur in reduced-hotness atmospheres, all cellular parts must fit to the cold (Elleuche 2014). Mesophilic & psychrophilic bacteria, as well as hyperthermophilic and halophilic archaea can change their membrane lipid contents to keep constant and low proton permeability at their specific growth temperatures. Thermophilic microorganisms, in another way, have a harder time confining proton infiltration through their membrane at extreme hotness, and these organisms must depend on less penetrable sodium ions to maintain an extreme sodium-cause in order to drive their strength-intensive membrane-bound movements. Enzymes from thermophilic animals have found ultimate efficient commercial use to date by way of their overall genetic stability (Demirjian 2001). Basically, to maintain function at extreme hotness, thermophilic proteins have an important hydrophobic gist and reinforced electrostatic contacts (Stetter 1999). Basic ATP-compelled transport systems mainly mediate the solute transport across the bacterial and archaeal sheath and or subordinate transport methods compelled by proton or sodium motive forces drive it. Hyperthermophilic microorganisms and archaea favour primary ATP-compelled assimilation processes for carbon and energy. Several ABC transporters accompanying high similarity for sugars from hyperthermophiles have been labelled and characterized. ABC transporters help these individuals to develop in a nutrient-inadequate environment. Different microorganisms like bacteria, yeast cyanobacteria, and algae from specific surroundings specify a valuable reserve that not only can be exploited sustainably in novel biotechnological processes but also as study models for identifying the biomolecules helping them to survive through extreme conditions (Herbert 1992).

Extremozymes – Industrial relevance

Extremozymes and extremolytes produced from extremophiles are having applications in different sectors of biotechnology including white, red and grey biotechnologies with potential to increase the biobased economy (Raddadi 2015).

Currently, very small number of microorganisms (1-2%) on the earth have been commercially exploited and most efficient ones among these are from extreme environments (Gomes & Steiner 2004). Extremozymes have been used and found very important in processes of biofuel production, pharmaceutical and chemical compound synthesis & food industries. The understanding of particular biochemical or metabolite that is responsible for adaptation to extreme habitats like specific enzymes have been targeted for biotechnological uses and applications (Dalmaso 2015). Currently and in the past also biocatalysis has been improved using natural enzymes but there are few reports available on uses of extremozymes in industria developments. Microbial extremozymes and their genetic consistency, reproducibility and increased yields in harsh environments, have led their use in a variety of industrial procedures.

Extremophile-derivative enzymes, or extremozymes, can proceed biochemical reactions in extreme circumstances, such as those visualized in technical processes, where enzymatic action was earlier thought to be impossible. Extremozymes offer novel catalytic options for current mechanical applications on account of their superior action and balance under harsh surroundings. For example, most of the universal industrial strains including bacterial spp (Bacillus, Escherichia coli, Corynebacterium glutamicum and Pseudomonas spp.) and yeast are grown in mild environments (pH of 5–7 and 30–37 °C) and medium enriched with yeast

extract. These temperate conditions favours growth of most of the micro-organisms in air, water and soils (Shrestha 2018).

Enzymes are employed in the dairy business for cheese production and creamery product preparation; in the baking production, enzymes increase bread condition; in beverage manufacturing, enzyme is used to maintain especially of wine purity and colour while lowering Sulphur levels. Extremophilic hemicellulases (β -mannanase, β -mannosidase, gluconidase, galactosidase, feruloyl esterase, acetyl xylan esterase and α -arabinofuranosidase) are effective enzymes for the complete plant cell wall saccharification (Antranikian & Egorova 2007). Some modern enzymes can further be employed to boost the produced things filterability and flavour.

Arthrobacter, Acidithiobacillus, Micrococcus, Bacillus, Geobacillus, Caldicellulosiruptor, Clostridium, Enterobacter, Coprothermobacter, Paenibacillus, Picrophilus, Pseudoalteromonas, Penicillium, and Thermobifida are just a few of the extremophile sources for enzymes that have been isolated and tried for biomass processing. Table 2 enlists some of important extremophiles with their classification and extremozymes produced. Tetrathionate hydrolase, decarboxylase, -galactosidase, subtilase, xylanase, dehydrogenase, endoglucanase, α -amylase, β -glucosidase, enzymes were reported (Zhu 2020).

Many industries will more and more be benefitted from the exploitation of extremozymes. It has been recommended that low proportion of these organisms (below 10%) could be cultivatable and further improvement of molecular biology and gene expression studies will help in understanding the microbial diversity for sustainable exploitation (Gupta 2014).

ISOLATION OF THERMOPHILIC CELLULOLYTIC BACTERIA

Many workers have reported the isolation of thermophiles in past. Based on the reports we have tried to compile the important aspects of isolations. According to a published method, sterile containers with various compost samples (temperature > 50 °C) were taken. To minimize mesophiles and anaerobic isolates, the compost piles were air-dried and heated to a temperature of 55°C for one week before being dried. Two techniques were employed to isolate thermophilic bacteria. After serial dilution, both straight spreads improved or plated on CMC (Carboxy methyl

Table 2. Classification of extremophiles and modern use of few enzymes.

Types	Growth Characteristics	Source	Enzymes	Applications
Acidophiles	can growth at or beneath pH 3-4	Volcanic springs, Acid mine drainage, USA	Amylase Cellulases	Single cell protein, starch processing Removal of hemi cellulosic material from feed
Halophile	can grow in elevated salt concentrations	Salty Lakes, saline soils	Proteases	Peptide synthesis
Alkaliphile	Growth at elevated pH value (more than 10)	salty lakes	Cellulases	Fermentation
Thermophile	Can survive between 60 degrees Celsius and 85 degrees Celsius	Hot springs	Lipases, cellulases	Additive to detergents for washing at room condition Breaking lipid stains, to breakdown lignocellulose

cellulose) agar using cellulose broth. All incubations were carried out in a controlled atmosphere at 55°C for two-four weeks with shaking at 120 rpm (Ibrahim & El-diwany 2007).

SELECTION OF CELLULOLYTIC THERMOPHILIC ISOLATES

The cellulolytic bacterial isolates were screened using a 1% congo red indicator. The plates were soaked with 1% Congo red indicator for 15 minutes before being soaked with 1M NaCl solution for another 15 minutes. The presence of a halo zone around the colony indicated that cellulose hydrolysis had occurred. If the zone was too cloudy, 0.1N HCL was added (Wood & Bhat 1998)

Effect of pH & Temperature

The temperature profile for cellulase activity can be determined between 30°C and 80°C. At different temperatures (30–80°C), the soluble enzyme extract along with the substrate (CMC) are subjected to assay the maximum activity. Various studies have been carried out at different pH by different workers to find the best assay pH for cellulase activity: 0.05 M sodium acetate (pH 3–4.5), 0.05 M sodium citrate (pH 5–5.5), and 0.05 M sodium phosphate buffer (pH 5–5.5) (Oyekola 2003; Ariffin et al. 2006; Ray et al. 2007)

Thermal Stability and Production of Cellulases

Thermal stability is important for industrial applications. One study indicated that *Bacillus subtilis* cellulase enzyme activity was highest at 50°C. The selection and formulation of an ideal cellulose basal medium is research-intensive and highly required for industrial production. One such study for the optimization using *Bacillus subtilis* in four distinct cellulose basal media for enzyme production has been described Ray et al. (2007). *Bacillus subtilis* produced the greatest enzyme activity.

Applications

For many decades, cellulases have been employed as key biocatalysts in variety of industries. Fabrics, pulp & paper, laundry and detergents, agriculture, pharmaceuticals, and food industry are just a few examples that employ bacterial cellulases. CMI (Coherent market insights) reported textile sector was the largest market for cellulases in 2017. Further enzyme market research findings included food and beverages, livestock, textile industry and bioenergy as the important application areas. Extremophiles, especially archaea and bacteria, provide an excellent platform for treating industrial waste streams that were previously thought to be hostile to the model organisms in microbial electrochemical systems (MESs) expanding the application from industry to environmental remediation (Shrestha 2018).

Fabrication Manufacturing

The fabrication industry is one of the world's most important industries. Cellulase enzymes are flexible enzymes that may be used to efficiently replace non-eco-friendly chemical treatments in textile manufacturing (Shah 2013). Customers are increasingly demanding individuality in terms of styles, colours, and the clothing they wear. As a consequence of rising client demand, this business has experienced tremendous expansion in recent decades. In these applications, this enzyme is currently the third most often used group of enzymes. Manufacturers that are constantly seeking for environmentally friendly methods to differentiate their products will find this to be a very competitive market platform. In

the industrial sector, cellulase is utilised for a number of purposes. Some of the primary uses of this enzyme in the industry, notably for textile wet processing, include bio stoning of textiles, biopolishing of fabric fibres, smoothing of cloths, and excess textile colour removal. Cellulases from *Trichoderma reesei* are the most often used enzyme in the textile industry. *Streptomyces* and *Thermobifida* are two genera of actinomycetes., as well as bacteria from the genera *Pseudomonas* and *Sphingomonas*, are further sources of enzymes for textile dye decolorization and deterioration.

Paper and Pulp Industry

According to the World Wildlife Fund (WWF), the paper sector consumes more than 40% of all industrial wood marketed worldwide, including items such as office and catalogue paper, glossy paper, tissue, and paper-based packaging. Paper and pulp are both renewable natural resources (Shah 2013). As a result, two common ideas in this industry are recycling and reuse. The employment of microbial cellulases is commonly used to accomplish this. In this industry, cellulases are employed in a number of ways. From the 1980s to the present, the variety of possible applications has grown significantly. Deinking, pulping, industrial waste bioremediation, bleaching, and fibre enhancement (Kuhad 2011) are some key processes of this industry where cellulases are employed. Considering these processes as harsh conditioned reactions, these will be more reproducible if extremophilic cellulases that can be more effective in these conditions are employed.

Laundries & Detergents

Enzymes have been used to generate enzymatic washing agents or biological detergents since the 1960s. Enzymes are often employed in detergent compositions generally. According to market data, the largest single market for enzymes was the detergent sector in 2014, accounting for 25–30% of total sales (Zhang & colleagues 2013). To date, cellulases from fungi such as *Humicola* (*H. insolens* and *H. griseothermoidea*), *Aspergillus niger*, *Trichoderma* sp. (*T. longibrachiatum*, *T. reesei*, *T. viride*, and *T. harzi-anum*) and *Bacillus* sp. have been intensively investigated for use in detergents. The greatest addition to conventional detergents is alkaline cellulases. It's due to their capacity to remove dirt and soil particles from the fabric's interfibrillar regions. Cellulases break down the rough projections of cellulose fibres or cellulose aggregates on the cloth. As a result, the material's shine and smoothness could be improved.

Agriculture

In agriculture, cellulases are often used to increase crop growth or in disease management. Combination of cellulases, hemicellulases, and pectinases is commonly used for this purpose. Certain fungal cellulases have the capacity to break down plant pathogen cell walls. Several studies using bacteria to increase plant performance, such as plant growth-promoting rhizobacteria (PGPR) has been reported in the past and still counting. These bacteria are said to serve a key role in lowering the use of artificial fertilisers, promoting plant development, and regulating possible plant infections and disease protection. In addition, numerous fungi, such as *Geocladium* sp., *Trichoderma* sp., *Chaetomium* sp. and *Penicillium* sp. promote seed germination, quick plant growth, faster flowering, stronger root systems, and increased crop yield. However, the specific mechanisms behind these reactions remain uncertain. All of these species, however, may produce cellulase and other enzymes, which may play a direct part in these processes. Some studies have found probable synergies between the

development of bacterial cellulase and the production of bacterial antibiotics against plant harmful fungi. Extremozymes are of great interest for a variety of industrial processes, in addition to starch and lignocellulose degradation. Chitinases are enzymes that work together to degrade the 1,4-glycosidic linked N-acetylglucosamine units of chitin. Chitinolytic enzymes are used as bio fungicides and bioinsecticides since this structural polysaccharide is found in the exoskeletons of fungus, insects, and crustaceans (Elleuche 2014).

In terms of climate change, microbial communities and plants from harsh habitats are being tested as biotechnological tools to increase cereal crop production and development of tree species tolerant to unfavourable climate events (droughts, flooding, frosts, heat, and cold waves, and so on) (Jorquera 2019).

Applications in Medicine

Medical pharmacology is a very busy field of research right now, with new findings being made all the time. One such sector is development and use of cellulases for medicinal purposes. The survival mechanisms of extremophiles are being studied in order to address difficulties related to human health; knowing these processes might be beneficial in management of human ailments (Babu 2015). Many extremophilic bio-products have already been employed as life-saving medications (Singh 2012). Although humans cannot produce cellulases, a recent study in health and medicine has found that ingesting enzyme blends that include cellulase offers health advantages. Cellulases produced from natural fermentation processes of *Trichoderma reesei* and *Bacillus licheniformis* has been added to commercially available enzyme mixes in response to global demand for enzyme blends. Fruits and vegetables, cereals, legumes, grains, nuts and seeds, soy, dairy, nutritious greens, sprouts, and herbs, as well as fats (lipids), sugars, proteins, carbs, and gluten, are all targets for these enzyme combinations. VeganZyme is one such example. Aside from that, there are digestive aids (such as Digestin, P-A-L Plus Enzymes, Polyzyme Plus, and others) gaining global attention as viable medical treatment for metabolic illnesses. Antimicrobial peptides have been discovered in both *Halobacteriaceae* and *Sulfolobus* species (phylogenetic family including all halophilic archaea). Halophilic archaea peptides (halocins) are considered to be found in all members of the family. Although halocins have been proven to destroy archaeal cells, there is no evidence that they kill bacteria that are dangerous to people (Coker 2016). DNA polymerases from thermophiles are being used in PCR-based diagnostics for a wide spectrum of animal diseases, considered as most well-known use of an extremophile product in veterinary medicine (Irwin 2010).

Biofuels and Bioenergy Production

Biofuels are a renewable source of energy. Second-generation bioethanol production is becoming increasingly popular due to the availability of low-cost raw ingredients. Pre-treatment is an important stage in the production of bioethanol from lignocellulosic biomass (Sindhu et al. 2016). Lignocellulosic biomass includes agricultural waste (corn stover, crop straws, and bagasse), herbaceous and weed crops (alfalfa, switch grass), short-rotation woody crops, forestry residues, wastepaper, etc. is among the most promising raw material for fuel production. The lignocellulosic biomass is the most abundant renewable biomass. Global lignocellulosic cellulose output is expected to exceed 200 billion metric tonnes per year (Sindhu et al. 2016). The benefits of producing bioethanol from these feedstocks are numerous. Removal of lignocellulosic materials, which are

non-edible plant parts is one such benefit. It is eco-friendly and most importantly as no food crops are eaten before harvesting, bioethanol production from lignocellulosic biomass does not contribute to food insecurity or food vs fuel controversy. Further its availability throughout the year as a raw material is beneficial for industrial production.

The structural complexity of lignocellulosic biomass, on the other hand, is a significant constraint of this production approach. Lignin cellulose, and hemicellulose form a very stable and complex structure when united. This makes it difficult to break the stable structure and support fermentation., Therefore the substrate must be pre-treated for efficient production. However, the pre-treatment procedures are neither eco-friendly nor cost-effective. But the novel or extremophilic cellulases can be used to de-stabilise this lignocellulosic biomass. Researchers are finding such efficient cellulose which can alone or in combination can be useful to degrade lignocellulosic biomass and bioethanol production.

SOURCE

Cellulases are enzymes that break down cellulose chains' -1,4 bonds. Fungi, bacteria, protozoans, plants, and mammals all make them. Based on their amino acid sequences and transparent constructions, cellulase catalytic modules are differentiated into many classifications. At the N- or C-end of catalytic modules in cellulases, noncatalytic carbohydrate-binding modules (CBMs) and/or other operationally recognised or mysterious modules are created.

Many cellulose-degrading enzymes have existed cloned, and signified from a variety of cellulolytic thermophilic bacteria. Conversely, a search for cellulose-degrading enzymes in hyperthermophilic bacteria indicated that such enzymes are uncommon in this group. Furthermore, only the Archaea genera *Pyrococcus* and *Sulfolobus* have been discovered to metabolise thermoactivated cellulases. In comparison to anaerobic microbes, aerobic thermophilic microorganisms have also been found to produce cellulases. *Rhodothermus marinus*, an aerobic thermophile isolated from a subsurface natural hot water spring in Reykjanes, NW Iceland produced thermostable cellulase (Cel12A) showing 50% activity after 3.5 h hours at 100°C.

The thermophilic filamentous bacteria *Thermobifida fusca* (previously *Thermomonospora fusca*) are a prominent cellulose degrader. Cel9B, Cel6A, Cel5A (earlier E1, E2, and E5), two exoglucanases Cel6B and Cel48A (already E3 and E6), and an endo/exoglucanase Cel9A are all secreted by this actinomycete and have been well described. More in-depth research is required to understand better the catalytic mechanism using computational and experimental methods. The crystal structure of this enzyme in association with substrate and inhibitor has also been determined. Table 3 compiles the different temperature rhymes and environmental conditions.

FUNGAL CELLULASES

Few thermophilic fungi have been identified as cellulase producers and listed in table 4.

Properties of Some (energetic) thermophilic cellulolytic microorganisms.

Microorganism	Enzyme	Mol mass (kDa)	Optimal T (°C)	Optimal pH
<i>Acidothermus cellulolyticus</i>	E1	72.0	81	5.0
<i>Anaerocellum thermophilum</i>	CelA	230.0	85-95	5.0-6.0
<i>Caldibacillus cellulovorans</i>	CMCase	174.0	80	6.5-7.0
<i>Clostridium thermocellum</i>	CelI	98.5	70	5.5
<i>Pyrococcus furiosus</i>	EglA	35.9	100	6.0

Table 3. Thermophilic cellulolytic Bacteria and Archaea showing growth at different temperature and in different environmental conditions.

Microbe Name	Domain	Gram Reaction	Growth T (°C)	Growth conditions
<i>Acidothermus cellulolyticus</i>	Bacteria	+	55	Aerobic
<i>Alicyclobacillus acidocaldarius</i>	Bacteria	+	60	Aerobic
<i>Caldibacillus cellulovorans</i>	Bacteria	+	68	Aerobic
<i>Clostridium stercorarium</i>	Bacteria	+	65	Anaerobic
<i>Clostridium thermocellum</i>	Bacteria	+	60	Anaerobic
<i>Dictyoglomus thermophilus</i>	Bacteria	-	73	Anaerobic
<i>Dictyoglomus turgidus</i>	Bacteria	-	72	Anaerobic
<i>Pyrococcus abyssi</i>	Archaea	-	96	Anaerobic
<i>Pyrococcus furiosus</i>	Archaea	-	98	Anaerobic

Table 4. Properties of different thermophilic fungi.

Microorganism	Enzyme	Mol mass (kDa)	Optimal T (°C)	Optimal pH (pH)
<i>Chaetomium thermophile</i>	EG	67.8	60	4.0
<i>Humicola grisea</i> var. <i>thermoidea</i>	EGI	58.0	55-60	5.0
<i>Myceliophthora thermophile</i>	EG	100.0	65	4.8
<i>Talaromyces emersonii</i>	EGI-III	68.0	75-80	5.5-5.8
<i>Thermoascus aurantiacus</i>	EGI	78.0	75	5.0
	EGII	49.0	68	5.0

Several cellulases have been reported to be produced by the thermophilic filamentous fungus *Humicola* sp., and several of the genes have been cloned, sequenced, and expressed. The thermophilic fungus *Humicola insolens* has a cellulase system with enzymatic machinery for effective cellulose consumption. This order, that is related to *T. reesei*'s, has five endoglucanases: EGI (Cel7B), EGII (Cel5), EGIII (Cel12), EGV (Cel45A), and EGVI (Cel6B), in addition to two cellobiohydrolases: CBHI (Cel7A) and CBHII (Cel6A) showed optimum activity between pH 5.5-9.0. Among these Cel7B was found to be highly active across a wide pH range showing over 60% activity between pH 5.0 -10.0. Cel45A exhibited a pH optimum of 9.0, while the other three cellulases had pH optimums of 6.0 to 8.0. There was no information regarding the ideal temperature and stability. The explanation for the abundance of enzymes produced by *H. insolens*, *T. reesei*, and many other cellulolytic microbes is unknown. According to the most widely accepted view, each enzyme plays a singular role concerning the substrate's assortment (solubility, degree of substitution or polymerization).

Biotechnological interventions to increase the production

Developing and establishing routes to enhance the cellulase production at industrial level involved different microorganisms and different methods. Every step in the production of cellulase is important, isolation of the suitable microorganism, pre-treatment, inoculation, fermentation, extraction of the enzyme and enzyme assay. Biotechnology is particularly interested in salt and cold-active enzymes (Karan 2012). Most of the industrial enzymes are obtained from using submerged fermentation (SmF) as it is easier to handle the environment such as pH and temperature. Enzyme production cost can be reduced, and yield can be improved by using Solid state fermentation. Optimal conditions are very important for enhanced production, *A. niger* was proved to be productive at pH of 6, and temperature of 30°C.

Inducible ion outflow systems reduce the intracellular accumulation of a particular ion through active transport, which is how heavy metal

ions are usually detoxified. Because these bacterium's metal resistance determinants are all involving reasoning from facts, their regulatory structures maybe exploited to assemble biosensors that assess biologically appropriate heavy metal concentrations in the environment. Only the cytoplasm of the relevant cell is detoxified when resistance is based on metal ion efflux. As a result, this resistance mechanism can't be directly used to the development of biotechnological methods. (Nies 2000).

Soil microorganisms such as *Pseudomonas fluorescens*, *Bacillus subtilis*, *E. coli*, and *Serratia marcescens* are potential cellulase produces (Sethi 2013). For maximum cellulase production culture medium and culture conditions were was optimized for such as pH 10 and temperature 40°C was reported as efficient for production n. Among all microorganisms *Pseudomonas fluorescens* was found to be better cellulase producer.

Adaptive development is an effective approach to customize the strains and genes that includes the degeneration of biomass, this method has been used to produce the mutant strain (N402) of *Aspergillus niger*, the transcriptomic study revealed that the expression of noxR, encoding the regulatory subunit of the NADPH oxidase complex, was lowered in the mutant version in contrast to the maternal strain (Patyshakuliyeva 2016). The properties of this mutant showed that it has five-time higher potential of producing cellulase than its parent strain.

Challenges

Biotechnological production and development possess greater challenges and vary between every isolation technique, development strategy and so on. Understanding existence under extreme environments is challenging on account of the troubles of artificial sophistication and observation because most of the structures cannot be refined. Many challenges are faced when we work with extremophilic microorganisms as these organisms live in extreme environments that are not suitable for our human survival. Extreme environments involve high pH, temperatures, salt concentrations, pressures and low temperatures, pH and salt concentrations, and pressures. Such harsh environments are intolerably hostile and can also be lethal to earthly life forms. These microorganisms thrive in extreme hot slots, ice, and alkali fluids, as well as acid and salty conditions, few may evolve in hazardous waste, organic solvent, and several other habitats. They have happened to be at 6.7 km inside the Earth's coating, in addition 10 km deep inside the sea at pressures of until 110 MPa from extreme acid (pH 0) to extreme fundamental environments (pH 12.8); and from hydrothermal vents at 122 °C to iced salt solution, at -20 °C. Extremophiles have a great phylogenetic diversity and are difficult to investigate in general. Only extremophiles are found in some orders or genera, whereas together non-extremophiles and extremophiles are found in others (Rampelotto 2013).

The optimum temperatures, pH and pressures of extremophilic organisms are very challenging, so for the survival they should meet the optimum conditions. Some extremophilic organisms need more than two extreme conditions for their growth and some can tolerate one though they are growing in normal conditions. For example, the archaeal *Methano pyruskandleri* strain 116 evolves at 122°C (the maximal recorded hotness), while the type *Picrophilus* (for instance, *Picrophilus torridus*) include ultimate acidophilic now known, accompanying the strength to evolve at a pH of 0-6. In conditions of extreme resistance to extreme environments, individuals of the most influential eukaryotic polyextremophiles are tardigrade. Tardigrades can participate through an inaction mode, named the tun state, whereby it can survive the conditions from -272 °C to 151 °C, vacuum environments (imposing extreme aridity), pressure of

6,000 ATM plus disclosure to X-rays and gamma-beams (Rampelotto 2013).

As studying these extremophiles is challenging one, research on these gives a key to research of new areas like astrobiology or outer terrestrial environments. These organisms can be considered as model organisms when research goes on extra-terrestrial existence of life. These possess remarkable adaptation mechanisms for their survival. To allow growth at extreme heats, nucleic acids may be shielded by various designs. Nucleotides are the construction blocks of deoxyribonucleic acid molecules, and the bases adenine and thymine link through two hydrogen bonds, while cytosine and guanine are affiliated by three hydrogen bonds. Since extreme genomic GC content, particularly at the tertiary codon position, confers better establishment, it is assumed that this may be the main method of protecting double-stranded DNA from denaturation in extremophiles (Wang 2006).

Recent Advances

The microbial capability to live in harsh and extreme environments led many investigators to study the adaptive characteristics of these microorganisms to further exploit them sustainably (Tango & Islam 2002). Many industries and researchers are committed to work on microorganisms and to engineer its genetic makeup to produce desirable characteristics. Mostly commercially available common enzymes have less industrial applicability as they could not withstand pH, high temperatures and pressures. In recent times extremozymes have received more attention. Cold-suitable proteases and amylases with potential to remove starch stains have been commercialized by industrial giants like Genesco & Novozymes. Industrial enzymes with application in biorefineries are being considered as specialized enzymes with an estimated value of \$ 1 billion in 2010 to \$5.0 billion in 2021 at a rate of 4.0% every year. This has surpassed the former, as they attained \$5.5 billion in 2018 and are presently calculated to reach \$7.0 billion by 2023 (Zhu 2020).

Extremozymes having application in delignification and subsequent usage of lignocellulosic biomass for bioenergy have been isolated and identified (Zhu 2020). Thermophilic microorganisms and their enzymes have been reported for excellent use in bioenergy production and anaerobic digestion. Some of these include *Caldicellulosiruptor bescii*, *Geobacillus proteiniphilus*, *Thermoanaerobacterium*, *Pyrococcus*, and *Caldicellulosiruptor* (Zhu 2020).

A gene cluster for biosynthesis of glycoicin from a thermophilic *Aeribacillus pallidus* has been transferred and expressed heterologously in *E. coli* for the increased production of glycoicin with potential in biofuel manufacturing (Kaunietis 2019).

In another research bioaugmentation process has been exploited for the improvement of a *Clostridium* sp. strain WST. This has considerably enhanced the butanol yield to 0.54 g/g by 98-fold. This hike offers an eco-friendly and cost effective approach to use lignocellulose for production of biofuels and bioenergy by reducing the manufacturing cost (Shanmugham et al. 2019).

Arsenic immune nematodes have existed found in Mono reservoir. Researchers revived eight variety from the salted, alkaline environment—increasing the acknowledged biodiversity of organisms in the California pond five-fold.

CONCLUSIONS

Microbial communities are still being found in conditions that are unfriendly for life to exist. The viruses of several of these extremophiles are

frequently neglected, despite their importance in influencing microbial community or as extremozyme developers. Studying unreachable locations such as the deep sea and ice-covered oceans has never happened smoothly because of the growth of revolutionary culturing sciences and new designs for exploring improbable regions such as the deepest oceans and ice-covered oceans (Podar & Reysenbach 2006).

Extremophiles – microorganisms that evolve in extreme salt or heavy metal concentrations, or at limits of heat, pressure, or pH — may soon play a bigger role in biotechnology. Microorganisms and microbial consortia have a considerable impact on pH, from the nano- to macro-scale. (Merino 2019). These creatures and their natural components are attractive as they allow process working in more circumstances than their classical counterparts (Ludlow & Clark 1991). Among the possible enzyme technologies conversion to glucose from cellulose by process of hydrolysis is salient of all processes. The range of industries impacted by the application these elements are innumerable. This is true when we evaluate plant-based industries being that at least 60% of plant mass is cellulose, thus developing other means of breaking it down are paramount to advancements. Extremophile research has yielded huge scientific discoveries, but it is now time to assess whether these results are sustainable and can be used to improve industrial operations to get new products or to undergo biotransformatics (Schiraldi & De Rosa 2002). Nowadays research on extremophiles focuses on screening and isolation of potential strains which are sources of novel enzymes with increased industrial potential and viability in critical conditions. Further extremophiles play a key function in biorefinery applications by providing novel metabolic pathways and catalytically resistant/strong enzymes functional under rough industrial conditions.

The application of extremophiles and their enzymatic elements has brought forth a range of versatile applications which are otherwise perceived to be difficult to perform. The most remarkable observation is that extremophiles exist in environments too strident for most organisms (these include but are not limited to extreme temperatures, pressures, pH, etc.), thus making it even more interesting to observe how some extremophilically derived enzymes turn out to be polyextremophilic exhibiting stability and activity in one or more extreme states, including high salt concentrations and alkaline pH, low temperatures, and non-aqueous environments. Keeping aforementioned in mind, the future applications of many of these enzymatic elements derived from extremophiles open new insights to the realm of modern enzymology and many industries further perpetuating and incentivizing the transition toward sustainable economies and industries. These proteins, which have adapted to function within extreme sets of conditions, are less prone to denaturing, opening doors to applications like the use of anaerobic and aerobic extremophiles second hand either as whole cells or their enzymes alone in the result of different biofuels, containing biodiesel, biomethane, bio butane, and bio hide in more recent times with promising long-term applications. The primary industries that advanced as a result of blending extremophile-based processes into their framework initially were food, agriculture, cosmetic, synthetic and fabric industries. Modern endeavours have also seen the fields of bioremediation of contaminated environments where much research considers extremophiles as a promising candidate due to their specific metabolic activities and the strength to indulge harsh habitats. Recently, various extremophiles have researched for their capability to produce extremolytes like biopterin, mycosporine like amino acids (MAA), palythine, porphyra-344 and phlorotannin that play pertinent roles in several applications in relation to agents that block cell cycle,

drugs of anti-cancer, antioxidants, and commercial products like sunscreen. In addition to that, multiple extremozymes were clarified and recognized from extremophiles for their industrial and biotechnological applications. This illustrates to some extent the vast and versatile extent to which extremophiles can be utilized in a means move toward a bioeconomy, while at the same time providing new aspects to researching the origin of life and astrobiology. With the advancement of biological tools, such as CRISPR-CAS9, the boundaries of extremophile-based utilities and research are practically endless.

FUTURE PROSPECTIVES

To address the depleting fossil fuel resources and the need for environmental protection and alternative energy resources, a number of biorefinery based applications and methods have been developed and proposed by researchers globally, but most of them are still in the pilot stage. Extremophiles and their enzymes have a significant market share that is anticipated to continue expanding because of their proven commercial success in the diverse biotechnology fields. To further use this immense potential sustainably, however, a lot of research has to be done to address problems associated with their industrial scale production, activity enhancement, novel sources etc.

AUTHOR CONTRIBUTION

S.M. written and prepared the manuscript, M.B. written and reviewed the manuscript, J.D.B. written and reviewed the manuscript, S.S. edited and reviewed the manuscript; V.S. designed and conceptualized the research and supervised all the process.

ACKNOWLEDGMENTS

The authors acknowledge the support of Head and Faculties of Molecular Biology and Genetic Engineering domain, School of Bioengineering and Biosciences, Lovely Professional University, Jalandhar, India.

CONFLICT OF INTEREST

The authors declare that they have no conflict of interest.

REFERENCE

- Antranikian, G., & Egorova, K., 2007. Extremophiles, a unique resource of biocatalysts for industrial biotechnology. *Physiology and biochemistry of extremophiles.*, pp.359-406. doi: 10.1128/9781555813.ch27.
- Ariffin, H. et.al., 2006. Production and Characterisation of Cellulase by *Bacillus pumilus* Eb3. *International Journal of Engineering and Technology*, 3(1), pp. 47-53.
- Arora, N.K. & Panosyan, H., 2019. Extremophiles: applications and roles in environmental sustainability. *Environmental Sustainability*, 2(3), pp.217-218. doi: 10.1007/s42398-019-00082-0.
- Babu, P., Chandel, A.K. & Singh, O.V., 2015. *Extremophiles and their applications in medical processes*. New York, NY: Springer International Publishing. pp.25-35.
- Berlemont. R. & Gerday, C., 2011. *Comprehensive Biotechnology (Second Edition)*. UK: Pergamon Press Inc.
- Cavicchioli, R. et al., 2002. Low-temperature extremophiles and their applications. *Current opinion in Biotechnology*, 13(3), pp.253-261. doi: 10.1016/s0958-1669(02)00317-8

- Charlesworth, J. & Burns, B.P., 2016. Extremophilic adaptations and biotechnological applications in diverse environments. *AIMS Microbiology*, 2(3), pp.251-261. doi: 10.3934/microbiol.2016.3.251
- Chen, G.Q. & Jiang, X.R., 2018. Next generation industrial biotechnology based on extremophilic bacteria. *Current opinion in Biotechnology*, 50, pp.94-100. doi: 10.1016/j.copbio.2017.11.016
- Coker J.A., 2016. Extremophiles and biotechnology: current uses and prospects. *F1000Research*, 5. doi: 10.12688/f1000research.7432.1
- Canganella, F. & Wiegel, J., 2011. Extremophiles: from abyssal to terrestrial ecosystems and possibly beyond. *Naturwissenschaften*, 98(4), pp.253-279. doi: 10.1007/s00114-011-0775-2
- Dos Reis, L. et al., 2013. Increased production of cellulases and xylanases by *Penicillium echinulatum* S1M29 in batch and fed-batch culture. *Bioresource technology*, 146, pp.597-603. doi: 10.1016/j.biortech.2013.07.124
- Dalmaso, G.Z.L., Ferreira, D. & Vermeelho, A.B., 2015. Marine extremophiles: a source of hydrolases for biotechnological applications. *Marine drugs*, 13(4), pp.1925-1965. doi: 10.3390/md13041925
- Demirjian, D.C., Morís-Varas, F. & Cassidy, C.S., 2001. Enzymes from extremophiles. *Current opinion in Chemical biology*, 5(2), pp.144-151. doi: 10.1016/s1367-5931(00)00183-6
- Dumorné, K. et al., 2017. Extremozymes: A Potential Source for Industrial Applications. *Journal of Microbiology and Biotechnology*, 27(4), pp.649-659. doi: 10.4014/jmb.1611.11006.
- Elleuche, S. et al., 2014. Extremozymes—biocatalysts with unique properties from extremophilic microorganisms. *Current opinion in Biotechnology*, 29, pp.116-123. doi: 10.1016/j.copbio.2014.04.003
- Gomes, J. & Steiner, W., 2004. The biocatalytic potential of extremophiles and extremozymes. *Food technology and Biotechnology*, 42(4), pp.223-225.
- González-González, R., Fucinos, P. & Rúa, M.L., 2017. An overview on extremophilic esterases. In *Extremophilic enzymatic processing of lignocellulosic feedstocks to Bioenergy*. Springer Cham. pp.181-204. doi: 10.1007/978-3-319-54684-1_10
- Gupta, G.N. et al., 2014. Extremophiles: an overview of microorganism from extreme environment. *International Journal of Agriculture, Environment and Biotechnology*, 7(2), pp.371-380.
- Herbert, R. A., 1992. A perspective on the biotechnological potential of extremophiles. *Trends in Biotechnology*, 10, pp.395-402. doi: 10.1016/0167-7799(92)90282-z
- Herbert, R.A. & Sharp, R.J., 1992. *Molecular biology and biotechnology of extremophiles*. Glasgow: Blackie.
- Ibrahim, A.S.S., El-diwany, A.I., 2007. Isolation and identification of new cellulases producing thermophilic bacteria from an egyptian hot spring and some properties of the crude enzyme. *Australian Journal of Basic and Applied Sciences*, 1(4), pp. 473-478.
- Irwin, J.A., 2010. Extremophiles and their application to veterinary medicine. *Environmental technology*, 31(8-9), pp.857-869. doi: 10.1080/09593330.2010.484073.
- Jayasekara, S., & Ratnayake, R., 2019. Microbial cellulases: an overview and applications. In *Cellulose*. doi: 10.5772/intechopen.84531
- Jorquera, M.A., Graether, S.P. & Maruyama, F., 2019. Bioprospecting and biotechnology of extremophiles. *Frontiers in Bioengineering and Biotechnology*, 7, 204.

- Karan, R., Capes, M.D. & Das Sarma, S., 2012. Function and biotechnology of extremophilic enzymes in low water activity. *Aquatic biosystems*, 8(1), pp.1-15. doi: 10.1186/2046-9063-8-4
- Karlsson, J. et al., 2002. Enzymatic degradation of carboxymethyl cellulose hydrolyzed by the endoglucanases Cel5A, Cel7B, and Cel45A from *Humicola insolens* and Cel7B, Cel12A and Cel45Acore from *Trichoderma reesei*. *Biopolymers: Original Research on Biomolecules*, 63(1), pp.32-40.
- Kaunietis, A. et al., 2019. Heterologous biosynthesis and characterization of a glycoicin from a thermophilic bacterium. *Nature communications*, 10(1), 1-12. doi: 10.1038/s41467-019-09065-5.
- Kuhad, R.C., Gupta, R. & Singh, A., 2011. Microbial cellulases and their industrial applications. *Enzyme research*, 2011, 280696. doi: 10.4061/2011/280696.
- Kvesitadze, G., 2017, Cellulases from Extremophiles, Durmishidze Institute of Biochemistry and Biotechnology of Agricultural University of Georgia, Goergia USA.
- Li, Duo-Chuan, Li, An-Na & Papageorgiou, Anastassios., 2011. Cellulases from Thermophilic Fungi: Recent Insights and Biotechnological Potential. *Enzyme research*, 308730. doi: 10.4061/2011/308730.
- Ludlow, J.M., & Clark, D.S., 1991. Engineering considerations for the application of extremophiles in biotechnology. *Critical reviews in Biotechnology*, 10(4), pp321-345. doi: 10.3109/07388559109038214
- Lynd, L.R. et al., 2002. Microbial cellulose utilization: fundamentals and biotechnology. *Microbiology and Molecular Biology Review*, 66(4), pp.739. doi: 10.1128/MMBR.66.3.506-577.2002
- Merino, N. et al., 2019. Living at the extremes: extremophiles and the limits of life in a planetary context. *Frontiers in Microbiology*, 10, pp.780. doi: 10.3389/fmicb.2019.00780. eCollection 2019
- Mrudula, S. & Murugammal, R., 2011. Production of cellulase by *Aspergillus niger* under submerged and solid-state fermentation using coir waste as a substrate. *Brazilian Journal of Microbiology*, 42(3), pp.1119-1127. doi: 10.1590/S1517-838220110003000033.
- Neifar, M. et al., 2015. Extremophiles as source of novel bioactive compounds with industrial potential. *Biotechnology of bioactive compounds: sources and applications*. Wiley, Hoboken, pp.245-268. doi: 10.1002/9781118733103.ch10
- Nies, D.H., 2000. Heavy metal-resistant bacteria as extremophiles: molecular physiology and biotechnological use of *Ralstonia* sp. CH34. *Extremophiles*, 4(2), pp.77-82. doi: 10.1007/s007920050140.
- Nicolaus, B., Kambourova, M. & Oner, E. T., 2010. Exopolysaccharides from extremophiles: from fundamentals to biotechnology. *Environmental Technology*, 31(10), pp.1145-1158. doi: 10.1080/09593330903552094
- O'sullivan, A. C., 1997. Cellulose: the structure slowly unravels. *Cellulose*, 4(3), pp.173-207.
- Oyekola, O.O., 2003. *The enzymology of sludge solubilisation under biosulphidogenic conditions: isolation, characterisation and partial purification of endoglucanases*. Rhodes University.
- Patyshakuliyeva, A. et al., 2016. Improving cellulase production by *Aspergillus niger* using adaptive evolution. *Biotechnology letters*, 38(6), pp.969-974. doi: 10.1007/s10529-016-2060-0
- Podar, M. & Reysenbach, A.L., 2006. New opportunities revealed by biotechnological explorations of extremophiles. *Current opinion in Biotechnology*, 17(3), pp.250-255. doi: 10.1016/j.copbio.2006.05.002

- Raddadi, N. et al., 2015. Biotechnological applications of extremophiles, extremozymes and extremolytes. *Applied Microbiology and Biotechnology*, 99(19), pp.7907-7913. doi: 10.1007/s00253-015-6874-9
- Rampelotto, P.H., 2013. Extremophiles and extreme environments. *Life*, 3(3), pp.482-485. doi: 10.3390/life3030482
- Ray A.K. et.al., 2007. Optimization of fermentation conditions for cellulase production by *Bacillus subtilis* CY5 and *Bacillus circulans* TP3 isolated from fish gut. *Acta Ichthyologica Et Piscatoria*, 37(1), pp.47-53.
- Sarmiento, F., Peralta, R. & Blamey, J.M., 2015. Cold and hot extremozymes: industrial relevance and current trends. *Frontiers in Bioengineering and Biotechnology*, 3, pp.148 doi: 10.3389/fbioe.2015.00148
- Schiraldi, C. & De Rosa, M., 2002. The production of biocatalysts and biomolecules from extremophiles. *Trends in biotechnology*, 20(12), pp.515-521. doi: 10.1016/s0167-7799(02)02073-5
- Sethi, S. et al., 2013. Optimization of cellulase production from bacteria isolated from soil. *ISRN Biotechnology*.doi: 10.5402/2013/985685
- Shah, S.R., 2014. Chemistry and application of cellulase in textile wet processing. *Research Journal of Engineering Sciences*, 3(2), pp.1-5
- Shanmugam, S. et al., 2019. Enhanced bioconversion of hemicellulosic biomass by microbial consortium for biobutanol production with bioaugmentation strategy. *Bioresource technology*, 279, pp.149-155. doi: 10.1016/j.biortech.2019.01.121
- Shrestha, N. et al., 2018. Extremophiles for microbial-electrochemistry applications: a critical review. *Bioresource technology*, 255, pp.318-330. doi: 10.1016/j.biortech.2018.01.151
- Sindhu, R., Binod, P. & Pandey, A., 2016. Biological pretreatment of lignocellulosic biomass—An overview. *Bioresource technology*, 199, pp.76-82. doi: 10.1016/j.biortech.2015.08.030
- Singh, O.V., 2012. *Extremophiles: sustainable resources and biotechnological implications*. John Wiley & Sons.
- Stetter, K.O., 1999. Extremophiles and their adaptation to hot environments. *FEBS letters*, 452(1-2), pp.22-25. doi: 10.1016/s0014-5793(99)00663-8
- Tango, M.S.A., & Islam, M.R., 2002. Potential of extremophiles for biotechnological and petroleum applications. *Energy Sources*, 24(6), pp.543-559. doi: 10.1080/00908310290086554
- Wang, H.C., Susko, E., & Roger, A. J., 2006. On the correlation between genomic G+ C content and optimal growth temperature in prokaryotes: data quality and confounding factors. *Biochemical and biophysical research communications*, 342(3), pp.681-684. doi: 10.1016/j.bbrc.2006.02.037
- Wood, T.M. & Bhat, K.M., 1998. Method for measuring cellulase activities. In *Methods in Enzymology, Cellulose and Hemicellulose*, Vol. 160, pp. 87-112. New York: Academic Press.
- Xia, L. & Cen, P., 1999. Cellulase production by solid state fermentation on lignocellulosic waste from the xylose industry. *Process Biochemistry*, 34(9), pp.909-912. doi:10.1016/S0032-9592(99)00015-1
- Zhang, Z.J. et al., 2013. The beatability-aiding effect of *Aspergillus niger* crude cellulase on bleached simao pine kraft pulp and its mechanism of action. *BioResources*, 8(4), pp.5861-5870. doi: 10.15376/biores.8.4.5861-5870
- Zhu, D. et al., 2020. Recent Development of Extremophilic Bacteria and Their Application in Biorefinery. *Frontiers in Bioengineering and Biotechnology*, 8, pp.483